Regional hydrogeology and groundwater budget modeling in the arid Middle Drâa Catchment (South-Morocco)

Dissertation

zur

Erlangung des Doktorgrades (Dr. rer. nat.)

der

Mathematisch-Naturwissenschaftlichen Fakultät

der

Rheinischen Friedrich-Wilhelms-Universität Bonn

vorgelegt von

Stephan Klose

aus Brühl

Bonn, am 12. November 2012

Angefertigt mit Genehmigung der Mathematisch-Naturwissenschaftlichen Fakultät der Rheinischen Friedrich-Wilhelms-Universität Bonn

1. Gutachter: Prof. Dr. Barbara Reichert

2. Gutachter: Prof. Dr. Lhoussaine Bouchaou

Tag der Promotion: 21. Dezember 2012

Erscheinungsjahr 2013

For my parents, my wife and my children!

Acknowledgements

This work is realized as a part of the IMPETUS project that was funded by the Federal German Ministry of Education and Research (BMBF) under grant No. 01 LW 06001B and by the Ministry of Innovation, Science, Research and Technology (MIWFT) of the federal state of Northrhine-Westfalia under grant No. 313-21200200.

First, I convey my sincere thanks to my supervisor Prof. Dr. B. Reichert, who made this thesis possible, assisted my work always open-minded and provided a reliable framework even beyond the period of the IMPETUS project. I warmly thank co-supervisor Prof. Dr. L. Bouchaou for the deep interest in my work and for his experienced support. I express my grateful thanks to Prof. Dr. B. Diekkrüger, who was always ready to support me and spend very instructive advice.

I sincerely thank Dr. S.-O Franz and the laboratory team for their indispensable and valuable work, namely B. Schulte-van Berkum, C. Kurth, S. Berkau, L. Schlüter (from INRES) and Dr. H. Wörmann.

My special thanks go to all colleagues who provided data and support for this thesis, namely H. Busche, C. Heidecke, A. Klose, O. Schulz, A. Kunert, S. Breuer, K. Haaken, R. Stumpf, K. Born, M. Finckh, A. Roth and Christina Rademacher-Schulz.

I express my cordial gratitude to our Moroccan partners for their lasting help in terms of local expertise, data and advice contributed from among the experts of the Direction del la Rechèrche et Planification de l'Eau, Service Eau Ouarzazate, Direction Générale de l'Hydraulique and the Office Regionale de Mise en Valeur Agricole Ouarzazate.

I have to thank a lot the IMPETUS head office for the support and cooperativeness.

I am grateful for the people who helped me in in Morocco and during fieldwork, namely Aziz Labdi, J. Ait El Hadj, Rachid Essafi, Abdessalam, Abdallah, Nour-Eddine, Fatima and Redouan, M. El Sabbar, Si Ahmed, L. Ait Ahmed among others.

I very specialy thank H. Busche, A. Klose, O. Schulz, C. Heidecke, A. Kocher and G. Steup for their ideas and enduring willingness to discuss my thesis. Without those, this thesis would have never finished!

Very warm thanks goes out to all colleagues around helping me professionally and personally, e.g. A. Kocher, P. Fritzsche, S. Giertz, H. Hölzel, K. Graf, K. Haaken, R. Stumpf, S. Breuer, U. Kutsch, S. Beuel, I. Görlich, J. Staisny, L. Bohnenkämper, Dr. M. Valdivia-Manchego and A. Waidosch.

I express my deep thanks to my family, namely my parents, Rosemarie and Gerd Braun, my wife Anna and her parents for their patience and their unconditional support.

Abstract

This study deals with the regional hydrogeology in Middle Drâa Catchment (MDC) in South-Morocco that features 15,000 km² of semi-arid to hyper-arid conditions and a heterogeneous geological setting. The MDC covers the southern flank of the central Anti-Atlas Mountains reaching the southerly adjacent Saharan Foreland. Pasture and migration are of significant meaning for existence. Important agriculture and settlement concentrate mainly in six date palm oases along the Wadi Drâa relying on both stream flow and uncontrolled groundwater pumping for irrigation. The dominant groundwater exploitation taps the most important alluvial Drâa aquifers that relate to the six Drâa oases. The Drâa aquifers form an interrupted chain of shallow groundwater reservoirs embedded in a hard rock aquitard system veined by a tributary wadi network.

The pressure of climate and global change particularly demands the analysis of the groundwater system, the quantification of water availability and scenario projections to derive options of adaptation and mitigation.

Accordingly, results of the analysis of groundwater level data, hydrogeochemical and hydrogeological information lead to the characterization of the current state of the groundwater system and the development of the groundwater budget model BIL. The BIL model simulates the lumped annual groundwater availability and response at the Drâa aquifers.

Lithological information from mapping surveys and bore log descriptions form the basis of a hydrofacies framework refining the existing concept of the aquifer system in the MDC. The groundwater level response of the Drâa aquifers relates to the re-interpreted distribution of specific yield values. The recent recharge of the Drâa aquifers depends mostly on transmission losses from the regulated inflow from the Upper Drâa Catchment to the Wadi Drâa. Indirect recharge from floods generating after intense rainfall within the MDC is another source of aquifer replenishment. The analysis of inorganic groundwater composition and stable isotope signature verifies the interpretation of the aquifer system and the main groundwater flow paths. The distribution of the hydrochemical facies and the state of hydrogeochemical evolution hint on significant influence of groundwater pumping for irrigation.

Based on the preceding analysis, items of the groundwater balance are pre-processed for each Drâa aquifer individually considering groundwater discharge from one aquifer to another. Accordingly, the BIL model assesses the annual groundwater budget of the Drâa aquifers for the 33 year period 1974-2006. The model results are highly sensitive to changes in indirect recharge from stream flow infiltration, aquifer properties and irrigation-related parameters. The plausibility tests of the model results reveal satisfying accordance with observed piezometric data as available.

So, scenarios of climate and global change are analyzed using the BIL model. As climate change has a significant impact on the groundwater availability of the Drâa aquifers and global change even worsens the situation, options of groundwater management are derived from the hydrogeological analysis and the groundwater budget modeling.

Zusammenfassung

Gegenstand der Untersuchungen ist die regionale Hydrogeologie im 15,000 km² großen mittleren Einzugsgebiet des Wadi Drâa in Süd-Marokko, das durch semi-aride bis hyper-aride Bedingungen und einen heterogenen geologischen Aufbau gekennzeichnet ist. Das Einzugsgebiet erstreckt sich über die südliche Flanke des Anti-Atlas Gebirges und reicht bis in das südlich angrenzende Vorland der Sahara. Extensive Weidewirtschaft und Migration stellen hier wichtige Stützen der Existenz dar. Landwirtschaft und Ansiedlungen konzentrieren sich im Bereich der sechs Dattelpalm-Oasen entlang des Wadi Drâa. Die Bewässerungslandwirtschaft als bedeutungsvollste Aktivität beruht auf der Verfügbarkeit von Flusswasser und unkontrolliert gefördertem Grundwasser. Die Hauptmenge an Grundwasser wird in den alluvialen Drâa-Aquiferen entnommen, den wichtigsten Aquiferen der Region. Dabei unterlagert je ein Aquifer eine der sechs Drâa-Oasen. Die Drâa-Aquifere bilden somit eine gestaffelte Kette von flachen Grundwasserspeichern, die in das umgebende System aus hydraulisch geringleitenden Festgesteinen eingebettet sind. Ein Netzwerk aus Wadis entwässert den Festgesteinsbereich zum Wadi Drâa hin.
Insbesondere die Auswirkungen des Klimawandels und des Globalen Wandels fordern sowohl aktuelle Untersuchungen des Grundwassersystems in der Drâa-Region als auch die Quantifizierung der Wasserverfügbarkeit und die Analyse von möglichen Zukunftsszenarien, um daraus angepasste Strategien des Wassermanagements abzuleiten. Demzufolge werden die Auswertungen von Grundwasserstandsdaten sowie hydrogeochemische und hydrogeologische Informationen genutzt, um den aktuellen Zustand der Grundwasserresourcen abzubilden und das Grundwasserbilanzmodell BIL zu entwickeln. Das Model BIL simuliert die jährliche regional integrierte Grundwasserverfügbarkeit und Grundwasserspiegelschwankungen in den Drâa-Aquiferen. Lithologische Informationen aus Kartierungen und Beschreibungen von Bohrprofilen stellen die Grundlage für die Erstellung einer hydrostratigraphischen Gliederung dar, mit deren Hilfe die bestehende hydrogeologische Modellvorstellung verbessert wird. Die Grundwasserspiegelschwankungen in den Drâa-Aquiferen sind von der neu interpretierten Verteilung der spezifischen Speicherkoeffizienten abhängig. Die aktuelle Grundwasserneubildung wird in hohem Maße durch die Flussbettversickerungen des regulierten Zuflusses aus dem oberen Einzugsgebiet des Wadi Drâa bedingt. Abfluss nach intensiven Niederschlägen innerhalb des Einzugsgebiets des mittleren Drâa führt ebenfalls zur indirekten Grundwasserneubildung. Die Auswertung der Analysen der anorganischen Beschaffenheit des Grundwassers und der stabilen Isotope an Wasserproben bestätigt die Interpretation zu Aquiferbau und -eigenschaften sowie zu den Hauptströmungspfaden des Grundwassers. Die Verteilung der hydrochemischen Fazies und die Deutung der hydrogeochemischen Entwicklung entlang der Hauptfließpfade des Grundwassers weisen auf deutliche Einflüsse durch die Entnahmen für die Bewässerung hin.
Aufbauend auf diesen Analysen wird die Berechnung der einzelnen Posten für die Grundwasserbilanz für jeden Drâa-Aquifer vorbereitet. Dabei wird der Grundwasserabfluss zwischen den Aquiferen berücksichtigt. Im Folgenden simuliert das Model BIL die jährliche Grundwasserbilanz der Drâa-Aquifere für 33 Jahre in der Periode 1974-2006. Die Sensitivität der Modelergebnisse ist hoch gegenüber der Veränderung der indirekten Grundwasserneubildung aus Flussbettversickerung, den Aquifereigenschaften und den Parametern, die mit der Bewässerung verknüpft sind. Die Prüfung der Plausibilität der Modellergebnisse fällt zufriedenstellend aus, gemessen an lückenhaft verfügbaren Grundwasserstandsdaten. Somit wird das Model BIL eingesetzt, um Szenarien zum Klimawandel und zum Globalen Wandel zu analysieren. Da der Klimawandel eine deutliche Reduzierung der Grundwasserverfügbarkeit in den Drâa-Aquiferen zur Folge hat und der Globaler Wandel die Situation verschärfen oder verbessern kann, werden aus der hydrogeologischen Analyse und der Grundwasserbilanzmodellierung Optionen für das Grundwassermanagement abgeleitet.

Résumée

Objet de cette enquête est l'hydrogéologie régionale dans le bassin versant du moyen Oued Drâa au sud du Maroc, caractérisée par 15 000 km² des conditions d'aridité semi aride et hyper et une structure géologique hétérogène. Le bassin versant couvre le flanc sud de l'anti Atlas et plages dans l'avant-pays d'adjacentes du sud du Sahara. Pâturage extensif et la migration est ici des piliers importants de l'existence. L'agriculture et les établissements sont concentrés dans la région de l'oasis de palmiers dattiers six le long de l'oued Drâa. L'agriculture irriguée comme l'activité la plus importante est basée sur la disponibilité de l'eau de rivière et incontrôlée a parrainé des eaux souterraines. Le montant en principal des eaux souterraines est retirée dans l'alluviale du Drâa aquifères, les aquifères les plus importants de la région. Il sous-tend un aquifère chacune des oasis du Drâa six. Les nappes Drâa ainsi former une chaîne en quinconce des aquifères peu profonds, qui sont incorporés dans le système de roche environnante hydraulique faiblement conducteur. Un réseau d'oueds drainé vers la zone de hard rock de l'oued Draa. En particulier, les effets du changement climatique et du changement global nécessitent que les deux enquêtes en cours du système des eaux souterraines dans la région du Draa et la quantification de la disponibilité de l'eau et de l'analyse de scénarios futurs possibles afin d'en tirer des stratégies appropriées de gestion de l'eau.
Par conséquent, l'analyse des données au niveau des eaux souterraines et d'information hydrogéochimique et hydrogéologique est utilisée pour cartographier l'état actuel des ressources en eaux souterraines, et de développer la BIL modèle des eaux souterraines équilibre. Le modèle simule la BIL annuelle régionalement intégrée des eaux souterraines disponibilité et les fluctuations de la nappe phréatique dans les aquifères du Drâa. L'information lithologique à partir des cartes et des descriptions des diagraphies de puits sont la base pour la création d'une structure hydrostratigraphique qui permet à l'actuel modèle hydrogéologique conceptuel est améliorée. Les fluctuations de la nappe d'eau dans les aquifères du Drâa dépendent de la distribution du coefficient de stockage nouvellement interprété spécifique. La recharge des eaux souterraines en cours est en grande partie causée par l'infiltration rivière de l'afflux réglementé de la zone de chalandise du Draa supérieure. Les eaux de ruissellement après des pluies intenses dans le bassin versant du Drâa centre mènent aussi à la recharge des eaux souterraines indirecte. L'évaluation de l'analyse de la composition minérale de l'eau souterraine et les isotopes stables d'échantillons d'eau confirmé l'interprétation de la structure de l’aquifère et des propriétés de l’aquifère ainsi que les voies d'écoulement principales de la nappe phréatique. La répartition des faciès hydrochimiques et l'interprétation de l'évolution hydrogéochimique le long des principales voies d'écoulement des eaux souterraines indiquent une influence significative par les prélèvements pour l'irrigation. Sur la base de ces analyses, le calcul des éléments pour l'équilibre des eaux souterraines pour chaque aquifère du Drâa est en cours de préparation. Ici, l'écoulement des eaux souterraines entre l'aquifère est considéré. Dans ce qui suit, le modèle simule BIL, l'équilibre des eaux souterraines des aquifères Drâa depuis 33 ans dans la période 1974-2006. La sensibilité des résultats du modèle est élevée par rapport à la variation de la recharge des eaux souterraines indirecte de la rivière infiltration, la nappe phréatique et les paramètres associés à l'irrigation. L'examen de la plausibilité des résultats du modèle est satisfaisant, compte tenu des données disponibles inégales niveau des eaux souterraines. Ainsi, la BIL modèle est utilisé pour analyser des scénarios sur le changement climatique et le changement climatique. Le changement climatique a un impact significatif sur la disponibilité des eaux souterraines dans les aquifères du Drâa et le changement mondial exacerbé la situation, à partir de l'analyse hydrologique et les options de base de bilans hydriques de modélisation pour la gestion des eaux souterraines sont dérivés.

Content

List of Figures

List of Tables

Abbrevations

DRPE	Direction de Recherche et Planification de Ressource en Eau, Rabat
ORMVAO	Office Nationale de Mise en Valeur d'Agricole Ouarzazate
DRE	Division des Ressources en Eau, Rabat
BIL model	Bilan hydrique de la Vallée du Drâa Moyen (model name)
IWEGS	Interaction of Water Exploitation on Groundwater and Soil (SDSS name)
SDSS	Spatial Decision Support System
SE	Service Eau Ouarzazate
CEM Drâa	Consommation d'Eau Ménagère (modul name of the BIL model)
SahysMod	Finite Difference Model to assess soil and groundwater salinity
CMB	Chloride Mass Balance method
WTF	Water Table Fluctuation method
IAH	International Association of Hydrogeologists
IAHS	International Association of Hydrolgical Sciences
GLOWA	Globaler Wandel des Wasserkreislaufs (Name of a research program)
BMBF	German Federal Ministry of Education and Research
MIWFT	Ministry of Innovation, Science, Research and Technology
DEM	Digital Elevation Model
HDI	Human Development Index
PAGER	Programme d'Approvisionnement Groupé en Eau Potables en Zones Rurale
GPS	Global Positioning System
XDA	X-ray Diffractometer Analysis
XFA	X-ray Fluorescence Analysis
PHREEQC	(Name of a numerical hydrochemical model)
HDPE	High Density Poly-Ethyl
LDPE	Low Density Poly-Ethyl
EC	(Specific) Electric Conductivity
GWML	Global Meteoric Water Line
LMWL	Local Meteoric Water Line

1 Introduction

The quantification of groundwater resources at the regional scale is a scientific challenge in particular in drylands under the threats of global change. Therefore, there is a desperate need for sound scientific expertise to support efficient groundwater management in dry environments. The understanding of mechanisms of current groundwater table fluctuations and aquifer response is crucial, as groundwater is one tessera of the hydrological cycle. Groundwater may also connect the recent hydrological cycle to "fossile" water resources in the ground providing a buffer reservoir and influencing water quality. The synthesis leads to the development of simulation models helping to better deal with the recent and future developments of the groundwater resources.

1.1 Motivation

The Middle Drâa Catchment (MDC) in South-Morocco features 15,000 km² of semi-arid to hyper-arid conditions, heterogeneous hydrogeological setting and selectively concentrated agriculture relying on both stream flow in the Wadi Drâa and uncontrolled groundwater pumping for irrigation. The pressure on water resources increases due to climate change and global change. Therefore, it is essential to identify the pressures and the current state of the groundwater system. The estimation and classification of future developments of groundwater resources support farsighted groundwater management. Accordingly, strategies of adaptation to and mitigation of impacts of global change can be found. In this context, research seeks to enhance knowledge and analysis techniques forming the basis to develop robust simulation tools for scientific and practical application.

1.2 Aim

This study aims on the analysis of the current state of the groundwater resources in the Middle Drâa Catchment. Therefore, it focuses on the characterization of the aquifer response and the groundwater evolution to prepare the modeling of the annual groundwater budget of the Drâa aquifers, which are the most important aquifers related to the oases along the Wadi Drâa. The impact of global change is assessed according to scenarios analyses using the groundwater budget model. Accordingly, the central research questions are:

- Which are the mechanisms of aquifer response?
- How much drainable groundwater is available?
- How the groundwater resources will develop under the pressure of global change?
- Which management options can be derived?

The following obligatory aspects are focused to answer the main research questions:

- Groundwater occurrence
- Groundwater flow patterns
- Quality of groundwater
- Groundwater recharge – processes and localization
- Groundwater discharge
- Groundwater use and consumption

1.3 Approach

The study follows a classical hydrogeological investigation concept (see Kovalevsky et al., 2004) enhanced by groundwater balance modeling. Therefore, the approach is subdivided in two parts providing

practical outcomes for a long-term groundwater management at the regional scale (cf. Blöschl & Sivapalan, 1995; Figure 1-1 Figure 1-2; chapter 8 & 9):

- Analysis of aquifer response, main flow paths and evolution of groundwater composition (chapter 6)
- Modeling of the groundwater budget of the Drâa aquifers (chapter 7).

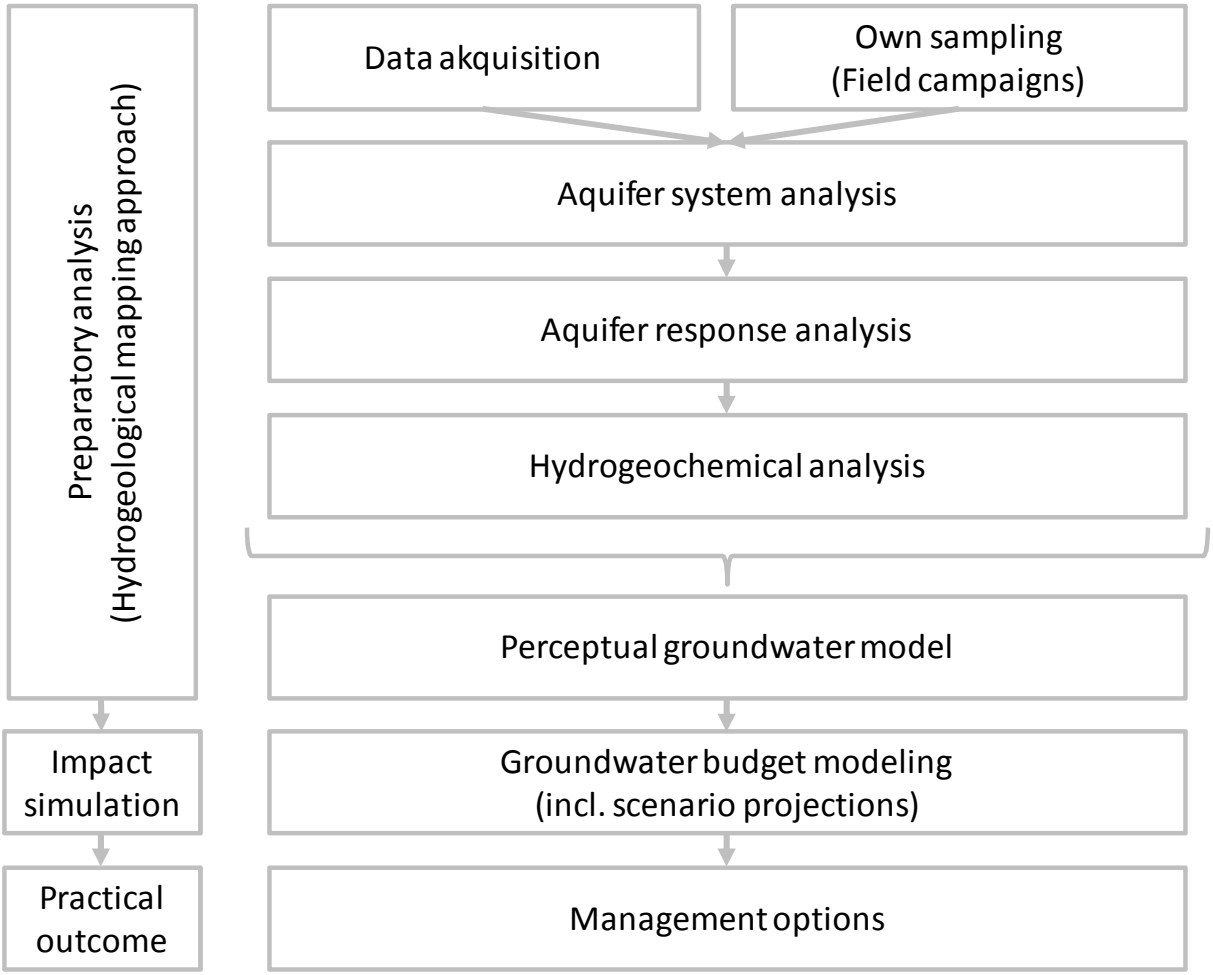

Figure 1-1: Abstract flow chart of the study approach.

The first part of the study is adapted to common mapping approaches that provide parameters for water resources modeling (Ad-Hoc-Arbeitsgruppe Hydrogeologie, 1997; Masuch-Oesterreich, 2000; Hannappel et al., 2003; Struckmeier, 2005). The methods applied to develop a perceptual groundwater model (chapter 7.2) are listed in brief below:

- Realization of recurrent surveys (2005-2007) inclusive analysis of water and rock samples
- Interpretation of geological maps, bore logs and sampling protocols (the latter are provided by the Service Eau Ouarzazate)
- Analysis of groundwater level observations (provided by the Service Eau Ouarzazate and the regional agricultural authorities ORMVAO) including the Water Table Fluctuation (WTF) method (after Healy & Cook, 2002)

- Hydrogeochemical interpretation of water and rock analyses including the Chloride Mass Balance (CMB) approach and stable isotope analysis
- Development of a perceptual groundwater model

The choice of methods is widely limited by the data availability and the research is based on both, own field campaigns and existing data (chapter 4). Own water sampling offers an actualized data base for hydrogeochemical analysis. At exemplary test sites the hydrogeological processes are explained at the sub-regional scale which are comparable with hill slope scale to catchment scale according to Blöschl & Sivapalan (1995; Figure 1-2). Results are then transferred to the regional scale following a lithofacies approach. Therefore, lithological and hydrogeological information is translated to a hydrofacies concept against the background of existing data and expertise.

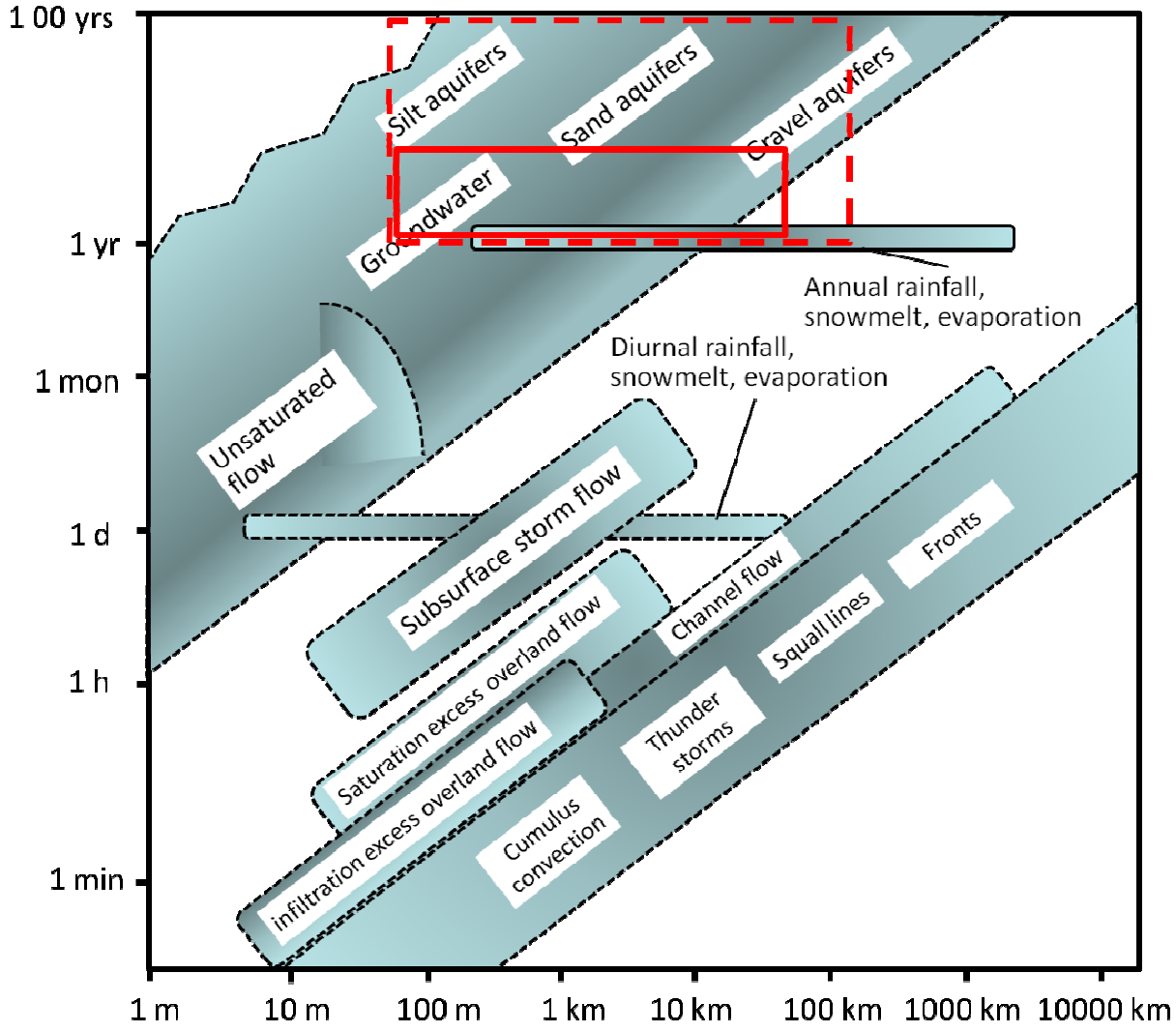

Figure 1-2: Range of characteristic spatial-temporal scales of hydrological processes; the dashed-lined red window marks the approximately the spatial-temporal scale of the study approach and the lined red window marks the sub-regional scale applied to describe the exemplary test sites (adapted from Blöschl & Sivapalan, 1995).

The second part of the study is the assessment of the lumped annual groundwater availability of the Drâa aquifers using a specially developed conceptual groundwater budget model, called BIL (BILan hydrique de la Vallée du Drâa Moyen; Water balance of the Middle Drâa Valley). The groundwater balance modeling includes the following tasks:

- Preprocessing of the water balance components for the Drâa aquifers (being largely congruent with the Drâa oases)
- Simulation of lumped annual groundwater availability (including sensitivity analysis and uncertainty assessment)
- Scenario analysis of global change

1.4 The IMPETUS Project

The IMPETUS research project as a part of the GLOWA research program provided the framework for this study. IMPETUS stands for "Integratives Management Projekt für einen Effizienten und Tragfähigen Umgang mit Süßwasser" in West-Afrika, i.e. integrated approach to the efficient management of scarce water resources in West Africa (http://www.impetus.uni-koeln.de/). IMPETUS was one of five projects within the German GLOWA research program (GLObaler Wandel des WAsserkreislaufs; Global Change and the Hydrological Cycle) under the grant of the German Federal Ministry of Education and Research (BMBF) and the Ministry of Innovation, Science, Research and Technology (MIWFT) of the federal state of Northrhine-Westfalia. IMPETUS started in 2000 and ran over nine years up to July 2009. The research focus was devoted to the impact of global change on the water cycle in two river catchments north and south of the Saharan desert. Accordingly, the Wadi Drâa in Morocco and the river Ouémé in Benin were chosen. Several institutes participated, mainly hosted at the University of Cologne and the University of Bonn. Different disciplines provide insight into the water cycle components from their point of view (e.g. hydrology, pedology, hydrogeology, agricultural sciences, botany, meteorology and anthropology). The research activity was divided into 3 phases starting with process analysis and quantification of water balance components using models in the first phase (2000-2003). The second phase dealt with the analysis and quantification of global change scenarios (2003-2006). The development and implementation of the results via decision support tools was the aim of the third project phase (2006-2009). A consecutive project (2009-2011) ensured the long-term implementation of the outcomes of the IMPETUS project at the relevant institutions in Morocco and Benin (e.g. water authorities).

2 Study area

This study deals with the arid to hyper-arid Middle Drâa Catchment (MDC) in South Morocco. The MDC covers about 15,000 km² on the southern flank of the central Anti-Atlas Mountains and reaches the southerly adjacent Saharan Foreland. The area of interest coincides widely the province of Zagora bordering on Algeria in the South (Figure 2-2 & Figure 2-2). As typical for a dry environment, stream flow appears mostly intermittent in a wadi network. The hydrogeological setting is complex made up of a discontinuous geological record starting around 2 Ga ago. Quaternary sediments form the most important hydrogeological units. Soils are typically poorly developed and the vegetation cover is sparse. The MDC is a marginal region with around 300,000 inhabitants. Human activity is mostly limited by water availability and the main land use is extensive pasture. Settlement and husbandry is concentrated at six date palm oases alongside the Wadi Drâa. Irrigation agriculture is the main activity depending on the controlled stream flow regime of the Drâa and on uncontrolled groundwater pumping.

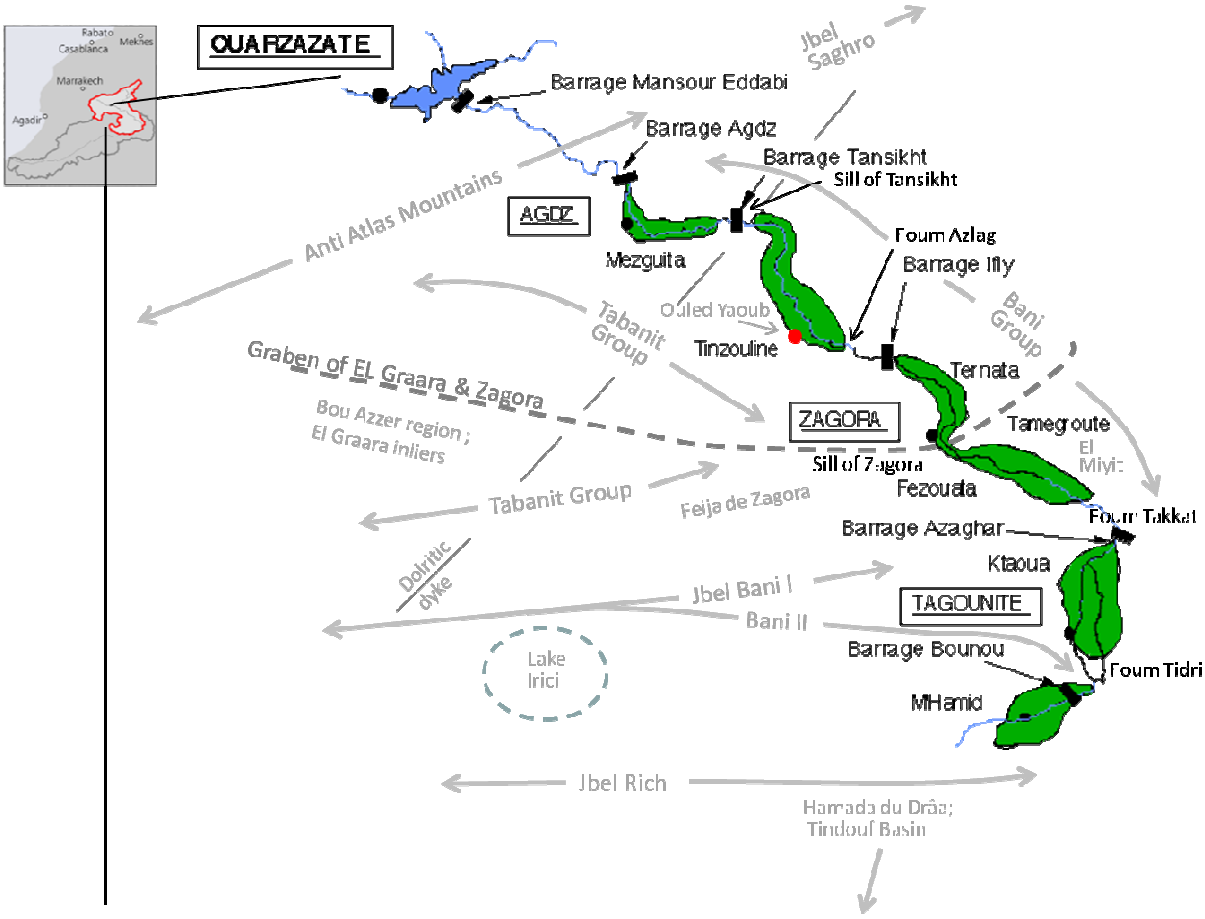

Figure 2-1: Scheme of the study area with the oases belt along the Wadi Drâa and the adjacent main features of landscape and geology.

In this study, four test areas are focused to identify exemplary aquifer settings and flow paths where groundwater is observed and sampled:

- Ternata and Fezouata oasis (spring 2005, see Figure 2-2)
- Basin of Feija de Zagora (West of Fezouata oasis; autumn 2005, see Figure 2-2: red oval “Feija”)
- Ouled Yaoub (downstream end of Tinzouline oasis; autumn 2005 and spring 2007, Figure 2-2: see red oval “OY”)
- Plain of El Miyit (East of Fezouata oasis; spring 2007, see Figure 2-2: red oval “EMY”)

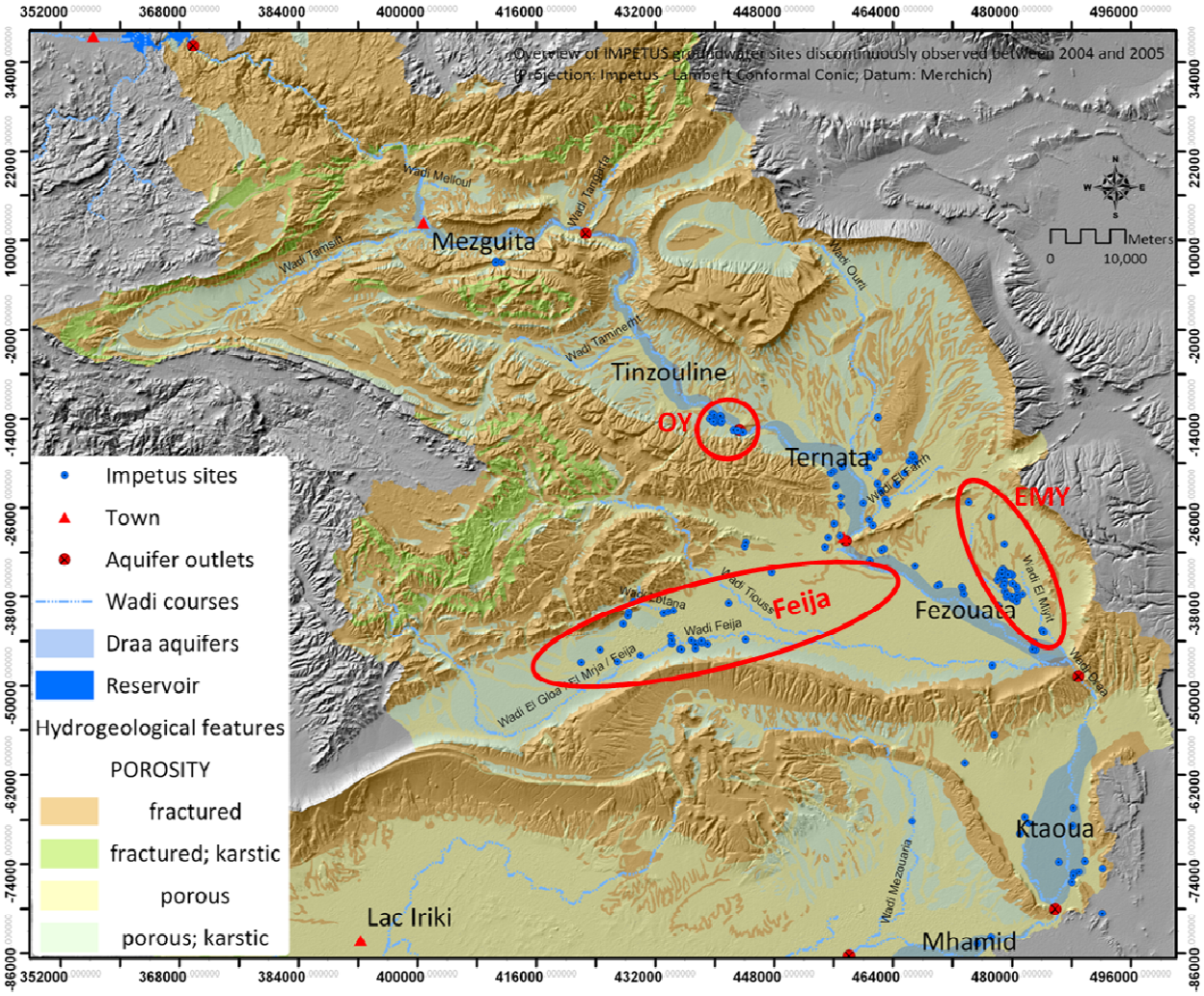

Figure 2-2: Overview of the test areas (see labeling and red ovals: Ternata and Fezouata, Feija, OY (Ouled Yaoub) and EMY (Plain of El Miyit) and distribution of 148 IMPETUS groundwater sites variably observed and sampled in the period 2004-2007.

2.1 Climate

Since the late Tertiary, climate in North Africa has been subject to strong variations between markedly humid periods ("pluvial") and dry periods ("interpluvial"; Michard, 1976; Fontes & Gasse, 1991; Szabo et al., 1995; Maley, 1997; Sultan et al., 1997; Zuppi & Sacchi, 2004). These climate variations influenced strongly the environment leading to the current shape of landscape and forcing temporal variations in groundwater recharge (Edmunds, 2003; Riser, 1988; Cappy, 2006; Arboleya et al., 2008).

Nowadays, the climate in the Middle Drâa Catchment (MDC) is markedly dry. The aridity index after Middleton and Thomas (1992) (ratio of rainfall and potential evapotranspiration) ranges between 0.01 and 0.03, i.e. hyper-arid at all meteorological stations in the MDC (Figure 2-3; Table 2-1). The region south of the High Atlas reveals predominantly arid B climates according to Köppen (1963). South of the Anti-Atlas, climate is mainly characterized as BWh desert climate (warm with mean temperature > 18°C). Typical weather is dominated by locally highly varying situations due to the orogenic barrier of the High Atlas and to lower extend of the Anti-Atlas Mountains. Precipitation is related with southerly and southwesterly winds evading the High Atlas Mountains (Fink et al., 2008; Knippertz, 2003). They can bring rainfall from the Atlantic Ocean. Additionally, easterly winds originating in continental Africa result

in scarce precipitation. Especially in summer, rainfall can arise from the south due to tropical-extratropical interactions. These summer rainfalls provide the largest share of the total annual precipitation accounting for around 40 % (Knippertz, 2003b).

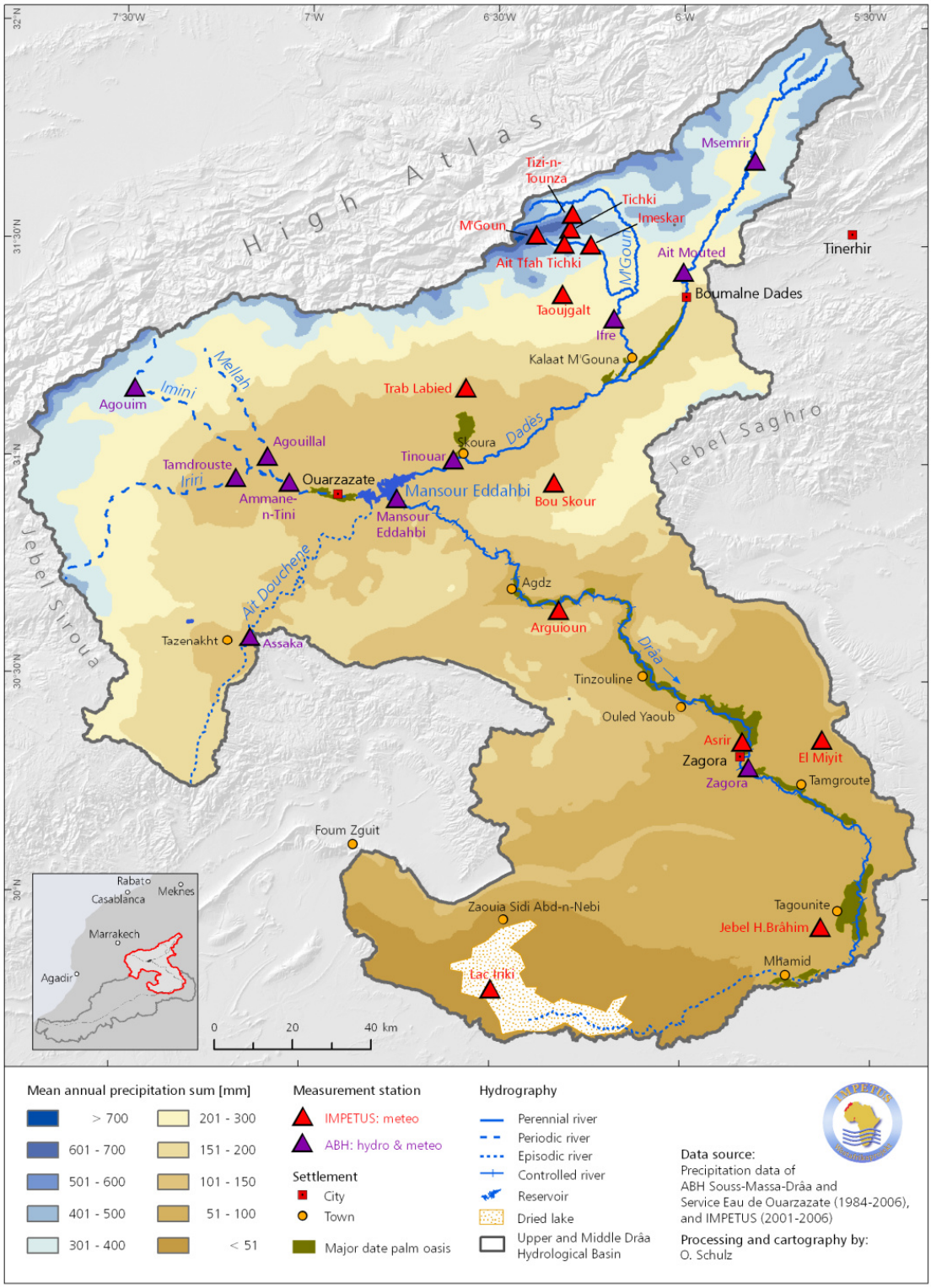

Figure 2-3: Precipitation map of the Upper and Middle Drâa Catchment (Schulz, 2008).

The inter-annual dynamic of precipitation in the region follows a decadal variability revealing distinct humid and dry periods (Schulz et al., 2008; Figure 2-4; Figure 2-3). The annual precipitation in the MDC

is distributed in a bimodal pattern where the rainy seasons are in spring and autumn (Figure 2-4; Müller-Hohenstein & Popp, 1990; Hulme, 1992; Knippertz et al., 2003). The annual rainfall within the catchment ranges roughly between 200 mm in the North and 30 mm in the South. In the same direction, aridity increases (Schulz, 2006; Table 2-1). The mean annual precipitation amounts to 66 mm at the Zagora station in the period 1963/64-1994/95 (data from DRPE; 55 mm for 1963/64-2004/05). The mean annual temperature accounts for 22 °C in the same period (Figure 2-4; data from DRH Agadir).

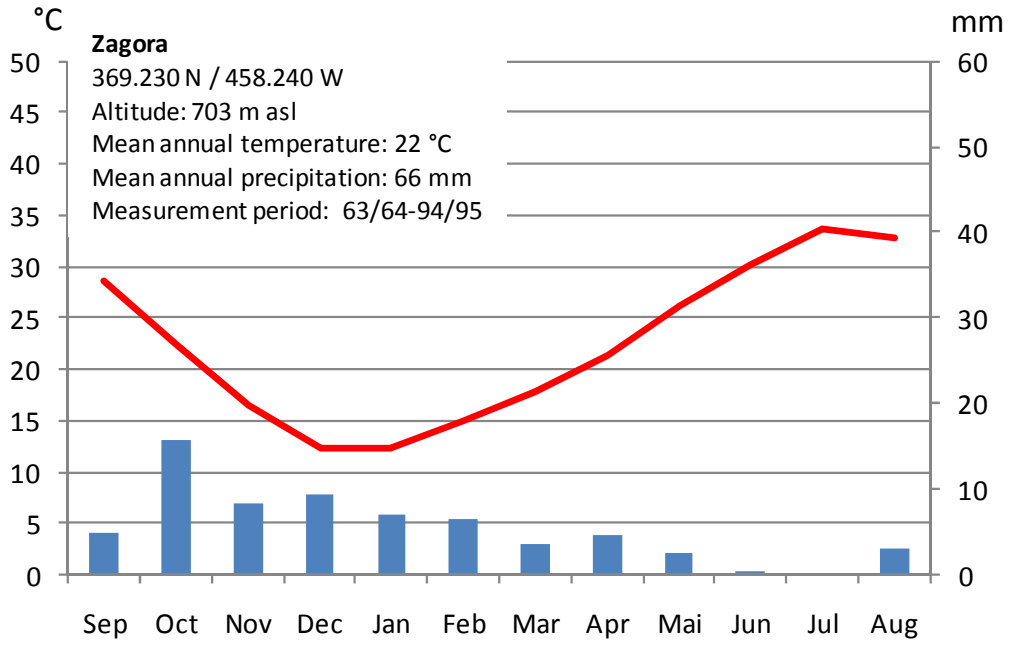

Figure 2-4: Climate diagram of meteorological station at Zagora.

The temporal and spatial variability of rainfall is very pronounced. At the Lac Iriki e.g. 84 % of precipitation fell in 2003 in three events on three days (Figure 2-3). The mean annual potential evaporation reaches around 3000 mm (DRH, 2001). Table 2-1 displays an overview of some characteristic climatic parameters measured at the meteorological stations run by IMPETUS in the MDC.

Table 2-1: Altitude and annual climate characteristics (e.g. aridity) measured the meteorological stations run by IMPETUS in the Middle Drâa Catchment (period 2000-2006; for localization of the stations see figure 3-1).

Station	Altitude [m asl]	Precipitation [mm]	Number of rain days	Evapotranspiration (Pennman-Monteith) [mm]	Aridity Index	Aridity class
Argioun	1020	78	19	2702	0.03	Hyper-arid
El Miyit	792	49	15	2704	0.02	Hyper-arid
Jbel B.-Hssaine	725	33	15	2730	0.01	Hyper-arid
Lac Iriki	450	55	13	2964	0.02	Hyper-arid

In the Drâa oases, actual evapotranspiration is increased due to an “oasis effect” (Huebner et al., 2004). So, the gradient of temperature, relative humidity and wind velocity get steeper between the oasis area and the adjacent scarcely vegetated environment. Additionally, the water use for flood irrigation on the fields enhances actual evapotranspiration.

2.2 Hydrology

The Wadi Drâa is the main drain of the MDC. It starts at the outlet of the reservoir Mansour Eddahbi at Zaouia-N-Ourbaz southeast of the town Ouarzazate. It passes the Anti-Atlas Mountain chain in south-eastern direction and goes down to the endorheic Lake Iriki (Figure 2-4). The further course of the wadi is directed to the south-west towards the Atlantic Ocean. This latter reach of the Wadi Drâa drains the Lower Drâa Catchment, which is tributary to the Atlantic Ocean. The altitudinal difference of the Wadi Drâa accounts for around 450 m between the outlet of the reservoir Mansour Eddahbi and Mhamid near Lake Iriki (Figure 2-5). The length is around 280 km. The hydraulic gradient of the Wadi Drâa ranges between 2.2 ‰ at the oasis Ternata and 1.5 ‰ at the most downstream oases Ktaoua and Mhamid (Figure 2-2; Chamayou et al., 1977). So, the mean gradient is about 1.75 ‰.

The Wadi Drâa drains the southern flank of the central Anti-Atlas Mountains and the Saharan Foreland through a network of ephemeral tributaries. The hydrographic network is widely subject to tectonic lineaments and the occurrence of less resistant rock formations. Runoff generating within the MDC occurs episodically. Base flow is very rare and arises only locally in the Anti-Atlas Mountains. Wadi discharge is usually triggered by intensive precipitation events, which can typically lead to flash floods. ORMVAO (1995) give a range of 20 - 40 Mm^3 of annual wadi discharge, which generates within the Middle Drâa Catchment. Chamayou (1966) found a discharge coefficient of around 8 % related to the station at Zagora (1937/38; 1954/55). Thereby, he relates his estimations to a catchment size of around 9,000 km^2 (between Zaouia-N-Ourbaz and Mhamid). He analyzed the hydrological system for a period before the reservoir Mansur Eddahbi was put in operation. Chamayou (1966) states that the stream flow generating within the MDC plays a secondary role for the regional water balance.

Since 1972, the MDC receives controlled inflow from the Upper Drâa Catchment (UDC) via the reservoir Mansour Eddabhi that is the only outlet. The main inflow comes from periodic water releases several times a year depending on the filling level of the reservoir (Schulz et al., 2008; Busche, in prep.). The water releases are used for agricultural purposes (ORMVAO, 1995). Furthermore, the dam crest can be overflowed after very humid years when the reservoir capacity was exhausted. The mean annual inflow from the reservoir Mansour Eddahbi to the MDC amounts to 261 Mm^3 according to the period of 1973/74-2005/06 while the mean annual volume of the controlled water releases accounts for 214 Mm^3 (data from ORMVAO). In dry years (e.g. 1983/84) the total annual inflow can decrease far below 100 Mm^3 and can exceed 1,300 Mm^3 in very humid years (e.g. 1989/90; Figure 2-6). The illustration of the marked quantiles (10 % and 90 %) elucidates the high variability in surface water availability. It shows both, the bottlenecks due to droughts and the relative surplus of water during humid periods. Furthermore, the deviation of the actual annual inflow from the planned amount of 250 Mm^3 is evident (Figure 2-6). Therefore, the planned annual inflow to the Wadi Drâa is met or exceeded in 40 % of the 33 years according to the total inflow of the period 1973/74-2005/06 but in 60 % of the years it stays unmet.

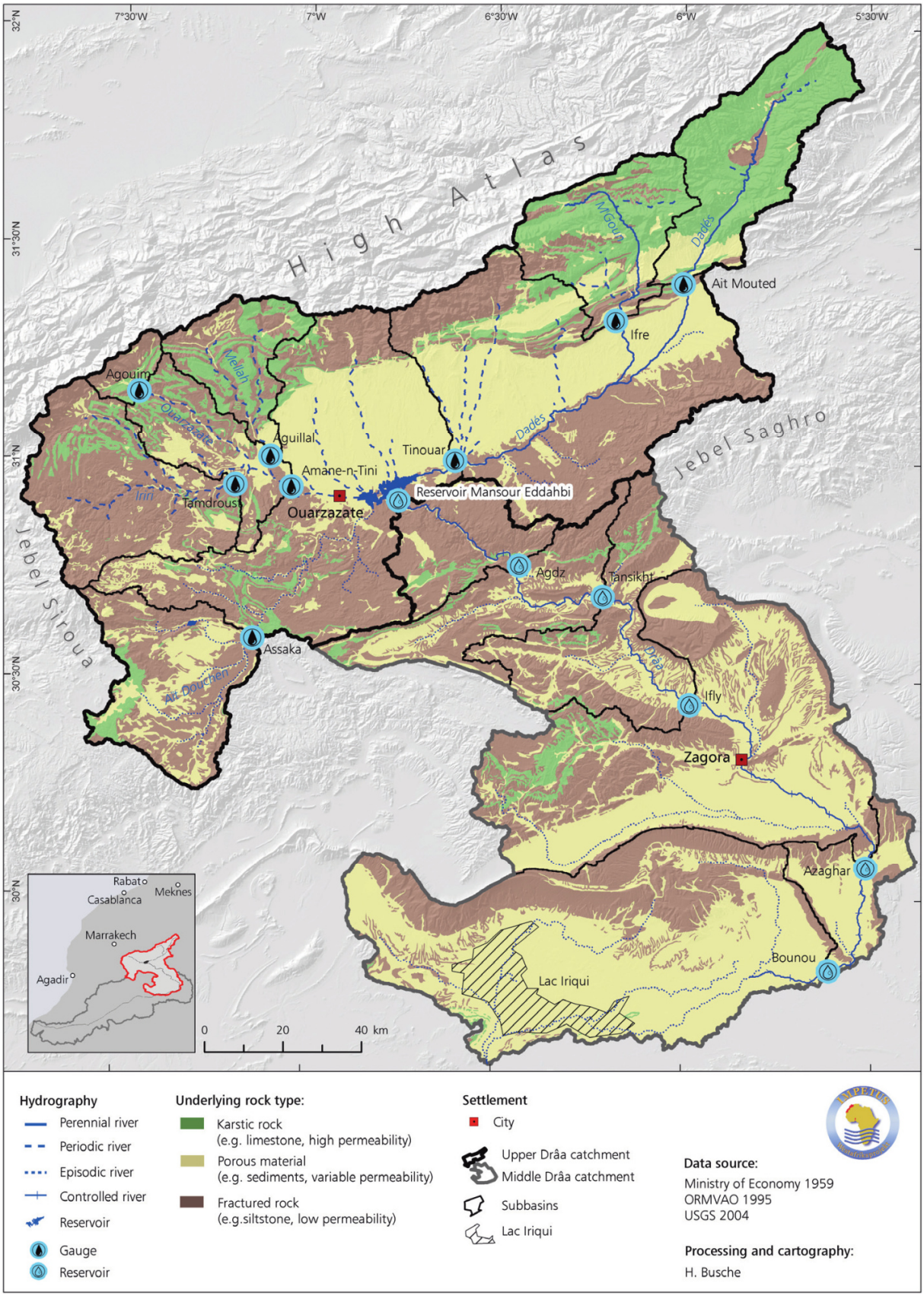

Figure 2-5: Hydrological setting in the Upper and Middle Drâa Catchment.

The water releases are planned to meet both the temporal and quantitative irrigation demand in the Drâa oases. In the majority of the cases, the volume of one water release amounts to 30 to 35 Mm³. So, the water releases last for around 15 days mostly. The inflow from the upstream reservoir is usually let

pass to a barrage at the lowermost oasis Mhamid. Therefore, the water is dammed up along the course of the Wadi Drâa. On the way to Mhamid, the stream flow can be retained in four further barrages to derive water to the oases for agricultural purposes (Figure 2-5; ORMVAO, 1995; Ouhajou, 1996; Doukkali, 2005; Martin, 2006). Water is derived to a hierarchical structured channel network for irrigation. In very dry years, the inflow from the reservoir may be dammed up at one of the barrages upstream of Mhamid to supply only a part of the oases belt along the Wadi Drâa.

Before 1972, the Wadi Drâa drained as an ephemeral river into the endorheic Lac Iriki. The mean annual stream flow was 416 Mm³ (1937/38-1963/64) measured at the gage Zaouia-N-Ourbaz (today's reservoir outlet). A theoretic mean annual stream flow of about 205 Mm³ is depicted based on fragmentary data measured at Zagora in the periods 1940/41-1950/51 and 1962/63-1963/64 (Chamayou, 1966).

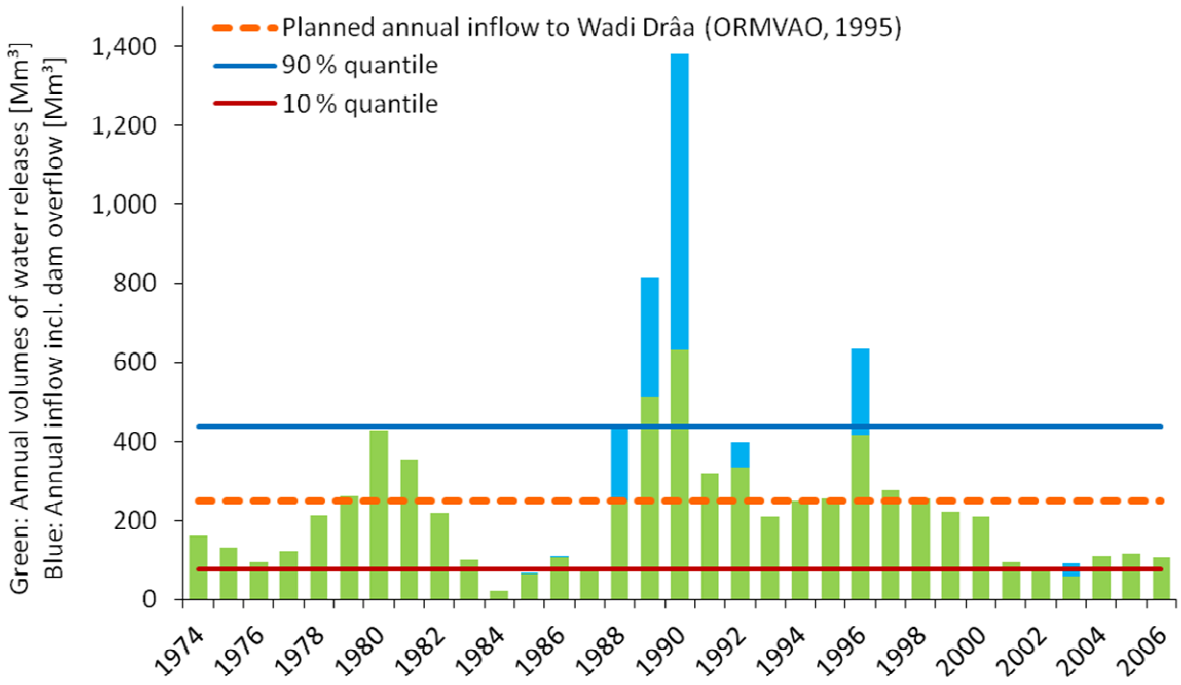

Figure 2-6: Annual amount of controlled water releases (green bars) from the reservoir Mansour Eddabhi and total annual inflow to the Wadi Drâa including the overflow of the dam crest in very humid years (blue bars) with thresholds of planned annual inflow to Wadi Drâa, the 10% quantile and the 90% quantile according to the total annual inflow (data from ORMVAO).

The role of transmission losses by infiltration of stream flow in the wadi bed and the resultant groundwater recharge has rarely been investigated. Chamayou et al. (1977) roughly estimate the losses due to infiltration and evaporation by a water balance approach using an observation period of 17 years. According to this estimate, 38 % of the discharge at Zaouia-N-Ourbaz is lost down to Mhamid. Chamayou (1966) states that losses due to infiltration of water derived for irrigation are more important than losses due to wadi bed infiltration. This may be due to the rapid return flow of water to the wadi bed by interflow.

Surface water quality of the controlled stream flow in the Wadi Drâa depends strongly on the water composition in the reservoir Mansour Eddahbi. The water quality in the reservoir, in turn, depends on

the tributaries from the High Atlas Mountains. The water quality of these tributaries is influenced by leaching of highly soluble minerals such as halite and gypsum occurring in rocks and soils. Thereby, the mineral load can vary with the preceding rainfall pattern and the resulting amount of river discharge (Bouidida, 1990; ORMVAO, 1995; Cappy, 2006). The water quality released from the reservoir Mansour Eddahbi is mostly of good quality in reference to the national classification scheme (750 to 1300 µS/cm; Secreteriat d'état charge de l'eau, 2001; Bouidida, 1990). The composition of the stream flow in the Wadi Drâa evolves along its flow path. So mineralization increases mainly due to evapotranspiration effects (Bouidida, 1990). Runoff generated within the MDC is of low solute content due to its relatively short travel time. Additionally, highly soluble minerals occur seldom along the wadis in the MDC. Pollution from point sources is negligible as the region is mostly extensively used and e.g. industrial emitters are absent.

2.3 Geology

The Middle Drâa Catchment (MDC) is located in the central Anti-Atlas which is a bulge of the northwestern edge of the West African Craton (Michard, 1976; Frizon de Lamotte et al. 2000; Piqué, 2001). The underground is made up of a Proterozoic orogen (the Anti-Atlas itself) with a Paleozoic overburden and a discontinuous Quaternary cover (Figure 2-7).

The out crops of the Anti-Atlas crops stretch along 750 km from the Atlantic Ocean to the Northeast. Towards the Northeast the main axe plunges below the Mesozoic sedimentary rocks of the Hamada du Guir (Algeria). In the North, the Anti-Atlas is bordered by the High Atlas orogen separated by the South-Atlas-Fault (SAF; Figure 2-7; Ennih & Liégeois, 2001). Towards the South, the Anti-Atlas orogen dips beneath the adjacent Tindouf basin (Hamada du Drâa) consisting of Paleozoic to recent fillings (Figure 2-7; Piqué, 2001; Burkhard et al., 2006). The Anti-Atlas orogen developed mainly during the Pan-African orogenesis (Thomas et al., 2004; Burkhard et al., 2006). It consists of two major rock sequences, in which crystalline metamorphic rocks are overlain by a metamorphic volcano-sedimentary sequence. Granites intrude the latter. The Paleozoic overburden represents a Variscan fold belt with a unique tectonic style (Burkhard et al., 2006; Ismat, 2008). It is mainly made up of sedimentary rocks of shallow marine origin (Michard, 1976; Piqué, 2001; Thomas et al., 2004; Collins & Pisarevsky, 2005; Burkhard et al., 2006). Fluvial and lacustrine Quaternary deposits complete the geological record and represent important aquifers in the MDC (Margat 1958; Chamayou, 1966; DRE, 1976; Aoubouazza & El Meknassi, 1996).

Geodynamic evolution

The geodynamic evolution is a key to understand the geological setting, which determines the aquifer system primarily. The discontinuous geological record includes a time span of around 2 Ga. Orogenic imprints determine the orientation of the lineament network representing a substantial feature of groundwater pathways. The Anti-Atlas is located on the **Eburnean** West African craton. It went through the **Pan-African** orogeny and was moderately overprinted by the **Variscan** orogeny. The **Alpine** orogeny had only slight impact within this region (Heinitz, 1984; Helg et al., 2004; Cartig et. al, 2004; Gasquet et al, 2005; Burkhard et al., 2006; Ismat, 2008). The precise geodynamic evolution of the Anti-Atlas is still a matter of debate, especially in cases of dating the latest Pan-African orogenic phase and the interpretation of tectonic style and architecture. The earliest tectonic signal in the Anti-Atlas region stems from the Eburnean (Birimian) orogeny but the Pan-African orogeny (~800 – 530 Ma) and the Variscan orogeny (320 – ?270 Ma) are decisive for the structural setting (Thomas et al., 2004; Gasquet et al., 2005).

Gasquet et al. (2005; 2008) find that the Pan-African orogeny represents a four-stage process, which starts with rifting followed by ocean opening. As a result, the Amazonian craton and terranes such as Avalonia split off from the Paleo-Gondwana continent.

- This first orogenic stage is accompanied by forming volcano-sedimentary sequences and ophiolitic crust (Taghdout group and Bou Azzer group; Gasquet et. al., 2008).
- Subduction takes effect during the second stage documented by calc-alkaline magmatism (Gasquet et al., 2005).
- Next, the basin is compressed and closed in terms of the collision of the West African Craton and formerly split-off terranes (Collins & Pisarevsky, 2005; Burkhard et al., 2006). Because of this third stage, ophiolitic fragments are obducted. Furthermore, a low-grade metamorphism is documented (Gasquet et al, 2005). Subsequently, the sedimentary-volcanoclastic rocks of the Saghro Group generate (Thomas et al., 2004).
- The fourth stage of the orogeny is a post-tectonic extension marked by intermediate to felsic intrusives and mainly alkaline magmatism (Gasquet et al, 2005). In the same period, the Ouarzazte Supergroup, then the Taroudant Group, and the Tata Group develop (Thomas et al., 2004).

The **Anti-Atlas orogen** is as a complex structure of blocks and massifs due to the Pan-African orogeny. The structures in the Anti-Atlas strike WSW-ENE in the eastern part, W-E in the central part and WNW-ESE in the most eastern part of the Anti-Atlas (Burkhard et al., 2006). During the Pan-African orogeny the formerly developed Anti-Atlas-Major-Fault (AAMF) including the Bou-Azzer Graben and Zagora Graben is active as a sinistral strike-slip fault. The AAMF stays virtually inactive since then (Ennih & Liégeois, 2001).

A Paleozoic overburden forms **Anti-Atlas fold belt**. It emerged during the Variscan orogeny after the Cambrian – Early Ordovician rifting (Michard et al., 2008). It is part of the larger Appalachian-Ouachita-Mauritanides orogen system (Robert-Charrue & Burkhard, 2005; Ismat, 2008). The Anti-Atlas fold belt represents an inverted intra-cratonic basin. A severe inversion of the basement structures and a simultaneous poly-harmonic buckle folding takes place due to the Paleozoic compression (Burkhard et al., 2006; Ismat, 2008). Studies of Burkhard et al. (2006) reveal that the basement is uplifted along inverted normal faults (40 – 60°) and outcrops in isolated “boutonnières”. The architecture of the Paleozoic strata changes from West to East in number, amplitude, tightness and cylindricity of upright folds (Burkhard et al., 2006). The resulting shortening is about 17 km. The alternation of quartzites and siltstones in the Paleozoic succession determines an individual stress behavior of the competent strata. Accordingly, the folding of the competent strata varies in frequency and altitude (Burkhard et al., 2006; Ismat, 2008).

The Alpine orogeny represents the latest deformation causing a slight impact (Heinitz, 1984). It comes along with the opening of the Atlantic Ocean and the High Atlas formation (see Table 2-2). Initially, faults are reactivated marked by dolerite dykes (cp. dyke of Foum Zguid; Helg et al., 2004). Subsequently, the Anti-Atlas fold belt is compressed to some extent in NW-SE direction.

Table 2-2: Summary of the geodynamic evolution of the Drâa region (compiled from Beauchamp et al., 1999; Michard et al., 2008).

Stratigraphic age		Geologic evolution
Cenozoic	Neogene - Quaternary	Continuous uplift of the High Atlas; erosion and sedimentation in the Drâa Catchment
	Neogene - Paleogene	Inversion of "Atlas rift" and alpine deformation, compression and major uplift of the High Atlas, faults reactivated and reversed along up-thrusts in the High Atlas; only slight impact in the Anti-Atlas by re-activation of faults; varying shallow marine to continental facies
Mesozoic	Lower Jurassic – Upper Cretaceous	Continuous rifting north of the Anti-Atlas, varying subsidence of the rift basin mosaic and finally isostatic uplift of rift margins of the Atlas system; varying facies from initially deep to shallow marine to continental deposits
	Triassic	Rifting north of the Anti-Atlas, fault-block mosaic; sedimentation of redbeds, evaporates, eruption of basalts
Paleozoic - Mesozoic	Permo - Triassic	Erosion and peneplain generation
Paleozoic	Permo - Carboniferous	Variscan orogenesis, inversion of the intra-cratonic basin, folding and mild metamorphism of the Paleozoic sedimentary rocks
Proterozoic - Paleozoic	Late Ediacaran - Carboniferous	Post Pan-African rifting in the Anti-Atlas (Early Cambrian), transtension, sedimentation in shallow marine facies
Proterozoic	Late Cryogenian – Late Ediacaran	Pan-African Mountain building; transpression, sedimentation of flysch facies, granitic intrusion and volcanism
	Early Cryogenian - Middle Cryogenian	Pan-African orogen, obduction, arc accretion, synmetamorphic folding
	Tonian	Rodinia break up (?), sedimentation of silici-clastic facies and volcanism
	Eburnean	West African Craton consolidation, metamorphism and granitic intrusion

Lithostratigraphical framework

The lithostratigraphical framework and the lithofacies distribution offer insight to the geodynamic evolution and the exogenous processes. The lithofacies determine the hydrogeological properties by far. In the following sections, the occurring geological units are briefly described in stratigraphical order.

Paleo-Proterozoic rocks occur at the western limit of the MDC (Bou Azzer and Zenaga inlier; Figure 2-7). Layered supracrustal schist, paragneisses and migmatite are intruded by granitic or granodioritic rocks. This complex builds the oldest basement of ~2 Ga age representing a product of the Eburnean orogeny (Thomas et al. 2004). Gasquet et al. (2008) compiled a lithostratigraphical framework of the Anti-Atlas orogen.

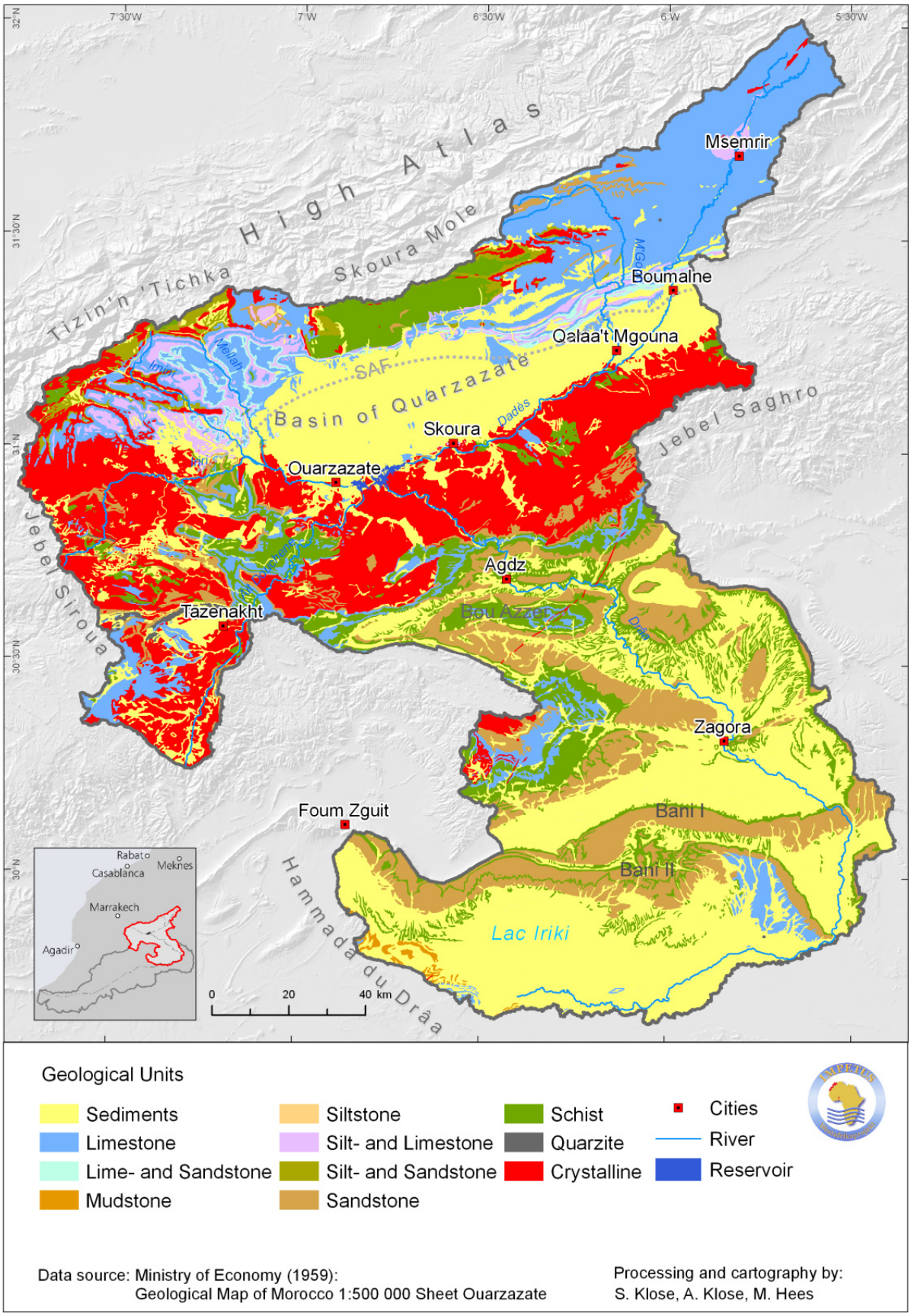

Figure 2-7: Lithological map of the Upper and Middle Drâa Catchment (Data source: Abdeljali et al., 1959: Carte Géologique 1:500000 – Feuille Ouarzazate).

The **Neoproterozoic** rocks are moderately metamorphic (greenschist facies). They are roughly divided into 4 lithostratigraphical groups, the Taghdout group (1), the Bou Azzer group (2), the Saghro group (3) and the Ouarzazate Supergroup (4) (Thomas et al., 2004; Gasquet et al., 2008):

(1) The Taghdout group occurs at the Bou Azzer inlier (see also Tizi'n Tarhatine group) (Thomas et al., 2004; Bouougir & Saquaque, 2004). It composites a sedimentary succession followed by a volcanic sequence and closes up by further sedimentary sequences. Quartzarenites and fine-grained siliciclastic deposits overlie the basal siliciclastic-carbonate successions. Tholeiitic basalts and dolerites follow next associated with gabbros. Siltstones close up this sequence of the Taghdout group interbedded by tholeiitic basalts, exhalative facies and sulphide deposits (Bouougir & Saquaque, 2004).

(2) The Bou Azzer Group is made up of an ophiolitic facies. A fault-bound ophiolitic fragment in the Bou Azzer region (Bou Azzer Group; Thomas et al., 2004) documents the formation of ocean floor.

(3) The Saghro Group outcrops locally in the Jbel Saghro (Fekkak et al, 2000; Figure 2-7). It is an upward coarsening sedimentary-volcanoclastic succession. Siliciclastic turbidites developing from shales to siltstones and sandstones alternate with basaltic beds (Gasquet et al., 2008).

(4) Further volcano-sedimentary sequences occur grouped to the Ouarzazate Supergroup (Thomas et al., 2004). They can be further subdivided by an unconformable contact to the Bou Salda and the Ouarzazate Group (Gasquet et al., 2008). The Ouarzazate Supergroup outcrops in the Jbel Saghro and the Bou Azzer inlier. It consists of rhyolites and meta-andesites alternating to conglomerates and sandstones. Recurrent intrusions are mainly of calc-alkaline composition (Thomas et al, 2004; Gasquet et al., 2008). In total, the Neoproterozoic units account for maximum 11 km of thickness. Mesoproterozoic record is missing (Figure 2-7; Thomas et al., 2004; Gasquet et al., 2008).

The **Paleozoic** successions of sedimentary rocks overlay the basement discontinuously. They cover the southern flank of the Anti-Atlas dipping generally southwards. So, the youngest Palaeozoic strata occur in the most southern part of the MDC, where the Devonian rocks are found (Figure 2-7). Overall, the Palaeozoic sequence accounts for 8-9 km of thickness in the western part and 4-5 km in the eastern part of the Anti-Atlas region (Figure 2-8). The series start with a basal conglomerate changing over to dolomites ("Calcaires inferieur"). They, in turn, end up with siltstones (cp. "Série de base"; Piqué, 2001; Gasquet et al., 2008). This first series is dated to overstep the Neoproterozoic - Cambrian border (cp. "Adoudounian"; Piqué, 2001; Ewen, 2004; Gasquet et al., 2008). Further, Early Cambrian series consist of reddish-purple siltstones intercalated by carbonates, evaporitic rocks and tuff layers ("Série lie-de-vin"). A sequence of limestones follows next ("Calcaires supérieur"). Alternating siltstones and limestones go after ("Série schisto-calaire") and a series of sandstones close up the sequence of Early Cambrian age (Helg et al., 2004). The Middle Cambrian begins with a fine-grained series of schists ("Schistes à Paradoxides") changing over to a sequence of sandstones and quartz-arenites ("Tabanit"). A hiatus separates the Cambrian sediments. Ordovician deposits composite of a siltstone series ("Schistes de Fezouata") followed by a succession of sandstones and quartz-arenites ("Tachilla" and "Bani I"; Destombes, 1985; Steenpaß, 2007; Kunert, 2008). Another succession of siltstones ("Schistes de Ktaoua") overlain by sandstones and quartz-arenites ("Bani II") terminates the Ordovician record (Destombes, 1985). The Silurian record is represented by fine grained sedimentary rocks followed by alternating series of shales, sandstones and limestones of Devonian age.

The upper Palaeozoic record is not documented within the study area. Mesozoic and Tertiary rocks are neither observed in the MDC. Only in the southerly adjacent Hamada du Drâa lacustrine limestones, marls with gypsum and conglomerates of Eocene, Oligocene as well as Mio-Pliocene age occur (Riser, 1988).

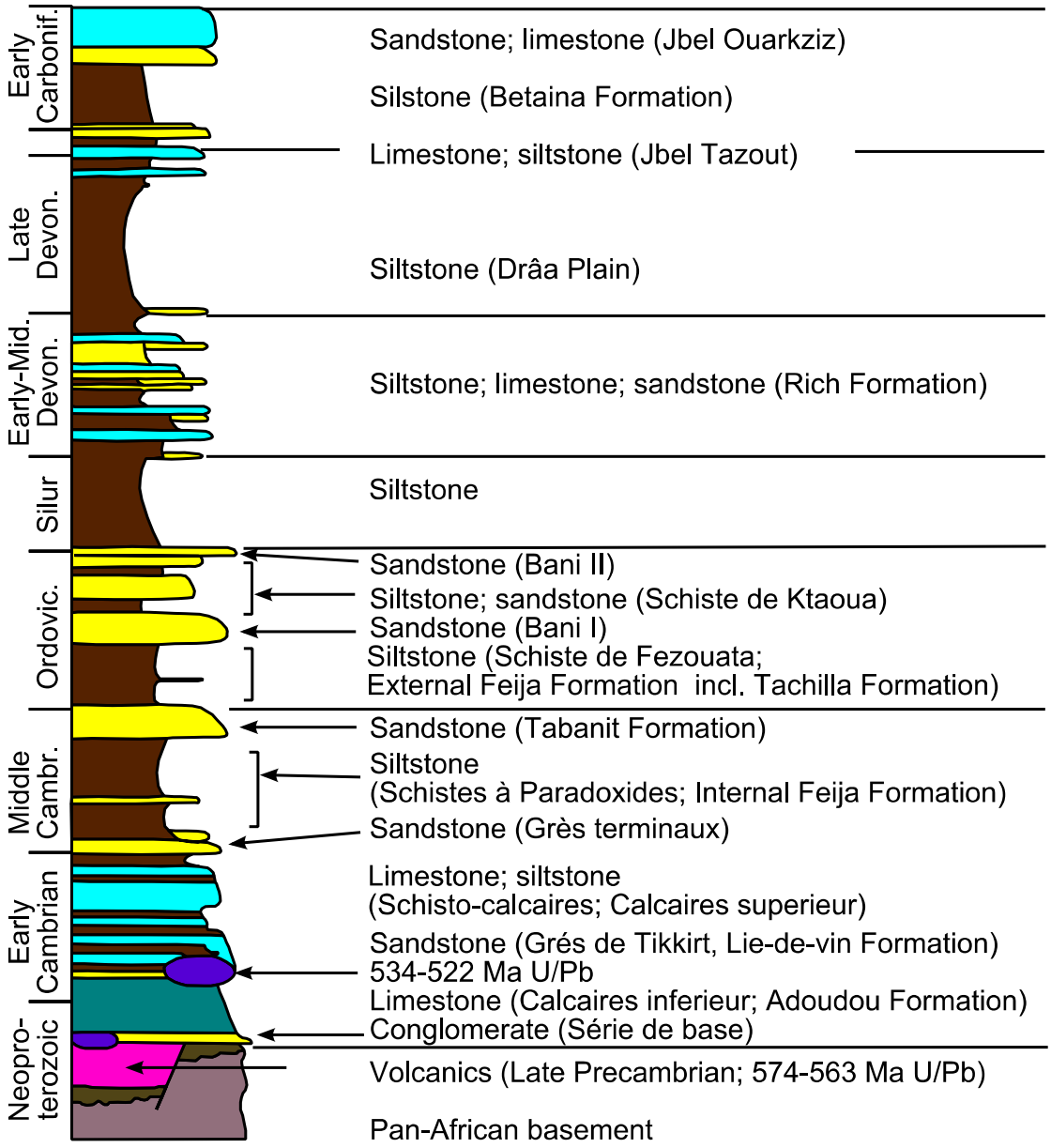

Figure 2-8: Generalized lithological column of the Variscan record in the western and central Anti-Atlas (modified from Gasquet et al., 2008)

On final top, **Quaternary** deposits occur after a hiatus mostly as alluvial terraces, slope debris and costal deposits. The reconstruction of the environment and the correlation of terrestrial and marine records is difficult and rarely investigated (Michard, 1976; Arboleya et al., 2008; Hssaine & Bridgland, 2009). Even the correlation of different sections and bore logs from the same region appears to be complicated (Riser, 1988). In the more humid interglacial periods (pluvial), incision was the dominant catchment process. This is due to the stabilization of hill slopes by a wooded vegetation cover and enhanced surface water availability at the same time. In the more arid glacial periods (interpluvials), sedimentation was the ma-

jor catchment process. In periods of more arid conditions, the stabilizing vegetation cover is missing and hence erosion prevails at the hillsides. In combination to reduced transport energy in the river network, sediments can accumulate in depressions and basins (Arboleya et al., 2008). These processes were most active in the transition times between pluvials and interpluvials.

The Quaternary record of Morocco is subdivided into six stratigraphic stages, Regrégurien, Saletien, Amirien, Tensiftien, Soltanien and Gharbian (Table 2-3). The Lower Pleistocene comprises the stages Regrégurien and Salétien whereas the demarcation of the Villafranchian to the Post-Villafranchian is difficult. During the Regrégurien erosive activity leads to slightly incised valleys into the Villafranchian plateaus. At the same time, calcareous encrustation of the existing strata develops (Michard, 1976). Alluvial deposits from this period are broadly consolidated by limy cement. The Middle Pleistocene (Amirien and Tensiftien) comprises terraces of red-colored and very clayey material incorporating blocks as well as grey-colored sediments with less clay content. These sediments are cemented to a large extend. During the Middle Quaternary lakes and swamps formed proven by lacustrine limestones, marls and marsh land. In the marshy soils, fossils are found such as the terrestrial mollusk *Rumina decollata* and the reed *Phragmatites australis* (Ait Hssaine & Bridgland, 2009; Breuer, 2007). In the later Middle Quaternary, the lakes and Marchhlands dried out. They were changing over to sebkhas proven by the formation of evaporitic rocks, e.g. carbonates and gypsum. The lacustrine deposits cop out e.g. in the sedimentary basin south-west of Zagora (Figure 2-7). During the Upper Pleistocene (Soltanien) lacustrine limestones, marls and fluvial red-colored silty deposits formed. The Lower and Middle Holocene (Gharbien) is often represented by grey to red-colored alluvial loam forming levees along channels (Michard, 1976). In addition to these marker units, slope debris and lacustrine sediments are found according to the respective relief position.

Table 2-3: Stratigraphic stages of the Quaternary (compiled from Awad, 1963; Michard, 1976; Riser, 1988; Arboleya et al., 2008; Hssiane & Bridgeland, 2009).

Sub-Era	Stag (Pluvial)	Geological record	Dominant catchment process	General climatic characteristic
Upper Holocene	(Actual)	Loam, aeolian sand, alluvial deposit	Enhanced erosion on hill sides and sediment supply	Arid
Middle Holocene	Gharbian	Loam, aeolian sand, lacustrine sediment and evaporite	Incision of hydrological network, lacustrine environments, stabilizing vegetation cover	Arid → humid
Lower Holocene		Loam, aeolian sand, lacustrine sediments		Humid
Upper Pleistocene	Soltanian	Loam, sand, gravel, fan deposits, lacustrine sediment, evaporite	Alternating incision of hydrological network and sedimentation, alternating lacustrine and sebkha (daya) environments, changing vegetation cover	Humid → arid
Middle Pleistocene	Tensiftien	Cemented sand and gravel, fanglomerate, conglomerate, lacustrine sediment, evaporite, paleosoils		Strongest changes including most arid phase
	Amirien			
Lower Pleistocene	Saletien	Cemented sand and gravel, fanglomerate, conglomerate	Alternating incision of hydrological network and sedimentation, changing vegetation cover	Alternating humid and moderate arid conditions
	Regrégurien			
Plio-Villafranchian	Hamadien	Lacustrine limestones, marls with gypsum and conglomerates	Peneplain formation	(Tropic)-humid

2.4 Relief

The Anti-Atlas mountain range trends mainly WSW-ENE. It forms the northern limit of the Middle Drâa Catchment (MDC) with highest altitudes of around 2500 masl. The landscape slopes generally from north to south roughly corresponding to the dipping of the underground. The lowest altitude of 450 m asl is found at Lac Iriki. The research area reveals a rejuvenated relief with close similarities with the Appalachian range (Alleghany chain, USA;Burkhard et al., 2006; Ismat, 2008). Medium to high ridges are found in the Anti-Atlas Mountains and a cuesta landscape prevails in the Saharan Foreland. Ridges and cuestas alternate to valleys mainly in the northern part of the catchment. Towards the South, the valleys are increasingly replaced by mostly fault-bordered sedimentary basins where less resistant schist occurs (Riser, 1988). These basins are furrowed by wadis, which may end up in pans without drain.

The crystalline basement forms narrow valleys, rounded hills and smooth ridges. The Paleozoic resistant sedimentary rocks shape relatively sharp ridges and cuestas, such as the Jbel Bani. Wadis are deeply incised where the less resistant schist is distributed. The valleys often follow faults and fractured zones. Besides tectonic lineaments, the ridges and cuestas form natural hydraulic barriers for both surface water and groundwater flow.

The Wadi Drâa forms the most prominent valley within the catchment. It can be subdivided into three distinct morphological sections. In the crystalline rocks of Anti-Atlas Mountains the Wadi Drâa shapes a narrow valley. As the underground is made up of Paleozoic sedimentary rocks, the Drâa Valley is moderately narrow and flanked by Ordovician sandstones and quartzites. At the lower wadi course goes through a more open the as it passes the sedimentary basins between the ridges and cuestas.

Six terraces are observed along the middle and lower wadi course. They are of Quaternary age according to the geological record and altitudinal levels. Slope debris shapes ramps, foot and toe slopes along the ridges and cuestas. Alluvial fans can occupy widespread smoothly sloping areas, especially in the sedimentary basins. In the southern part of the research area isolated fields of sand dunes complete the topographic inventory of a desert environment (Gerrard, 1990).

The recent landform developed as a result of a sequence of mainly two processes:

1. incision
2. formation of peneplains
3. incision again

Pre-Variscan polycyclic processes form the basement building the backbone of landscape. The Variscan orogeny creates gentle southward dipping folds as a basis for cuestas in the Paleozoic sedimentary rocks. Peneplains are generated due to intensive weathering driven by tropical climate conditions during an acyclic phase between Triassic and Miocene. Cyclic incision and sedimentation begins again in the late Miocene accompanied by the major uplift of the High Atlas surely triggered by the Alpine orogeny. Climate variations control the formation of the recent river network, terraces and basin fillings during Quaternary. The base level of the wadi Drâa, as the main drain, drops successively in Quaternary times. Sedimentation prevails during the “interpluvials”, whereas incision is the dominant process during the “pluvials” focusing at the catchment scale (Riser, 1988; Sebrier et al., 2006; Arboleya et al., 2008).

2.5 Soils

The soils in the Middle Drâa Catchment (MDC) are typical for drylands. They mostly have low content of organic matter (less than 1 %), high skeleton content and often reveal crusting and stone pavements (A. Klose, 2009). The most frequent soil type in the MDC is the Regosol as recent research reveals (A. Klose, 2009; Figure 2-9). Calcisols amount for 23 % of observed soils. Solonchaks accounts for a proportion of 15 %, the same as Leptosols, which is most frequent soil type worldwide. Luvisols account for 11 % of soils (A. Klose, 2009).

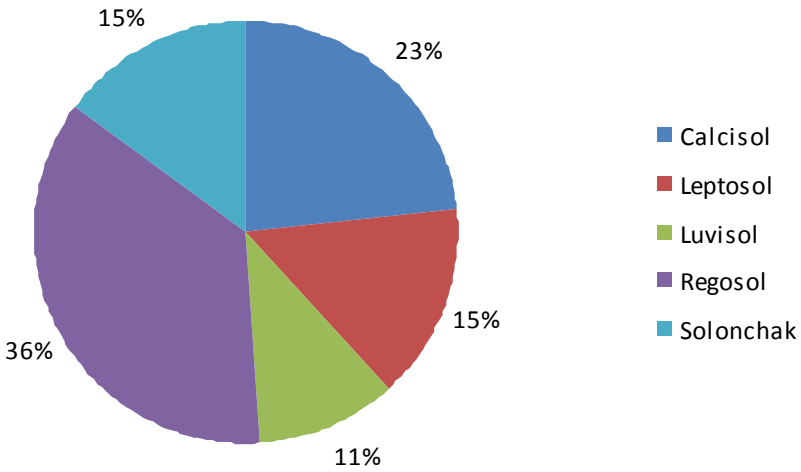

Figure 2-9: Proportion of soil types observed in the Middle Drâa Catchment (after A. Klose, 2009).

The spatial distribution of soils is highly variable. In the sedimentary basins (e.g. Feija de Zagora, Lac Iriki), sandy soils with high skeleton contents dominate, whereby shallow soils rich in skeleton characterize the summits and slopes (Cavallar, 1950). The agriculturally used oasis soils (Anthrosols) are different, as they are formed on loamy loess-like river sediments of up to 8 m thickness. Therefore, they are nearly free of skeleton (e.g. Brancic, 1968). Figure 2-10 shows a typical catena for the study area. Poorly developed Regosols prevail on the silt- and sandstones as well as on quartzites. Luvisols, highly developed Regosols, Solonchaks and Vertisols are found covering alluvial and lacustrine deposits. The limit between sediment layer and soil appears often to be a smooth transition due to the weak development of arid soils. Furthermore, the local existence of Paleo-soils is undoubtedly. Paleo-soils developed in more humid periods of the Quaternary and can be preserved in natural sediment traps (Riser, 1988; Ait Hssaine & Bridgland, 2009).

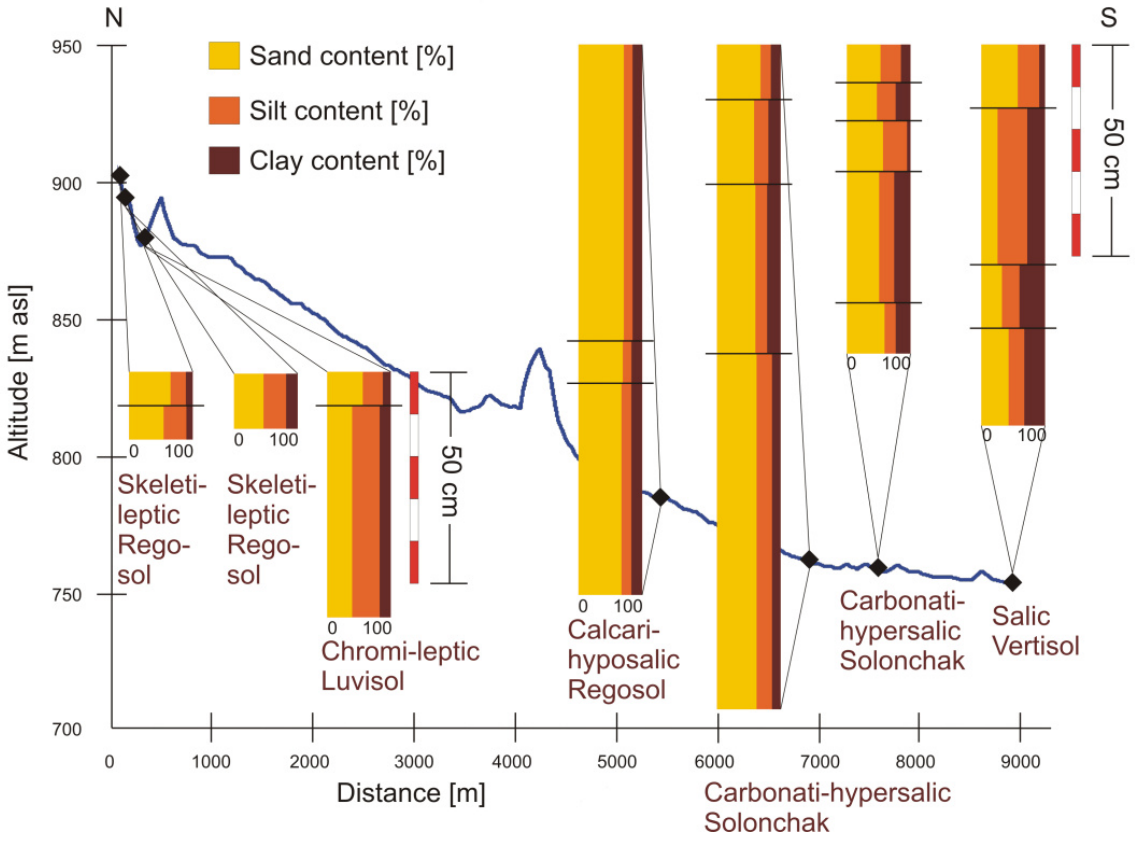

Figure 2-10: Typical catena in the Middle Drâa Catchment near the town of Zagora (from A. Klose, 2009).

Noticeably high carbonate contents are found in each soil type due to aeolian input (A. Klose, 2009). So, fractures and cracks could be refilled by secondary carbonate (chapter 6.1.2). Carbonate can precipitate from percolating water even in the substratum depending on climatic and chemical conditions. At many places crusts and caliches are observed influencing the soils hydrological properties and thus influencing groundwater recharge. Furthermore, the generally high skeleton content and stone pavement have an impact on infiltration (A. Klose, 2009). In addition to occurrence, mobilization and precipitation of minerals the sand content plays an important role for soil salinity. The higher the sand content the better the drainage of the soil and the less the salinization (A. Klose, 2008; Stuhldreher, 2008).

2.6 Land cover and land use

The study area is characterized by an arid desert ecosystem. The vegetation cover is composed of pre-Saharan associations forming steppe land (Finckh & Staudinger, 2002; Le Houérou, 2001). Dwarf-shrub dominated Saharan rock and Saharan wadi communities occupy the research area increasingly to the south. In addition, Artemisia and Hamada steppe occurs and *Acacia raddiana* trees concentrate along the wadis (Finckh & Poete, 2008). Large and medium specimen of Acacia trees can be connected to groundwater by their deep reaching roots (Gresens, 2006). *Tamarix amplexicaule* is found at the margins of the oasis and around dunes. Halophytes are spread on clay-salty soils, especially in pans without active drain.

The sparse natural vegetation cover is the basis for extensive grazing dominating the MDC. So, transhumance and even nomadism exists. Information on livestock is rare. In North African steppes livestock density is estimated to the mean of 0.7 sheep equivalents per hectare (Le Houérou, 2001), surely vary-

ing locally. Because of grazing, the vegetation cover is degraded and desertification appears to be a severe hazard in the study area (Finckh & Staudinger, 2002; Finckh & Poete, 2008; Roth, 2010). Cropping depends generally on irrigation is basically related to the occurrence of loamy Quaternary deposits with favorable soils (chapter 2.3). It concentrates in the belt of six date palm oases along the Wadi Drâa and secondarily along the tributaries. Here irrigation is practiced since many centuries depending on both surface water and groundwater. The main crops are date palms, wheat, barley, alfalfa and henna. Additionally, vegetables and stone fruits are cultivated. The cropping areas are traditionally subdivided into small parcels of land rugged by irrigation canals (Ouhajou, 1996). The irrigated surface varies seasonally depending on crop rotation and water availability (ORMAVAO, 1995). On average, the irrigated surface accounts for around 250 km², i.e. around 1.7 % of the catchments surface.

2.7 Infrastructure, population and economy

The Middle Drâa Catchment (MDC) is a marginal region with agriculture, migration and tourism as principal sources of income. The human development index (HDI) for the Saharan Foreland amounts to a maximum of 0.52 (Belfkih et al., 2006). In comparison to this, the HDI on the national level of Morocco accounts for 0.65 and is classified as medium. The Middle Drâa Catchment (MDC) is accessible by the national road N10 from Marrakech and Errachidia. The next international airport is in the town Ouarzazate. Additionally, a small launching and landing site exists near the town of Zagora. The main traffic axis of the study area is the national road N9 traversing from North to South and passing the belt of the Drâa oases. It connects the town Ouarzazate with the town Zagora and further Mhamid (Figure 2-2 & Figure 2-2). A secondary traffic axis is the road to the town of Tazenakht in the East. Within the MDC, minor roads and tracks prevail.

The research area overlaps widely the province of Zagora counting around 283,000 inhabitants in 2004 (Province of Zagora, 2004, in Martin, 2006). Around 85 % of the inhabitants live in the rural zones, i.e. 241,000. Thereby, more than 90 % of the rural zone inhabitants concentrate on the six Drâa oases, i.e. minimum 217,000 (Ouhajou, 1996). The only urban agglomerations are Agdz and Zagora with around 42,000 inhabitants in total. A clear urbanization trend is observed for the middle Drâa valley (Platt, 2008b). The annual population growth rate accounts for 2.1 % based on inquiries in 1994 and 2004 (ORMVAO, 1995; Province of Zagora, 2004; Platt, 2008a).

The socio-economic fabric of the research area has rarely been analyzed. The agriculture provides little income ranging below the subsistence level in many cases (Heidecke; 2009; Rademacher-Schulz, 2010). Dates and henna are nearly the only cash crops produced for local markets and agriculture is generally low developed except at single farms. Generally, inorganic fertilizer input and mechanization ranges on a low level. The agricultural production is closely linked to water management because of an enormous irrigation demand (see below). Moreover, migration is known to be a major source of income, but a precise quantification remains to be an open question (Rademacher, 2010). In addition to agriculture and migration, tourism represents an important economic activity. The evaluation of the exact economic value of tourism still needs to be analyzed (Martin, 2006). Employment in the public service is another source of income, Industry is absent except of mining gold, iron, barite and other minerals mainly in the Bou-Azzer zone.

Water management figures a very important issue because human activities are mainly restricted by water availability. In particular, the rural water supply needs to be developed. Therefore, a national master plan for the installation of tap water systems, called PAGER (*Programme d'Approvisionnement Groupé en Eau Potables en Zones Rurale*) was launched in 1995 (Bzioui 2004; Graf, 2009). As a result,

59 % of the rural households in the Province of Zagora were connected to tap water systems in 2001, by contrast to only 14 % in 1992. Domestic water consumption differs widely depending on type of access, family size, living standard and especially social space. Rough estimation of local data reveals mean daily consumption per capita of 30 L in rural areas and 50 L in urban zones (IMPETUS, 2006; Graf, 2009). Considering around 300,000 inhabitants, domestic water use is still a little amount in comparison to agricultural water consumption. The water demand for irrigation is estimated to approximately 98 % of the total water demand (DRPE, 1998). Irrigation depends on surface water from the reservoir Mansour Eddahbi and on individually pumped groundwater. Additionally, groundwater is pumped for irrigation at small irrigated perimeters along the tributaries of the Wadi Drâa and in the adjacent sedimentary basins. Thereby, both surface water and groundwater are free of charge. Contrarily, the costs for well drilling and motor pump must be borne by the owner just like recurrent costs for fuel and maintenance (Heidecke, 2009). Most of the irrigation wells are dug wells, but also combinations of dug and drilled wells are observed. Although the actual number of wells and pumps is not exactly known, it appears to be likely that the amount of groundwater extraction has increased within the last decade. DRH (2001) give a number of inventoried pumps in the Middle Drâa Valley of about 700. The recently estimated number of all wells is about 5000 (pers. communication Service Eau Ouarzazate). Finally, water use and groundwater pumping remain uncontrolled and rarely observed in the MDC.

3 Synthesis on groundwater research in drylands

The following sections are a synthesis of background information on groundwater studies in drylands. In literature a uniform title or common definition of what is e.g. a “dry environment” is hard to find. The use of the attribute “arid” is sometimes inconsistent to further aridity classes and other classifications of “dry environments”. For that reason, the term “drylands” is used to bridge the in variety in definitions. Drylands are understood as terrestrial regions of climatic water scarcity classified by the aridity index AI (ratio of mean annual precipitation and mean annual potential evapotranspiration; Middleton & Thomas, 1997). So drylands are characterized by four aridity classes: hyper-arid (AI: <0,05), arid (AI: 0,05<0,2), semi-arid (AI: 0,2<0,5) und dry sub-humid (AI: 0,5<0.65) in accordance to Safriel et al. (2005). Overall, 41.5 % of the total land surface is counted among drylands.

3.1 Brief history of groundwater studies in drylands

Research on hydrogeology and groundwater systems in drylands emerged globally since the early 20th century (Hibbs, 2008; Wheater & Al-Weshah, 2002; Simmer, 2003). Early studies were linked to the assessment of water availability for irrigation purposes and municipal use. Through time, the question of water balance became a priority because the development in irrigation agriculture (e.g. use of motor pumps) and urbanization entailed increased water use. Parallely, groundwater recharge studies advanced. Mathematical groundwater models were developed and used to support conjunctive resource management (chapter 7.1). More and more, interdisciplinary work made headway to examine the sustainability of groundwater systems at different scales. Accordingly, since the late 1980s the field of ecohydrology emerged through studies on stream-aquifer interconnections and soil-vegetation-atmosphere transfer approaches (chapter 3.2.2; 3.2.3). At the same time, the number of publications on groundwater recharge began to rise (chapter 3.2.5). Hydrogeochemical investigations and tracer techniques develop as analysis technology got more sensitive (Sanford & Pope, 2010; Herzceg & Leaney, 2010). Contamination and the question of nuclear waste disposal was and is a motivation for hydrochemical modeling (water-rock interactions, redox processes etc.; Appelo & Postma, 2007). Overall, groundwater studies aim at multi-parameter approaches, especially in drylands where the data

availability is often scarce. Enhanced computational power and further development of mathematical models made it possible to handle larger data sets, e.g. at the watershed scale. Triggered by enhanced groundwater flow modeling, transport modeling advanced increasingly. In parallel, data management and regionalization turned to be more and more important (Simmers, 1984; Blöschl & Sivapalan, 1995; Noetinger et al., 2005). Geographic Information Systems (GIS) and remote sensing techniques grew to be indispensable tools (Batelaan & De Smedt, 2001; Jackson, 2002; Kellgren, 2002; Sander 2007; Tweed et al., 2007). Furthermore, hybrid geophysical methods were developed to increase insight to groundwater systems including the unsaturated zone (Hibbs, 2008). Because of the differentiation of methods, research tends to follow complementary approaches. Thereby, the analysis of fluxes across interfaces is a current challenge of regional hydrogeology, e.g. the investigation of lateral recharge from a mountain massif to a sedimentary basin (Bakker et al., 1999; Wahi et al., 2008). Questions of climate and global change recently dominate a large proportion of research (Dragoni & Sukhija, 2008). In this context, scenario analysis provides a tool to simulate possible future developments. Recently, the assessment of managed aquifer recharge and contributions in the context of food security and mining are important issues of applied research in arid regions (Dillon, 2005; Gale, 2005; Steenbergen & Tuinhof, 2009; Stroßnider et al., 2010).

Research focused on densely observed test sites and watersheds, such as the Walnut Gulch (USA; e.g. Goodrich et al.1997; Keefer et al., 2008) and the Murray basin (Australia; e.g. Leaney & Herzceg, 1999; Cartwright et al., 2008). Thereby, detailed knowledge on the function of arid hydrological systems was gained. The United States Geological Survey (USGS) and the Australian Commonwealth Scientific and Industrial Research Organization (CSIRO) provide comprehensive studies on arid basins. International institutions, such as the International Hydrological Program of the United Nations Educational, Scientific and Cultural Organization (UNESCO-IHP), the International Association of Hydrological Sciences (IAHS) and the International Association of Hydrogeologists (IAH), play an important role by providing comprehensive assessments. Moreover, valuable suggestions on investigations of arid zones and drylands are found in special issues of scientific journals, particularly the Hydrogeology Journal (Volume 10, 2002) and Groundwater (Volume 46/3, 2008). Beside common research projects, multidisciplinary research programs offered new insights. The investigation of groundwater resources of North Africa and the Middle East progressed strongly since the middle of the 20^{th} century. Insight to the function of arid groundwater systems was gained in numerous scientific projects in North Africa, in the Middle East, in South-East Asia and more recently in South Africa and Central Asia (Table 3-1).

Table 3-1: Selective history of summarizing publications on groundwater studies in drylands at various scales.

Authors	Study areas	Targets
Barica (1972)	Middle East	Salinization of groundwater
Lloyd (1986)	Various	Aridity and groundwater
Gee & Hillel (1988)	various	Groundwater recharge
Fontes & Edmunds (1989)	various	Environmental isotope techniques
Lerner et al. (1990)	various	Groundwater recharge
Simmers et al. (1997)	various	Groundwater recharge
Coram et al. (1999)	Australia	Groundwater flow, dryland salinity
IAEA (2001)	various	Isotope techniques
Wheater & El-Weshah (eds) (2002)	various	Wadi hydrology
Simmers (ed) (2003)	various	Hydrological processes
Xu & Beekman (eds) (2003)	South Africa	Groundwater recharge
Margane (2003a)	Arab region	Groundwater monitoring
Margane (2003b)	Arab region	Groundwater resource management
Gale (ed) (2005)	various	Managed aquifer recharge

3.2 Hydrogeological characteristics of drylands

Characteristics and processes of dry environments relevant to hydrogeological interpretation are briefly addressed in this section. The environmental setting, especially the geological setting, provides the framework for groundwater regimes. Simmers (2003) compiled the general environmental features of arid and semi-arid zones relevant for hydrological and hydrogeological processes supplemented by characteristics of groundwater in desert areas (after Fetter, 2001), as listed below:

- High levels of incident solar radiation
- High diurnal and seasonal temperature variation
- Evaporation is prominent in the hydrological cycle (thereby potential evapotranspiration may be many times higher than precipitation)
- Low relative air humidity at short distance from the sea
- Highly variable, often strong winds with frequent dust and sand storms
- Sporadic rainfall of high temporal and spatial variability
- Hortonian overland flow is the dominant run-off process
- Extreme variability of short-duration runoff events in ephemeral drainage systems
- High sediment transport rates and highly mobile channel beds
- High rates of transmission loss due to infiltration in channel alluvium
- Relatively large groundwater and soil moisture storage changes
- Poorly developed soil profiles linked to highly variable geomorphologic characteristics
- Sparse or absent vegetation
- Strong soil water uptake due to high potential evapotranspiration
- Very low groundwater recharge is very low (often virtually zero)

- Mainly indirect and localized groundwater recharge (from stream flow infiltration, at pans and colluviums)
- Important stream-aquifer interactions
- Paleo-groundwater (due to recharge during more humid periods e.g. in Pleistocene)
- High mineralization and salinization of groundwater due to slow flow and high evapotranspiration rates (including phreatic evaporation, directly from aquifers)

Besides geological prerequisites and natural driving forces (climatic processes), anthropogenic influences are important. Land cover and land use are among the key factors of hydrogeological processes such as groundwater recharge. In particular, irrigation agriculture has a considerable impact on water resources and is often linked to groundwater extractions. Figure 3-1 represents an overview of hydrogeological and hydrochgeochemical processes in drylands at the “landscape scale”.

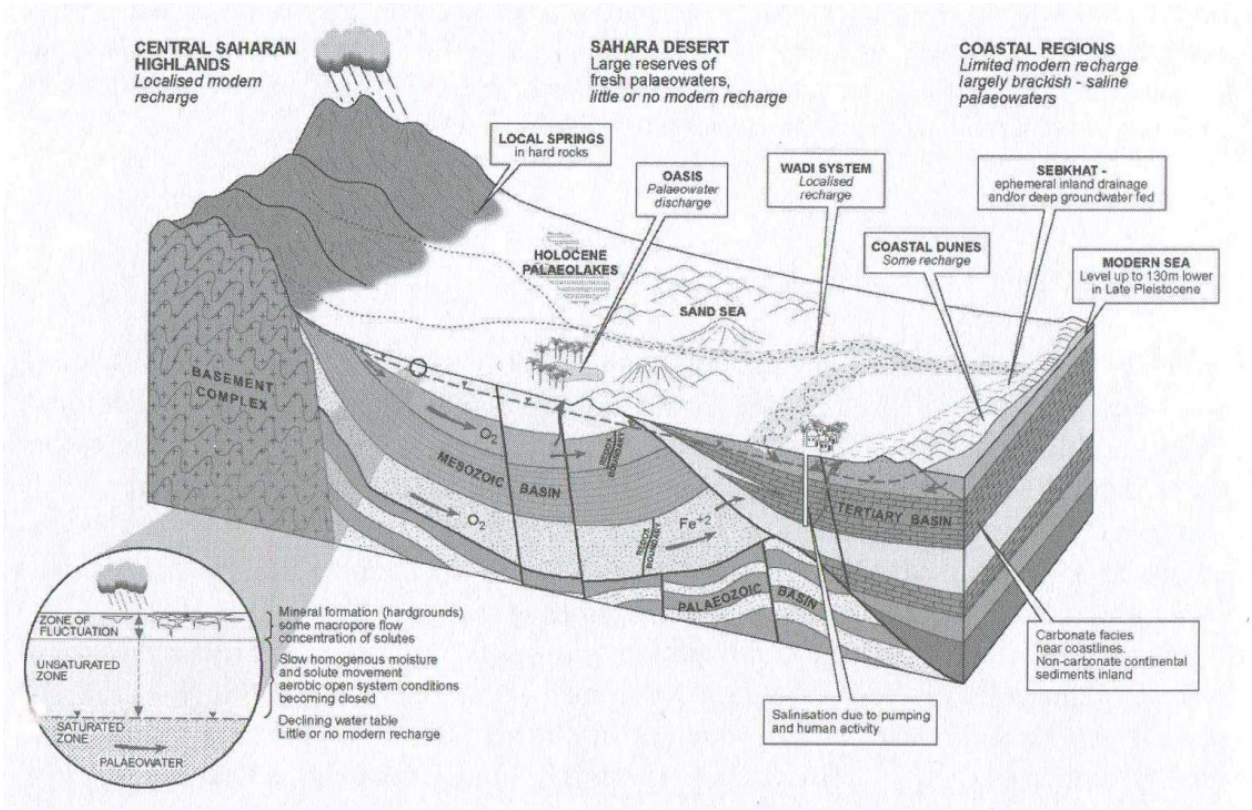

Figure 3-1: Landscape hydrogeology and hydrogeochemical processes in drylands reflecting the geological environment in North Africa (from Edmunds, 2003).

In the following sections, hydrogeological-relevant characteristics of drylands are highlighted to determine the meaning of technical terms in the context of this study. The description of methods and techniques mirrors the current state of process understanding. Additionally, selected literature is listed in tables to portray a reasonable range of characteristic parameters for water resources in drylands.

3.2.1 Precipitation

Rainfall is the major hydrological input, whereas snowfall can also be important, e.g. in mountainous regions. Precipitation occurs extremely spotty in dry environments (Sharon, 1972; Wheater, 2002). In addition, the temporal variability is very high in terms of intensity, frequency and duration. Patchy and short-duration rainfall is observed to be dominant. Also small amounts of long-duration rainfall events are detected which are widely distributed. They can be substantially important in terms of groundwater

recharge (Wheater, 2002). Intensive storm events are known to result in flash floods and enhanced groundwater recharge (Lewis & Walker, 2002; Schulz et al., 2008; Morin et al., 2009). Still a major restriction for the investigations of hydrological processes in drylands is the lack of high quality observations of precipitation regarding both density of weather stations and long-term surveillance. For hydrological process studies the density of rain gauges should be high.

Methods to analyze the spatiotemporal occurrence of precipitation, which are suitable for humid areas, may not be appropriate in arid zones, because of the distinct and highly variable character of rainfall. Approaches to model rainfall in arid zones are thus highly challenging no matter which scale is selected. Even conventional regionalization techniques (e.g. Thiessen polygons) may lead to skewed results of hydrological and hydrogeological modeling (Wheater, 2002). Therefore, it is still a challenge to find appropriate techniques. Consequently, relationships between elevation and rainfall intensity or rainfall duration as well as frequency of rain days should always be checked for the actual mechanisms. Thereby, data scarcity is often limiting the application more sophisticated methods in drylands, such as geo-statistic approaches or weather generators (Wheater, 2002).

In addition to purely physical approaches, isotopic and chemical tracers can help to characterize and quantify the hydrological input from rainfall. Therefore, the combination of groundwater dating methods and tracer methods on rainfall can reveal insight to paleo-hydrologic conditions and groundwater recharge during more humid periods in Holocene and Pleistocene (e.g. Sultan et al., 1997; Jouzel et al., 2000; Taupin et al., 2000; Taupin et al., 2002; Goni et al., 2001; Zuppi & Sacchi, 2004).

Selected examples of rainfall studies linked to regional hydrogeological investigations in drylands are listed in Table 3-2.

Table 3-2: Selected examples of rainfall studies linked to regional hydrogeological research in arid zones.

Authors	Study location	Spatial scale	Approach
Jouzel et al. (2000)	Earth	Global	Stable isotopic data / model comparison
Taupin et al. (2000)	West Africa	Regional	Direct measurements / stable isotope methods
Zuppi & Sacchi (2004)	Northwest Africa and Northern Italy	Regional	Direct measurements / stable isotope methods
Fink & Knippertz (2003)	Northwest Africa (Morocco)	Regional	Direct measurements from stations
Born et al. (2008)	Northwest Africa	Regional	Modeling (REMO) and dynamic-statistical downscaling

3.2.2 Runoff, infiltration and vadose zone processes

Dryland hydrology is characterized by high spatial and temporal variability due to irregular precipitation patterns, variable conditions of runoff generation, highly dynamic sediment transport and the effects of transmission losses (Tooth, 2000). As a rule of thumb, the hydrological response of dryland catchments becomes increasingly non-linear with increasing catchment size, because the variability in channel processes dominates the hydrological system more and more. Thus, conventional rainfall-runoff approaches (e.g. classical unit hydrograph analysis) may lead to biased results in drylands (Wheater, 2002).

In drylands, Hortonian overland flow is the typical process leading to runoff and is caused by the combination of high intensity, short duration convective rainfall (chapter 3.2.1) and weak infiltration capacities of dryland soils (Wheater, 2002; Lange & Leibundgut, 2003).

The following typical factors determine dryland infiltration in time and space (Toth, 1963; Allison et al., 1990):

- Short duration and high intensity of rainfall (chapter 3.2.1)
- High evaporation and transpiration losses
- Locally highly variable soil properties, e.g. sealing and crusting.
- Relief features like braided wadi beds, fans and pans (chapter 3.2.3 & 3.2.5)
- Sparse or missing vegetation cover
- Locally high intensive irrigation agriculture
- Low antecedent state of soil moisture

The antecedent state of soil moisture is often neglected in dryland studies, because it is assumed zero due to relatively long dry periods between the rare rainfall events. However, in areas with irrigation agriculture the antecedent state of soil moisture may be an important factor.

The sparse or non-existing vegetation cover diminishes protection from soil erosion. The splash effect of raindrops is much higher on bare soils than on vegetated surfaces. Consequently, bare soils are more susceptible for sealing and crusting which can lead to reduced infiltration capacity (Le Bissonais et al., 2005).

The locally varying factors of infiltration complicate the clear determination of the dominant processes, especially for regional scale studies (A. Klose, 2009). As an example, stone pavements and high stone contents can have a wide-ranging influence on infiltration as typical for dryland soils. Stones can either reduce or enhance infiltration considerably according to their position upon, beneath or embedded in the soil surface (Poesen & Lavee, 1994). Infiltration estimates are usually obtained from direct observations, e.g. with soil moisture probes, or from numerical modeling (Issar & Resnick, 1996; Dunkerley, 2002).

In drylands, a large percentage of rainfall and infiltrated water is lost by evaporation as analyzed in soil moisture investigations (Wheater, 2002; Weber, 2004). High evapotranspiration losses in arid zones can reduce the specific retention within the vadose zone to zero. Vapor transfer outweighs then capillary rise (Healy & Cook, 2002). Thus, processes of the vadose zone are of crucial importance in estimating runoff and groundwater recharge, but in fact they are rarely understood (Hendrickx et al., 2003). For further information on vadose zone fluxes in dry environments refer to Allison & Hughes (1983), Scanlon et al. (1997), Bellot et al. (1999), Dong et al. (2003), Scanlon (2000), Ji et al. (2006) among others. Scanlon et al. (2002) compared several soil water balance models often used to evaluate land-atmosphere interactions. Scanlon et al. (2007) focus on the global impacts on water resources due to land use change directly affecting the soil water balance.

3.2.3 Stream - aquifer interactions

Stream flow in drylands is characterized by intermittent and mostly episodic discharge in wadis due to sparse rainfall (chapter 3.2.1). The wadis beds are made of course material predominantly revealing high infiltration rates and hence water losses to the underlying aquifer. Overland flow may concentrate in a wadi channel network leading to stream flow and often to flash flood due to intense rainfall (Wheater, 2002; chapter 3.2.1 & 3.2.2). Interflow can contribute to stream flow as water, which passed through the vadose zone depending on local conditions, e.g. preferential paths and impervious horizons.

In drylands, the flood volume decreases downstream due to transmission losses. Transmission losses can be divided into two parts:

- Direct evaporation from water surface
- Infiltration in the wadi bed (including subsequent evapotranspiration)

Direct evaporation losses from floodwater seem to play a minor role (e.g. Lange, 2005) but evapotranspiration losses from the riverbed and the flood plain after the flood event can have substantial effects even on the regional water balance (Sorman & Abdulrazzak, 1995; Shentsis et al., 1999). Wadi bed infiltration dominates the processes of transmission loss and is often the major source of groundwater recharge in dry environments (chapter 3.2.5).

Generally, there are four types of how streams can interact with an underlying aquifer:

- Gaining
- Loosing (connected or disconnected)
- Flow-through (perpendicular)
- Parallel-flow.

All types of stream – aquifer interactions can be observed along wadis in which the loosing stream is predominant.

Woessner (2000) discussed conceptual models of streams – aquifer interaction focusing on the processes from an eco-hydrologic perspective. These conceptual models can be applied for humid and dry environments. Subjects of stream - aquifer exchange studies should be the fluvial plain system containing the stream channel, flood plain and associated fluvial sediment in which the hyporheic zone corresponds to the direct mixing zone.

To sum up, the key factors of stream – aquifer interactions are (after Winter, 1999; Woessner, 2000; Sophocleous, 2002; Morin et al., 2009):

- Hydraulic properties of the channel, e.g. roughness
- Texture and geohydraulic properties of the channel bed and the associated fluvial sediments; concerning e.g. hydraulic conductivity and drainage
- Stream stage relative to the adjacent groundwater gradients - peak discharge, flood frequency, hydrograph shape and type
- Geometry and position of the stream channel within the fluvial plain, especially reach length.

The structure and the geohydraulic properties of dryland channels can vary largely spatially and in time, even from one flood event to another, due to very dynamic erosion and sedimentation processes during flash floods. This may also relate to the associated alluvial sediments. Consequently, it becomes more uncertain to fix hydraulic parameters for the characterization and quantification stream – aquifer interactions in drylands. Various factors also influence stream – aquifer interactions in different ways. The typically low antecedent moisture of the wadi bed and the associated alluvial sediments may cause an enhanced air entrapment and delayed infiltration and percolation (Parissopoulos & Wheater, 1992). Substantial clogging effects are observed due to the sedimentation of fine particles at the final state of the flood event and locally, e.g. on flood plains. That is why infiltration rates in wadi beds may differ largely (Dunkerley, 2008). Sophocleous (2002) gives a comprehensive review on the state of science on interactions between groundwater and surface water including aspects of human impact.

Common investigation methods comprise direct measurement of groundwater levels, river discharge, soil moisture and various modeling approaches (Table 3-3; Table 3-4). Special techniques such as channel routing are required for the distributed interpretation and quantification of transmission losses in drylands (Wheater, 2002). In addition, hydrogeochemical and tracer techniques proved to be very helpful (Edmunds, 2003). The comparison of studies shows a very wide range for rates of wadi bed infiltration due to the method approached and the scale of investigation. As an example, Lange (2005) and Morin et al. (2009) found diverging results applying different methods in the same area (Table 3-4). In literature effective wadi infiltration is often given as lumped parameter, i.e. as percentage of upstream flow for a specific reach length (Table 3-3) and values range from 1.5 to 57 % of upstream flow for reaches between 2 and 147 km of length. Further application of values of wadi bed infiltration as percentage of upstream flow is acceptable as a rough estimation.

Table 3-3: Some selected studies of wadi bed infiltration in arid regions as percentage of upstream flow.

Authors	Study location	Spatial scale (reach length)	Approach	Result
Hughes & Sami (1992)	South Africa (Goba River)	Local (2 km)	Soil moisture dynamics (neutron probe observations)	Effective infiltration 22 % of upstream flow
Sharp & Saxton (1962; in Cataldo et al.; 2004)	USA (Cheyenne River)	Sub-regional (48 km)	Direct measures from gauges	Effective infiltration per event 1.5 - 30 % of upstream flow
Shentsis et al. (1999)	Israel (Wadi Tsin)	Sub-regional (69 km)	Hydrologic-lithostratigraphical modeling (water balance)	Mean annual effective infiltration 45 % of upstream flow
Lange (2005)	Namibia (Kuiseb River)	Regional (147 km)	Flow routing modeling (diffusion wave method)	Effective infiltration 57 % of upstream flow

Wadi bed infiltration can also be found as effective infiltration rates mostly derived from distributed modeling (Table 3-4).

Table 3-4: Some selected evaluations of transmission losses in arid regions as infiltration rates.

Authors	Study location	Spatial scale (reach length)	Approach	Result
Parissopoulos & Wheater (1992)	Wadi Habawanah (Saudi Arabia)	Plot (3x3m)	Infiltration tests and numerical modeling	Mean infiltration rate: 720 mm/h
Osterkamp et al. (1995)	Abu-Dhabi	Sub-regional (various)	run-off modeling	Constant infiltration rate: 46-285 mm/h
Lange (2005)	Kuiseb River (Namibia)	Regional (147 km)	Flow routing modeling (diffusion wave method)	Constant infiltration rate: 40-400 mm/h
Morin et al. (2009)	Kuiseb River (Namibia)	Regional (240 km)	Flow routing modeling (kinematic wave method)	Constant infiltration rate: 8.5 mm/h

Dunkerley (2008) proves the spatial variability of wadi bed infiltration by clogging even at the scale of a wadi bank profile. Accordingly, infiltration rates vary from 0.7 to 75 mm/h depending on the position along the wadi bank profile and thus, the degree of clogging.

A major outcome of research appears to be that floods of medium and high stages lead to significant transmission losses (Shentsis et al., 1999; Morin et al., 2009). Additionally, during very high floods a sig-

nificant amount of water can be stored in the flood plain (Knighton & Nanson, 1994; Lange, 2005). Nevertheless, site-specific investigations are indispensable to gain reliable quantification of transmission losses.

3.2.4 Groundwater dynamics

Groundwater dynamics depend strongly on aquifer properties but also on driving forces such as climatic conditions as well as land and water use (Fetter, 2001; Gehrels & Gieske, 2003). Aquifer properties determining groundwater dynamics are listed below:

- Boundary conditions inclusive geomorphologic setting
- Aquifer geometry
- Hydraulic conductivity
- Storage coefficient
- Physic-geochemical characteristics (specific gravity differences, saturation etc.).

Furthermore, examples for natural and anthropogenic driving forces are given according to Gehrels & Gieske (2003):

- Climatic processes (triggering naturally water flow and mass transport)
- Land cover and land use (natural / anthropogenic)
- Groundwater use (anthropogenic).

Mechanisms that lead to groundwater table fluctuations are summarized by Freeze and Cherry (1979; Table 3-5). In semi-arid regions, groundwater dynamics are often highly variable. Various mechanisms determine aquifer response. Each of these mechanisms can take place nearly everywhere and at each temporal scale. Healy and Cook (2002) examined reasons for water table fluctuations beside the concept of specific yield that is crucial to groundwater recharge estimations (chapter 3.2.5). They distinguish reasons for rise and fall of groundwater levels for long-term, seasonal and short-term conditions. Long-term water table changes may be mainly driven by external influences such as natural climate change and anthropogenic land use change. Seasonal variations in water levels often arise from seasonality in evapotranspiration, precipitation and irrigation. Short-term fluctuations may be the result of rainfall, barometric pressure variations and pumping.

Table 3-5: Summary of mechanisms leading to groundwater table fluctuations distinguished for aquifer conditions and driving forces (modified after Freeze and Cherry, 1979).

Mechanisms	Aquifer conditions		Driving forces	
	Unconfined	Confined	Natural	Anthropogenic
Groundwater recharge	X	X	X	
Air entrapment during recharge	X		X	
Evapotranspiration and phreatophytic consumption	X		X	X
Bank-storage	X		X	
Tidal effects	X	X	X	
Atmospheric pressure effects	X	X	X	
External loading of confined aquifers		X		X
Earthquakes		X	X	
Groundwater pumpage	X	X		X
Deep-well injection		X		X
Artificial recharge	X			X
Irrigation	X			X
Agricultural drainage	X			X
Geotechnical drainage	X			X

According to Thoth (1963; 1995; 1999), groundwater systems can be spatially divided into flow systems of regional, intermediate and local scale. In this regard, Carillo-Rivera (2000) showed the importance of the superposition of groundwater flow systems for water balance estimations. Focusing at one site, the flow system can change in scale throughout time (Meyboom, 1967). Accordingly, local flow systems can overprint an intermediate flow system in the shallow aquifer section e.g. after substantial groundwater recharge.

Geomorphological features can be determined from mapping and DEM (Digital Elevation Model) evaluation e.g. using GIS. Aquifer geometry can also be derived from mapping surveys as well as geophysical sounding and remote sensing approaches. Aquifer properties can be identified using various methods such as aquifer tests, laboratory tests, groundwater level observations or inverse by numerical modeling (e.g. Johnson, 1967; Rushton & Howard, 1983; Nwankwor et al., 1984; Neumann, 1987; Krusemann & De Ridder, 2000; Moench, 2008). High spatial heterogeneity in aquifer media can lead to large uncertainties in quantifying groundwater dynamics. Nilson et al. (2007) give examples to consider and quantify uncertainties concerning hydrogeological variables, geological model structure and scale.

Statistical evaluation of groundwater hydrographs provides punctual insight to the hydraulic response. The results of point scale analysis can be regionalized to interpret intermediate and regional flow systems (chapter 7.1). In arid regions data scarcity and high spatial variability often limits the use of regionalization techniques and the finding of robust relationship to controlling factors (Wheater, 2002). Including geohydraulic properties and the respective driving forces, groundwater dynamics can be studied and simulated using numerical models (Haitjema, 1995; Scanlon et al., 2003). Gehrels & Gieske (2003) give an overview on approaches to analyze aquifer response:

- Purely stochastic impulse-response approaches
- Stochastic impulse-response approaches including aquifer properties

- Purely deterministic physically-based 1D unsaturated zone models
- Spatially distributed 3D groundwater flow models.

Recently, more and more complementary approaches are applied to adequately address the complexity of aquifer systems. Complementary approaches incorporate e.g. geochemical tracers to bridge the lack of data by providing integrating information (chapter 3.2.6; 7.1; Flint et al., 2002; Earman et al., 2008). In Table 3-6 selected studies on groundwater dynamics are listed to show the spectrum of approaches at varying scales mainly with focus on arid zones.

Table 3-6: Selected studies on groundwater dynamics.

Authors	Study location	Spatial scale	Approach
Leduc et al. (1997)	HAPEX-Sahel test site (Niger)	Regional	Groundwater level observations, hydrochemical analyses, water budget of pools
Carillo-Rivera (2000)	Baja California & Central Mexico	Regional	Water balance
Flint et al. (2002)	Yucca Mountains (USA)	Regional	Numerical modeling (Richards equation), flux estimation by Darcy equation, neutron moisture monitoring, Inverse modeling to match thermal profiles in boreholes, modified Maxey-Eakin transfer method (precipitation-recharge response function), chloride mass balance, global fallout radio nuclides (tritium, carbon-14, chlorine-36), natural atmospheric radio nuclides (carbon-14, chlorine-36), profile analyses of perched-water chemistry including isotopes
Scanlon et al. (2003)	Edwards aquifer (USA)	Sub-regional	Lumped parameter modeling, distributed numerical modeling
Dahan et al. (2008)	Kuiseb River (Namibia)	Local	Monitoring of vadose zone moisture, flood and groundwater levels (water balance)
Gehrels & Gieske (2003)	Various	various	Time series analysis, stochastic forcing of a linear reservoir, 1D numerical soil water flow modeling, 2D/3D numerical groundwater flow modeling
Abdalla (2008)	Central Sudan Rift Basin Aquifer	Regional	2D numerical groundwater flow modeling (steady state)
Park & Parker (2008)	Hongcheon area (South Korea)	Local	1D semi-analytical model
Hutchison & Hibbs (2008)	Hueco Bolson (USA)	Regional	Hydrogeochemistry, isotopic tracers, numerical modeling

3.2.5 Groundwater recharge

Groundwater recharge can be defined as downward flux of water through the unsaturated zone (Xu & Beekman, 2003). Thereby, net recharge is the actual replenishment of ground water reservoir, whereas potential recharge is leachate, which leaves a prior defined soil column or compartment in the vadose zone. Groundwater recharge is classified to direct and indirect processes. Direct recharge (synonymous: diffuse or local) is a result of vertical percolation of effective precipitation (*in situ*). By contrast, indirect recharge results from infiltration of surface water in channel beds (chapter 3.2.3). Localized groundwater recharge portrays a class of intermediate processes. Thus, water percolates from horizontal (near-) surface water concentrations in absence of well-defined channels (Lerner et al., 1990). Investigations of groundwater recharge mainly focus on vertical flow processes at different spatial (point, line and areal) and temporal scales (short-term and long-term), therefore always depending on site conditions and data availability.

Conventionally, recharge is expressed as annual rate in millimeters or percentage of precipitation.

The principal factors controlling groundwater recharge are listed below representing mostly complex assemblies of conditions and processes:

- Precipitation
- Evapotranspiration
- Relief position
- Soil depth and properties
- Soil moisture
- Aquifer properties
- Depth to groundwater
- Groundwater flow system / aquifer system
- Vegetation and land cover
- Land use and irrigation.

Soil properties determine the pathway of water and the processes following infiltration. The approaches of investigation of vertical flow are dictated by the data availability on soil properties and their respective temporal resolution, especially at the small scale (chapter 3.2.2). Generally, piston flow and preferential flow have to be distinguished (Figure3-2; Simmers et al., 1997; Wood et al., 1997).

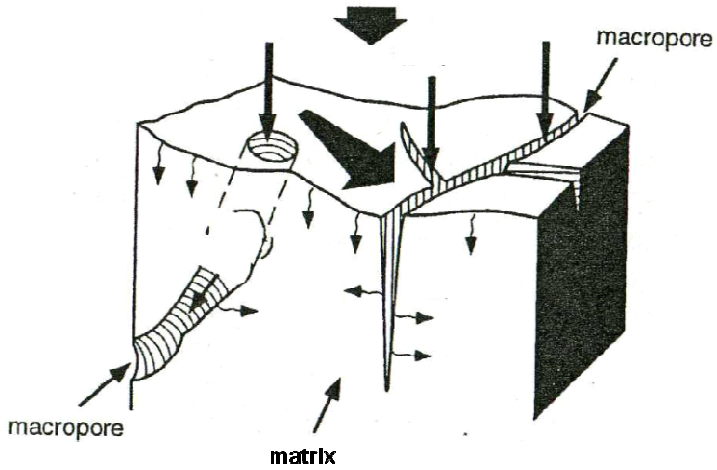

Figure3-2: Description of pathways of water through soil (after Simmers et al., 1997).

Three spatial scales of preferential pathways are defined: “micro” (shrinking cracks, borrowing etc.), “meso” (gullies, classic dikes etc.) and “macro” (streambeds, karstic sinks etc.; Gee & Hillel, 1988).

Kuells (2003) and Zagana et al. (2007) give integrative conceptual models of groundwater recharge taking into account factors such as relief position, run-off formation and properties of the vadose zone (Figure3-3).

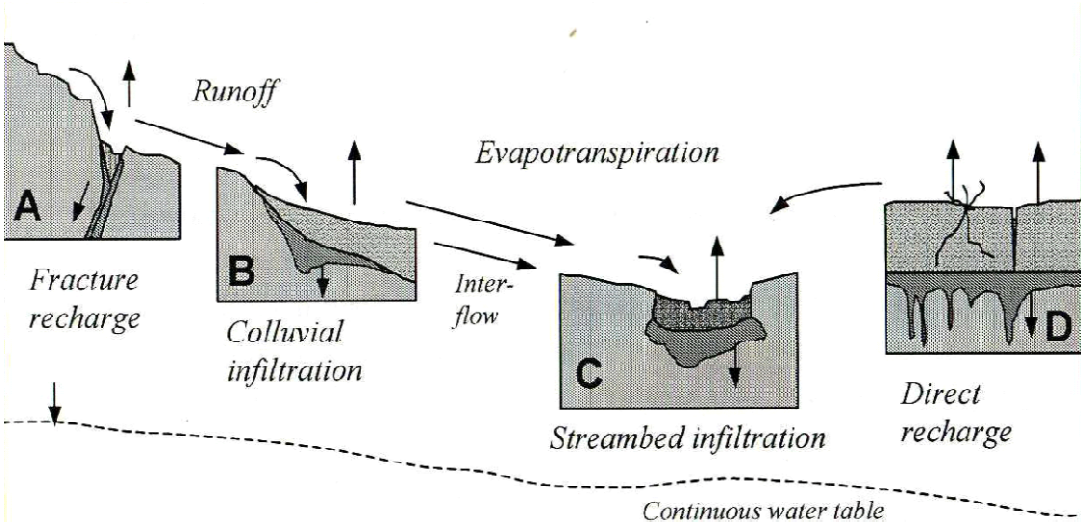

Figure3-3: Conceptual models of groundwater recharge (from Kuells, 2003).

"Mountain-front recharge" is established as concept for groundwater recharge along a mountain front towards an adjacent basin in dry environments (Wilson & Guan, 2004). This incorporates the hydrological processes entirely and within the contributing "mountain block", i.e. the hard rock body associated with the adjacent basin. Mountain block, mountain front, basin floor and discharge zone are defined as hydrological distinct areas (basin riparian areas etc.; Wilson & Guan, 2004). Mountain-front recharge is split up in two components, groundwater recharge through the vadose zone (mountain-front recharge) and lateral afflux of groundwater from the mountain block through the saturated zone (mountain-block recharge). Wahi et al. (2008) refer to mountain-front recharge in a broader sense as "mountain system recharge" also including mountain block recharge. Mountain-front recharge in a narrow sense is almost comparable to the concept of "colluvial recharge" at the feet of the slopes (Figure3-3; Külls, 2000). Sanford (2002) gives an overview on groundwater recharge and mathematical models. Thereby, various determining factors on recharge are described which can be directly translated into boundary conditions. Accordingly, a climate-controlled mountainous recharge system can be represented by assigning constant-head boundary conditions in the valley and specific-flux conditions in the uplands.

Groundwater recharge is generally low in arid environments and indirect recharge is the dominant process. Estimations of groundwater recharge are crucial to quantify groundwater resources and the development of management strategies (Misstear, 2000). Particularly in arid regions, the need for reliable estimation of groundwater recharge is high, but very difficult because of the large variability in its controlling factors (Simmers, 1997; Edmunds, 2003). Additionally, fossil groundwater resources occur due to substantial recharge in the Pleistocene and Holocene and slow circulation (De Vries, 2000; Edmunds, 2003). Estimation of groundwater recharge in arid zones follows the rule of thumb: "The greater the aridity, the smaller and potentially more variable the natural flux" (Gee & Hillel, 1988). For a brief summary on groundwater recharge processes it is referred to De Vries & Simmers (2002).

Groundwater recharge rates in arid zones vary largely from 0.2 to 35 mm per year, representing 0.1–5 % of long-term average annual precipitation. Recharge rates can extremely locally vary due to transmission losses from ephemeral streams and preferential flow (Scanlon et al., 2006; chapter 3.2.3).

Scanlon et al. (2002) summarize appropriate techniques to quantify groundwater recharge including space and time scales, range and reliability of estimations. Further technical and critical review on re-

charge estimations can be withdrawn from Sharma (1986), Gee & Hillel (1988), Cook & Herzceg (1998), Simmers et al. (1997), Wood (1999), Scanlon (2000), Timlin et al. (2003) and Edmunds (2003) among others. Commonly, methods for groundwater recharge estimations are subdivided by the target zone. Thus, techniques are developed for the vadose zone, the saturated zone or surface water bodies (Scanlon et al., 2002). The approaches can be subdivided to physical methods and tracer techniques or different spatial and temporal scales. As an example, the water table fluctuation (WTF) method can be used for the estimation of actual recharge at the local scale (Healy & Cook, 2002; Delin et al., 2007). The WTF method is applicable in humid and arid environments. The combination of the WTF method with water balance approaches enhances the field of application, as documented by Sophocleous (1991) and Marechal et al. (2006). Xu & Beekmann (2003) give a broad overview on methods for the estimation of groundwater recharge applied in southern Africa. Selected case studies on groundwater recharge in (semi-)arid regions using different techniques are listed in Table 3-7.

In drylands groundwater recharge is mostly so low that the recharge rates are smaller than the errors of other items of the water balance (Gee & Hillel, 1988). Because of this, the water balance approach may not be appropriate and its application has to be checked carefully. Numerical modeling provides a tool for quantification, parameter estimation and process understanding (Flint et al. 2002; Seyfried et al., 2005; chapter 7.1).

Table 3-7: Selected case studies on groundwater recharge in (semi-)arid regions using different techniques.

Authors	Study location	Spatial scale	Target	Approach
Wood et al. (1997)	Southern High Plains (USA)	Local and regional	Macro-pore recharge	Watershed modeling (rainfall-runoff, evapotranspiration) and infiltration tests, Chloride and ^{18}O profile analysis
De Vries et al. (2000)	Kalahari (Namibia)	Regional	Paleo-recharge	Environmental tracers including profile analysis & groundwater dating, groundwater modeling
Healy & Cook (2002)	Various	Point scale	Actual groundwater recharge	Water table fluctuation method
Flint et al. (2002)	Yucca Mountains (USA)	Various	Comparison of groundwater recharge estimation methods	Numerical modeling (Richards equation), flux estimation via Darcy equation, neutron moisture monitoring, inverse modeling of thermal profiles, modified Maxey-Eakin transfer method, chloride mass balance, global fallout radio nuclides (^{3}H, ^{14}C, ^{36}Cl), natural atmospheric radio nuclides (^{14}C, ^{36}Cl), geochemical profile analyses including isotopes
Seyfried et al. (2005)	Various	Various	Ecohydrological control of deep drainage (since Holocene)	Finite element heat and mass transfer modeling, soil moisture and geochemical profiles, water balance

Tracer methods are applied to estimate the residual percolation, and thus actual groundwater recharge (Simmers et al. , 1997; Cook & Herczeg, 2000; Edmunds, 2003). Furthermore, tracers integrate recharge variability over catchment areas and periods of time, and thus Paleo-recharge (Kendall & Caldwell, 1998; chapter 3.2.6). Consequently, tracer techniques for recharge estimations are often used in combination to groundwater dating (De Vries, 2000; Edmunds, 2003). A method widely used in (semi-)arid environments is the chloride mass balance approach (CMB; Table 3-8). CMB is appropriate at the point scale (profile analysis) and the regional scale (zero-dimensional approach; Allison & Hughes, 1983; Gaye &

Edmunds, 1994; Wood & Sanford, 1995; Scanlon et al., 2002; Scanlon et al., 2007). The investigation of vadose zone profiles is mostly applied in combination with other tracers and dating techniques (^{14}C, ^{3}H etc.; Cook & Herczeg, 2000). CMB is also developed for horizontal one- and more dimensional application (Cook & Herczeg, 2000; Sumioka & Bauer, 1999).

Table 3-8: Examples of studies using CMB (Chloride Mass Balance) in (semi-)arid zones.

Authors	Approach	Study location	Area [km²]	Mean annual precipitation [mm]	Groundwater recharge [mm; %]
Wood & Sanford (1995)	Zero-dimensional	Texas / USA	80,000	330-560	11; 3
Bromley et al. (1997)	Profile analysis	Niger	10,000 (1 profile)	564	13; 2
Sami & Hughes (1996)	Zero-dimensional	South Africa	665	460	4.5; 1
Bazuhaire & Wood (1996)	Zero-dimensional	Saudi Arabia (various basins)	135,000	121 (135*)	4 (8*); 3 (6*)

* including an extraordinary high recharge rate in one of the studied basins.

Moreover, studies on quaternary geology, paleo-climate and paleo-hydrology can be very informative for interpretation, if exact data on groundwater ages and residence times are lacking. Although uncertainties remain, a multi-scale and multi-disciplinary investigation should be approached to optimize the reliability (Cook & Herczeg, 2000).

3.2.6 Hydrogeochemistry and isotope hydrology

Studies on groundwater chemistry are an interdisciplinary approaches coping with the characterization of the geological and hydrological factors controlling groundwater composition. The groundwater composition is determined by the chemical changes of infiltrating water along its pathway through the vadose zone and within the saturated zone. Chemical changes of groundwater are mainly due to water-rock interactions and mixing processes occurring naturally. Furthermore, anthropogenic influences may be observed, e.g. contamination.

The groundwater composition is evaluated in terms of predefined objectives. Kovalevsky et al. (2004) define the objectives of chemical hydrogeological investigations as “to determine the sources, concentration, and fate of dissolved constituents within the physical framework of flow and transport”. A combination of hydrogeochemical methods and isotopic techniques is frequently used to understand the evolution of groundwater quality (Edmunds, 2003; Edmunds et al., 2003). Thereby, the overall aim is to understand the groundwater system better. Glynn & Plummer (2005) give a review on geochemistry and understanding of groundwater system. Kovalevsky et al. (2004) listed the basic hydrogeological knowledge should exist to interpret site-specific hydrochemical data (see also Alley, 1993):

- Basic concepts of organic and inorganic chemistry
- Appropriate use of environmental isotopes and geochemical modeling
- Principles of advective/dispersive transport and the coupling with reactions
- Consequences of surface water - groundwater interaction or soil moisture - groundwater interaction on groundwater quality
- Effects of land use on water quality
- Application of geochemical principles to regional aquifer systems

- Salt water intrusion
- Specific contamination problems in karst aquifers

A four-fold general procedure includes description, identification, explanation and monitoring (Figure 3-4).

Description	**Identification**
Horizontal and vertical distribution of dissolved constituents Relationships between constituents and hydrogeological factors	Source and flow of groundwater (1. Natural, 2. Anthropogenic) mineralogical controls Probable chemical reactions Source of contaminants Significant parameters to monitor
Explanation	**Monitoring**
Source of constituents Hydrochemical heterogeneity Concentration and distribution of constituents	Spatial chemical changes Temporal chemical changes Rate of chemical changes

Figure 3-4: General procedure of groundwater quality studies following no specific order in workflow (after Kovalevsky et al., 2004).

Comprehensive studies and reviews on chemical hydrogeology including principles of hydrochemistry and modeling are amongst others provided by Hem (1985), Sigg & Stumm (1996), Domenico & Schwartz (1997), Appelo & Postma (2005) and Merkel & Planer-Friedrich, (2008). Comprehensive analysis on isotope hydrology and reviews on isotope techniques in semi-arid zones is carried out by Fontes & Edmunds (1989), Fritz & Clark (1997), Kendall & McDonnel (1998), Cook & Herzceg (2000), IAEA (2001).

Groundwater chemistry studies in drylands often have to deal with evapotranspiration, paleo-groundwater systems, surface water - aquifer interaction and impacts from irrigation agriculture. In this context, salinization represents a frequent problem for groundwater use (Fritz, 1997; Coram et al., 1999; Yechieli & Wood, 2002; Farber et al., 2004; Cartwright et al., 2004; Krimissa et al., 2004; Hogan et al., 2007; Jalali, 2007; Bouchaou et al., 2008).

Hydrogeochemical studies are carried out in form a feedback loop between interpretation of the aquifer system, the groundwater dynamics and the mineralogical-geochemical setting. This is especially the case for studies in drylands because data scarcity often makes supporting interpretation from neighboring disciplines important. Thus, preliminary and recurrent interpretations of aquifer systems and groundwater flow patterns have to be checked and revised by results from the hydrogeochemical evaluation. The revised system comprehension represents then again the basis for investigations of groundwater quality studies. Reliability of techniques varies largely according to data availability, the system comprehension and the scale of investigation. Especially in the case of fossil groundwater resources often occurring in semi-arid regions, the interpretation groundwater composition depends on further analysis such as residence time assessment and dating (Table 3-9).

Data acquired from archives are an important source beside own sampling and monitoring, but must always be checked very carefully in terms of their plausibility, spatial and temporal resolution and respresentativity. Hydrogeochemical methods are often applied to problems on the regional scale (Table 3-9). The classical concept of hydrochemical facies mapping represents a common approach to initially characterize groundwater quality distribution. It is used to work out homogeneous compartments (Domenico & Schwartz, 1997; Kovalevsky et al., 2004; Glynn & Plummer, 2005).

Against the background of the identification of groundwater flow patterns, the spatial and temporal evolution of groundwater chemistry is interpreted. Thus, hydrochemical cross-sections illustrate the groundwater evolution in downgradient direction using indicators such as reduction / oxidation-values (Edmunds, 2003). Tracer techniques, particularly isotope tracers, provide a powerful tool for hydrological process study. Contrary to point data, tracers integrate at least small-scale variability. Therefore, tracer techniques indicate catchment-scale responses over respective time steps without the need for regionalization (Kendall & Caldwell, 1998; chapter 7.1). Isotopic approaches contribute e.g. to residence time evaluations (Zuber & Maloszewski, 2001; Bouhlassa & Aiachi, 2002; Weissmann et al., 2002; Matter et al., 2005; Bouhlassa et al., 2007; Vengosh et al., 2007; Bouchaou et al.; 2008).

The modeling of mixing of different water bodies and hydrochemical reactions become more and more important along with enhanced data availability (Uliana & Sharp Jr., 2001; Stigter et al. 2006; Matter et al., 2005). Examples of combined groundwater flow and transport modeling including chemical reactions are rarely found for dry environments probably due to the lack of data (Fryar et al., 2002; Hutchison & Hibbs, 2008; chapter 7.1). Selected publications on hydrogeochemical studies in arid environments are listed in Table 3-9. Investigations of North African aquifers concerning groundwater chemical and isotopic issues are published by Soltan (1998, 1998), Guendouz et al. (2003), Edmunds et al. (2003), Gaaloul & Cheng (2003), Guendouz et al. (2006) and Kamel et al. (2008) among others. Numerous studies on chemical groundwater evolution in Southern Morocco are available, such as Bouchaou et al. (1995), Hsissou et al. (1996a, b), Hamidi et al. (1999), El Ouali et al. (1999), Boutaleb et al. (2000), Bouhlassa & Aiachi (2002), Fakir et al. (2002), Dindane et al. (2003), Bouhlassa et al. (2007), Bouchaou et al. (2009), Tagma et al. (2009) and El Yaouti et al. (2009).

Table 3-9: Selected publications on integrated hydrogeochemical studies in arid zones.

Authors	Study location	Spatial scale	Targets	Approach
Nativ et al. (1997)	Negev desert (Israel)	Regional	Salinization	Hydrogeochemical analyses (solutes, ^{18}O, ^{2}H, ^{3}H isotopes), profile analyses
Fryar et al. (2002)	Southern High Plains (USA)	Sub-regional	Hydrochemical evolution, groundwater recharge, flow system	Hydrogeochemical analyses (solutes, ^{18}O, ^{2}H, ^{14}C isotopes), modeling (MODFLOW / MODPATH, PHREEQC, NETPATH)
Edmunds (2003)	North Africa (various)	Regional	(Paleo-)groundwater recharge, salinity, flow system, sustainability	Hydrogeochemical analyses (downgradient groundwater evolution, major ion ratios, red-ox-conditions, CMB*, isotopic signatures)
Cartwright et al. (2004)	Murray Basin (Australia)	Regional	Salinity, origin of solutes, flow systems,	Groundwater chemistry analyses (facies, ratios), stable isotope analyses (^{18}O, ^{2}H, ^{14}C isotopes)
Cherkaoui et al. (2005)	Drâa Valley (Morocco)	Sub-regional	Groundwater quality, groundwater balance	Groundwater chemistry analyses (facies; SAR**), water balance
Rueedi et al. (2005)	Continental Terminal Aquifer (Niger)	Regional	Aquifer - aquifer interaction	Hydrogeochemical analyses (solutes, ^{18}O, ^{2}H, ^{4}He isotopes), (geo)statistical analysis, mixing calculation
Khayat et al. (2006)	Jericho area (Palestine)	Local	Salinity	Groundwater chemistry analyses (fingerprinting), Tritium analysis
Matter et al. (2005)	Halfayn aquifer (Oman)	Regional	Flow system, groundwater availability	Multiple isotopic and geochemical tracer analyses (major ions, ^{18}O, ^{2}H, ^{3}H,^{14}C isotopes); hydrochemical modeling (PHREEQC, NETPATH)
Kattan (2008)	Euphrates (Syria)	Regional	Hydrochemical evolution, irrigation return flow	Stable isotope analysis (^{18}O, ^{2}H isotopes); CMB*
Bouchaou et al. (2008)	Souss-Massa (Morocco)	Regional	Recharge, salinization, residence time	Multiple isotopic and geochemical tracer analyses (Br^-/Cl^-, ^{18}O, ^{2}H, ^{3}H, $^{87}Sr/^{86}Sr$, ^{11}B, ^{14}C isotopes)

*CMB – Chloride Mass Balance; **SAR -Sodium Adsorption Ratio

4 Data basis

Groundwater studies in the Middle Drâa Catchment (MDC) are reported since the middle 20th century (e.g. Compagnie Africaine Géophysique, 1947; Margat 1958). Main focus was put on the Drâa aquifers in the intensively used areas along the Wadi Drâa (Chamayou, 1966; Chamayou et al., 1977; DRE, 1976; DRH, 2001). The work of Chamayou (1966) represents a milestone in hydrogeological research in the Middle Drâa Valley. He analyzed the groundwater system for the period before the reservoir Masour Edhabbi was put in operation in 1972. So, it serves for the comparison of the uncontrolled hydrological system to the recent system. The publication of Chamayou et al. (1977) forms another basis even for recent groundwater studies. Further systematic aquifer investigations have been examined in the sedimentary basin in the West of Zagora (Feija de Zagora; ORMVAO, 1981; Aoubouazza & El Meknassi, 1996).

The local water authority *Service Eau Ouarzazate* is mainly responsible for collection, monitoring and storing hydrological data.

The data basis for the present study can roughly be subdivided into two sets:

- Primary data (specifically observed; Table 4-1)
- Secondary data (acquired from literature and colleagues of the IMPETUS-Project; Table 4-2)

Primary data come from own field campaigns and surveys in the period 2005 to 2007 providing sampling of water and rocks. These own data are used to supplement the secondary data basis (see below). Additional local hydrogeological mapping and field observations help the interpretations (Steenpaß, 2007; Kunert, 2008; Breuer 2007; Haaken 2008; Stumpf, 2008).

Further data is acquired from various articles, books and reports based on a critical literature review. Colleagues of the IMPETUS – Project and our Moroccan partners, provide in turn further fundamental data. Table 4-2 shows the revised and selected data used in this study. Additionally, personal communications received from our Moroccan partners and inhabitants during face-to-face surveys and field campaigns helped to develop a regional knowledge and are incorporated into this work.

Table 4-1: List of primary data used in this study according to the MDC with 15,000km².

Theme & Attributes	Type	Resolution
Lithofacies, geochemical composition	Descriptive, Point data (numerical)	Outcrop scale, 26 samples at 22 outcrops
Groundwater levels	Point data (numerical)	163 observations at 68 sites
Hydrochemistry: Major ions, physico-chemical parameters	Point data (numerical)	97 samples at 67 sites
Meteorology: ^{18}O, ^{2}H signature and chloride concentration in precipitation	Point data (numerical)	66 samples at four Impetus stations, eight samples at Trab Labied station Figure 2-3)

Table 4-2: List of secondary data and information used in this study.

Attributes	Type	Spatial & temporal resolution	Sources
Planimetry: Altitude	Raster map (DTM)	90 x 90 m (re-sampled. 30 x 30 m)	SRTM (re-sampled and re-projected by IMPETUS)(USGS (2004), http://www2.jpl.nasa.gov/srtm/index.html)
Topography	Images	1 / 100,000	Topographic Map of Morocco (1953)
Geological structure, Stratigraphy, Lithology	Analogue maps, descriptive	1 / 500,000, 1 / 200,000	Geological Map of Morocco (Abdeljali et al., 1959)
	Descriptive, numerical	117 bore logs, , Vertical accuracy: ±0.1 m;	Compagnie Africaine de Geophysique (1947), Chamayou (1966), bore logs (SE, ORMVAO, 1981)
Aquifer system: Distribution, Nature	Descriptive		Margat (1958), Chamayou (1966), DRE (1976)
Type	Descriptive, numerical	57 sampling sites; 117 bore logs, , Vertical accuracy: ±0.1 m;	Chamayou (1966), DRH (2001), ORMVAO (1995), field protocols (SE, Ouarzazate)
Properties	Numerical		Chamayou (1966), Chamayou et al. (1977)
Groundwater levels	Numerical	2406 observations at 38 sites (1973-2002); daily at two sites (2005-2007)	SE and ORMVAO
Groundwater recharge	Descriptive	(partly incomprehensible)	Chamayou (1966), Aoubouazza & El Meknassi (1996), DRE (1976)
Groundwater flow	Descriptive	Selective per Drâa oasis	Chamayou (1966), DRPE, ABH, SE (and ORMVAO)
Wadi-aquifer interactions	Descriptive	Uneven (along the wadi Drâa)	Chamayou (1966), ORMAVAO (1995)
Hydrochemistry: Major ions and physico-chemical parameters	Numerical	211 samples at 57 sites	Chamayou (1966), Bouidida (1990), DRH (2001), field protocols and data (Service Eau Ouarzazate and ORMVAO)
Groundwater development: Casing etc.	Descriptive, numerical	Casing at 59 sites of 117 bore logs, Vertical accuracy: ±0.1 m;	Chamayou (1966), DRH (2001), ORMVAO (1995), field protocols (SE, ORMVAO)
Stream flow (Drâa)	Numerical	Daily (1986-2006)	ORMVAO
Surface water usage	Descriptive		Ouhajou (1996), ORMVAO (1995)
Precipitation	Numerical	Daily at the Zagora station (1962-2006), Impetus stations (2002-2006; Figure 2.2)	DRH and IMPETUS, Schulz (2006)
Temperature	Numerical	Daily at Impetus stations (2002-2006; Figure 2.2)	DRH and IMPETUS, Schulz (2006)
Wind velocities, directions and intensities, humidity	Numerical	Daily at Impetus stations (2002-2006; Figure 2.2)	DRH and IMPETUS, Schulz (2006)
Population, income etc.	Descriptive, numerical		Ouhajou (1996), DRH (2001), Martin (2006), Oubalkace (2007), Platt (2008a), Heidecke (2009), Rademacher, (2010), DRPE (1998), ORMVAO (1995)

4.1 Hydrogeological data

Hydrogeological data is derived from own mapping, descriptions in literature (Table 4-2), bore logs and the geological maps of Morocco 1/200,000 and 1/500,000 (Abdeljali, et al., 1959; chapter 5.1). 80 bore logs are available tapping the Drâa aquifers and further 37 bore logs for the sedimentary basin of Feija de Zagora even all including the aquifer basis (ORMVAO, 1981). Thereby, 56 bore logs represent the geological record down to the aquifer basis. The repartition of the bore logs to the hydrogeological units is uneven for the middle Drâa valley as shown in Table 4-3 (Figure 4-1).

The bore log data from the Feija de Zagora provide thickness of the weathered fringe of schisty sandy siltstones beneath alluvial deposits and supplementary information for interpretation (Table 6-7;).

Table 4-3: Overview of number and reparation of bore logs providing information on the Drâa aquifers.

Aquifer unit	Number of bore logs	Number of bore logs including basis of Drâa terraces
Mezguita	9	7
Tinzouline	6	2
Ternata	11	9
Fezouata	30	29
Ktaoua	13	8
Mhamid	11	1

Data on aquifer test are rarely comprehensible and thus mostly excluded from the analysis.

4.2 Groundwater level data

Own manual observations provide 162 groundwater levels at 58 sites. They help to describe the piezometric state during simultaneous water sampling.

The Service Eau Ouarzazate provides two piezometric data sets concentrating on the Drâa aquifers:

- 2,406 Irregular, monthly to annual, observations at 38 sites between 1973 and 2002 (chapter 6.2.1)
- Daily observations at two sites between 2005 and 2007 (chapter 6.2.3)

The fragmentary monthly to annual groundwater level record is applied to assess the response of the Drâa aquifers.

The repartition of the fragmentarily observed groundwater sites is shown in Table 4-4:

Table 4-4: Overview of the repartition of the fragmentarily observed groundwater sites.

Aquifer unit (Oasis)	Number of observation sites
Mezguita	6
Tinzouline	4
Ternata	10
Fezouata	8
Ktaoua	4
Mhamid	6

The selective daily groundwater level data provide the estimation of groundwater recharge using the WTF (Water Table Fluctuation) method.

4.3 Hydrogeochemical data

Hydrogeochemical data was mainly collected during key date samplings of water in spring and autumn 2005 and spring 2007. At 67 sites, 95 water samples were taken. At 23 sites, sampling was carried out repeatedly. At 20 sites, a two-fold sampling is available and three sites were sampled three. Three exemplary test sites are selected for this study such as the area around the village Ouled Yaoub (OY), The basin of the Feija de Zagora and the Plain of El Miyit (Figure 4-1).The local Moroccan water authorities, the Service Eau Ouarzazate (SE), provide hydrochemical data. The 57 selected Moroccan sampling sites concentrate within the Drâa aquifers and are scanned for seven key date sampling campaigns providing 211 samplings (Figure 4-1; Table 4-5). These data are partly useful. Their relation to controlling factors cannot be checked due to a lack of spatial and temporal data resolution.

Table 4-5: Overview of selected 211 samplings from 56 sites of the local Moroccan water authorities, the Service Eau Ouarzazate (SE), for the description of temporal variations of groundwater composition supplemented by hydro-meteorological period (chapter 6.2.1).

Month of sampling	Number of samplings	Relative hydro-meteorological state
October 1977	11	Dry
December 1978	39	Dry to humid
November 1979	47	Humid
July 1980	31	Humid
June 1981	31	Humid to dry
November 1981	32	Humid to dry
June 1983	20	Dry

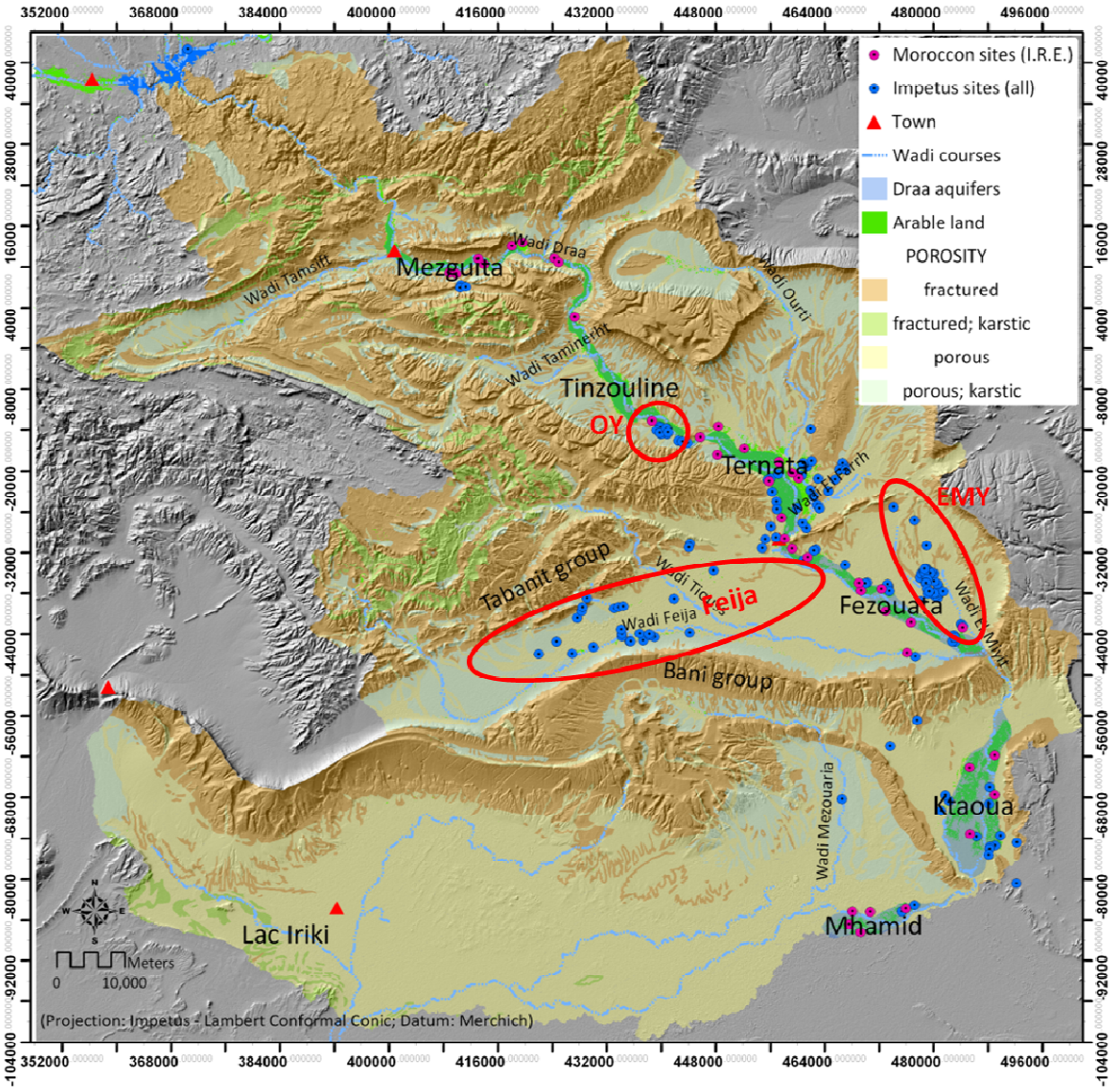

Figure 4-1: Overview map of Impetus groundwater sites (blue circles) and sites of the Service Eau Ouarzazate (pink circles).

Own precipitation samples were collected at the Impetus meteorological stations to analyze the stable isotopes (cf. Cappy, 2006; Figure 2-3).

Along with groundwater samples, the selective precipitation samples are used to estimate approximately regional groundwater recharge applying the chloride mass balance method. Due to a lack of accuracy, only eight samples from the Impetus meteorological station Trab Labied in the Upper Drâa Catchment (UDC) could be used. Although the Trab Labied station is located in the UDC, the data is applied in this study approximately because no other data is available. The Service Eau Ouarzazate provides the precipitation amount at the Zargora station (Table 4-6).

Table 4-6: Data applied for the estimation of lumped annual groundwater recharge in the Middle Drâa Catchment using the CMB (Chloride Masse balance).

Data	Source	Temporal resolution
Mean annual precipitation	Zagora Station provided by the Service Eau Ouarzazate	Daily between September 1962 and April 2006
Chloride concentration in precipitation	IMPETUS meteorological station Trab Labied (Figure 2-3)	8 samples in 2007 at meteorological
Mean chloride concentration in groundwater	Own field campaigns	53 samples at 20 wells in 2005-2007

Additionally, at 22 outcrops in the MDC 26 rock samples were collected.

5 Methods of groundwater system analysis

The study follows a classical hydrogeological investigation concept (Kovalevsky et al., 2004) enhanced by regional groundwater balance modeling. Accordingly, this research is subdivided into two parts:

- Groundwater system investigation including groundwater composition analysis
- Modeling of regional groundwater availability

The first part of this work follows a modern hydrogeological mapping approach focusing on the MDC (Ad-Hoc-Arbeitsgruppe Hydrogeologie, 1997; Masuch-Oesterreich, 2000; Hannappel et al., 2003; Struckmeier, 2005). Thereby, the choice of methods is widely limited by the data availability (see Wheater & Al-Weshah, 2002). The methods applied to develop the conceptual groundwater model are listed in brief below:

- Interpretation of geological maps, bore logs and sampling protocols (the latter are provided by the Service Eau Ouarzazate)
- Realization of recurrent surveys (2005-2008) inclusive analysis of water and rock samples
- Evaluation of groundwater level observations (provided by the Service Eau Ouarzazate and the regional agricultural authorities ORMVAO) inclusive the Water Table Fluctuation method
- Hydrogeochemical evaluation of water and rock analyses inclusive the Chloride Mass Balance approach and stable isotope analysis

Modern hydrogeological mapping requires the following aspects:

- Systematic survey
- Centralized data collection inclusive structuring of data and results to distinct information levels (and layers)
- Standardized evaluation and representation of hydrogeological information
- User-oriented and problem-oriented organization

For this study, the mapping approach is adapted to be the initial step of a groundwater investigation preparing for groundwater balance assessment. Geographical Information System (GIS) techniques are used to process and visualize the hydrogeological parameters. All sample sites were located by a Global Positioning System-device (GPS; Garmin III plus). According to the hydrogeological mapping approach,

primary and secondary data and results are stored in a relational data structure to be processed and presented in a Geographical Information System (GIS; ESRI ARCGIS). Figure 5-1 shows the general relational data structure of point information. The data is linked by an "1:n" relation using the identifying name of each site (ID) as a key. The data set is twofold subdivided in properly mapped sites and acquired site information. Sites mapped for the IMPETUS project are named individually whereas the existing Moroccan identification is used for the acquired sites. All data is projected in the mediating IMPETUS projection connecting two projection surfaces of the Lambert Conformal Conic projection (date: Merchich).

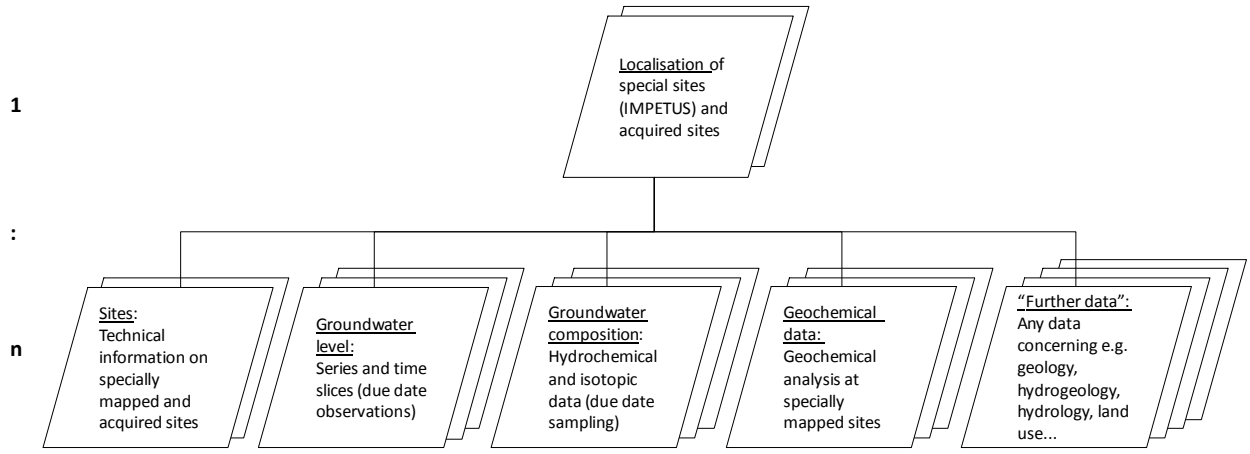

Figure 5-1: Scheme of the relational data structure linked by "1:n" relation.

The aquifer system is represented in maps (ground plans) and cross sections. The distribution of hydrogeological units serves as reference level of the maps. Data of different scaling and varying resolutions are included in this study (chapter 4). So, the hydrofacies approach is applied as common regionalization approach. It is based in the assumption that lithological properties determine the hydrological characteristics of a certain lithological facies (Anderson, 1999; Klingbeil et al., 1999). Consequently, a regional lithofacies concept is compiled and translated to a hydrofacies concept (Anderson, 1999; Klingbeil et al., 1999). Hydrogeological attributes are allocated to lithological map units. Therefore, the allocation is reconsidered based on comparative hydrofacies description in similar environments and stratigraphic order. The hydrofacies concept is then verified at supporting points observed during field campaigns.

5.1 Aquifer system analysis

Geological investigations provide the basis for hydrogeological interpretations. Geological maps bore logs and sampling protocols are interpreted. Moreover, local mapping and field observations were recurrently realized in spring and/or autumn 2005-2007. Geological field mapping was carried out at selected local sites to verify the occurrence and the structure of Paleozoic and Quaternary strata for hydrogeological purposes (cf. Ewen, 2004; Steenpaß, 2007; Breuer, 2007; Kunert, 2008; Figure 2-2). Additionally, rock sampling was conducted in spring and/or autumn of 2005 to 2008 to gain geochemical data (chapter 5.3).

Important information is derived from bore log data provided by the Service Eau Ouarzazate (chapter 6.1.4). 80 bore logs are available tapping the Drâa aquifers. Thereby, 56 bore logs represent the geological record down to the aquifer basis (Table 6-5). Further 37 bore logs are available for the sedimentary basin Feija de Zagora including the aquifer basis and considering the weathered fringe of the schisty substrata (ORMVAO, 1981).

Lithological data is interpreted for hydrogeological purposes. So, rock types with similar geohydraulic properties are summarized to homogeneous hydrogeological units using the standard section and the bore logs. Each hydrogeological unit is then attributed by lumped characteristic values, e.g. hydraulic conductivity and specific yield. The geohydraulic characteristics are allocated in comparison with the description of the hydrogeological properties of similar rocks in similar environments and stratigraphical order. Consequently, the lithological facies description is translated to a regional hydrofacies concept (see Ad-Hoc-Arbeitsgruppe Hydrogeologie, 1997; Anderson, 1999; Klingbeil et al., 1999).

The regional distribution of aquifer properties is compiled and visualized using a Geographical Information System (GIS; ESRI ARCGIS). Therefore, the themes of the Hydrogeological Map of Germany (1/200,000) are taken as a directive (e.g. Figure 2-2; Masuch-Oesterreich, 2000; Hannappel et al., 2003; Struckmeier, 2005; http://www.bgr.bund.de/cln_109/nn_324514/DE/Themen/Wasser/Projekte/Berat__Info/Huek200/huek200__projektbeschr.html, cited 29.12.2010):

- Lithology
- Consolidation
- Porosity
- Geochemical rock type
- Hydraulic conductivity

Therefore, consolidation is classified into *loose*, *cemented* and *hard rock*. In respect to the porosity, the common classification of *porous*, *fractured* and *karstic* is used as well as combinations of these categories. The basic categories of geochemical type of rocks are *siliceous*, *carbonate*, *sulfatic*, *halitic* and *organic*. Hydraulic conductivity is attributed by classified K-values. Both, possible minimum and maximum K-values are assigned based on the range of values of hydraulic conductivities given by Freeze & Cherry (1979). Accordingly, classes of hydraulic conductivities are adjusted based on the classification of the hydrogeological map of Germany 1/200,000 (Table 5-1).

Table 5-1: Classification of hydraulic conductivity following Hannappel et al. (2003).

Class of hydraulic conductivity	K-value [m/s]
Very high	$>10^{-2}$
High	$>10^{-3} – 10^{-2}$
Medium	$>10^{-4} – 10^{-3}$
Moderate	$>10^{-5} – 10^{-4}$
Moderate to low	$>10^{-6} – 10^{-4}$
Low	$>10^{-7} – 10^{-5}$
Very low	$>10^{-9} – 10^{-7}$
Ultralow	$<10^{-9}$
Low to ultralow	$<10^{-5}$
Highly variable	If range of K-values does not fit the classes mentioned above

The differentiation between aquifer and aquitard is adopted from Fetter (2001). Thus, an aquifer is defined as hydrogeological unit with a lumped hydraulic conductivity greater or equal $1 \cdot 10^{-5}$ m/s.

In addition, several spot tests contribute to the geohydraulic data basis. Thus, transmissivity and hydraulic conductivity are proofed applying the Copper & Jacob method for recovery tests at several selected wells (Kruseman & De Ridder, 2000; Koziorovsky, 1985, see also Haaken, 2008). Furthermore, the number and aperture of fractures is exemplary counted at 1 m² plots to estimate roughly the maximum fracture volume at the very shallow subsurface. Values for the specific yield (S_y) of the alluvial deposits are assigned to the lithological units represented in the bore logs. Therefore, the values from literature for similar deposits are compared based on statistical analysis provided by Johnson (1967; Table5-2) compiled from 17 studies. Healy & Cook (2002) discussed the principal of specific yield and furthermore the uncertainties involved. Specific yield values for consolidated material are adopted from Mattheß & Ubell (2003) and Freeze & Cherry (1979).

Table5-2 : Minimum, maximum and mean values of specific yield (S_y) according to texture (from Johnson, 1967).

Texture	Minimum S_y [%]	Maximum S_y [%]	Mean S_y [%]	Coefficient of variance [%]	Number of determinations
Clay	0	2	5	59	15
Silt	3	19	8	60	16
Sandy clay	3	12	7	44	12
Fine sand	10	28	21	32	17
Medium sand	15	32	26	18	17
Coarse sand	18	35	27	18	17
Gravelly sand	20	35	25	21	15
Fine gravel	21	35	25	18	17
Medium gravel	13	26	23	14	14
Coarse gravel	12	26	22	20	13

The horizontal aquifer distribution is extracted from the digitized geological map 1/500,000 after the hydrogeological attribution. The distribution of aquifers along the wadi Drâa is again extracted from the digitized geological map 1/500,000. The outcropping aquifer surfaces are then planimetered using a GIS (ESRI ARCGIS).

Moreover, regional geological cross-sections are interpreted to get an overview of the vertical hydrogeological structures. Therefore, the legend is adopted from the International Hydrogeological Map of Europe (1:1,500,000; http://www.geozentrum-hannover.de/nn_326806/DE/Themen/Wasser/Projekte/Berat__Info/Ihme1500/ihme1500__projektbeschr.html; sited 29.12.2010). Furthermore, the vertical structure of the Drâa aquifers is exemplarily represented in cross-sections. Thereby, bore logs are used as fix points to hint on the sedimentological architecture of the Drâa aquifers. The lower surface of the geological strata is reconstructed based on the existing geological concept (see Chamayou, 1966). The hydrogeological interpretation of the regional stratigraphy provided the delineation of aquifer types. The uncertainties of the hydrogeological reconstruction are discussed following relevant literature, e.g. Nilsson et al (2007).

The potential volume of the Drâa aquifers is assessed and compared to the estimations of Chamayou (1966) and Chamayou et al. (1977) as well as ORMVAO (1995). The official geological maps of Morocco (1/500,000 and 1/200,000) and bore logs (provided by the Service Eau Ouarzazate) supplement the assessment (chapter 6.1.4). The groundwater budget modeling is based on these estimations (chapter 7).

5.2 Groundwater dynamic analysis

The aquifer response is evaluated based on fragmentary monthly to annual groundwater level data available for the period 1973 and 2002 (chapter 6.2.1). Based on this data set, groundwater pathways and the change in gradients are evaluated (chapter 6.2.2). Moreover, continuously measured groundwater level data from two points are interpreted for the period 2005 to 2007 using the Water Table Fluctuation method (WTF; chapter 6.2.3).

5.2.1 Groundwater level observation

Systematically collected groundwater level data exists only for the area of the Drâa oasis provided by the Service Eau Ouarzazate. The groundwater levels were measured manually at key dates. The temporal resolution of the observations is irregular but bi-monthly data is available for several periods. The spatial resolution of the observation points is quite uneven and to sparse to apply geostatistical methods. Overall, the data from 38 sites is evaluated qualitatively with a focus on the period 1973 to 2002.

Moreover, the continuously recorded groundwater level data is interpreted on a daily basis for the period 2005 to 2007. These continuous data stems from automatic observations provided by ORMVAO.

Further supplementing data was collected during field surveys in spring and/or autumn in the years 2005 to 2007. Thereby, groundwater levels were manually measured using a contact meter. These measurements were organized simultaneously to key date sampling for hydrochemical analysis. Additional information for interpretation was gained by oral communications from inhabitants.

5.2.2 Evaluation of groundwater level data

Fragmentary monthly to annual groundwater level data from 38 sites are described in comparison with precipitation, stream flow and hydrofacies. Therefore, the data is rescaled to a monthly time line accepting gaps within the fragmentary series. The observed points change over time, so that none of the series covers the whole observation period between 1973 and 2002. Simultaneous observations are only available in a bi-monthly mode for a succession of maximum 8 month at in turn maximum 18 points. Thus, the manually observed aquifer response cannot directly be correlated to their influencing factors, such as precipitation or stream flow in the Wadi Drâa (chapter 3.2.4). Furthermore, these groundwater level fluctuations can neither be allocated to long-term, seasonal or short-term processes precisely. Consequently, the fragmentary recorded aquifer response is studied based on the comparison of mean values for distinct hydro-meteorological periods (humid vs. dry).

Main pathways of groundwater and the change hydraulic of gradients are derived from the fragmentary groundwater level data and by the help of a GIS (ESRI ARCGIS). The simultaneous groundwater level observations are compared spatially considering influences due to precipitation and stream flow. Additionally, correlations between the groundwater level responses of different observation points were realized to check e.g. spatial interdependencies and aquifer heterogeneity. Furthermore, maps of groundwater level contours are designed manually based on own observations in spring 2005, October 2005 and spring 2007 (chapter 5.3.1 & 6.2.2). Groundwater discharge is assessed approximately along the main flow paths for the simultaneous groundwater level observations based following Darcy (1857).

5.2.3 Water table fluctuation method

The water table fluctuation method (WTF) is applied to estimate groundwater recharge rates at two sites on a daily basis (2005-2007; data provided by ORMVAO; chapter 6.2.3).

The WTF method is adopted from the water balance equation:

$$R = \Delta S^{gw} + Q^{bf} + ET^{gw} + Q_{off}^{gw} - Q_{on}^{gw}$$

With:		
	R	Groundwater recharge [mm/d]
	ΔS^{gw}	*Change in groundwater storage [mm/d]*
	Q^{bf}	*Baseflow [mm/d]*
	ET^{gw}	*Evapotranspiration from groundwater [mm/d]*
	Q_{off}^{gw}	*Groundwater discharge including pumping [mm/d]*
	Q_{on}^{gw}	*Groundwater inflow [mm/d]*

As a prerequisite for the WTF method, groundwater recharge is defined as water actually arriving at the groundwater table of unconfined aquifers, i.e. inducing a water level rise at a piezometer. Groundwater recharge is thus calculated as follows:

$$R = S_y \cdot \frac{\delta h}{\delta t} = S_y \cdot \frac{\Delta h}{\Delta t}$$

With:		
	R	*Rate of* groundwater recharge *[mm/d]*
	S_y	*Factor of specific yield*
	h	*Water table height [mm]*
	t	*Time [d]*

Thereby, it is assumed that recharge to the water table goes instantaneously into storage and that all other components of above presented equation are negligible during the recharge period. Because this assumption is nearly only valid for short time spans (hours or several days), the application of the WTF method is most adequate for such short recharge periods (Healy & Cook, 2002). The total recharge is estimated by setting Δh equal to the difference between the peak of the water level rise and the extrapolated antecedent recession curve at the time of the peak (Figure 5-2). Healy & Cook (2002) describe the antecedent recession curve as the trace that the well hydrograph would have followed in absence of the rise-producing recharge (Figure 5-2). The trace is drawn manually in this case keeping in mind that it is a subjective matter (see chapter 6). Further approaches to draw antecedent recession curves are presented for example by Arnold et al. (1995), Heppner & Nimmo (2005) and Delin et al. (2007).

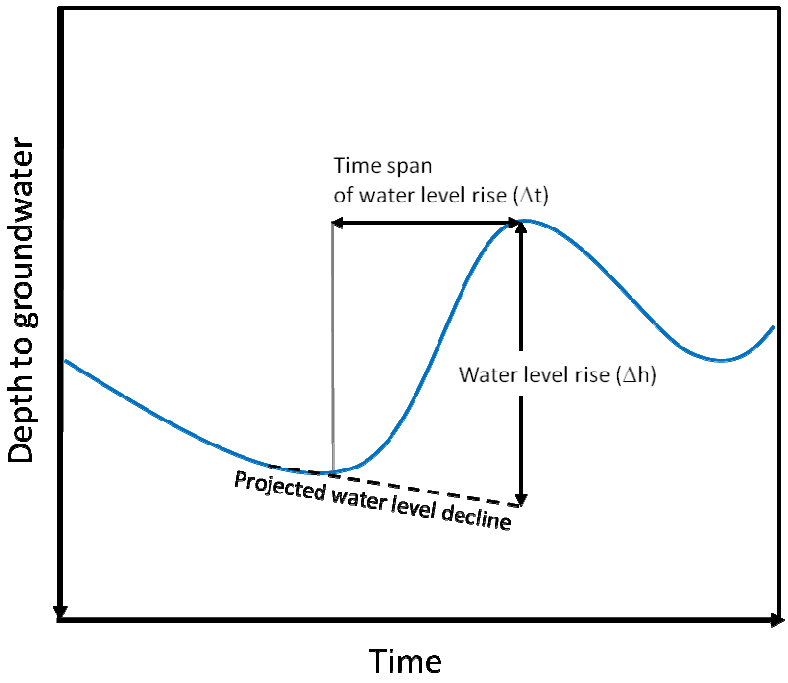

Figure 5-2: Schematic groundwater hydrograph with the projected trace of the antecedent recession curve ("projected water level decline") and the perpendicular at the time of the peak.

The application of the WTF method involves the following major limitations (after Healy & Cook, 2002):

- The hydrograph should reveal sharp water level rises and declines which is most occurring in shallow aquifers.
- The observed hydrographs should be representative for the focused area or aquifer.
- The WTF method is an event-based method and thus, it cannot for a steady state of recharge.
- Difficulties arise in relation to identifying the cause(s) of groundwater level fluctuations and determining the value for specific yield (S_y)

5.3 Hydrogeochemical investigation

The hydrogeochemical investigation follows the classical approach of hydrochemical facies mapping (Domenico & Schwartz, 1997; Kovalevsky et al., 2004; Glynn & Plummer, 2005; chapter 6.3.1). Thus, inorganic water constituents and geochemical characteristics of the rocks are interpreted based on hydrochemical, geochemical and isotopic analysis (Hötzl & Witthüser, 1999; Edmunds 2003; chapter 6.3.2, 6.3.3, 6.3.4 & 6.3.5).

Spatial and stratigraphic distribution of dissolved constituents is analyzed against the background of groundwater dynamics (chapter 6.3.2 & 6.3.3). Thereby, geochemical analyses, i.e. x-ray diffraction analysis (XDA) and x-ray fluorescence analysis (XFA) help to explain provenance, concentrations and distribution of inorganic solutes. Relations of solutes to hydrogeological parameters are determined using specific ions ratios and saturation indices. Furthermore, signatures of stable isotopes from precipitation, groundwater and surface water are analyzed.

Groundwater evolution is studied along regional pathways. Anthropogenic impact is assessed based on (quasi-)geogenic solutes. Consequently, long-term variability in groundwater composition is evaluated

using indicators and indicator ratios. Subsequently, monitoring options are deduced (Kovalevsky et al. 2004). Additionally, the Chloride Mass Balance approach (CMB) is applied to assess regional groundwater recharge (chapter 6.2.4).

5.3.1 Water sampling

Surface water and groundwater samples were taken at the beginning and/or the ending of the hydrological year in order to monitor states of highest and lowest water levels (chapter 4). Sampling was realized as key date sampling (Margane, 2004; Hötzl & Witthüser, 1999).

Surface water samples were taken as scoop samples. Groundwater samples were taken from wells either as scoop samples or after pumping depending on the equipment of the site. Sampling after pumping was executed after the balance in EC (electric conductivity) and in pH-value was achieved. Physicochemical parameters such as EC, pH-value, redox-potential as well as saturation and concentration of oxygen were measured directly within the dispensing vessel using the multi probe WTW Multi 340i/Set. Samples were filtered in two successions (200 µm and 0.45 µm) and bottled to HDPE vials for different analysis (Table 5-3).

Sampling of rainwater was carried out to detect the ratios of stable isotopes (18-Oxygene (^{18}O), Deuterium (D)) as well as chloride. Therefore, rainwater was collected at the meteorological stations run by IMPETUS using a funnel collector (Figure 5-3; Cappy, 2006). Directly after each rain event a local employee of IMEPTUS bottled the sample to a 30 ml HDPE vial. The funnel collector was also employed to sample rainwater for chloride analysis. Chloride samples were taken at the meteorological station at Trab Labied in the year 2007 (Figure 2-3).

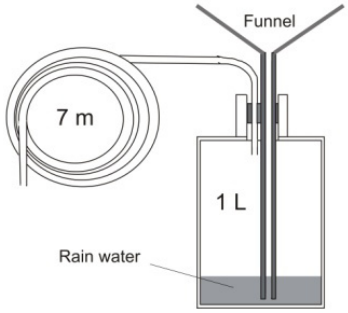

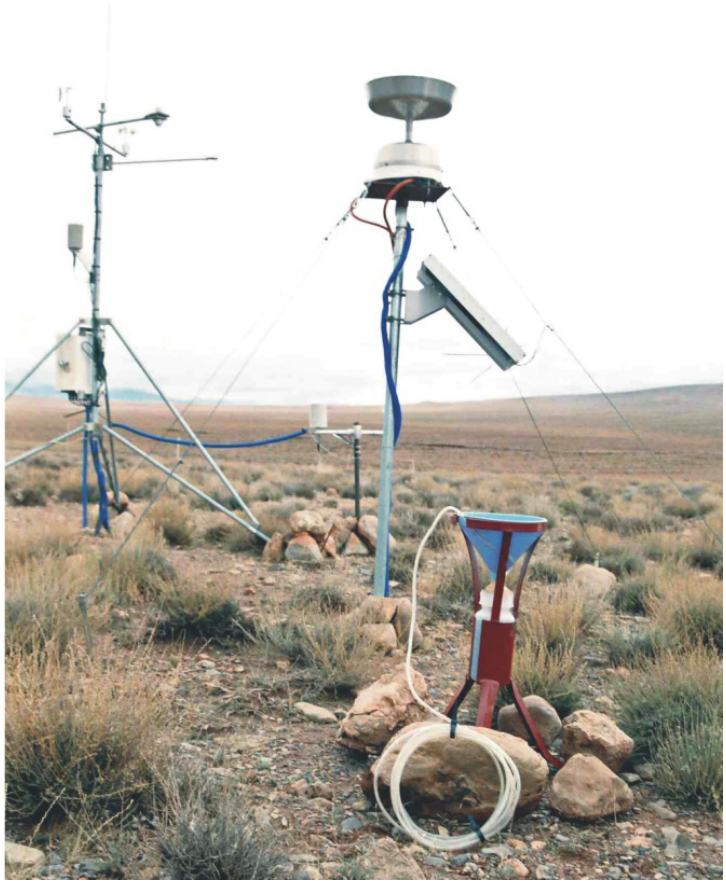

Figure 5-3: Scheme and illustration of a funnel collector to sample precipitation for stable water isotope analysis (from Cappy, 2006).

5.3.2 Rock sampling

Rock samples of around 200 g were withdrawn in situ from rock mass directly and from excavated material from dug wells. At the same time, the respective rock type, stratification and orientation were determined. All samples were packed in LDPE bags. The sample sites were located using a GPS-device (see above).

5.3.3 Soil sampling

Soil samples were collected in the context of the IMPETUS project. A. Klose (2009) provides a detailed description of the soil sampling procedure. Selected soil samples were analyzed for their mineral content using x-ray diffraction. Furthermore, extracts of selected soils samples were analyzed for their major ion content (chapter 5.3.5 & 5.3.6).

5.3.4 Water analysis

Bicarbonate and carbon dioxide was determined on the spot by acid-base titration with 0.1 M HCl against pH-value of 4.3 and with 0.02 M NaOH against pH-value of 8.2 respectively under the use of distilled water. Samples were preserved by sulphuric acid and nitric acid for cation analyses with photometry and spectroscopy. Anion analyses were done on non-treated water using chromatography (Table 5-3).

Hydrochemical analyses of surface water and groundwater include major ions and trace metals (Table 5-3). These analyses were done in the laboratory of the Steinmann Institute – Geology following the

German guideline of Hötzl & Witthüser (1999). Metallic cations and trace metals were detected with Atomic Absorption Spectroscopy (AAS; Perkin –Elmer AAnalyt 700). Ammonium and phosphate as well as silicon (as meta-silicic acid) were analyzed using photometry (Dr. Lange CADAS 100). Anion concentrations were determined using ion chromatography (Shimadzu HIC-A6). Analytes, sample preparation procedures and analysis are listed in Table 5-3.

Analyses of the stable water isotopes 18-Oxygene (^{18}O) and Deuterium (D) were carried out at the Institute of Groundwater Ecology of the Helmholtz Zentrum München – German research centre of environmental health. The $\delta^{2}H$ and the $\delta^{18}O$ ratios are measured according to the Vienna standard meteoric ocean water (VSMOW).

Table 5-3: Overview of analytes, sample preparation procedures and analysis methods.

Sample volume	Analytes	Filtration	Preservation	Analysis method (Analyzer)
20 ml	$SO_4^{2-;}$ Cl^- F^-; NO_3^-; Br^-	-	-	Ion Chromatography (IC; Shimadzu HIC-A6)
100 ml	PO_4^-	200 µm and 0.45 µm	H_2SO_4 (supra-pure)	Photometry (Dr. Lange CADAS 100)
100 ml	NH^{4+}; H_2SiO_4 (meta)	200 µm and 0.45 µm	H_2SO_4	Photometry (Dr. Lange CADAS 100)
100 ml	Na^+; K^+; Mg^{2+}; Ca^{2+}; Fe^{2+}; Mn^{2+}; trace metals	200 µm and 0.45 µm	HNO_3	Atomic Absorption Spectrometry (AAS; Perkin –Elmer AAnalyt 700))
500 ml	HCO_3^-	-	-	Field titration with 0.1 M HCl
500 ml	CO_2	-	-	Field titration with 0.02 M NaOH
30 ml	$\delta^{18}O$; δD	-	-	Mass Spectrometry (MS)

The detection limits of analytes depend on the analysis method (given with hardware details) and any calibration procedure (Table 5-4). The high detection limit in respect to chloride is due to hardware-dependent measurement uncertainty for low chloride values (B. Schulte-van Berkum, Laboratory of the Steinmann Institute – Geology, personal communication, 2007).

Table 5-4: Detection limits of parameters and their source.

Analytes	Detection limits	Sources
Na^{+}; K^{+}; Mg^{2+}; Ca^{2+}	0.01 mg/l -	Hardware details
NO^{3-}	2.72 mg/l	Calibration DIN 32645 (Schmitt; 2003)
Fe^{2+}; Ni^{2+}; Cd^{2+}; Pb^{2+}	0.001 mg/l	Hardware details
SO_4^{2-}	4.68 mg/l	Calibration DIN 32645 (Schmitt; 2003)
Sr^{2+}; Cu^{2+}; Mn^{2+}	0.002 mg/l	Hardware details
Cl^{-}	14.07 mg/l	Calibration DIN 32645 (Schmitt; 2003)
As^{2+}	0.005 mg/l	Hardware details
PO^{4-}	0.05 mg/l	Calibration DIN 32645 (Schmitt; 2003)
$NH4^{+}$	0.26 mg/l	Calibration DIN 32645 (Schmitt; 2003)
H_2SiO_4 (meta)	0.22 mg/l	Calibration DIN 32645 (Schmitt; 2003)
δD	1.0 ‰	Hardware details
$\delta^{18}O$	0.1 ‰	Hardware detail

The ion balance (charge balance error) is applied to check the plausibility of the hydrochemical analyses. Therefore, the international ion balance equation is chosen and an error of 10 % is accepted (Fetter, 2001; Güler et al., 2002):

$$Charge\ Balance\ Error\ [\ \%] = \frac{\sum[cations] - \sum[anions]}{\sum[cations] + \sum[anions]} \cdot 100$$

5.3.5 Rock analyses

The x-ray diffraction analyses (XDA) were done at the Steinmann Institute – Geology using a Bruker Axs D8 Advance apparatus and the MacDiff software (Petschick, 2000). The XDA allows a semi-quantitative evaluation of measurements. Thus, a detection limit cannot be determined. The interpretation follows rather the rule that minerals or groups of minerals are proportionally determined if they exceed the range of 5 to 10 % (S.-O. Franz, Steinmann Institute – Geology, personal communication, 2007).

Soil samples were analyzed for their mineral content using x-ray diffraction following the same procedure as described above.

The x-ray fluorescence analyses (XFA) were done at the Steinmann Institute – Mineralogy using Phillips 1480 apparatus and the X40 Oxiquant measuring program. The samples were prepared as borate fusion beads. The detection limits for all trace elements is 0.1 ppm. Concerning the major element analysis, the reasonable range of measurement is determined by calibration against standard samples.

5.3.6 Soil extract analysis

Soil extracts were analyzed for their inorganic soluble content to detect whether chloride is present or not (prerequisite to approach the chloride mass balance; chapter 5.3.7.1 & 6.2.4). Soil samples were collected in the context of the IMPETUS project (chapter 5.3.3).

The soil extract analysis was carried out following the international standard of soil analysis (Van Reeuwijk (Ed.), 1995).

The dried soil samples were admixed with distilled water to a relation of 1:5 using PE bottles. Subsequently the prepared samples were shaken (two hours) and stored for twelve hours. Then the samples were centrifuged and filtered. Finally, the extract was titrated and analyzed for the major ion content (chapter 5.3.4).

The ion balance (charge balance error) is applied to check the plausibility of the soil extract analyses same as for the hydrochemical analyses. The ion balance can only be a approximate plausibility check because for soil extract analyses are known to be prone of artifacts (Van Reeuwijk (Ed.), 1995).

5.3.7 Hydrogeochemical evaluation

The determination of (quasi-)background composition or “natural groundwater” or pre-developed composition of groundwater constitutes a basis or reference state to evaluate aquifer structure, groundwater dynamics and influences on groundwater quality. That means that the mainly lithology-dependent water composition without anthropogenic constituents has to be identified. “Natural groundwater” is defined as groundwater composition of purely geogenic origin or as groundwater composition revealing imprints of a normal, century old cultural landscape and being free of synthetic substances. In reality, shallow groundwater are rarely of purely geogenic origin, but commonly quasi-background compositions can be defined. In this study a threshold query is performed in respect to typical indicators of anthropogenic influences such as nitrate. Furthermore, the concentrations of dissolved constituents are compared referring to typical lithogenic groundwater compositions such as water purely from sandstone.

To describe the inorganic hydrochemical composition at different sites and moments graphical methods are applied following Piper (1944) and Schoeller (1955; see also Fetter, 2001; Güler et al., 2002; Kovalevsky et al., 2004; chapter 6.3.1). Water is classified according to Furtak & Langguth (1967) and Black (1961, 1966) based on Piper diagrams (see Fetter, 2001; Domenico & Schwartz, 1997). Moreover, the dominant proportion of cations and anions serve for characterizing water types.

The influence of upwelling water from deeper aquifer zones is tested by a comparison of indicator and the mean groundwater composition of the respective aquifer unit (chapter 6.3.3.5). The indicators for the upwelling are withdrawn from literature and listed below:

- Elevated electric conductivity
- Lowered pH value
- Elevated temperature
- Lowered Redox potential
- Elevated (bi-)carbonate and (free) carbon dioxide content
- Elevated sodium content
- Elevated potassium content
- Elevated chloride content
- Lowered bromide - chloride ratio

- Elevated sulfide (and sulfate) content
- Elevated iron content
- Elevated boron content
- Elevated ammonium content (reduced nitrate content)

Probable chemical reactions are identified along groundwater paths using ions ratios and saturation indices in comparison to the geochemical analysis using the hydrochemical model PHREEQC (Hem, 1985; Merkel & Friedrich-Planer, 2008; Appelo & Postma, 2005).

The interpretation of spatial distribution of water types and groundwater evolution is based on the prior hydrogeochemical characterization (chapter 6.3.2 & 6.3.3). Furthermore, specific ion ratios and saturation indices (SI) referring to selective mineral phases are applied. The analysis of the stable isotope signatures from precipitation, groundwater and surface water supplements the interpretation of groundwater provenance and groundwater evolution along main flow paths. Therefore, the signatures of stable isotopes of precipitation are used to draw a Local Meteoric Water Line (LMWL; Fontes & Edmunds, 1989; Clark & Fritz, 1997; Cook & Herczeg, 2000).

The anthropogenic influence on groundwater and water quality aspects are described based on common indicators and the Moroccan Water Quality Standard (chapter 6.3.4 & 6.3.5).

The signatures of stable isotopes of precipitation are used to draw a Local Meteoric Water Line (LMWL; Fontes & Edmunds, 1989; Clark & Fritz, 1997; Cook & Herczeg, 2000). The analysis of the stable isotope signatures from groundwater and surface water are evaluated to determine the provenance of groundwater and evaporation effects to supplement the interpretation of groundwater evolution (Figure 5-4).

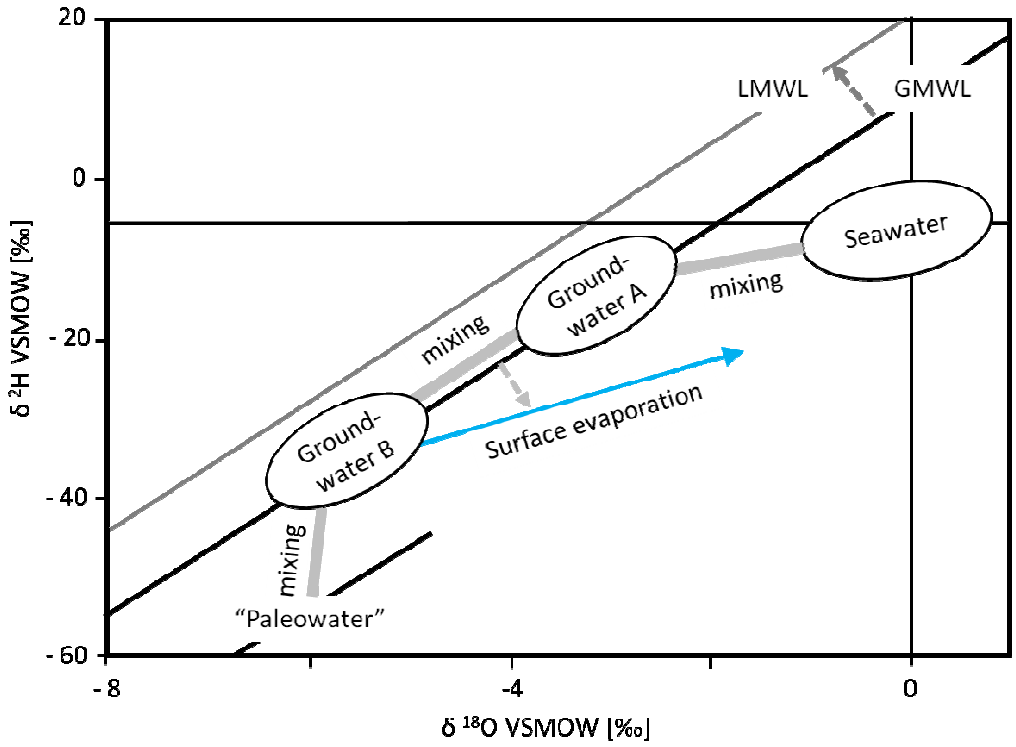

Figure 5-4: Selected processes of deviation from the Global Meteoric Water Line and a Local Meteoric Water Line illustrating evaporation effects and mixing (adapted from Clark & Fritz (1997) and Mook (2000)).

5.3.7.1 Chloride mass balance

The chloride mass balance approach (CMB) is applied to estimate regional groundwater recharge. Therefore, primary data is used except for precipitation (data provided by Service Eau Ouarzazate). Additionally, field protocols and site descriptions on the hydrogeological and pedological situation provide as interpretative help (Steenpaß, 2007; Breuer, 2007; Kunert, 2008; Haaken, 2008; Stumpf, 2008).

CMB results in rates of actual groundwater recharge. It is developed for assessments of long-term conditions at the areal scale. Following this approach the input of chloride into a system is balanced by the output of the system. CMB is based on the water balance equation and can be applied as zero- to three-dimensional mixing cell model (Herczeg & Edmunds, 2000; Cook & Herczeg, 2000). In this context, chloride is a conservative tracer. It has nearly the same mobility in water as water molecules itself due to very similar self-diffusion coefficients (Hill, 1984; Herczeg & Edmunds, 2000). The geochemical cycle of chloride equals to that of water except in terms of evapotranspiration. Chloride is enriched by the amount of water, which is removed, because it remains in the residual solution. Based on this, the chloride concentration is used to assess the net water loss compared to rainfall and thus, the amount of recharge (Herczeg & Edmunds, 2000).

The conservativeness of chloride in the system is a basic prerequisite for valid application of a zero-dimensional CMB approach. Precipitation (wet and dry fallout) has to be the only source of chloride; i.e. input or loss via rock weathering; anthropogenic input and recycling of chloride has to be negligible. Run-off has to be negligible too and atmospheric input has to remain constant. Also, the focused aquifer has to be a homogeneous unit as CMB is a mixing cell model (Table 5-5). There are further conditions to check as the spatial variability of the mean groundwater recharge within the study area and the changes in chloride concentration along flow paths. If significant changes in chloride occur along a path way, a

one- or more dimensional mixing cell model would be the choice. If mean groundwater recharge varies significantly over a region, this region would have to be subdivided according to conceptual models (Figure3-3). There are more assumptions to consider according to zero- to three-dimensional CMB respectively (Cook & Herczeg, 2000).The validity of application of CMB in this study is checked referring to the prerequisites and assumptions listed in Table 5-5.

Table 5-5: Check list of prerequisites and assumptions for the CMB as a steady state zero-dimensional mixing cell model (according to Herczeg & Edmunds, 2000; Cook & Herczeg; 2000).

Pre-requisite	Check
Negligible runoff	Discharge measurements; historical data / reports
Precipitation is the only source of chloride	Hydrogeochemical investigation (incl. XDA; XFA); hydrochemical modeling
Conservativeness of chloride in the system	assumed
Constant atmospheric input	investigation of Quaternary deposits; literature on Quaternary geology and climate
Aquifer is a homogeneous unit	Based on drilling logs (data provided by Service Eau Ouarzazate and ORMVAO)

In the present study, a zero-dimensional approach of the CMB for steady state conditions is chosen following the equation:

$$GWR = \frac{[Cl]p \cdot PCP}{[Cl]gw}$$

With : GWR *Annual rate of groundwater recharge [mm/yr]*

$[Cl]p$ *Concentration of chloride in precipitation [mg/l]*

PCP *Annual average rate of precipitation [mm]*

$[Cl]gw$ *Concentration of chloride in groundwater [mg/l]*

The results can be given as rate of groundwater recharge or recharge coefficient, e.g. in percent of mean annual precipitation.

Sampling sites are classified according to the key factors of recharge and conceptual models to check the dominant mechanisms (chapter 3.2.6, Figure3-3). Statistically significant differences between the classes are clarified using whisker box plots (Kovalevsky et al. 2004). As a result, main processes of groundwater recharge are determined.

The estimated recharge coefficients are applied in the groundwater budget modeling to assess lateral groundwater flow caused by regional recharge (chapter 7.3).

6 Regional hydrogeology of the Middle Drâa Catchment

6.1 Aquifer structure and properties

The heterogeneous geological setting of the southern flank of the central to eastern Anti-Atlas (see chapter 2.3) is determinant for a complex aquifer structure and varying aquifer properties (Figure 6-1; Figure 6-2; Figure 6-3).

The regional aquifer system is characterized regarding the following aspects:

- Hydrogeological properties
- Aquifer distribution (horizontal aquifer structure)
- Hydrostratigraphy (vertical aquifer structure)

The description of the aquifer system follows broadly the differentiation of fractured media and porous media. These classes are further subdivided to the regional main aquifers types.

Fractured hard rock including karstified rocks:

- Fractured aquitard system

Porous sediments including slightly consolidated sediments:

- Drâa aquifers
- Tributary aquifers
- Basin aquifers

The alluvial aquifers along the Wadi Drâa, the Drâa aquifers, are described separately because there water availability is highest (Chamayou, 1966). In addition, the information density is much higher for the Drâa aquifers in comparison to other hydrogeological units.

6.1.1 Overview of aquifer system

The underground of the Middle Drâa Catchment (MDC) is made up of crystalline successions overlaid with various series of sedimentary rocks (chapter 2.3). A discontinuous cover of Quaternary deposits is related to the wadi network (Figure 6-1). The hydrogeological data is fragmentary concerning the strata older than Quaternary. The compilation of secondary data and verifying field mapping allows the attribution of at least a part of the geological formation.

According to the geological map of Morocco 1/500,000, in the MDC the surface distribution of the hydrological units is dominated by 53 % of fractured media followed by 42 % of porous media. Further 5 % are occupied by fractured and partly karstic rocks (Figure 6-1).

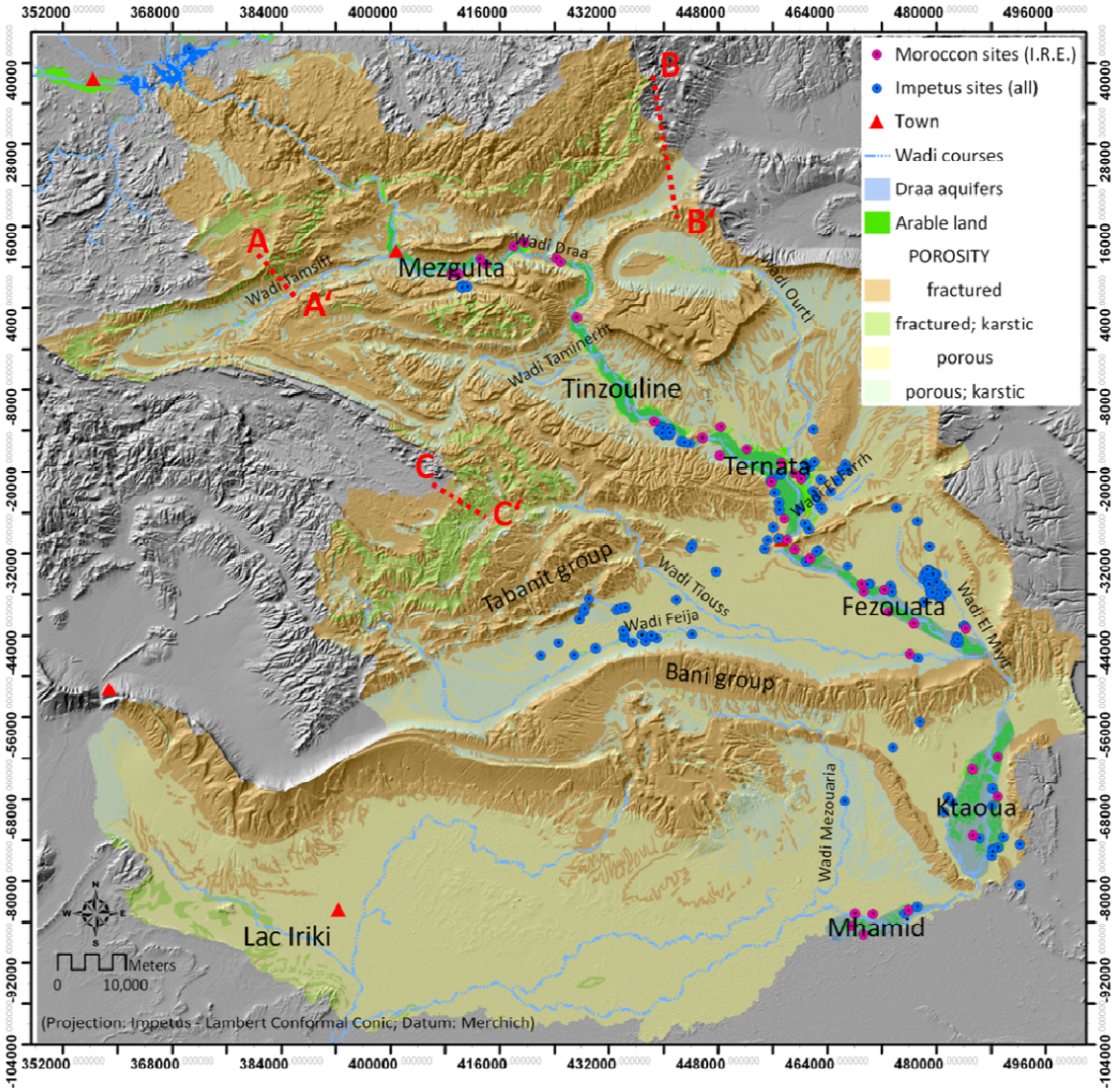

Figure 6-1: Hydrogeological map of the Middle Drâa Catchment with the IMPETUS groundwater sites, the underground's porosity according to the hydrogeological map of Germany 1/200,000 (Hannappel et al., 2003) and the approximate location of the regional cross-sections (Figure 6-2).

Because of the heterogeneous lithofacies distribution and the complex geological structure, the variability in aquifer properties is high (chapter 2.3). Media with a lumped hydraulic conductivity of greater or equal than $1 \cdot 10^{-5}$ m/s are defined as aquifers as opposed to aquitards (according to Fetter, 2001). So, the aquifers are made up of loose and slightly consolidated Quaternary sediments and slightly karstified Paleozoic carbonate rocks (cf. Chamayou, 1966; DRE, 1976). To give an overview, the distribution of hydraulic conductivity and type of porosity is represented in a hydrogeological map, which is deduced from the geological map 1/500,000 (Figure 6-1; chapter 5.1). Hydraulic conductivity is classified according to the hydrogeological map of Germany 1/200,000, which is a contribution to the International Hydrological Program (IHP) of UNESCO (Hannappel et al., 2003; Table 5-1; chapter 5.1). For further hydrogeological maps it is referred to following chapters.

Regionally connected aquifer systems are restricted to the alluvial deposits. These are embedded in the fractured media of sedimentary rocks and crystalline formations. The fractured media represents a heterogeneous aquitard system with varying groundwater residence times between 500 and 2,800 years in the Precambrian formations of the Skoura Mole in the Upper Drâa Catchment (Cappy, 2006). The inter-

pretation of regional geological cross-sections provides an overview of the vertical aquifer structure of the southern flank of the central Anti-Atlas. The aquifer geometry can roughly be depicted from these hydrogeological cross-sections (Figure 6-2; Michard, 1976). The thickness of porous media ranges between 4 to 40 m. A thickness of approximately more than 10 m appears to be limited to the wadi courses and the sedimentary basin West of Zagora (Feija de Zagora).

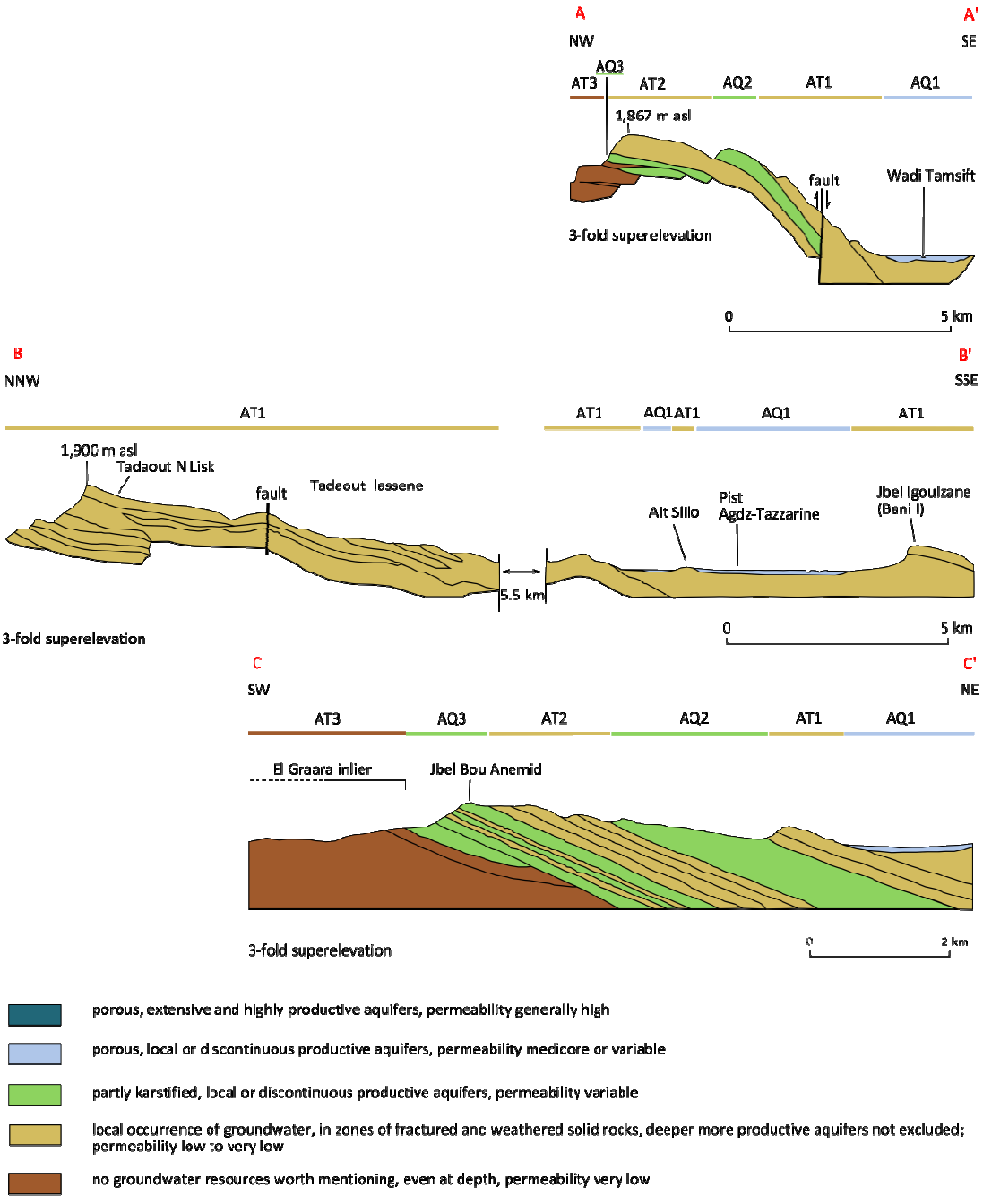

Figure 6-2: Regional hydrogeological cross-sections of southern flank of the central Anti-Atlas Mountains (according to Clariond, Choubert and Hindermayer in Chamayou et al., 1977; Figure 6-1); thereby, AQ1 means most upper Aquifer, AT1 mean most upper Aquitard, AQ2 means next lower Aquifers and so on according to the regional hydrostratigraphical concept from Table 6-1.

The interpretation of the geological data results in a regional hydrostratigraphical concept (Table 6-1).

Table 6-1: Regional hydrostratigraphical concept for the middle Drâa catchment according to the Geological map of Morocco 1/500,000 and the aquifer classification after Fetter (2001; aquifer is defined as hydrogeological unit with a lumped hydraulic conductivity greater or equal $1 \cdot 10^{-5}$ m/s); for color scheme see Figure 6-2.

Era	System	Lithology	Porosity	Aquifer/ Aquitard	Hydro-stratigra-phy
Neogenic	Recent; Upper Quaternary	Loose sediment	Porous	Aquifer	AQ1
	Lower Quaternary; Middle Quaternary	Loam; sand; gravel; lacustrine sediment; evaporites; calich-es; conglomerate; paleosoils	Porous; karstic		
	Lower Quaternary	Conglomerate; cemented sandy gravel			
	Upper Tertiary; Lowest Qua-ternary (Plio-Villafranchian)	Conglomerate; lacustrine limestone; marl with gypsum			
Paleozoic	Siluri-Ordovician	Siltstone	Fractured	Aquitard	AT1
	Siluri-Ordovician	Quartzite			
	Siluri-Ordovician (Caradoc; Llandovery; Bani II)	Sandstone			
	Ordovician (Llandeilo; Caradoc; Schistes de Ktaoua)	Schisty siltstone			
	Ordovician (Upper Llandeilo; Tachilla; Bani I)	Sandstone; siltstone			
	Ordovician (Trémadoc; Llandei-lo; Schistes de Fezouata)	Siltstone			
	Cambrian (Acadien; Grés de Tabanit)	Sandstone			
	Cambrian (Acadien; Schistes à Paradoxides)	Siltstone			
	Cambrian (Géorgien)	Sandstone			
	Cambrian (Géorgien; Grés términaux)	Sandstone; siltstone			
	Cambrian (Géorgien; Schisto-calcaire)	Limestone; schist	Fractured; karstic	Aquifer	AQ2
	Cambrian (Géorgien; Schistes lie-ve-vin)	Siltstone; sandstone	Fractured	Aquitard	AT2
	Early Cambrian (Calcaires inferieurs)	Limestone	Fractured; karstic	Aquifer	AQ3.1
	Early Cambrian (basis)	Conglomerate	Fractured	Aquifer	AQ3.2
Proterozoic	Precambrian	Crystalline rock	Fractured	Aquitard	AT3

The Quaternary lithofacies is hydrogeologically interpreted and transformed to hydrofacies at the regional scale. Basic information on the Quaternary lithofacies is provided by Chamayou (1966) as he distinguishes four units:

- Gravel with blocs (regs)
- Fan deposits and slope debris
- Gravelly to loamy terraces
- Dunes

Focusing on the alluvial aquifers, the lithofacies clearly determines the aquifer system (Figure 6-3).

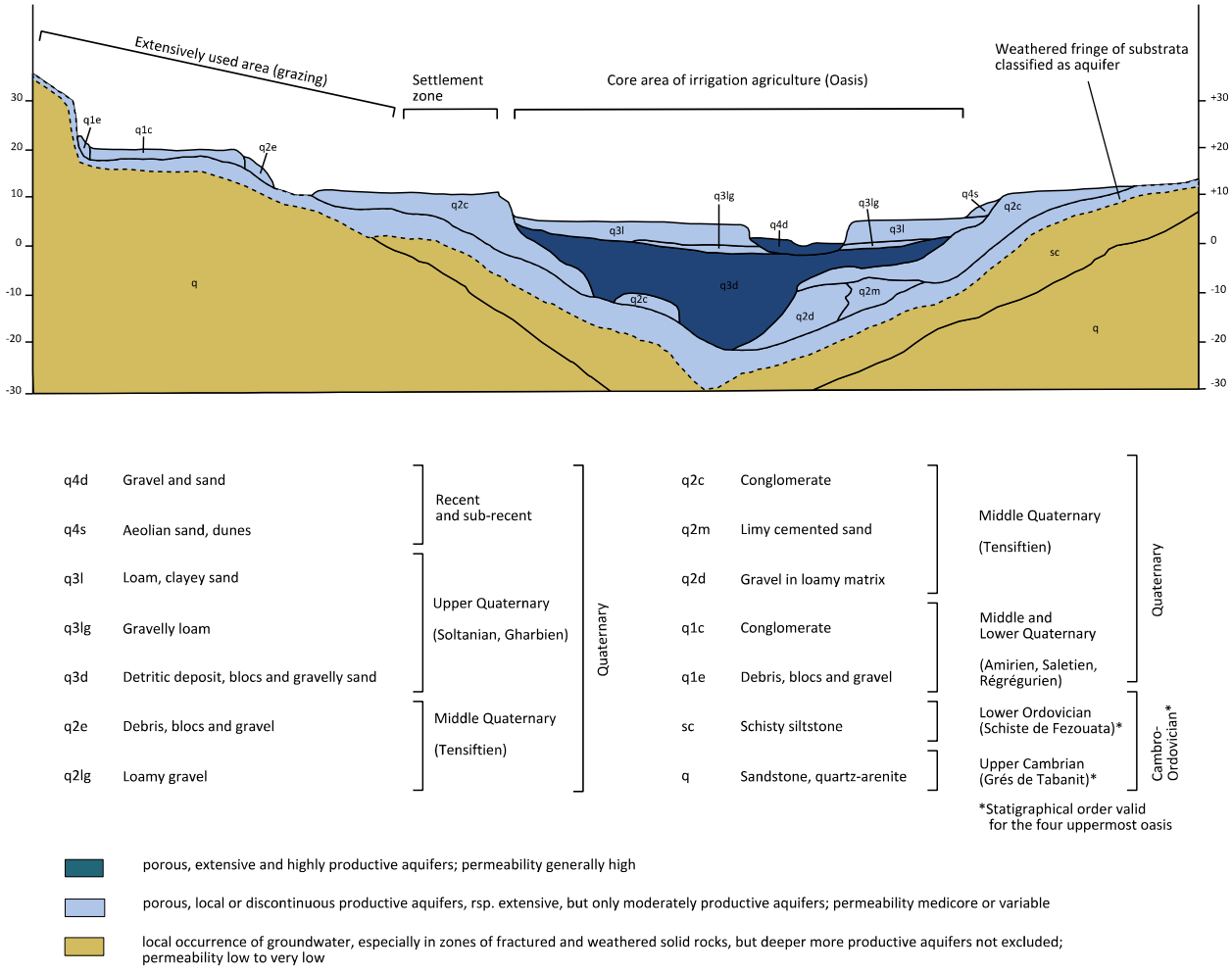

Figure 6-3: Schematic cross-section of the hydrogeological structure of the alluvial aquifers according to the Quaternary facies (after Chamayou, 1966).

Quaternary the deposition conditions varied highly ranging from high energy flash floods to sedimentation in stagnant water or lacustrine environments.

A recapitulatory hydrostratigraphical concept is developed for the alluvial aquifers based on the hydrogeological interpretation of lithofacies, bore log data and former expertise (Table 6-2). It represents mainly the hydrogeological properties and interpretation rather than the stratigraphical order changing over time due to progress in dating. Furthermore, verifying information on aquifer thickness and characterizations of the aquifer material was gained by own hydrogeological mapping during IMPETUS field

campaigns supported by several Diploma-theses (Steenpaß, 2007; Kunert, 2008; Breuer, 2007; Haaken, 2008; Stumpf, 2008).

Table 6-2: Hydrostratigraphical concept of the alluvial deposits in the Middle Drâa Valley based on the stratigraphic stages of Quaternary (compiled from Awad, 1963; Chamayou, 1966; Michard, 1976; Riser, 1988; Arboleya et al., 2008; Hssiane & Bridgeland, 2009 and bore logs from Service Eau Ouarzazate; see Table 2-3).

Lithology	Mean maximum thickness	Distribution	Hydrofacies	Dominant lithofacies along the wadi Drâa	Hydrogeological interpretation
Loam; alluvial sand and gravel; aeolian sand;	2-3 m (dunes: -10 m)	Limited to wadi beds	Very low to very high hydraulic conductivity; porous; unconfined	Sand, gravel	Aquifer of high transmissivity, partly moderate
Succession of coarse gravel (basis) to sand with loamy lenses (often with anthrosol); aeolian sand; lacustrine sediment; evaporite	2-3 m	Mostly limited to wadi beds	Very low to very high hydraulic conductivity; porous; unconfined	Loam, sandy gravel	Aquifer of moderate transmissivity, partly high
Fining up succession of sand (basis) to gravelly loam to loam (partly with anthrosol); fan deposits; lacustrine sediment; evaporite	5 to 10 m (max. 25 m)	Quite wide; locally in direct contact to underlying hard rocks	Low to high hydraulic conductivity; porous; unconfined; possibly locally (semi-)confined	Loam, sand	Aquifer of moderate transmissivity, partly high
Alluvial sand and gravel with loamy and marly lenses; conglomerate; fanglomerate; slightly cemented sand; lacustrine sediment; evaporite; paleo-soils (partly with anthrosol)	15-20 m max: 25 m	Widespread; widely in direct contact to underlying hard rock **most important formations**	Very low to high hydraulic conductivity; porous with secondary porosity by dissolution; unconfined; possibly locally (semi-) confined; sub-regional aquitard	Gravelly sand, conglomerate	Aquifer of variably high transmissivity; sub-regional aquitard **most important sub-unit**
Cemented alluvial sand and gravel; fanglomerate; conglomerate	4 to 15 m	Patchy occurrence due to erosion; thicker in the northern area	Low to high hydraulic conductivity; porous with possibly secondary porosity by dissolution; unconfined; possibly locally (semi-)confined	Conglomerate	Aquifer of variable transmissivity (moderate to high)
Alternating lacustrine limestones and marls with gypsum; conglomerate	variable		Very low to high hydraulic conductivity; porous with possibly secondary porosity by dissolution; unconfined; possibly locally (semi-) confined; layered aquifer		Aquifer of variable transmissivity (moderate to high); inclusive subjacent weathered fringe of substrata
Siltstone (sandy schist)	800 m	Discordant contact	High hydraulic conductivity within the weathered fringe (mean thickness: 5 to 8 m); low to very low hydraulic conductivity; fractured; unconfined-confined	Siltstone	Aquitard; weathering fringe acts as aquifer with moderate to high transmissivity

6.1.2 Fractured aquitards

The fractured aquitards are made up of Proterozoic crystalline series and Paleozoic sedimentary rocks. The **crystalline formations** (Proterozoic) outcrop mainly in the Anti-Atlas Mountain range in the northern part of the Middle Drâa Catchment (MDC). Furthermore, they are found in fault-bordered inliers, e.g. in the Bou-Azzer region (Figure 2-7). Their low to ultra low hydraulic conductivity characterizes them as aquitards. Two Precambrian limestone formations play a special role. They may form local aquifers due to karstification and hence enhanced hydraulic conductivity. At the surface of migmatic granite a fracture volume of less than 1 % was found based on own field observations taken randomly. For the same rock type a fracture volume of up to 5 % is observed within a fractured zone. All fractures were superficially refilled by aeolian sand. Prevalently, the fractures are filled by re-crystallized quartz and subordinately by calcite. The observation of fracture volumes hint on the variety in aquifer productivity due to fractioning. Still the values of fracture volume are very small and fractured zones appear to be locally limited. Consequently, the observed granite functions as an aquitard without groundwater resources worth mentioning for regional water management. Even at depth no further groundwater resources are expected because of generally decreasing fracture volume with depth. Furthermore, the crystalline formations represent the basement and thus the lowest unit in the hydrostratigraphical order (Table 6-1; Figure 6-2). From this example it is clear, that the interpretation of fracture observations carries a high degree of uncertainty and can only be considered as rough estimation for regional classification. Data on the connectivity of fractures or fracture zones in the crystalline basement are not available for this study.

The series of **sedimentary rocks** (Paleozoic) are made up of alternating sandstone, siltstone and carbonate rocks. They are folded dipping southwards and south-eastwards (Destombes; 1985; Helg et al.; 2004). The sandstone and siltstone formations represent aquitards of low to ultra low hydraulic conductivity. The partly karstified carbonate rocks form aquifers of probably enhanced hydraulic conductivity. Individual observations during own field campaigns reveal a fracture volume up to 7 % at the surface of dolomitic limestone (Cambrian; Calcaires inferieurs). These fractures are only superficially opened. At deeper levels the fractures are refilled mainly by calcite. Successions of schisty siltstone, violet sandstone and conglomerate (Cambrian; Schistes lie-ve-vin) have a fracture volume of around 1 % observed in individual outcrops. All observed fractures contain calcite filling of porous and fine to medium grained texture. It is assumed that the fissures can function as flow paths but it cannot be excluded that fractures are blocked by clayey veins formed as a result of weathering. The same as for the crystalline formations, the interpretation of fracture observations are highly uncertain and can only be an approximate indication on the groundwater productivity of the very shallow part of the sedimentary rocks. The fracture volume of the limestone formations appears to be larger than for siltstone and granite. The calcite veins may be subject to dissolution even in greater depth. Accordingly, the limestone formations are classified as partly jointed and possibly karstified aquifers of local and discontinuous nature (Table 6-1; Figure 6-2).The productivity is assumed to be low to moderate but special investigations have to be undertaken to verify these interpretations. Investigations of the connectivity of fractures are missing, but Ismat (2008) studied the fracture pattern of the quartzitic sandstone and schisty siltstone of the Bani Group in the Tata region (around 280 km West of Zagora). The maximum length of fractures is stated to be 1 to 2 m. This is for the most prominent fractures steeply dipping approximately vertical and striking sub-perpendicular to the overall NE–SW trend of folds. So, the main advective groundwater flow is assumed to be directed NW-SE depending on dip and connectivity. The thin soil cover and the almost vertical dip of the main fractures makes it probable that infiltration and groundwater recharge is enhanced in comparison loose sediments where partly capillary rise and evaporation losses reduce percolation.

Overall, the fracture pattern reveals a dense network of fissures being capable to serve as a local aquifer as it occurs in the Zagora region (Figure 6-4; Figure 6-5).

Figure 6-4: Fracture pattern of quartzitic banks of the Ouininirhen Formation (Bani I Group) at the Jbel Zagora (foto by A. Kunert).

Additionally, it is assumed that the schisty siltstone can function as impervious layers cutting groundwater flow paths (Figure 6-5).

Figure 6-5: Fracture pattern of the alternating silt- and sandstone of the Igzert Formation (Bani I Group) at the Jbel Zagora (foto by A. Kunert).

Further local hydrogeological surveys support these assumptions (Ewen, 2004; 82007; Kunert, 2007; Breuer, 2007; Haaken 2008; Stumpf, 2008). Finally, the siltstone and sandstone formations are classified as aquitard with locally occurring groundwater (Table 6-1; Figure 6-2).

6.1.3 Porous aquifers

Loose and slightly consolidated deposits of Quaternary age shape the alluvial aquifer system of shallow thickness and varying hydraulic conductivity (Table 6-1; Figure 6-2). Three sub-systems of alluvial aquifers exist in the Middle Drâa Catchment (MDC):

- Drâa aquifers (main aquifers consisting of Drâa terraces) - see Chapter 6.1.4
- Tributary aquifers (secondary aquifers embedded in the Fractured aquitards)
- Basin aquifers (mediating aquifers beneath flat relief)

The **Drâa aquifers** are lined up along the Wadi Drâa. They are flanked by Fractured aquitards to the East and to the West. Cambrian quartzite and sandstone (Tabanit Group) occur to the West and quartzarenites of the Bani I Group down to the cuesta of the Jbel Bani to the East. The two most upstream Drâa aquifers (Tinzouline and Mezguita) have a quite slim form. Downstream, the Basin aquifers and Tributary aquifers are spread forming an intermediary element to the flanking aquitards. South of the Jbel Bani, the cuesta of the Bani II Group borders the terraces of the wadi Drâa to the West and to the East (Figure 6-6; Figure 6-1; Figure 2-7). The delimitation of the Drâa aquifers from the Lower Drâa Catchment is not clearly identified. The Drâa aquifers have an internal structure dependent on the succession of sedimentary terraces, their varying texture and grade of cementation (Table 6-2). Therefore,

older deposits are slightly consolidated having lower permeabilities than the superposed or embedded loose sediments (Chamayou et al., 1977). Blocky slope debris outcrop at the steep hillsides representing mostly unsaturated cover layer. The Drâa aquifers overlay the Fractured aquitard of Ordovician schisty siltstone (Figure 6-7). A fringe of weathered material occurs at the top of the aquitard forming effectively a part of the alluvial aquifers. The Drâa aquifers can be directly connected with aquifers beneath the tributary wadis and aquifers in adjacent basins (feijas). These basins play locally a mediating role between the aquitard system of hard rock aquitard and the Drâa aquifers. The Drâa aquifers are the most important aquifers within the MDC. This is mainly due to the inflow from the reservoir Mansour Edhabbi and the relatively favorable hydraulic conductivities of the terrace sediments (chapter 2.2). For further characterization of the Drâa aquifers it is referred to chapter 6.1.4.

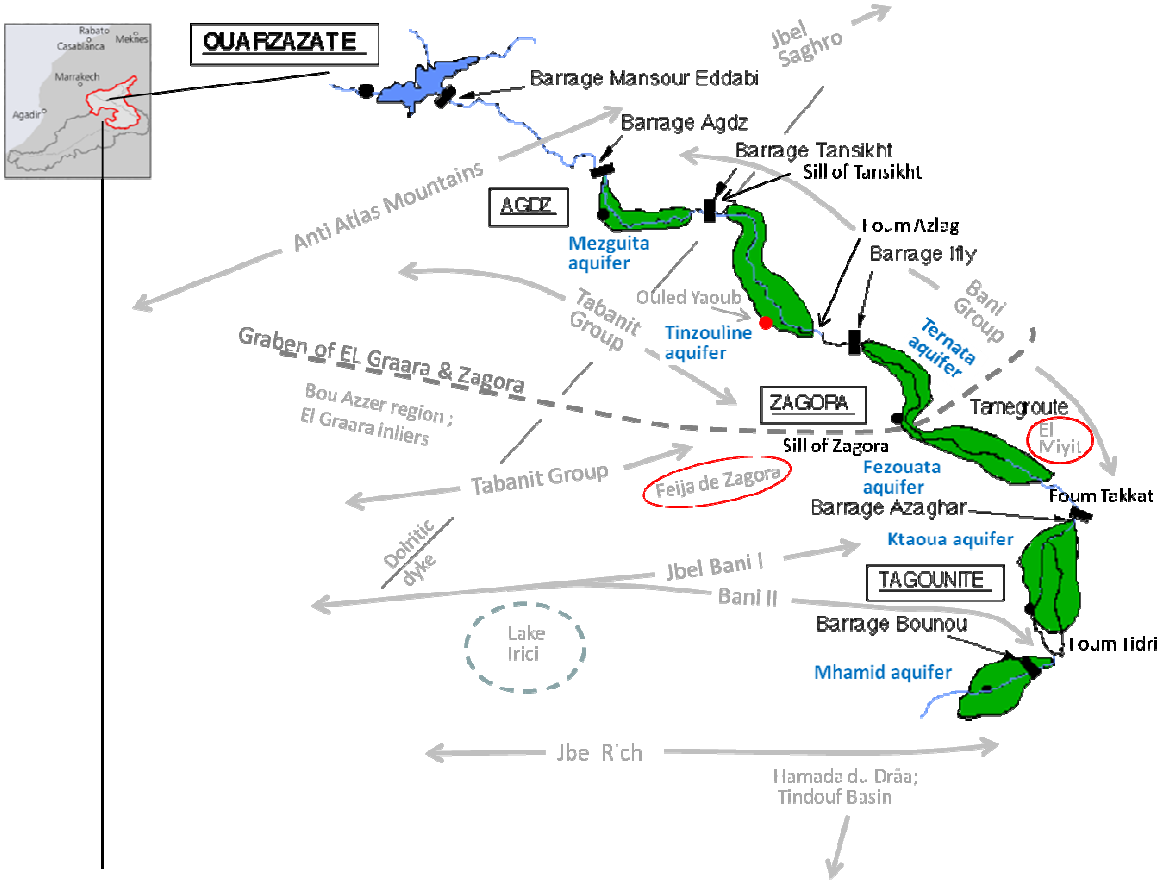

Figure 6-6: Scheme of the oases belt along the wadi Drâa and the adjacent main features of landscape and geology.

The **Tributary aquifers** are very shallow and narrow alluvial aquifers embedded in the Fractured aquitards beneath the tributaries of the Wadi Drâa. The Tributary aquifers provide hydraulic connection between the Fractured aquitards and the Drâa aquifers forming groundwater veins (Table 6-1; Figure 6-2). Fault zones in the Fracture aquitards can form preferential pathways resulting in inflow to the secondary aquifers and further on to the Drâa aquifers (chapter 6.2.2). It can be assumed that the Tributary aquifers are replenished by indirect recharge after heavy rainfall and discharge within the wadi beds. This is supported by the properties of the channels. The wadi gradients are relatively steep and zones of stagnant water are not extended so that clogging of the wadi bed is of secondary importance. The wadi beds are rough consisting mostly of coarse sandy gravel and blocks so that the infiltration capacity is enhanced. The Tributary aquifers are of secondary importance for regional groundwater flow and water

supply because of their small effective volume and storage capacity in comparison to the Drâa terraces (Chamayou et al., 1977).

Figure 6-7: Outcrop of weathered schisty siltstone (Schistes de Fezouata, Ordovician; Breuer, 2007).

The **Basin aquifers** feature terrace sediments of tributary wadis of the Drâa, evaporate-bearing lacustrine deposits, paleo-soils and most commonly a vast flat relief. Chamayou (1966) classifies the Basin aquifers and the Tributary aquifers as one. In this study, the Basin aquifers are understood to play a special role because they connect the fractured aquitards and the Drâa aquifers as mediating unit. They differ from the Tributary aquifers due to potentially longer flow paths and vast flat morphology being partly responsible for smoother hydraulic gradients in the Basin aquifers (chapter 6.2.2). Furthermore, the hydrogeochemical characteristics are different (chapter 6.3.4 & 6.3.3) and in particular, thick sedimentary series of the Basin aquifers have higher reservoir capacity (Chamayou et al., 1977; DRE, 1976). So, two types of Basin aquifers are distinguished:

- Thick Basin aquifers (> 10 m of mean thickness of sediments), e.g. Feija de Zagora,
- Thin Basin aquifers (< 10 m of mean thickness of sediments), e.g. El Miyit (Figure 6-6)

The Thick Basin aquifers are defined as morphological basins containing a sedimentary filling of a mean thickness of more than 10 m (locally adapted classification). The Basin of Feija de Zagora reveals quaternary sediments of a mean thickness of around 20 m ranging from 2 to 54 m (based on 40 bore logs from the Service Eau Ouarzazate; chapter 6.2.2.5). In contrast to this, the mean thickness of sediments in the Basin of El Miyit account for 3 m ranging from 1.5 to 5 m (based on mapping at 11 wells; Stumpf, 2007; chapter 6.2.2.6). In particular, the thick Basin aquifers have a multi-layered hydrostratigraphy, which is influenced by the Paleo-relief of the underlying schists. Furthermore, caliche formations during Quaternary are characteristic (Chamayou et al., 1977). So, intercalated lacustrine fine sediments, marls and

dense carbonates (caliches) can act as local aquitards. The enhanced importance of the Basin aquifers as groundwater reservoir becomes obvious through the increasing development of individual farms and competitive use for drinking water supply e.g. in the Basin of the Feija de Zagora (Aoubouazza & El Meknassi, 1996; Breuer, 2007; Rademacher, 2009, Heidecke, 2009).

6.1.4 Drâa aquifers

Downstream of the outlet of the reservoir Mansour Edhabbi the Wadi Drâa forms a canyon passing the Anti Atlas Mountain range before flowing through a landscape of ridges and cuestas. In this canyon very shallow alluvial deposits developed, which are not important for the regional aquifer structure. But downstream of the Anti-Atlas Mountain range six alluvial aquifers are lined up along the wadi Drâa, the Drâa aquifers (Figure 6-6). The Drâa aquifers are the most important aquifers due to their structure and properties, but also because of the surface water inflow from the upstream reservoir Mansour Edhabbi (chapter 2.2). The Drâa aquifers are flanked by Paleozoic aquitards. The Paleozoic aquitards and tectonic lineaments form barriers separating each Drâa aquifer from the further downstream one. The wadi Drâa connects the aquifers across the barriers forming a six-fold aquifer-cascade. A dolerite dyke functions as hydraulic sill in the wadi course representing the downstream limit of the Mezguita aquifer (Sill of Tansikht). A ridge of Cambrian quartzarenites (Tabanit Group) limits the Tinzouline oasis to the downstream Ternata oasis (Foum Azlag). The Zagora Graben separates the aquifers of Ternata and the Fezouata oasis (Sill of Zagora). Thereby, the reversal relief of the Zagora Graben forms a chain of quartzarenites (Bani I Group). Further downstream, the double chain of the Jbel Bani (Bani I & II) shapes a cuesta of quartzarenites delimiting the Fezouata oasis from the Ktaoua oasis (Foum Takkat). A braced sub-chain of the Jbel Bani (Bani II) forms another cuesta between Ktaoua and the Mhamid oasis (Foum Tidri). The downstream limit of the most southern oasis Mhamid is not clearly defined (Figure 6-1, Figure 6-6). So, the Drâa aquifers are divided into six units named same as the date palm oases (downgradient order):

- Mezguita aquifer
- Tinzouline aquifer
- Ternata aquifer
- Fezouata aquifer
- Ktaoua aquifer
- Mhamid aquifer

Geohydraulic properties as transmissivity and hydraulic conductivity are withdrawn from literature summarized in Table 6-3. Moreover, the IMPETUS project provides single values of hydraulic conductivities in the Feija of Zagora and the village Ouled Yaoub (Oasis Tinzouline) through rough recovery tests at irrigation wells (Breuer, 2007; Haaken, 2008). Results of these spot tests fall within the range of values from literature (Chamayou, 1966; Chamayou et al., 1977; DRH, 2001). The data basis is sparse in spatial resolution and only very few aquifer tests are comprehensible. Therefore, data from Chamayou (1966) is used for this study (Table 6-3).

Table 6-3: Geohydraulic properties of the alluvial deposits along the wadi Drâa as mean transmissivity and mean hydraulic conductivity (Chamayou, 1966).

Aquifer unit	Mean transmissivity (Chamayou, 1966) [m²/s]	Median hydraulic conductivity (Chamayou, 1966) [m/s]	Number of aquifer tests
Mezguita	$6 \cdot 10^{-3}$	$1 \cdot 10^{-3}$	2
Tinzouline	$5 \cdot 10^{-2}$	$7 \cdot 10^{-3}$	18
Ternata	$5 \cdot 10^{-2}$	$3 \cdot 10^{-3}$	15
Fezouata	$2 \cdot 10^{-2}$	$2 \cdot 10^{-3}$	17
Ktaoua	$7 \cdot 10^{-3}$	$3 \cdot 10^{-4}$	18
Mhamid	$5 \cdot 10^{-3}$	$3 \cdot 10^{-4}$	8

Information on the flow sections at the downgradient contacts of the Drâa aquifers stem from own mapping using GIS-techniques with transmissivities from Chamayou (1966) (Table 6-4; Figure 6-6).

Table 6-4: Characteristics of flow sections at the downgradient hydraulic contact of the Drâa aquifers (foums and sills; from Chamayou, 1966; Figure 6-6).

Downgradient contact of Drâa aquifers (foums and sills)	Flow section [m²]	Hydraulic conductivity [m/s]
Sill of Tansikht	4,000	$6 \cdot 10^{-4}$
Foum Azlag	3,000	$5 \cdot 10^{-3}$
Sill of Zagora	6,000	$8 \cdot 10^{-3}$
Foum Takkat	13,000	$2 \cdot 10^{-3}$
Foum Tidri	150,000	$2 \cdot 10^{-4}$

The internal structure of the Drâa aquifers is based on the hydrogeological interpretation of lithofacies description and bore log data conscious of the inherent uncertainties (Table 6-2). Thereby, bore logs give indispensable clues for regional differentiation of the aquifer system. The internal aquifer structure is sparsely known from borehole descriptions provided by the Service Eau Ouarzazate. For the present work, 80 bore logs are available tapping the Drâa aquifers whereas the delimitation of these is based on the geological map 1/500,000 and thus a regional estimation. 56 bore logs represent the geological record down to the aquifer basis. The repartition of the bore logs to the hydrogeological units is uneven for the middle Drâa valley as shown in Table 6-5.

Table 6-5: Overview of number and reparation of bore logs providing information on the Drâa aquifers.

Aquifer unit	Number of bore logs	Number of bore logs including basis of alluvial deposits
Mezguita	9	7
Tinzouline	6	2
Ternata	11	9
Fezouata	30	29
Ktaoua	13	8
Mhamid	11	1

Further 37 bore logs are available for the sedimentary basin Feija de Zagora even all including the aquifer basis (ORMVAO, 1981). The bore log data from the Feija de Zagora provide thickness of the weathered fringe of schisty sandy siltstones beneath alluvial deposits and supplementary information for interpretation (Table 6-7).

Values for specific yields (S_y) are derived from bore logs provided by Service Eau Ouarzazate (chapter 5.1). Chamayou (1966) already mentioned that the data basis concerning the storage term of the aquifers is very sparse. Furthermore, he distinguished between two S_y dependent on a loamy lithofacies and a gravelly lithofacies respectively. So, the storage of drainable groundwater is dependent on the thickness of the respective lithofacies unit. In the present study, values for the specific yield are assigned to the lithological units represented in the bore logs. Therefore, the values from literature are compared to similar lithological units in bore logs (Johnson, 1967; Table5-2).

Box plots reveal two main groups of reservoir capacity subdivided in the two upper Drâa aquifers (Mezguita and Tinzouline) and the four lower ones (Ternata to Mhamid; Figure 6-8). This may be due to the different environmental conditions during the formation of the deposits. The relatively slim shape of the two uppermost oases indicates on sedimentological conditions which differ from these in oases connected to the Feijas (Riser, 1988). The sedimentation is determined by relatively short distances to the source area and high relief energy. Thereby, Precambrian and Early Cambrian rocks are tapped in the Anti-Atlas Mountain range. Material is further transported and sorted downgradient by the wadi Drâa. The more distal sedimentation areas of the lower four oases receive additionally eroded material from the El Graara inlier (Bou Azzer region) and local source areas via the feijas (Figure 6-6). The feijas function as buffer and sediment trap, but still contributing depending on the prevailing hydrological system during Quaternary (Table 2-3). So, the change in sedimentation dynamic, consolidation processes and source areas via the feijas may be a reason for the two-fold grouping of the specific yield along the wadi Drâa. But it cannot be excluded that the grouping is an artifact and hence a result of sparse data availability and resolution (Table 6-5). However, the box plots show the high variability and hence the uncertainty of specific yield assessments (Figure 6-8; Healy & Cook, 2002).

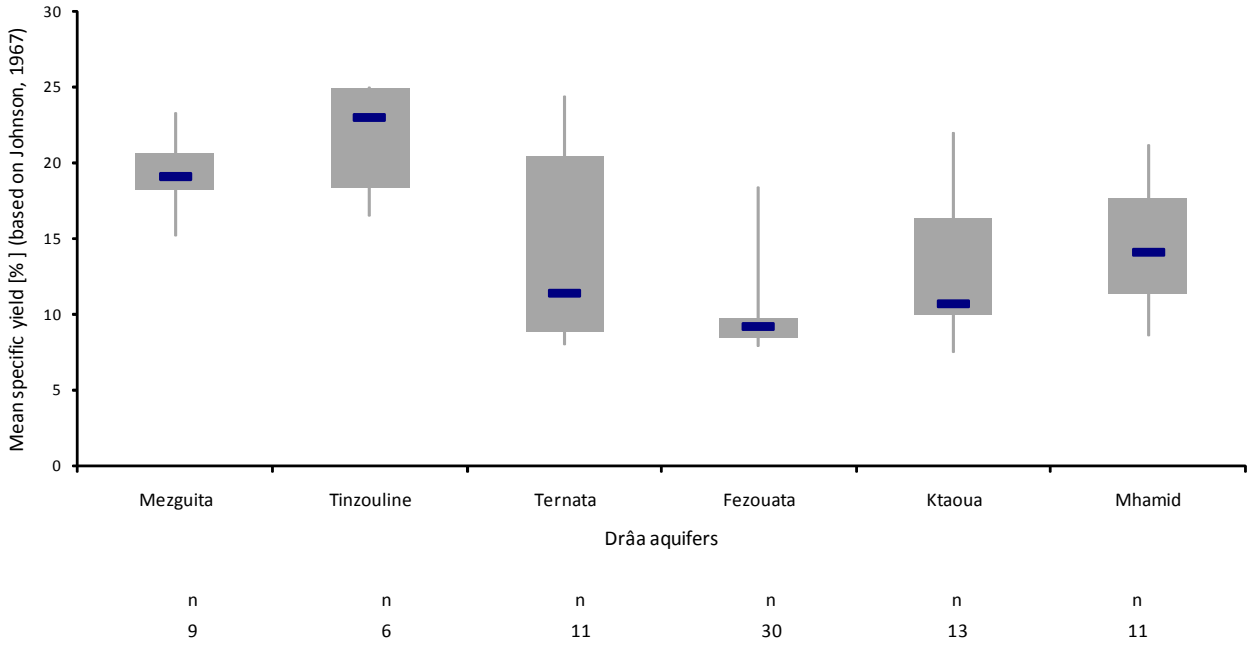

Figure 6-8: Box plots representing statistical measures for the specific yield allocated to 80 bore logs (after Johnson; 1967) in order to compare the oasis aquifers (grey vertical lines display minima and maxima; grey boxes represent the 25 % to 75 % quantile range; blue horizontal lines portray the median values).

In comparison to Chamayou et al. (1977), the assigned values of specific yield are systematically higher (Table 6-6). In contrast to former expertise, a successive downgradient decline in specific yield is unconfirmed. The differences in comparison to former assessments may be due to the respective method used to determine the value for specific yield. Chamayou et al. (1997) carried out pumping tests. Accordingly, the assessment of specific yield relies on the saturated thickness. In this study, specific yield values are assigned over the entire length of each bore log, which is significantly larger than the saturated thickness. Consequently, this can have an influence on the difference in specific yield compared to Chamayou et al. (1977). Furthermore, field test reveal systematically lower values of specific yield compared to laboratory experiments (Healy & Cook, 2002). The specific yield values allocated to bore logs contain data gained by laboratory experiments as based on Johnson (1967). As mentioned before, the data availability and resolution limits the interpretation strongly (Chamayou, 1966; Chamayou et al., 1977). Overall, the values allocated to bore logs appear to be realistic, as the data provided by Johnson (1967) remain valid since decades (Healy & Cook, 2002). The uncertainty in bore log documentation appears to be one of the most important sources of error.

Table 6-6: Comparison of specific yield values from Chamayou et al. (1977) on the left hand and from own estimations based on bore log analogue assignment after Johnson (1967) on the right hand.

Drâa aquifers	Mean specific yield (Chamayou et al. (1977) [%]	Mean specific yield [%]	Minimum specific yield [%]	Maximum specific yield [%]
Mezguita	n.d.	19	14	29
Tinzouline	16	22	16	31
Ternata	9	15	8	23
Fezouata	n.d.	10	5	18
Ktaoua	3	13	7	19
Mhamid	5	15	8	21

The potentially drainable volumes of the Drâa aquifers are determined based on the specific yield estimation, the bore loge data and the outcrop area. The geometric calculations follow the multiplication of the outcrop area of the aquifer with the mean thickness and the specific yield (Table 6-7).

The delimitation of aquifer outcrop is assessed using a GIS based on own mapping, the synthesis of literature and the bore log data (Figure 6-1). The mean thickness of the alluvial deposits of the Drâa aquifers are derived from bore log data (Table 6-5). In order to estimate drainable volume of the complete Drâa aquifers and not only of the alluvial deposits, the weathered fringe of the substrata is considered. Therefore, the mean value of thickness of the weathered fringe is added and the mean specific yield is applied as before (Table 6-6). The mean thickness of the weathered fringe accounts for 5.5 m and is taken from 37 bore logs from the Feija de Zagora, because they are the only available source of information. In this study, the Drâa aquifers represent rectangular bodies as a generalized abstraction by using the mean value of the aquifer thickness. The discrete reconstruction of the aquifer geometry carries large uncertainties, as very sparse data is available on the anastomosing or anabranching architecture of the deposits of the Wadi Drâa. Furthermore, the alluvial fans and debris cones intersect the fluvial terraces. Nilsson et al. (2007) found that the estimation of the drainable volume of groundwater could be biased to more than 100 % because of uncertainties in the hydrogeological concept. Referring to this, the present study provides a low parameterized and robust approximation of the aquifer geometry and hence the potentially drainable aquifer volumes. The minimum, mean and maximum values of specific yield are applied to show the widest range of drainable alluvium volumes (Table 6-7).

Table 6-7: Potentially drainable volumes of the alluvial deposits including the mean thickness of weathered fringe of the substrata (5.5 m) based on own estimations with specific yield values based on bore log data and Johnson (1967; Table 6-6).

Aquifer unit	Mean thickness [m]	Outcrop area [km²]	Minimum drainable aquifer volume [Mm³]	Maximum drainable aquifer volume [Mm³]	Mean drainable aquifer volume [Mm³]
Mezguita	20.5	30.5	87.5	181.2	118.7
Tinzouline	20.5	56.4	185.1	358.6	254.5
Ternata	19.5	56.8	88.6	254.8	166.2
Fezouata	21.5	72.5	77.9	280.5	155.9
Ktaoua	31.5	127.2	280.4	761.0	520.7
Mhamid	50.5	44.0	177.7	466.4	333.1

Estimations of drainable aquifer volumes based on based on Chamayou (1966) and Chamayou et al. (1977; Table 6-8) as well as based on ORMVAO (1995; Table 6-9) are compared to the own estimations (Table 6-10). Thereby, the two literature sources reveal the potentially drainable volumes of alluvial deposits along the Drâa. Own estimations consider additionally the weathered fringe of substratum as it contributes to the drainable aquifer volume (Table 6-7).

Table 6-8: Potentially drainable volumes of the alluvial deposits based on Chamayou (1966) and Chamayou et al. (1977).

Aquifer unit	Mean specific yield [%]	Mean thickness [m]	Outcrop area [km²]	Mean drainable volume of alluvial deposits [Mm³]
Mezguita	5	25	45.0	56.3
Tinzouline	16*	25	69.0	276.0
Ternata	9*	25	45.4	102.2
Fezouata	5	30	72.1	108.2
Ktaoua	3*	40	79.0	60.0
Mhamid	5*	50	124.6	311.5

** Specific yield values from Chamyou et al. (1977)*

The estimations of potentially drainable volumes of alluvial deposits based on Chamayou (1966) and Chamayou et al. (1977) as well as based on ORVMAO (1995) differ from own estimations due to distinct specific yield values and alternative aquifer dimensions (Table 6-8; Table 6-9).

Table 6-9: Potentially drainable volumes of the alluvial deposits based on ORMVAO (1995).

Aquifer unit	Mean specific yield [%]	Mean thick-ness [m]	Outcrop area [km²]	Mean drainable volume of alluvial deposits [Mm³]
Mezguita	5	14	36.0	25.2
Tinzouline	11	17	58.6	109.7
Ternata	11	20	78.3	172.3
Fezouata	8	18	55.8	75.3
Ktaoua	4	30	110.3	132.8
Mhamid	5	18	33.1	29.7

In Table 6-10 the range of potentially drainable aquifer volumes from different sources is summarized. The drainable aquifer volumes based on Chamayou (1966) and Chamayou et al. (1977) and in particular based on ORMVAO (1995) are much lower than the result of own assessments. This is due to the consideration of the weathered fringe of the substrata on the one hand and the generally higher specific yield values on the other. The differences in outcrop area are of minor importance. The difference between own estimation and the results based on Chamayou (1966) and Chamayou et al. (1977) are half because of the consideration of the weathered fringe of the substrata and half because of higher specific yield values. The difference between own estimations and results based on ORMVAO (1995) constitutes to one third of the consideration of the weathered fringe of the substrata. However, supplement to the geological data basis is required to improve water resources assessments. Regarding differences in specific yield values, improved data availability would probably reduce uncertainties. Thereby, specific yield remains difficult to determine and can vary in time (Healy & Cook, 2002).

Table 6-10: Comparison of mean drainable volumes of the Drâa aquifers based on Chamayou (1966) and Chamayou et al. (1977), ORMVAO (1995) and own estimations including the mean thickness of weathered fringe of the substrata (5.5 m).

Drâa aquifer	Mean drainable aquifer volume [Mm³]	Mean drainable volume of the weathered fringe of substrata (5.5 m)	Mean drainable alluvium volume (following Chamayou, (1966 & Chamayou et al. ,1977) [Mm³]	Mean drainable alluvium volume (following ORMVAO, 1995) [Mm³]
Mezguita	118.7	31.8	56.3	25.2
Tinzouline	254.5	68.3	276.0	109.7
Ternata	166.2	46.9	102.2	172.3
Fezouata	155.9	39.9	108.2	75.3
Ktaoua	520.7	90.9	60.0	132.8
Mhamid	333.1	36.3	311.5	29.7
Total	1,549.1	314.1	914.1	544.6

The generalized description of the aquifer system forms the basis for the lumped quantification of annual groundwater availability and aquifer response of the Drâa aquifers using the BIL groundwater balance model (chapter 7). Therefore, the mean aquifer capacity is applied based on the mean specific yield.

6.2 Aquifer response and groundwater flow paths

The characteristic geohydraulic behavior of an aquifer is commonly determined based on geometric measures and physical properties, such as volumetric structure of the aquifer, transmissivity, hydraulic conductivity and storage coefficients (chapter 6.1). Thereby, the aquifer response to inflow and outflow is time dependent, especially concerning the storage term. In the arid study area, the high evaporation potential is assumed to enhance the temporal dynamic in the aquifer response. Furthermore, hydrogeochemical processes such as precipitation or solution of minerals can alter properties such as effective porosity within decades (chapter 6.3.3.3).

The aquifer response in the Drâa aquifers is described based on the aquifer system analysis and groundwater level data provided by the Service Eau Ouarzazate and the ORMVAO. Specially measured groundwater level data provides new complementary information collected during own field campaigns.

Two piezometric data sets are available concentrating on the Drâa aquifers:

- Irregular, monthly to annual, observations at 38 sites between 1973 and 2002
- Daily observations at two sites between 2005 and 2007

The irregular groundwater level data is interpreted qualitatively due to irregular gaps of observation. These gaps do not allow correlation analyses of groundwater level response in relation to determining factors, such as direct recharge through precipitation or wadi discharge after releases of the Mansour Eddahbi reservoir.

Furthermore, flow paths towards the Drâa aquifers are determined based on the fragementary record for key dates at individual pairs of sites. Data from own field surveys is used to assess exemplary groundwater flow paths for spring 2005, autumn 2005 and spring 2007 in the Zagora region.

Based on daily aggregated groundwater level data, the water table fluctuation method is applied to estimate groundwater recharge locally (chapter 6.2.3). As a result, the groundwater flow system of the Drâa aquifers can be described conceptually (chapter 6.2.2).

6.2.1 Response of the Drâa aquifers

The observations of groundwater level fluctuations are used to evaluate the aquifer response. The data resolution (temporal and spatial) reveals only a long-term overview of the aquifer response at 38 well sites. Observations are selected for the period of October 1973 to September 2002. The sites are located within or at the rim of the Drâa oases and thus tap the Drâa aquifers. The observation concept of the Moroccan water authorities is obviously implemented to monitor the development of groundwater levels in the intensively used and relatively densely inhabited oasis areas. The spatial resolution of the observations points is highly irregular (Figure 6-9).

Table 6-11 gives an overview of the repartition of the fragmentarily observed groundwater sites.

Table 6-11: Overview of the repartition of the fragmentarily observed groundwater sites.

Aquifer unit (Oasis)	Number of observation sites
Mezguita	6
Tinzouline	4
Ternata	10
Fezouata	8
Ktaoua	4
Mhamid	6

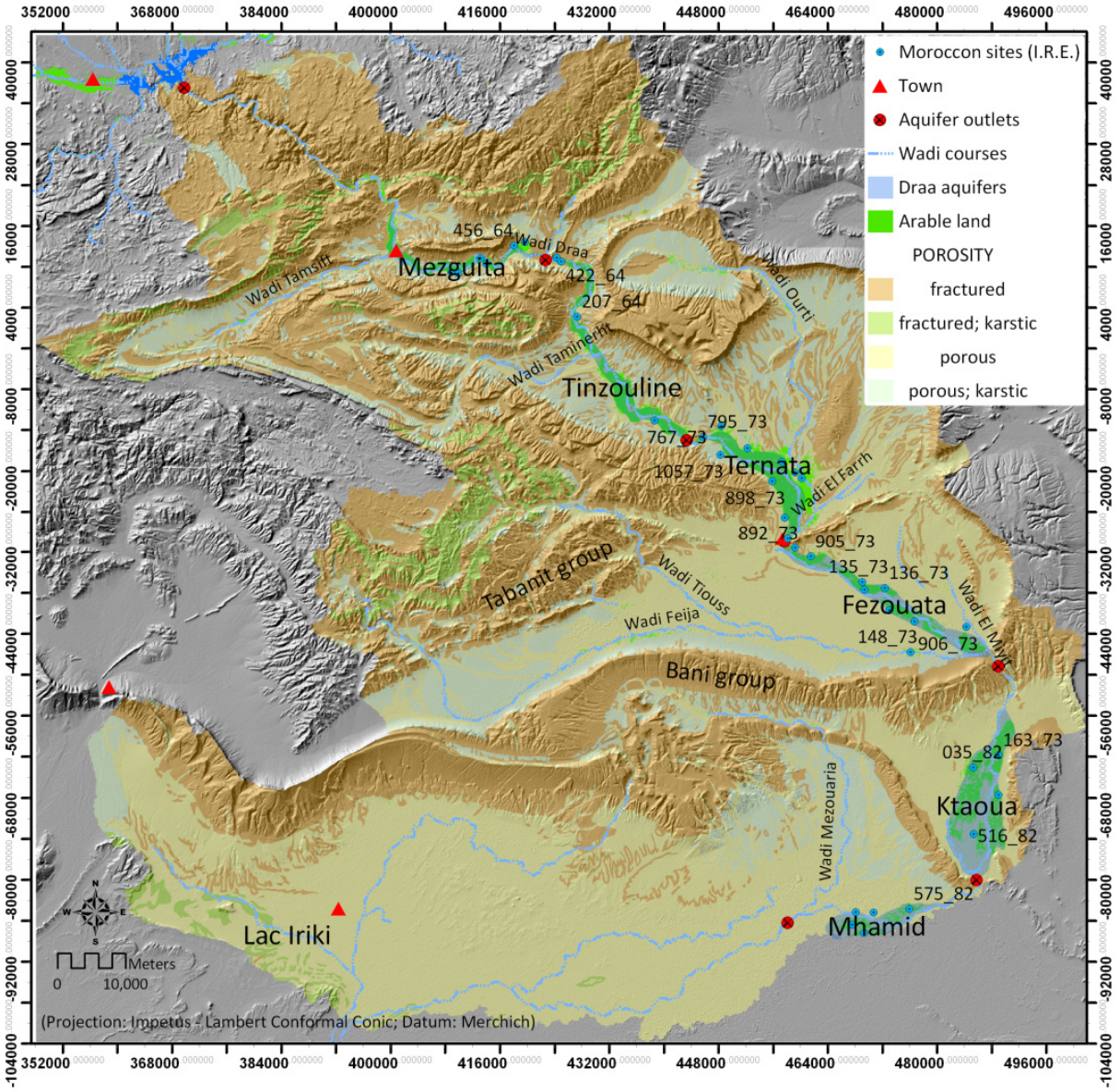

Figure 6-9: Overview of the distribution of 38 Moroccan groundwater sites revealing fragmentary monthly to annual groundwater level observations between 1973 and 2002.

Groundwater level record is temporal irregular and partly inconsistent. The data is rescaled to a monthly time line (Figure 6-10). Thereby, four global gaps of observations are found which last longer than eight months:

- November 1979 to July 1980
- September 1980 to June 1981
- October 1993 to June 1994
- December 1996 to February 1998

A further prominent gap is found between December 1985 and October 1986 subdividing approximately 75 % of the data set into two measurement phases. After December 1985 observation was stopped at nine sites and at further five even before. Additional 14 sites were observed after October 1986, whereas at one of them measurements started in 2000. At least, ten discontinuous observations go beyond

the gap between December 1985 and October 1986. Shorter gaps are considered as discontinuity in observations.

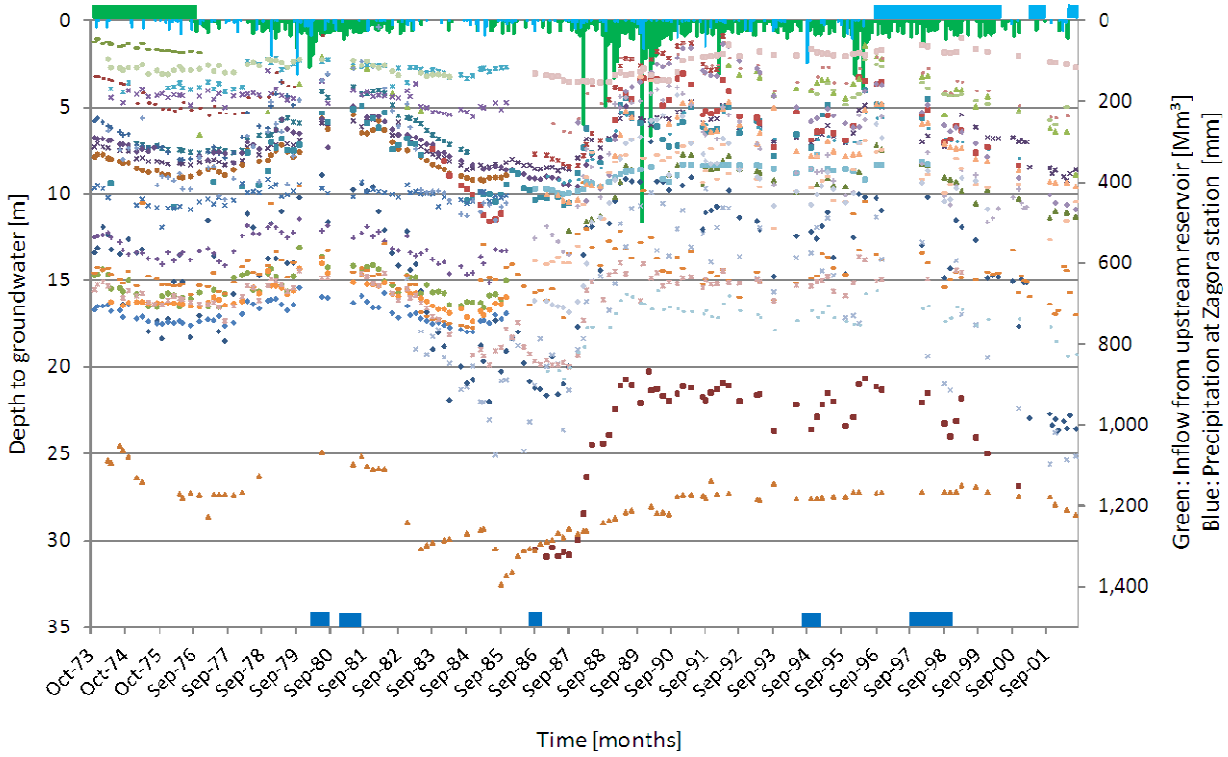

Figure 6-10: Overview of the groundwater level record at 38 sites as depth to groundwater against a monthly time line with stream flow from the reservoir Mansour Eddahbi (green columns) and precipitation at Zagora station for the period October 1973 - September 2002 (light blue columns; Source: ORMVAO). Data gaps are Blue bars lines along the lower x-axes mark gaps in groundwater level data, green bar along upper x-axis marks a gap in stream flow data, light blue bars mark gaps in precipitation data.

The observed groundwater levels show distinct discharge and recharge periods obviously depending on the wadi discharge in the Drâa after water releases from the upstream reservoir Mansour Eddabhi and rainfall. Thus, natural climatic variations influence the medium to long-term aquifer response. The Drâa aquifers show a dynamic behavior due to their shallow structure and limited storage capacity (chapter 6.1). Water releases from the upstream reservoir lead to pronounced recharge. Generally, groundwater levels appear to rise quickly after strong rainfall within the catchment mainly due to indirect recharge. The groundwater level fluctuations vary from site to site. This can be explained by locally varying aquifer structure and properties (chapter 6.1). A statistic relation between amplitude of groundwater level fluctuation and distance to Wadi Drâa is not found based on the discontinuous data set. But it is probable that local and intermediate groundwater systems change over time in relation to indirect and localized recharge processes along the wadi course.

As an example for a recharge period, a global groundwater level rise is observed in the period September 1977 – November 1979 (27 months). The groundwater levels show an overall increase interrupted by interim lows in summer times (Figure 6-10). Observations of 16 sites are selected to show the groundwater level rise. Criteria for selection are the availability of data at the beginning and the ending of the period and high temporal density of observations. The observations of September 1977 – November 1979 show rising groundwater levels by 0.79 to 8.26 m. Thereby, the mean value is 2.14 m whereas the median accounts for 2.84 m. These values exclude data from the Mhamid aquifer because

the observations begin in or after 1986. The other Drâa aquifers are represented by the 16 selected data sets (Table 6-12).

Table 6-12: Representation of groundwater level data for the period September 1977 – November 1979 in relation to the Drâa aquifers.

Drâa aquifer (Oasis)	Number of data sets September 1977 – November 1979
Mezguita	5
Tinzouline	3
Ternata	3
Fezouata	4
Ktaoua	1
Mhamid	non

The global recharge of September 1977 – November 1979 appears to be mainly triggered by precipitation within the Middle Drâa Catchment (MDC). That is shown by the comparison of the statistical characteristics of the recharge period September 1977 – November 1979 and the complete observation period in relation to mean monthly inflow from the reservoir Mansour Eddabhi and the mean monthly precipitation at Zagora station (Figure 6-11). The statistical measures of the mean monthly inflow differ only slightly for the observation periods. The difference in mean precipitation appears to be more pronounced but remains unclear. The comparison also reveals high variability of inflow and especially rainfall as the box plot shows (Figure 6-11).

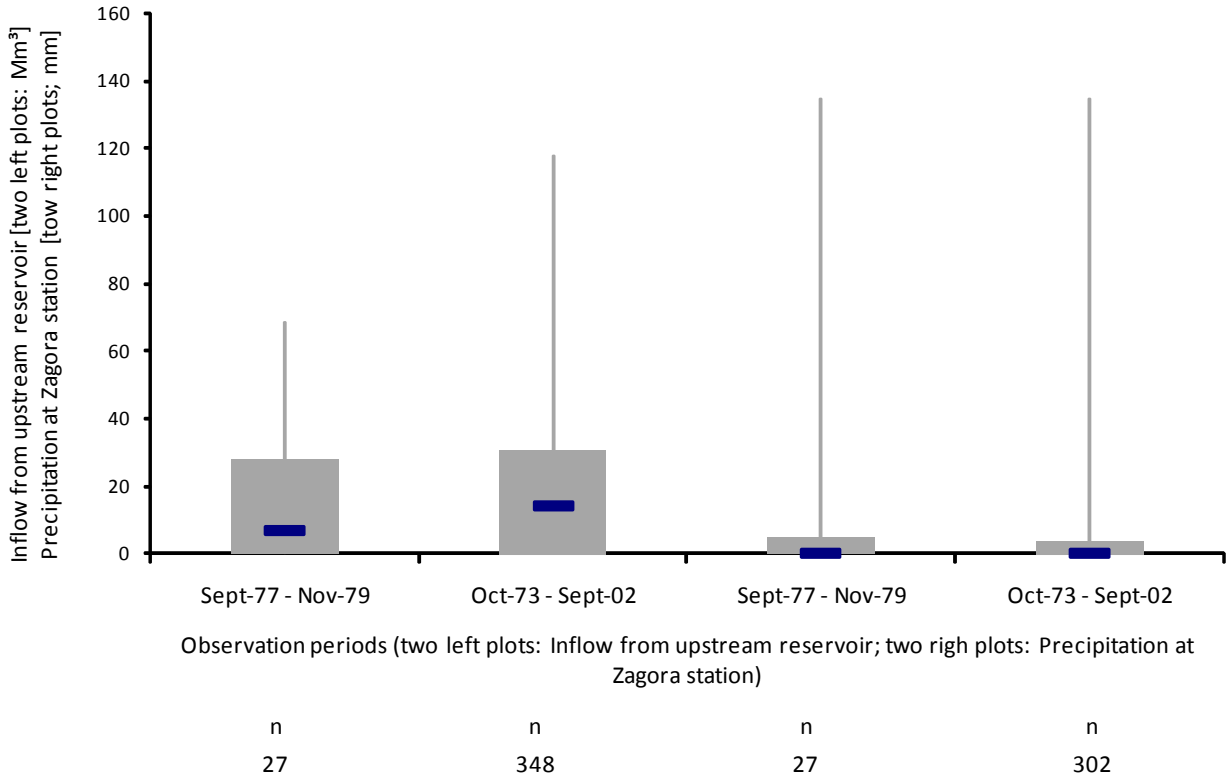

Figure 6-11: Box plots of mean monthly inflow from the reservoir Mansour Eddabhi and mean monthly precipitation at Zagora station to compare the periods September 1977 - November 1979 and October 1973 – September 2002 (grey vertical lines display minima and maxima; grey boxes represent the 25 % to 75 % quantile range; blue horizontal lines portray the median values).

The mean monthly value of water releases from the reservoir Mansour Eddabhi for September 1977 – November 1979 accounts for 15.0 Mm³. By comparison, the mean value of the time span October 1973 – September 2002 amounts to 17.8 Mm³. So, the inflow is 0.8 times less in the recharge period. The mean value of precipitation accounts for 11.4 mm at Zagora station whereas the mean value of the entire observation periods amounts to 5.5 mm. Accordingly, precipitation is approximately 2.1 times higher in this recharge period. Application of the Mann Whitney U-test reveals that the mean monthly inflow from the reservoir Mansour Eddabhi is not significantly different concerning the period September 1977 – November 1979 and the complete observation period October 1973 – September 2002. Accordingly, the null hypothesis is confirmed at a significance level of 95 % ($P \geq 0.05$; two-tailed test; $n_1 = 348$; $n_2 = 27$; $U = 4870.5$). The difference of mean monthly precipitation at the Zagora station is neither significant at the 95 % level regarding the recharge period and the period October 1973 – September 2002 at a level of 5 % ($P \geq 0.05$; two-tailed test; $n_1 = 348$; $n_2 = 27$; $U = 5098$). Accordingly, the hydrometeorological input to the aquifer system in the period September 1977 – November 1979 does not significantly differ than that in the total observation period. Even if the results of the U-test failed the significance level, the mean monthly precipitation in the recharge period is 2.1 times higher than in the entire observation period, i.e. 11.4 mm versus 5.5 mm. Particularly, some mean monthly values of precipitation in autumn and winter times are extraordinary high (30.9 mm in January 1978, 86 mm in January 1979 and 134.9 mm in October 1979). Therefore, the increased precipitation can be assumed the main trigger for the observed overall groundwater level rise. This complies with further recent causal research results (Herczeg & Leaney, 2011). A precise threshold of effective precipitation could not be determined due to a lack of data concerning temporal and spatial resolution and less supplementary in-

formation. As a concluding result, it is assumed that precipitation within the catchment is the dominant trigger for groundwater recharge in relation to inflow from the upstream reservoir for the period September 1977 – November 1979. Intensive rainfall is supposed to lead to Hortonian overland flow, which converges in wadi beds and subsequently in the Wadi Drâa (Figure 6-12). A varying fraction of discharge can infiltrate along the wadi course leading to percolation and actual groundwater recharge. The precise proportion of indirect recharge resulting from rainfall cannot be quantified.

Figure 6-12: Hortonian overland flow converging in channels (left photo) and leading to wadi discharge (right photo) in the Feija northeasterly of Foum Zguid in spring 2005 (photos by A. Klose).

Another global but more pronounced groundwater level rise is observed between the years 1987 and 1992. The groundwater levels show an overall increase whereas the sharpest rise is observed between 1987 and 1989. The overall groundwater level rise is interrupted by interim lows in summer times (Figure 6-10). 15 observations are selected from the period October 1987 - March 1990 (30 months) for the same reasons as for the previous recharge period. They show rising groundwater levels by 0.36 to 12.97 m. Thereby, the mean value is 5.14 m whereas the median accounts for 6.05 m. These values exclude data from the Ktaoua oasis because the observations reveal a lack around March 1990. However, the two sites in Ktaoua show also an increase in groundwater levels by 2.16 to 4.66 m between October 1987 and August 1989.

Table 6-13: Representation of groundwater level data for the period October 1987 – March 1990 in relation to the Drâa aquifers.

Drâa aquifer (Oasis)	Number of data sets October 1987 – March 190
Mezguita	1
Tinzouline	2
Ternata	6
Fezouata	4
Ktaoua	non
Mhamid	2

The cause for groundwater recharge between October 1987 and March 1990 is an enhanced inflow from the upstream reservoir Mansour Eddabhi and increased precipitation within the MDC. Consequently, this period represents pronounced humid conditions. The comparison of this recharge period

with the entire observation time span (October 1973 – September 2002) reveals a pronounced increase in inflow from the reservoir Mansour Eddhabbi and a moderate increase in precipitation (Figure 6-13).

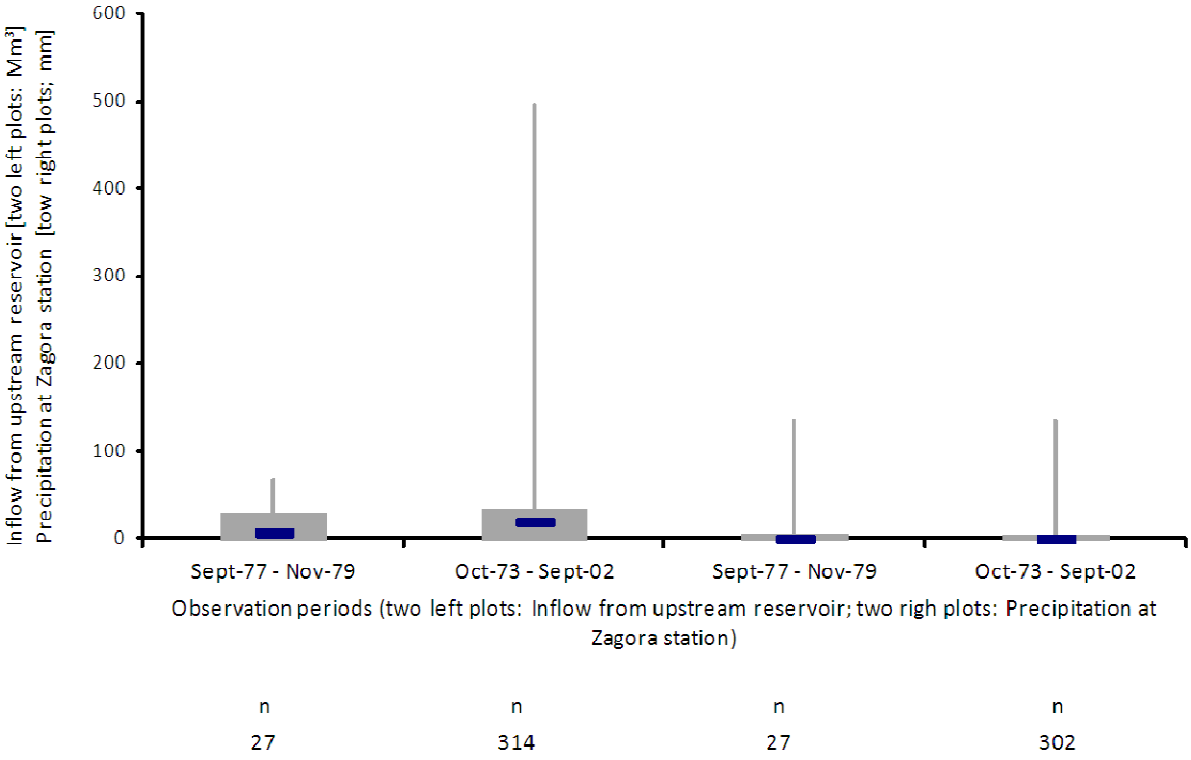

Figure 6-13: Box plot of mean monthly inflow from the reservoir Mansour Eddhabbi and mean monthly precipitation at Zagora station to compare the periods October 1987 - March 1990 and October 1973 – September 2001 (grey vertical lines display minima and maxima; grey boxes represent the 25 % to 75 % quantile range; blue horizontal lines portray the median values).

Mean monthly values of inflow and precipitation are compared for the periods October 1987 - March 1990 and October 1973 – September 2001. The mean value of inflow from the reservoir accounts for 76.2 Mm³ for October 1987 - March 1990 (median: 34.9 Mm³). By comparison, the mean value over the time span October 1973 – September 2002 amounts to 24.8 Mm³ (median: 19.1 Mm³). So, the inflow from the reservoir is three times higher during the recharge period October 1987 - March 1990 (Table 6-14). Thereby, the mean precipitation at the Zagora station within the MDC shows slightly increased values for this recharge period in comparison to the period October 1973 – September 2002. The mean value of precipitation accounts for 7.4 mm at the station Zagora (median: 1.81 mm), whereas the mean value over the period October 1973 – September 2002 amounts to 5.5 mm (median: 0.00 mm). Thus, mean monthly precipitation at the Zagora station is approximately 1.3 higher in the recharge period October 1987 - March 1990 (Table 6-14). Application of the Mann Whitney U-test verifies the difference between the mean values of monthly inflow from the reservoir Mansour Eddabhi to be highly significant (significance level = 99.9 %) concerning the period October 1987 – March 1990 and October 1973 – September 2002 ($P < 0.001$; two-tailed test; $n_1 = 348$; $n_2 = 30$; $U = 7895$). The difference between mean values of monthly precipitation within the catchment is tested to be significant at a 99 % level regarding the recharge period and the period October 1973 – September 2002 ($P < 0.01$; two-tailed test; $n_1 = 348$; $n_2 = 27$; $U = 6728$). Consequently, recharge in October 1987 - March 1990 is triggered by the combination of increased mean monthly inflow from the upstream reservoir and mean monthly precipitation. Thereby, inflow from the upstream reservoir is supposed to be the dominant component.

In conclusion, the combination of inflow from the upstream reservoir and precipitation within the catchment triggers global groundwater recharge in the period October 1987 - March 1990. Thereby, constantly high inflow rates from the reservoir Mansour Eddabhi are the main cause for groundwater level rise. Due to this, a varying fraction of discharge can infiltrate along the wadi course leading to actual groundwater recharge. The groundwater is not recharged continuously during this period. This is a hint on overprinting discharge mechanisms such as evapotranspiration and pumping. The discharge mechanisms remain unclear due to a lack of information as explained further below.

The comparison of the inflow conditions and the precipitation within the catchment reveal the variance in principal driving forces for global groundwater recharge in the MDC. That means that recharge in the Drâa aquifers can be predominantly depending on external conditions, i.e. precipitation within the Upper Drâa Catchment and afflux to the reservoir Mansour Eddabhi. But recharge can also be triggered by high monthly precipitation within the catchment. The precise ration between recharge from infiltration in the wadi bed in comparison to recharge from infiltration of irrigation water derived from the wadi bed remains unknown, due to temporal and spatial data scarcity. Furthermore, the proportional impact of indirect recharge resulting from rainfall cannot be regionally quantified (chapter 6.2.3).

Table 6-14: Mean monthly values of inflow from the reservoir Mansour Edddhabi and precipitation at Zagora station within the Middle Drâa Catchment for the periods September 1977 - November 1979 and October 1987 - March 1990 in comparison to the respective mean values for the period October 1973 - September 2002 including the significance level of difference between the samples (Mann Whitney U-test).

Period	Mean monthly inflow to wadi Drâa from reservoir Mansour Eddabhi [Mm³]	Significance of distinction between recharge period and entire record (Mann Whitney U-test)	Mean monthly precipitation at Zagora station [mm]	Significance of distinction between recharge period and entire record (Mann Whitney U-test)
Sept-1977 – Nov-1979	15.0	Not significant ($P \geq 0.05$; two-tailed test; $n_1 = 348$; $n_2 = 27$; $U = 4870.5$)	11.4	Not significant ($P \geq 0.05$; two-tailed test; $n_1 = 348$; $n_2 = 27$; $U = 5098$)
Oct-1987 – Mar-1990	37.3	Highly significant ($P < 0.001$; two-tailed test; $n_1 = 348$; $n_2 = 30$; $U = 7895$)	7.4	Significant ($P < 0.01$; two-tailed test; $n_1 = 348$; $n_2 = 27$; $U = 6728$)
Oct-1973 – Sept- 2002	24.8	Reference period	5.5	Reference period

The statistical characteristics of the two phases of recharge are compared to underline the difference in the recharge mechanisms. They can be compared because they are nearly of the same duration (27 and 30 months). The box plot of groundwater level rise displays a differentiation of the two recharge phases in range, variation and median. The recharge phase triggered by high precipitation within the catchment (September 1977 – November 1979) is characterized by smaller values of median, quantiles and range. Thereby, the range overlaps widely (Figure 6-14). So, the mean values of groundwater level rise do not differ significantly between the two recharge periods (Mann Whitney U-test: $P \geq 0.05$; two-tailed test; $n_1 = 16$; $n_2 = 15$; $U = 167$). Nevertheless, the two recharge phases differ apparently clear in values of median with 2.84 and 6.05 m (Figure 6-14). Against the background of the prior interpretation, the distinction in median values is taken as another proof that recharge only caused by precipitation within the catchment is less effective than in combination with enhanced inflow from the upstream reservoir depending on the absolute amount of water. Furthermore, other site specific influences of the groundwater level fluctuation (e.g. pumping) are very likely but remain unknown concerning nature and severity

of effect. These site specific influences are assumed to cause the overlapping range of the samples. Overall, the indications for interpretation of the described medium to long-term overall groundwater recharge mechanisms are coherent and robust. This is because the definition of attributes for classification is adapted to the temporal and spatial data resolution considering the lack of supplementary information. As an example, the location of sites tapping the Drâa aquifer is unambiguous and important to clearly detect recharge due to wadi bed infiltration after water releases from the upstream reservoir (Figure 6-9). Furthermore, the hypotheses of causalities are checked against comparable studies (chapter 3).

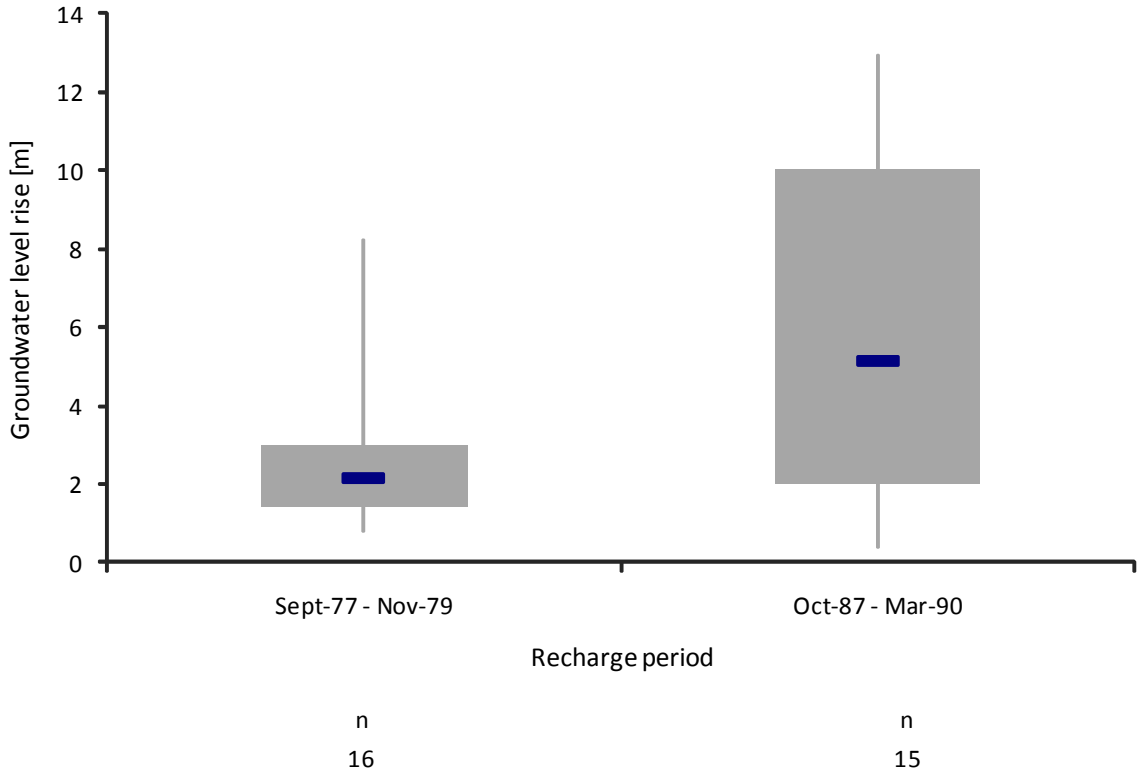

Figure 6-14: Box plot of groundwater level rise to compare the periods September 1977 – November 1979 and October 1987 - March 1990 (grey vertical lines display minima and maxima; grey boxes represent the 25 % to 75 % quantile range; blue horizontal lines portray the median values).

Regarding to discharge, decreasing groundwater levels are the result of reduced inflow from the reservoir Mansour Eddabhi and precipitation within the catchment (Zagora station). In the period January 1983 – March 1985 (27 month) the mean monthly inflow from the upstream reservoir is 3.2 Mm^3. In comparison to this, the mean monthly inflow amounts to 24.8 Mm^3 for October 1973 – September 2002, i.e. 7.7 times more than in the discharge period. Mean monthly precipitation in this period accounts for 3.8 mm. Mean monthly precipitation in October 1973 – September 2002 is 5.5 mm, i.e. 1.5 times more than in the discharge period of January 1983 – March 1985. The difference between mean values of monthly inflows from upstream reservoir is highly significant (significance level = 99.9 %) concerning the discharge period January 1983 – March 1985 and the entire record of October 1973 – September 2002 based on the Mann Whitney U-test ($P < 0.001$; two-tailed test; $n_1 = 348$; $n_2 = 27$; $U = 6971.5$). Mean values of monthly precipitation at Zagora station do not differ significantly at a 95 % level for the same periods based on the Mann Whitney U-test ($P > 0.05$; two-tailed test; $n_1 = 348$; $n_2 = 27$; $U = 4848$). So, reduced mean monthly inflow from the upstream reservoir represents the domi-

nant cause for falling groundwater level. Furthermore, it is main trigger for medium to long-term groundwater level fluctuation considering additionally the analysis of groundwater recharge periods above. As a summarizing result, climate variations have a distinct impact on groundwater resources of the Drâa aquifers.

Table 6-15: Mean monthly values of inflow from the reservoir Mansour Edddhabi and precipitation at Zagora station within the Middle Drâa Catchment for the period January 1983 – March 1985 in comparison to the respective mean values for the period October 1973 - September 2002 including the significance level of difference between the samples (Mann Whitney U-test).

Period	Mean monthly inflow to wadi Drâa from reservoir Mansour Eddabhi [Mm³]	Significance of distinction between discharge period and entire record (Mann Whitney U-test)	Mean monthly precipitation at Zagora station [mm]	Significance of distinction between discharge period and entire record (Mann Whitney U-test)
Jan-1983 – Mar-1985	3.2	Highly significant ($P < 0.001$; two-tailed test; $n_1 = 348$; $n_2 = 30$; $U = 7895$)	3.8	Not significant ($P > 0.05$; two-tailed test; $n_1 = 48$; $n_2 = 27$; $U = 6728$)
Oct-1973 – Sept- 2002	24.8	Reference period	5.5	Reference period

Pumping is supposed to be the dominant cause for short-term groundwater level fluctuations. Irrigation wells are numerous and show high pumping rates (4 to 6 L/sec; see Breuer, 2007; Haaken, 2008; Stumpf, 2008). This, among further reasons, is because of low irrigation efficiencies in relation to the commonly applied flood irrigation. Even if the hydraulic conductivity is high (Table 6-3; chapter 6.1.4), irrigation wells may appear as pumping centers leading to overlapping local cones of drawdown. Pumping can induce also seasonal or even long-term effects in aquifer response at the local and sub-regional scale depending on exploitation rate, aquifer properties, climatic situation and groundwater recharge. Furthermore, the number of motor pumps for irrigation has increased since the 1970-ties. This development towards a more intensive and individualized groundwater use strategy is comparable to land use change resulting in a long-term impact on the groundwater level fluctuations (Ouhajou, 1996; DRH, 2001; Healy & Cook, 2002).

Crop rotation is expected to influence the seasonal groundwater fluctuations via evapotranspiration effects. Thereby, varying irrigation schemes are supposed to have the largest impact.

The observed aquifer response can hardly be allocated to long-term, seasonal or short-term processes precisely because superposing processes cannot be distinguished. In terms of groundwater recharge, the importance of the stream flow – aquifer interaction is evident beside intensive rainfall within the catchment. Thus, the replenishment of the Drâa aquifers depends on the inflow from the Upper Drâa Catchment and thus also on the management of the reservoir Mansour Eddabhi. In terms of discharge, the arid climate conditions play the major role in combination to relatively small aquifer potential and intensive groundwater use for irrigation within the oases.

The influence of further factors has to be assumed such as recharge from (re-)infiltrating irrigation water at the field plot. But the effect of those further influences cannot directly be proofed due to the incomplete observations. The interpretation of the discontinuous groundwater level data represents a qualitative analysis completed by statistical proofs. The data gaps (temporal, spatial and regarding supplementary information, e.g. pumping) bias the signal of aquifer response to an uncertain part. Further, uncertainties can appear due to the design and casing of the observation points for which the function and

hydraulic connection remains unchecked. Thus, they remain to be further checked causally. Based on this, further integrated observations of hydro-meteorological parameters and data on groundwater withdrawal are required. Further uncertainties arise due to the lack of information on the measurement procedure. The precise measuring point and eventually height of measuring point above ground remain mostly unknown, but are assumed to be the same at each site for all measurements.

The differentiation between the groundwater level data for the Drâa aquifers reveals diversification in the dynamic of aquifer response. The most dynamic fluctuations are found at Ternata selected by-eye. In all other Drâa aquifers the groundwater level response appears relatively dammed fluctuating from site to site around different mean levels. The above mentioned periods of rising and falling groundwater levels are documented at each aquifer and site.

The aquifer response is a result of various mechanisms representing both natural and human origin. The specific yield as indicator for storage capacity is assumed to have naturally an effect on groundwater level fluctuations. Generally, highly dynamical aquifer response would reflect low specific yield values and vice versa as hydraulic conductivity and potential aquifer volume remain constant. Thus, different mean specific yield values cause distinct groundwater level response in relation to the aquifer unit. Therefore, the overall groundwater level rise from the recharge periods in September 1977 – November 1979 and October 1987 – March 1990 are compared to mean values of specific yield for the Drâa aquifers individually (chapter 6.1.4; Figure 6-15; Figure 6-16). Thereby, the exemplary sites are used which are already mentioned above. The comparison of both recharge periods prove the general hypothesis of dammed aquifer response due to high mean specific yield values concerning Mezguita and Tinzouline. The reverse effect is found for Ternata. Furthermore, a large range in specific yield determines a large range in groundwater level fluctuation. Intermediate groundwater level dynamics are found due to intermediate specific yield values in Mhamid. In Fezouata, specific yield appears not to be the dominant determinant for the groundwater level dynamic. Enhanced lateral groundwater inflow from the Feija aquifers in combination to the specific aquifer volume may be a reason. Distinct groundwater recharge response caused by different distribution of the controlled discharge in the wadi Drâa is assumed to play a minor role because the discharge period shows also dammed aquifer response. Overall, the explanations for the distinct aquifer response in Fezouata remain speculative due to sparse data availability (temporal, spatially and additional information). Data from Ktaoua are not available for this comparison.

The comparison of groundwater level rise and mean values of specific yield hints on the relationship between aquifer response and storage term. It cannot provide quantitative evidence but allows robust statements about the dominance of the influence of specific yield. A deeper look on the dynamic behavior of groundwater levels would not be appropriate due to lacking data concerning the temporal and spatial resolution and additional information (e.g. groundwater use). Without doubt, other factors have an effect and require further surveys and monitoring.

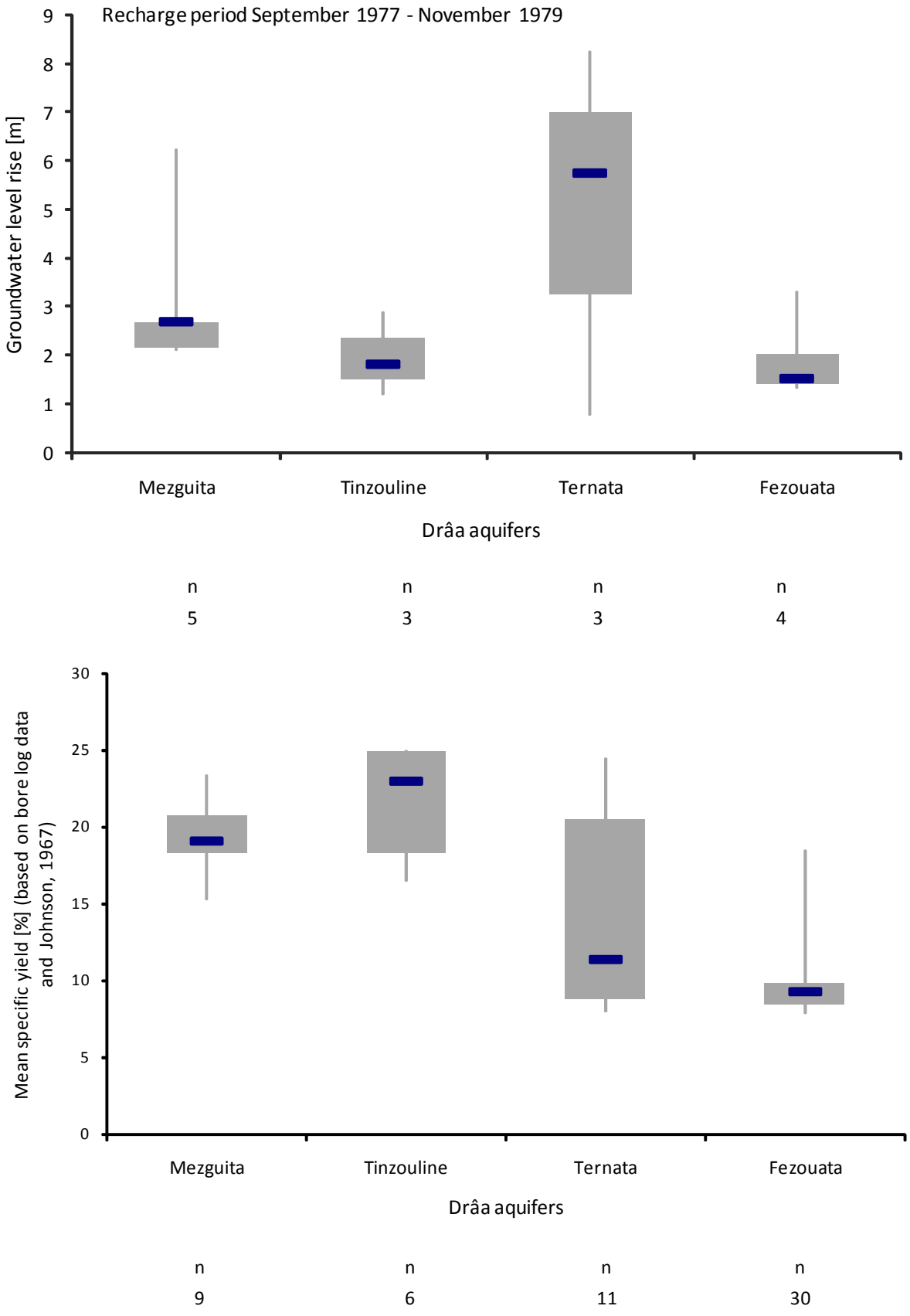

Figure 6-15: Comparison of groundwater level rise in the period September 1977 – November 1979 and mean values of specific yield (based on bore log data and Johnson, 1967; grey vertical lines display minima and maxima; grey boxes represent the 25 % to 75 % quantile range; blue horizontal lines portray the median values).

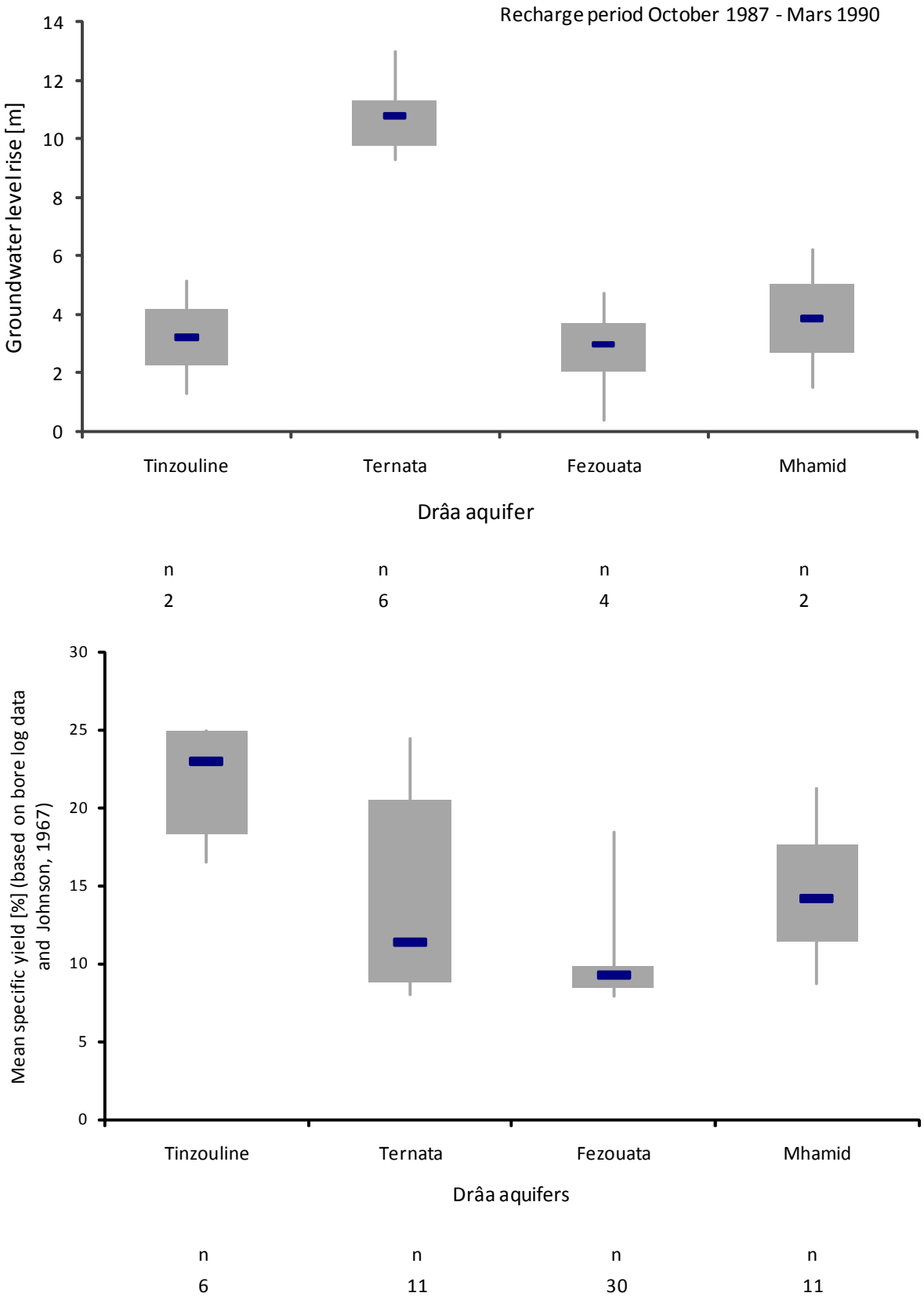

Figure 6-16: Comparison of groundwater level rise in the period October 1987 – March 1990 and mean values of specific yield (based on bore log data and Johnson, 1967; grey vertical lines display minima and maxima; grey boxes represent the 25 % to 75 % quantile range; blue horizontal lines portray the median values).

The identified relation between the dynamic of groundwater level response and specific yield testifies in turn the preferable application of own estimations of specific yield (based on bore log data and Johnson, 1967) in distinction to literature values (Chamayou, 1966; ORMVAO, 1995).

6.2.2 Main flow paths

The groundwater flow in the six Drâa aquifers is the main groundwater drain (chapter 6.1.3). Thereby, the agricultural water consumption and evapotranspiration in the Drâa oasis represents main groundwater discharge (chapter 7). Groundwater flow systems develop at different spatiotemporal scales around the Drâa aquifers depending on the aquifer setting and varying recharge and discharge conditions.

The Drâa aquifers receive continuous inflow to a minor amount from the subjacent Fractured aquitards representing a regional groundwater flow system (Mountain Block Recharge; see Wilson & Guan, 2004). Generally, the fractured hard rock terrain with a thin soil cover provides a subordinate recharge zone (chapter 6.2.4; Klose, A., 2009; Kutsch, 2008; Külls, 2000; Wilson & Guan, 2004). Based on estimations of groundwater residence time, the contribution from the Fractured aquitards towards the Drâa aquifers is made up of water older than 50 years hinting on very slow flow, mostly not participating the current hydrological cycle (Cappy, 2006; withdrawn from an exemplary Tritium dating, Annex XXX). The tributary aquifers provide temporal variably inflow to the Drâa aquifers by forming intermediate to local groundwater flow systems (see Toth, 1995; chapter 6.1.3 & 6.3.3). At the same time, the Tributary aquifers can continuously receive minor inflow from the subjacent Fractured aquitards (see chapter 6.3.5). The main current actual recharge is assumed to develop as indirect recharge triggered by intensive precipitation events mainly contributing to the Tributary aquifers (chapter 6.1.3, 6.2.3 & 6.2.4). The Basin aquifers may form partly individual or mediating groundwater reservoirs between the Fractured aquitards and the Drâa aquifers. They differ from the Tributary aquifers in their transit function due to longer pathways and larger reservoir capacity (chapter 6.1.3, 6.3.5). The Feija aquifers receive continuous inflow of water older than 50 years from the adjacent aquitard system (Cappy, 2006; chapter 6.3; Table 6-16; chapters 6.2.2.3, 6.2.2.5, 6.2.2.6, 6.3.5). Furthermore, they are replenished by localized and indirect recharge such as colluvial and wadi bed recharge (chapter 6.2.4).

In agreement to this, Chamayou (1966) states inflow towards the alluvial aquifers (in this study: Tibutary, Basin and Drâa aquifers) from the subjacent hard rock aquitards (in this study: Fractured aquitards) verified by observations at hill foots in the Bou-Azzer region. Chamayou (1966) distinguishes further on flow systems in the quartzitic sandstone – siltstone series of the Tabanit and the Bani Group:

- Advective flow at the wadi bank (local)
- Flow along fault lines (local to regional)
- Preferential flow at the wadi bank (e.g. fault lines; local)

In the present study, the “advective flow at the wadi bank” is interpreted as local groundwater flow system connecting the Tributary aquifers and the Fractured aquitards. The “flow along fault lines” represents the main path in the regional flow system. Chamayou (1966) assumes groundwater stratification concerning recharge age due to the monoclinic structure of the southern flank of the Anti-Atlas, which could not be verified by groundwater level analyses. The “preferential flow at the wadi bank” develops in the loose aquifer material and in the fractured media. It represents the rapid flow component of the local groundwater system. Furthermore, it is the most rapid connection between local flow system at the wadi banks and the regional groundwater system within the Fractured aquitards. So, upwelling of

groundwater from deeper zones is possible (chapter 6.3.3.5). By contrast, fault lines in the Fractured aquitards are closed at a certain depth and can be filled by calcite, quartz or clay (chapter 6.1.2). The most productive flow paths appear to be fault zones. The groundwater flow in the carbonate rock aquifers of Paleozoic age remains uninvestigated. Chamayou (1966) states explicitly that the Basin aquifers receive inflow from the Fractured aquitards, which is verified in this study (chapter 6.3.3.3).

Selective sites from the fragmentary groundwater level data (October 1973 – September 2002) support the hypothesis of continuous groundwater inflow from the adjacent porous aquifers and Fractured aquitards towards the Drâa aquifers at several sites (Table 6-16).

Supplementary knowledge on groundwater flow paths is gained from the analyses of own groundwater level observations during field campaigns. Groundwater levels were manually measured at the same key dates of groundwater sampling in spring 2005, autumn 2005 and spring 2007 (Figure 2-2). In conclusion, Figure 6-17 depicts an overview of the main groundwater flow paths.

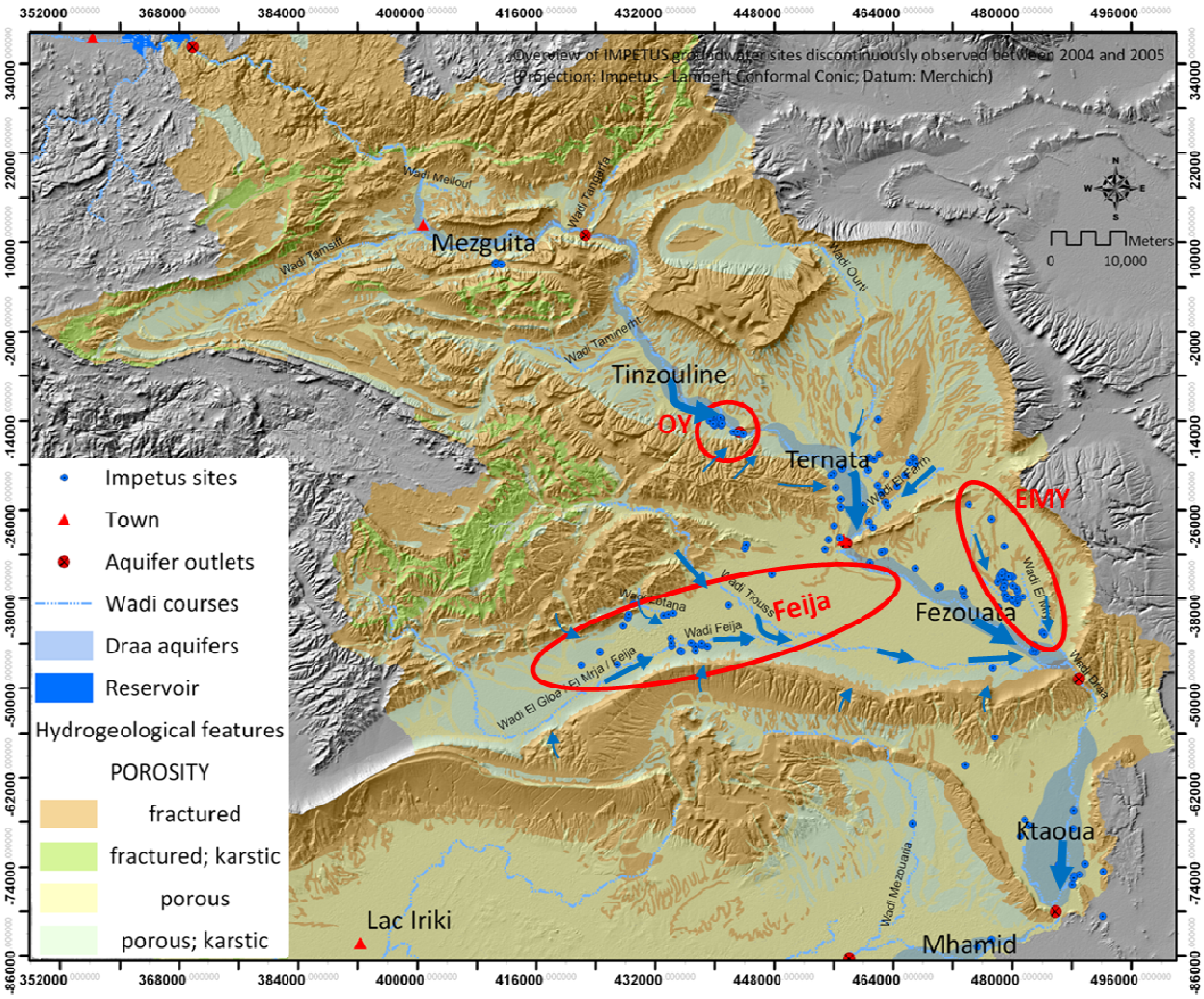

Figure 6-17: Overview of the main groundwater flow paths: bold blue arrows: main drain and thin blue arrows: minor lateral flow to the Drâa aquifers including the test areas (see labeling and red ovals: Ternata and Fezouata, Feija, OY (Ouled Yaoub) and EMY (Plain of El Miyit).

6.2.2.1 Hydraulic gradients towards Fezouata

Two hydraulic gradients are determined towards the Fezouata aquifer at different key dates (Table 6-16). One of these verifies inflow from the Feija de Zagora via underflow of the wadi Feija in May 1978. The hydraulic gradients along the downstream section of wadi Feija (148/73 – 892/73) is smooth accounting for 1.1 ‰. Contrarily, Chamayou (1966) describes steep hydraulic gradients directed from the Feijas towards the Drâa aquifers. A reason for the divergence in this case may be the backwater at the lower end of Fezouata in front of the narrow natural outlet (Foum Takkat) through the Jbel Bani (Figure 6-6). The hydrogeological properties in the Feija aquifer can also have an influence as the alluvial deposits are made up of slightly cemented conglomerate intercalated by rigid conglomerate. Especially the hydraulic conductivity of the slightly cemented conglomerates can be enhanced due to secondary porosity caused by solution of cement. In addition, the thickness of the alluvial aquifers amount to 14.5 m so that the aquifer properties may promote a generally smooth hydraulic gradient in this zone. Further proofs are not available. The analysis of change in hydraulic gradients due to distinct groundwater recharge remains unknown due to lacking observations.

The hydraulic gradient from the plain of El Miyit towards the middle part of the Fezouata aquifer accounts for 1.6 ‰ in December 1984. Thus, inflow from the plain of El Miyit towards the Drâa aquifer is verified. December 1984 is within a distinct overall discharge period (Figure 6-10; chapter 6.2.1) and the inflow gradient is expected to be steep because groundwater discharge in the main aquifers is enhanced due to water use and evapotranspiration. Thereby, the inflow from the regional groundwater system of adjacent hard rock aquitards is expected to remain constant even if no recharge due to precipitation is observed. The general slope of land surface around is smooth (around 2.5 ‰) only interrupted by slightly incised secondary wadis. As an unevaluated hypothesis, the hydraulic gradient is probably accordingly smooth without considering the aquifer structure in detail. Further hypothesis concerning the hydrodynamic behavior at this site would be invalid due to a lack of observations. Moreover, information on the site outside the Fezouata oasis is scarce.

Table 6-16: Hydraulic gradients between selected sites portraying inflow from the hard rock aquitard system towards the Drâa aquifers of Fezouata observed at key dates.

Key date	Site label (outside - inside Drâa aquifer)	Groundwater level outside [m asl]	Groundwater level inside [m asl]	Groundwater level difference [m]	Distance between sites [m]	Hydraulic gradient [‰]	Setting
May-78	148/73 – 882/73	664.57	656.44	8.13	7580	1.1	Inflow as underflow of wadi Feija
Dec-84	1069/73 – 136/73	678.40	675.85	2.55	1580	1.6	Inflow from plain of El Miyit

The backwater in front of the hydraulic barrier at the downstream end of the Fezouata aquifer is proven by inverted gradients between the downstream zone of the El Miyit plain and the eastern bank of the wadi Drâa near Foum Takkat (Figure 6-6; see also chapter 6.2.2.4). Therefore, at five key dates the "backwater gradients" are evaluated. The values of inverted hydraulic gradients are very low ranging between 0.2 and 0.9 ‰ (Table 6-17). The first two key dates are within the overall recharge period of 1977 – 1979 (Figure 6-10) revealing the lowest values of inverted hydraulic gradients. This can be due to a comparably enhanced inflow from the adjacent El Miyit plain caused by groundwater recharge triggered by extraordinary high monthly rainfall in this area (23 mm in August 1978, 86 mm in January 1979 and 135 mm in October 1979 observed at Zagora station; see chapter 6.2.1). Chamayou (1996) presents

similar conclusions concerning enhanced lateral inflow from the tributary aquifers towards the Drâa aquifers. The highest values of inverted hydraulic gradients are found in the period June 1980 – July 1981 after the global recharge period. This may be due to obviously high monthly inflow from the upstream reservoir resulting in enhanced actual recharge in the Drâa aquifers. This interpretation is underlined by the comparison between mean monthly inflows from the upstream reservoir of the period June 1980 – July 1981 with the mean monthly inflow during the entire observation period September 1973 – October 2002. The Mann Whitney U-test confirmed a significant difference between the mean monthly inflows from the upstream reservoir concerning the periods June 1980 – July 1981 and September 1973 – October 2002 at a level of 99 % ($P < 0.01$; two-tailed test; $n_1 = 348$; $n_2 = 14$; $U = 3516$). The same statistical test for mean monthly precipitation at Zagora station reveal that the samples of the periods June 1980 – July 1981 and September 1973 – October 2002 are not significantly different at a level of 95 % ($P > 0.05$; two-tailed test; $n_1 = 348$; $n_2 = 14$; $U = 2468$). Consequently, the inflow from the reservoir Mansour Eddabhi is once again proven to play a dominant role for the groundwater dynamic within the Drâa aquifers.

Table 6-17: Hydraulic gradients of backwater in front of the hydraulic barrier at downstream end of the Fezouata aquifer between the downstream zone of the El Miyit plain (site label 906/73) and the eastern bank of the wadi Drâa near Foum Takkat (site label: 895/73) at key dates.

Key date	Groundwater level 906/73 [m asl]	Groundwater level 895/73 [m asl]	Groundwater level difference [m]	Distance between sites [m]	Hydraulic gradient [‰]
Dec-78	653.95	655.04	1.09	3800	-0.4
Nov-79	645.94	655.42	0.48	3800	-0.2
Jul-80	654.80	657.60	2.80	3800	-0.9
Jun-81	655.10	657.95	2.85	3800	-0.9
Nov-81	658.00	661.00	1.85	3800	-0.6

The hypothesis of Chamayou (1966) that the Drâa aquifer looses water at the respective downstream hydraulic barrier to subjacent aquitards remains unevaluated due to a lack of hydrogeological data and groundwater observations.

6.2.2.2 Hydraulic gradients towards Ktaoua

Hydraulic gradients towards the Ktaoua aquifer are estimated for one lineament between the Moroccan site 435/82 (outside Drâa aquifer) and 516/82 (inside Drâa aquifer) at six key dates (Table 6-18). The hydraulic gradient varies slightly around the value of 1.3 ‰ and testifies generally inflow from the Feija aquifer towards the Drâa aquifer. Thereby, the land surface dips evenly with a gradient of 1.7 ‰. Thus, surface morphology is assumed to have varying influence on groundwater dynamics along the flow path. Influences of aquifer structure remains unchecked due to lacking information.

Table 6-18: Hydraulic gradients towards the Ktaoua aquifer between the western feija (site label 435/83) and the western bank of the wadi Drâa (site label: 516/82) at six key dates.

Key date	Groundwater level 435/82 [m asl]	Groundwater level 516/82 [m asl]	Groundwater level difference [m]	Distance between sites [m]	Hydraulic gradient [‰]
Sept-77	595.58	586.50	9.08	7530	1.2
Nov-79	597.04	587.65	9.39	7530	1.3
Jun-81	598.57	589.87	8.70	7530	1.2
Nov-81	598.66	588.72	9.94	7530	1.3
Aug-82	598.70	588.11	10.59	7530	1.4
Dec-82	598.37	588.78	9.59	7530	1.3

Referring to the change of inflow the variation in hydraulic gradients is not meaningful. A deeper look on the groundwater level fluctuation for the individual sites gives hints on different aquifer response concerning the feija and the Drâa aquifer. The box plot of groundwater level change at the end points of the observed hydraulic gradient between the feija (435/82) and the Drâa aquifer of Ktaoua (516/82) shows wider range of fluctuation within the Drâa aquifer as in the Feija aquifer (Figure 6-18). Thereby, the median values of groundwater level changes differ distinctively by 0.58 m. Thus, they appear to portray different trends in groundwater level fluctuation. This may be due to distinct aquifer responses on differing recharge and discharge mechanisms.

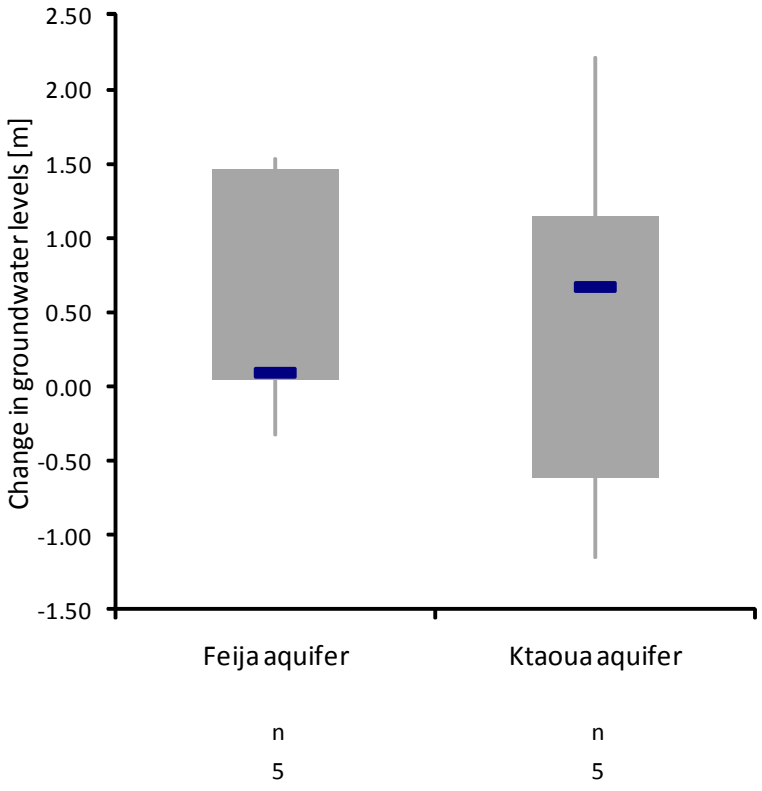

Figure 6-18: Box plot of groundwater level change at the end points of the observed hydraulic gradient between the feija (435/82) and the Drâa aquifer (516/82) of Ktaoua for five observations between September 1977 and December 1982 (grey vertical lines display minima and maxima; grey boxes represent the 25 % to 75 % quantile range; blue horizontal lines portray the median values).

Groundwater levels rise increasingly in the Drâa aquifer from September 1977 to November 1979 and finally June 1981. The same is observed for the Feija aquifer whereas the rise in groundwater level remains constant. Thus, overall recharge is evident in this period which is verified by the analysis of hydro-meteorological input (see Figure 6-10; chapter 6.2.1). Referring to the following three observations, the groundwater level response varies comparing the Feija aquifer and the Drâa aquifer. In the Drâa aquifer the groundwater level falls from June 1981 to November 1981. This can be explained by seasonally enhanced groundwater discharge. The same applies to the fallen groundwater level in August 1982. Furthermore, the overview of observations in the Drâa aquifers shows overall stagnant groundwater levels in 1981 and slightly falling levels from 1982 on. Thus, a global groundwater discharge is obvious. Contrarily, the western Feija aquifer of Ktaoua shows slightly rising groundwater levels from June 1981 to November 1981 and further on to August 1982. Groundwater levels in the two aquifer compartments show diverging trends from August 1982 to December 1982. Therefore, the Drâa aquifer reveals a rising groundwater level again whereas the Feija aquifer is discharged (Figure 6-19).

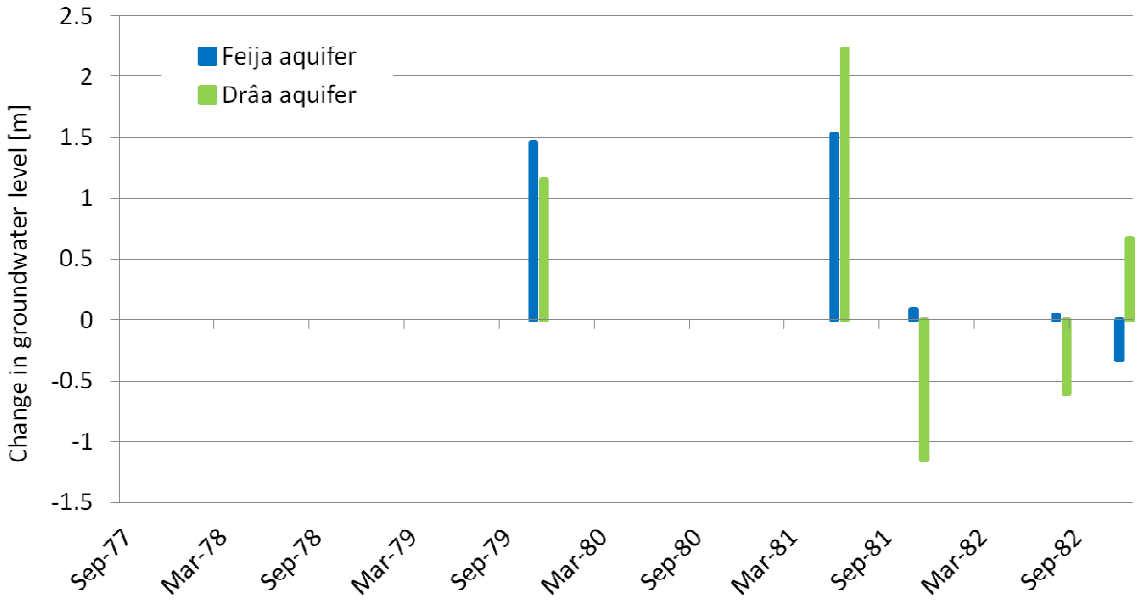

Figure 6-19: Groundwater level change data at the end points of the observed hydraulic gradient between the feija (435/82) and the Drâa aquifer (516/82) of Ktaoua for five observations between September 1977 and December 1982.

Consequently, the response of the Feija aquifer on hydro-meteorologically dry conditions is dammed and delayed in comparison to the Drâa aquifer. This is a clear hint on the buffer effect of the Feija aquifers with regard to the inflow to the Drâa aquifer. The slow circulation in the regional groundwater flow system of the hard rock aquitards is assumed to contribute constantly to the Feija aquifer supporting the delay in discharge to a small proportion due to low specific yield and hydraulic conductivity. In the Drâa aquifer a local groundwater flow system is characterized by relatively quick and more dynamic recharge triggered by wadi bed infiltration. Seasonally enhanced pumping and evapotranspiration losses must influence the similarly dynamic discharge. In conclusion, human activity particularly irrigation enhances the dynamic in the response of the Drâa aquifer whereas a constant inflow from the Feija aquifer is verified.

Based on the derived hydraulic gradients, a rough estimation of monthly western groundwater inflow towards the Ktaoua aquifer is carried out using the Darcy equation. The hydraulic gradient is therefore roughly assumed to be constant over one month. The front of the flow section is approximated based on own field observations and GIS techniques. A value for transmissivity is adopted from Aoubouazza & El Meknassi (1996) accounting for $3 \cdot 10^{-4}$ m²/s. The influence of spatially varying aquifer properties is not possible because according data lacks.

Accordingly, the approximate monthly western inflow ranges between 17,968 and 21,872 m³ (Table 6-19). The variation is low considering the hydro-meteorological conditions approximately. This clarifies the influence if the assumed slow circulation in the regional groundwater flow system of the hard rock aquitards contributing quasi-constantly to the groundwater flow towards the Drâa aquifers. An approximate mean annual value of western inflow is 239,933 m³ considering the discontinuous monthly values between September 1977 and December 1982.

Table 6-19: Approximate estimation of monthly groundwater inflow from the western Feija aquifer towards the Ktaoua aquifer based on discontinuous Moroccan groundwater level and using a transmissivity of $1 \cdot 10^{-4}$ m²/s adopted from Aoubouazza & El Meknassi (1996).

Date	Hydro-meteorological conditions	Hydraulic gradient [‰]	Front of flow section [m]	Approximate monthly inflow [m³/month]
Sept-77	humid	1.2	20,000	18,753
Nov-79	humid	1.2	20,000	19,394
Jun-81	intermediate	1.2	20,000	17,968
Nov-81	dry	1.3	20,000	20,529
Aug-82	dry	1.4	20,000	21,872
Dec-82	dry	1.3	20,000	19,807

6.2.2.3 Groundwater flow paths in the Ternata and Fezouata aquifer in April 2005

The Ternata aquifer is the third unit within the aquifer chain along the wadi Drâa. It is separated to the downstream Fezouata aquifer by the Anti Altas Major Fault (AAMF), locally called Graben of Zagora (chapter 2.3; 6.1). The Ternata aquifer spreads as bent oblong body between the Foum Azlag at the upstream end and the sill of Zagora (Graben of Zagora) at the downstream end. The lower part adjoining the Graben of Zagora appears to be widened striking in N-S direction. Wadi Ourti in the Northeast drains into this lower part of Ternata. Wadi El Farrh and wadi Ben Dlala go to lower eastern part of Ternata (Figure 6-20). Own field observations of the aquifer structure exposed in dug wells give hints that the alluvial deposits beneath wadi El Farrh and wadi Ben Dlala form relatively thick tributary aquifers. Therefore, the thickness of alluvial deposits exceeds 8 m in all observed wells. Further smaller wadis contributing to Ternata are not explicitly mentioned here.

Manually measured groundwater levels provide information on groundwater flow paths in April 2005 based on a groundwater contour map (Figure 6-20). April 2005 represents a phase shortly after a water release from the upstream reservoir Mansour Eddabhi. The prior water release of 35 Mm³ is documented at the reservoir outlet between 3. - 20. March 2005. Thus, this period is a phase of potential groundwater recharge to the Drâa aquifers due to wadi bed infiltration. The groundwater level observations cannot provide detailed information on the recharge effect and process because spatial resolution is too sparse for that. The groundwater level contours reveal the main groundwater flow path approximately beneath the wadi Drâa. Groundwater flow in the lower part of Ternata follows a hydraulic gradient of

around 2.6 ‰. Thereby, the hydraulic gradients in the middle part of the Ternata aquifers amount to 4 ‰ in comparison to 1.9 and 2.4 ‰ at its downstream end. The moderate hydraulic gradient in the lower part of Ternata is assumed to be caused by a backwater effect in front of the “sill of Zagora” which means the Graben of Zagora and its inverted relief at Jbel Zagora. Therefore, the groundwater path is narrowed resulting in a backwater in combination with reduced aquifer thickness at the sill of Zagora (chapter 6.1.3). Relatively low values of depth to groundwater and an almost permanent effluent seepage in the wadi bed of the Drâa in front of the “sill of Zagora” support the hypothesis of backwater (chapter 6.3; see also Chamayou, 1966). The groundwater level contours of the aquifer of wadi Ourti show a hydraulic gradient of around 7.3 ‰ towards the Drâa aquifer. Thereby, the relatively steep relief of the wadi bed appears to influence the hydraulic gradients. The underflow of wadi El Farrh and wadi Ben Dlala follow gradients of around 3.0 ‰. This comparably smooth hydraulic gradient may be due to the relatively thick alluvial deposits as mentioned above.

In conclusion, the hydraulic gradients within the lower part of the Ternata aquifer provide further evidence for backwater due to narrowing of the flow section at the “sill of Zagora”. Easterly groundwater inflow towards the Ternata aquifer is traced by hydraulic gradients beneath the main tributaries (Ourti, Ben Dlala and El Farrh). Even if groundwater recharge due to infiltration in the wadi Drâa is assumed to result in a flow component towards the rim of the Drâa aquifer in March to April 2005, Ternata receives inflow from the eastern tributary aquifers. Consequently, a constant lateral groundwater inflow towards the Drâa aquifer of Ternata is assumed.

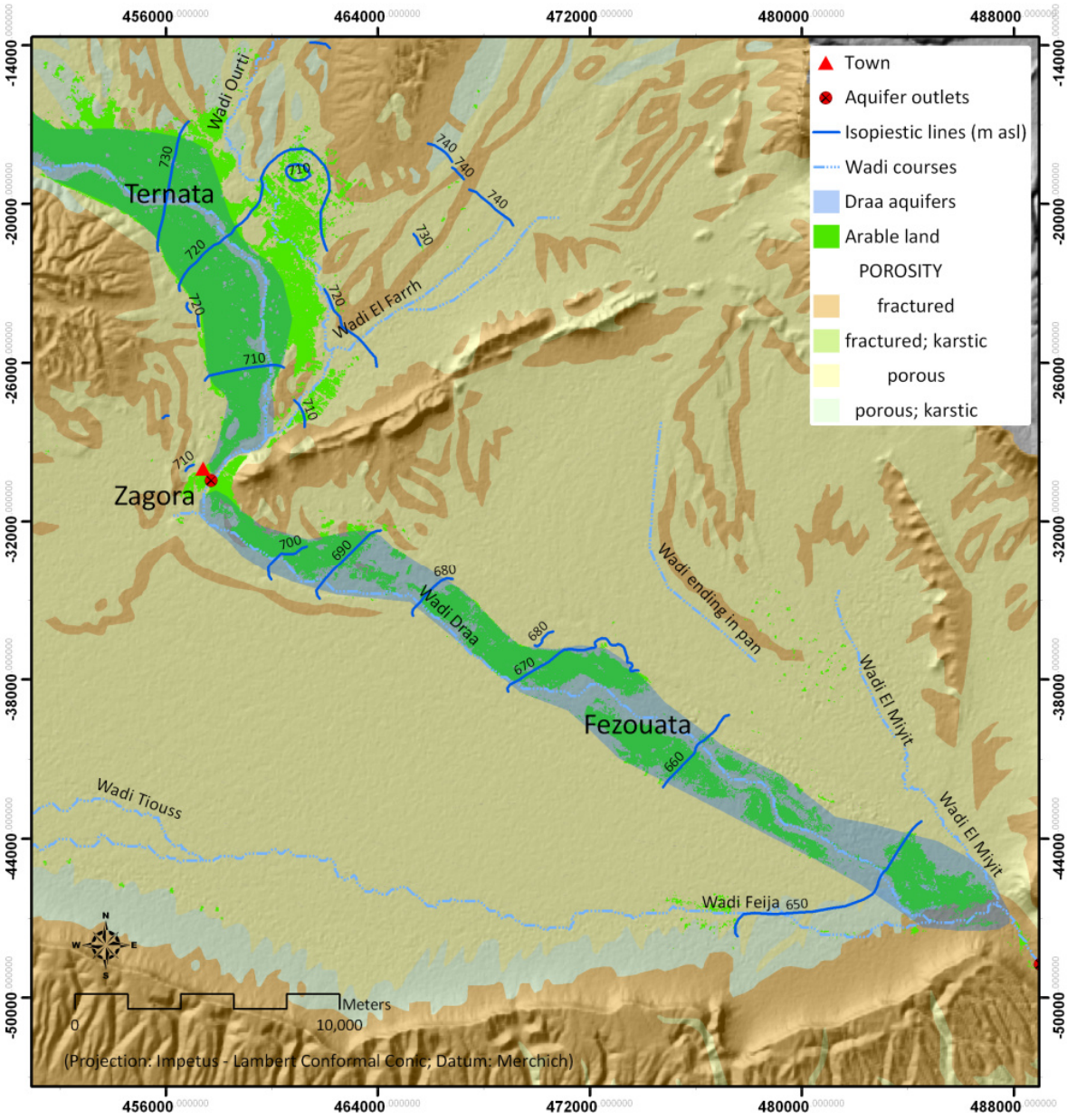

Figure 6-20: Map of manually designed groundwater level contours in the Ternata and Fezouata oasis showing a cone depression in the North-East of Ternata (based on manually observed groundwater levels at 37 wells in April 2005).

Based on the observed hydraulic gradients, a rough estimation of respective lateral inflow towards the Drâa aquifers is carried out using the Darcy equation. Thereby, the flow sections are approximated based on own field observations and GIS techniques. The height of the flow section is estimated based on bore log information and the mean value of available groundwater level data in April 2005. Thereby, the weathered fringe of the substratum is included accounting for 5.5 m (chapter 6.1.4). So, the saturated thickness at the flow section is assumed 5 m beneath wadi Ourti and 7.5 m beneath wadi Ben Dlala and El Farrh. Values for hydraulic conductivity are compiled from literature and own spot tests of well recovery after pumping. Therefore, the Darcy estimations are based on lumped minimum and maximum values of hydraulic conductivity for the secondary alluvial aquifers:

- Lumped minimum value of hydraulic conductivity: $1 \cdot 10^{-4}$ m/s
- Lumped maximum value of hydraulic conductivity: $1 \cdot 10^{-3}$ m/s

Accordingly, a reasonable range of results is covered at the observed sites. The resulting inflow from the eastern tributary aquifers varies throughout one order of magnitude due to the applied range of hydraulic conductivity. Approximate annual inflow ranges between 150,742 and 1,507,421 m³ assuming the observed hydraulic gradients to be constant over one year. The approximate mean value of eastern underflow is 829,081 m³ (Table 6-20).

Table 6-20: Approximate estimation of annual inflow from the main tributary aquifers in the East (Ourti, Ben Dlala and El Farrh) towards the Ternata aquifer based on groundwater level observations in April 2005 and using lumped minimum and maximum values of hydraulic conductivity ($1 \cdot 10^{-4}$ m/s and $1 \cdot 10^{-3}$ m/s).

Upstream aquifer	Hydraulic gradient [‰]	Flow section [m²]	Approximate minimum DARCY flow [m³/yr]	Approximate maximum DARCY flow [m³/yr]	Approximate mean DARCY flow [m³/yr]
Ourti aquifer (tributary)	7.3	1,000	23,021	230,213	126,617
Ben Dlala aquifer (tributary)	3.0	6,000	56,765	567,648	312,206
El Farrh aquifer (tributary)	3.0	7,500	70,956	709,560	390,258
Sum of eastern tributary underflow			150,742	1,507,421	829,081

These values exclude direct inflow from the subjacent fractured hard rock aquitard towards the Ternata aquifer. Consequently, the total inflow from the East towards the Ternata aquifer must be slightly greater. The inflow from the subjacent aquitard remains unknown due to lacking data. The estimation of inflow from the eastern tributary aquifers towards Ternata aquifer is not temporally representative because the observations only reveal a snapshot. Furthermore, the hydraulic gradients observed at key dates are taken to estimate annual groundwater flow approximately. Despite this bias, the present rough estimations provide an assessment of the order of magnitude concerning the underflow of tributaries in 2005 (Table 6-20). Furthermore, the Darcy flow assessment provides measures for approximate comparison with existing estimations of lateral groundwater inflow (Chamayou, 1966). Accordingly, Chamayou (1966) gives a longtime average value of 2.2 Mm³ for the lateral annual groundwater inflow towards Ternata aquifer based on the assessment of groundwater recharge by wadi bed infiltration and areal precipitation. Own estimations of around 0.8 Mm³ for 2005 are not directly comparable with the results of Chamayou (1966) because the western inflow remains uninvestigated in the present study. However, assuming the double amount of annual groundwater inflow concerning own estimations (~1.7 Mm³) the results range in the same order of magnitude. Furthermore, 2005 is one of the dry years considering precipitation leading to a potential underestimation of long-term mean lateral inflow (October 2004 – September 2005: 21.2 mm at El Miyit station; Figure 2-3).

Chamayou (1966) states substantial lateral inflow from the western Graben of Zagora (Bou-Azzer region). This inflow could not be verified due to a lack of spatial and temporal data on groundwater levels.

6.2.2.4 Groundwater flow paths in Ouled Yaoub in October 2005 and April 2007

The village Ouled Yaoub is located at the lower end of the Tinzouline oasis west of the wadi Drâa. More in detail, the settlement stretches along the main road to Zagora westerly adjacent to the oasis gardens.

Ouled Yaoub has around 1,000 inhabitants mostly depending on subsistence agriculture (Rademacher, 2009). Thus, the village is located in the area of the hard rock aquitard (schisty siltstone and sandstone) at the outer rim of the Tinzouline aquifer. Groundwater observations are available from own field surveys in October2005 and April 2007 (see Haaken, 2008). Therefore, the Tinzouline aquifer drains generally southwards. It receives inflow from preferential path such as tributary aquifers. Furthermore, lateral inflow from the adjacent hard rock aquitard is assumed. Backwater is observed at the lower end of the Tinzouline aquifer caused by a hydraulic barrier of Tabanit sandstone (Foum Azlag, Figure 6-21; Haaken, 2008).

A first manually designed groundwater level contour map reveals the groundwater flow paths in October 2005. A second groundwater level contour map is found below representing the flow pattern in April 2007 (see also Haaken, 2008). In October 2005 the isopiestic lines portray diverging flow paths within the Tinzouline aquifer southeast of the village Ouled Yaoub. Thus, a part of the groundwater flows parallel to the wadi Drâa in southeastern direction. Another part flows in southwestern direction towards the rim of the Tinzouline aquifer. This may be due to effects of the internal structure of the Drâa aquifer (Figure 6-3). The groundwater flow towards the rim of the Tinzouline aquifer is opposed to the lateral inflow. Consequently, a zone of convergence develops at the edge of the Drâa aquifer. The flow pattern in October 2005 represents low flow conditions, as precipitation and inflow from the upstream reservoir are low. Annual precipitation accounts for 21.2 mm at El Miyit station in the period October 2004 – September 2005 in comparison to an approximate mean annual value of 60 mm at Zagora station (Figure 2-3). Furthermore, the annual inflow from the upstream reservoir to the wadi Drâa is 110 Mm^2 in the same period in comparison to a long-term annual average of 211 Mm^3 between 1974 and 2006 (data provided by ORMVAO).

The hydraulic gradient parallel to the wadi Drâa accounts for around 4.5 ‰ in October 2005. The hydraulic gradient directing to the southwestern edge of the Tinzouline aquifer amounts to around 8.0 ‰. Thereby, it gets even steeper the nearer it is to the inner limit of the Drâa aquifer represented by the accumulation of isopiestic lines (Figure 6-21). This may be due to groundwater drawdown caused by pumping from irrigation wells. These irrigation wells are lined up along the inner rim of the oasis gardens east of the road as observed during field campaigns (see also Haaken, 2008). Thereby, the aquifer limit may function as a negative boundary condition because the adjacent hard rock aquitard is less productive than the Tinzouline aquifer. The hydraulic gradient beneath the tributary in the south-west of Ouled Yaoub appears to be very steep accounting to around 11 ‰ near the outer limit of the Tinzouline aquifer. This can be explained by a convex groundwater table due to the convergence of the lateral inflow from the fractured aquitard. Furthermore, the drainage situation just before flowing into the deeper incised Drâa aquifer can steepen gradient. Similar flow pattern are known from tectonic step faults where groundwater in alluvial deposits falls over the edge of a fault-bloc made of less permeable hard rock.

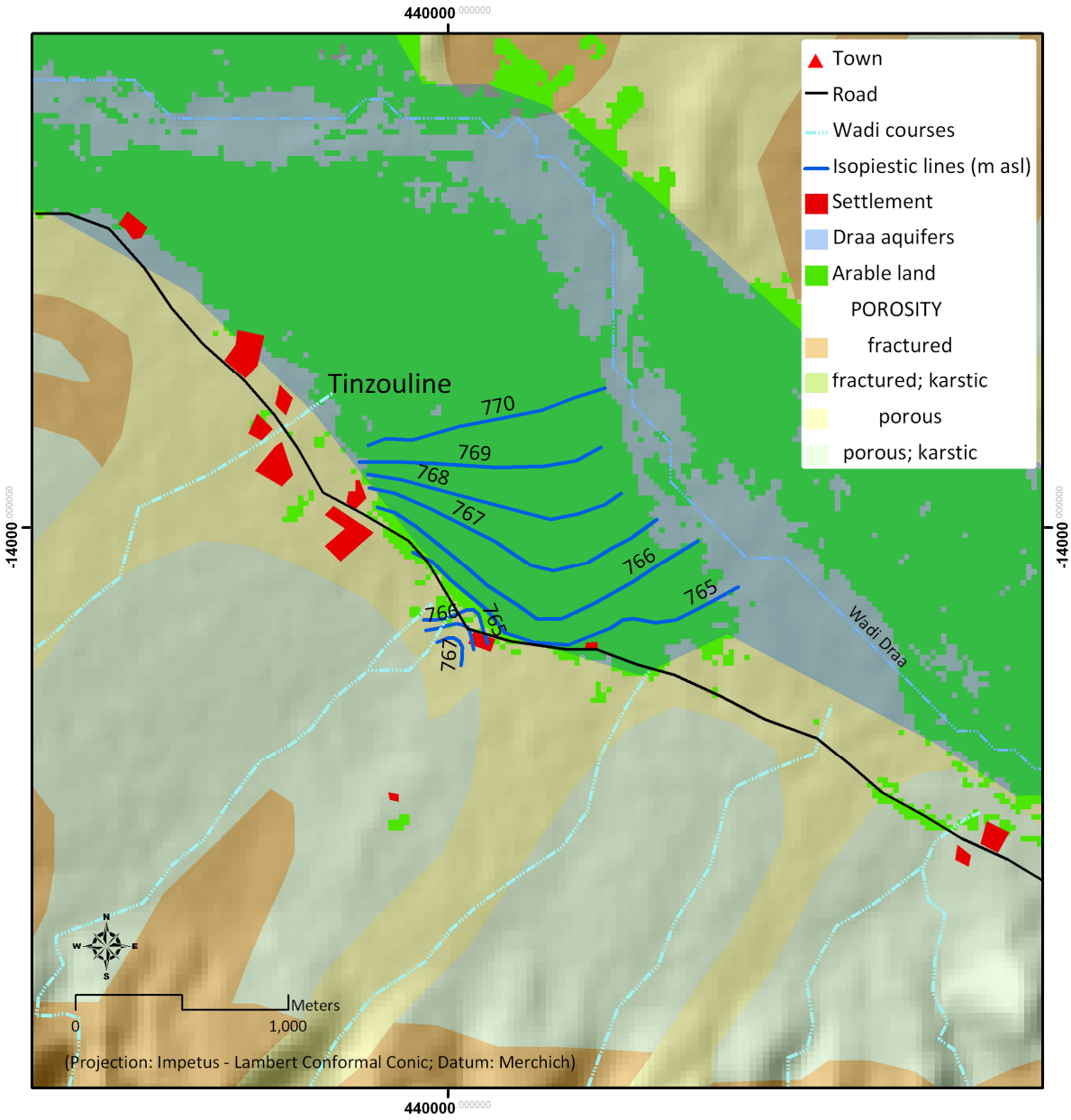

Figure 6-21: Map of manually designed groundwater level contours around the village Ouled Yaoub in the Tinzouline oasis based on manually observed groundwater levels at nine wells in October 2005.

Referring to the interpretation of groundwater flow pattern of October 2005, the minimum values of the estimated hydraulic gradients are assumed reasonable to assess the annual inflow from the preferential path beneath the tributary roughly (Table 6-21). The flow section is approximated based on own field observations and GIS techniques. The height of the flow section is assumed based on own field observations and the mean value of available groundwater level data (Haaken, 2008). Thereby, the width of the wadi bed is taken as width of flow section. The saturated thickness could not be determined because the structure of the tributary aquifer remains unknown. So, an altered zone of the substratum in combination to the alluvial deposits of the tributary is assumed to provide a preferential pathway (chapter 6.1.4). An approximate transmissivity of $3 \cdot 10^{-4}$ m²/s is adopted from Aoubouazza & El Meknassi (1996).

As a result, the approximate annual preferential inflow towards the Tinzouline aquifer at Ouled Yaoub is 3,504 m³. In comparison to this, the 1,000 inhabitants consume around 11,000 m³ applying an approximate mean daily per capita demand of 30 L per day (Rademacher, 2009). These estimations can only provide an approximation to give some idea on the components of a local groundwater balance. Further investigation is needed to assess groundwater flow and local water balances definitively. Therefore, groundwater observation, water consumption and further hydro-meteorological data are required (see also Graf, 2009). As an example, data on precipitation is only available at El Miyit station, which is located south of Zagora, and hence too far away to assess groundwater recharge at the local scale precisely.

Table 6-21: Rough estimation of annual inflow from the south-western tributary towards the Tinzouline aquifer based on groundwater level observations in October 2005 using transmissivity of $3 \cdot 10^{-4}$ m²/s (approximately adopted from Aoubouazza & El Meknassi, 1996).

Upstream site and aquifer	Hydraulic gradient [‰]	Front of flow section [m]	Approximate annual DARCY flow [m³/yr]
Southwestern tributary Ouled Yaoub	11	100	3,504

In April 2007, the groundwater level contours show more uniform flow pattern as in October 2005. Therefore, the groundwater flow is generally directed southwards nearly parallel to the wadi Drâa. As before, an opposed flow paths are obvious at the limit of the Tinzouline aquifer representing the convergence of lateral groundwater inflow beneath the tributary and flow within the Drâa aquifer (Figure 6-22).

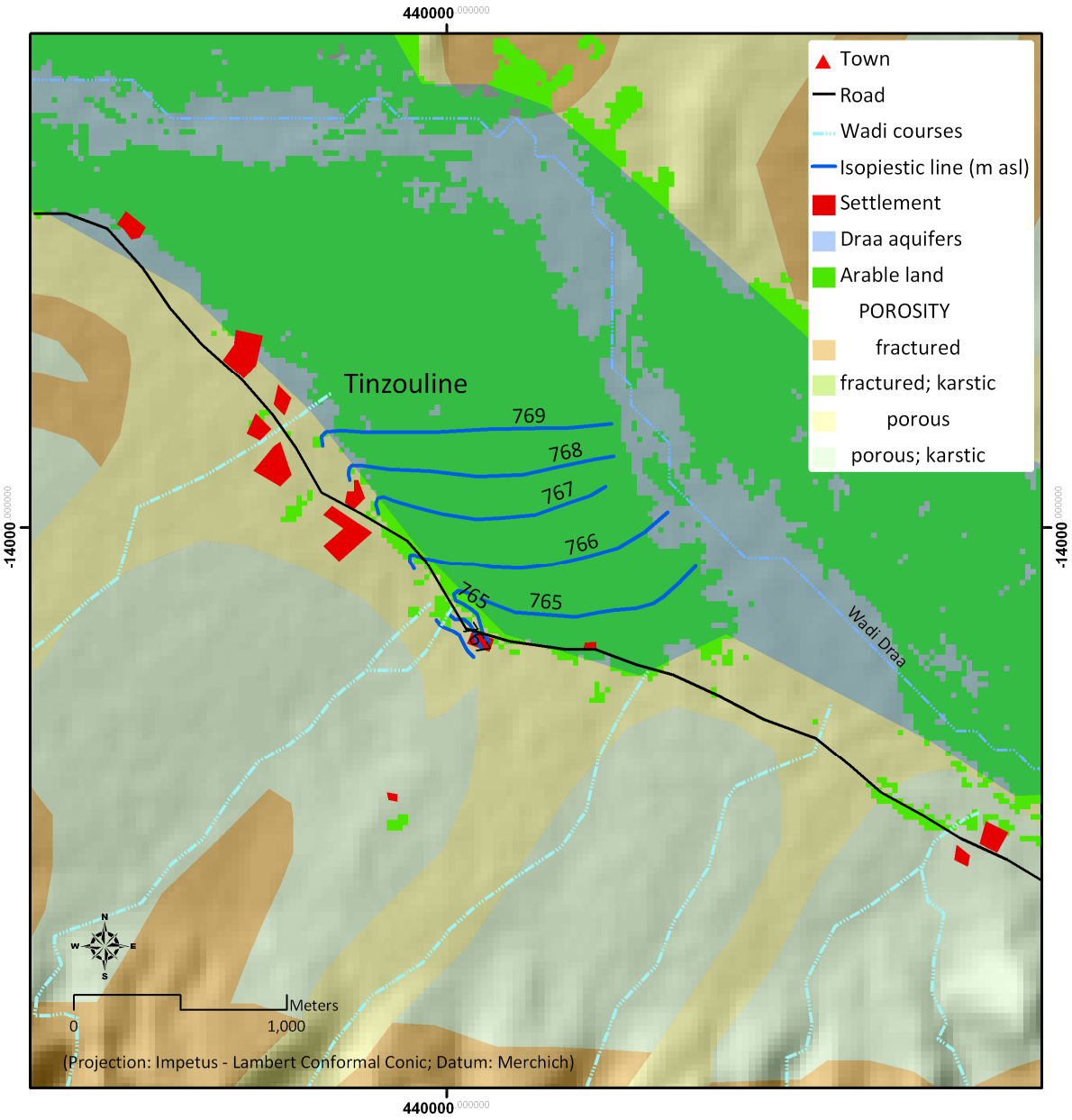

Figure 6-22: Map of manually designed groundwater level contours around the village Ouled Yaoub in Tinzouline oasis based on manually observed groundwater levels at ten wells in April 2007.

Based on the groundwater level contour map for April 2007 the hydraulic gradients are derived. Therefore, the groundwater table slopes with around 4.4 ‰ within the Tinzouline aquifer. The hydraulic gradient accounts for about 14 ‰ beneath the southwestern tributary in Ouled Yaoub.

Furthermore, the approximate annual preferential flow beneath the southwestern tributary in Ouled Yaoub is assessed same as for October 2005 (Table 6-22). The inflow accounts for around 4,500 m³ per year. In comparison to October 2005, the inflow is enhanced probably due to increased groundwater recharge caused by precipitation. This hypothesis is proven by increased precipitation of about 40 mm between October 2006 and March 2007 observed at El Miyit station (Figure 2-3). In comparison to this, precipitation is about 21 mm between October 2004 and September 2005 at El Miyit station (Figure 2-3). Haaken (2008) states a hydraulic gradient of around 7 ‰ beneath that tributary in Ouled Yaoub.

Consequently, the approximate annual inflow towards the Tinzouline aquifer is about 2,113 m³ (Table 6-22).

Table 6-22: Comparison of own estimations and an assessment based on Haaken (2008) concerning approximate annual inflow from the south-western tributary towards the Tinzouline aquifer for 2007 using transmissivity of $3 \cdot 10^{-4}$ m²/s (approximately adopted from Aoubouazza & El Meknassi, 1996).

Upstream site and aquifer	Hydraulic gradient [‰]	Front of flow section [m]	Approximate annual DARCY flow [m³/yr]
Southwestern tributary Ouled Yaoub (own estimations)	14	100	4,505
Southwestern tributary Ouled Yaoub (Haaken, 2008)	7	100	2,113

In conclusion, the rough estimations of approximate annual groundwater flow along the preferential path beneath a tributary in Ouled Yaoub give a general idea on values for a local water resources assessment. The results remain invalidated due to a lack of spatial and temporal resolution of groundwater data. As mentioned before, water consumption and supplementary data has to be analyzed in the respective social and institutional context to gain a reasonable basis for local water planning and management.

6.2.2.5 Groundwater flow paths of the Feija de Zagora in October 2005

The Feija de Zagora is an asymmetric intra-mountainous basin westerly adjacent to the Fezouata aquifer (Figure 6-6). It reveals a filling of fluvial and lacustrine Quaternary deposits. The substratum is the Ordovician schisty siltstone of the Schistes de Fezouata Formation. The Feija de Zagora is bordered by Cambrian sandstone and quartz-arenite of the Tabanit Formation on the one hand and by the Jbel Bani on the other (Figure 2-8; Table 6-1; Table 6-2). After Chamayou (1966), the feija aquifers and the tributary aquifers are treated as one though the feija aquifers are addressed separately as less productive and shallow in thickness. 37 bore logs provided by ORMVAO (1981) show that the alluvial deposits of the Feija de Zagora range between 2 m and 54 m in thickness. Thereby, the mean thickness accounts for approximately 20 m. The ephemeral wadi Feija is the main drain running alongside the basin near its southern boundary. Accordingly, the Feija de Zagora represents a very similar hydrological setting as the Drâa valley except the controlled discharge from the upstream reservoir Mansour Eddabhi (chapter 2.2). The Feijas provide alternative zones for cropping solely based on irrigation by pumped groundwater. These zones are increasingly occupied since the mid-80-ties. Furthermore, the feijas reveal a comparable natural hydrogeological setting to the Drâa aquifers except for the controlled discharge of the wadi Drâa. Thus, the feijas represent the modern land use and some kind of quasi-background condition for the characterization of the groundwater system at the same time.

Information from three recurrent field surveys is available carried out in spring 2005, autumn 2005 and spring 2007, whereas the field campaign in autumn was the most extensive observation. Groundwater level measurements stem from key dates of simultaneous groundwater sampling. The groundwater level data from October 2005 is processed to manually design a groundwater level contour map (Figure 6-23).

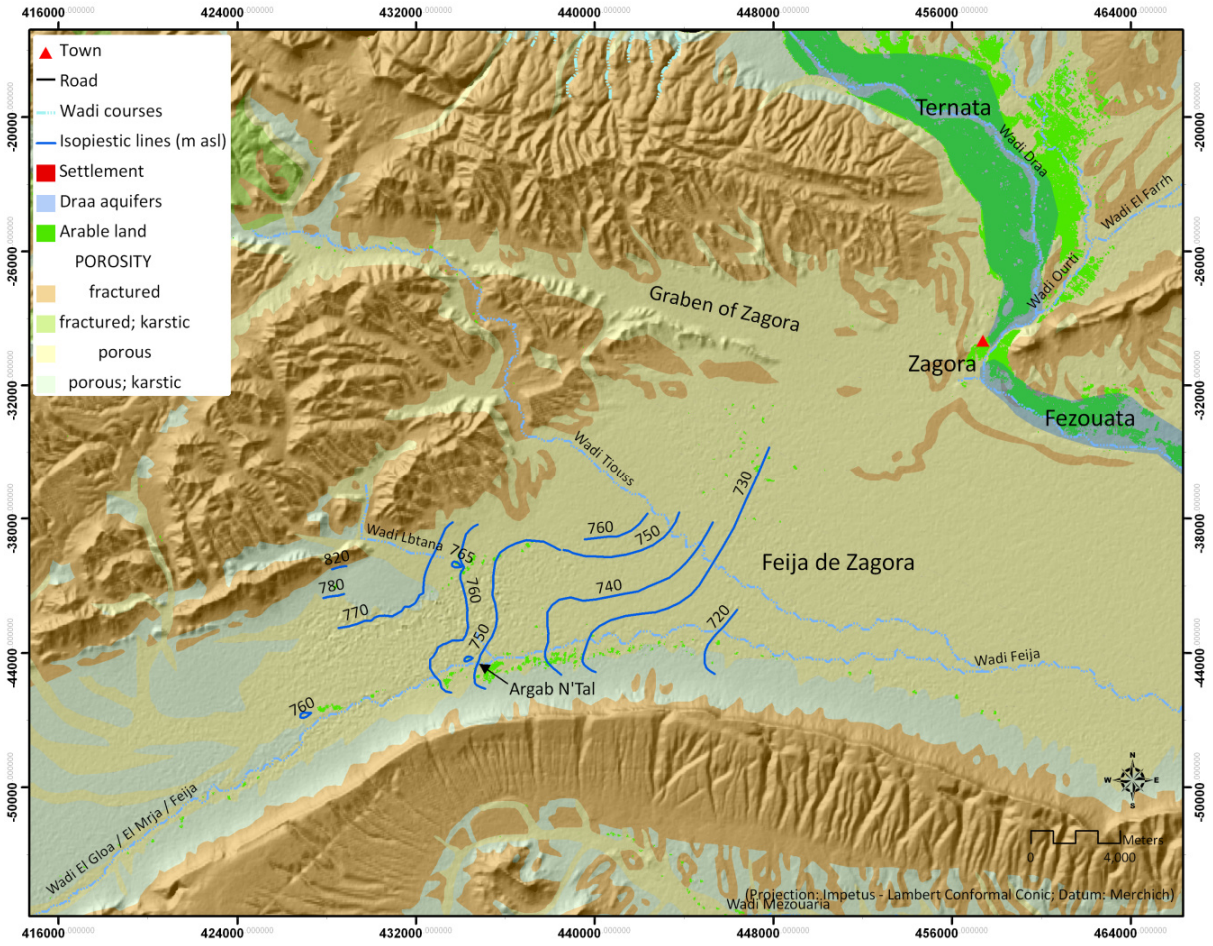

Figure 6-23: Map of manually designed groundwater level contours of the area around the village Argab'N-Tal in the Feija de Zagora based on manually measured groundwater levels at 23 wells in the alluvial Feija aquifer in October 2005.

Groundwater discharges mainly in easterly direction along the wadi Feija. The configuration of the groundwater level contours displays converging groundwater flow towards the main drain wadi Feija. Thereby, groundwater flow follows the principal slope of the landscape. But there appears to be other influences such as heterogeneity in aquifer structure and properties particularly in the center of the basin. The shape of the groundwater level contours may be due to paleo-relief. Zones of different hydraulic conductivity are determined by the multi-layered aquifer structure of terraces and lacustrine limestones intercalated by clayey marls. Lateral afflux from the northern boundary appears to be proofed in terms of underflow of the wadi Lbtana. A clear hint on inflow from the Jbel Bani is not found but appears to be probable. Obviously, extraction for irrigation results in local drawdown around the concentration of pumping wells. This groundwater level contour map is a snapshot of flow conditions and must not be interpreted for transient conditions directly. But based on the recurrent field surveys and the evaluation of a questionnaire on agricultural practice and groundwater use, it is assumed that the observed drawdown is manifest. Iit remains doubtful if the groundwater use in the Feija de Zagora is sustainable, particularly mindful of the increasing number of pumping wells and farms (Breuer, 2007).

The hydraulic gradient tracing the flow path from the northern boundary (wadi Lbtana) towards the wadi Feija is relatively steep accounting for 4.9 ‰ in October 2005. The hydraulic gradient along the wadi Feija at Argab N'Tal is approximately 3.8 ‰ in October 2005.

The hydraulic gradient from October 2005 is applied to estimate roughly the groundwater inflow towards the Fezouata aquifer based on the Darcy equation. Same as before, the flow sections are approximated based on own field observations and GIS techniques. The height of the flow section is estimated based on bore log information and the mean value of available groundwater level data. The weathered fringe of the substratum is considered accounting for 5.5 m (chapter 6.1.4). Therefore, the saturated thickness at the flow section is assumed to be 14.65 m in October 2005. Hydraulic conductivity is assessed using a transmissivity of $3 \cdot 10^{-4}$ m²/s adopted from Aoubouazza & El Meknassi (1996). Consequently, hydraulic conductivity accounts for around $2 \cdot 10^{-5}$ m/s.

As a result, the approximate annual groundwater inflow from the Feija de Zagora towards the Fezouata aquifer is around 1.1 Mm³ assuming the hydraulic gradient of October 2005 to be constant over one year.

Table 6-23: Approximate estimation of annual inflow from the Feija de Zagora aquifer towards the Fezouata aquifer based on groundwater level observations in October 2005 and using transmissivity of $3 \cdot 10^{-4}$ m²/s (based on Aoubouazza & El Meknassi, 1996).

Upstream site and aquifer	Hydraulic gradient [‰]	Flow section [m²]	Approximate annual DARCY flow [m³/yr]
Feija de Zagora aquifer	3.8	439,500	1,078,531

For May 1978, a hydraulic gradient towards the Fezouata aquifer is derived from a key date measurement at two sites. This gradient represents the underflow of wadi Feija in a distinct humid period (chapter 6.2.1). Same as before, the annual lateral groundwater flow from the Feija de Zagora towards the Fezouata aquifer is assessed roughly. The saturated thickness is estimated based on bore log information and the mean value of available groundwater level data. It is assumed to be 16.50 m in May 1978 including weathered fringe of the substratum (5.5 m). Hydraulic conductivity is assessed using a transmissivity of $3 \cdot 10^{-4}$ m²/s adopted from Aoubouazza & El Meknassi (1996). Consequently, hydraulic conductivity accounts for around $2 \cdot 10^{-5}$ m/s. Therefore, the approximate annual western groundwater inflow towards the Fezouata aquifers is about 0.31 Mm³ assuming the hydraulic gradient of May 1978 to be constant over one year.

Table 6-24: Approximate estimation of annual inflow from the Feija de Zagora aquifer towards the Fezouata aquifer based on Moroccan groundwater level observations in May 1978 and using a transmissivity of $3 \cdot 10^{-4}$ m²/s (based on Aoubouazza & El Meknassi, 1996).

Upstream site and aquifer	Hydraulic gradient [‰]	Flow section [m²]	Approximate annual DARCY flow [m³/yr]
Feija de Zagora aquifer	1.1	495,000	312,206

The comparison of results of 1978 and 2005 reveals higher inflow for 2005 due to a steeper hydraulic gradient (1978: 1.1 ‰; 2005: 3.8 ‰). The hydraulic gradient for 2005 is taped around 30 km west of the Fezouata aquifer. Consequently, it carries an undetermined degree of uncertainty concerning the Darcy flow estimations. On the other hand, the bore log data give hints on hydraulic connectivity within the Feija de Zagora and towards the Fezouata aquifer. The hydraulic gradient observed in October 2005 is assumed to drive the inflow to the Drâa aquifer. The smoother hydraulic gradient in May 1978 is mainly caused by the backwater effect at the lower end of Fezouata in front of the Jbel Bani (Table 6-17). Consequently, the groundwater inflow in 2005 is taken as inflow to the upper part of the Fezouata aquifer.

Accordingly, the inflow in 1978 represents the inflow to the lower part of Fezouata. A lumped value for the upper and lower inflow is calculated based on the mean hydraulic gradient of 2.5 ‰ to give a general idea of the probable total inflow from the Feija de Zagora to the Fezouata aquifer. As a result, the western annual inflow to Fezouata is approximately 0.7 Mm³. In comparison to this, Aoubouazza & El Meknassi (1996) calculate approximately the same approximate an annual groundwater flow from the Feija de Zagora in the year 1979. More in detail, the own estimation and the assessment of Aoubouazza & El Meknassi (1996) differs slightly due to varying parameters. The mean value of two hydraulic gradients accounting for 2.5 ‰ is a little higher in comparison to Aoubouazza & El Meknassi (1996). They give an overall hydraulic gradient of 2.0 ‰ for 1979 (Table 6-25). The shorter front of flow section applied in own estimations (30,000 m versus 37,600 m) compensates the effect of the steeper hydraulic gradient. The approximate annual lateral inflow amounts to around 0.9 Mm³ applying the longer front of flow section to the higher hydraulic gradient (Table 6-25).

Table 6-25: Comparison of approximate estimation of annual inflow from the Feija de Zagora aquifer towards the Fezouata aquifer concerning own estimations and the assessment of Aoubouazza & El Meknassi (1996).

Source	Transmissivity [m²/s]	Hydraulic gradient [‰]	Front of flow section [m]	Approximate annual groundwater flow [m³/yr]
Aoubouazza & El Meknassi (1996)	$3 \cdot 10^{-4}$	2.0	37,600	711,452
Own estimations	$3 \cdot 10^{-4}$	2.5	30,000	695,369
Own estimations	$3 \cdot 10^{-4}$	2.5	37,600	871,529

A definitive assessment of groundwater inflow to the Fezouata aquifer remains to be done because temporal and spatial data resolution is insufficient at this time. Generally, both assessments appear to be in reasonable range of results.

6.2.2.6 Groundwater flow path in the plain of El Miyit in April 2007

The plain of El Miyit stretches between the Fezouata oasis and the easterly adjacent Jbel Bani. Alluvial deposits outcrop and form the aquifer overlaying the aquitard of the schisty siltstone. In the plain of El Miyit the thickness of alluvial deposits range between 1.5 m and 5 m as the mean value is 3 m (Stumpf, 2008). Therefore, the plain of El Miyit reveals a different aquifer structure in comparison to the Feija de Zagora. Consequently, El Miyit represents mainly a tributary aquifer. Whether the alluvial deposits form a feija aquifer in the lower part of the El Miyit plain remains unknown. Even if a feija aquifer exists, its buffer role concerning the lateral groundwater inflow is minor in comparison to the Feija de Zagora aquifer due to the smaller aquifer extension. Even in comparison to the tributary aquifers of wadi Ben Dlala and El Farrh in the East of lower Ternata (chapter 6.2.2.3), the productivity of the El Miyit aquifer appears to be low because of the smaller superficial catchment (Figure 2-2).

Based on own observations and Stumpf (2008), a groundwater level contour map of the uppermost aquifer in the El Miyit plain is designed for April 2007. Therefore, the Plain of El Miyit receives inflow from the Northeast via minimum two parallel-oriented tributary aquifers, wadi El Miyit in the East and another wadi more West. These two tributary aquifers are assumed to be hydraulically separated due to the outcrop of the subjacent aquitard (schisty siltstone) in-between (Figure 6-24). The subjacent aquitard outcrops in a westward sloping ridge, which rises above the incised wadi beds in the upper part of the

plain. In the middle part of the El Miyit plain the tributary aquifers appear to merge probably forming a feija-like alluvial aquifer of very shallow structure (mean thickness: 3 m; see Stumpf, 2008). The groundwater discharge converges in front of the Jbel Tadrart and Jbel Bani and the downstream outlet Foum Takkat. Thereby, the main groundwater flow paths point towards the Fezouata aquifer in an acute angle (Figure 6-24).

According to the groundwater level contour map for April 2007, the hydraulic gradients range approximately between 6.3 ‰ and 7.3 ‰ in the upper part of the tributary aquifers of the El Miyit plain. The steep gradients hint on moderate hydraulic conductivity and storage capacity in combination to the influence of the relief ascending towards the northern and eastern edge of the plain (Figure 6-24). Furthermore, the ridge-like outcrop of the subjacent aquitard causes a narrow form particularly of the eastern tributary aquifer. The groundwater table slopes with approximately 2.8 ‰ to 3.0 ‰ in the middle part of plain where the two main tributaries merge and the main accumulation of farm gardens are found (Figure 6-24). The gradient is smoother here due to the lateral connection and widening of the aquifer. As observed during the field campaign in April 2007, numerous pumps are in use for irrigation in the farm gardens. Thereby, it remains unclear which influences pumping takes. It is probable that the increasing number of pumps since the 1980-ties results in a long-term transient groundwater drawn down comparable to land use change impacts. This hypothesis is supported by the shallow structure of alluvial deposits (mean thickness: 3 m, Stumpf, 2007) and the consequential low aquifer productivity. Furthermore, the mean depth to groundwater is about 13 m in April 2007. Therefore, the pre-defined alluvial aquifer appears to be completely discharged even if the weathered fringe of the substrata is considered (mean thickness: 5.5 m). Inhabitants in turn underline via oral information as groundwater depth was found at around 5 m in the mid 1980-ties when first irrigation wells had been dug. Thus, the groundwater level contour map appears to portray the groundwater potentials of the subjacent aquitard in the upper and middle part of the El Miyit plain (zone within the grey dashed line, Figure 6-24). In the lower part of the El Miyit plain the hydraulic gradient flattens accounting for about 1.3 ‰. It is assumed that backwater leads to the smooth hydraulic gradient in front of the Jbel Bani and the Foum Takkat referring to inverted gradients at downstream end of the El Miyit aquifer system (Table 6-17). In the lower part of the El Miyit plain the groundwater table is found in the alluvial aquifers (including the weathered fringe of substrata of 5.5 m) revealing a saturated thickness of around 3.60 m.

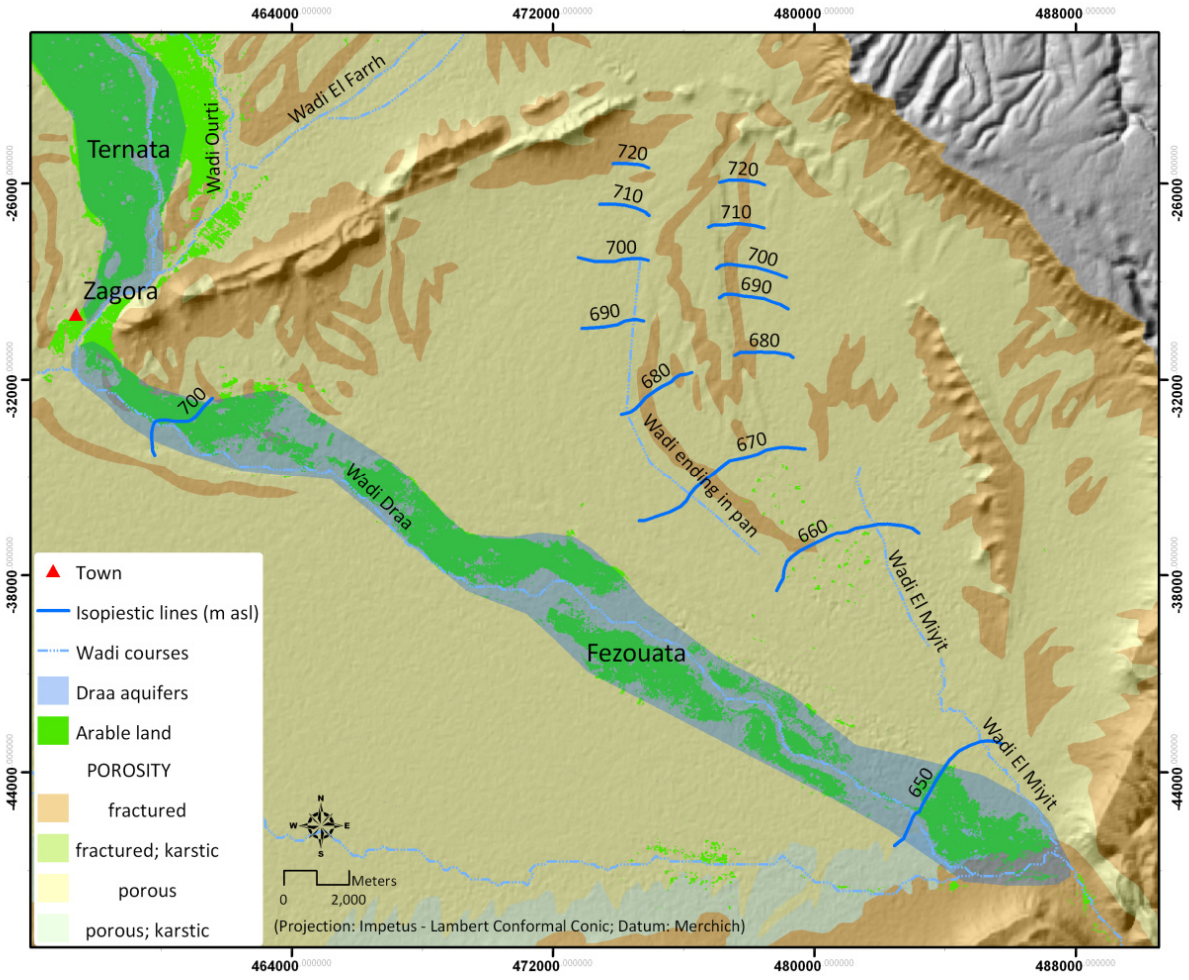

Figure 6-24: Map of manually designed groundwater level contours along the wadi El Miyit and in the Fezouata based on manually observed groundwater levels at 39 wells in April 2007.

Groundwater inflow towards the Fezouata aquifer is assessed roughly based on the hydraulic gradients from April 2007 using the Darcy equation. Thereby, the inflow is only calculated for the lower third of the front of the Fezouata aquifer (~10,000 m) because the alluvial aquifer system of the El Miyit plain appears to be completely discharged in its middle and upper part in April 2007. Accordingly, the flow sections are estimated based on own field observations and GIS techniques. The height of the flow section is assessed based on bore log information, own field observations and the mean value of available groundwater level data (see Stumpf, 2008). The weathered fringe of the substratum is considered accounting for 5.5 m (chapter 6.1.4). Thus, the saturated thickness at the flow section is assumed 3.60 m in April 2007. Hydraulic conductivity is assessed using a transmissivity of $3 \cdot 10^{-4}$ m²/s adopted from Aoubouazza & El Meknassi (1996).

Table 6-26: Approximate estimation of annual inflow from the El Miyit aquifer system towards the lower third of the Fezouata aquifer based on groundwater level observations in April 2007 and using transmissivity of $3 \cdot 10^{-4}$ m²/s (based on Aoubouazza & El Meknassi, 1996).

Upstream aquifer	Hydraulic gradient [‰]	Flow section [m²]	Approximate annual DARCY flow [m³/yr]
Lower third of El Miyit aquifer system (Apr-07)	1.3	36,000	163,987
Entire El Miyit aquifer system (lumped:Dec-84 & Apr-07)	1.5	150,000	548,726

Comparably, a lumped annual groundwater inflow from the El Miyit plain amounts to around 0.5 Mm³ from inflow assessments based on own observations (Table 6-26) and hydraulic gradients of December 1984 (Table 6-16). Thereby, groundwater inflow is assumed over the entire front of the Fezouata aquifer (~30,000 m). Referring to general flow conditions, December 1984 belongs to a distinct dry period with overall falling groundwater levels in the middle Drâa valley (chapter 6.2.1).

As a result, the groundwater inflow from the El Miyit plain towards the Fezouata aquifer remains to be definitively assessed due to a lack of data on aquifer system and groundwater observations. Furthermore, the geohydraulic role of the Graben of Zagora remains uninvestigated. It is assumed that the groundwater flow within the El Miyit plain is influenced by exploitation for irrigation. Thereby, the derived values of approximate annual inflow (0.2 to 0.5 Mm³; Table 6-26) appear to be reasonable representing low flow conditions.

6.2.2.7 Resulting approximate groundwater inflow towards the Fezouata aquifer

A lumped value for annual lateral inflow towards the Fezouata aquifer is carried out based on the rough assessments of annual groundwater discharge from the Feija de Zagora (chapter 6.2.2.5; 6.2.2.6) and the El Miyit plain. Thereby, the results for the inflow from the Feija de Zargora represent a mean value of high flow conditions (May 1978) and low flow conditions (October 2005). There may be a bias due to the fact that the low flow conditions are represented by another locality than the high flow conditions influenced and probably dammed by backwater in front of the Jbel Bani. The estimation of inflow from the El Miyit plain represents low flow conditions. In comparison to this Chamayou (1966) estimates the lateral inflow to the Fezouata aquifer as long-term average applying a mean annual precipitation of 75 mm. More recent precipitation observations reveal a long-term average of 60 mm at Zagora station. Thus, the estimation of Chamayou (1966) represents average to high flow conditions concerning precipitation.

The comparison of own estimations and those of Chamayou (1966) appear to reflect the flow conditions referring to each assessment (Table 6-27). Therefore, the lateral groundwater inflow ranges approximately between 1.2 Mm³ during low to average flow conditions and 2.9 Mm³ during average to high flow conditions.

Table 6-27: Lumped assessment of the total lateral groundwater inflow towards the Fezouata aquifer in comparison to long-term estimations of Chamayou (1966).

Upstream site and aquifer	Flow conditions	Approximate mean inflow [Mm³/yr]
Feija de Zagora (own estimations)	Lumped average	0.7
El Miyit plain (own estimations)	Low flow	0.5
Total inflow to Fezouata (own estimations)	Low to average	1.2
Long-term inflow to Fezouata (Chamayou, 1966)	Average to high	2.9

6.2.3 Groundwater recharge assessment based on water table fluctuations

The water table fluctuation method is applied to assess the order of magnitude of groundwater recharge from river water infiltration to the Drâa aquifers (chapter 5.2.3). Groundwater data is available at two sites in the upper section of the middle Drâa valley, one at Tarmast in the Mezguita aquifer and one at Tansikht at the upstream end of the Tinzouline aquifer (Figure 6-25). The piezometers were equipped with automatic data logger by the Office Regional de Mise en Valeur Agricole Ouarzazate (ORMVAO).

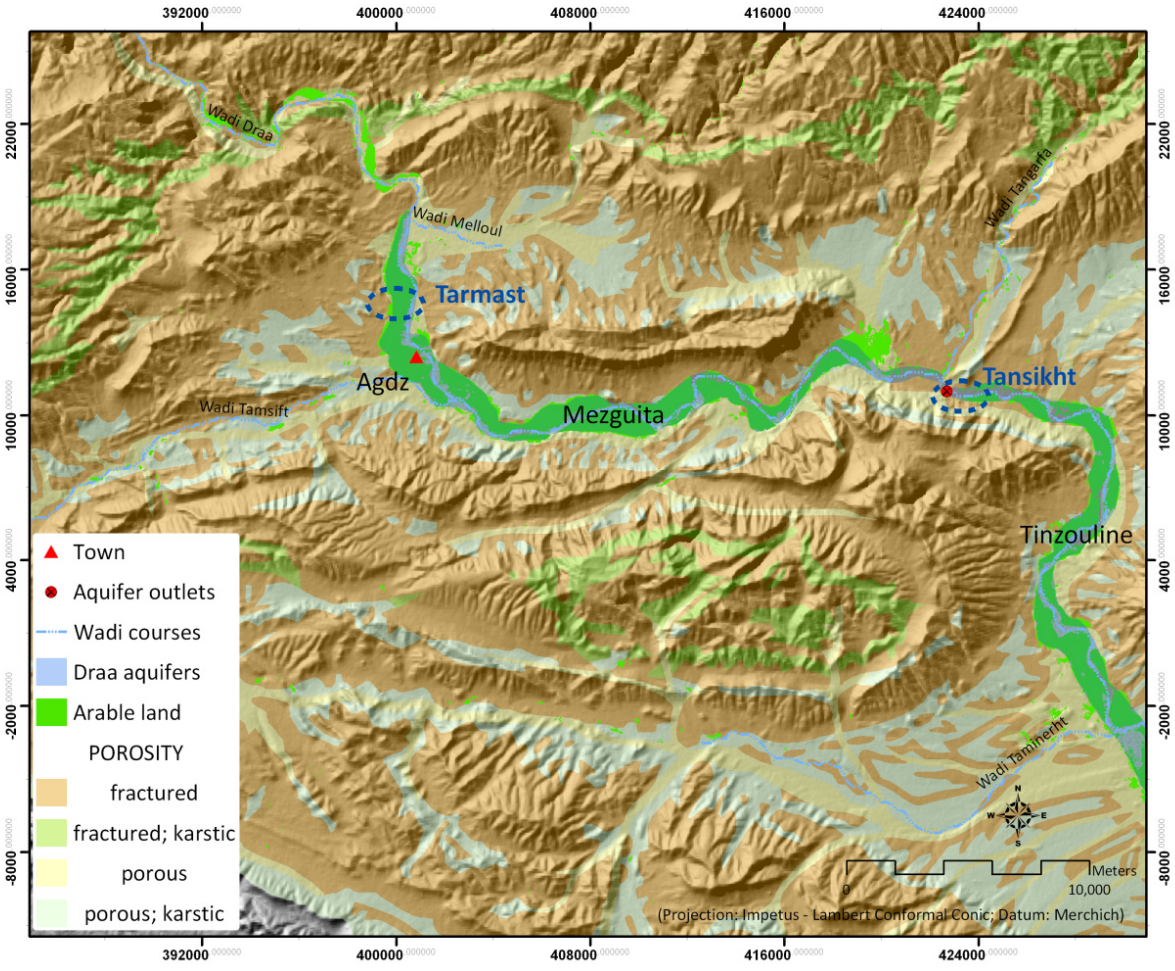

Figure 6-25: Approximate localization of the piezometers equipped with data loggers of the ORMVAO.

The estimation of hydraulic gradients between the wadi Drâa and the piezometer could not be evaluated because the precise localization of the piezometers is lacking.

Table 6-28: Site-specific information on the piezometers chosen to apply the water table fluctuation method (data provided by the ORMVAO).

Drâa aquifer	Site	Riverside	Situation	Approximate distance to Drâa	Altitude [m asl]
Mezguita	Tarmast	West	2 - 3 km Nord of Agdz	800 m	923,01
Tinzouline	Tansikht	West	At the bridge	100 m	850,36

At Tarmast, the series of daily depth to groundwater from 12/2004 to 07/2007 describes a clear fluctuation with distinct peaks and dips (Figure 6-27). Groundwater depth ranges from 6.78 to 12.65 m with a mean of 10.20 m (Figure 6-26, left).

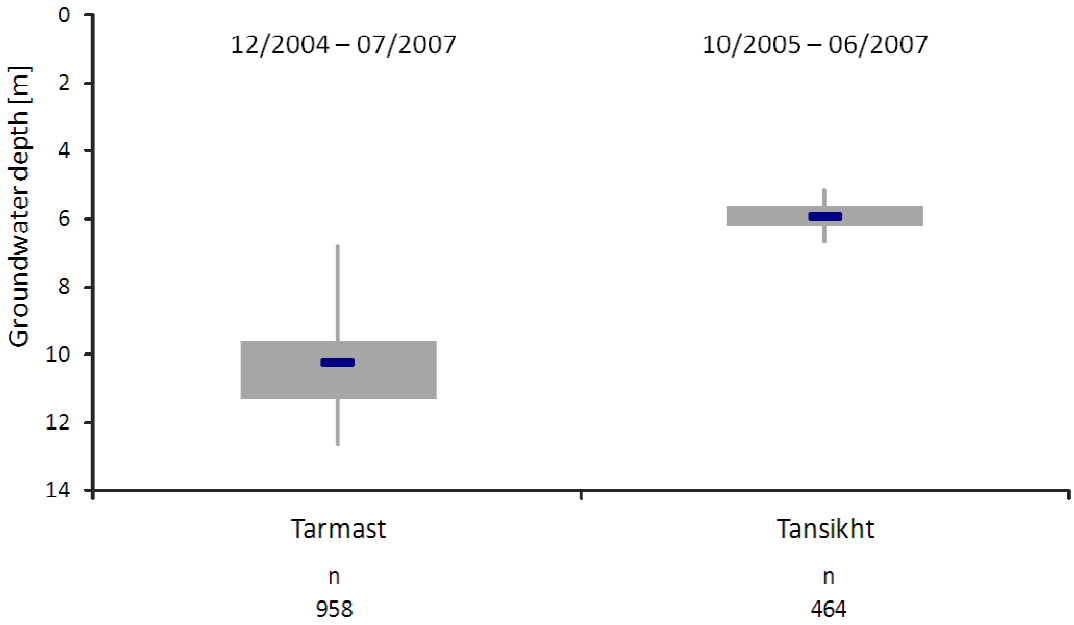

Figure 6-26: Box plots of depth to groundwater at the piezometers Tarmast and Tansikht; grey vertical lines display minima and maxima; grey boxes represent the 25 % to 75 % quantile range; blue horizontal lines portray the median values.

The curve shape exhibits sharp groundwater level rises and slightly smoother recessions. The groundwater level rises relate apparently to inflow from the reservoir Mansour Eddahbi and secondarily on precipitation within the catchment (measured at the IMPETUS station Argioun; Figure 2-3). These precipitation events lead to wadi discharge and to groundwater recharge from transmission losses subsequently. A threshold could not be found concerning precipitation amount or intensity, which can lead to indirect groundwater recharge. This is because further discharge observations and precise data on precipitation distribution are lacking.

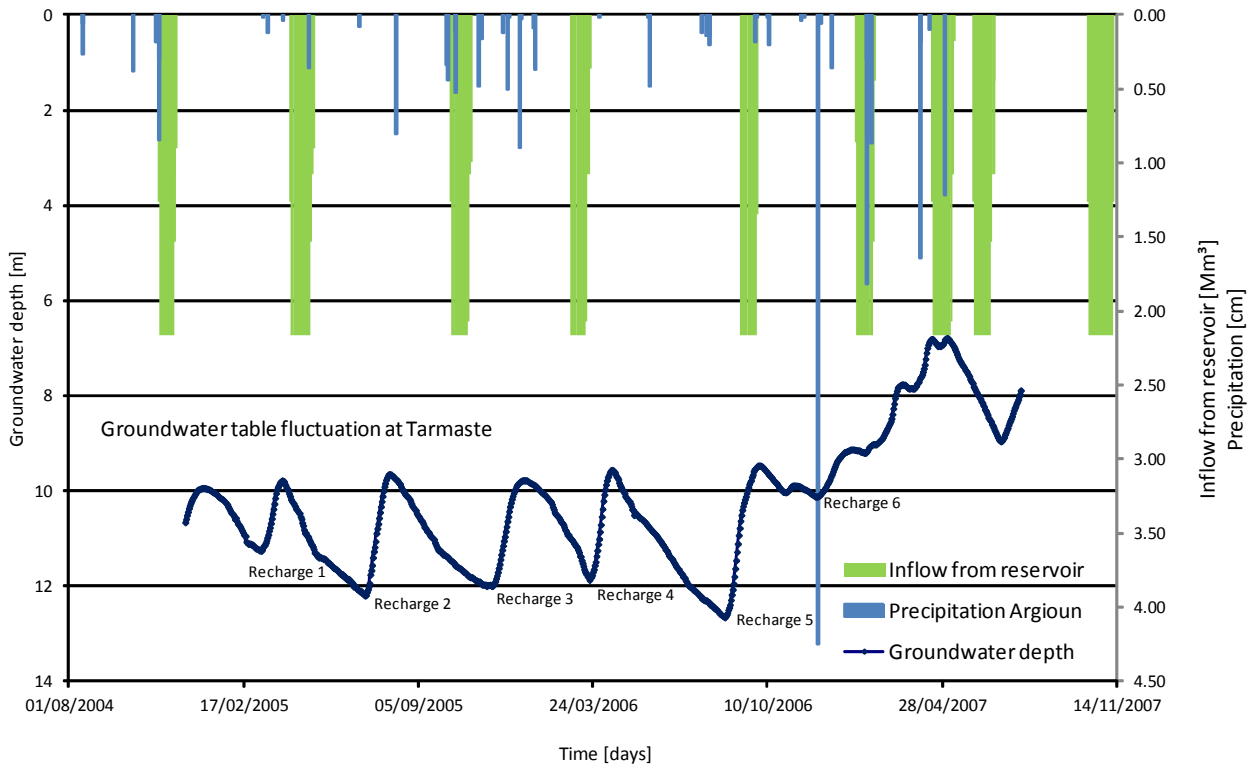

Figure 6-27: Daily time series of groundwater levels at Tarmast (Mezguita aquifer) with stream flow and precipitation data for the period 08/2004 – 11/2007.

The results of the water table fluctuation method are listed in Table 4-6 subdivided for the groundwater level rises marked in Figure 6-27.

Table 6-29: Actual groundwater recharge at the piezometer Tarmast / Mezguita aquifer (2004- 2007) subdivided for the groundwater level rises marked in Figure 6-27 as a result of estimations using the water table fluctuation method.

Recharge period (Figure 6-27)	*Days of water level rise*	*Difference in groundwater level [m]*	*Total groundwater recharge [mm]*	*Recharge rate [mm/d]*
(1)	24	1.36	245	10
(2)	26	2.40	433	17
(3)	33	2.25	405	12
4) purely inflow	25	1.85	332	13
(5)	37	3.83	689	19
(6) purely PCP	8	0.66	119	15
			Mean	14

As a result, the mean net groundwater recharge at the piezometer Tarmast is 14 mm per day over 153 days in the period 02/2005 to 11/2006. The annual recharge of the Mezguita aquifers in the hydrological year 2005/2006 is accordingly about 2.6 Mm³ based on the rough assumption that the piezometer Tarmast represents the hydrogeological setting of Mezguita. So, the length of the section of the Wadi Drâa going over the Mezguita aquifers is around 36 km taken from the SRTM DEM using GIS. The

mean width of the wadi bed is roughly assessed to be 50 m. The area available for transmission losses from the Wadi Drâa is then calculated and multiplied by 95 days of recharge (groundwater level rise) in 2005/06 and the mean recharge rate of 14 mm per day. The recharge coefficient in relation to transmission losses of inflow from the reservoir accounts approximately for 2.4 % of the inflow volume. This appears to be an underestimation by one order of magnitude in comparison to values given by Chamayou (1966) postulating a recharge coefficient of around 20 %. This may be due to the distance of in 800 m between the piezometer and the Wadi Drâa (data from ORMVAO; Table 6-28). Overall, this assessment of groundwater recharge should be applied without being verified. So, further data needs to be collected such as precise localization, aquifer properties and longer series.

At Tansikht the daily depth to groundwater is redorded for the period 03/2005 – 07/2005 and 10/2005 - 06/2007. Only later observation period is used to apply the water table fluctuation method because only one peak is found in the prior observation period. Furthermore, the falling limb of the peak in March 2005 looks biased describing an abrupt cutoff. The series of groundwater depth between 10/2005 and 06/2007 reveals also a clear fluctuation dependent on inflow from the reservoir Mansour Eddahbi and secondarily on precipitation within the catchment (measured at the IMPETUS station Argioun; Figure 2-3; Figure 6-28). Groundwater depth ranges from 5.11 to 6.69 m with a mean of 5.88 m (Figure 6-26, right). At Tansikht, the groundwater depth is shallower and shows a smaller range in comparison to the Tarmast piezometer. This may be due to the local aquifer structure and a larger specific yield at Tansikht, but data is lacking to interpret the differences in groundwater depth between Tarmast and Tansikht. The groundwater level rises are sharp and the falling limbs of the curve are smoother than rising ones.

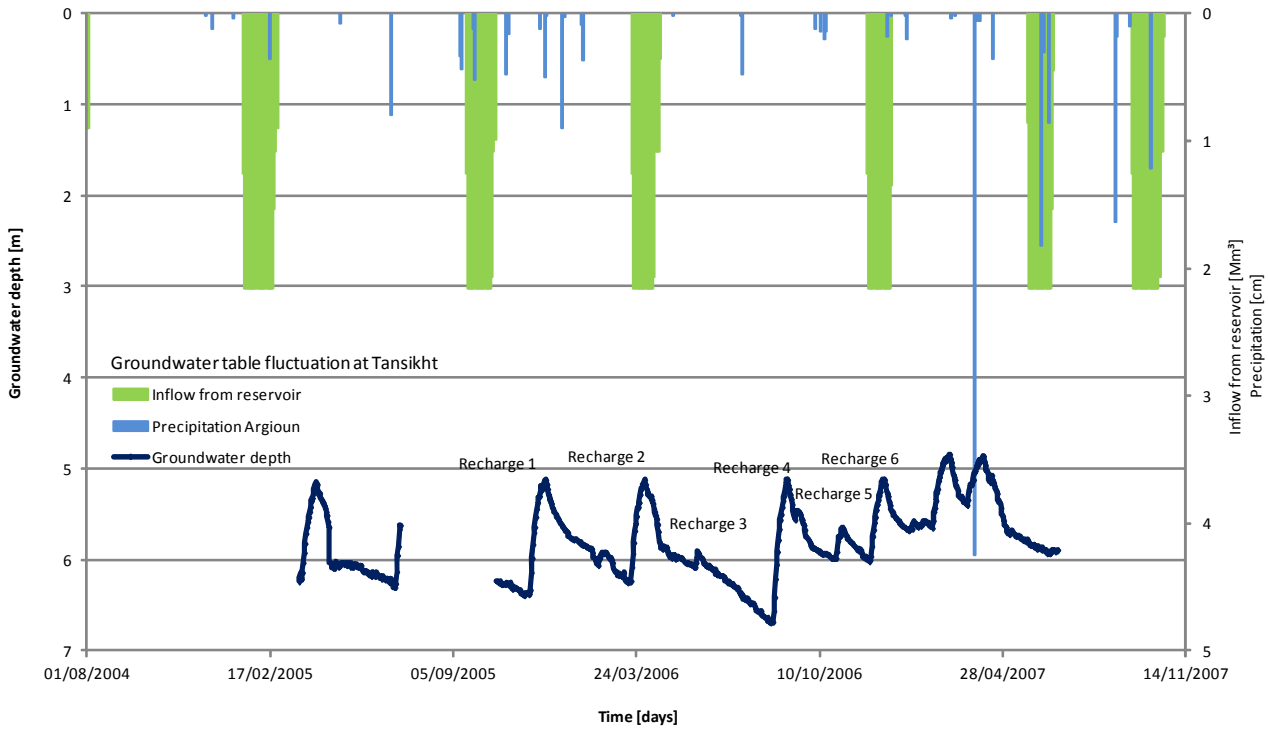

Figure 6-28: Daily time series of groundwater levels at Tansikht (Tinzouline aquifer) with stream flow and precipitation data for the period 03/2005 – 07/2005 and 10/2005 - 06/2007.

The results of the water table fluctuation method are listed in Table 6-30 subdivided for six groundwater level rises for which the method was applicable (Figure 6-28).

Table 6-30: Actual groundwater recharge at the piezometer Tansikht / Tinzouline aquifer for six valid events in 2005 - 2007 marked in Figure 6-28 as a result of estimations using the water table fluctuation method.

No. of recharge event (Figure 6-28)	Period of water level rise [days]	Difference in groundwater level [m]	Total groundwater recharge [mm]	Recharge rate [mm/d]
1	18	1.36	252	14
2 purely inflow	15	1.34	240	16
3 purely PCP	3	0.18	33	11
4	15	1.75	315	21
5	7	0.37	70	10
6	16	1.08	192	12
			Mean	14

The mean net groundwater recharge at the piezometer Tansikht is 14 mm per day over 58 days in the period 10/2005 to 09/2006. The annual recharge of the Tinzouline aquifers in the hydrological year 2005/2006 is accordingly about 2 Mm³ based on the very rough assumption that the piezometer Tansikht is representative for the hydrogeological setting of Tinzouline. So, the length of the flow section of Wadi Drâa is around 45 km. The mean width of Wadi Drâa is assumed 50 m. The reacharge fpr 2005/06 is then assessed applying 58 days of recharge (groundwater level rise) and the mean recharge rate of 14 mm per day. The recharge coefficient related to transmission losses of inflow from the reservoir accounts approximately for 1.9 % of the inflow volume. Same as mentioned for Tarmast, this appears to be an underestimation by one order of magnitude in comparison to values given by Chamayou (1966) postulating a recharge coefficient of around 20 %. This is surprising because the distance between the piezometer and the Wadi Drâa is around 100 m (data from ORMVAO; Table 6-28). The assessment of groundwater recharge at the Tansikht piezometer can neither be used without being verified. Therefore, further investigation is necessary such as precise localization, studies on aquifer properties and observations of longer series.

6.2.4 Regional groundwater recharge assessment using chloride mass balance

The chloride mass balance is applied to estimate approximately regional groundwater recharge using own precipitation and groundwater samples. The recharge rates are compared for the hydrogeological units excluding the Drâa aquifers (Figure 6-29). The Drâa aquifers are strongly influenced by recharge from transmission losses in the wadi bed. So, the zero-dimensional approach of the chloride masse balance must not be applied. The recharge rates are given as percentage of the annual precipitation of 63 mm (observed at Zagora station; Figure 2-3). The highest recharge rate is found for the Basin aquifers. Recharge is lower in the Tributary aquifer and lowest in the Fractured aquitard (Figure 6-29). The differences in recharge rates are not great. So, the rock type and the type of opening of the parent material do not dominantly influence recharge.

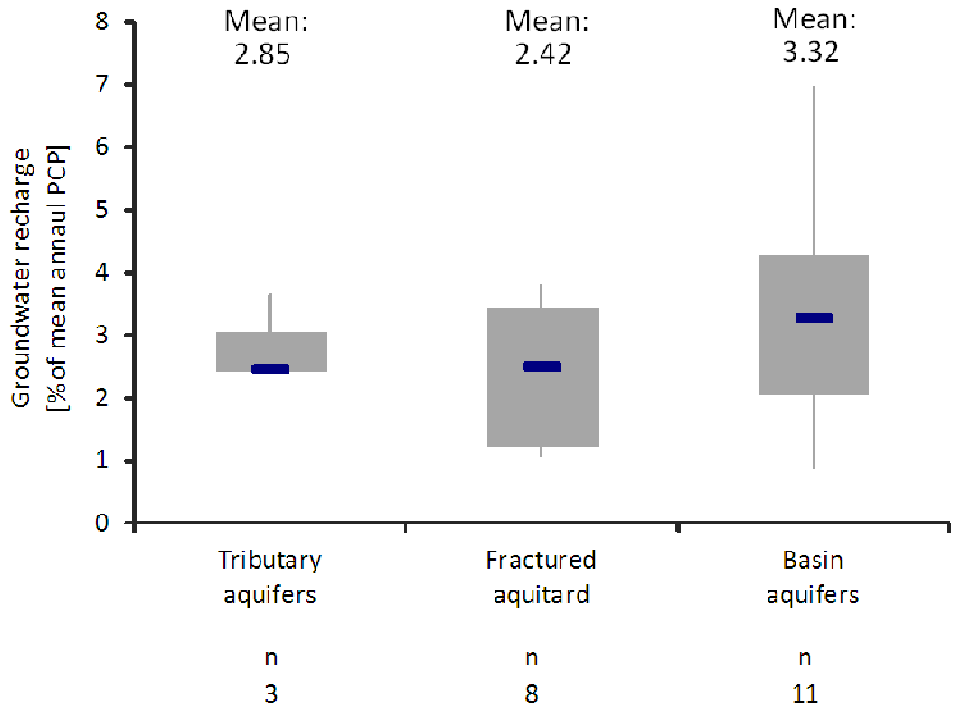

Figure 6-29: Box plot of the groundwater recharge rate (as percent of mean annual precipitation 63 mm) for fractured media and porous media; grey vertical lines display minima and maxima; grey boxes represent the 25 % to 75 % quantile range; blue horizontal lines portray the median values.

The recharge rate gained by the chloride mass balance is re-classified to proof perceptual models of groundwater recharge in the dry environment of the Kalahari / S-Africa found by Külls (2000). The results of the classification of sites modified after Külls (2000) is shown in Figure 6-30. The classes of wadi losses, fracture infiltration, colluvial infiltration and direct percolation is enhanced by the group of localized percolation as pans are observed in the area of the Basin aquifers.

The sites near the main wadi in the Basin of the Feija de Zagora show the highest recharge rate. These sites are also located near to the colluvial deposits of the Jbel Bani bordering the Basin to the South. As a result, wadi losses and colluvial infiltration represent the most important processes triggering groundwater recharge. That means recharge is systematically higher in settings where overland flow and wadi discharge is dominant. So, a one-dimensional approach of the chloride masse balance should be applied next. Recently data concerning run off and surface water chemistry is lacking. The differences are little between the Tributary aquifers, the Fractured aquitard and the sites tapping the Basin aquifer far from the main wadi. The results may be biased due to the influence of water of longer residence time and from deeper zones particularly concerning the Fractured aquitards. Cappy (2006) found groundwater residence ages between recent and 3,000 years. So, groundwater may have increased chloride content which leads to an underestimation of groundwater recharge. Longer residence time can also mean that the groundwater was recharged during times of different climatic conditions. So, the chloride input into the system could have been another in comparison to the data observed recently. Assuming inflow from the Fractured aquitard, the results for the Tributary aquifers and the Basin aquifers can be biased too. Furthermore, samples from sites tapping the Fractured aquitard west of Mezgiuta may bias the result (Figure 6-25). These northern sites receive more precipitation due to the altitudinal gradient (Schulz, 2006). Further differentiation of recharge rates within the Fractured aquitards cannot be made due to the lack of long-term data along that altitudinal gradient. The sample number of three for the Tributary aquifers allows only graphical representation and first comparison based on the representative sam-

pling. Further statistic evaluation is excluded. All data used in for the chloride mass balance is geochemically tested for further sources of chloride. Upstream of the sites included in this study the absence of halite and chloride is verified approaching XRA and XRF. Data from other aquifer zones are excluded from the chloride mass balance because irrigation activity may function as a further source of chloride leading to an underestimation of recharge (chapter 6.3.3.3).

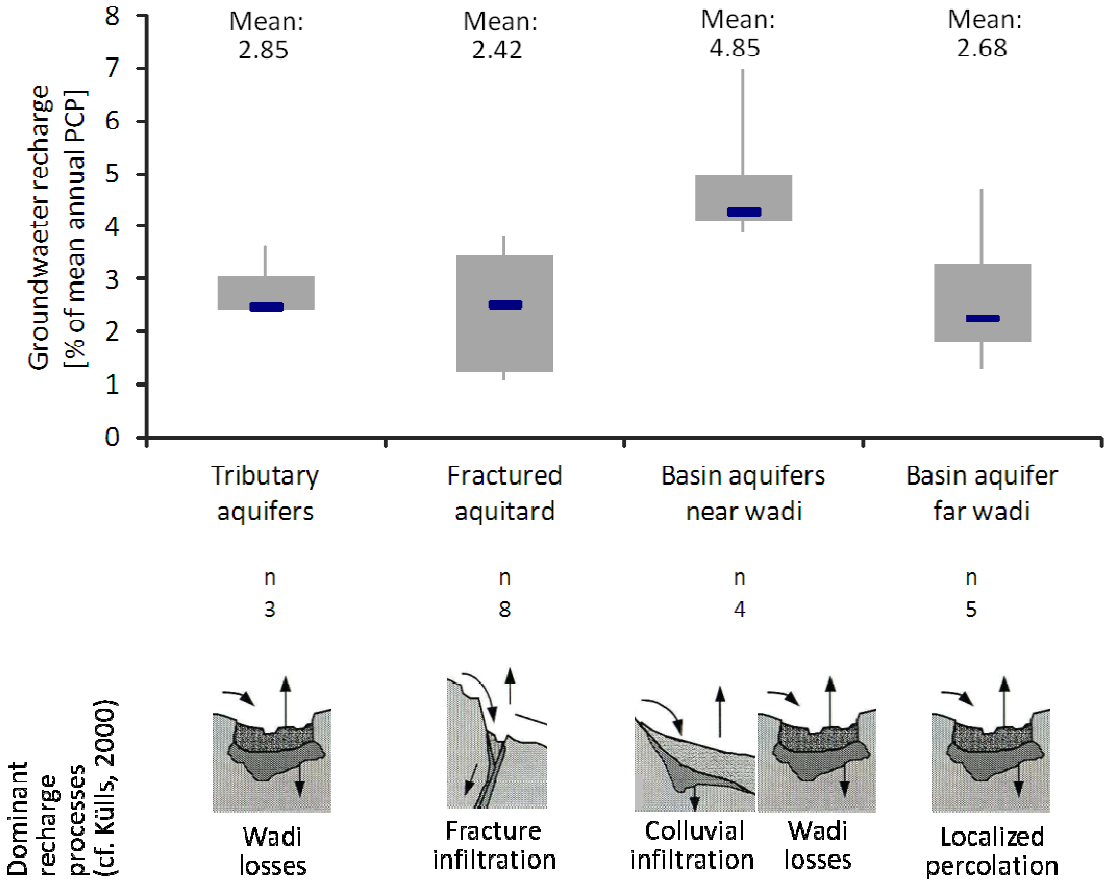

Figure 6-30: Box plot of the groundwater recharge rate (as percent of mean annual precipitation 63 mm) classified according to perceptual models of recharge modified after Külls (2000); grey vertical lines display minima and maxima; grey boxes represent the 25 % to 75 % quantile range; blue horizontal lines portray the median values.

Further IMPETUS expertise on groundwater recharge focuses on potential recharges (Weber; 2004; Kutsch; 2008). Results of Weber (2004) focus on a relatively small spatial and temporal scale and cannot be directly compared with the results of the CMB approach. Results of Kutsch (2008) display potential direct groundwater recharge for a relatively short period. So, they cannot directly be compared to the results of the CMB. CMB results can neither directly be compared with data from the Moroccan Ministry of Environment because they used “infiltration coefficients” related to specific geological units to estimate groundwater recharge (DRE; 1976).

6.3 Hydrogeochemistry

Hydrogeochemical investigation is used to supplement and verify the interpretation of the aquifer system (chapter 6.1) and the groundwater system (chapter 6.2) of the MDC.

In this context, the following objectives are focused:

- Characterization of groundwater composition (inventory),
- Identification of spatial patterns of hydrochemical facies,
- Explanation of hydrogeochemical processes,
- Understanding groundwater evolution along main path ways

More in detail, hydrogeochemical analysis of inorganic groundwater composition and stable water isotopes is carried out to obtain enhanced information on groundwater recharge sources, groundwater flow directions and anthropogenic influences. So, salinization processes are depicted as typical problem of arid environments. The evaluation of influences and impacts on groundwater quality is an interesting by-result helping to understand the potential groundwater use strategies. Water quality aspects are depicted for both drinking water production and irrigation purposes (chapter 6.3.5).

The present hydrogeochemical analysis is mainly based on own key date samplings of water in spring and autumn 2005 and spring 2007 (chapter 4.3 & 5.3). In total 95 water samples were taken from 67 stations. At 23 sites, sampling was carried out repeatedly. Two-fold sampling is available for 20 sites and three sites were sampled three times. Additionally 26 rock samples were taken at 22 outcrops in the MDC to supplement the interpretation of hydrochemical analyses. Exemplary test sites (around Ouled Yaoub and Fezouata; Figure 6-31) are selected to study hydrogeochemical processes and to upscale the findings to the regional aquifer systems following a hydrofacies approach (chapter 5.1).

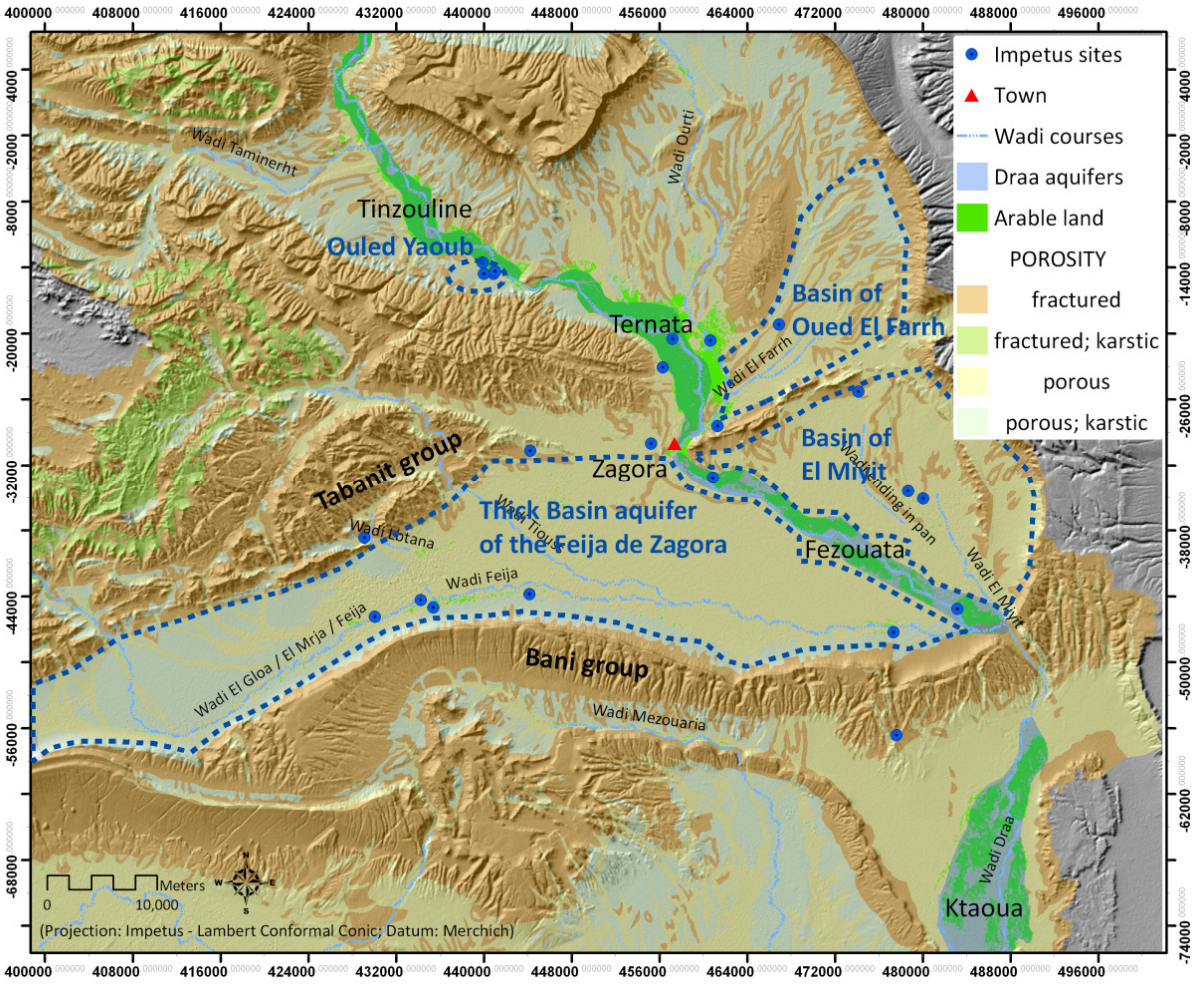

Figure 6-31: Map of test areas and groundwater sites repeatedly sampled spring and autumn 2005 and spring 2007.

6.3.1 Inorganic groundwater composition

The inorganic chemistry of groundwater from the Middle Drâa Catchment (MDC) is represented by selected parameters in terms of descriptive statistic and hydrogeological causality. All parameters are presented as mean values of repeated samples in spring and autumn 2005 and spring 2007 at 23 sites. So the following aspects a chosen to characterize the groundwater composition:

- Specific electric conductivity
- Water type after Davies & De Wiest (1967)
- Water type by dominant ions
- Hydrochemical classifications using Piper diagrams based on Furtak & Langguth (1967) and Back (1960)

Some parameters such as dissolved oxygen, redox potential and temperature are excluded from the characterization because samples were taken both as scoop samples and after pumping. Concerning the scoop samples, it cannot be ruled out that the observed values are influenced due to the contact of groundwater to the atmosphere for indeterminate duration.

6.3.1.1 Specific electric conductivity

The specific electric conductivity of groundwater ranges from 570 to 7063 µS/cm around a mean of 2238 µS/cm and a median of 2000 µS/cm (Figure 6-32).

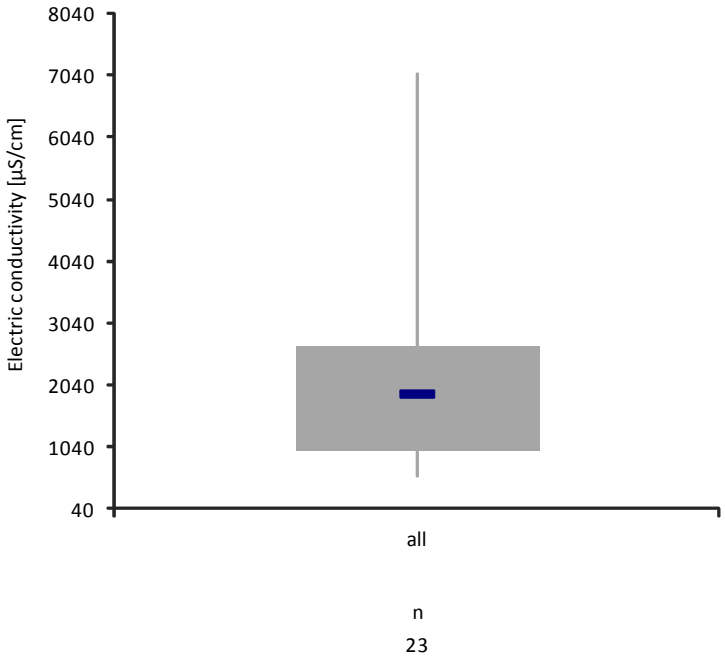

Figure 6-32: Whisker box plot of mean values of repeated observations of specific electric conductivity of groundwater in spring and autumn 2005 and spring 2007 at 23 sites (grey vertical lines display minima and maxima; grey boxes represent the 25 % to 75 % quantile range; blue horizontal lines portray the median values).

In the MDC the water of fresh and brackish type occurs after the classification scheme of Davies & De Wiest (1967). According to this, the most common water type is brackish observed at 16 of 23 sites. Seven sites reveal fresh water (Table 6-31).

Table 6-31: Results of the groundwater classification after Davies & De Wiest (1967) for 23 sites in the MDC (repeated sampled in spring and autumn 2005 and spring 2007).

Classes after Davies & De Wiest (1967)	Range of electric conductivity [µS/cm]	Number of sites
Brackish	1,000 to 10,000	16
Fresh	< 1,000	7

Highest values are found at the lower end of the Drâa aquifers verifying the hydraulic separation (Figure 6-33; here from North to South: Tinzouline, Ternata and Fezouata). Lowest values are found mostly in extensively used areas in wells tapping the tributary aquifers, which are embedded in the fractured aquifer.

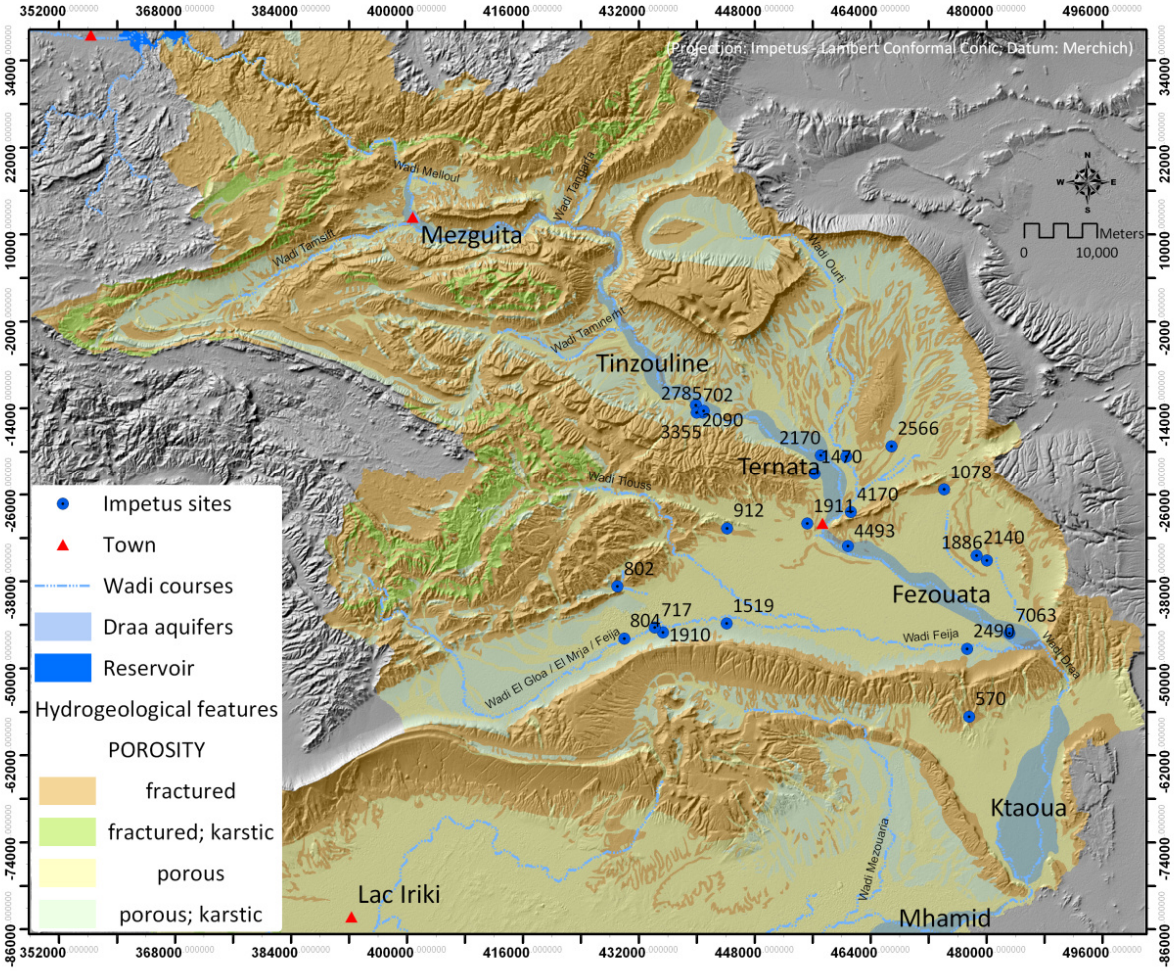

Figure 6-33: Mean values of specific electric conductivity of groundwater observed in spring and autumn 2005 and spring 2007 at 23 sites.

The classification of aquifer units is based on various aspects including expert knowledge from field-work. The aquifer units are regional units and correspond to lithofacies units of the geological map of Morocco 1/500,000 and 1/200,000 (chapter 6.1):

- Fractured aquitards
- Tributary aquifers (embedded in the Fractured aquitards)
- Basin aquifers (beneath flat plains)
- Drâa aquifers (terrace sediments of the Wadi Drâa including the altered fringe of underlying silt-stones)

Fresh water is never found in the Drâa aquifers. Four of seven fresh water observations are done in the Basin aquifer of the Feija de Zagora. Further fresh water samples are drawn from the Tributary aquifer and the fractured aquitard. So, this first look on the distribution of the water types appears to support the interpretation of the aquifer system (chapter 6.1 & 6.2).

6.3.1.2 Water type by dominant cation and anion

The definition of water types by the dominant cation and anion shows eight of 23 sites of Calcium-Bicarbonate as most common type. Seven of these eight represent fresh groundwater with less than

1,000 µS/cm of electric conductivity according to the classification of Davis & De Wiest (1967; chapter 6.3.1.1). Sodium-Sulfate is the second most type observed at four sites respectively. Calcium-Chloride and Calcium-Sulfate types occur three times and one time the closely related type of Sodium/Calcium-Chloride. Furthermore, Magnesium-Sulfate type is found two times same as the Sodium-Bicarbonate type.

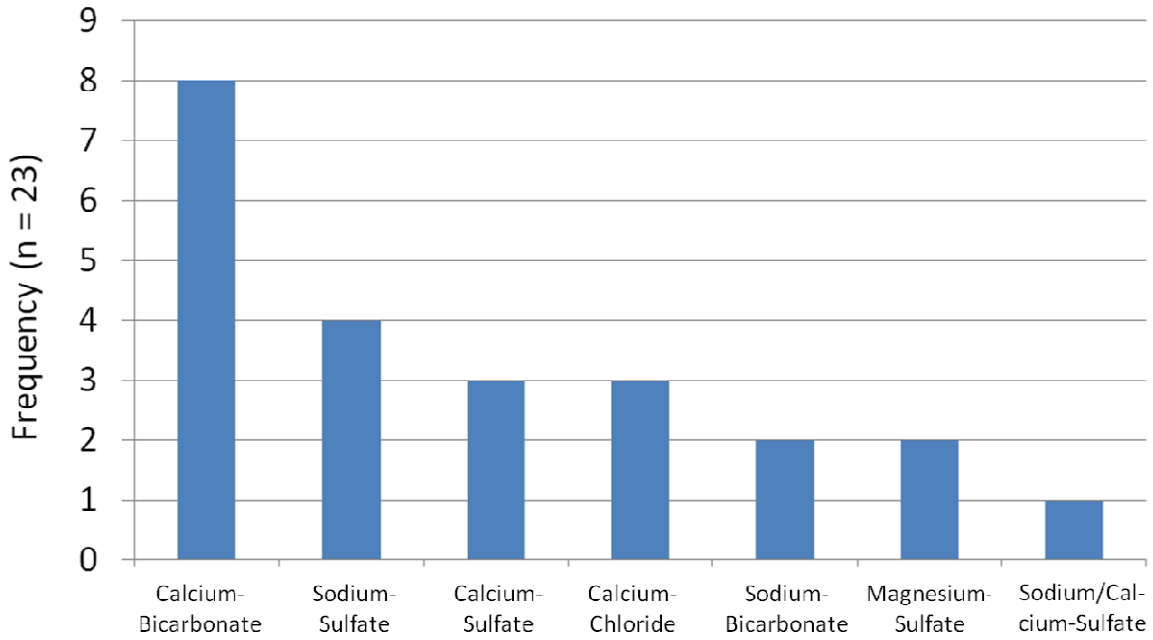

Figure 6-34: Frequency of water types occurring in the MDC based on repeated samplings in spring and autumn 2005 and spring 2007 at 23 sites.

Similar to the results presented in chapter 6.3.1.1 different water types tend to group in distinct areas of the MDC such as the Calcium-Bicarbonate type which is only found outside the Drâa oases. This observation gives a hint on the distribution of hydrochemical zones, which appears to be related to the predefined aquifer units (chapter 6.1 & 6.2).

6.3.1.3 Hydrochemical characterization after Furtak & Langguth (1967)

The hydrochemical characterization after Furtak & Langguth (1967) is based on the diamond plot of the Piper diagram subdivided to seven fields of dominant hydrochemical types. This approach reveals five hydrochemical classes in the MDC (Table 6-32; Figure 6-35).

Table 6-32: Results of the groundwater classification after Furtak & Langguth (1967) for 23 sites in the MDC (repeated sampled in spring and autumn 2005 and spring 2007).

Class after Furtak & Langguth (1967)	Cation type	Anion type	Number of sites
e	Alkaline-earth water with increased alkaline share	Mainly sulfatic	15
d	Alkaline-earth water with increased alkaline share	Mainly bicarbonate	3
a	Alkaline-earth water	Mainly bicarbonate	2
b	Alkaline earth water	Bicarbonate-sulfatic	2
f	Alkaline water	Mainly (bi-)carbonate	1

The seven water samples of bicarbonate type or shared bicarbonate type (Table 6-32: a, d & b) are the same which are classified as fresh water after Davies & De Wiest (1967; chapter 6.3.1.1). According to this the classification after Furtak & Langguth (1967) seems to reflect the distribution of hydrochemical facies in relation to the pre-defined aquifer units too (chapter 6.1 & 6.25.1). The sample, which lies in the field f, is of noticeably different hydrochemical facies than all other samples due its high alkaline share with bicarbonate dominance (pH value of 7.1). This sample and the sample, which plot far below the others in the field d, should be checked for an influence of upwelling water of saline type and high carbon dioxide content.

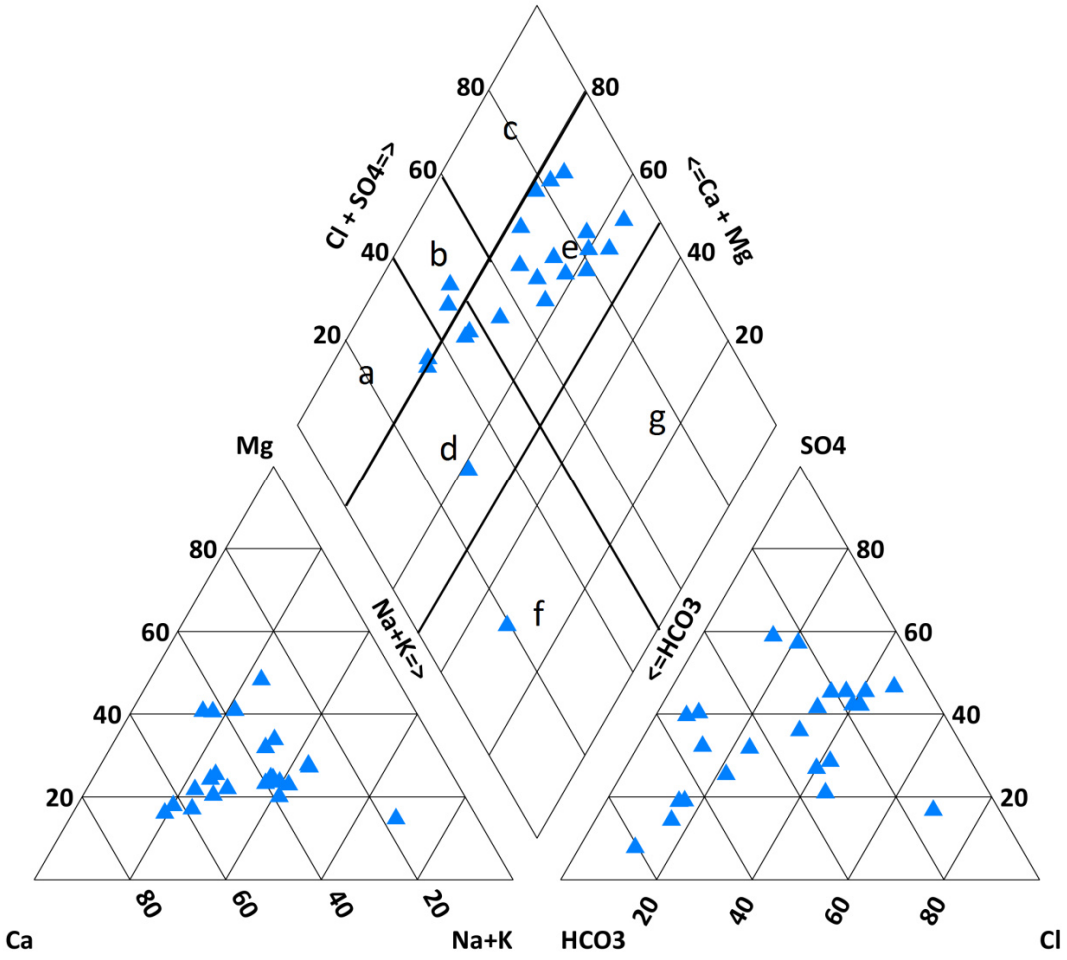

Figure 6-35: Piper diagram with the groundwater classification scheme afte Furtak & Langguth (1967) representing the mean values of inorganic composition of groundwater from repeated samplings in spring and autumn 2005 and spring 2007 at 23 sites; Alkaline-earth water: a = mainly bicarbonate, b = bicarbonate-sulfatic c = mainly sulfatic; Alkaline-earth water with increased alkaline share: d = mainly bicarbonate, e = mainly sulfatic; Alkaline water: f = mainly (bi-) carbonate, g = mainly chloride.

6.3.1.4 Hydrochemical characterization after Back (1960)

The hydrochemical characterization after Back (1960) is based on the Piper-diagram subdivided to eight fields of hydrochemical types. It application reveals basically four hydrochemical classes for the MDC (Table 6-33; Figure 6-36).

Table 6-33: Results of the groundwater classification after Back (1960) for 23 sites in the MDC (repeated sampled in spring and autumn 2005 and spring 2007).

Classes after Back (1960)	Number of sites
Sodium-Potassium Chloride-Sulfate type	14
Calcium-Magnesium Bicarbonate type	7
Chloride-Sulfate type	1
Sodium-Potassium Bicarbonate type	1

The seven water samples of calcium-magnesium bicarbonate type are the same which are classified as fresh water after Davies & De Wiest (1967; chapter 6.3.1.1) and same as classified as bicarbonate type or shared bicarbonate type after Furtak & Langguth (1967; chapter 6.3.1.3). According to this in turn all classifications reflect the distribution of hydrochemical facies in relation to the pre-defined aquifer units (chapter 6.1 & 6.2).

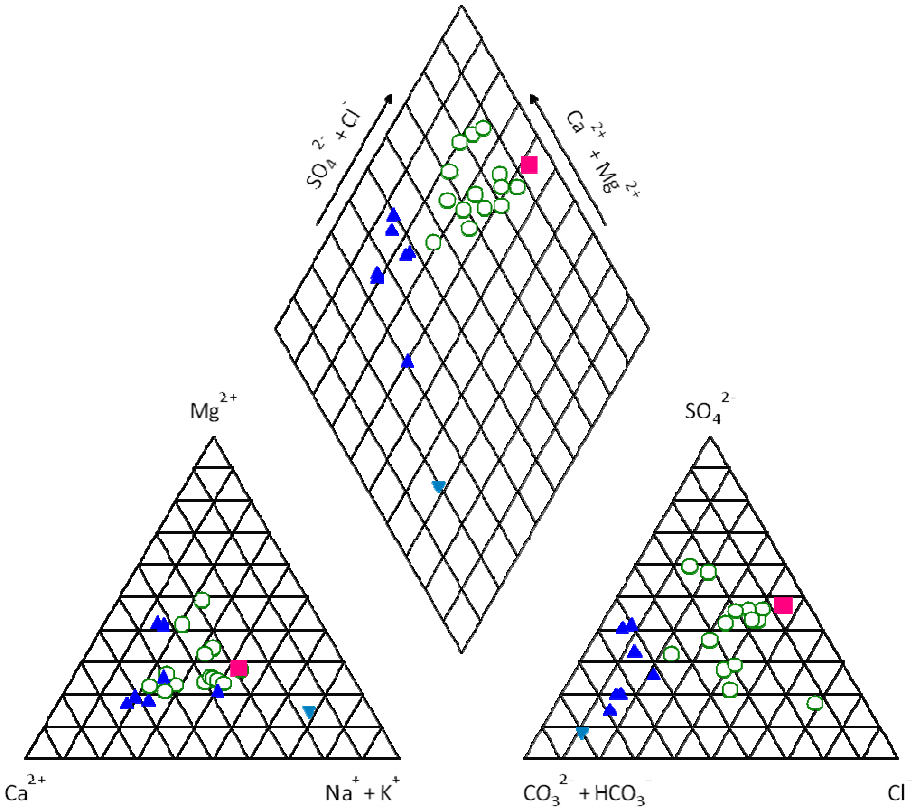

Figure 6-36: Piper diagram with the groundwater classification scheme after Back (1960) representing the mean values of inorganic composition of groundwater from repeated samplings in spring and autumn 2005 and spring 2007 at 23 sites; blue triangles = Calcium-Magnesium Bicarbonate type, hollow green circles = Sodium-Potassium Chloride-Sulfate type, pink square = Chloride-Sulfate type, inverted blue triangle = Sodium-Potassium Bicarbonate type.

6.3.2 Hydrochemical characterization of the hydrogeological units

Knowledge on the groundwater flow system including vertical flows and groundwater stratification is also important when testing the hypothesis that the hydrogeochemical patterns reflect the aquifer structure and the groundwater flow system. In this context, the interpretation of the vertical structure of the shallow aquifers remains incomplete and this study focuses on the horizontal regional structure of the aquifers in the MDC. This is because the vertical resolution of lithological information is sparse (chapter 6.1; 6.2). Most information is drawn from selective bore logs. The groundwater samples represent an effective mixing of water from the respective aquifer unit tapped by the respective well. This is due to the mostly free inflow of water to the wells, which are mainly open boreholes, or dug wells. Even if a multi-layered structure of the aquifer is apparent, the hydrochemical finding can be assumed a mix signal from all groundwater-bearing layers.

6.3.2.1 Groundwater composition of the Tributary aquifers

Groundwater from the Tributary aquifers shows only fresh water of Calcium-Bicarbonate type and the electric conductivity ranges slightly from 570 to 802 µS/cm with a mean of 691 µS/cm (Figure 6-37 & Figure 6-70).

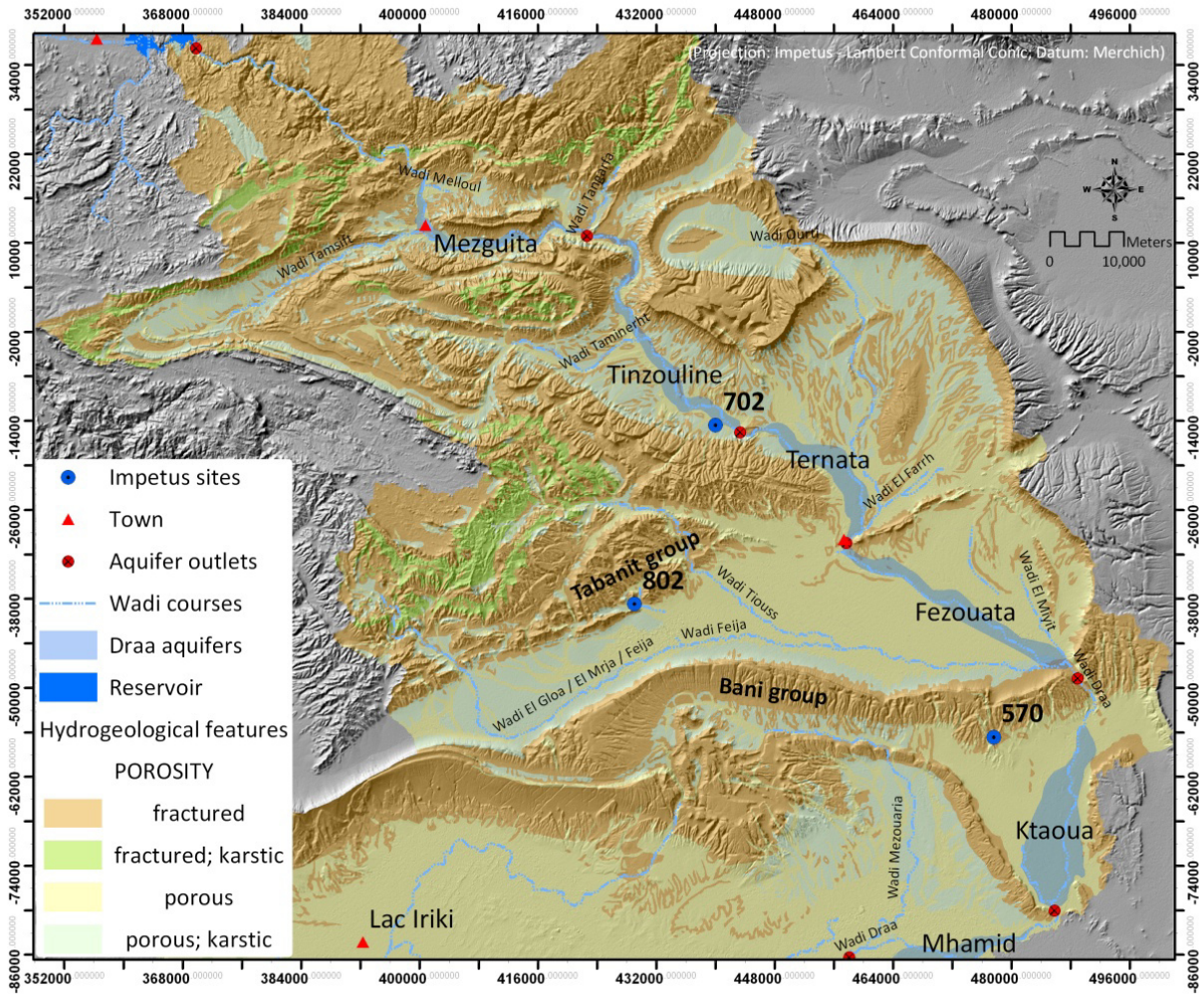

Figure 6-37: Map of the sites tapping the Tributary aquifers with their mean electric conductivity in µS/cm (based on repeated sampling in spring and autumn 2005 and spring 2007).

The hydrochemical facies of the Tributary aquifers are shown in a Piper diagram (Figure 6-38). Two sites reveal approximately the same facies coming from the Cambrian siliciclastic formation of the Tabanit Group (chapter 2.3). The third site plotting more in the upper centre of the Piper diamond plot represents groundwater from a catchment within the Ordovician siliciclastic formation of the Bani I Group (Figure 6-38; chapter 2.3). So, the slight difference in water composition of these three sites can be due to geochemical variations between the geological Groups and enhanced aridity at the site in the Bani group more south (chapter 2.1). More sites would have to be sampled to check the water composition for other influences such as local geochemical variability and residence time.

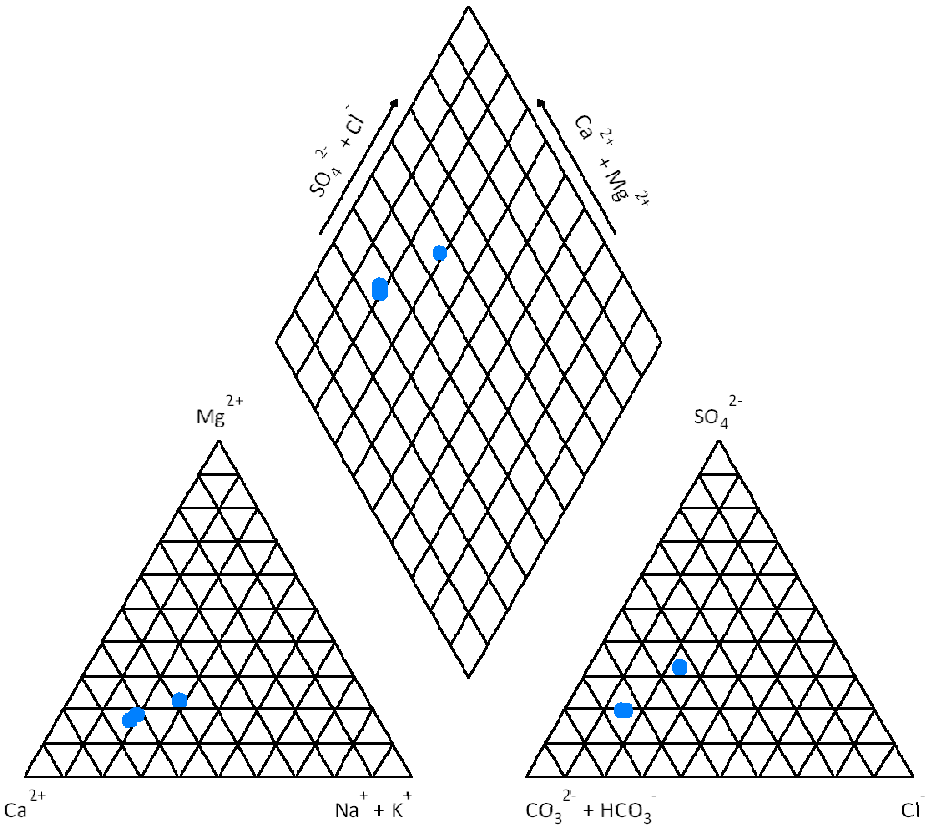

Figure 6-38: Piper diagram of sites in the Tributary aquifers embedded in the Tributary aquifers.

Same as the Piper diagram, the semi logarithmic fingerprint plot reveals both the similarity of the groundwater composition at the three sites and the differentiation of the drains of Tabanit and Bani Group (Figure 6-39). The difference within the class Tributary aquifers is mainly caused by a difference concerning the sodium and the bicarbonate concentration leading to slightly modified ion ratios in relation to the other ions.

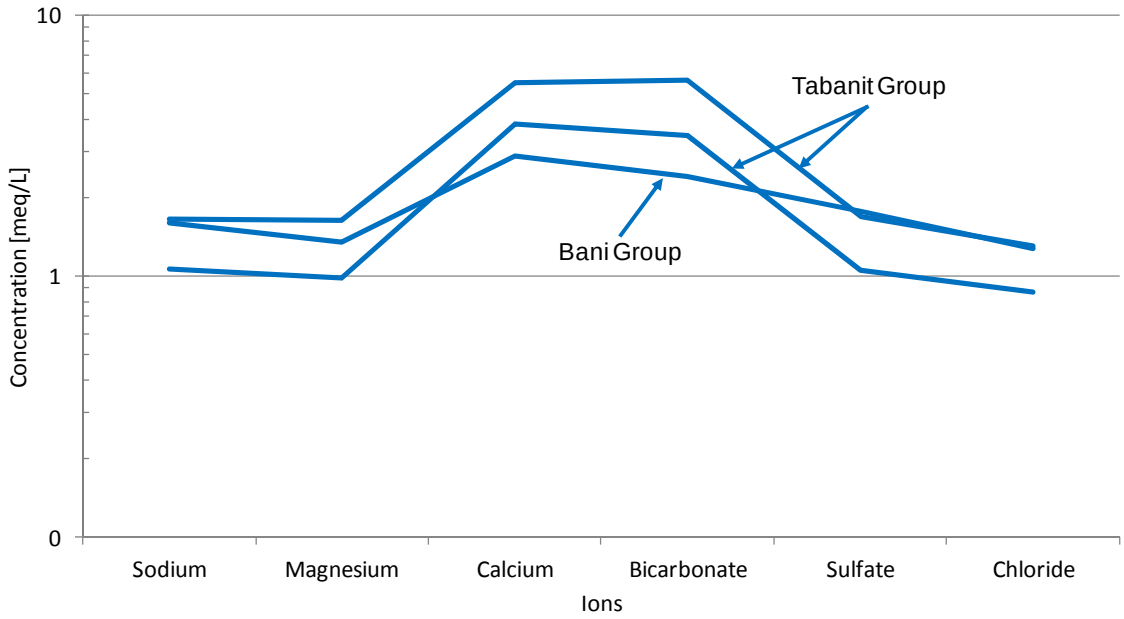

Figure 6-39: Schoeller semi logarithmic diagram of representative sites of the Tributary aquifers draining different geological units as the Cambrian Tabanait Group (quartzitic sandstone and siltstone) and the Ordovician Bani Group (sandstone and siltstone).

6.3.2.2 Groundwater composition in the Fractured aquitards

The groundwater the Fractured aquitards is fresh water of Calcium – Bicarbonate type with a mean electric conductivity of 995 µS/cm excluding an anthropogenically influenced site near the town Zagora and a site influenced by upwelling (Figure 6-40; chapter 6.3.3.5; Figure 6-68). The anthropogenically influenced groundwater is brackish and of Calcium – Chloride type.

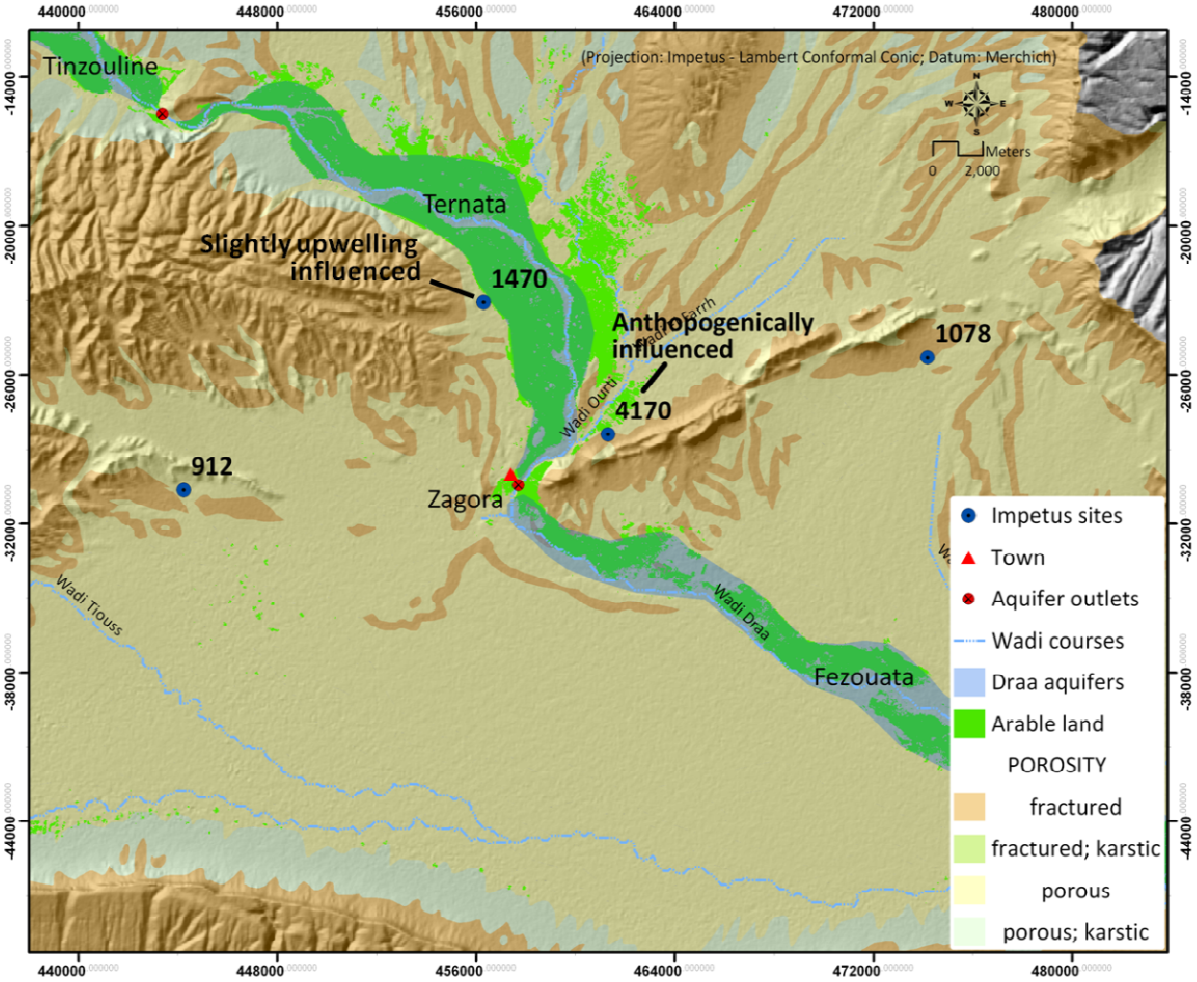

Figure 6-40: Map of the sites tapping the Fractured aquitard with their mean electric conductivity in µS/cm (based on repeated sampling in spring and autumn 2005 and spring 2007).

The water composition from the sites tapping the Fractured aquitard is represented in a Piper diagram (Figure 6-41). The deviation in composition is greatest in terms of anions. So, sulfate and chloride contents may be an indicator for anthropogenic influences and not only the nitrate concentration.

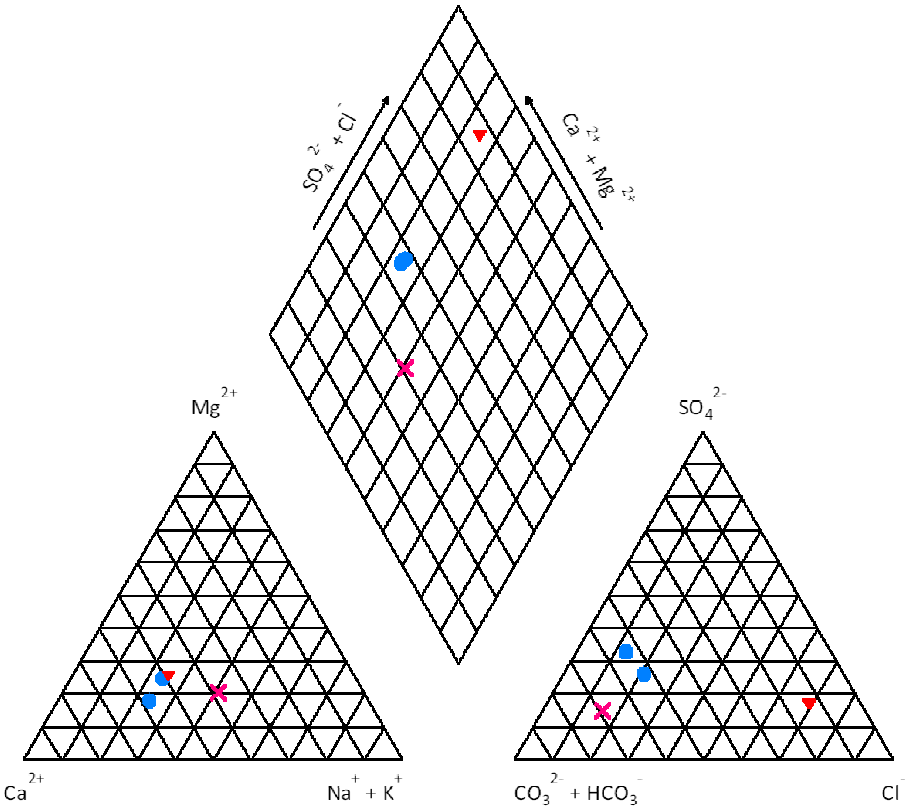

Figure 6-41: Piper diagram of sites tapping direct the Fractured aquitard, colored: geogeneous background = light blue circles, anthropogenically influenced = red inverted triangle, influenced by upwelling = red cross.

The semi logarithmic fingerprint plot of ions (Figure 6-42) illustrates the quasi-background composition of groundwater from the Fractured aquitard as opposed to the anthropogenically influenced water (chapter 6.3.4.2) and a site influenced by upwelling (chapter 6.3.3.5).

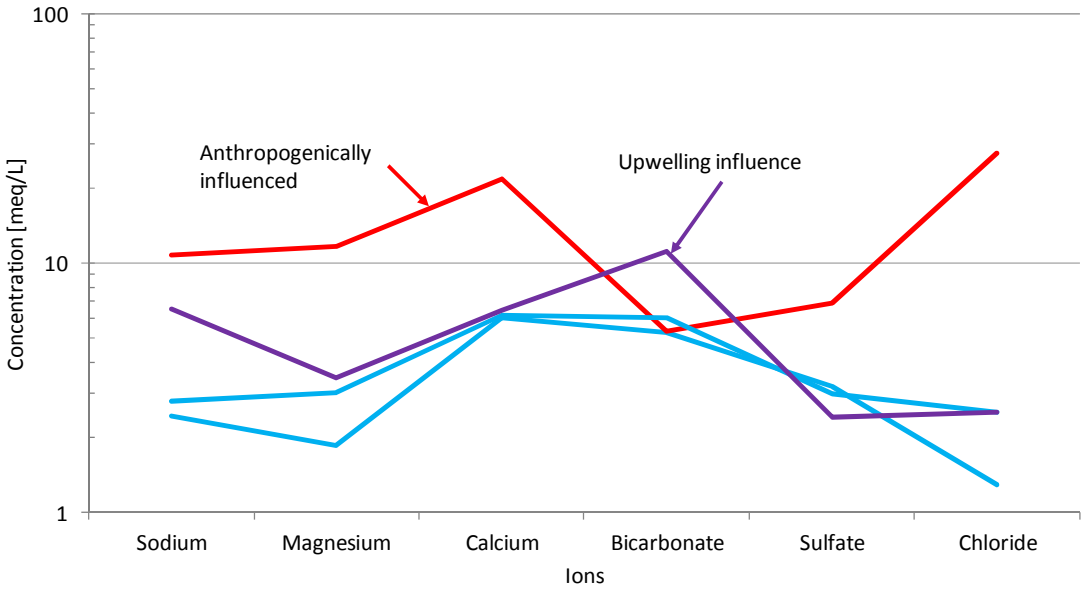

Figure 6-42: Schoeller semi logarithmic diagram of repeatedly sampled sites (spring and autumn 2005; spring 2007) in the Fractured aquitard with outliers influenced by human activity (chapter 6.3.4.2) and upwelling (chapter 6.3.3.5).

6.3.2.3 Groundwater composition in the Basin aquifers

Sites tapping the Basin aquifers reveal various groundwater types caused by a wide range of hydrogeochemical processes and / or varying groundwater flow pattern (Figure 6-48; chapter 6.3.3.3). The groundwater within the Basin aquifers ranges from fresh to brackish water and from 717 to 3120 µS/cm in electric conductivity (Figure 6-43). The groundwater types vary broadly from Calcium – Bicarbonate type to Calcium – Sulfate type, Calcium – Chloride type and Magnesium – Sulfate type. One site with Sodium – Bicarbonate water plays a special role. It is located in a basin east of Ternata but influenced by upwelling and which is not represented here (chapter 6.3.3.5).

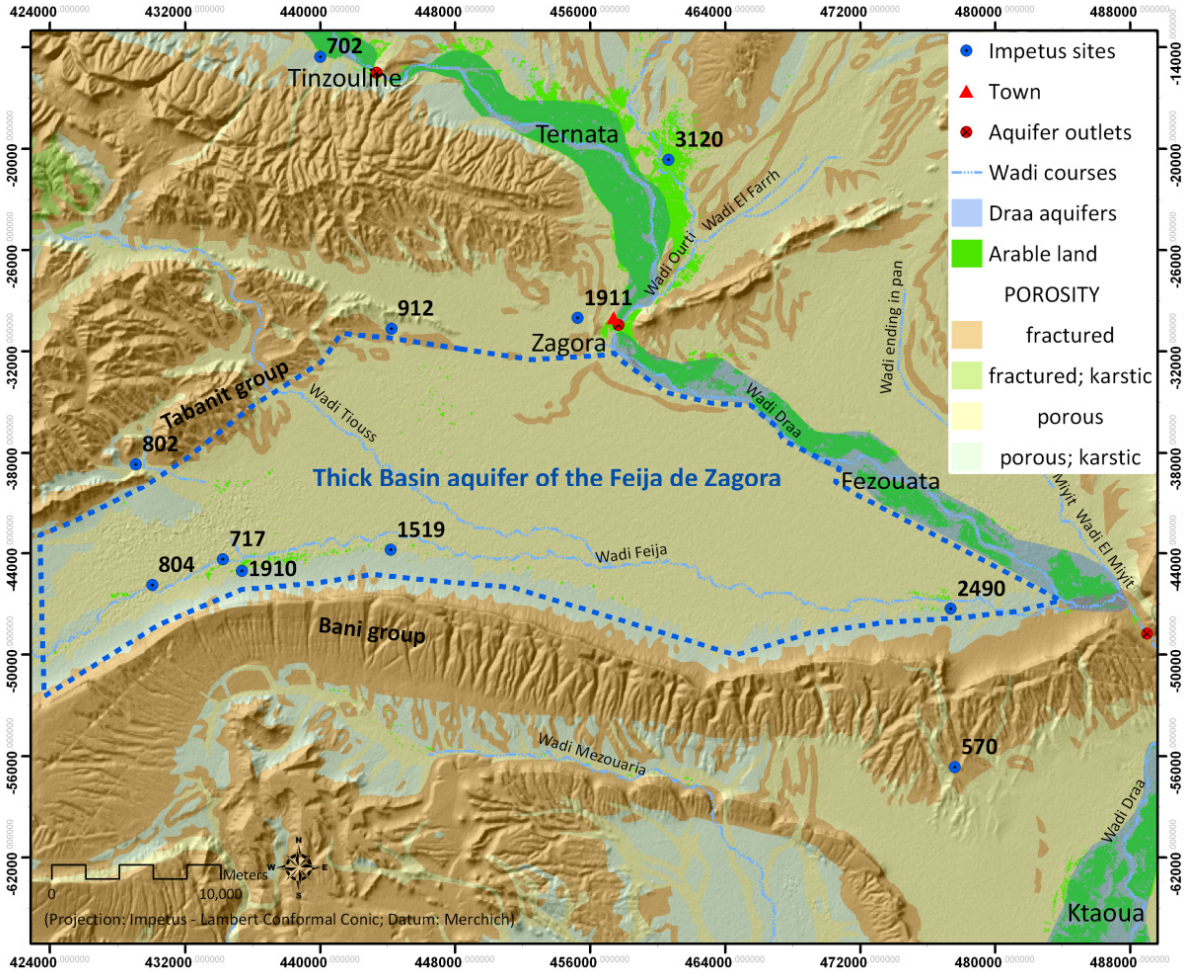

Figure 6-43: Map of the Basin Feija de Zagora with mean electric conductivity in µS/cm at sites repeatedly sampled in spring and autumn 2005 and spring 2007.

The groundwater compositions of the Basin aquifers are shown in a Piper diagram (Figure 6-44). The hydrochemical facies varies strongly within the class of Basin aquifers. There is a subdivision of different basins and along the main hydraulic gradient particularly depicted for the Basin of Feija de Zagora and the Basin of El Miyit (chapter 6.3.3.3, 6.2.2.5 & 6.2.2.6).

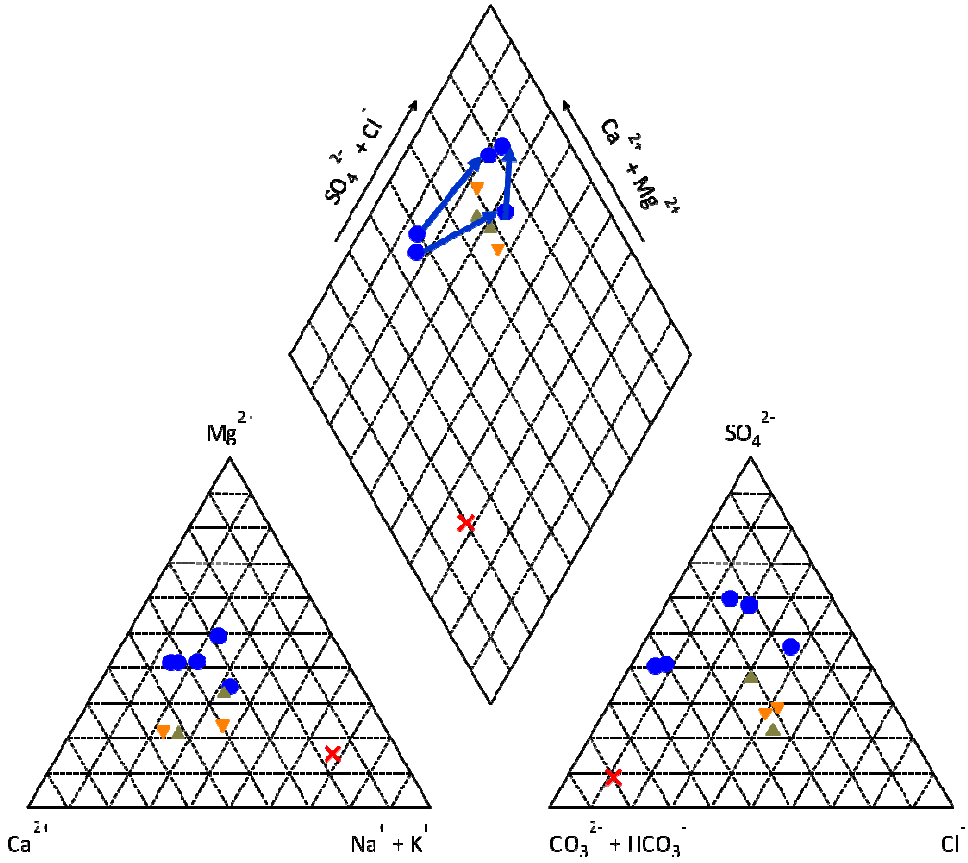

Figure 6-44: Piper diagram of sites tapping direct the Basin aquifers with the outlier influenced by upwelling (red x); blue circles = Basin of Feija de Zagora; yellow inverted triangles = Basin of El Miyit; grayish triangles = Basin NE' adjacent to Ternata; blue arrows = main groundwater flow paths (chapter 6.2.2).

So, the sites located at the outer rim of the Basins are assumed to represent the quasi-background type of groundwater in the pasture area (Figure 6-45). More downgradient along the groundwater flow path locally varying geochemical composition of the sediments and cropping may have an impact on the water composition (chapter 6.3.3.3).

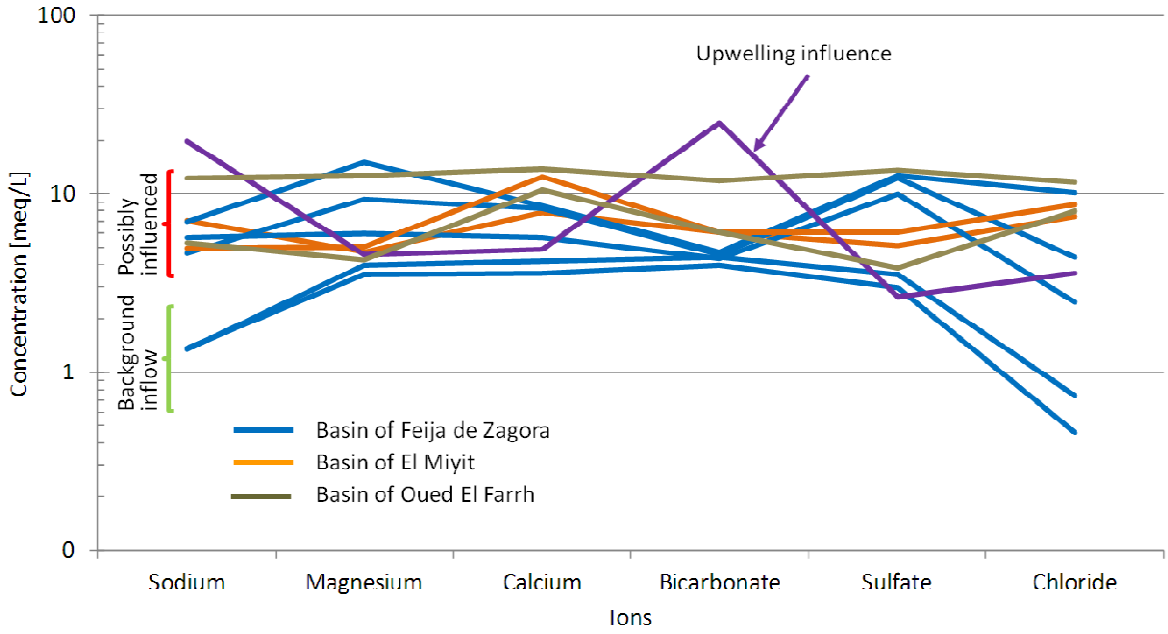

Figure 6-45: Schoeller semi logarithmic diagram of repeatedly sampled sites (spring and autumn 2005; spring 2007) in the Basin of Feija de Zagora, the Basin of El Miyit and the Basin of Oued El Farrh with an outlier influenced by upwelling (chapter 6.3.3.5).

6.3.2.4 Groundwater composition in the Drâa aquifers

The groundwater within the Drâa aquifers is characterized by brackish water of Calcium / Sodium - Sulfate / Chloride and Sodium - Sulfate / Chloride type (dominant cations and anions).

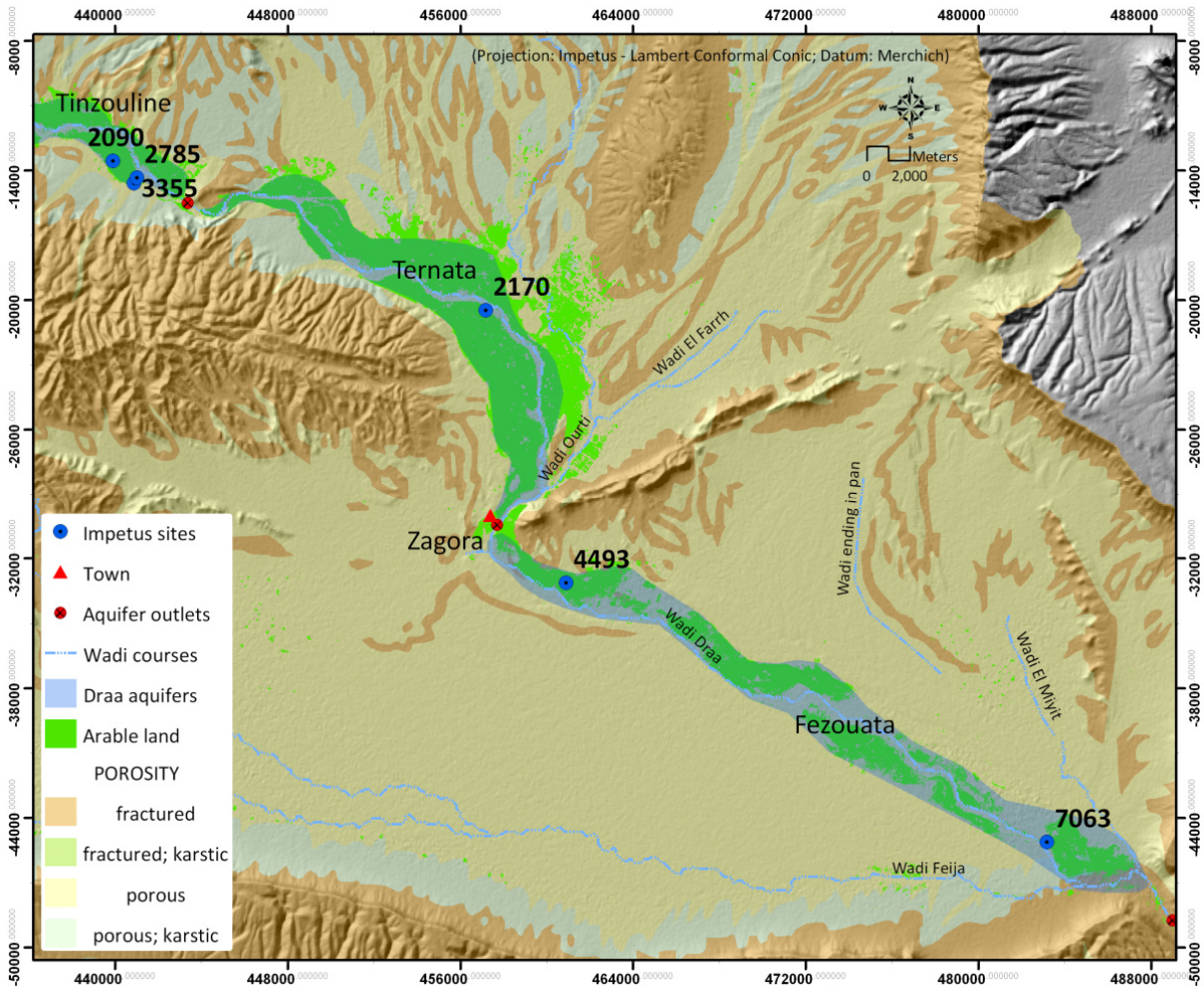

Figure 6-46: Map of the sites tapping the Drâa aquifers Tinzouline, Ternata and Fezouata with their mean electric conductivity in µS/cm (based on repeated sampling in spring and autumn 2005 and spring 2007).

The typical groundwater composition is shown in a Piper diagram (Figure 6-47). It shows a differentiation of the sites outside of the Drâa aquifers as opposed to the sites tapping the Drâa aquifers where irrigation is based on both surface water and groundwater. The sites in the most southern Drâa aquifer considered are within the Fezouata aquifer marked by red squares. They plot near to the right upper rim of the diamond plot revealing medium contents of alkaline earth ions. The lower left end of the group of the Drâa aquifer sites is made up of sites within the Tinzouline and Ternata aquifers (Figure 6-46). So, the hydrochemical facies develops towards higher sulfate and chloride dominance along the main flow path. In the same direction a salinization trend becomes evident along with the increasing aridity of the environment towards the South (see also Figure 6-50; chapter 2.1).

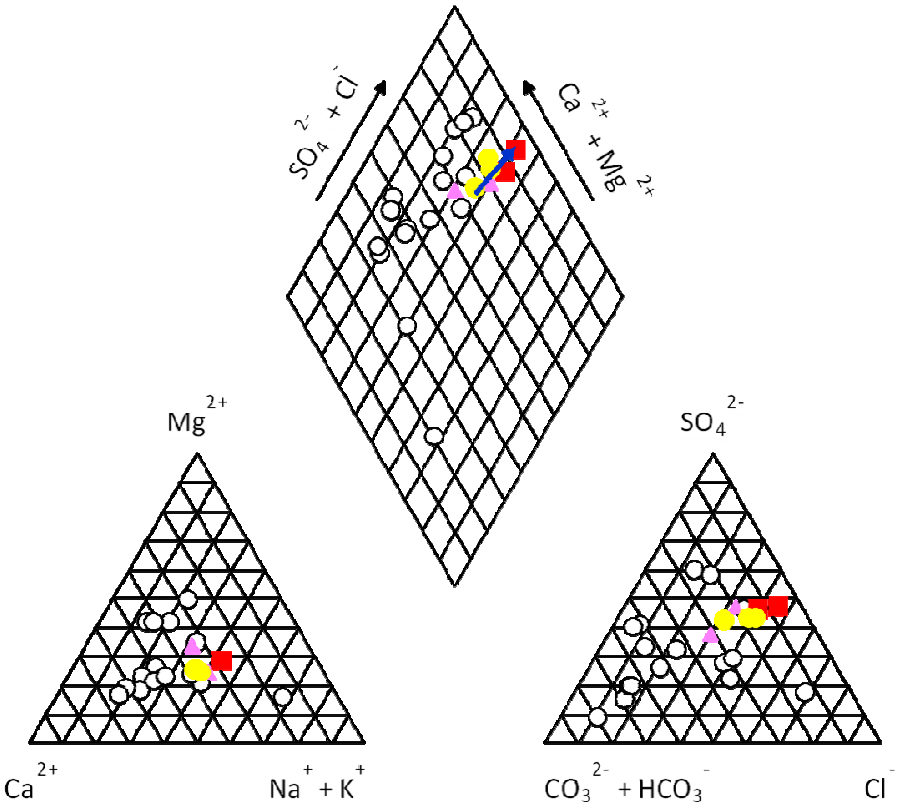

Figure 6-47: Piper diagram for sites tapping the Drâa aquifers colored: Tinzouline aquifer = yellow circles, Ternata aquifer = pink triangles, Fezouata aquifer= red squares, sites outside of Drâa aquifers = open circles; main flow path = dark blue arrow (based on repeated sampling in spring and autumn 2005 and spring 2007 at 23 sites in the MDC).

The hydrochemical facies of the northern Drâa aquifers form a transition to the sites outside of the Drâa aquifers. At this point, the aspect of land use comes into play and overprints the interpretation of the hydrochemical facies, which is only based on the distribution of the aquifer units. As Figure 6-48 shows, there is a separation between the sites in areas of extensive land use (blue circles) and all other plots. The pink triangles mark sites in areas where irrigation agriculture based on groundwater pumpage practiced since less than 20 years. These sites plot in transition to the hydrochemical facies of the Drâa aquifers. As a conclusion, the implementation of irrigation agriculture and groundwater pumping has a significant impact on the hydrochemical facies within less than 20 years. The hydrochemical facies marked with the red cross is clearly anthropogenically influenced as evidenced by an increased nitrate content (chapter 6.3.4.2). The plots marked with a red x stand for sites significantly influenced by upwelling water from deeper zones (chapter 6.3.3.5).

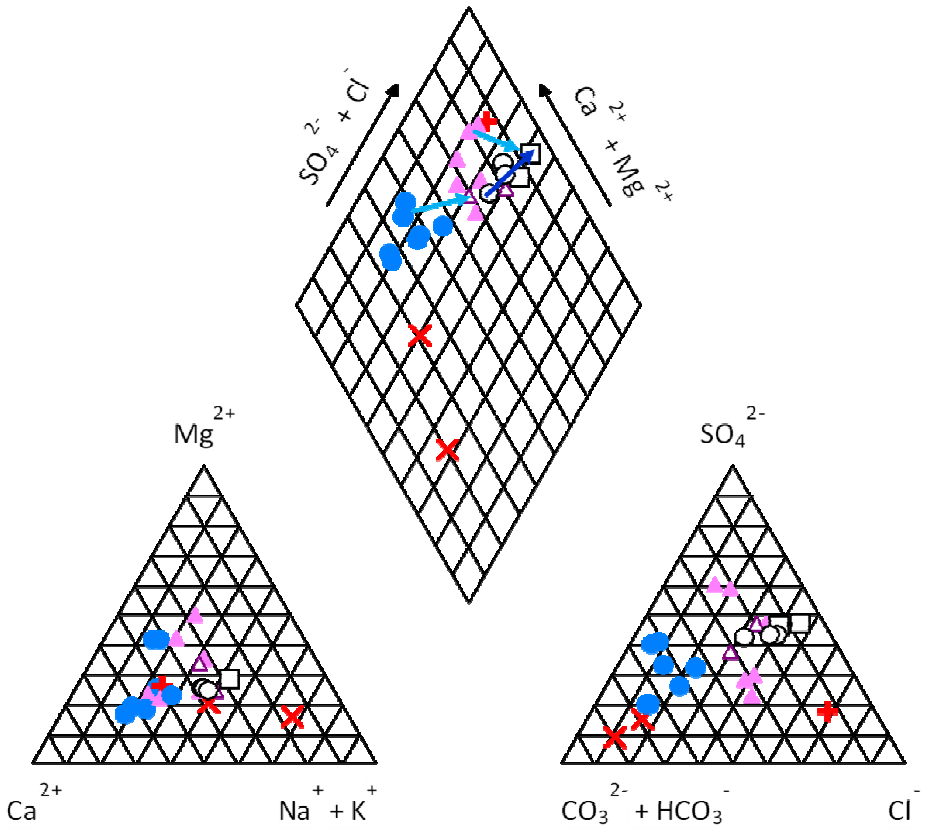

Figure 6-48: Piper diagram for sites outside the Drâa aquifers colored: Extensive land use = blue circles, < 20 years intensive land use = pink triangles, anthropogenic influence = red cross, outliers = red x (chapter 6.3.3.5), sites tapping the Drâa aquifers = open forms; main flow path = dark blue arrow; lateral inflow = light blue arrow (based on repeated sampling in spring and autumn 2005 and spring 2007 at 23 sites in the MDC).

The interpretation of piper diagrams based on the local hydrogeological setting differs as opposed to the characterization after Furtak & Langguth (1967) and Back (1960). So, the consideration of local knowledge on the aquifer setting, main flow path and land use pattern results in the differentiation of the water type e and the Sodium-Potassium Chloride-Sulfate type respectively. This differentiation in turn verifies the delimitation of the Drâa aquifers from the Fractured aquitards, the Tributary aquifers and the upstream parts of the Basin aquifers. The downstream part of the Basin aquifers shows similar hydrochemical facies in comparison with the Drâa aquifers except an increased sulfate content (chapter 6.3.3.3).

The separation between Basin aquifers on the one hand and the Tributary aquifers and Fractured aquitards on the other hand is apparent when comparing the downstream areas of the Basins aquifers to the Tributary aquifers and the Fractured aquitards. For sites located in the upstream parts of the Basin aquifer the distinction against the Tributary aquifer and the Fractured aquitards is not clear. This is due to the lateral inflow from the Fractured aquitards and the Tributary aquifers to the Basins (chapter 6.3.3 & 6.2.2). As a further hypothesis, the impact of irrigation agriculture outside the Drâa aquifers should be visible in the hydrochemical signature in comparison to the pre-developed sites in areas of extensive pasture (chapter 6.3.3).

The groundwater composition within the Drâa aquifers is quite homogeneous. This is shown by a diagram of mean values of inorganic composition of groundwater from two samplings at 3 stations in the

Tinzouline aquifer, two stations in the Ternata aquifer and the two stations in the Fezouata aquifer (from north to south; Figure 6-49).

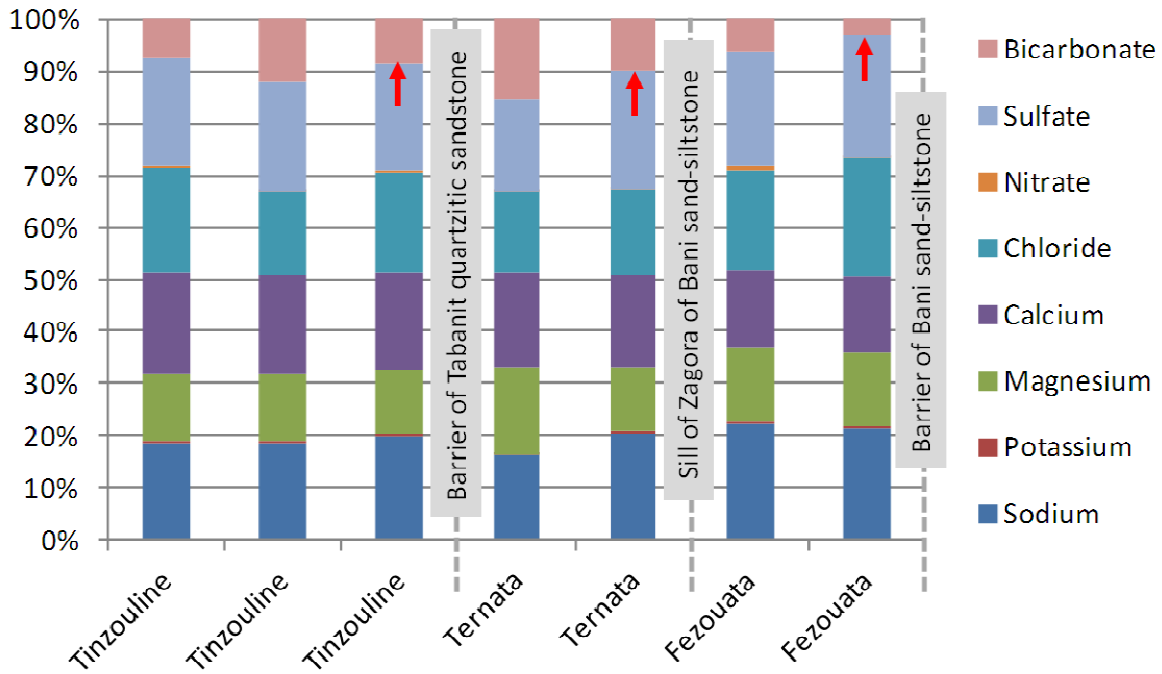

Figure 6-49: Stacked column chart of mean inorganic composition of groundwater from two samplings at 3 stations in the Tinzouline aquifer, two stations in the Ternata aquifer and two stations in the Fezouata aquifer (from north to south); red arrows mark the lowest bicarbonate concentrations at the downstream end of each Drâa aquifer.

Differences show up in respect to the bicarbonate concentration, which appears to be lowest at downstream end of each of the represented Drâa aquifers (Figure 6-49). Overall, the bicarbonate content seems to decrease from north to south, i.e. downstream. This may be due to increasing aridity, which forces calcite precipitation (chapter 6.3.3).

Groundwater salinity increases downstream along the course of the Wadi Drâa due to an increase of all solute constituents indicating evaporation effects and increasing aridity (Figure 6-50). More in detail, in each of the Drâa aquifers increase in salinity is depicted (cf. Bouidida, 1990; Figure 6-49 & Figure 6-50). This is caused by accumulation of solutes in groundwater due to the downstream delimitation of each Drâa aquifer by aquitard outcrops and tectonic lineaments (Figure 6-6).

As salinity increases generally towards the South, a line of hydrochemical separation strikes within the Fezouata aquifer (Figure 6-50). This change in hydrochemical signature can be caused by hydrogeochemical processes within the aquifer and changed inflow conditions (chapter 6.3.2.4 & 6.3.3.3).

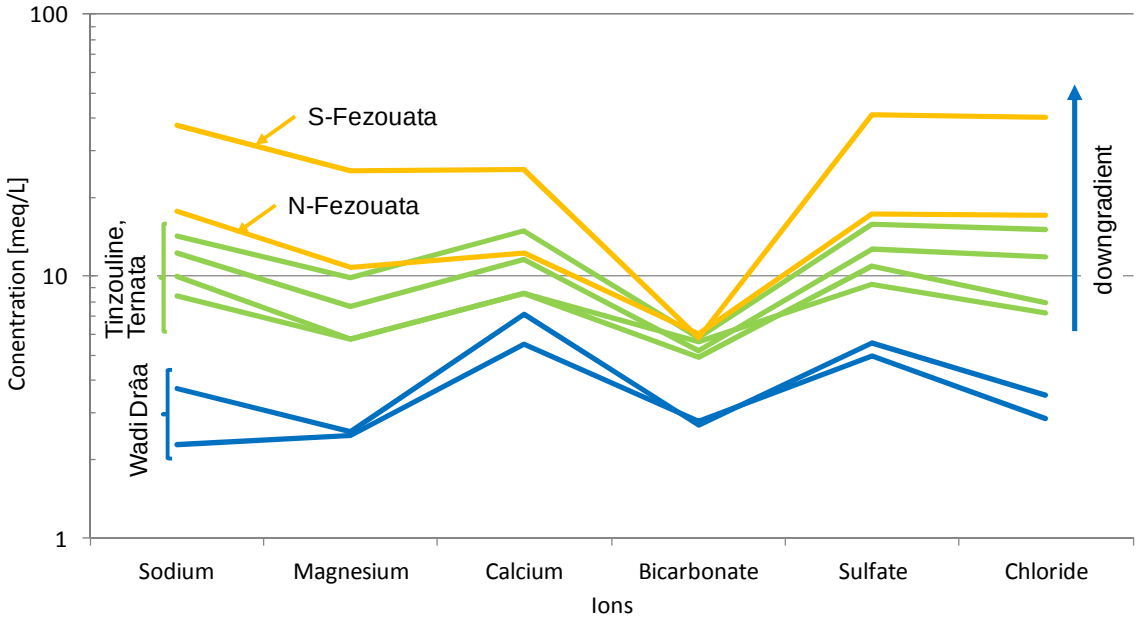

Figure 6-50: Adapted Schoeller plot of mean inorganic composition of groundwater at sites within the Tinzouline, Ternata and Fezouata aquifer sampled in spring and autumn 2005 and spring 2007.

6.3.3 Spatial Groundwater evolution within the hydrogeological units

In the following sections, the dominant hydrogeochemical processes are depicted for the hydrogeological units: Tributary aquifers, Fractured aquitards, Basin aquifers and Drâa aquifers. Symptomatic pathways of groundwater are selected to reconstruct sources of solutes and the groundwater evolution (chapter 6.2.2). The hydrochemical signature is used to characterize and compare the hydrogeological units (cf. chapter 6.3.4). Indicative ion ratios are applied to assess the rock sources referring to water – rock and water – rock – gas interactions. Thermodynamic non-equilibrium states, e.g. of the carbonate-equilibrium-system, indicate short-term changes and may be interpreted as effect of human activity. Uncertainties appear due to the spatially limited 'spot sampling' as local effects of e.g. human activity may bias the interpretation of the hydrochemical facies.

6.3.3.1 Hydrogeochemical processes in the Tributary aquifers

The hydrochemical facies of the Tributary aquifers embedded in the Fractured aquitards is similar to that of the Fractured aquitards itself (chapter 6.3.2.1 & 6.3.2.2). This supports the basic assumption that the Fractured aquitards drain to the Tributary aquifers (chapter 6.2.2). The decreased mineralization of groundwater from the Tributary aquifer in comparison to that from the Fractured aquitards hints on mixing and dilution of water from the aquitards with leaking wadi discharge after rainfall by indirect recharge (Figure 6-51). So, the lumped residence time appears to be shorter in the Tributary aquifers than in the Fractured aquitard. Furthermore, the hydraulic conductivity is higher in the Tributary aquifers.

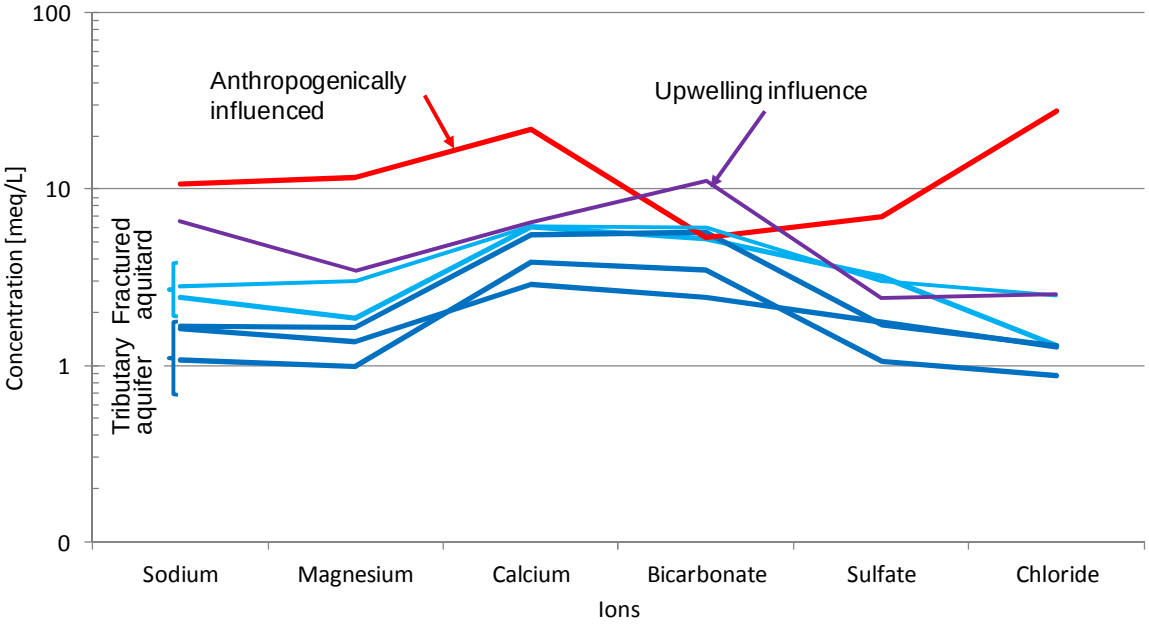

Figure 6-51: Schoeller semi logarithmic diagram of sites in the Fractured aquitard around Ternata and Fezouata and the Tributary aquifers; Fracured aquitard = light blue; Tributary aquifer = dark blue; influenced by upwelling water from deeper zones = violet; anthropogenically influenced = red (Zag 10).

Indicative ion ratios hint on interactions of water – rock and water – rock – gas compartments, which should be comparable to these in the Fractured aquitard (chapter 6.3.3.2).

The equivalent ratio $Ca^{2+}/(Ca^{2+}+SO_4^{2-})$ of >0.5 hints on carbonates and silicates as main sources of calcium ions. The equivalent ratio of $HCO_3^-/(meta)SiO_2$ of >10 hints clearly on carbonate weathering and the equivalent ratio of $Mg^{2+}/(Ca^{2+}+Mg^{2+})$ of <0.5 indicates that the main sources of calcium ions are limestone and dolomite (Table 6-34; chapter 5.3.4). The Ca^{2+}-content originates mainly from the dissolution of the carbonate cement of the slightly consolidated terraces and conglomerates (chapter 6.1.3; Haaken, 2008; Figure 6-52). Another source of the calcium ions may be aeolian calcite deposits in soils (A. Klose, 2009). The weathering of Paleozoic carbonate rocks can provide a source of bicarbonate in groundwater if the catchment of the respective site taps these carbonate rocks even by regional flow systems of the Fractured aquitards (Figure 2-7; Figure 6-1).

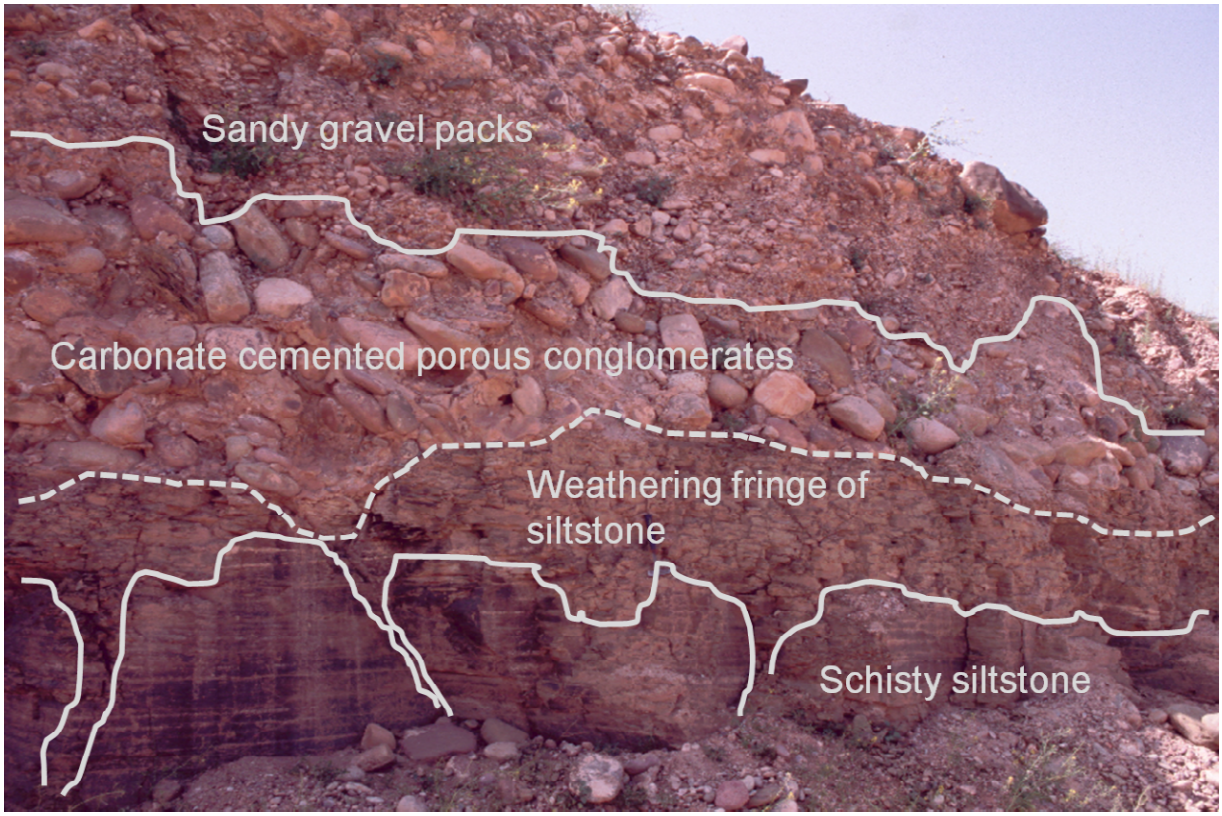

Figure 6-52: Photo of fluvial Quaternary formations near Ouled Yaoub near the southwestern rim of the Tinzouline oasis (Figure 6-33; Photo by K. Haaken).

Cation exchange is clearly pointed out by the equivalent ratio of meta-SiO_2/(Na^+ + K^+ -Cl^-) as Plagioclase weathering is unlikely based on the equivalent ratio of (Na^++K^+-Cl^-)/(Na^++K^+-Cl^-+Ca^{2+}) (Table 6-34). So Sodium mainly comes from cation exchange. Sampling of the Paleozoic Tabanit group of alternating quartzitic sandstone and schisty siltstone from the southwestern rim of the Tinzouline oasis reveals Plagioclase content of around 10 % as X-ray diffraction analysis shows. So, Sodium may come secondarily from albite weathering if the catchments of the sites are open to plagioclase-bearing rocks.

Table 6-34: Selected ion rations to deduce rock sources of solutes in groundwater of the Tributary aquifers.

Ion ratio [meq/L]	Value (range)	Conclusion
HCO_3^-/meta-SiO_2	17 to 24	Carbonate weathering
meta-SiO_2/(Na^++K^+-Cl^-)	0.6 – 0.9	Cation exchange
(Na^++K^+-Cl^-)/(Na^++K^+-Cl +Ca^{2+})	0.06 – 0.07	Plagioclase weathering unlikely

The near equilibrium conditions and slight oversaturation in respect to calcite and dolomite underline the dissolution of carbonate (Figure 6-53; cf. Bakalowicz, 1994). The oversaturation of the site tapping the northern rim of the Feija de Zagora hints on enhanced carbonate dissolution in the catchment zone of this site west of Fezouata (Figure 6-43). This can be caused by relatively long groundwater residence time, a larger catchment in comparison to the other sites and tapping a regional flow system with contact to the Paleozoic carbonate rocks (Figure 2-7; Figure 6-1).

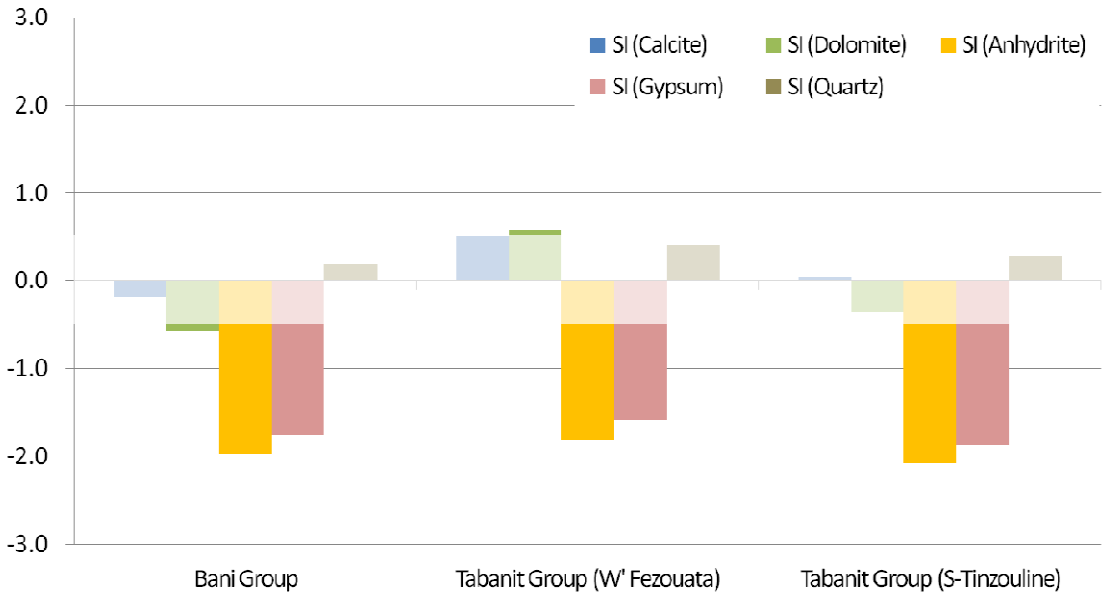

Figure 6-53: Distribution of saturation indices in relation to calcite, dolomite, anhydrite, gypsum and quartz at sites tapping the Tributary aquifers embedded in the Fractured aquitards; the transparent white band marks the thermodynamic equilibrium range of -0.5 to 0.5 after Bakalowicz, 1994.

In conclusion the essential hydrogeochemical processes within the Tributary aquifers are:

- Mixing and dilution of water from the Fractured aquitard with leaking wadi discharge through indirect recharge
- Carbonate weathering (limestone-dolomite weathering)
- Cation exchange

6.3.3.2 Hydrogeochemical processes in the Fractured aquitards

As described in chapter 6.3.3.1 the fractured aquitard reveals very similar groundwater composition in comparison to the Tributary aquifers and the increased mineralization is due to longer residence times within the Fractured aquitard.

The equivalent ratio $Ca^{2+}/(Ca^{2+}+SO_4^{2-})$ of >0.5 indicates that carbonates and silicates have to be the source of calcium ions. The equivalent ratio of $HCO_3^-/(meta)SiO_2$ of >10 hints clearly on carbonate weathering. More in detail the equivalent ratio of $Mg^{2+}/(Ca^{2+}+Mg^{2+})$ of <0.5 means that limestone and dolomite are the main source of calcium ions in groundwater. Although the sand- and siltstones do not contain carbonate in their matrix, fracture fillings are made up of calcite (chapter 6.1.2). X-ray diffraction analysis of the siliceous sedimentary rocks verifies the field observations as all analysis fall below the detection limit for calcite and dolomite in the matrix. The interaction of groundwater and carbonate Paleozoic rocks may have further influence in the MDC. Referring to the catchment area of the sampled sites groundwater can be influenced by dissolution of the carbonate Paleozoic rocks as the formation of regional flow systems is assumed (Figure 2-7; Figure 6-1). Further investigation of the flow systems of the fractured aquitard are needed to verify the assumption of regional flow, residence times and hydrogeochemical influence of the carbonate Paleozoic formations on the sampled sites. Furthermore, the soils have generally high carbonate contents which may be leached particularly under more humid paleo-hydrological conditions (A. Klose, 2009; cf. residence times between 500 and 2,800 years in the Precambrian rocks of the Skoura Mole in the Upper Drâa Catchment, Cappy, 2006).

The equivalent ratio of $(Na^+ + K^+ - Cl^-)/(Na^+ + K^+ - Cl^- + Ca^{2+})$ ranges from 0.05 to 1.66 indicating that plagioclase weathering is unlikely at two of three sites (chapter 5.3.4). One site diverges as it reveals a higher $(Na^+ + K^+ - Cl^-)/(Na^+ + K^+ - Cl^- + Ca^{2+})$ –ratio of 0.4 indicating that plagioclase weathering is possible (Table 6-35). This site is located in the south-west of Ternata tapping the Paleozoic quartzitic sandstone and siltstone series of the Tabanit Group and shows a slight influence by upwelling of water from deeper zones containing e.g. relatively high carbon dioxide concentrations (chapter 6.3.3.5). The upwelling influence causes more intensive weathering of minerals and consequently leads to an increasing mineralization of groundwater downgradient of this site.

Table 6-35: Selected ion rations to deduce the dominant rock sources of solutes in groundwater of the Fractured aquitards.

Ion ratio [meq/L]	Value (range)	Conclusion
HCO_3^-/meta-SiO_2	20 to 54	Carbonate weathering
meta-SiO_2/$(Na^+ + K^+ - Cl^-)$	0.05 – 0.22	Cation exchange

The finding for more aggressive water at the upwelling-influenced 'Tabanit site' west of Ternata is supported by the distribution of saturation indices. So, the groundwater is generally under-saturated in respect to calcite, dolomite, anhydrite and gypsum (Figure 6-54). In particular, the saturation index referring to calcite is within the thermodynamic between -0.5 and 0.5. This equilibrium band is stated by Bakalowicz (1994) indicating that near-equilibrium conditions (-0.5 >> 0.5) must not lead to dissolution or precipitation practically. The oversaturation of groundwater in respect to quartz at the 'Tabanit site' west of Ternata may be interpreted as effect of a relatively long residence time and supports in turn the hypothesis of an influence of upwelling water from deeper zones (chapter 6.3.3.5).

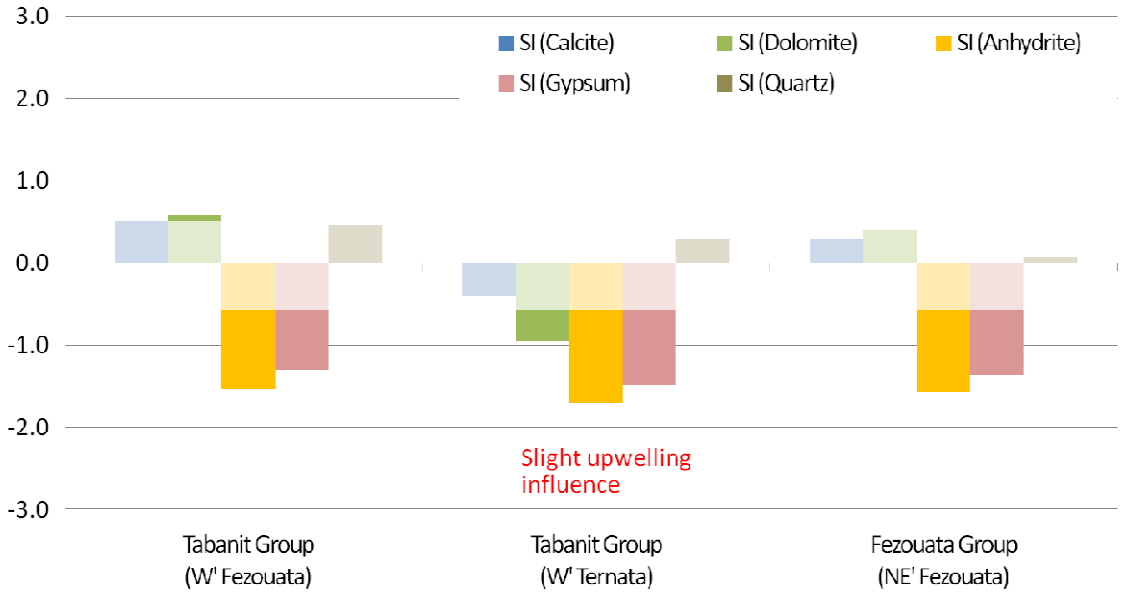

Figure 6-54: Distribution of saturation indices in relation to calcite, dolomite, anhydrite, gypsum and quartz at sites tapping the Fractured aquitards; the transparent white band marks the thermodynamic equilibrium range of -0.5 to 0.5 after Bakalowicz, 1994.

In conclusion the essential hydrogeochemical processes within the Fractured aquitard are:

- Carbonate weathering (limestone-dolomite weathering)
- Cation exchange

6.3.3.3 Hydrogeochemical processes in the Basin aquifers

Groundwater can strongly evolve along the flow lines of the Basin aquifers depending on inflow conditions, water-rock-atmosphere interactions and human activity. As described in chapter 6.1.3, the Basin aquifers connect the fractured aquitards and the Drâa aquifers as mediating unit. The vast flat morphology is partly responsible for smoother hydraulic gradients in the Basin aquifers potentially longer residence times in comparison to the Tributary aquifers (chapter 6.2.2). Two types of Basin aquifers are distinguished in respect to the thickness of the sedimentary deposits. The Thick Basin aquifers are defined as morphological basins containing a sedimentary filling of a mean thickness of more than 10 m (locally adapted classification).

It can be assumed that all Basin aquifers play a similar hydrogeochemical role at the regional scale. High internal heterogeneity in the geogeneous setting and husbandry may lead to bias of interpretation for the local scale. So, two local examples of flow paths are chosen to explain the dominant hydrogeochemical processes in the Basin aquifers:

- Feija de Zagora as “Thick Basin aquifer” with > 10 m of mean thickness of sediments
- El Miyit as “Thin Basin aquifer” with < 10 m of mean thickness of sediments

In contrast to this, the mean thickness of sediments in the Basin of El Miyit account for 3 m ranging from 1.5 to 5 m (based on mapping at 11 wells; Stumpf, 2007; chapter 6.2.2.6).

The **Thick Basin aquifer of the Feija de Zagora** provides an exemplary hydrogeological setting, which is very similar to the Drâa aquifers, i.e. the Basin is flanked by Cambrian sandstone series (Tabanit Group) at one site and by Siluri-Ordovician siltstone-sandstone series (Bani Group) at the other site (Figure 6-43; chapter 2.3 & 6.1.3). Quaternary sediments occur in the Basin of Feija de Zagora revealing a mean thickness of around 20 m ranging from 2 to 54 m (based on 40 bore logs from the Service Eau Ouarzazate; chapter 6.2.2.5). The land use is apparently different in contrast to the Drâa aquifers as pasture is dominant interrupted by patches of arable land mainly depending on the distribution of loamy soils (A. Klose, 2009).

The Schoeller semi logarithmic plot of the sites in the Basin of Feija de Zagora shows spatially different hydrochemical fingerprints for the sites from the northern rim (Tabanit Group), the southern rim (Bani Group) and along the main drain of the Basin (Wadi Feija, basin sediments, Figure 6-55). As lateral inflow from the Fractured aquitard towards the Basin can be assumed, groundwater from the Tabanit Group and the Bani Group contribute slightly different water composition to the Feija de Zagora. The groundwater compositions along the Wadi Feija reveal different water types in comparison to the inflow components and have higher mineralization and larger variety. So, mixing and /or groundwater evolution can be assumed for the flow path within this Basin aquifer (chapter 6.3.3.3). The three groups of groundwater compositions are named according to their spatial distribution (Figure 6-51):

- “Bani sandstone” is found in the southern rim and western part of the Feija de Zagora.
- “Tabanit sandstone” is found at the northern rim.
- “Feija sediments” is found within the basin and along the Wadi Feija

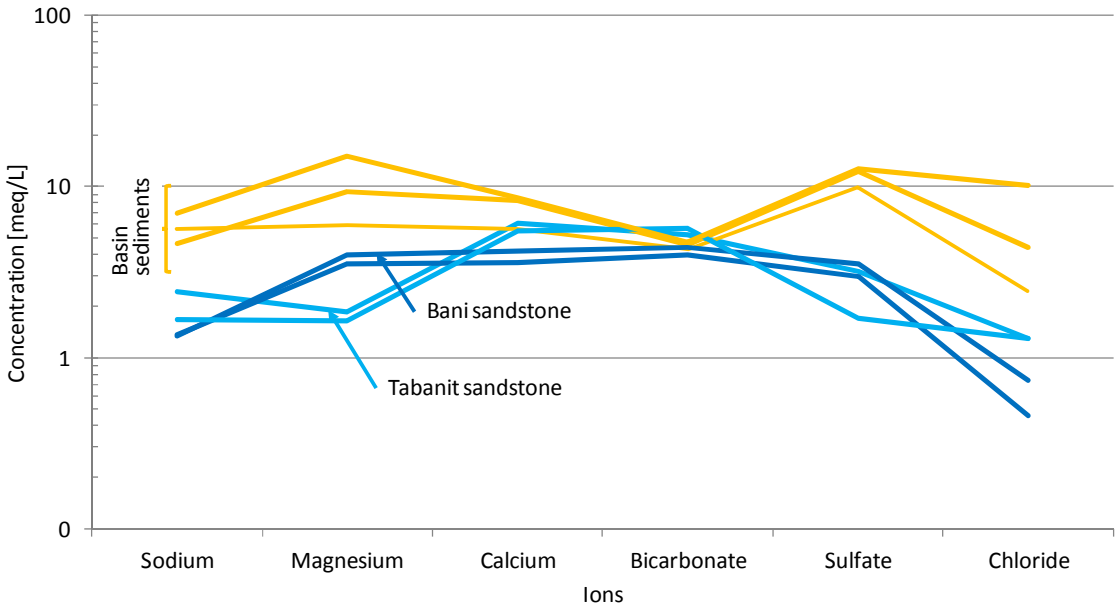

Figure 6-55: Schoeller semi logarithmic diagram of repeatedly sampled sites (spring and autumn 2005; spring 2007) in the Basin aquifer of the Feija de Zagora reveal three groups of groundwater composition reflecting different hydrochemical zones according to groundwater gradients: "Bani sandstone" influenced by western and southern inflow; "Tabanit sandstone" influenced by northern inflow; "Basin sediments" (calcite precipitation and gypsum / anhydrite dissolution probable).

So, "Bani sandstone" and "Tabanite sandstone" are end members of mixing. Freshly percolating water mainly from indirect recharge and irrigation return flow may be further end members in the mixing system of the Basin aquifers.

After a relatively short distance to the rim of the Basin of Feija de Zagora, the dolomite weathering becomes dominant in comparison to the limestone-dolomite weathering along the lateral inflow to the Basin (chapter 6.3.2.1 & 6.3.2.2). This can be seen in the equivalent ratio of $Mg^{2+}/(Ca^{2+}+Mg^{2+})$ of 0.5 in combination to an equivalent ratio of $HCO_3^-/(meta)SiO_2$ of >10. This finding is verified by the development of the saturation indices in respect to calcite and dolomite along the main flow path in the aquifer of the Feija de Zagora (Figure 6-56). So the groundwater becomes oversaturated in respect to calcite and dolomite after a passage of few kilometers in the Basin aquifer. If dolomite can precipitate practically depends on the thermo-dynamic equilibrium with calcite, which forms first. The precipitation of dolomite may happen locally if enough calcium ions remain in groundwater (molar ratio of Mg^{2+}/Ca^{2+} >5, depending on further system conditions as temperature and pH-value; Folk & Land, 1975). The source of calcite and dolomite are the partly evaporitic lacustrine Quaternary sediments, the older Quaternary carbonate cemented terrace sediments and the recent evaporitic pan sediments being leached due to localized recharge and irrigation return flow (as described below for the Basin of El Miyit; cf. Figure 6-57 & Figure 6-58 & Figure 6-59). Further downstream the findings are ambiguous as for the upstream part of the Basin of the Feija de Zagora, because of local effects of intensive agriculture, a multi-layered aquifer structure and a heterogeneous geochemical setting. Locally the ratio $Ca^{2+}/(Ca^{2+}+SO_4^{2-})$ of 0.5 indicates that the main source of calcium ions is the dissolution of gypsum. The development of the saturation indices in respect to gypsum verifies changing conditions of gypsum and anhydrite weathering along the main hydraulic gradient (Figure 6-56). The gypsum dissolution appears to be the dominant process in the whole of the Basin aquifer probably depending on the occurrence of anhydrite and gypsum. Gypsum occurs in the evaporitic lacustrine Quaternary deposits and in recent evaporitic pans (cf.

Figure 6-58). In the Upper Drâa Catchment, de-dolomitization is observed caused by gypsum dissolution (Cappy, 2006). This can be excluded in the Basin aquifers because a typical molar ratio of $Ca^{2+}/Mg^{2+} > 1.3$ and at the same time a molar ratio of Mg^{2+}/SO_4^{2-}magnesium of 0.4 is not found (cf. Kuells, 2000).

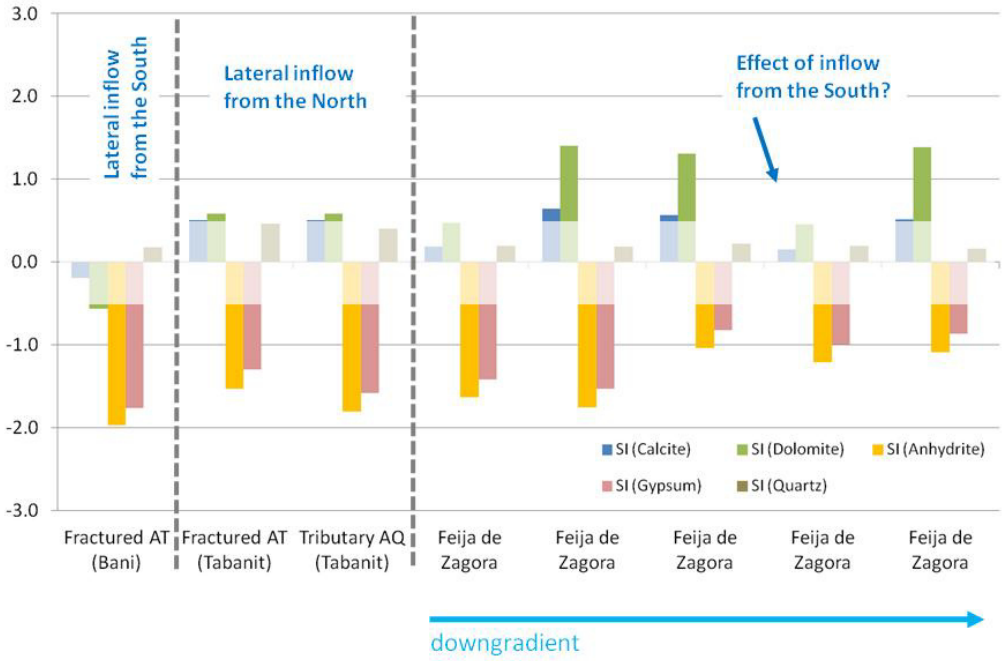

Figure 6-56: Distribution of saturation indices in relation to calcite, dolomite, anhydrite, gypsum and quartz along the main flow path in the Thick Basin aquifer of the Feija de Zagora including the lateral inflow (Figure 6-43); the transparent white band marks the thermodynamic equilibrium range of -0.5 to 0.5 after Bakalowicz, 1994.

The hydrogeochemical processes change in dominance along the flow path through the Basin of the Feija de Zagora as a Thick Basin aquifer (chapter 6.1.3). In conclusion, the basic groundwater evolution can be grouped to upstream processes and downstream processes. In the upstream part the following processes dominate:

- Mixing and dilution with inflow from the Tributary aquifers and the Fractured aquitard (at the rim of the Basin)
- Dolomite weathering
- Gypsum dissolution (locally)
- Cation exchange

The following processes dominate in the downstream part:

- Gypsum dissolution (locally)
- Calcite precipitation
- Cation exchange

In the **Thin Basin aquifer of El Miyit** provides another example for accentuated groundwater evolution in the Basin aquifers (Figure 6-58). Leaching of the lacustrine deposits has a significant influence on

groundwater composition. X-ray analyses of the lacustrine sediments in the downstream part of the basin reveal contents of evaporitic minerals (e.g. bassanite) up to 70 %. Dissolution processes increase downstream of irrigated areas because of enhanced leaching by return flow as observed in the affluences of the oases Fezouata. So, agricultural activity intensifies natural salinization of groundwater in the Basin aquifers. An increase in sulphate concentration downstream of irrigated fields of El Miyit points to enhanced leaching of gypsum and anhydrite by intensified by irrigation. This hypothesis is mainly based on a detailed field survey carried out in spring 2007 (Stumpf, 2007). Accordingly, the signature of stable water isotopes in groundwater indicates an increasing evaporation effect along the hydraulic gradient in the plain of El Miyit in comparison to the LMWL (Local Meteoric Water Line; Figure 6-57). The smoother slope of the regression of the signature of stable isotopes in groundwater represents the evaporation effect. Even if the precipitation signature is scattered the clear plot of the the groundwater sampled along the hydraulic gradients provides robust proof.

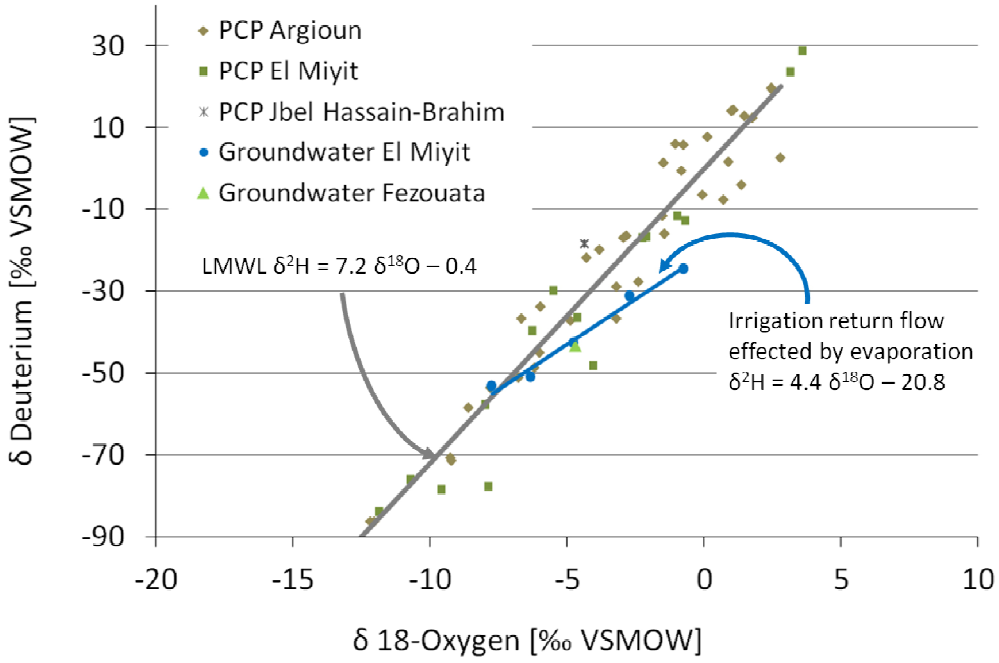

Figure 6-57: Stable isotopic signature of precipitation (PCP) from diverse stations and groundwater from El Miyit Basin (blue circles) and the in the southern part of the Fezouata aquifer (green triangle): grey line = LMWL (Local Meteoric Water Line; grey line), blue line = regression of groundwater along the main flow path in the El Miyit Basin representing the effect of irrigation return flow which is effected by evaporation during flood.

The evaporation is assumed to be enhanced in the last 20 to 25 years. This hypothesis is supported by several findings. The stable isotope signature of groundwater upstream and outside of the cropping area shows no influence of evaporation and lower sulfate concentrations. Groundwater is too deep to have an effect of direct evaporation from the aquifer because capillary rise is not possible (mean depth to groundwater was 14 m based on nine observations in spring 2007). According to oral communication of inhabitants, depth to groundwater never rose higher than 5 m since the early 1980-ties when cropping was introduced. So it can be assumed that even in humid periods the groundwater depth would not fall below 5 m considering that the mid of 1980-ties represent a distinct humid period (chapter 6.2.1). Evapotranspiration of quasi-natural vegetation appears to play a minor role in comparison to the irrigated crops. Scattered Acacia trees are almost the only groundwater consuming vegetation taking up a rela-

tively little amount of water (Weber, 2004; Gresens, 2006; Fritzsche, 2010). In conclusion, to this the evaporation effects are caused by irrigation reflux of pumped groundwater considering that flood irrigation is applied. Flood irrigation is very water consuming in comparison to other irrigation techniques such as drip irrigation and allows a high amount of water both to percolate and to evaporate due to downtimes of hours upon the fields. The irrigation wells are approximately lined up along the groundwater gradient (Figure 6-24; Figure 6-58). So water from the irrigation reflux can flow again downstream and can be pumped several times while being influenced by evapotranspiration each time used for irrigation (cf. Stumpf, 2007). The irrigation reflux dissolves minerals, in particular gypsum, and assimilates soluble constituents (Figure 6-58). Under natural conditions groundwater recharge and percolating water amounts to be much lower than under irrigation agriculture. As a result, irrigation is a reason for enhanced gypsum leaching in the plain of El Miyit depending on the occurrence of gypsum in the vadose zone and irrigation agriculture since the 1980-ties. The volume of groundwater taking part in the irrigation induced cycling is assessed for the main flow path in the Basin of El Miyit based on own field observations and surveying (cf. Stumpf, 2007, Heidecke 2009). So, the pumping rate amounts to 4 to 6 L/sec, i.e. around 18 m^3/h. Farmers pump groundwater at around 150 days/year (main agricultural season) and two times per day for around two hours as possible. That means that the annual pumping rate per well is about 10,000 to 11,000 m^3. Assuming a recharge coefficient of around 2.7 % (chapter 6.2.4) nearly 300 m^3/a may re-percolate from an irrigation well to the aquifer in the Basin of El Miyit.

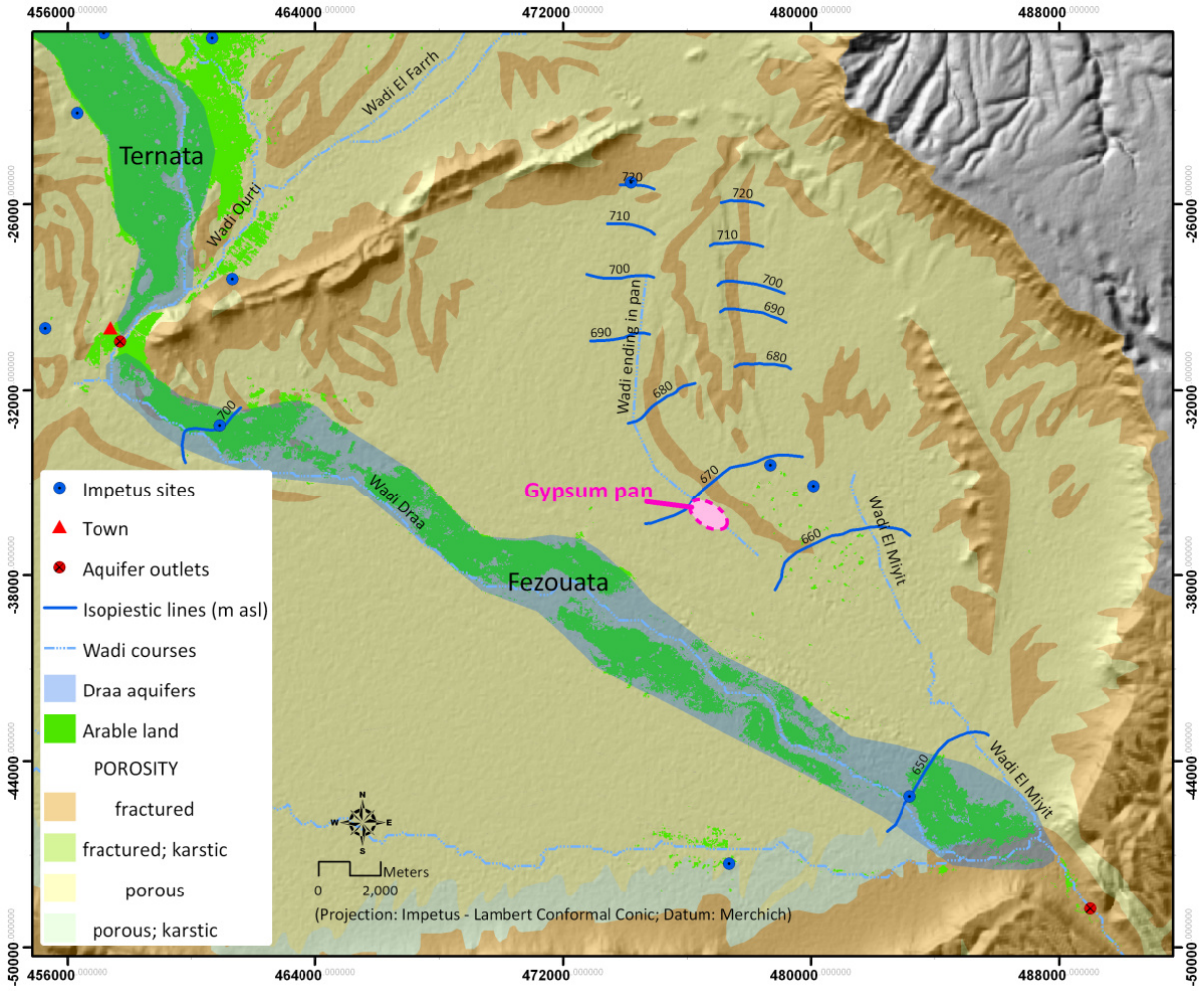

Figure 6-58: Map of manually designed groundwater level contours along the wadi El Miyit and in the Fezouata based on manually observed groundwater levels at 39 wells in April 2007; red oval marks a gypsum pan in the plain of El Miyit.

The evaluation of hydrogeochemical data based on sampling in spring 2007 provides further proofs for this conclusion. Along the groundwater gradient, the saturation indices in respect to gypsum and anhydrite show under-saturation in the upstream area of the irrigation well field and the gypsum outcrop (Figure 6-59). When groundwater passes this area, the saturation indices reveal equilibrium state in respect to gypsum and anhydrite. The increase in saturation indices in respect to calcite and dolomite supplement the hypothesis of leaching of gypsum and anhydrite, which leads to a surplus of calcium and magnesium ions, which in turn can lead to precipitation of calcite and eventually dolomite (Figure 6-59). The precipitation of minerals e.g. calcite can lead to a reduction of the effective porosity and aquifer storage capabilities, which play a major role for measures such as, managed aquifer recharge.

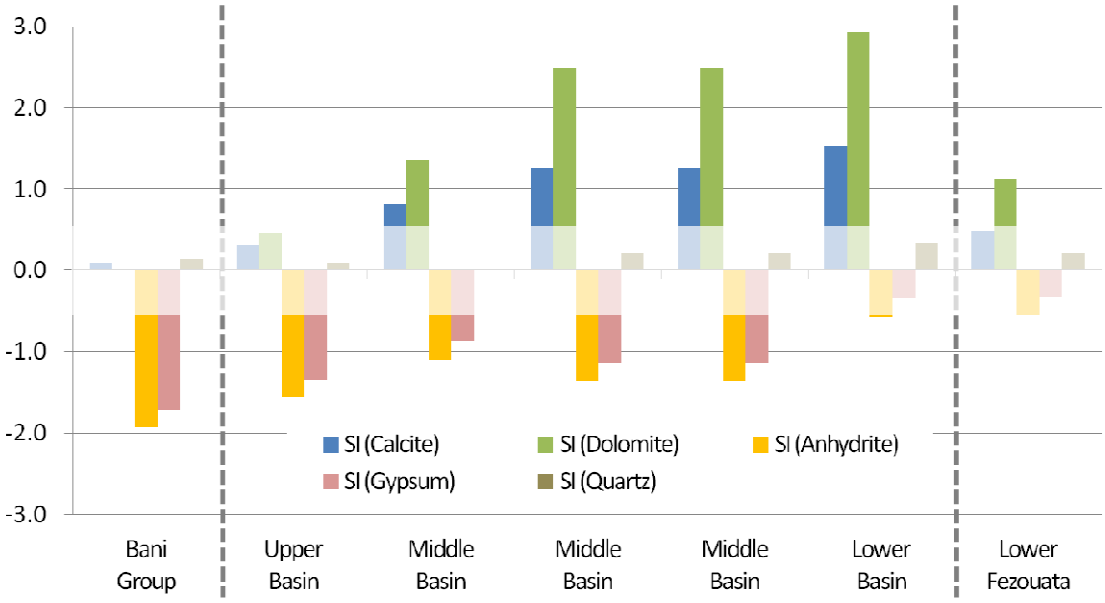

Figure 6-59: Saturation indices in respect to calcite, dolomite, anhydrite, gypsum and quartz along the main hydraulic gradient in the El Miyit Basin in spring 2007.

The groundwater evolution along the main flow path of the El Miyit Basin is also observed based on the mean values of repeated hydrochemical analysis (sampling in spring and autumn 2005 and spring 2007). So the development of the saturation indices in respect to calcite, dolomite, anhydrite, gypsum and quartz reveal broadly the same hydrogeochemical processes as described into detail for spring 2007 (Figure 6-60).

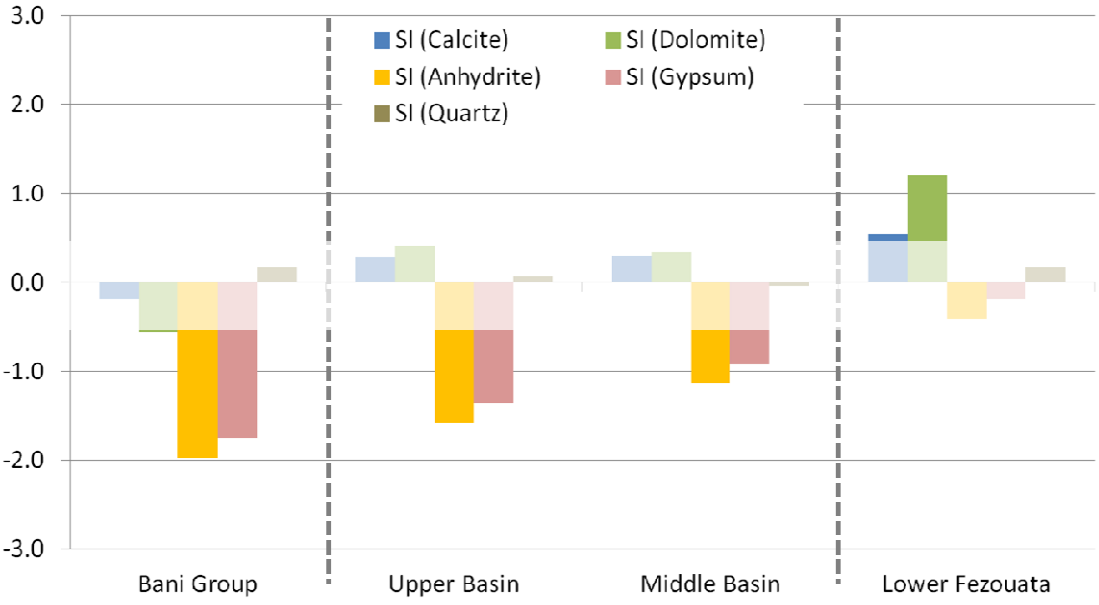

Figure 6-60: Saturation indices in respect to calcite, dolomite, anhydrite, gypsum and quartz along the main hydraulic gradient in the El Miyit Basin based on repeated sampling in spring and autumn 2005 and spring 2007.

Further evaluation of the stable isotopes reveals that the groundwater in the Plain of El Miyit is probably a mix of paleo-water depleted signature in stable isotopes and inflow from recent recharge. The altitude of the recharge area is about 1,749 m asl (±50 m) based in 2005 and 2007 (Stumpf, 2007). The surround-

ing highest mountain is the Jbel Bani reaching a mean altitude of about 1,100 m asl. Consequently, the depleted signature in stable isotopes cannot solely come from recent groundwater recharge. An influence of infiltrated water from the Wadi Drâa is excluded because of the far distance to the Wadi Drâa and hydraulic gradients towards the Fezouata aquifers (chapter 6.2.2.7). In conclusion, the depletion in stable isotope signature is due to an inflow of paleo-water recharge during a cooler climate in Quaternary. This is in accordance to groundwater dating in the Anti-Atlas Mountains revealing groundwater residence times of up to 3,000 years (Cappy, 2006).

The estimated flow velocity in this area accounts roughly for 1 to 1.5 km/a (chapter 6.2.2.6). So, at first stagnant groundwater seems to be negligible as a reason for increased residence time and enhanced mineralization due to water-rock interactions. It cannot be excluded that an internal stratification of groundwater exists, which is not detected because samples were taken as mix samples from the wells (no depth-oriented sampling). In areas of enhanced irrigation, return flow density driven mixing in the aquifer can be assumed. An internal stratification of less mineralized groundwater overlaying higher mineralized groundwater is conceivable as a result from stagnant water in front of the Jbel Bani, which is a hydraulic barrier at the lower end of the Fezouata aquifer. Further interpretations are not possible because of the lack of depth-oriented hydrochemical data, groundwater age data and more detailed geohydraulic information.

In conclusion, various hydrogeochemical processes determine the groundwater evolution within the Thin Basin aquifer of El Miyit. In the upstream part and at the rim of the basin the following basic hydrogeochemical processes are identified:

- Linear mixing and dilution with leaking wadi discharge through indirect recharge
- Carbonate weathering
- Cation exchange

In the downstream part of the Basin aquifer, the basic hydrogeochemical processes depend more and more on the distribution of gypsum and agricultural activity:

- Linear and local mixing and dilution with leaking wadi discharge and leakage from pans and depressions through indirect and localized recharge
- Gypsum dissolution
- Calcite precipitation
- Anthropogenically enhanced salinization through irrigation return flow

6.3.3.4 Hydrogeochemical processes in the Drâa aquifers

Groundwater evolves along the main flow path in the MDC and within each aquifer as the analysis of hydrochemical data from the Tinzouline, Ternata and Fezouata aquifers and as well from the Ktaoua and Mhamid aquifers show. The mineralization increases along the chain of Drâa aquifers, which is due to increasing aridity, decreasing groundwater recharge and potentially increasing groundwater residence times and thus dissolution of minerals. Strong evapotranspiration losses take effect particularly from backwater in front of hydraulic barriers (e.g. Sill of Zagora; chapter 6.1.4) where depth to groundwater is relatively low (less than 5 m). This interpretation is supported by observations of soil salinization in relation to upward water flow via capillary rise (Breuer, 2007; Stuhldreher, 2008). Furthermore, a salt adapted plant community is observed in areas of relatively low depth to groundwater (pers. communication Dr. M. Finckh). Furthermore, irrigation enhances the groundwater salinity particularly in areas where direct evaporation from the aquifer is missing and as the depth to groundwater exceeds the critical depth of capillary rise. The leachate from flood irrigation can dissolve and transport soluble constituents from the vadose zone, e.g. from quaternary lacustrine deposits or active evaporation pans as described for the Basin aquifers exemplarily (chapter 6.3.3.3).

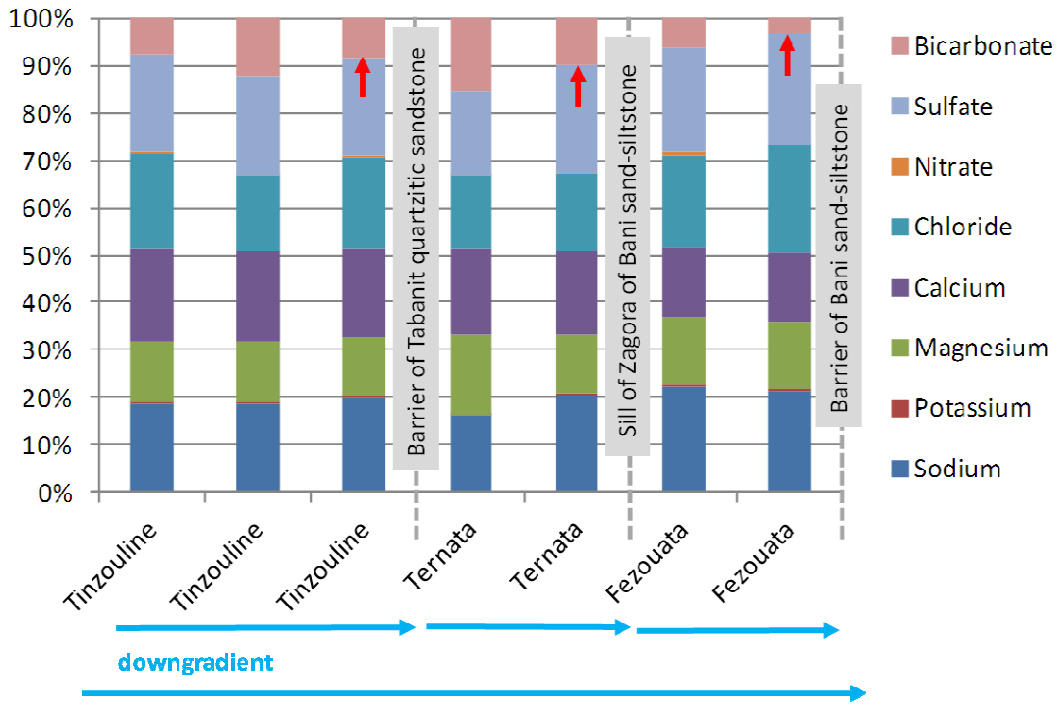

Figure 6-61: Stacked column chart of mean inorganic composition of groundwater from samplings in the Tinzouline, Ternata and Fezouata aquifers with the respective downstream barrier; red arrows mark the lowest bicarbonate concentrations each at the downstream end of a Drâa aquifer (cf. Figure 6-49).

Groundwater sampling in spring 2005 reveals a sharp increase in mineralization between the Ternata aquifer and the aquifers more south, Fezouata and Ktaoua. This finding verifies the separation of the aquifers by the hydraulic barriers at the lower and of each Drâa aquifer (Figure 6-61). A sharp rise of mineralization within the Fezouata aquifer is observed forming an intermediate step of the salinization trend along the main flow path of the MDC (Figure 6-62 & Figure 6-64). The water composition of stream flow in the Wadi Drâa is added to the following semi-logarithmic fingerprint plots to clarify the

end member of low mineralized surface water inflow from the Upper Drâa Basin (Masour Eddahbi reservoir; Figure 6-62, Figure 6-64 & Figure 6-65).

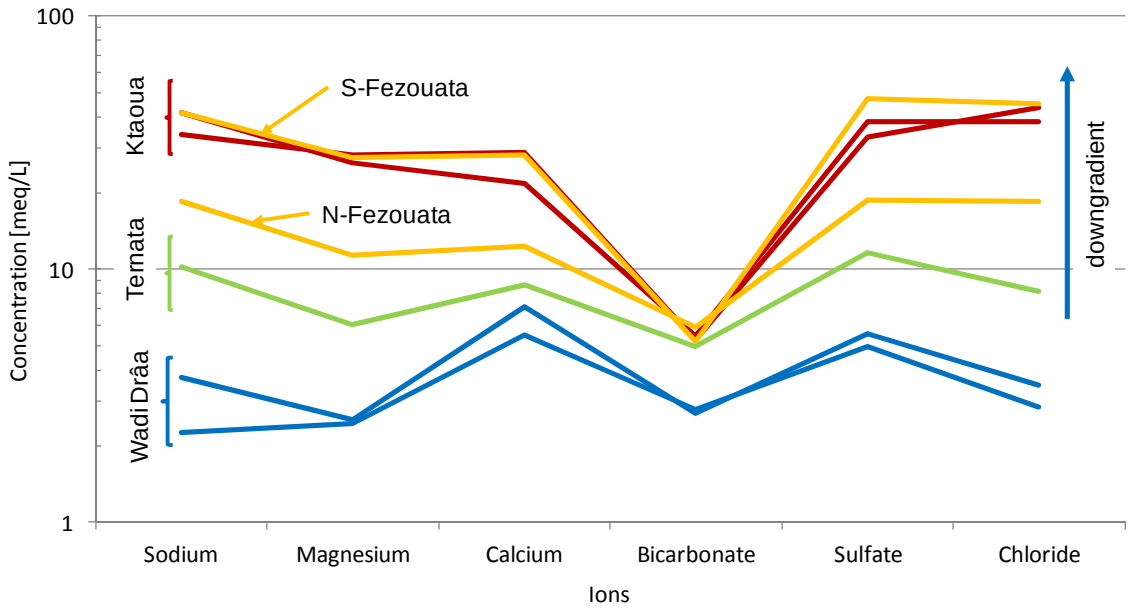

Figure 6-62: Adapted Schoeller plot of inorganic composition of groundwater at sites within the Ternata, Fezouata and Ktaoua aquifer sampled in spring 2005.

A quite similar result is found for the sampling in autumn 2005 (Figure 6-64). The groundwater samples taken in the northern part of the Fezouata aquifer and from the Tinzouline and Ternata aquifer group between 2,110 and 3,500 µS/cm in electrical conductivity in autumn 2005. The samples from the southern part of the Fezouata aquifer and the Ktaoua and Mhamid aquifer show values beyond 6000 µS/cm marking a sharp increase in electric conductivity over a distance of around 20 km within the Fezouata aquifer. The sharp increase in sulfate ions in combination to the sharp decrease in bicarbonate and moderate increase in calcium indicates the dissolution of gypsum while calcite precipitates (chapter 6.3.3.3). There are unverified hints on the occurrence of evaporites within the Fezouata aquifer withdrawn from bore log descriptions (Soletanche, 1980) but the increase in sulfate can also be caused by a change in (lateral) inflows (chapter 6.3.3.3). Upwelling of water from deeper zones can be excluded as reason for salinization as the upwelling is assumed to be concentrated along the course of faults and deep rooting fractures (chapter 6.3.3.5). So, the increase in mineralization within the Fezouata aquifer is mainly interpreted as an effect of the lateral inflow of relatively high mineralized groundwater from the adjacent Basin aquifers, i.e. the Thick Basin aquifer of the Feija de Zagora in the West and the Thin Basin aquifer of El Miyit in the East. The analysis of hydrogeochemical data provides indication for the actual continuous lateral inflow towards the Drâa aquifers because the phenomenon occurs in spring and autumn 2005 (chapter 6.2.2). The effect of mixing with high-mineralized backwater in front of the barrier of the Jbel Bani (Bani sand-siltstone) may be an alternative or complementary explanation of the increase of mineralization at the lower end of the Fezouata aquifer. Furthermore, the signatures of stable isotopes in groundwater in April 2007 and precipitation indicate a ternary mixing referring to the groundwater composition in the southeastern part of the Fezouata aquifer (Figure 6-58; Figure 6-63). Groundwater from the southern part of the Fezouata aquifer plots at the lower third of the regression line of the groundwater samples along the main flow path in the Basin of El Miyit. It is influenced by

evaporation in comparison to precipitation but less than groundwater from the southern part of the Basin of El Miyit (Figure 6-57). Evaporation directly from the aquifer can be excluded because of depth to groundwater significantly more than 5 m. So, the southeastern part of the Fezouata aquifer receives inflow from the developed part of the Basin of El Miyt (Figure 6-63: c.), from the adjacent undeveloped aquifers and aquitards (Figure 6-63: b.) and from current recharge mainly after wadi bed infiltration (Figure 6-63: a.).

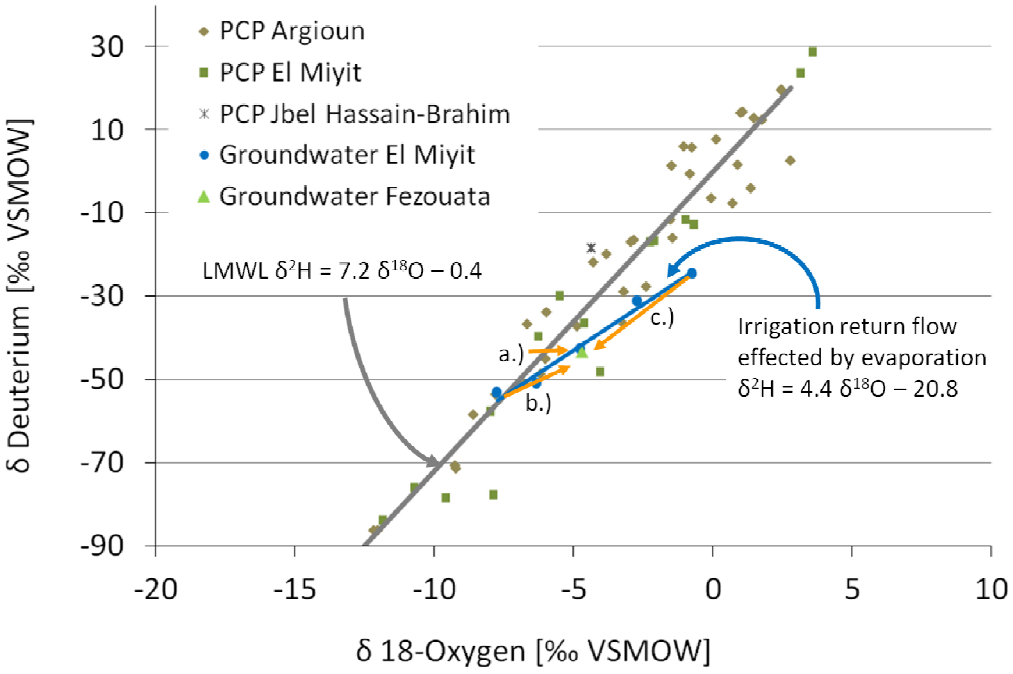

Figure 6-63: Stable isotopic signature of precipitation (PCP) from diverse stations and groundwater from El Miyit Basin (blue circles) and the in the southern part of the Fezouata aquifer (green triangle): grey line = LMWL (Local Meteoric Water Line; grey line), blue line = regression of groundwater along the main flow path in the El Miyit Basin representing the effect of irrigation return flow which is effected by evaporation during flood irrigation and organge lines = inflows to the Fezouata aquifer (a.) Recent recharge, b.) pre-developed lateral inflow, c.) developed lateral inflow).

Further investigation is needed to assess the share of both mechanisms itself and their temporal variance.

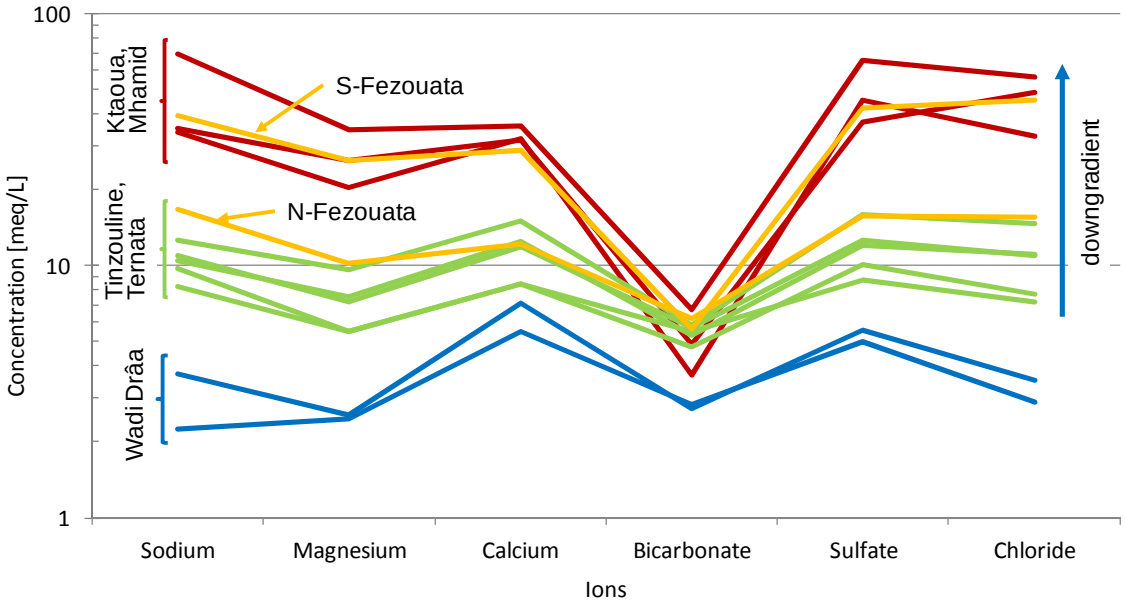

Figure 6-64: Adapted Schoeller plot of inorganic composition of groundwater at sites within the Tinzouline, Ternata, Fezouata, Ktaoua and Mhamid aquifer sampled in autumn 2005.

The groundwater sampling in spring 2007 reveals again a similar distribution of mineralization along the main flow path in the MDC from north to south (Figure 6-65). The sharp increase in mineralization within the Fezouata aquifer is observed because the site in North-Fezouata was locked and could thus not be sampled.

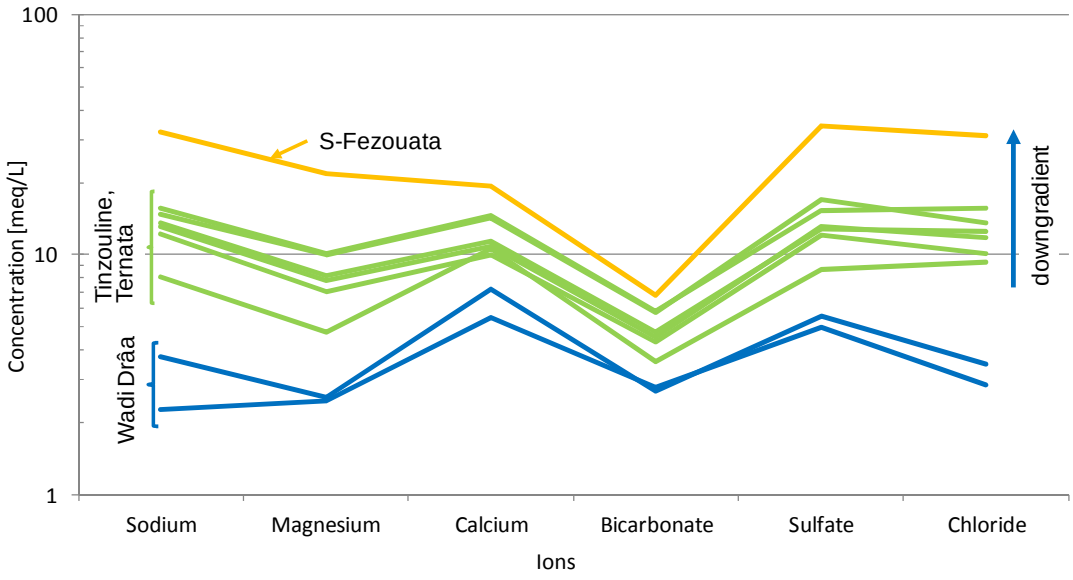

Figure 6-65: Adapted Schoeller plot of inorganic composition of groundwater at sites within the Tinzouline, Ternata and Fezouata aquifer sampled in spring 2007.

The basic hydrogeochemical processes leading to the increased mineralization along the main flow path in the MDC group into Northern MDC down to Ternata and Southern MDC from Fezouata on. The

groundwater evolution in Ternata reveals characteristics of both groups the Northern MDC and the Southern MDC.

The equivalent ratio of $HCO_3^-/(meta)SiO_2$ of >10 hints clearly on carbonate weathering at sites in South-Tinzouline and Ternata. More in detail the equivalent ratio of $Mg^{2+}/(Ca^{2+}+Mg^{2+})$ of <0.5 means that limestone and dolomite are the main source of calcium ions in groundwater whereas at the site in Ternata the molar ration of $Ca^{2+}/(Ca^{2+}+SO_4^{2-})$ indicates calcium ion removal due to cation exchange or calcite precipitation. Calcite precipitation can be excluded as far as possible because the saturation of groundwater in respect to calcite and dolomite is in the near-equilibrium range (Figure 6-66).

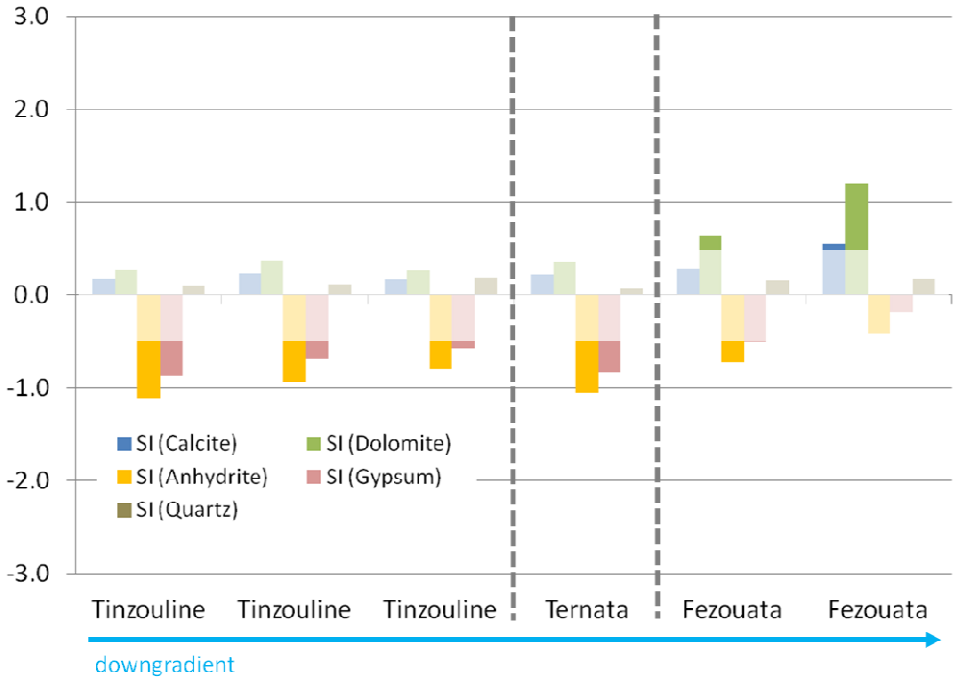

Figure 6-66: Saturation indices in respect to calcite, dolomite, anhydrite, gypsum and quartz along the main hydraulic gradient in the Middle Drâa Catchment from Tinzouline to the Fezouata aquifer based on repeated sampling in spring and autumn 2005 and spring 2007.

The dilution of groundwater by recharge from infiltrated wadi discharge is observed immediately after water releases from the upstream reservoir Masour Eddahbi according to the temporal variation of electric conductivity at the lower end of the Fezouata aquifer. The electric conductivity is around 7,690 µS/cm and 7,300 µS/cm at sampling dates, which were 33 and 73 days after the end of a water release from the reservoir. In contrast to this, the electric conductivity is 6,200 µS/cm at a sampling date one day before the ending of a water release from the reservoir (Table 6-36).

Table 6-36: Comparison of electric conductivity in groundwater at the lower end of Fezouata in relation to the end of water releases from the reservoir Manour Eddahbi to show the effect of dilution by indirect recharge after infiltration of wadi discharge.

Electric conductivity of groundwater [µS/cm]	Sampling date	Start of water release from reservoir Masour Eddahbi	End of water release from reservoir Masour Eddahbi	Total volume of water release [Mm³]	Days between sampling and end of water release
7,690	21.04.2005	3.03.2005	20.03.2005	35	33
7,300	3.10.2005	1.07.2005	23.07.2005	45.8	73
6,200	27.02.2007	8.02.2007	1.03.2007	42.4	-2
1,051*	12.03.2007	--	--	--	--

*Electric conductivity of surface water in the reservoir Mansour Eddahbi

So, the decrease in mineralization is caused by dilution with relatively low mineralized surface water from the reservoir, which infiltrates in the wadi bed and forms indirect net groundwater recharge. This process is particularly described by Bouidida (1990) whose study focused on salinity in the MDC.

Furthermore, hydrochemical data from the local Moroccan water authorities, the Service Eau Ouarzazate (SE) are examined to verify the influence of the water releases on the groundwater composition in the Drâa aquifers. So, sporadic samples from the most upper Drâa aquifer Mezguita are represented (Figure 6-67). The temporal development of electric conductivity indicates that the groundwater salinization is broadly influenced by salt leaching from the vadose zone and dilution by percolation of fresh water from wadi bed infiltration.

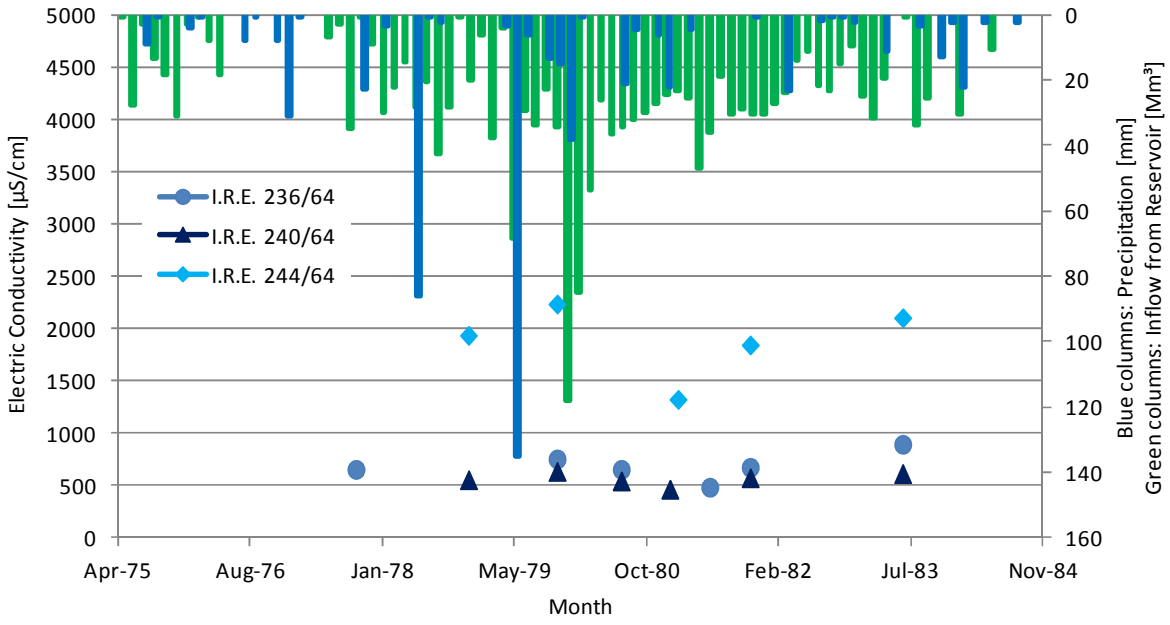

Figure 6-67: Temporal development of electric conductivity at the Mezguita aquifer in comparison to monthly wadi inflow from the reservoir and monthly precipitation at the Zagora Station; I.R.E. is the short term for Moroccan groundwater stations (chapter 4.3).

The electric conductivity first increases after a period with heavy rainfall and high inflow rates from the reservoir in 1979. This should be due to leaching of salts from the vadose zone after a drier period before. In the continuing period of high inflow rates from the reservoir and a large amount of precipitation

in spring time 1980 electric conductivity begins to decrease. This is due to dilution of groundwater caused by wadi bed infiltration and hence percolation of relatively fresh water. The following increase in electric conductivity is may be caused by decreasing water input from the reservoir and by anthropogenic salinization from irrigation return flow. Further interpretation requires a higher temporal resolution of groundwater measurements is needed to differentiate overlaying processes of salinization and dilution. Parallel to this, further studies on soil salinity and vadose zone processes are required. The development of electric conductivity within the other aquifers shows very similar pattern and thus supports the interpretation of the example of the Mezguita aquifer.

In conclusion the fundamental hydrogeochemical processes within the Northern Drâa aquifers (Mezguita, Tinzouline & Ternata) are:

- Mixing and dilution with leaking wadi discharge through indirect recharge in particular in succession of water releases from the upstream reservoir Masour Eddahbi
- Limestone-dolomite weathering
- Cation exchange
- Anthropogenic salinization by enhanced leaching of soluble from the vadose zone caused by irrigation return flow

Within the Southern Drâa (Fezouata, Ktaoua & Mhamid) aquifers the basic hydrogeochemical processes are:

- Dilution of groundwater with leaking wadi discharge through indirect recharge in particular in succession of water releases from the upstream reservoir Mansour Eddahbi
- Stalinization of groundwater by lateral groundwater inflow influenced by gypsum dissolution (in opposite to the dilution)
- Cation exchange / reverse softening
- Calcite precipitation
- Anthropogenic salinization by enhanced leaching of soluble from the vadose zone caused by irrigation return flow

6.3.3.5 *Upwelling from deep aquifer zones*

A distinct hydrochemical signature is assumed to indicate upwelling of water from deeper zone. It is found at two sites tapping the Fractured aquitard in comparison to all other sites tapping the Fractured aquitard too. One site is located in the Plain of Oued El Farrh northeast of the town Zagora. The other site is tapping the Tabanit sandstone west of Ternata (Table 6-37; Figure 6-68 & Figure 6-69).

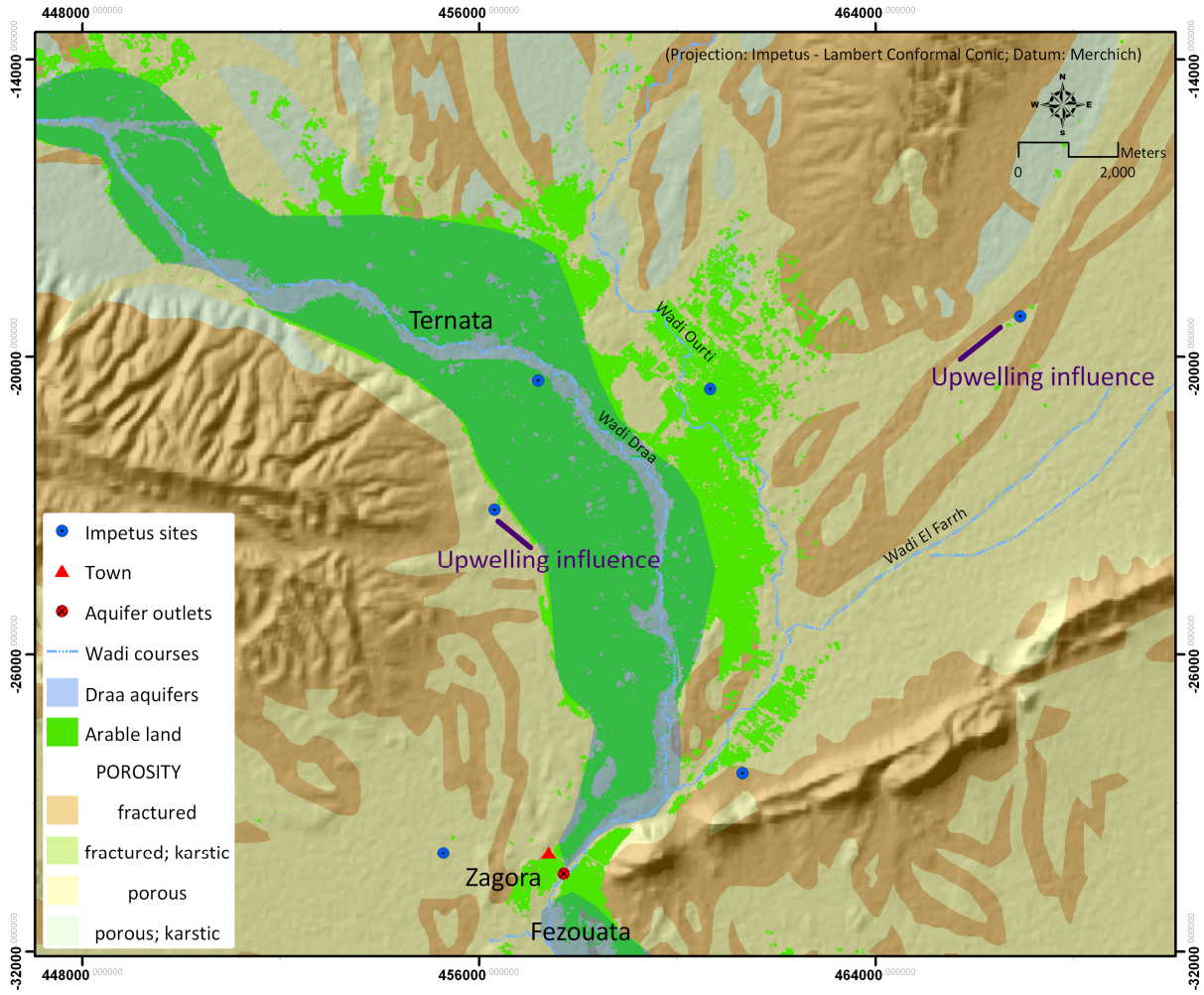

Figure 6-68: Map highlighting the sites influenced by upwelling of water from deeper zones (based on repeated sampling in spring and autumn 2005 and spring 2007).

Firstly, the water was slightly sparkling when being spilled on the ground during sampling. The comparison of hydrochemical fingerprints supports the hypothesis of the upwelling influence with increased grade in mineralization and higher contents of free carbon dioxide and bicarbonate (chapter 6.3.1.3; Figure 6-69).

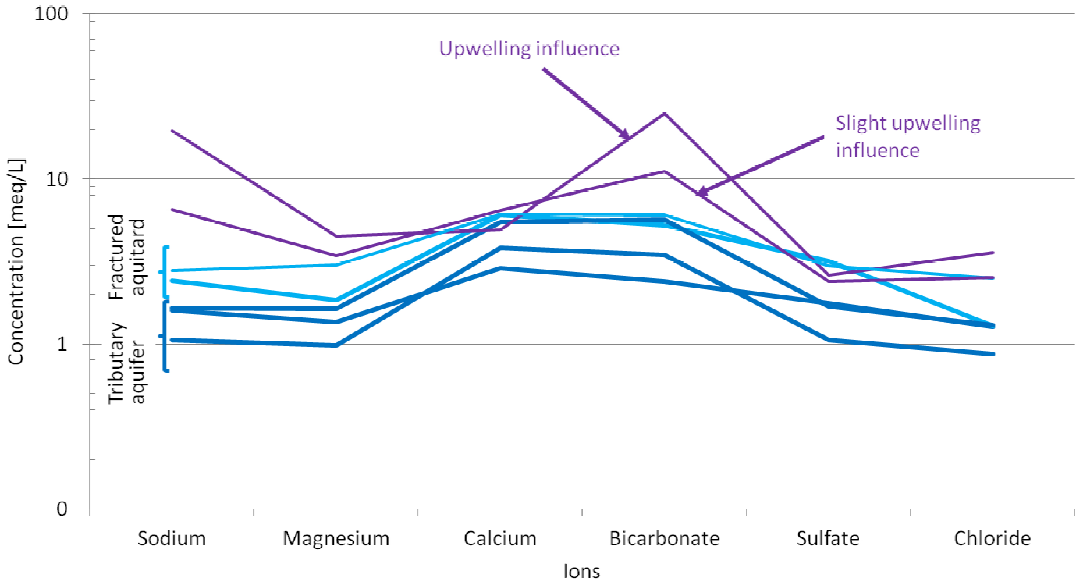

Figure 6-69: Schoeller semi logarithmic diagram of sites influenced by upwelling water from deeper zones and from the Fractured aquitards and the Tributary aquifers; Fractured aquitard = light blue; Tributary aquifer = dark blue; Influenced by upwelling = violet.

More in detail, upwelling influence is shown by comparing indicators at the two influenced sites and the mean values of repeated samplings (spring and autumn 2005, spring 2007) at the other sites tapping the Fractured aquitard (Table 6-37).

Table 6-37: Indicators for the influence of upwelling water from deeper zones of a site in the Plain of Oued El Farrh tapping Ordovician siltstone in comparison to the mean values from the Fractured aquitard (sampling: n = 5; chapter 5.3.7).

Potential indicator	Upwelling site Plain of Qued El Farrh NE' Zagora	Upwelling site Tabanit sandstone W' Ternata	Mean values Fractured aquitard
Elevated free carbon dioxide content	30 mg/L	286 mg/L	23 mg/L
Elevated (bi)carbonate content	1528 mg/L	681 mg/L	350 mg/L
Lowered Redox potential	109 mV	86 mV	177 mV
Elevated electric conductivity	2566 µS/cm	1470 µS/cm	1011 µS/cm
Elevated temperature*	22.8 °C	25.9°C	24.3
Lowered pH value	7.1	6.2	7.3
Elevated sodium content	451 mg/L	151 mg/L	60 mg/L
Elevated potassium content	15 mg/L	12 mg/L	5.56 mg/L
Elevated iron content	0.001 mg/L	0.04 mg/L	0.02 mg/L
Elevated ammonium content	1.7 mg/L	0.9 mg/L	0.35 mg/L
Elevated chloride content	126 mg/L	90 mg/L	72 mg/L
Depleted signature in 18-oxygen	-7.3 ‰	-8.0 ‰	-7.81 ‰
Depleted signature in deuterium	-54.9 ‰	-56.1 ‰	-53.98 ‰

*not interpreted due to partly scoop sampling (chapter 5.3.1)

Some indicators verify the hypothesis of upwelling, such as (Table 6-37):

- Elevated free carbon dioxide content (in case of the Tabanit site west of Ternata)
- Elevated bicarbonate content
- Lowered redox potential
- Elevated electric conductivity
- Elevated alkali content

The elevated bi-carbonate content may interpreted as effect of enhanced carbonate weathering due to carbon dioxide upwelling. The larger carbonate occurrence is found within the thin Quaternary sediments of the Plain of the Oued El Farrh in comparison to the Tabanit sandstone west of Ternata. This is the reason that the free carbon dioxide content at the Tabanit site is not consumed due to carbonate dissolution. The elevated mineralization and thereby elevated alkali content is caused by increased residence time of groundwater from deeper zones. The lowered redox potential hints on reducing aquifer conditions. An anthropogenic organic contamination cannot be excluded as a reason for lowered redox potential values because investigations of organic constituents are missing so far. Other indicators do not show a clear evidence of upwelling but based on the sum of parameters the hypothesis of local upwelling is confirmed.

Detailed interpretation cannot be carried out without further investigations regarding the source of upwelling and the quantification of upwelling. Also the mechanism of upwelling cannot be further interpreted. It may be that the upwelling is in relation with near Neogene volcanism (Jbel Siroua, Michard et al. 2008). It may also be that the upwelling is mainly caused by geohydraulic by-pass along fault lines. Further findings concerning upwelling are presented by Cappy (2006) characterizing the Upper Drâa Catchment hydrogeologically.

6.3.4 Influences on groundwater chemistry

As an outcome of the hydrogeochemical analyses, the spatial distribution of hydrochemical facies reflects the aquifer structure and the regional compartments of the groundwater system in the MDC. So, the sampled sites are grouped to aquifer units as they are presented in chapter 6.1.

Furthermore, the analyses of groundwater evolution reveal that anthropogenic influences change quality and mass flow of water significantly in different ways throughout time and space. It is exemplarily examined that small scale effects can overprint the regional hydrochemical signal and hint on anthropogenic temporal imbalances in the groundwater flow system based on local studies. As an example, irrigation with surface water leads to groundwater recharge by percolation. This is evident considering that farmers use water when available and not only corresponding to the need of the plants (Heidecke, 2009). The increasing use of groundwater for irrigation to meet irrigation demands better enhances salinity by irrigation return flow.

In the following section, findings are compiled to show the meaning of anthropogenic influences based on indicators such as electric conductivity and hydrochemical facies represented in Piper diagrams.

6.3.4.1 Distribution of electric conductivity

The horizontal distribution of specific electric conductivity in groundwater can be used to represent the regional aquifer structure and the groundwater flow directions as described in chapter 6.1 and 6.2. Whisker box plots show a quite clear differentiation of the electric conductivity referring to the aquifer

units (Figure 6-70). The largest overlap is found for the Fractured aquitard and Basin aquifer. The measures of the groups cannot be further analyzed statistically because the sample numbers are too small (e.g. n = 3 for the Tributary aquifers) but based on the assumption of representative sampling the box plots provide an indicative verification of the interpretation of the aquifer system and the groundwater flow paths (chapter 6.1 & 6.2).

So, groundwater from the Tributary aquifers embedded in the Fractured aquitard shows the lowest electric conductivity representing short residence time of water in the underground. Next higher values are found in the Fractured aquitard hinting on longer groundwater residence times. The rock material of the Fractured aquitard is mainly siliceous and soil covers are thin which makes a hydrogeochemical comparison with the Tributary aquifers possible. Cappy (2006) found residence times between 500 and 2,800 years in the Precambrian rocks of the Skoura Mole in the Upper Drâa Catchment and thus supports the interpretation. The wide range of electric conductivity of 570 to 7063 µS/cm (Figure 6-32) is due to local effects of high heterogeneity in the fractured flow system and probably anthropogenic influences (chapter 6.3.4.2). The electric conductivity in the Basin aquifers shows also a wide range of values with an increased median in comparison to the Fractured aquitard. This is because the sediments contain more solubles and reveal a larger inner surface being available for water rock interactions. The residence time of groundwater in the Basin aquifers is assumed to be intermediate in comparison to the Fractured aquitards and the Drâa aquifers featuring high hydraulic conductivity. The electric conductivity in the Drâa aquifers is the highest revealing a wide range of values although hydraulic conductivity is high and effective mixing is assumed. The reason for the high electric conductivity may be caused by influences of land and water use for centuries. The mineralization of the Drâa aquifers is depicted more in detail in the following sections (chapters 6.3.2.4, 6.3.3.4 & 6.3.3.3).

The overlapping range of values of the groups hints on further aspects influencing electric conductivity in the groundwater. This may be due to the fact, that the classification of the aquifer unit integrates further potential influencing aspects, which are not precisely quantified amongst each other. These aspects are e.g. the precise capture zone, advective mixing, vertical flow components and local variations in land use. This in turn refers to the importance of defining background wells and the quasi-natural hydrogeochemical processes e.g. in terms of thermo-dynamic equilibrium (chapter 6.3.3.5).

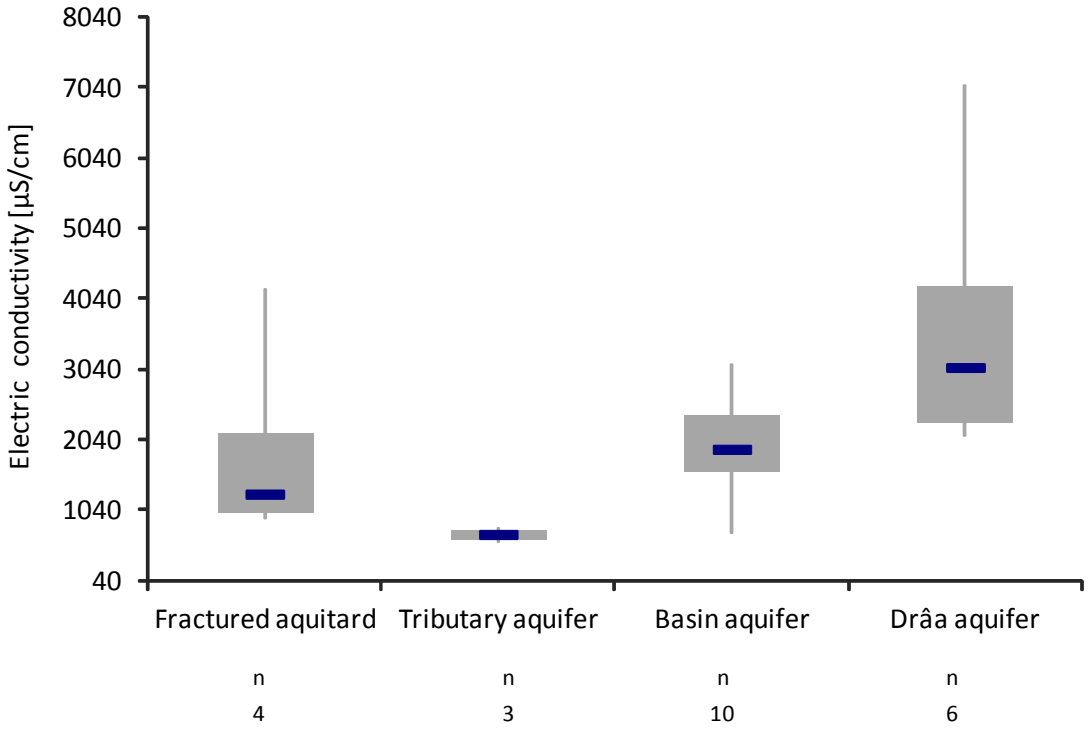

Figure 6-70: Whisker box plot of mean values of repeated observations of specific electric conductivity of groundwater in spring and autumn 2005 and spring 2007 at 23 sites subdivided by the tapped aquifer unit (grey vertical lines display minima and maxima; grey boxes represent the 25 % to 75 % quantile range; blue horizontal lines portray the median values).

The classification of sites by type of lithofacies indicates that water-rock interactions have a strong influence on the electric conductivity in the MDC. The wide range of values within the groups suggests also that further aspects have impact on the degree of mineralization (Figure 6-71). The class sandstone is presented for illustrative purposes due to the small number of samplings (n = 3). If the siltstone and sandstone would be summed up to one group, the influence of lithofacies on electric conductivity appears to be more significant. This may indicate that the sites largely represent equilibrium or quasi-background conditions.

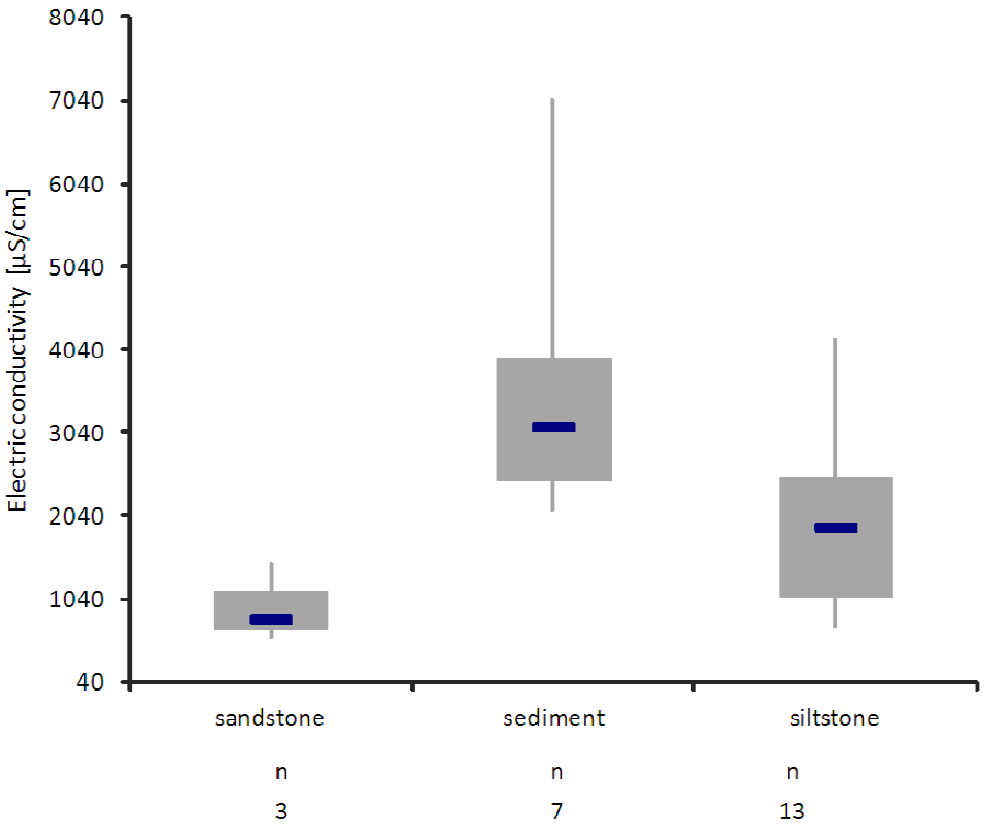

Figure 6-71: Whisker box plot of mean values of repeated observations of specific electric conductivity of groundwater in spring and autumn 2005 and spring 2007 at 23 sites subdivided by the tapped lithofacies unit (grey vertical lines display minima and maxima; grey boxes represent the 25 % to 75 % quantile range; blue horizontal lines portray the median values).

Land use can influence groundwater composition significantly. Usually land use change is a long-term process and lasts of decades (Lerner, 2002; Healy & Cook, 2002). In this context, land use may be taken as criteria for the definition of quasi-background sites representing groundwater, which is influenced since centuries in opposite to wells with geogeneous groundwater composition. So the class “pasture” is assumed to represent the mainly geogenous groundwater composition with relatively low electric conductivity. The class “cropping”, by contrast, stands for intensive land use since centuries which implicates relatively high electric conductivities for example due to anthropogenic salinization (Figure 6-72). The Whisker box plots reveal a distinction between the groups “pasture” and “cropping”. So, the nature of land use has an impact on the groundwater composition and in particular on salinity (cf. Bouidida, 1990). The distinction of the groups may be enhanced by the circular reference that land use in turn is dependent on the hydrogeological properties of the underground and the prevailing soil type (cf. A. Klose, 2009). In this case, almost all cropping sites are located in the sediments, which provide increased mineralization in comparison to sand- and siltstone. The largely overlapping range of values of the groups hints on further uncertainties of this classification. The land use may have changed faster than assumed which can lead to short-term impacts on electric conductivity and disequilibrium (chapter 6.3.3.5). The class “settlement” counts only three samples and is added for presentation purposes without further statistical implication. The variability is very high in this class. This appears mostly to be dependent on the location of the settlement inside or outside of a cropping area, which in turn supports the classification of “pasture” and “cropping” sites.

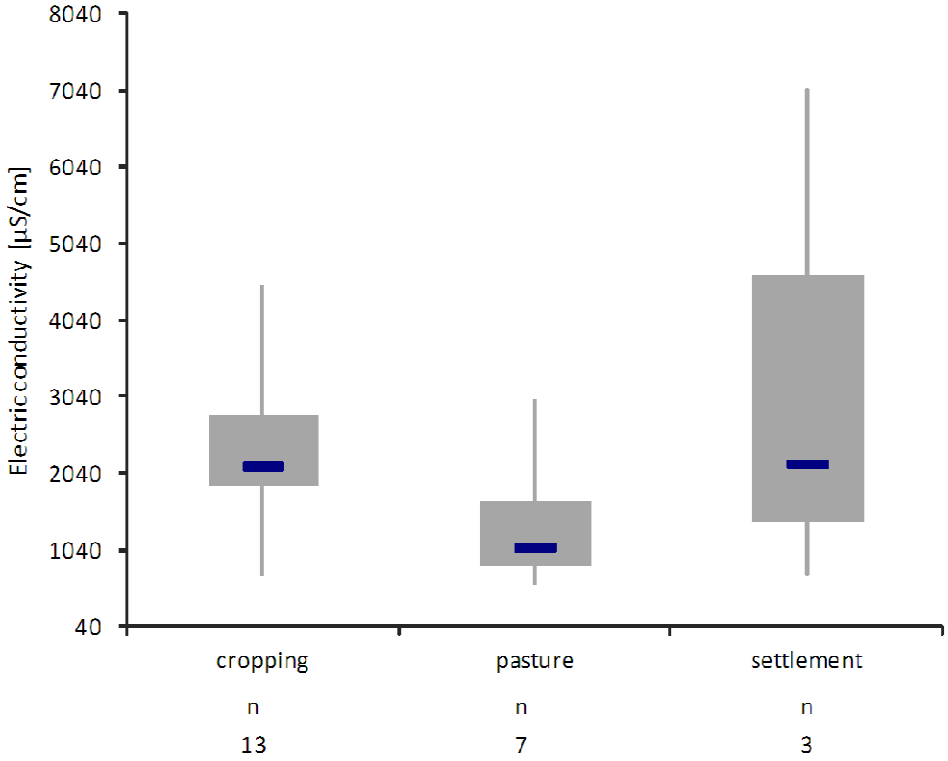

Figure 6-72: Whisker box plot of mean values of repeated observations of specific electric conductivity of groundwater in spring and autumn 2005 and spring 2007 at 23 sites subdivided by the land use class (grey vertical lines display minima and maxima; grey boxes represent the 25 % to 75 % quantile range; blue horizontal lines portray the median values).

The regional distribution of electric conductivity of groundwater shows significant distinction of sites classified by land use and rock type. Due to this a combined classification is tested to describe the dominance of aspects influencing groundwater composition and to identify the quasi–background compositions and the representatively of sites (Figure 6-73). The nature of land use takes into account if land use is extensive, i.e. pasture, or if it is intensive, i.e. irrigation agriculture. Furthermore, the period of intensive land use is distinguished regarding if cropping is practiced for less or much more than 20 years.

The differentiation of sites based on land use nature and hydrogeological aspects allows a robust regional differentiation of electric conductivity in groundwater even if detailed information e.g. on residence time of groundwater and local hydrogeochemical processes are lacking.

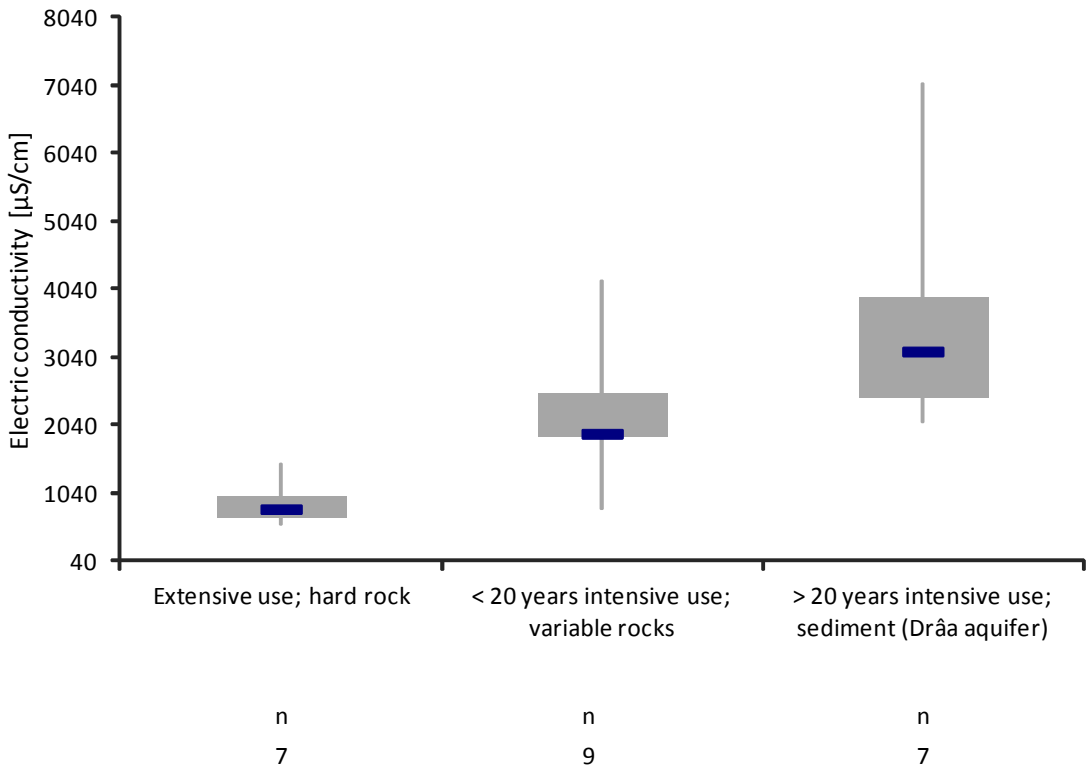

Figure 6-73: Whisker box plot of mean values of repeated observations of specific electric conductivity of groundwater in spring and autumn 2005 and spring 2007 at 23 sites subdivided by a combined classification of nature of land use and rock type (grey vertical lines display minima and maxima; grey boxes represent the 25 % to 75 % quantile range; blue horizontal lines portray the median values).

6.3.4.2 Representative hydrochemical facies

Representative groundwater compositions are identified to understand and explain their regional occurrence and the spatial distribution of a certain water type. So, the classifications of water types after Furtak & Langguth (1967) and Back (1960) are used to differentiate hydrochemical groups of sites and hydrogeochemical zones based on the repeated sampling (April 2005, October 2005 and April 2007) at 23 sites in the MDC (Table 6-32; Table 6-33).

The groundwater types a, b and d after Furtak & Langguth (1967) represent fresh water of quasi-geogenous background composition found in the extensively used areas. Accordingly, the classification 2d after Back (1960) includes the same sites. This group is named “pasture - hard rock” because the capture zones of the sites are largely located within the fractured aquitard (Figure 6-74 & Figure 6-75).

The groundwater type e after Furtak & Langguth (1967) and 1d and 1c after Back (1960) represent a large group of mostly brackish water from mostly loose sediments and agriculturally used areas. So the group is called “agriculture-sediment”. Within this group the sites tapping the Drâa aquifers tend to plot nearer or in the 1c class after Back (1960) revealing a higher sulfate and chloride content (Figure 6-74 & Figure 6-75). An outlier of the classification scheme is found in the fractured aquitard at the northern rim of the catchment of the Ktaoua aquifer (Figure 6-74 & Figure 6-75). The groundwater at this site is relatively low mineralized (570 µS/cm) but it carries high sodium content (27 % of cations) and high sulfate content (30 % of anions). This is may be due to local geochemical effects and high aridity. Furthermore, this site is an open public draw well for watering with animal excrement around. It shows slightly elevated nitrate concentrations (mean = 23 mg/L) which hint on the influence of pasture activity and

may be a reason for the bias of the classification. The groundwater type f after Furtak & Langguth (1967) and 4d after Back (1960) respectively plays a special role because it is representative for a strong influence of upwelling water from deeper zones (Figure 6-69; Figure 6-75; chapter 6.3.3.5).

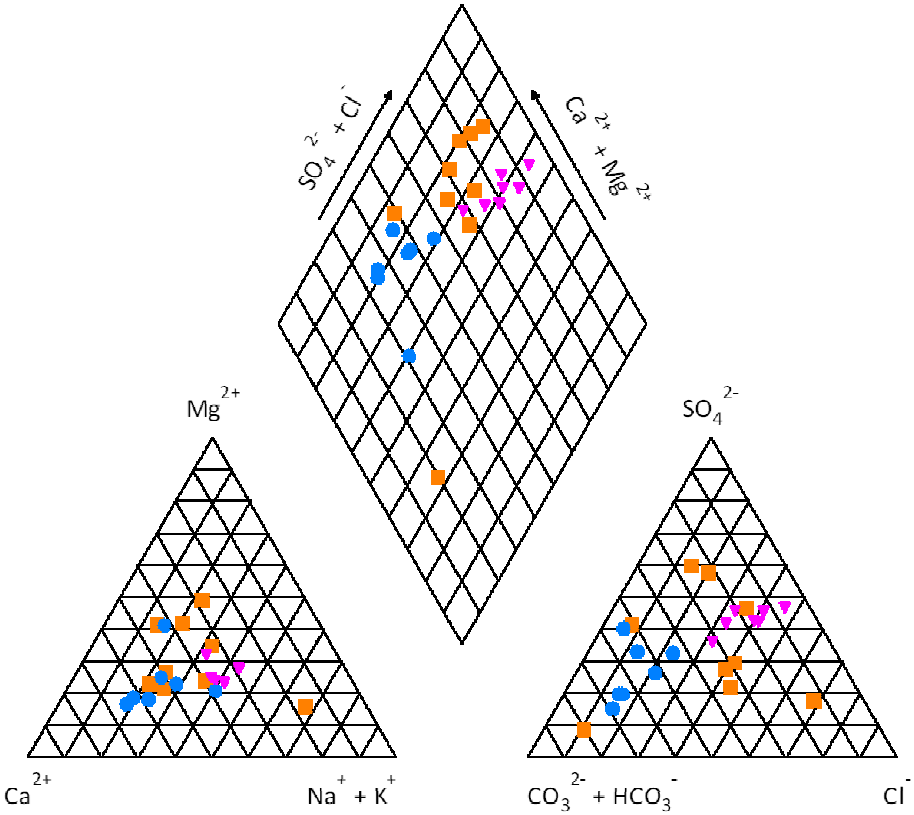

Figure 6-74: Piper diagram representing classification of nature of land use and rock type (Figure 6-73) based on the mean values of inorganic composition of groundwater from repeated samplings in spring and autumn 2005 and spring 2007 at 23 sites; blue circles = extensive land use, hard rock,; orange squares = < 20 years intensive land use, variable rocks; pink inverted triangles = > 20 years intensive land use, sediments (Drâa aquifers).

Overall, the classification of representative groundwater types based on Furtak & Langguth (1967) and Back (1960) is robust and provides a starting point to describe hydrogeochemical processes in the MDC.

This is due to water-rock interaction along the flow paths towards the Drâa aquifers. Furthermore, the irrigation return flow enhances salinization and particularly gypsum dissolution as shown in chapter 6.3.3.3. So, human activity influences the groundwater system significantly after approximately 20 years by changing pasture into cropland.

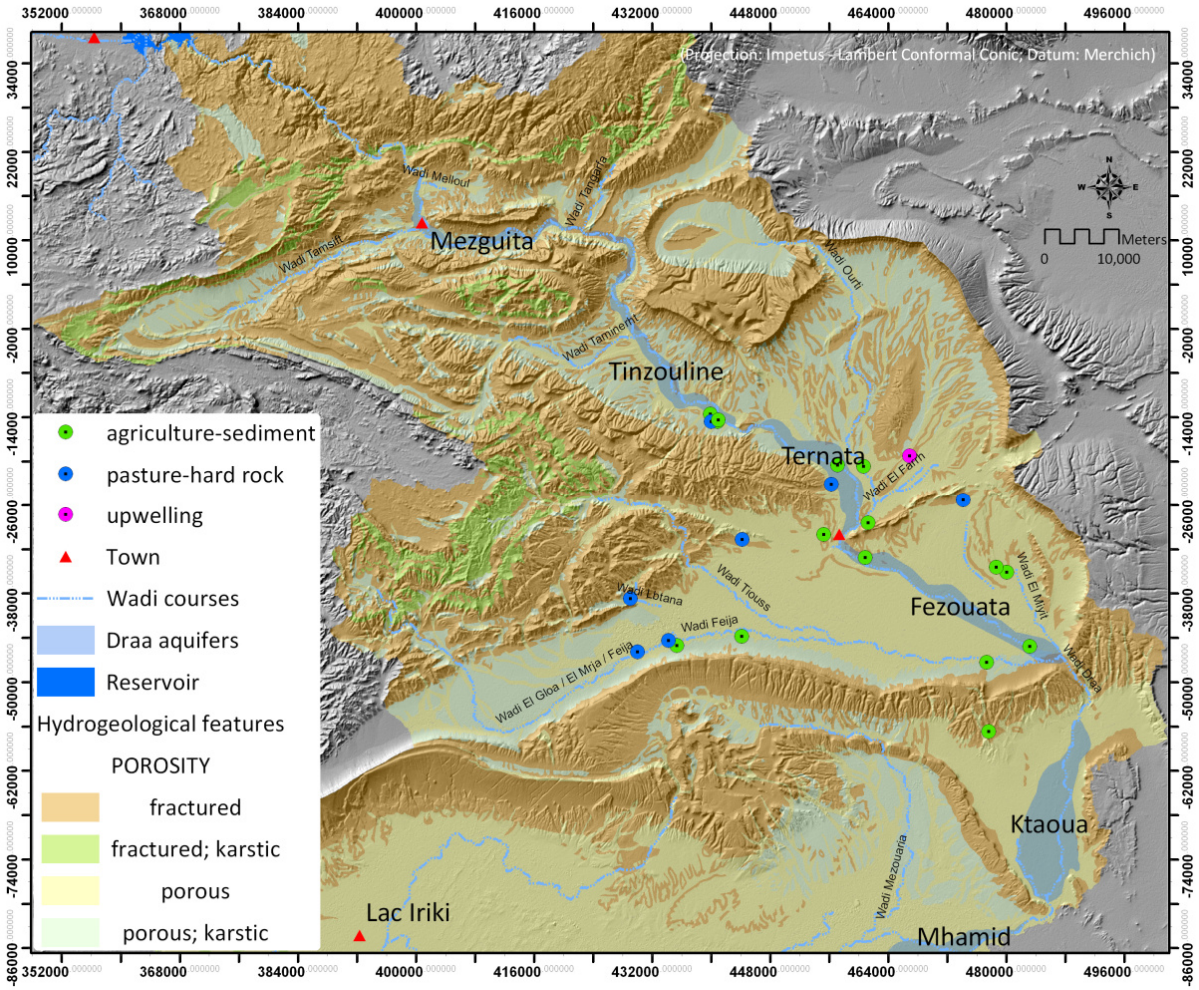

Figure 6-75: Map of the distribution of representative groundwater types according to land use and rock type (based on repeated sampling in April 2005, October 2005 and April 2007 at 23 sites in the MDC).

6.3.4.3 Nitrate content of groundwater

As an indicator of anthropogenic influences on groundwater composition the nitrate concentration is depicted. So typical geogenous concentrations of nitrate are compared to nitrate values of own samples to select quasi-background compositions of groundwater (chapter 5.3; Kunkel et al., 2004). So, at five sites significantly elevated nitrate concentrations of more than 30 mg/L hint on fecal contamination or influence from fertilizers due to improper storage (Figure 6-76). In the case of the presented sites evidence for anthropogenic influence was found during field observations. So, these five sites are open wells with excrements and domestic waste around (perimeter of 10 m). As further field observations reveal sanitation installations are lacking widely. So, it can come to local fecal contamination of groundwater. The inappropriate storage of fertilizer, pesticides, gasoline and oil in partly leaky cans directly around the wells is also a frequently observed phenomenon.

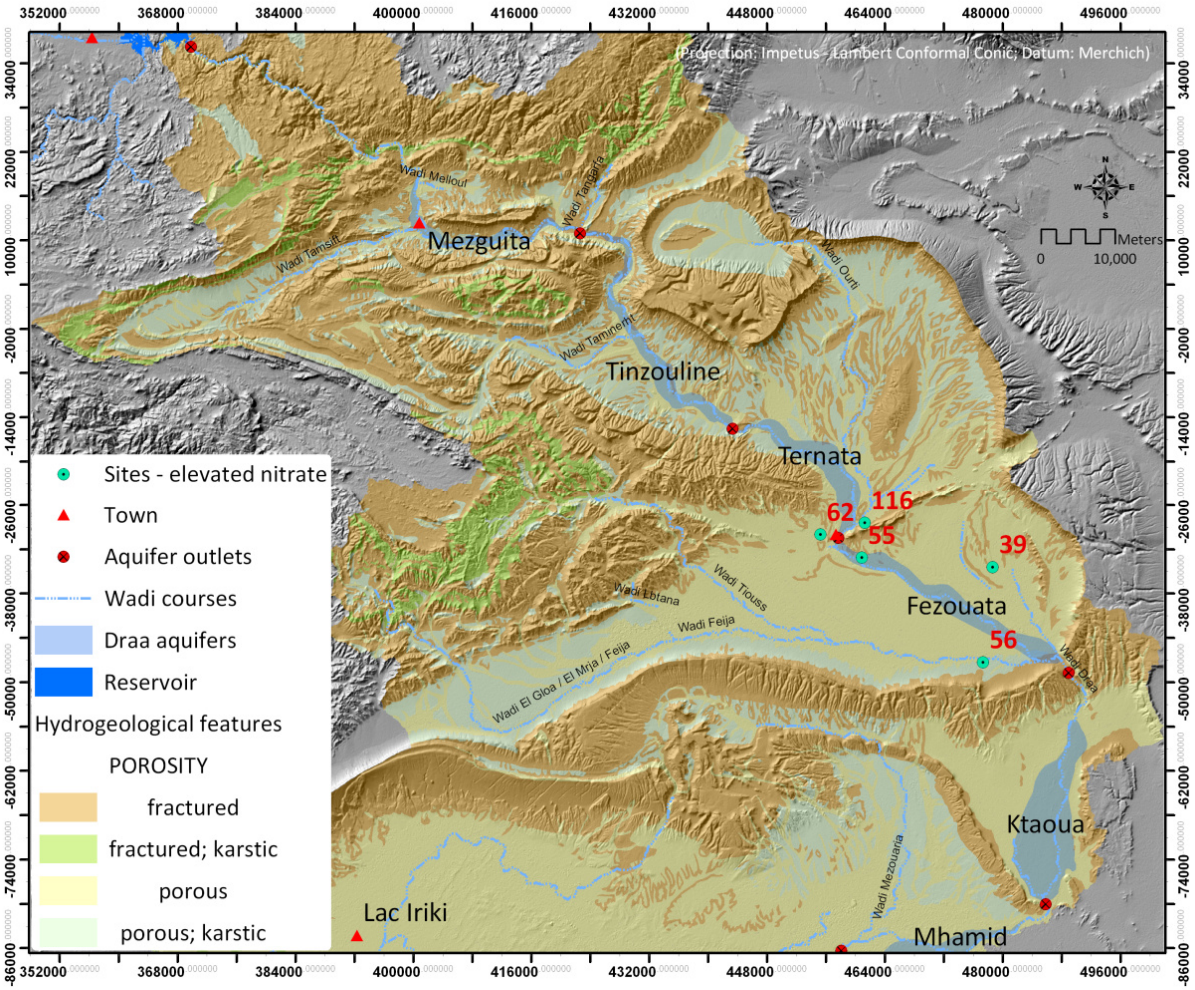

Figure 6-76: Map of the sites with significantly elevated nitrate concentrations in mg/L referring to a maximum geogenous nitrate value of 30 mg/L (based on repeated sampling in spring and autumn 2005 and spring 2007 at 23 sites in the MDC).

6.3.5 Water quality aspects

Water quality aspects are depicted for basic management reasons. The indicators of water quality mirror the aquifer system and flow path and the anthropogenic influence in particular.

6.3.5.1 Groundwater classification after Moroccan Water Quality Standard

The Moroccan standards of water quality provide a classification scheme based on thresholds for individual parameters. This classification scheme is applied to single inorganic parameters as electric conductivity, chloride content and nitrate content (Secréterait d'état charge de l'eau, 2003; Figure 6-77). So, most of the sites which reveal poor and very poor water quality are located in the Drâa aquifers where intensive land use (irrigation agriculture) is predominant. The main problem appears to be the salinization of groundwater caused by strong evapotranspiration (in particular from backwater in front of hydraulic barriers), lateral groundwater inflow influenced by gypsum dissolution and enhanced leaching of soluble from the vadose zone caused by irrigation return flow (chapter 6.3.3.4). The classification concerning chloride content is in relation to the classification of electric conductivity and thus salinity. Increased nitrate concentrations may be caused by fecal contamination from latrines or influence from fertilizers due to improperly storage and secondarily local over-fertilization (chapter 6.3.4.2)

Hydrogeological unit	Electric conductivity [µS/cm]	Chloride [mg/l]	Nitrate [mg/l]
Tributary aquifers	good	very good	good
	good	very good	very good
	good	very good	medium
Fractured aquitards	good	very good	good
	very poor	poor	very poor
	medium	very good	very good
	good	very good	good
Basin aquifers	medium	good	good
	medium	very good	good
	medium	very good	medium
	good	very good	good
	good	very good	good
	medium	medium	poor
	medium	medium	medium
	medium	very good	good
	very poor	medium	good
	medium	good	poor
Drâa aquifers	very poor	medium	good
	medium	good	good
	poor	medium	good
	very poor	medium	poor
	medium	good	good
	very poor	very poor	very good

very good	400	200	5
good	1300	300	25
medium	2700	750	50
poor	3000	1000	100
very poor	>3000	>1000	>100

Figure 6-77: Groundwater classification after the Moroccan Water Quality standard based on electric conductivity, chloride content and nitrate content (based on repeatedly sampled sites (n = 23) in spring and autumn 2005 and spring 2007).

At four sites, the quality standards of drinking water regulations are violated in terms of nitrate. So, the mean values of repeated sampling spring and autumn 2005 and spring 2007 show nitrate concentrations exceeding 50 mg/L (Table 6-38). This may be due to fecal contamination or influence from fertilizers due to improperly storage and secondarily local over-fertilization (chapter 6.3.4.2). At the site tapping the northern part of the Fezouata aquifer, a sharp increase of the nitrate content is observed in comparison

to the samplings in spring and autumn 2005. This must be due to a contamination between autumn 2005 and spring 2007.

Table 6-38: Sites showing nitrate concentrations exceeding 50 mg/L (based on repeated sampling in spring and autumn 2005 and spring 2007).

Site	Range of nitrate concentration [mg/L]	Mean nitrate concentration [mg/L]
Lower end of the Thick aquifer of the Feija de Zagrora	55 to 57	56
Fractured aquitard at the southern outer rim of the Ternata aquifer	114 to 118	116
Northern Fezouata aquifer*	6 to 150	55
North-eastern rim of the Thick aquifer of the Feija de Zagrora	58 to 65	62

*extraordinary high nitrate content in spring 2007

In conclusion, drinking water treatment appears to be of less effort in the Tributary aquifers and the Fractured aquitard than in the Basin and Drâa aquifers. Contrariwise, the Basin and Drâa aquifers are the most productive aquifer and settlements concentrate in the range of the Drâa aquifers. So, drinking water production appears to be challenging. Solar-driven distillation of high mineralized water may be an option for decentralized treatment of high mineralized water. Comprehensive evaluation of the groundwater quality is not possible yet because data on organic compounds are lacking.

6.3.5.2 Irrigation water quality

The quality of water for irrigation and the risk of soil structure break down because of irrigation are assessed applying the adjusted SAR (Sodium Adsorption Ratio; after Ayers & Westcot, 1994) and the RSC (Residual Sodium Content; Mattheß, 1990). The classification of groundwater for irrigation purposes concerning the adjusted SAR indicates that a moderate risk in yield reduction exists in the range of the Drâa aquifers. Groundwater from all other hydrogeological units appears to be applicable for irrigation without hesitation. One site of the Basin aquifers reveals moderate risk of groundwater use for irrigation. This site is located in the Basin of Oued El Farrh being influenced by upwelling water from deeper zones (6.3.3.5). So the latter site has to be treated as outlier.

The groundwater classification by RSC indicates a distinction of the Tributary aquifers in comparison to all other hydrogeological units. The groundwater from Tributary aquifers causes low and moderate risk of soil structure breakdown after irrigation. In contrast to this, the other sites reveal groundwater causing mainly high risk. The distinction of the Tributary aquifers concerning RSC may be due to relatively short groundwater residence times and a higher share in fast recharged water after intensive rainfall and consequently discharge in the wadis (chapter 6.1.3). Overall, the hydrochemical findings are consistent with the results of the aquifer structure and groundwater flow paths as presented in the chapters 6.1 & 6.2.

Hydrogeological unit	Irrigation risk adjSAR (Ayers&Westcot, 1994)	Soil structure breakdown risk, RSC (Mattheß, 1990)
Tributary aquifers	non	moderate
	non	moderate
	non	low
Fractured aquitards	non	high
	non	high
	non	high
	non	high
Basin aquifers	non	high
	non	high
	non	high
	non	moderate
	non	moderate
	non	high
	non	high
	moderate	high
	non	high
	non	high
Dråa aquifers	moderate	high
	non	high
	moderate	high
	moderate	high
	non	high
	moderate	high

non	3	low	1.25
moderate	9	moderate	2.25
severe	>9	high	>2.50

Figure 6-78: Classification of groundwater for irrigation purposes concerning the Adjusted Sodium Adsorption Ratio (adjSAR; after Ayers & Westcot, 1994) and the Residual Sodium Content (RSC; after Mattheß, 1990).

7 Groundwater budget modeling of the Drâa aquifers

Based on the previous investigation and mapping, the annual groundwater availability for the Drâa oases is assessed using a lumped parameter model developed for the MDC (BIL). The groundwater balance modeling includes following tasks:

- Preprocessing of the water balance components assigned to the Drâa oases
- Development of an analytical groundwater balance model using a MS Excel spreadsheet
- Simulation of groundwater availability (including sensitivity analysis and uncertainty assessment)
- Scenario analysis to assess the impact of global change

The groundwater balance model BIL is developed as MS Excel spreadsheet to assess the potentially drainable groundwater volume and the aquifer response at the scale of the Drâa aquifers (chapter 6.1). So, BIL simulates the annual groundwater budget for each Drâa aquifer considering the respective subcatchments. The temporal resolution is annual determined by the data availability (chapter 4 & 0). The input data of the aquifer budgets are based on our own hydrogeological studies and data provided by the Moroccan partners (DRPE; SE Ouarzazate; ABH Souss-Massa-Drâa; and ORMVAO) and literature. The model approach takes into account the hydraulic connection of the Drâa aquifers as one reservoir cascade using the DARCY equation. So, BIL is capable of projecting long-term scenarios for the whole aquifer chain.

In this chapter, the basic understanding of the groundwater flow system and the groundwater budget items is given first (section 7.2) followed by the description of the translation of the general system understanding into the BIL model (section 7.3). The parameterization of BIL is depicted in section 0. The results of the modeling including a sensitivity analysis, calibration, model plausibility and model uncertainties are discussed in section 0. Finally, scenarios of climate and global change are introduced and their impact on groundwater resources in the MDC is demonstrated in section 7.6.

7.1 Theory of modeling procedure

In the following sections, a brief descriptive introduction to the theory of the procedure groundwater modeling is given. Groundwater modeling a very important tool for system analysis and for water resources evaluation and thus a classification of the presented lumped bucket model approach is focused. Principally, modeling techniques for drylands are the same as for humid regions. In detail, the approaches have to be adapted to the particular setting. Particularly at the regional scale, the mechanisms and processes have to be specifically analyzed to create robust and appropriate models (Kirchner, 2006).

The complete modeling procedure incorporates the following main tasks (Peck et al., 1988; Refsgaard & Storm, 1996; Reilly, 2001; Mandle, 2002; Bear et al., 2005; Figure 7-1):

- Conceptualization based on a perceptual model
- Model construction,
- Parameterization
- Sensitivity analysis
- Calibration
- Validation
- Uncertainty analysis

The basis is the perceptual and conceptual model reflecting actual mechanisms and processes (Abbott & Refsgaard, 1996; Refsgaard, 1997; Reilly, 2001; Bredehoeft, 2004).

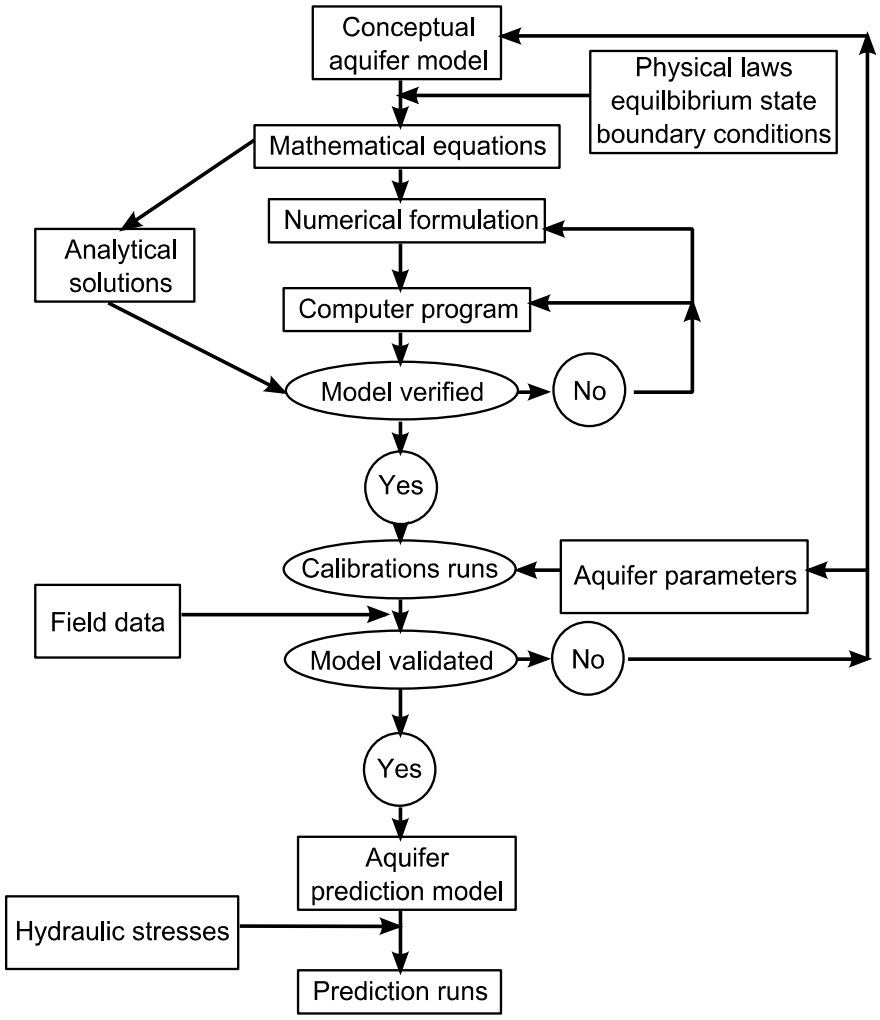

Figure 7-1: Schematic outline of stepwise modeling procedure for mathematical simulations of groundwater resources (from Peck et al., 1988).

In terms of model construction, scaling, regionalization and discretization are important. In combination with the respective data basis, this is the basis for choosing an appropriate modeling approach. The discretization of a groundwater model is specified by the hydrogeological structure of the modeled medium. Accordingly, it has to be schematized in both vertical and horizontal directions following hydrostratigraphical units (Sanz et al., 2009). Furthermore, aquifer properties have to be regionalized and scaled to the model distribution or summed up to lumped parameters. Starting and boundary conditions have to be defined (Franke et al., 1987). Scaling problems became a centre of focus in quantitative water resources research along with increasing size of studied systems (2D and 3D). For this reason, coupling of deterministic and stochastic approaches are increasingly applied to fulfill natural heterogeneity and non-linearity (Simmers, 1984; Schwarze et al., 1994; Blöschl & Sivapalan, 1995; Scanlon et al., 2002; Noetinger et al., 2005; Renard, 2007).

Furthermore, the model performance criteria have to be defined and checked (Refsgaard & Storm, 1996). The parameterization means the setting of fix parameters and temporarily variable model input. The model simulation practically includes sensitivity analysis and calibration. Sensitivity analysis is used to evaluate the influence of input parameters on the modeling result. Therefore, various approaches and tools exist, e.g. sensitivity indices among others (De Roo, 1993; De Roo et al., 1996; Grossmann & Lange, 1999; Saltelli, 2002; Tang et al., 2007). Validation and uncertainty analysis complete the process. Iterative procedures are usually employed spanning from conceptualization to validation if data is available. Calibration is defined as adjustment of parameters to improve the model results. Primarily, non-measured parameters should be adapted. The ultimate parameter set may not be found by calibration as various parameter sets can produce the same model results ("equifinality"), (Beven, 2006). Generally, manual and automatic calibration procedures can be distinguished (Refsgaard & Storm, 1996). Furthermore, combinations of manual and automatic calibration procedures are in use. The development of techniques made headway since the 1980s leading to complex methodology (e.g. GLUE), parameter estimation and inverse modeling approaches (Poeter & Hill, 1997; Beven & Freer, 2001; Rozos et al. 2004). Validation is the testing of the quality of model results. An overview of model validation is provided by Tsang (1991) focusing on the check of model results versus field and laboratory data. Validation is mostly approached in combination with calibration. Four categories of validation are subdivided referring to Refsgaard & Knudsen (1996) following Klemes (1985, 1986) as an example:

- Split sample test – calibration for a period of 3-5 years and validation for another period of similar length based on observed time series
- Differential split-sample test – calibration for certain catchment conditions (e.g. humid period) and validation for differing ones (e.g. dry period)
- Proxy-basin test – an existing model will be transferred to another catchment with similar conditions after initial calibration, and consequently it will be validated
- Proxy-basin differential split-sample test - an existing model will be transferred to another catchment with similar conditions after initial calibration, the model will be validated for both a parameter set of a period before and a parameter set after a catchment change.

A further option is the model-model comparison if validation data is lacking (Refsgaard & Knudsen, 1996). Konikow & Bredehoeft (2002) alert that groundwater models can only be invalidated, but not validated, because of ever-existing inherent errors (see below). They postulate a cautious use of model validation and a stronger commitment to system analysis instead. Model uncertainty can be due to "conceptual deficiencies, numerical errors, and inadequate parameter estimation" (Kinikov & Bredehoeft, 2002). Numerous studies deal with the evaluation of uncertainties (Beven & Binley, 1991; Nilsson et al., 2007; Krause et al., 2005; Beven, et al. 2008 among others). Once a model is calibrated and validated successfully, it can be used for scenario projection and prediction (Yu, 2002; Bear et al., 2005).

Physical (real) and especially mathematical (abstract) models are in use to quantify groundwater resources and to describe water fluxes at any scale (Boonstra & De Ridder, 1990; IAEA, 1996; Fetter, 2001). In coupled model systems, heat flux, solute transport and hydrochemical reactions are integrated (Glynn & Plummer, 2005). Thereby, groundwater flow modeling provides as a basis. The coupling of hydrological and groundwater models is important, especially in arid zones (Sophocleous & Perkins, 2000; see chapter 3.2.2; 3.2.3). More detailed information on hydrological models is provided e.g. by Maidment (1993). Hatton (1998) focused on water budget estimations. Comprehensive regional modeling studies deal with complex responses of watersheds and large aquifers (Brodie, 1999; Batelaan & De Smedt, 2001; Scanlon et al., 2003).

Groundwater modeling requires different techniques for porous media and fractured rocks, which are determined by differing aquifer properties and types of flow (Kellgren, 2002; Berkowitz, 2002; Scanlon et al., 2003; Cook, 2003; Neumann, 2005). Depending on the nature of the mathematical equation, three types of mathematical models can be distinguished, empirical (experimental), stochastic and deterministic (Kresic, 2007). The different approaches can be more or less physically based. In terms of deterministic models, analytical or numerical solutions are used to describe elements of groundwater flow. However, the classification of models is somewhat arbitrary and depends in fact on the system, which should be represented. Thus, models can include multiple approaches of different model classes.

In distributed numerical models, the area under investigation is subdivided into smaller cells or elements, for which the groundwater flow equation is solved for each cell or element. Therefore, the water balance is considered based on the continuum approach by converting differential flow equations into algebraic formulations (e.g. Navier-Stokes equation for porous media). Target value is thereby the distribution of hydraulic heads at points representing individual cells or elements. Two outstanding techniques are the finite differences method and the finite elements method (Kinzelbach & Rausch, 1995; Kresic, 2007). The development of modeling systems advances incorporating GIS and remote sensing techniques, even based on open source software (Batelaan et al., 1993; Carrera-Hernandez & Gaskin, 2006; Tweed et al., 2007). Mathematical models are the core of model-based Decision Support Systems (DSS) providing as a tool for scenario analyses and water resource management (Loucks, 1995; Margane, 2003b).

Analytical solutions for groundwater flow description reveal distributed information mostly based on the Theiss equation (Haitjema, 1995). Analytic element models (AEM) are available as computational engines and modeling systems. AEM are applied to arid environments with heterogeneous structure, e.g. mountain blocs linked to sedimentary basins (Bakker et al., 1999).

Lumped parameter models use linear or non-linear transfer functions to describe the steady state conditions of an aquifer compartment (Schwarze et al., 1994; Wittenberg, 1999; Schwarze, 1999; Zuber & Maloszewski, 2001; UNEP, 2002; Rödiger et al., 2009). They are often applied where data resolution is too sparse to use distributed models.

7.2 Perceptual groundwater model

The perceptual model gives a synopsis of the hydrogeological setting and processes in terms of forming a basis to simulate the annual groundwater budget and aquifers response of the Drâa aquifers.

Aquifer structure and properties

The outcrop surface of the six Drâa aquifers covers around 2 % of the entire surface of the Middle Drâa Catchment (MDC) accounting to approximately 15,000 km². The Drâa aquifers are aligned along the Wadi Drâa named same as the date palm oases (downgradient order, Figure 7-2):

- Mezguita aquifer
- Tinzouline aquifer
- Ternata aquifer
- Fezouata aquifer
- Ktaoua aquifer
- Mhamid aquifer

Principally, natural hydraulic barriers of outcropping aquitards at tectonic lineaments and cuestas separate the Drâa aquifers from each other (Foums and sills; Figure 7-2). The aquifers are still connected via very shallow and narrow alluvial filling at the principally separating aquitard outcrops. The Wadi Drâa itself represents a connecting vein between the Drâa aquifers via minor river-aquifer interactions. These are groundwater seepage in the wadi bed due to backwater and return flow in particular in front of the separating aquitard outcrops.

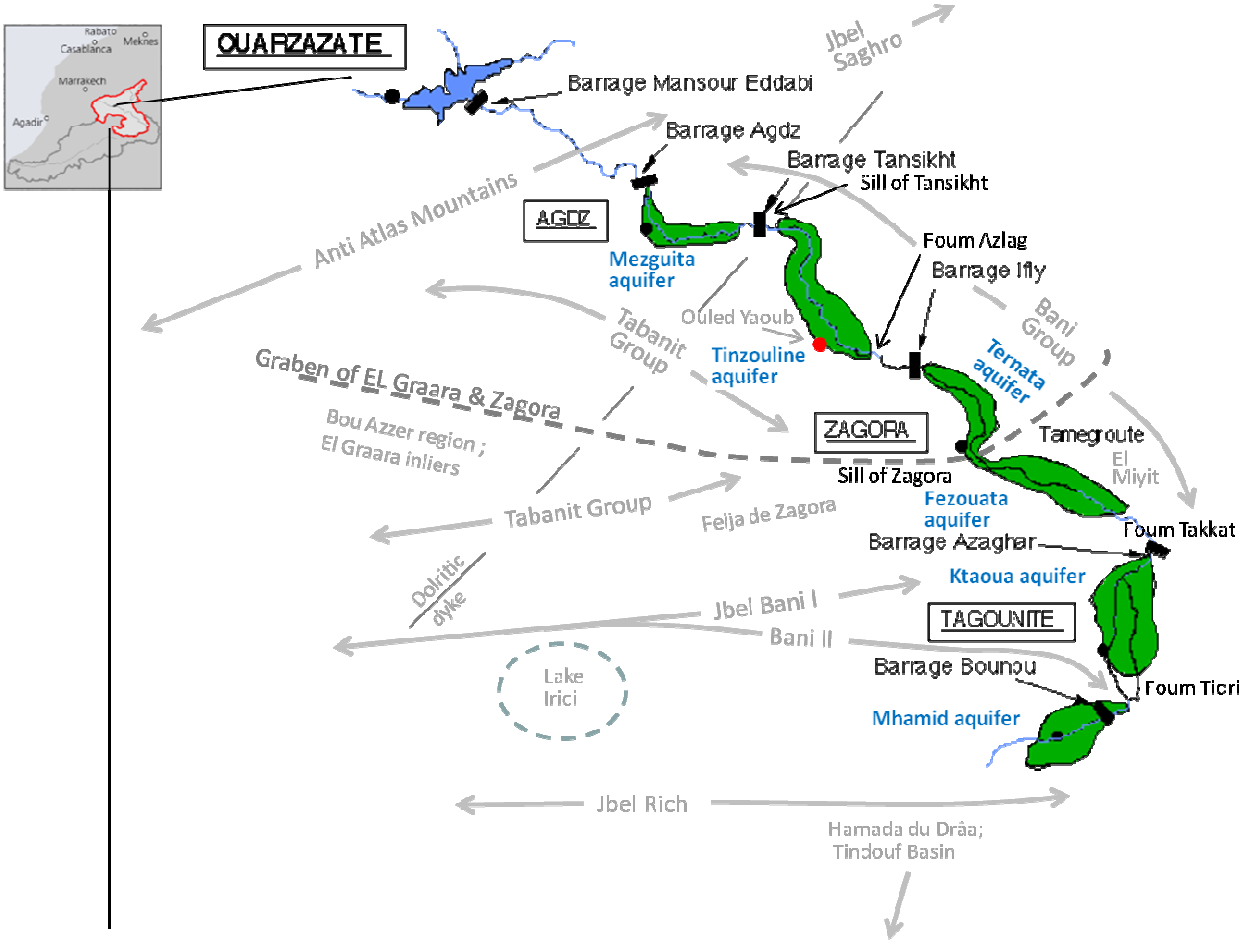

Figure 7-2: Scheme of the oases and the related aquifers along the Wadi Drâa with the main features of landscape and geology in the Middle Drâa Catchment.

The structure of the Drâa aquifers is typical for shallow alluvial aquifers made of Quaternary terrace sediments embedded in Paleozoic sedimentary bedrock forming a Variscan fold belt. The aquifer thickness is made up of the alluvial deposits and a highly weathered fringe in the schisty substrata accounting for around 5.5 m corresponding to bore log data (from the Service Eau Ouarzazate). So the vertical structure of the Drâa aquifers is summarized as one unit to allocate aquifers properties applicable for groundwater balance assessments at the regional scale (Table 7-1). The Drâa aquifers are essentially made up of sandy-gravelly deposits partly cemented and locally interposed by aquitards of loamy to marly composition. Variation in the internal aquifer structure influences the hydraulic aquifer response of each individual Drâa aquifer. The differences between the individual Drâa aquifers are clarified by the variation in specific yields (Table 7-1).

Table 7-1: Summarized information on the aquifer structure and main properties compiled from Chamayou (1966), bore log data and own investigations (chapter 6.1.4).

Aquifer unit	Surface distribution [km²]	Mean thickness [m]	Mean transmissivity (Chamayou, 1966) [m²/s]	Mean specific yield [%]	Mean drainable volume [Mm³]
Mezguita	30.5	20.5	$6 \cdot 10^{-3}$	19	59.3
Tinzouline	56.4	20.5	$5 \cdot 10^{-2}$	22	127.2
Ternata	56.8	19.5	$5 \cdot 10^{-2}$	15	83.1
Fezouata	72.5	21.5	$2 \cdot 10^{-2}$	10	77.9
Ktaoua	127.2	31.5	$7 \cdot 10^{-3}$	13	260.3
Mhamid	44.0	50.5	$5 \cdot 10^{-3}$	15	166.6

Groundwater recharge

The Drâa aquifers are mainly indirectly recharged by percolation after infiltration of stream flow (chapter 6.2.1 & 6.2.3). Seldom appearing long or intense rainfall within the MDC leads to stream flow rarely. The water releases from the reservoir Mansour Eddahbi in the Upper Drâa Catchment trigger the major amount of stream flow several times a year depending on the filling level of the reservoir and the agricultural water demand in the MDC (Busche, (in prep.); ORMVAO, 1995; Ouhajou, 1996; Heidecke, 2009). The magnitude of groundwater recharge rates linked to stream flow infiltration is assumed 8 – 20 % taken from literature (Chamyou, 1966; ORMVAO, 1995) because accurate knowledge on groundwater recharge is lacking. The infiltration of stream flow changes from upstream to downstream and also temporarily during a water release procedure because water is firstly dammed up on the whole length of the Wadi course to Mhamid, Ktaoua or even Ternata at four minor barrages (chapter 2.2). In a second step water is derived to the fields via channels of different order from the minor barrages (Ouhajou, 1996). The infiltration of irrigation water and the irrigation return flow of pumped groundwater leads also to groundwater recharge as exemplarily hydrogeochemical investigations in the Plain of El Miyit show (chapter 6.3.3.3). Flood irrigation is the most common irrigation technique. So percolation after irrigation is enhanced in contrast to areas where drip irrigation is applied. The arid climate forces evaporation losses from open water surfaces during water impounds in the bed of the Wadi Drâa and during the widespread flood irrigation. Therefore, leakage water increases salinity and all in all groundwater recharge is reduced.

Direct groundwater recharge after infiltration of precipitation is rare due to generally very low antecedent soil moisture, groundwater depth of mostly more than 5 m and little amount of precipitation (Weber, 2004; Kutsch, 2008). The annual rate of direct recharge is assumed to fall beneath the rate of localized recharge accounting for around 2.7 % of mean annual precipitation at the Zagora station (63 mm; Figure 2-3; chapter 6.2.4). The lumped annual groundwater recharge is about 2.4 % of mean annual precipitation at the Zagora station (63 mm) in areas of fractured media. Indirect groundwater recharge is estimated to range from 2.9 to 4.9 % of mean annual precipitation at the Zagora station (63 mm) outside of the Drâa aquifers and thus the zone of influence of indirect recharge of the Wadi Drâa (chapter 6.2.4). The comparison of inorganic hydrochemical analyses of the Tributary aquifers with these of the Fractured aquitards and the Basin aquifers verify that indirect recharge is a dominant recharge process (chapter 6.3.3.1 & 6.3.3.2). Investigation of groundwater residence time in the Upper Drâa Catchment leads to the assumption that an imprint of paleo-recharge biases the quantification of recent recharge rates (Cappy, 2006).

Groundwater recharge outside of the Drâa aquifers is assumed to contribute to lateral groundwater inflow to the Drâa aquifers via local and regional flow systems at recent and geological time scales.

Groundwater flow and groundwater discharge

The arid climate conditions control dominantly the processes of groundwater discharge in combination to relatively small aquifer potential and intensive irrigation agriculture within the Drâa oases (chapter 2.1, 6.1 & 6.1.4). The intensive groundwater use for irrigation within the oases represents a prominent aspect of groundwater discharge and the regional water balance (ORMVAO, 1995).

The groundwater flow in the Drâa aquifers is basically determined by relatively high transmissivities and medium to high specific yields (Table 7-1). Varying geohydraulic parameters of the individual Drâa aquifers cause differences in water table fluctuations and groundwater flow patterns. The relatively low specific yield of the Ternata aquifer causes for example a highly dynamic behavior of the groundwater level rise and thus influences the groundwater flow (Figure 6-15, Figure 6-16).

Pumping for irrigation purposes is assumed to influence the groundwater flow within the Drâa aquifers leading to an overall drawdown of groundwater levels. It is the main discharge mechanism in the Drâa aquifers. This is supported by estimations of evapotranspiration and agricultural water demand. So, flat cones of depression in the groundwater table can form concentrating around accumulation of irrigation wells (Figure 6-20). The rate of groundwater withdrawal must vary depending on the availability of both stream flow of Wadi Drâa and groundwater. The priority of water use lies on irrigation with surface water, which free of charge (Ouhajou, 1996, Heidecke, 2009). So, in times of drought the cropping area is reduced by the farmers to face the water scarcity (ORMVAO, 1995). The groundwater flow regime of the Drâa aquifers is represented broadly for the Ternata and Fezouata aquifer in spring 2005 (chapter 6.2.2.3). The isopiestic maps verify the main drainage along the main gradient of the Wadi Drâa (Figure 6-20). So the Drâa aquifers are assumed to represent the groundwater main drain at the regional scale. The Drâa aquifers receive groundwater inflow from the Tributary aquifers, the Basin aquifers and the Fractured aquitards (chapter 6.1.1, 6.2.2, 6.3.3 & 6.3.3.5). The groundwater inflow is caused by regional groundwater recharge. The Tributary and Basin aquifers contribute groundwater inflow after indirect recharge mainly and after leakage from the Fractured aquitard secondarily. The Fractured aquitards contribute minor inflow via faults and fracture zones. Upwelling appears to play a minor role for the groundwater flow pattern. As the Investigation of groundwater residence time in the Upper Drâa Catchment show, an imprint of paleo-recharge biases the estimation of regional recharge rates (Cappy, 2006) and thus the analysis of recent groundwater circulation. Nevertheless, the groundwater inflow towards the Drâa aquifers is evident based on the hydraulic gradients and the hydrogeochemical findings (chapter 6.2.2 & 6.3.3). Analysis of strontium isotopes in groundwater verifies the inflow to the Drâa aquifers even via a regional groundwater flow system (oral communication with L. Bouchaou, August 2012).

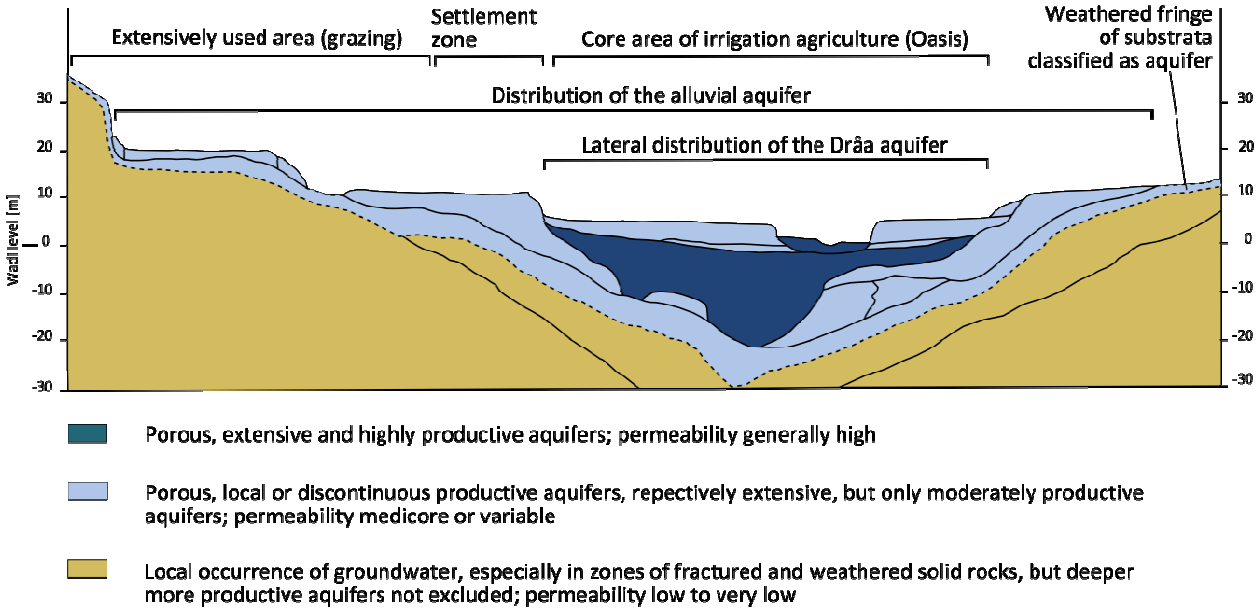

Figure 7-3: Schematic cross-section of a Drâa aquifer with a hydrogeological classification according to the alluvial facies and the substrata (after Chamayou, 1966).

7.3 Modeling approach

The BIL model is a simple lumped bucket model representing coupled annual groundwater balance estimations for the Drâa aquifers based on a detailed pre-processing of the individual items. The abstraction of the perceptual model and the mathematical representation of the dominant processes to estimate the annual groundwater availability and aquifer response are depicted in this section. The balance scheme portrays the perceptual model as a basis to describe the conceptual and procedural model (Figure 7-4). The water balance method is modified and adapted to the setting in the study area applying the concept of specific yield (Healy & Cook; 2002; Ruud et al.; 2004; Maréchal et al.; 2006). Varying methods were combined to pre-process each single component of the balance equation (see below). Target figure of the groundwater balance is the drainable annual groundwater volume as annual aquifer filling level.

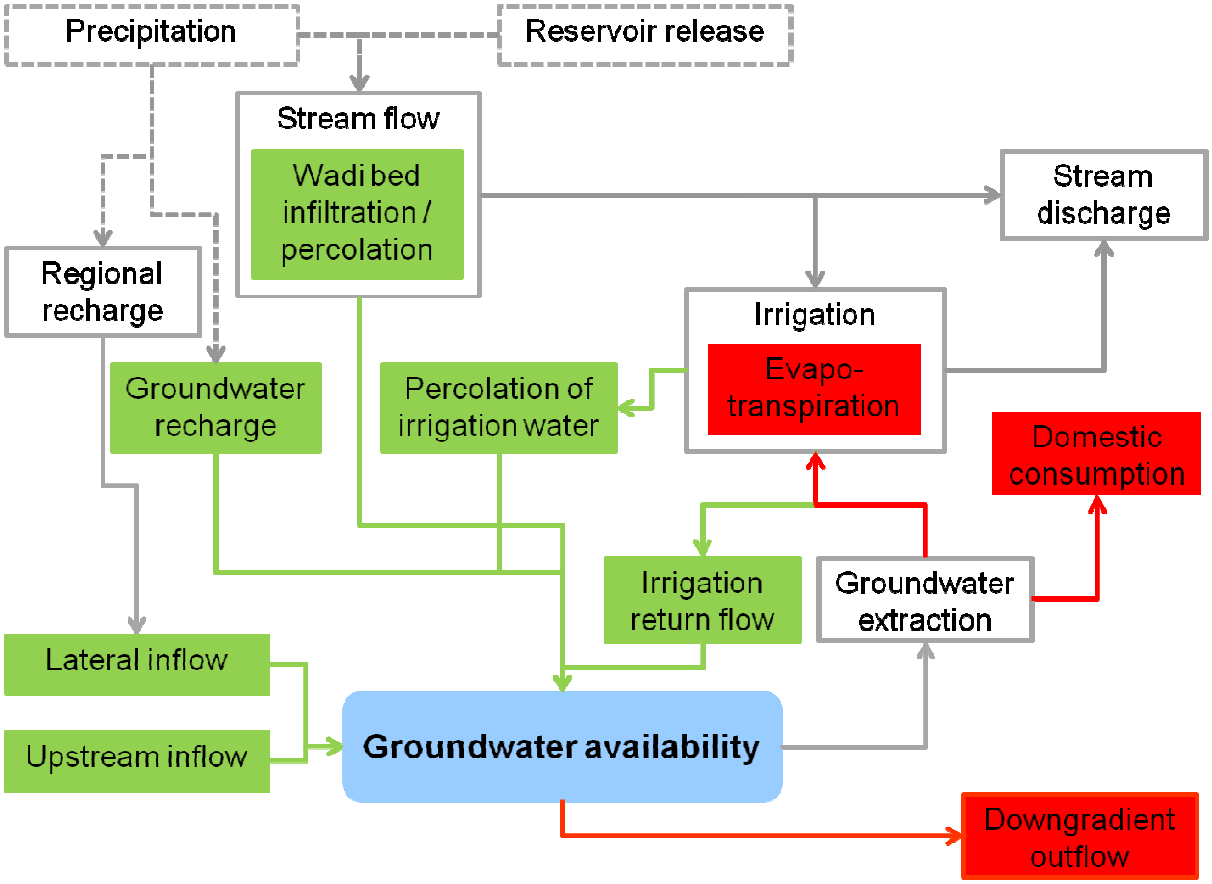

Figure 7-4: General groundwater balance scheme of one Drâa aquifer; green colored features represent estimations of inflow, red colored features represent estimations of discharge; grey colored features represent secondary estimations and pre-processing.

The basic equation to estimate the groundwater budget V_{GW} of each Drâa aquifer is given below:

$$V_{GW} = V_{GWprior} + R_{SF} + R_{PCP} + R_{Irri} + R_{Residual} + R_{Return} + Q_{lateral} + Q_{upstream} - Q_{Irri} - Q_{domestic} - Q_{downgradient}$$

With:	$V_{GWprior}$	*Volume of drainable groundwater of the prior year [m³/a]*
	R_{SF}	*Recharge from stream flow infiltration after water releases from the reservoir Mansour Eddahbi [m³/a]*
	R_{PCP}	*Recharge from precipitation infiltration [m³/a]*
	R_{Irri}	*Recharge from infiltration of irrigation water derived from the Wadi Drâa [m³/a]*
	$R_{Residual}$	*Recharge from resdiual stream flow after derivation of irrigation waterfrom Wadi Drâa [m³/a]*
	R_{Return}	*Recharge from irrigation return flow after groundwater pumping [m³/a]*
	$Q_{lateral}$	*Lateral groundwater inflow after regional recharge [m³/a]*
	$Q_{upstream}$	*Groundwater inflow from the upstream Drâa aquifer [m³/a]*
	Q_{Irri}	*Groundwater withdrawal for irrigation water supply [m³/a]*
	$Q_{domestic}$	*Groundwater withdrawal for domestic water supply [m³/a]*
	$Q_{downgradient}$	*Groundwater outflow to the downgradient Drâa aquifer /area ' [m³/a]*

Recharge from stream flow infiltration (R_{SF})

Neither infiltration from wadi bed nor evaporation losses during transmission and impounding in the wadi bed can be precisely determined. This is due to a lack of data on discharge rates, infiltration rates and others at an adequate spatial and temporal resolution. So lumped recharge coefficients are implemented stemming from literature (Chamayou 1966; ORMVAO 1995). The recharge coefficients range broadly from 8 % to about 20 % of stream flow and are revised in a manual calibration for each Drâa aquifer (chapter 7.5.2). The recharge is calculated by multiplying the stream flow of Wadi Drâa with the respective lumped recharge coefficient reach by reach for each Drâa aquifer after subtracting a lumped evaporation loss of 5 % (Chamayou, 1966). The stream flow is thus reduced from reach to reach by the amount of recharge getting lost to the respectively belonging Drâa aquifer.

The major amount of stream flow stems from the water releases of the reservoir Mansour Eddahbi. A minor amount of stream flow generates within the Middle Drâa Catchment (MDC). It is quantified by applying the run off coefficient of 8 % (according to Chamayou, 1966) to the mean annual areal precipitation of the respective sub-catchment of each Drâa aquifer. The two stream flow components are summed up for the annual water budget calculations at each Drâa aquifers:

$$R_{SF} = (\mathrm{SF_{Reservoir}} + \mathrm{SF_{MDC}}) \cdot LC_{\mathrm{EV}} \cdot \mathrm{RC_{Wadi}}$$

With:

$SF_{Reservoir}$	*Stream flow released from the reservoir Mansour Edahbbi [m³/a]*
SF_{MDC}	*Stream flow generated within the MDC [m^3/a]*
LC_{EV}	*1 - Coefficient of lumped evaporation loss from stream flow [-]*
RC_{Wadi}	*Recharge coefficient based on literature reference and calibrated manually [-]*

The remaining stream flow splits in irrigation and stream discharge (Figure 7-4; see below).

Recharge from infiltration of precipitation (R_{PCP})

Direct recharge caused by precipitation is very little and negligible for most of the time (cf. Weber, 2004; Kutsch, 2008). Nevertheless, the item is implemented in the water budget modeling because dry environments are well known for their extreme variability in amount, distribution and intensity of precipitation, which may lead to recharge after extreme events. Therefore, the model BIL should keep capable of considering direct recharge not at least because of the relatively small aquifer storage capacities and of being able to project scenarios of climate change.

The estimation of net groundwater recharge from precipitation infiltration is based on a lumped coefficient of recharge determined by the application of the zero-dimensional Chloride Mass Balance approach (chapter 6.2.4 & 7.2). Therefore, the representation of all further processes such as evapotranspiration is indirect. The respective annual areal precipitation relating to outcrop surface of each Drâa aquifer is multiplied by the recharge coefficient, which meets maximum recharge estimation with a rate of 2.7% of mean annual precipitation (chapter 7.2). The annual areal precipitation is estimated based on the annual precipitation at the Zagora station using a regression equation of the correlation between precipitation and elevation given by Schulz (2006).

The estimation of direct groundwater recharge for each Drâa aquifer follows the equation below:

$$R_{PCP} = RC_{\mathrm{PCP}} \cdot PCP_j$$

With:

RC_{PCP}	*Recharge coefficient [-]*
PCP_j	*Mean areal precipitation of the outcrop surface of Drâa aquifers [m³/a]*

Recharge from infiltration of irrigation water from Wadi Drâa (R_{Irri})

Groundwater recharge caused by irrigation with water derived from stream flow in the Wadi Drâa is estimated by multiplying a lumped recharge coefficient with the amount of annual irrigation demand satisfied by surface water. The BIL model considers additionally lumped evapotranspiration losses from the irrigation channels on the way from the Wadi Drâa to the fields based on Chamayou (1966).

$$R_{Irri} = SF_{Residual} \cdot LC_{channel} \cdot RC_{\mathrm{Irri}}$$

With:

RC_{Irri}	*Recharge coefficient [-]*
$SF_{Residual}$	*Residual stream flow after subtraction of upstream transmission losses derived to the fields [m³/a]*
$LC_{channel}$	*1 - Coefficient of lumped losses in irrigation channels [-]*

The amount of irrigation water derived to the fields from streamflow depends on the irrigation demand (see below) and the surface water availability, i.e. the residual stream flow after subtraction of transmission losses. Irrigation demand is first satisfied by surface water as long as it is available. The remaining irrigation demand is satisfied by groundwater pumping.

The amount of water derived from Wadi Drâa to the individual oases for irrigation purposes is a fraction of the remaining stream flow considering transmission losses. The fraction of water from the Wadi Drâa routed to the individual oasis follows the direction of a water management committee in the provincial capital Ouarzazate and traditional water rights (Ouhajou, 1996). Consistent data on the repartition of irrigation water were not available. So, the BIL model considers the indicative distribution targets of irrigation water to the Drâa oases defined by ORMVAO (1995) (Table 7-5).

$$SF_{Residual} = \left((SF_{Reservoir} + SF_{MDC}) \cdot (1 - RC_{Wadi}) \cdot LC_{EV}\right) \cdot \mathrm{SF}_{\mathrm{Repartition}}$$

With:

$SF_{Residual}$	*Residual stream flow [m³/a]*
$SF_{Repartition}$	*Fraction of stream flow routed to each individual oasis [-]*

This equation above is valid in the case of the uppermost aquifer, Mezguita. For all other oases, the residual stream flow of the upstream aquifer is subtracted from the total stream flow.

Irrigation demand

Although the irrigation demand is not an item of the groundwater budget, its estimation is crucial for the BIL model. Accordingly, it is treated separately here.

The irrigation demand is assessed indirectly considering three items: the annual crop water demand of the mean assemblage of crops in each oasis, the farmer's response on drought conditions via a reduction of cropping area, and the irrigation efficiency.

The crop water demand is calculated as actual evapotranspiration of crops under optimal water supply using the CropWat model. The CropWat model is based on the Pennman-Monteith equation after Allen et al. (1998) and is freely provided by the Food and Agriculture Organization of the United Nations (FAO; http://www.fao.org/nr/water/infores_databases_cropwat.html cited 24.09.2012). The evapotranspiration estimation implements crop specific K_c-values based on surveys in the Drâa oases (Ministère des travaux publics, 1998). In case of the date palms, the estimations are based on the number and a mean leaf area of the trees (data from ORMVAO and Gresens, 2006).

The water demand of the main crops is then multiplied with the respective annual area under cultivation and their surface percentage. The surface percentage of each crop within the individual oases is assumed constant and is based on the agricultural census (Source: ORMAVO). The cropping area in the Drâa oases varies from year to year indicating that the reduction of the cropping area is a farmer's response on drought conditions. Data on cropping area is only available as lumped area of arable land in the all Drâa oases for the period 1977/78-1993/94 (ORVMAO, 1995). Thereby, data is lacking for the year 1989. The variation in cropping area in the period 1977/78-1993/94 shows a robust correlation of $r^2 = 0.77$ to annual stream flow from reservoir Mansour Eddahbi as main source of irrigation water (Figure 7-5). Thereby, the extraordinary high stream flow value for 1990 is excluded as an outlier. The annual cropping area within BIL is extrapolated based on the regression function of the correlation for the periods 1973/74 to 1976/77, 1994/95 to 2005/06 and 1988/89 to 1989/90. Thereby, a lower threshold of minimum 30 % of cropping area is implementd because cropping for subsistence has always been done.

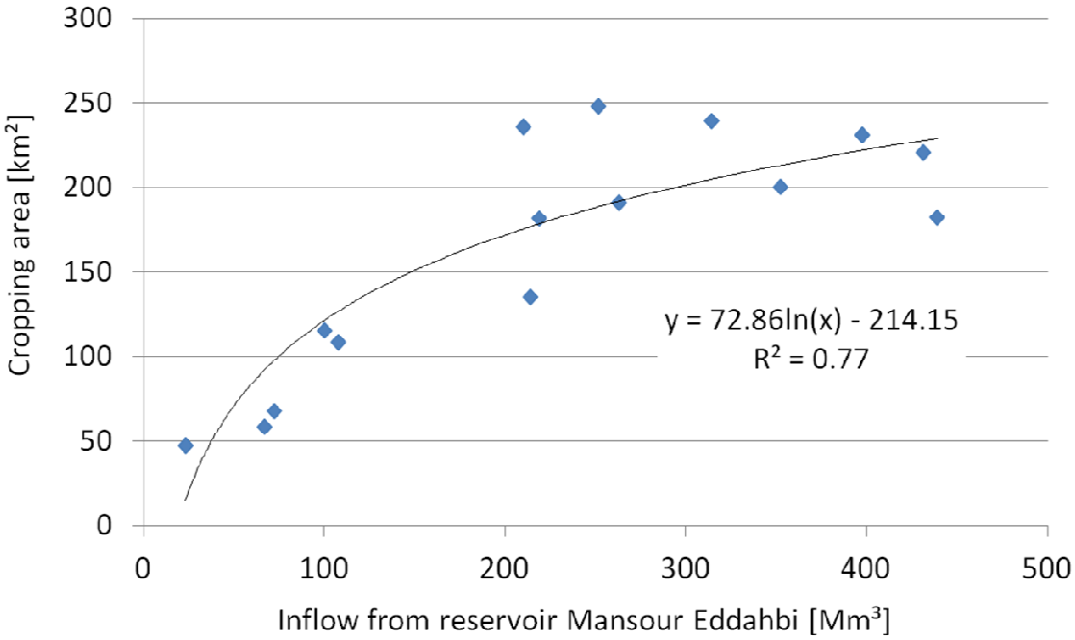

Figure 7-5: Relation between annual cropping area and stream flow from reservoir Mansour Eddahbi.

The combination of the basic assumption that crop water demand equals irrigation water demand and of the broad observation of growing crops leads to the simplified concept that irrigation demand equals extraction for irrigation purposes mindful of irrigation inefficiencies (cf. Ruud et al., 2004).

The irrigation demand is multiplied with a factor of the irrigation inefficiency that is the reciprocal value according to the irrigation efficiency. Therefore, an irrigation efficiency of ~ 40 % is taken as a basis for flood irrigation (Bos & Nugteren, 1990; Foster & Perry, 2010). Irrigation efficiency is manually calibrated because it includes aspects of the water use strategy precise and data is lacking. It is assumed that hence the water use strategy of the farmers is represented as they use more water as necessary if it is available. This may hint on the farmer's awareness of the risk of soil salinity. So, they intent to wash out salts from the root zone by the help of irrigation induced percolation.

$$ID = IIE \cdot \left(WaterDemand_P + \sum_{1}^{c} (WaterDemand_C \cdot CropArea_{Total} \cdot FAP_C) \right)$$

With:

ID	*Annual irrigation demand per oasis [m³]*
IIE	*Irrigation inefficiency factor [-]*
$WaterDemand_P$	*Annual water demand of the lumped number of date palms [m³]*
$WaterDemand_c$	*Annual water demand of crop c [m³ / m²]*
$CropArea_{Total}$	*Total crop area of the oasis in the respective year [m²]*
FAP_C	*Factor of area percentage of crop c [-]*

Recharge from residual stream flow ($R_{Residual}$)

The residual stream flow is the rest of water that stays impounded in the Wadi Drâa after the derivation of irrigation water (chapter 2.2). The residual amount of stream flow in the Wadi Drâa is estimated by subtracting the amount of water derived from the Wadi Drâa. The infiltration of residual stream flow leads to groundwater recharge. It is quantified by multiplying the residual stream flow with the same recharge coefficient that is the same to asses 'recharge from wadi bed infiltration'. Evapotranspiration losses are considered by implementing a coefficient of lumped evaporation of 0.95, i.e. 5 % of the water remaining in the bed of the Wadi Drâa is consumed by evaporation.

$$R_{residual} = \mathrm{SF}_{\mathrm{residual}} \cdot LC_{\mathrm{EV}} \cdot \mathrm{RC}_{\mathrm{Wadi}}$$

With:

LC_{EV}	*1 - Coefficient of lumped evaporation loss from stream flow [-]*
RC_{Wadi}	*Recharge coefficient based on literature reference and calibrated manually [-]*

Recharge from irrigation return flow after groundwater pumping (R_{Return})

Groundwater is pumped to cover the residual irrigation demand that remains unmet by the amount of irrigation water derived from the Wadi Drâa (see Q_{Irri} below). The recharge caused by irrigation return flow is estimated by multiplying the amount of pumped groundwater per Drâa aquifer (see Q_{Irri} below) with the same recharge coefficient that is used to assess the recharge caused by irrigation with water derived from the Wadi Drâa.

$$R_{Return} = \mathrm{Q}_{\mathrm{Irri}} \cdot \mathrm{RC}_{\mathrm{Irri}}$$

With:

Q_{Irri}	*Annual Groundwater withdrawal for irrigation water supply [m³]*
RC_{Irri}	*Recharge coefficient for irrigation water [-]*

Lateral groundwater inflow ($Q_{lateral}$)

Lateral groundwater inflow to each of the Drâa aquifers is assessed using linear storage units. These units correspond to the aquifer types fractured, porous, and fractured/karstic. The basic storage volume is estimated by multiplying the outcrop surface the respective aquifer type with its lumped maximum thickness and a lumped specific yield or storage coefficient taken from literature (Mattheß & Ubell, 2003). Therefore, the surface of the respective aquifer type is withdrawn from the SRTM DEM in combination to the hydrogeological map 1/500,000 (chapter 4 & 6.1.1). The difference between mean elevation of the outcrop area of a Drâa aquifer and the mean elevation of the outcrop area of the respective linear storage unit is taken to estimate the lumped thickness of the linear storage unit. Therefore, the data is derived from the SRTM DEM using GIS techniques (chapter 4). Annual areal recharge within the respective oasis sub-catchment replenishes the storage units. It is estimated based on annual areal precipitation and recharge coefficients gained from the chloride mass balance (CMB; chapter 6.2.4). The annual areal precipitation is extrapolated based on the annual precipitation at the Zagora station using a regression equation of the correlation between precipitation and elevation given by Schulz (2006). The lumped K-value of the respective aquifer type is chosen as recession coefficient to calculate the storage outflow and hence the lateral inflow to a Drâa aquifer (Figure 7-6).

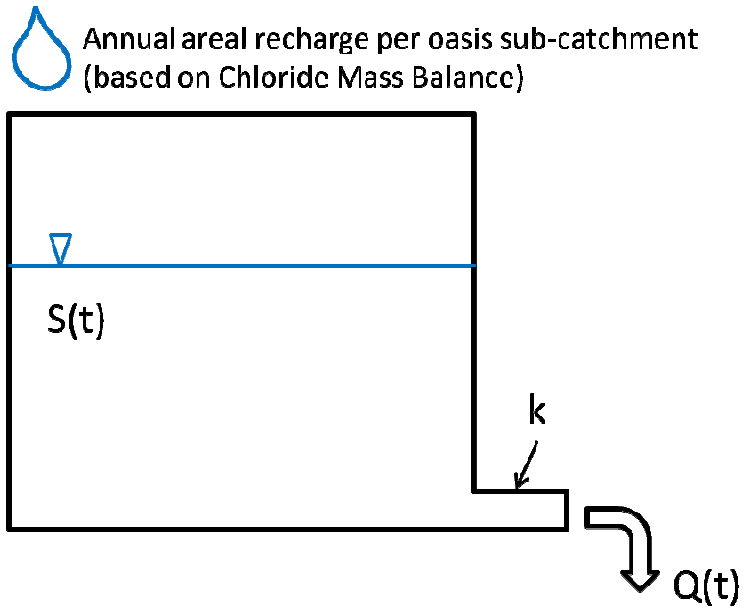

$$S(t) = k \cdot Q(t)$$

With:

S(t)	*Storage → Respective aquifer type*
k	*Recession coefficient → Lumped K-value*
Q(t)	*Outflow → Lateral inflow to Drâa aquifer*

Figure 7-6: Scheme of the linear storage approach used to estimate the lateral groundwater inflow to the Drâa aquifers.

Groundwater withdrawal for irrigation water supply (Q_{Irri})

The priority in using water from the Wadi Drâa for irrigation before using groundwater is the basic assumption to estimate the amount of pumped irrigation water from the aquifers. So, the pumped groundwater equals the residual irrigation demand that could not be covered by the amount of water derived from the Wadi Drâa. The amount of surface water applied to the fields (residual stream flow minus channel losses) is subtracted from the irrigation demand resulting in the residual irrigation demand.

$$Q_{Irri} = ID - (\mathrm{SF}_{\mathrm{residual}} \cdot LC_{\mathrm{channel}})$$

With:

ID	*Irrigation demand [m³/a]*
$SF_{residual}$	*Residual stream flow after the derivation of irrigation water [m³/a]*
$LC_{channel}$	*1 - Coefficient of lumped losses in irrigation channels [-]*

Groundwater withdrawal for domestic water supply ($Q_{domestic}$)

Groundwater withdrawal for domestic water supply is calculated in a pre-processing module developed together with the Ethnologist Ch. Rademacher of the IMPETUS project. The annual domestic water consumption per Drâa aquifer is based on the daily water consumption as per capita equivalent and the projected demographic development. Water consumption and population development are subdivided into urban and rural areas, as those differ considerably. Thereby, the only urban settlements exist in the systems of Mezguita, Ternata and Ktaoua. Ternata plays a special role for the estimation of the withdrawal for domestic water consumption because the water supply wells tapp the aquifers belonging to Fezouata. The data on per capita water consumption for both urban and rural areas stems from local survey carried out in the line of the IMPETUS and the Service Eau Ouarzazate. The data is assumed representative. The lack of demographic data is filled by a simple linear interpolation between survey dates.

$$Q_{domestic} = WC_{\mathrm{urban}} \cdot IH_{urban} + WC_{\mathrm{rural}} \cdot IH_{rural}$$

With:

WC_{urban}	*Urban water consumption as per capita equivalent [m³/a]*
IH_{urban}	*Number of urban inhabitants*
WC_{rural}	*Rural water consumption as per capita equivalent [m³/a]*
IH_{urban}	*Number of rural inhabitants*

Groundwater outflow to the downgradient Drâa aquifer / area ($Q_{downgradient}$)

The annual groundwater outflow to the downgradient Drâa aquifer or area (in case of Mhamid) is realized by the calculation of 1D groundwater flow based on the Darcy Equation. Therefore, the flow section at the respective hydraulic barrier at the lower end of each Drâa aquifer is taken as basis. The hydraulic gradient between the Drâa aquifers is estimated based on the mean elevation of the belonging oasis and the prior modeled groundwater levels. So, the six Drâa aquifers are coupled to form an aquifer cascade that reflects long-term changes as super-ordinate system.

$$Q_{downgradient} = K \cdot I \cdot A \cdot 31536000$$

With:

K	*Saturated hydraulic conductivity [m/s]*
I	*Hydraulic gradient based on water levels of the antecedent year [-]*
A	*Flow section area at downstream barrier [m²]*
31536000	Factor relating seconds to years

Groundwater inflow from the upstream Drâa aquifer ($Q_{upstream}$)

The annual groundwater outflow to the downgradient Drâa aquifer is the inflow of the next downstream Drâa aquifer.

7.4 Model parameterization

The model parameters stem from own surveying and pre-processing as well as reports and literature (chapter 4). Parameters are all input data, which stay fixed in the model runs. The model input is defined as annually variable input data driving the dynamic in the simulations.

Aquifer dimension & properties

The data on aquifer dimension and properties are fix parameters. The BIL model uses the outcrop surface, the mean elevation and the respective catchment area of the Drâa aquifers from own investigations. Thereby, the aquifer delimitation is arbitrary relating to Mhamid. Accordingly, the Mhamid aquifer represents the boundary condition at the lower end of the chain of the Drâa aquifers. The mean thickness and the specific yield data derives from bore logs provided by the Service Eau Ouarzazate. The initial saturated thickness is estimated based on groundwater level data. Rational for the parameterization is provided in chapter 6, the parameters selected for the BIL model are summarized in Table 7-2.

Table 7-2: Parameterization of the aquifer properties (see chapter 6.1).

	Mezguita	Tinzouline	Ternata	Fezouata	Ktaoua	Mhamid
Specific yield [-]	0.19	0.22	0.15	0.10	0.13	0.15
Outcrop surface [km²]	30.5	56.4	56.8	72.5	127.2	44
Aquifer thickness [m]	20.5	20.5	19.5	21.5	31.5	50.5
Catchment area [km²]	2,349	1,273	1,442	2,899	708	206
Mean elevation [m]	899	814	739	677	611	554
Initial saturated thickness [m]	8	6	5	14	22	40
Distance to downstream aquifer [m]	36500	34000	32250	35000	31750	30000

Precipitation

Annual precipitation data at the Zagora station is provided by the ORMVAO for the period 1973/74 to 2005/06. The BIL model uses extrapolated precipitation data of the Drâa oases based on a regression equation of the correlation between precipitation and elevation given by Schulz (2006).

Table 7-3: Annual precipitation [m³] at the Drâa oasis extrapolated based on the annual precipitation at the Zagora station using a regression equation of the correlation between precipitation and elevation given by Schulz (2006).

Year	Zagora station	Mezguita	Tinzouline	Ternata	Fezouata	Ktaoua	Mhamid
1973/74	0.034	0.042	0.037	0.034	0.031	0.028	0.025
1974/75	0.045	0.056	0.050	0.045	0.041	0.037	0.034
1975/76	0.081	0.100	0.089	0.081	0.074	0.067	0.061
1976/77	0.022	0.027	0.024	0.021	0.020	0.018	0.016
1977/78	0.076	0.095	0.085	0.076	0.070	0.063	0.058
1978/79	0.232	0.289	0.257	0.232	0.212	0.192	0.175
1979/80	0.072	0.089	0.080	0.072	0.065	0.059	0.054
1980/81	0.033	0.041	0.037	0.033	0.030	0.027	0.025
1981/82	0.050	0.062	0.056	0.050	0.046	0.042	0.038
1982/83	0.019	0.024	0.021	0.019	0.017	0.016	0.014
1983/84	0.031	0.039	0.035	0.031	0.029	0.026	0.024
1984/85	0.098	0.122	0.109	0.098	0.089	0.081	0.074
1985/86	0.024	0.030	0.027	0.024	0.022	0.020	0.018
1986/87	0.029	0.036	0.032	0.029	0.026	0.024	0.022
1987/88	0.246	0.306	0.273	0.246	0.225	0.204	0.186
1988/89	0.102	0.127	0.114	0.102	0.093	0.085	0.077
1989/90	0.077	0.096	0.086	0.077	0.071	0.064	0.058
1990/91	0.045	0.056	0.050	0.045	0.041	0.037	0.034
1991/92	0.080	0.100	0.089	0.080	0.073	0.066	0.061
1992/93	0.043	0.053	0.047	0.042	0.039	0.035	0.032
1993/94	0.037	0.046	0.041	0.037	0.034	0.031	0.028
1994/95	0.115	0.142	0.127	0.114	0.105	0.095	0.087
1995/96	0.126	0.156	0.139	0.125	0.115	0.104	0.095
1996/97	0.043	0.054	0.048	0.043	0.039	0.036	0.033
1997/98	0.114	0.141	0.126	0.113	0.104	0.094	0.086
1998/99	0.020	0.025	0.022	0.020	0.018	0.017	0.015
99/2000	0.059	0.074	0.066	0.059	0.054	0.049	0.045
2000/01	0.011	0.013	0.012	0.011	0.010	0.009	0.008
2001/02	0.040	0.050	0.045	0.040	0.037	0.033	0.030
2002/03	0.041	0.052	0.046	0.041	0.038	0.034	0.031
2003/04	0.101	0.126	0.112	0.101	0.093	0.084	0.077
2004/05	0.028	0.035	0.032	0.028	0.026	0.023	0.021
2005/06	0.068	0.085	0.075	0.068	0.062	0.056	0.051

Groundwater levels

Groundwater level data is available from the archives of the Service Eau Ouarzazate and the ORMVAO. Single data sets of fragmentary monthly to annual resolution are used to set the initial conditions of the model parameterization (Table 7-2; chapter 4 & 6.2.1). Furthermore, these data are used to check the model plausibility at the aquifers of Mezguita, Tinzouline, Ternata and Fezouata (chapter 7.5.3).

Stream flow

The total annual stream flow in the MDC comprises the inflow from the reservoir Mansour Edahbbi in the Upper Drâa Catchment (UDC) and the stream flow that generates within the MDC. The inflow from the UDC is provided by the ORMVAO. The stream flow generating within the MDC stems from the application of the run-off coefficient of 8 % given by Chamayou (1966).

Table 7-4: Annual stream flow as sum of inflow from the reservoir Mansour Edahbbi in the Upper Drâa Catchment (UDC) and stream flow forming within the MDC (Middle Drâa Catchment) based on the areal precipitation of the sub-catchments of the Drâa oasis and the run-off coefficient of 8 % given by Chamayou (1966).

Year	Inflow from UDC [Mm³]	Stream flow from MDC [Mm³]	Sum of stream flow in the MDC [Mm³]
1973/74	160	25	185
1974/75	133	33	166
1975/76	95	59	154
1976/77	124	16	140
1977/78	214	56	270
1978/79	263	170	433
1979/80	431	53	484
1980/81	352	24	376
1981/82	219	37	256
1982/83	100	14	114
1983/84	23	23	46
1984/85	67	72	139
1985/86	108	18	126
1986/87	72	21	93
1987/88	439	181	619
1988/89	815	75	890
1989/90	1,380	57	1437
1990/91	314	33	347
1991/92	398	59	456
1992/93	210	31	241
1993/94	251	27	279
1994/95	256	84	340
1995/96	634	92	726
1996/97	277	32	309
1997/98	257	83	340
1998/99	221	15	236
99/2000	211	43	254
2000/01	93	8	101
2001/02	71	29	101
2002/03	91	30	121
2003/04	110	74	184
2004/05	116	21	137
2005/06	107	50	157

Groundwater recharge

The BIL model estimates various items of groundwater recharge as listed below (chapter 7.3):

- Recharge from stream flow infiltration in the bed of the Wadi Drâa
- Recharge from precipitation infiltration (direct recharge)
- Recharge from infiltration of irrigation water derived from Wadi Drâa
- Recharge from residual stream flow
- Recharge from irrigation return flow after groundwater pumping

For each recharge pathway (via wadi bed, via irrigation water, and via precipitation at the aquifer surface) conceptual coefficients that describe the fraction of the water that recharge the aquifer are given (Table 7-5). However, in order to calculate the absolute amount of water reaching the aquifer, the amount of precipitation, streamflow and irrigation water must be estimated. Precipitation amount is given in Table 7-3 above and multiplied with the aquifer outcrop surface (Table 7-2). Stream flow data is given in Table 7-4 above. Thereby, the reparation fraction of irrigation water to the Drâa oases from the Wadi Drâa is taken as planned by the ORMVAO (1995) shown in Table 7-5. The irrigation demand is calculated based on the crop water demand (Parameterization see Table 7-6), the irrigation efficiency factor and the cropping area for each crop (Table 7-7, Figure 7-5). The irrigation efficiency of 40 % is taken from literature and calibrated subsequently (chapter 7.3 & 7.5.2).

Irrigation demand is first satisfied by the available stream flow (after taking into consideration recharge from stream flow, repartition of stream flow to the respective oasis, and evaporation from stream flow (Table 7-5). The remaining irrigation demand is covered from groundwater. Irrigation water from both sources recharges the aquifer assuming the coefficient given in Table 7-5.

Table 7-5: Recharge and evaporation loss coefficients and fraction of repartition of stream flow to the Drâa oases (indicative target value by the ORMVAO, 1995).

	Mezguita	Tinzouline	Ternata	Fezouata	Ktaoua	Mhamid
Recharge coefficient for stream flow infiltration [-]	0.08	0.08	0.08	0.08	0.10	0.10
Recharge coefficient for precipitation [-]	0.027	0.027	0.027	0.027	0.027	0.027
Recharge coefficient for irrigation water infiltration [-]	0.027	0.027	0.027	0.027	0.027	0.027
Evaporation loss coefficient for stream flow [-]	0.05	0.05	0.05	0.05	0.05	0.05
Coefficient for losses in irrigation channels between Wadi and field [-]	0.05	0.05	0.05	0.05	0.05	0.05
Fraction of irrigation water repartition from the Wadi Drâa [%]	8	8	30	14	28	12

Table 7-6: Crop water demand calculated based on the CropWat model. Climate parameters are extracted from the IMPETUS weather stations (IMPETUS, 2008)

	Mezguita	Tinzouline	Ternata	Fezouata	Ktaoua	Mhamid
Annual water demand of wheat [mm/m²]	426.97	437.73	439.10	443.84	450.71	455.45
Annual water demand of barley [mm/m²]	412.79	423.66	424.71	429.41	436.27	440.97
Annual water demand of alfalfa [mm/m²]	1344.96	1364.85	1372.01	1382.14	1396.42	1405.88
Annual water demand of henna [mm/m²]	1344.96	1364.85	1372.01	1382.14	1396.42	1405.88
Annual water demand of vegetables [mm/m²]	481.11	488.87	491.22	495.05	500.48	504.09
Annual water demand of maize [mm/m²]	662.72	669.25	674.08	678.35	683.72	687.69
Annual water demand of date palms [mm/tree]	2383.17	2439.60	2421.11	2518.04	2565.79	2600.80

Table 7-7: Distribution of crops [% of total cropping area] for each oasis (Ministère des travaux publics, 1998).

	Mezguita	Tinzouline	Ternata	Fezouata	Ktaoua	Mhamid
Fraction of wheat [%]	60.91	57.53	64.36	71.50	68.93	74.18
Fraction of barley [%]	5.08	6.77	4.78	6.18	15.51	13.91
Fraction of alfalfa [%]	21.57	18.61	17.51	18.01	9.48	9.27
Fraction of henna [%]	3.05	5.08	2.65	1.41	1.03	0.00
Fraction of vegetables [%]	4.31	3.38	0.00	0.00	0.00	0.00
Fraction of maize [%]	5.08	8.63	10.71	2.90	5.05	2.64
Number of date palms	271,000	184,660	330,600	254,400	245,240	131,100

Lateral groundwater inflow

Three general units are differentiated within the oases catchments: porous, fractured, and fractured/karstic rocks. Data on the dimension of the linear storage units are needed to estimate the lateral groundwater inflow to the Drâa aquifers. Furthermore, linear storage units use the effective porosity and fracture volume. The lumped K-value of the respective linear storage unit is taken as recession coefficient. The parameterization is summarized in Table 7-8 and 7-9. Precipitation data is taken from Table 7-3 above and multiplied with the area given in Table 7-9.

Table 7-8: Parameterization of the linear storage units in order to calculate lateral inflow.

	Fractured rocks	Porous rocks	Fractured/karstic rocks
Effective porosity [-]	0.01	0.12	0.08
Recession coefficient [-]	$1 \cdot 10^{-8}$	$1 \cdot 10^{-4}$	$1 \cdot 10^{-7}$
Groundwater recharge factor [-]	0.024	0.039	0.024

Groundwater in-/outflow along the main hydraulic gradient

The estimation of groundwater outflow from an upstream Drâa aquifer and hence the inflow to the downstream Drâa aquifer is based on the Darcy equation. The needed parameters are listed in Table 7-9. The hydraulic conductivity is based on the transmissivities given by Chamayou (1966). The other parameters are approximated based on own mapping and analysis of bore logs provided by the Service Eau Ouarzazate. The BIL model estimates the lumped annual hydraulic gradient dynamically. The mean elevation of the oases and distance to the downstream oasis (Table 7-2) together with the output filling level of the previous year is used to calculate the hydraulic gradient.

Table 7-9: Parameters to calculate 1D-groundwater flow along the main flow path beneath the Wadi Drâa from the respective upstream to the next downstream aquifer with transmissivity from Chamayou (1966).

Aquifer unit	Thickness of flow section [m]	Width of flow section [m]	Area of flow section [m²]	Mean transmissivity (Chamayou, 1966) [m²/s]	Hydraulic conductivity [m/s]
Mezguita	10	400	4,000	$6 \cdot 10^{-3}$	$6 \cdot 10^{-3}$
Tinzouline	10	300	3,000	$5 \cdot 10^{-2}$	$5 \cdot 10^{-3}$
Ternata	6	1,000	6,000	$5 \cdot 10^{-2}$	$8 \cdot 10^{-3}$
Fezouata	10	500	5,000	$2 \cdot 10^{-2}$	$2 \cdot 10^{-3}$
Ktaoua	10	1,300	13,000	$7 \cdot 10^{-3}$	$7 \cdot 10^{-3}$
Mhamid	25	12,000	150,000	$5 \cdot 10^{-3}$	$2 \cdot 10^{-4}$

Domestic water consumption

The daily domestic water consumption as per capita equivalent is different in rural and urban areas as the surveying of IMPETUS and the Service Eau Ouarzazate reveal (Rademacher, 2009). The BIL model uses approximate lumped values to estimate the annual domestic water consumption per capita:

- Rural areas: 30 L/d per capita
- Urban areas: 50 L/d per capita

The number of inhabitants stem from a population census in the year 2000. The demographic development is projected using a linear function based on growth rates for rural and urban areas given in the population census from the year 2000 (Table 7-10).

Table 7-10: Parameters to calculate 1D-groundwater flow along the main flow path beneath the Wadi Drâa from the respective upstream to the next downstream aquifer with transmissivity from Chamayou (1966).

	Mezguita	Tinzouline	Ternata	Fezouata	Ktaoua	Mhamid
Demographic development – rural [%/a]	0.80	1.12	1.07	0.90	0.36	-0.90
Demographic development – urban [%/a]	3.10	-	*	2.90	-	-

(- means that no urban area exists; * urban water consumption is covered by wells tapping the downstream system of Fezouata where no urban settlement exists)

7.5 Results of groundwater balance simulation

The results of the modeled annual lumped filling levels of the Drâa aquifers show differentiated aquifer response in the period 1973/74 – 2005/06 with a strong relation to the inflow to the Wadi Drâa from the reservoir Mansour Eddahbi and the total stream flow respectively (Figure 7-7).

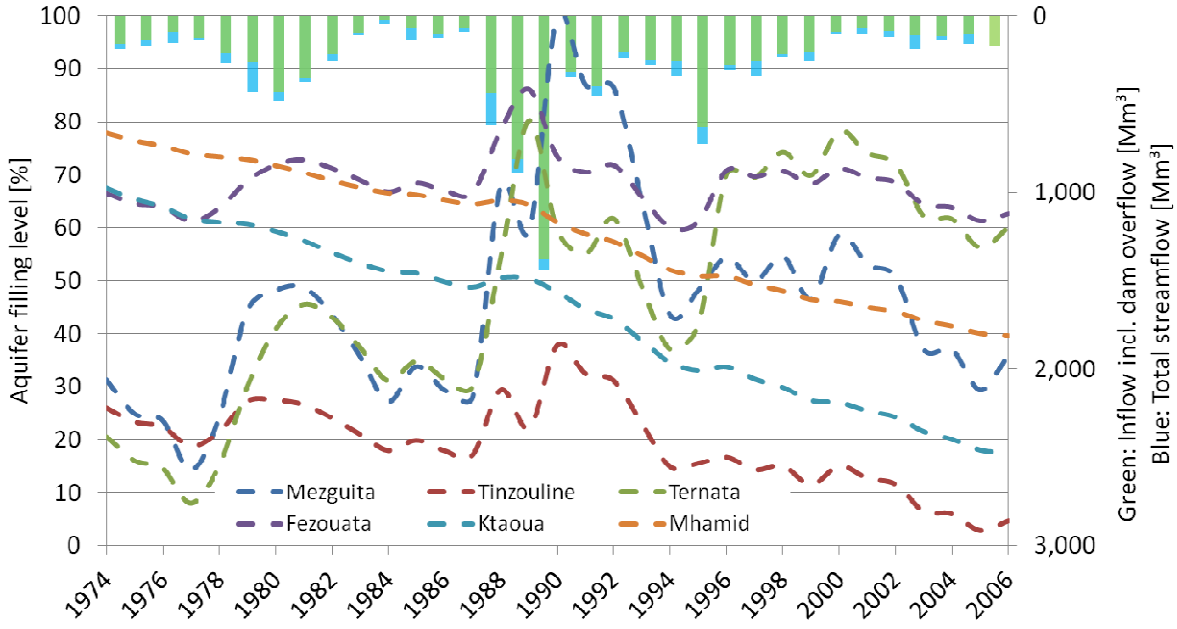

Figure 7-7: Overview of the modeled filling level of the Drâa aquifers in the period 1973/74 – 2005/06.

The model response of the Ktaoua and the Mhamid aquifer is dammed in comparison to all the others and show a clear decline of the groundwater reservoirs. This is partly an artifact caused by a lack of data relating to Ktaoua. In terms of Mhamid, the aquifer represents a generalized boundary condition of the chain of Drâa aquifers that hinders the modeling of the aquifer dynamic (chapter 7.2 & 7.3).

The modeled groundwater extraction for irrigation is compared to the modeled amount of irrigation water derived from stream flow to evaluate relative importance of source of irrigation water relating to the targeted repartition of water to the oases from the Wadi Drâa and without water pricing (Figure 7-8). Thereby, the groundwater extraction costs the purchase of the pump and its running expenses (Heidecke, 2009). The importance of groundwater extraction for irrigation in opposite to irrigation with surface water is high and varies from Drâa aquifer to Drâa aquifer. The reason for that is the strategy of farmers to expand arable land if relatively more stream flow is available in combination to the fact that different crop mix and climatic conditions result in different irrigation demands in the oases. Even if a lot of stream flow from the reservoir Mansour Eddahbi is available, the farmers have to pump relatively more groundwater for irrigation because the relation between cropping area and stream flow exceeds the 1:1 ratio by far (Figure 7-5).

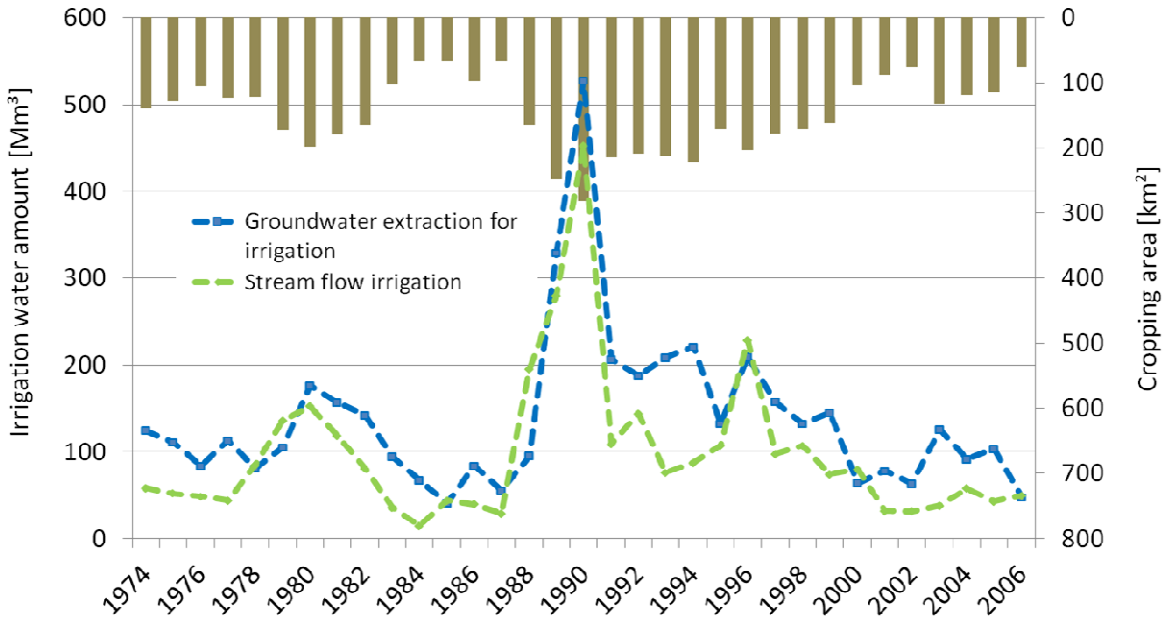

Figure 7-8: Modeled groundwater extraction for irrigation and modeled irrigation derived from stream flow with the cropping area as lumped mean values for all Drâa aquifers in the period 1973/74 – 2005/06.

The ratio of mean groundwater extraction for irrigation versus the mean amount of irrigation water from the Wadi Drâa over the period 1973/74 – 2005/06 represents the differences in the meaning of irrigation with groundwater. So, the higher the ratio, the more important is groundwater for irrigation over irrigation with surface water (Table 7-11).

Table 7-11: Ratio of mean groundwater extraction for irrigation versus the mean amount of irrigation water from the Wadi Drâa over the period 1973/74 – 2005/06.

	Mezguita	Tinzouline	Ternata	Fezouata	Ktaoua	Mhamid
Ratio of mean groundwater extraction for irrigation versus the mean amount of irrigation water from the Wadi Drâa	2.6	2.8	0.7	1.8	2.0	4.2
Mean irrigation demand [Mm³]	65.4	48.5	57.0	23.1	29.9	11.9
Ratio of mean groundwater volume versus mean irrigation demand	0.8	1.0	1.4	4.6	7.5	16.6
Ratio of maximum aquifer volume versus mean irrigation demand	1.8	5.3	2.9	6.7	17.4	28.0

Accordingly, irrigation with groundwater as opposite to irrigation with surface water plays the most important role in Mhamid because it receives the smallest amount of stream flow at the end of the oases chain in combination to the second-smallest repartition fraction of irrigation water from the Wadi Drâa (Figure 7-9; Table 7-11). The modeling of the Mhamid aquifer is based on scarce data particularly in terms of the aquifer dimensions (chapter 6.1.4). So, these results represent estimations that require to be verified.

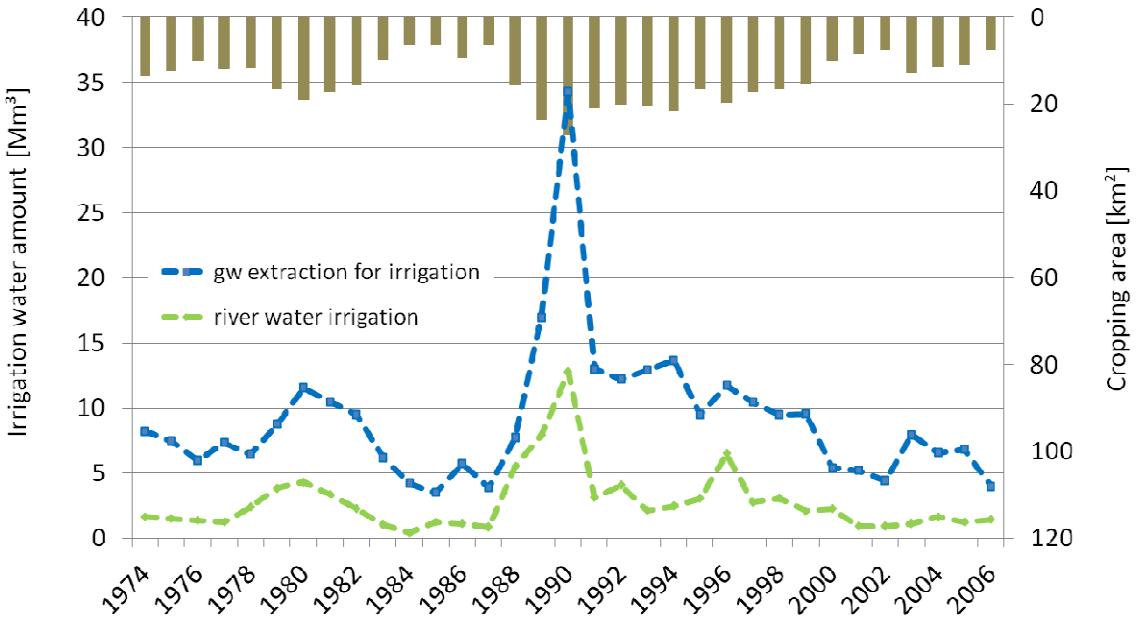

Figure 7-9: Modeled groundwater extraction for irrigation and modeled irrigation derived from stream flow with the cropping area at the Mhamid aquifer in the period 1973/74 – 2005/06.

For the Ternata aquifer, the irrigation with surface water is most important because the oasis receives the highest percentage of stream flow for irrigation (30 %) strongly linked to the cropping area (Figure 7-10; Table 7-11; Table 7-5; Table 7-1).

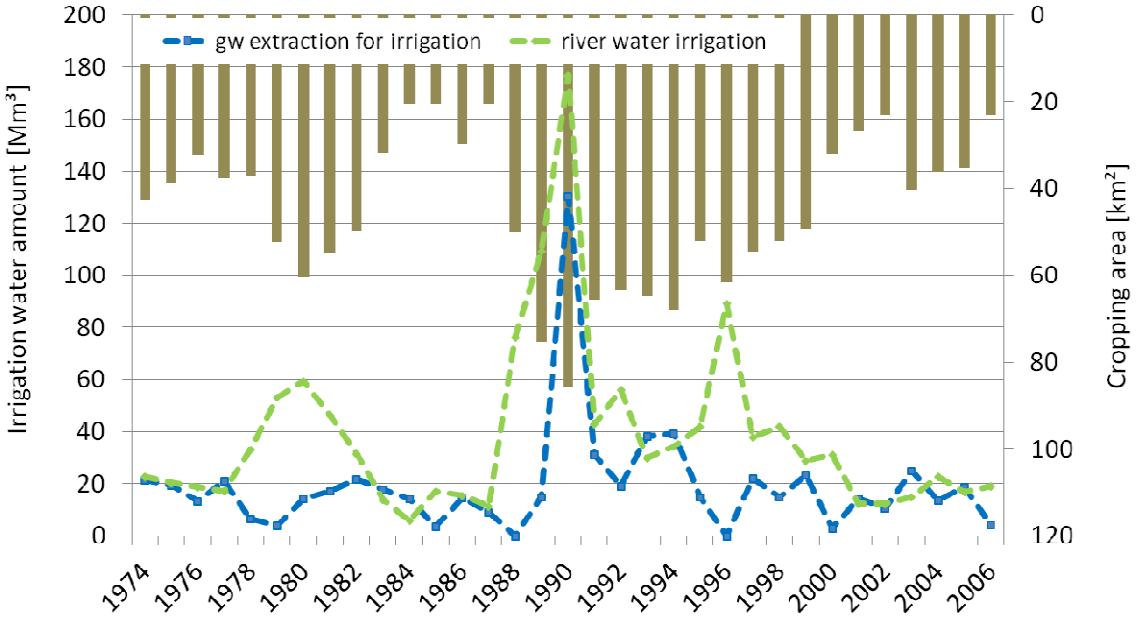

Figure 7-10: Modeled groundwater extraction for irrigation and modeled irrigation derived from stream flow with the cropping area at the Ternata aquifer in the period 1973/74 – 2005/06.

For all other Drâa aquifers, the ratio of mean groundwater extraction for irrigation versus the mean amount of irrigation water from the Wadi Drâa is between these of the Mhamid and the Ternata aquifer (Table 7-11).

The comparison of the agricultural water demand and the groundwater extraction for domestic supply verifies the dominance of irrigation demand relating to the overview of all Drâa aquifers. The share of domestic water extraction is about 1 % of the irrigation demand and exceeds never 3 % of the total water demand of all Drâa aquifers together (Figure 7-11).

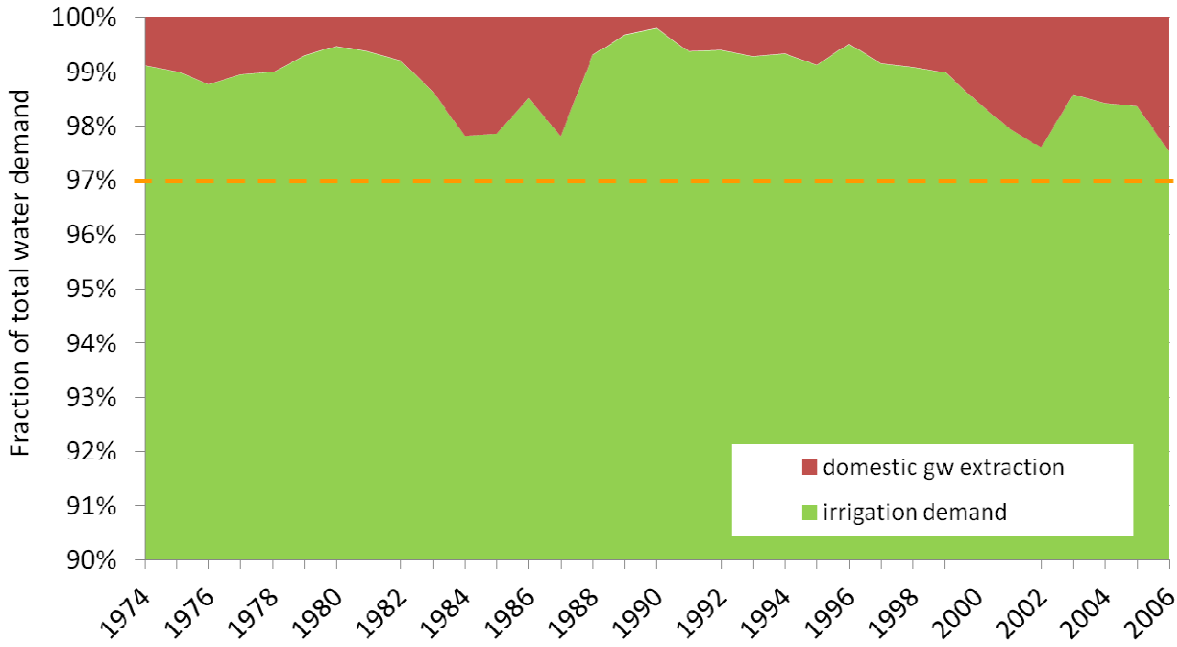

Figure 7-11: Comparison of modeled agricultural water demand (irrigation demand) and domestic groundwater extraction for all Drâa aquifer in the period 1973/74 – 2005/06.

Only at the Fezouata aquifer the share of domestic water supply is more than three percent ranging between less than 1 % and up to 9 % (Figure 7-12). This due to the circumstance that a series of wells is located in the catchment of the Fezouata aquifer producing drinking water for the town Zagora, which is located in the area of the Ternata aquifer (Figure 7-2). Accordingly, the only significant domestic water consumption relates to the urban water supply of Zagora according to the regional lumped model approach. At the local scale, the domestic water consumption can be strictly limited due to aquifer heterogeneity and mechanisms of groundwater flow, which is not represented in the BIL model.

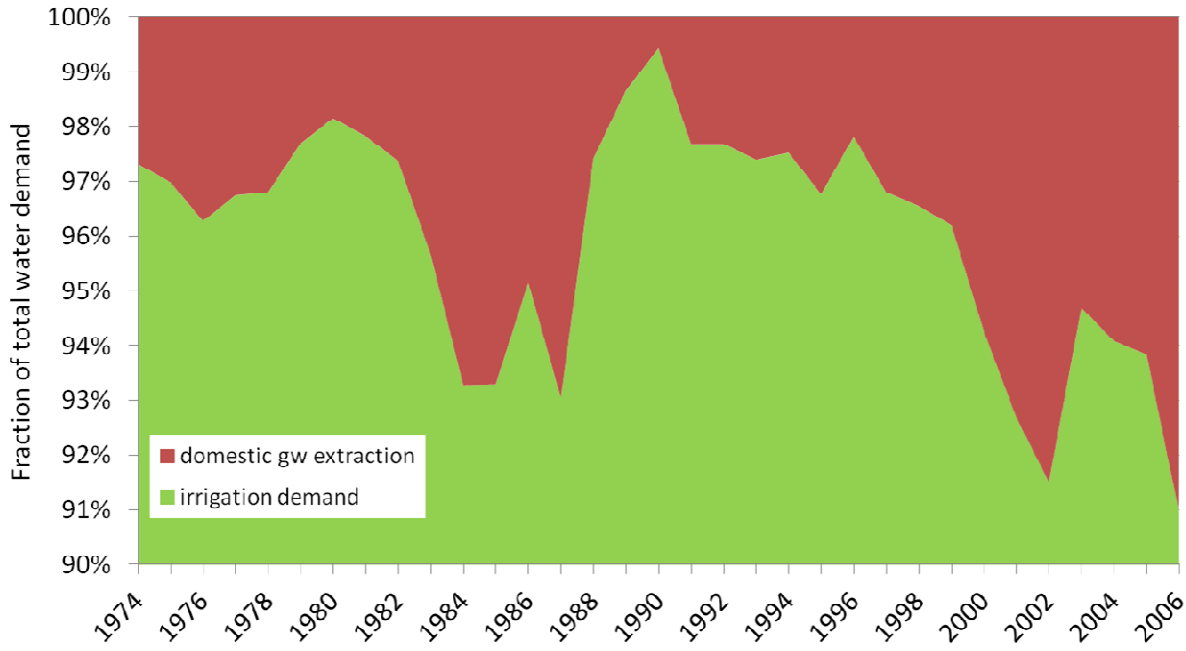

Figure 7-12: Comparison of modeled agricultural water demand (irrigation demand) and domestic groundwater extraction at the Fezouata aquifer in the period 1973/74 – 2005/06 (change scaling of the ordinate).

The representation of all components of annual aquifer inflow and groundwater recharge for all Drâa aquifers clarifies the significance of recharge from stream flow and wadi bed infiltration overall (Figure 7-13: “recharge from wadi bed infiltration” and “recharge from residual stream flow”). The share of total groundwater recharge from wadi bed infiltration ranges between approximately 65 % in dry years (1984) and 95 % in distinct humid years (1990). So, the managed aquifer recharge via the management of the water releases from the reservoir Mansour Eddahbi plays an important role for agriculture and existence in the Drâa oases. This becomes even more evident in relation to the share of irrigation demand over domestic water supply accounting generally for more than 97 % (Figure 7-13).

In the dry periods around 1984 and 2002, the lateral groundwater inflow (“gw afflux”) becomes increasingly important reaching more than 20 % of total aquifer inflow and recharge. Each other inflow and recharge component accounts generally for less than 5 % summing up for maximum 10 % of total aquifer inflow and recharge. As a result, the selective enhancement of infiltration of stream flow displays an option of enhanced managed aquifer recharge even if groundwater pumping is costly whereas surface water is free of charge (chapter 9).

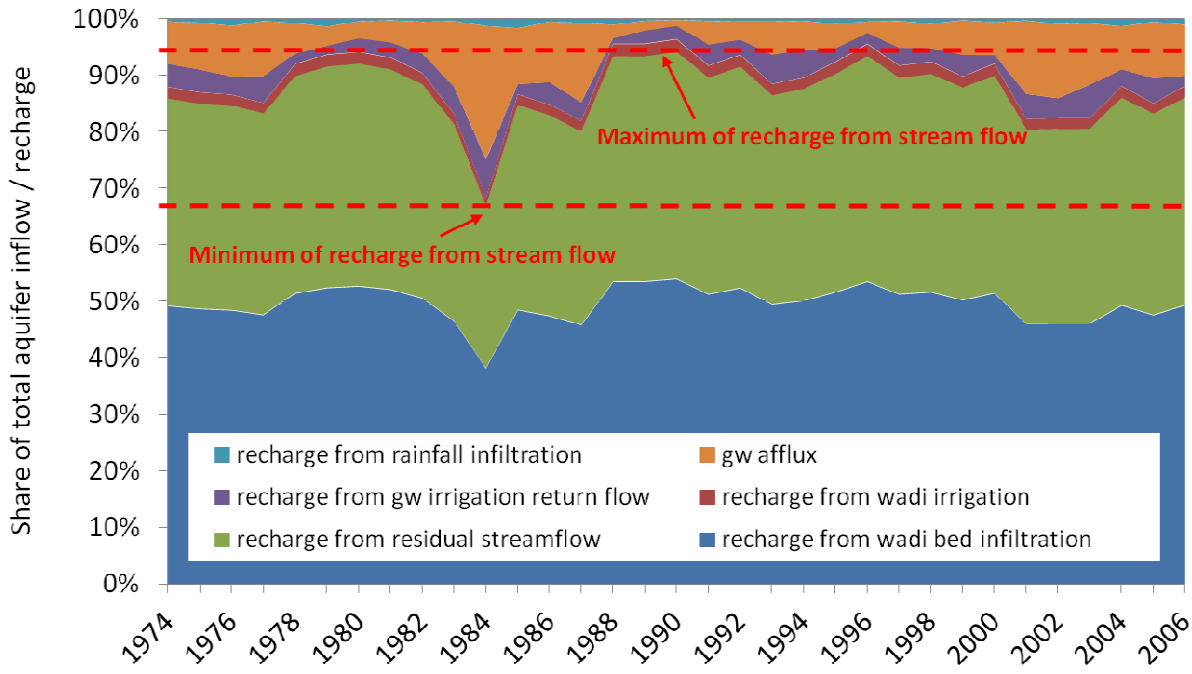

Figure 7-13: Modeled proportional components of annual aquifer inflow and groundwater recharge for all Drâa aquifers in the period 1973/74 – 2005/06.

The Fezouata aquifer forms an exception from the results for the Drâa aquifers overall. The recharge from stream flow and wadi bed infiltration overall at Fezouata ranges from around 40 % to 90 % and falls below the lumped values for all Drâa aquifers (Figure 7-13: 65 to 95 %; Figure 7-14: “recharge from wadi bed infiltration” and “recharge from residual stream flow”).

Thereby, the lateral groundwater inflow (“gw afflux”) rises in significance ranging largely between 3 % and 55 %. This is due to the large catchment of the Fezouata aquifer and the intermediating role of the Thick Basin aquifer of the Feija of Zagora (chapter 6.1.3 & 6.3.3.3). Accordingly, the lateral groundwater inflow buffers drought effects, which in turn leads to a subdued filling level response of the Fezouata aquifer in comparison to all other Drâa aquifers (Figure 7-7; Figure 7-19).

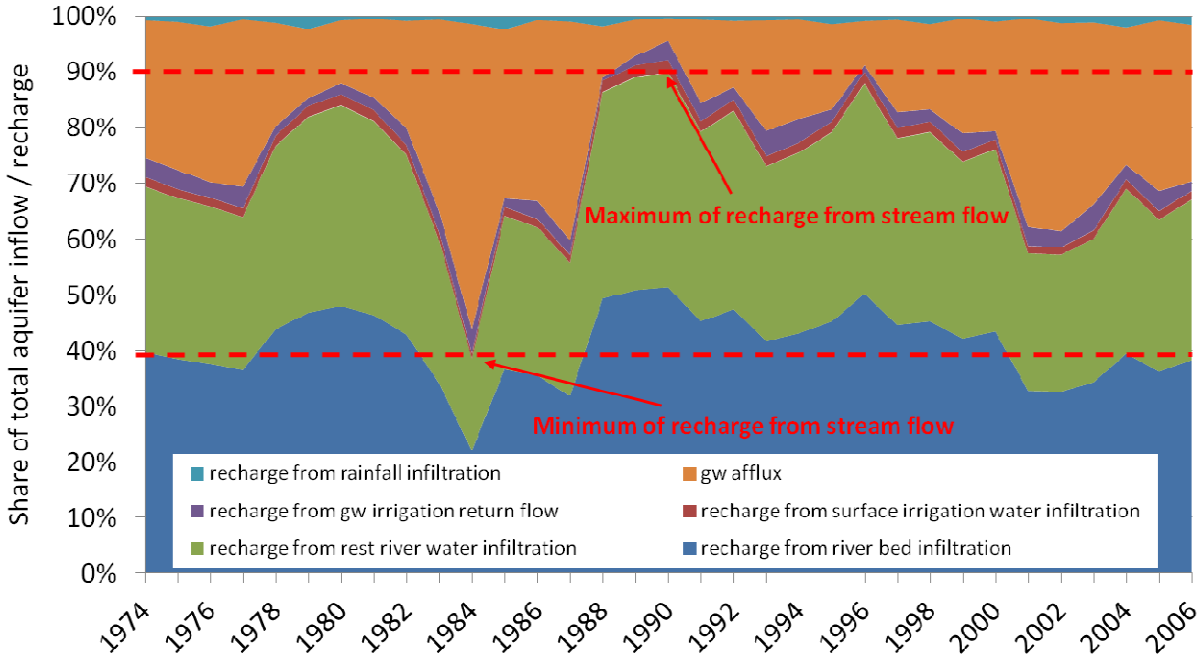

Figure 7-14: Modeled proportional components of annual aquifer inflow and groundwater recharge at the Fezouata aquifer in the period 1973/74 – 2005/06.

The Drâa aquifers show different trends in filling level over the whole model period. Accordingly, the sum of change in aquifer filling level is depicted as percent (Table 7-12). The water balance of the Tinzouline, Ktaoua and Mhamid aquifer is clearly negative. The Mezguita and Fezouata aquifer show a slight overall decline of filling level. As opposed, the overall change in filling level at the Ternata aquifer reveals a significant positive trend. In the following sections, the main model results for each Drâa aquifer are presented in terms of annual aquifer filling level and change in annual aquifer filling level.

Table 7-12: Sum of change in filling level of the Drâa aquifer over the whole model period 1974 – 2006.

	Mezguita	Tinzouline	Ternata	Fezouata	Ktaoua	Mhamid
Sum of change in aquifer filling level [%]	-3	-25	34	-6	-52	-39

The Mezguita aquifer

The modeled filling levels of the Mezguita aquifer range between 14 % and 100 %. The mean aquifer filling level is 46 % (median = 44 %; Figure 7-15). The aquifer response is highly dynamic although the mean specific yield value is high (19 %; Table 7-1). The dynamic aquifer behavior is caused by the combination of the smallest aquifer volume and the highest mean irrigation demand (65.4 Mm^3) accounting for a ratio of 1.8 (Table 7-11). Thereby, the overall water availability is the most in comparison to all other Drâa aquifers. Mezguita is the uppermost aquifer and thus receives inflow from the reservoir earlier than the lower Drâa aquifers. Furthermore, the mean lateral groundwater inflow to Mezguita is the second highest (1.3 Mm^3) only topped by the afflux to the Fezouata aquifer (2.3 Mm^3).

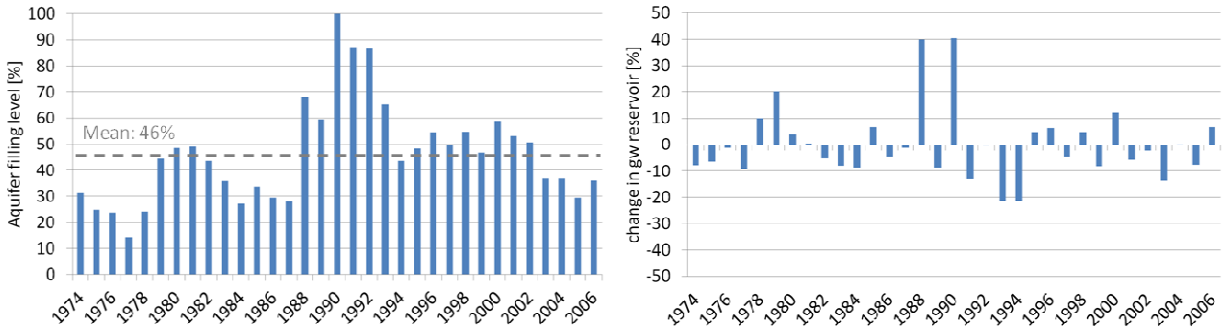

Figure 7-15: Modeled filling level Mezguita aquifer in the period 1973/74 – 2005/06 (mean = 46 %) and its change in groundwater reservoir.

The Tinzouline aquifer

The filling levels of the Tinzouline aquifer reveal the lowest value in comparison to all other Drâa aquifers ranging from 3 % to 38 % (Figure 7-17). The mean aquifer filling level is 19 % (median = 19 %). This is because of a relatively low initial filling level and smooth course of the aquifer response. The aquifer response is subdued in dynamic because the mean specific yield value is high (22 %; Table 7-1). Furthermore, Tinzouline reveals a medium ration of maximum aquifer volume versus irrigation demand and a relatively high annual lateral groundwater inflow accounting for around 1 Mm³ (Table 7-11).

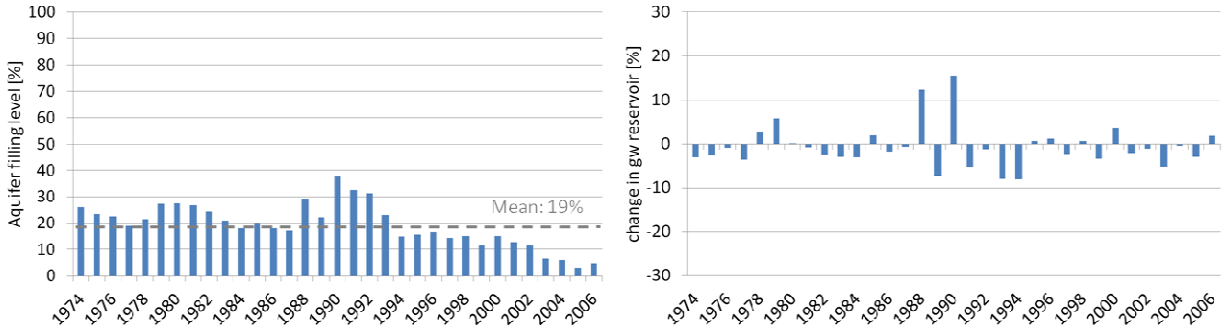

Figure 7-16: Modeled filling level Tinzouline aquifer in the period 1973/74 – 2005/06 (mean = 19 %) and its change in groundwater reservoir.

The filling level of the Tinzouline falls below the mean value in 16 of 33 years and four times, it is below 10 % of the aquifer capacity. Accordingly, Tinzouline suffers from severe water scarcity and the succession of dry years has a strong impact on groundwater resources.

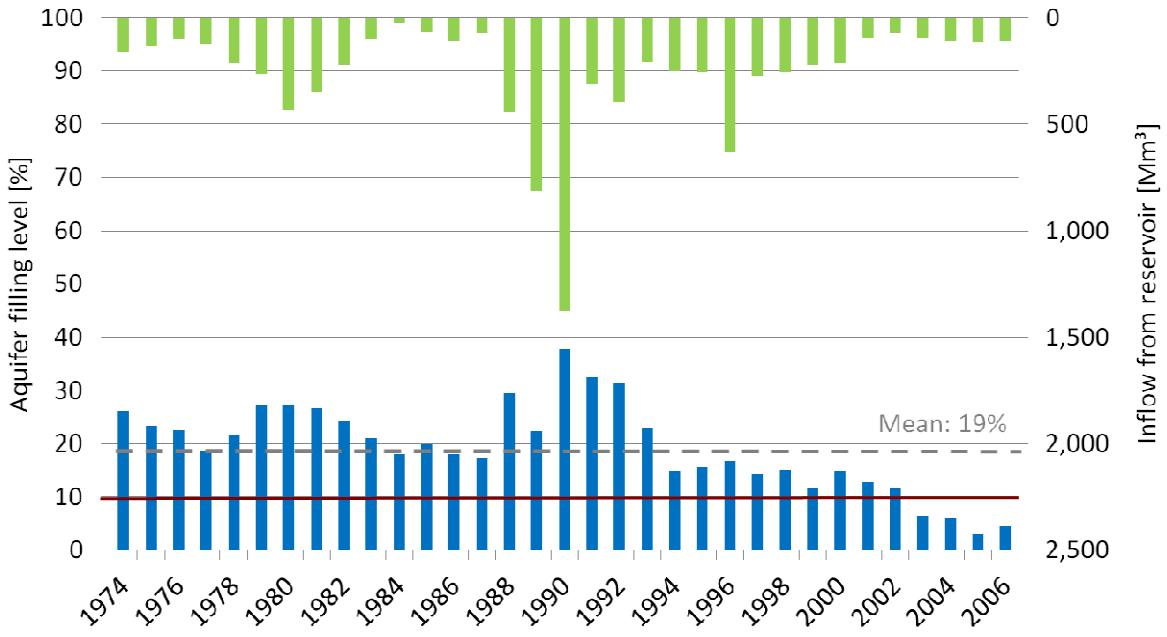

Figure 7-17: Modeled lumped annual filling level Tinzouline aquifer in the period 1973/74 – 2005/06 (mean = 19 %) with the inflow from the reservoir Mansour Eddahbi to the Wadi Drâa.

The Ternata aquifer

The modeled filling levels of the Ternata aquifer range from 8 to 80 % with a mean value of 48 % revealing a highly dynamic aquifer response (Figure 7-18). This is mainly due to the combination of a relatively small aquifer volume and the high mean irrigation demand (57.0 Mm³) accounting for a ratio of 2.9 (Table 7-11). Ternata receives 30 % of irrigation water from the Wadi Drâa, which is the greatest share in comparison to all other Drâa oases. Accordingly, the high significance of surface water for irrigation lowers the risk of aquifer draw down (Figure 7-10; Table 7-5). Thereby, the specific yield accounts for 15 % leading to a medium inherent aquifer dynamic (Table 7-1).

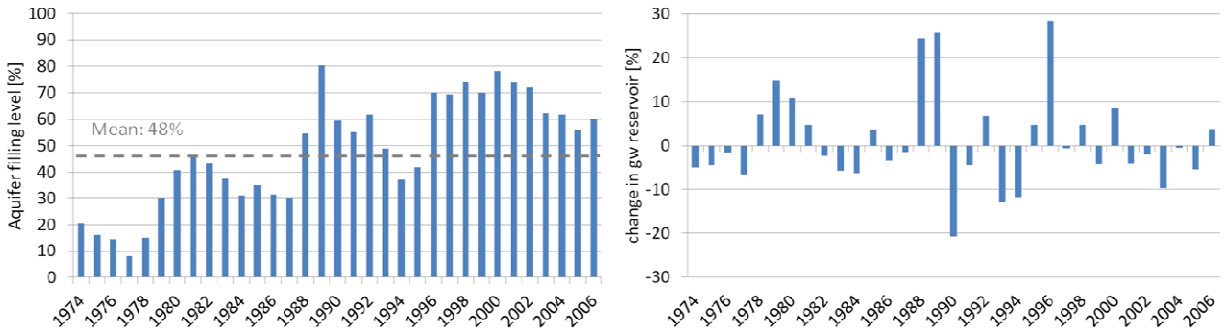

Figure 7-18: Modeled filling level Ternata aquifer in the period 1973/74 – 2005/06 (mean = 48 %) and its change in groundwater reservoir.

The Fezouata aquifer

The lumped annual aquifer response of the Fezouata aquifer is subdued represented by filling levels of 60 % to 86 % with a mean of 68 % (median = 68 %; Figure 7-19). The smooth course of the filling level development is due to strong annual lateral groundwater inflow (mean = 2.3 Mm³) buffering the impact

of droughts and the related decreased groundwater recharge from wadi bed infiltration. The ratio of maximum aquifer volume and mean annual irrigation demand is relatively high (6.7; Table 7-11) leading to a compensated aquifer response. Furthermore, Fezouata receives a medium share of 14 % of irrigation water from the wadi Drâa supporting the relative protection of groundwater resources (ratio of mean groundwater extraction for irrigation versus the mean amount of irrigation water from the Wadi Drâa = 1.8; Table 7-11).

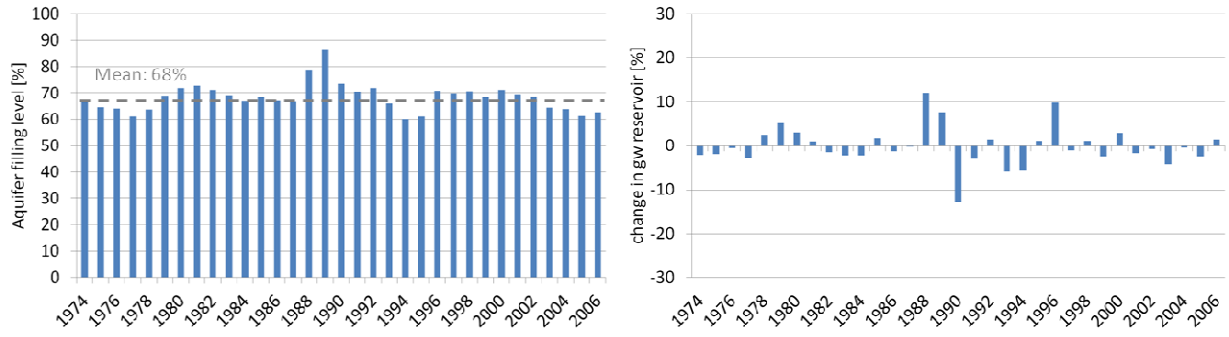

Figure 7-19: Modeled filling level Fezouata aquifer in the period 1973/74 – 2005/06 (mean = 68 %) and its change in groundwater reservoir.

The Ktaoua aquifer

The response of the Ktaoua aquifer is dammed in comparison to all the other Drâa aquifers (except Mhamid) and shows a clear decline of the groundwater reservoirs (Figure 7-20).

A lack of data is responsible for the unconventional model results being highly uncertain referring to the Ktaoua aquifer. Probably, the adaption of the cropping area in relation to surface water availability does not meet the farmer's strategy in the Ktaoua oasis. Furthermore, groundwater and soil salinity limits cropping, which the BIL model does not represent.

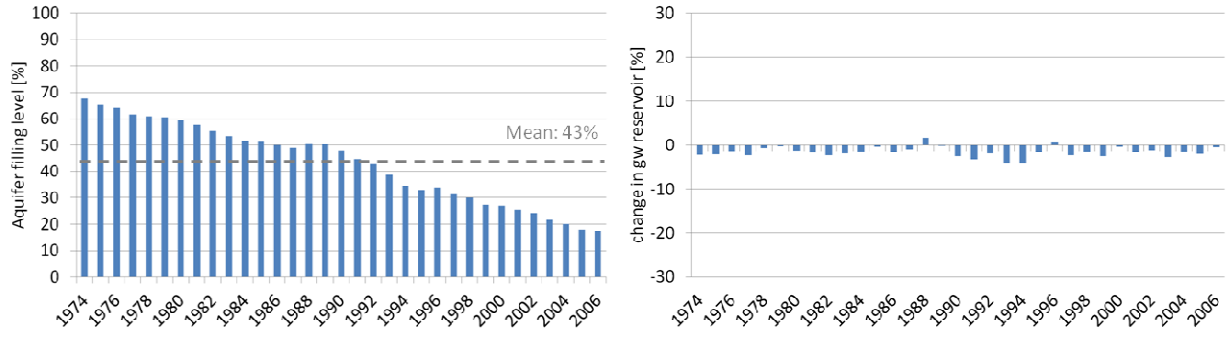

Figure 7-20: Modeled filling level Ktaoua aquifer in the period 1973/74 – 2005/06 (mean = 43 %) and its change in groundwater reservoir.

The Mhamid aquifer

Similar to the Ktaoua aquifer, the response of the Mhamid aquifer is subdued and shows a clear decrease in filling level (Figure 7-21). The Mhamid aquifer represents a generalized boundary condition at the lower end of the chain of Drâa aquifers. The high uncertainties in aquifer dimension and properties

and thus aquifer volume hinder the precise modeling of the aquifer dynamic. The model bias in terms of Mhamid is considered and accepted to be able to simulate the groundwater budget of the Drâa aquifers as coupled reservoir chain.

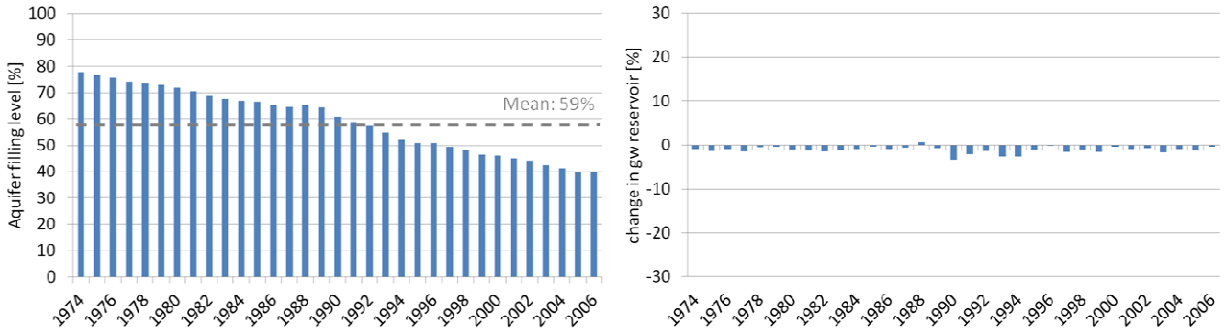

Figure 7-21: Modeled filling level Mhamid aquifer in the period 1973/74 – 2005/06 (mean = 59 %) and its change in groundwater reservoir.

7.5.1 Sensitivity analysis

The sensitivity analysis shows the susceptibility of the model results against modification of parameters. Accordingly, the parameters for that the modification leads to the largest deviation of model results represent target figures of further investigation to enhance the modeling. In this study, groups of parameters are determined whose modification has a strong effect on the modeling results referring to the six Drâa aquifers.

The procedure follows the “one at a time” principle. Thereby, one parameter is modified in a prior defined range, while all other parameters stay fixed. The range of parameters for the sensitivity analysis is defined on the widest range of reasonable values based on relevant literature and expertise (chapter 3.2 & 4). Some of the parameters are modified in the same range for all Drâa aquifers while others are changed within an individual range for each Drâa aquifer (Table 7-13).

Table 7-13: Parameters that are the same and that are modified in the same range for all Drâa aquifers.

Parameter	Parameter value	Parameter modification
Recharge coefficient - Precipitation	2.7 %	1 – 13 %
Recharge coefficient - Irrigation	2.7%	1 – 13 %
Run-off coefficient	8 %	0 – 14 %
Evaporation loss - Surface water	5 %	0 – 85 %
Recharge coefficient - Regional recharge	2.4 and 3.9 %	1 – 13 %
Recession coefficient - Lateral inflow fractured	$1 \cdot 10^{-7}$	$1 \cdot 10^{-5}$ - $1 \cdot 10^{-10}$
Recession coefficient - Lateral inflow fractured/karstic	$1 \cdot 10^{-8}$	$1 \cdot 10^{-2}$ - $1 \cdot 10^{-6}$
Recession coefficient - Lateral inflow porous	$1 \cdot 10^{-4}$	$1 \cdot 10^{-5}$ - $1 \cdot 10^{-10}$
Per capita water consumption - rural	10.95 m³/a	3.65 – 29.2 m³/a
Per capita water consumption - urban	18.25 m³/a	10.95 – 43.8 m³/a

The BIL model is run 250 times using the randomly modified parameters based on the Latin Hyper Cube sampling. The model sensitivity is tested for 32 parameters relating to the six Drâa aquifers, i.e. overall 192 tests are carried out. Therefore, a uniform distribution is assumed concerning the range of parameter modification. The sensitivity analysis is realized using the software SimLab (http://www.simlab-soft.com/; cited August 2012).

Diagrams represent the results of sensitivity analysis as percentage of parameter change versus percentage of change in groundwater volume. Thereby, the years 1983, 1985 and 1990 are chosen to show the model sensitivity for distinct hydro-meteorological conditions (Figure 2-6). The year 1983 represents a medium state of slightly falling groundwater levels after period of medium to slightly enhanced filling levels. The year 1985 represents a dry period concerning hydro-meteorological condition whereas the aquifer filling levels range around the mean. In the year 1990, the hydro-meteorological water availability is extraordinary high. Accordingly, the relation of parameter change and change in model output often reaches a plateau of filled up or run dry aquifers at different levels for dry, medium and humid periods. As expected, the plateau of the filled up aquifer is reached earlier referring to the humid periods because the antecedent filling level is higher in comparison to the dry and medium period

Table 7-14 shows the synthesis of the sensitivity analysis for each Drâa aquifer in terms of high, medium and low susceptibility of the BIL model to the modification of selective parameters. Thereby, the 1:1 relation of percentage of parameter change versus percentage of change in groundwater volume is the criterion of medium model sensitivity, i.e. if the result of the sensitivity analysis cover approximately the 1:1 relation, the model sensitivity is medium. Accordingly, if the result of the sensitivity analysis plots significantly below the 1:1 ratio, the model sensitivity low and high in the reverse case.

Table 7-14: Synthesis of model sensitivity at the Drâa aquifers (high, medium, low) in relation to the tested parameters.

Parameter	Mezguita	Tinzouline	Ternata	Fezouata	Ktaoua	Mhamid
Aquifer outcrop	Medium	Medium	Low	Medium	Medium	Medium
Aquifer Thickness	Medium	Low	Medium	Medium	Low	Low
Specific yield	Medium	Medium	Low	Medium	High	Medium
Recharge coefficient -Wadi	High	High	Medium	Low	Low	Low
Recharge coefficient - Precipitation	Low	Low	Low	Low	Low	Low
Recharge coefficient - Irrigation	Low	Low	Low	Low	Low	Low
Catchment area	Low	Low	Low	Low	Low	Low
Run-off coefficient	High	High	Medium	Low	Low	Low
Evaporation loss –Surface water	Low	Medium	High	Low	Low	Low
Recharge coefficient – Regional recharge	Low	Low	Low	Low	Low	Low
Recession coefficient – Lateral inflow fractured	Low	Low	Low	Low	Low	Low
Recession coefficient – Lateral inflow fractured/karstic	Low	Low	Low	Low	Low	Low
Recession coefficient – Lateral inflow porous	Low	Low	Low	Low	Low	Low
Fraction of wheat per cropping area	High	High	High	High	Medium	Low
Fraction of barley per cropping area	Low	Low	Low	Low	Low	Low
Fraction of alfalfa per cropping area	Low	High	High	Low	Low	Low
Fraction of henna per cropping area	Low	Low	Low	Low	Low	High
Fraction of vegetables per cropping area	Low	Low	Low	High	High	Low
Fraction of maize per cropping area	Low	Low	Low	Low	Low	Low
Number of date palms	Low	Low	Low	Low	Low	Low
Irrigation efficiency	High	High	High	High	High	High
Repartition of irrigation water from Wadi Drâa (for respective aquifer;)	High	High	High	Medium	Medium	Low
Demographic development - rural	Low	Low	Low	Low	Low	Low
Demographic development - urban	Low	Low	Low	Low	Low	Low
Domestic water consumption – rural	Low	Low	Low	Low	Low	Low
Domestic water consumption – urban	Low	Low	Low	Low	Low	Low
Initial saturated thickness	Medium	Medium	Low	Medium	High	Medium

The following sections present a description of modified parameters at each Drâa aquifer followed by a synthesis of the model sensitivities. Subsequently, selected examples illustrate the results more in detail.

For the Mezguita aquifer, the modified parameters are represented in Table 7-15.

Table 7-15: Parameters, parameter values and parameter modification at the Mezguita aquifer.

Parameter	Parameter value	Parameter modification
Aquifer outcrop	30,471,249 m²	15,235,625 – 60,942,498 m² (relative: half and double)
Aquifer Thickness	20.50 m	0 – 25.97 m (maximum from bore logs)
Specific yield	19 %	1 – 35 %
Recharge coefficient - Wadi	8 %	0 – 37.2 %
Catchment area	2,348,859,333 m²	1,163,552,127 – 4,654,208,508 m²
Fraction of wheat per cropping area	60.91 %	0 – 100 % for each Drâa aquifer, while the sum must be 100 %
Fraction of barley per cropping area	5.08 %	- „ -
Fraction of alfalfa per cropping area	21.57 %	- „ -
Fraction of henna per cropping area	3.05 %	- „ -
Fraction of vegetables per cropping area	4.31 %	- „ -
Fraction of maize per cropping area	5.08 %	- „ -
Number of date palms	271,000	135,500 – 542,000 (relative: half and double)
Irrigation efficiency	31 %	10 – 90 %
Repartition of irrigation water from Wadi Drâa	8 %	0 – 100 % for each Drâa aquifer, while the sum must be 100 %
Demographic development - rural	0.8 %	0.5 - 5 %
Demographic development - urban	3.1 %	0.5 - 5 %
Initial saturated thickness	8 m	Relative: ± 2 m

At the Mezguita aquifer the modification of the following five parameters has a high effect on the modeling results (Table 7-14):

- Coefficient of recharge from wadi bed infiltration
- Run-off coefficient for stream flow generating within the MDC
- Fraction of wheat
- Irrigation efficiency
- Repartition fraction of irrigation water from Wadi Drâa to the fields

Furthermore, the BIL model shows medium sensitivity for the following four parameters:

- Area of aquifer outcrop
- Aquifer thickness
- Specific yield
- Initial saturated thickness (starting condition)

The parameters and their modification applied to the Tinzouline aquifer are shown in Table 7-16.

Table 7-16: Parameters, parameter values and parameter modification at the Tinzouline aquifer.

Parameter	Parameter value	Parameter modification
Aquifer outcrop	56,427,757 m²	28,213,879 – 112,855,514 m² (relative: half and double)
Aquifer Thickness	20.50 m	0 – 25.97 m (maximum from bore logs)
Specific yield	22 %	0 – 35 %
Recharge coefficient - Wadi	8 %	0 – 37.2 %
Catchment area	1,272,996,217 m²	612,582,769 –2,450,331,076 m²
Fraction of wheat per cropping area	57.53 %	0 – 100 % for each Drâa aquifer, while the sum must be 100 %
Fraction of barley per cropping area	6.77 %	- „ -
Fraction of alfalfa per cropping area	18.61 %	- „ -
Fraction of henna per cropping area	5.08 %	- „ -
Fraction of vegetables per cropping area	3.38 %	- „ -
Fraction of maize per cropping area	8.63 %	- „ -
Number of date palms	184,660	92,330 – 369,320 (relative: half and double)
Irrigation efficiency	32 %	10 – 90 %
Repartition of irrigation water from Wadi Drâa	8 %	0 – 100 % for each Drâa aquifer, while the sum must be 100 %
Demographic development - rural	1.12 %	0.5 - 5 %
Demographic development - urban	0 %	0.5 - 5 %
Initial saturated thickness	6 m	Relative: ± 2 m

At the Tinzouline aquifer, the modification of the following seven parameters has a high effect on the modeling results (Table 7-14):

- Coefficient of recharge from wadi bed infiltration
- Run-off coefficient for stream flow generating within the MDC
- Evaporation loss from stream flow
- Fraction of wheat
- Fraction of alfalfa
- Irrigation efficiency
- Repartition fraction of irrigation water from Wadi Drâa to the fields

Further three parameters have a medium effect on the modeling results:

- Aquifer outcrop
- Specific yield
- Initial saturated thickness (starting condition)

For the Ternata aquifer, the parameters and their modification are represented in Table 7-17.

Table 7-17: Parameters, parameter values and parameter modification at the Ternata aquifer.

Parameter	Parameter value	Parameter modification
Aquifer outcrop	56,815,733 m²	28,407,867 – 113,631,466 m² (relative: half and double)
Aquifer Thickness	19.50 m	0 – 32.17 m (maximum from bore logs)
Specific yield	15 %	1 – 35 %
Recharge coefficient - Wadi	8 %	0 – 37.2 %
Catchment area	1,441,777,294 m²	687,252,939 –2,749,011,757 m³
Fraction of wheat per cropping area	64.36 %	0 – 100 % for each Drâa aquifer, while the sum must be 100 %
Fraction of barley per cropping area	4.78 %	- „ -
Fraction of alfalfa per cropping area	17.51 %	- „ -
Fraction of henna per cropping area	2.65 %	- „ -
Fraction of vegetables per cropping area	0 %	- „ -
Fraction of maize per cropping area	10.71 %	- „ -
Number of date palms	330,600	165,300 – 661,200 (relative: half and double)
Irrigation efficiency	61 %	10 – 90 %
Repartition of irrigation water from Wadi Drâa	30 %	0 – 100 % for each Drâa aquifer, while the sum must be 100 %
Demographic development - rural	1.07 %	0.5 - 5 %
Demographic development - urban	0 % (supply from Fezouata)	0.5 - 5 %
Initial saturated thickness	5 m	Relative: ± 2 m

The BIL model shows high sensitivity in terms of the modification of the following four parameters at the Ternata aquifer (Table 7-14):

- Fraction of wheat
- Fraction of alfalfa
- Irrigation efficiency
- Repartition fraction of irrigation water from Wadi Drâa to the fields

The modification of the following three parameters has a medium effect on the modeling results:

- Aquifer thickness
- Coefficient of recharge from wadi bed infiltration
- Run-off coefficient for stream flow generating within the MDC

Table 7-18 presents the parameters and their modification for the Fezouata aquifer.

Table 7-18: Parameters, parameter values and parameter modification at the Fezouata aquifer.

Parameter	Parameter value	Parameter modification
Aquifer outcrop	72,491,530 m²	36,245,765 – 144,983,060 m²(relative: half and double)
Aquifer Thickness	21.50 m	0 – 25.97 m (maximum from bore logs)
Specific yield	10 %	0 – 35 %
Recharge coefficient - Wadi	8 %	0 – 37.2 %
Catchment area	2,899,264,246 m²	1,436,557,832 – 5,746,231,329 m²
Fraction of wheat per cropping area	71.50 %	0 – 100 % for each Drâa aquifer, while the sum must be 100 %
Fraction of barley per cropping area	6.18 %	- „ -
Fraction of alfalfa per cropping area	18.01 %	- „ -
Fraction of henna per cropping area	1.41 %	- „ -
Fraction of vegetables per cropping area	0 %	- „ -
Fraction of maize per cropping area	2.90 %	- „ -
Number of date palms	254,400	127,200 – 508,800 (relative: half and double)
Irrigation efficiency	62 %	10 – 90 %
Repartition of irrigation water from Wadi Drâa	14 %	0 – 100 % for each Drâa aquifer, while the sum must be 100 %
Demographic development - rural	0.90 %	0.5 - 5 %
Demographic development - urban	2.90 % (supply for Zagora/Ternata)	0.5 - 5 %
Initial saturated thickness	14 m	Relative: ± 2 m

The BIL model shows high sensitivity in terms of the modification of the following four parameters at the Fezouata aquifer (Table 7-14):

- Evaporation loss from stream flow
- Fraction of wheat
- Fraction of vegetables
- Irrigation efficiency

Furthermore, modification of the following five parameters has a medium effect on the modeling results:

- Area of aquifer outcrop
- Aquifer thickness
- Specific yield
- Repartition fraction of irrigation water from Wadi Drâa to the fields
- Initial saturated thickness (starting condition)

Table 7-19 presents the parameters and their modification for the Ktaoua aquifer.

Table 7-19: Parameters, parameter values and parameter modification at the Ktaoua aquifer.

Parameter	Parameter value	Parameter modification
Aquifer outcrop	127,152,025 m²	63,576,012 –254,304,050 m² (relative: half and double)
Aquifer Thickness	31.50 m	0 – 38.27 m (maximum from bore logs)
Specific yield	13 %	1 – 35 %
Recharge coefficient - Wadi	10 %	0 – 37.2 %
Catchment area	707,708,141 m²	1,436,557,832 – 5,746,231,329 m²
Fraction of wheat per cropping area	68.93 %	0 – 100 % for each Drâa aquifer, while the sum must be 100 %
Fraction of barley per cropping area	15.51 %	- „ -
Fraction of alfalfa per cropping area	9.48 %	- „ -
Fraction of henna per cropping area	1.03 %	- „ -
Fraction of vegetables per cropping area	0 %	- „ -
Fraction of maize per cropping area	5.05 %	- „ -
Number of date palms	254,400	122,620 – 490,480 (relative: half and double)
Irrigation efficiency	80 %	10 – 90 %
Repartition of irrigation water from Wadi Drâa	28 %	0 – 100 % for each Drâa aquifer, while the sum must be 100 %
Demographic development - rural	0.36 %	0.5 - 5 %
Demographic development - urban	0 %	0.5 - 5 %
Initial saturated thickness	22 m	Relative: ± 2 m

The BIL model shows high sensitivity in terms of the modification of the following four parameters at the Ktaoua aquifer (Table 7-14):

- Specific yield
- Fraction of vegetables
- Irrigation efficiency
- Initial saturated thickness (starting condition)

Furthermore, modification of the following three parameters has a medium effect on the modeling results:

- Area of aquifer outcrop
- Fraction of wheat
- Repartition fraction of irrigation water from Wadi Drâa to the fields

Table 7-20 presents the parameters and their modification for the Mhamid aquifer.

Table 7-20: Parameters, parameter values and parameter modification at the Mhamid aquifer.

Parameter	Parameter value	Parameter modification
Aquifer outcrop	43,979,767 m²	21,989,884 –87,959,534 m² (relative: half and double)
Aquifer Thickness	50.50 m	0 – 52.77 m (maximum from bore logs)
Specific yield	15 %	0 – 35 %
Recharge coefficient -Wadi	10 %	0 – 37.2 %
Catchment area	206,102,520 m²	98,390,842 – 393,563,371 m²
Fraction of wheat per cropping area	74.18 %	0 – 100 % for each Drâa aquifer, while the sum must be 100 %
Fraction of barley per cropping area	13.91 %	**- „ -**
Fraction of alfalfa per cropping area	9.27 %	**- „ -**
Fraction of henna per cropping area	0 %	**- „ -**
Fraction of vegetables per cropping area	0 %	**- „ -**
Fraction of maize per cropping area	2.64 %	**- „ -**
Number of date palms	131,100	65,550 – 262,200 (relative: half and double)
Irrigation efficiency	75 %	10 – 90 %
Repartition of irrigation water from Wadi Drâa	12 %	0 – 100 % for each Drâa aquifer, while the sum must be 100 %
Demographic development - rural	-0.90 %	0.5 - 5 %
Demographic development - urban	0 %	0.5 - 5 %
Initial saturated thickness	40 m	Relative: ± 2 m

The BIL model shows high sensitivity in terms of the modification of the following two parameters at the Mhamid aquifer (Table 7-14):

- Fraction of vegetables
- Irrigation efficiency

Furthermore, the BIL model shows medium sensitivity for the following three parameters:

- Area of aquifer outcrop
- Specific yield
- Initial saturated thickness (starting condition)

Aquifer outcrop

The modification of the area of aquifer outcrop has a medium linear effect on the modeling result (Figure 7-22). This is because the aquifer outcrop is one large factor of the estimation of the aquifer capacity and the groundwater volume (chapter 6.1.4). The Ternata aquifer is an exception. Accordingly, the results reveal low sensitivity. At Ternata the groundwater resources and aquifer capacity are less important than surface water for irrigation, which in turn is the most important balance item (Table 7-11). This may lead to the reduced model sensitivity in terms of the aquifer outcrop at Ternata. Overall, the interest of investigation of the aquifer outcrop is of medium interest also because the narrow shape of the Drâa valley limits the expanse of the aquifer outcrop naturally.

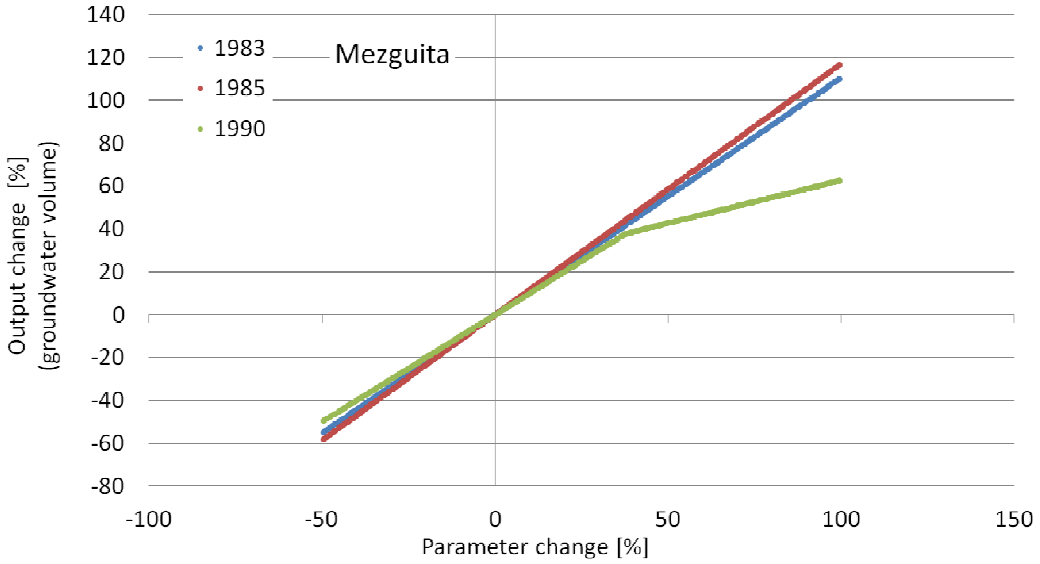

Figure 7-22: Medium model sensitivity for area of aquifer outcrop at the Mezguita aquifer as an example.

Aquifer thickness

In case of aquifer thickness, the BIL model shows low to medium sensitivities depending on the relations between the factors of the aquifer dimension (Table 7-14). In comparison to the aquifer outcrop, the aquifer thickness is a smaller factor of the estimation of the aquifer capacity and hence of less importance for the sensitivity. Thereby, only the reduction of the aquifer thickness has effect on the groundwater volume because a higher aquifer capacity does not mean that the actual groundwater volume is greater. As opposed, a lower aquifer capacity means that less groundwater can be in the aquifer. As an example, the model sensitivity at the Fezouata aquifer is illustrated (Figure 7-23; Table 7-14). Accordingly, the sensitivity is medium for the humid period and low for the dry and medium period. Even if the model sensitivity is low to medium, the aquifer thickness is of prior research interest because this parameter is prone of uncertainty and spatial data resolution is sparse.

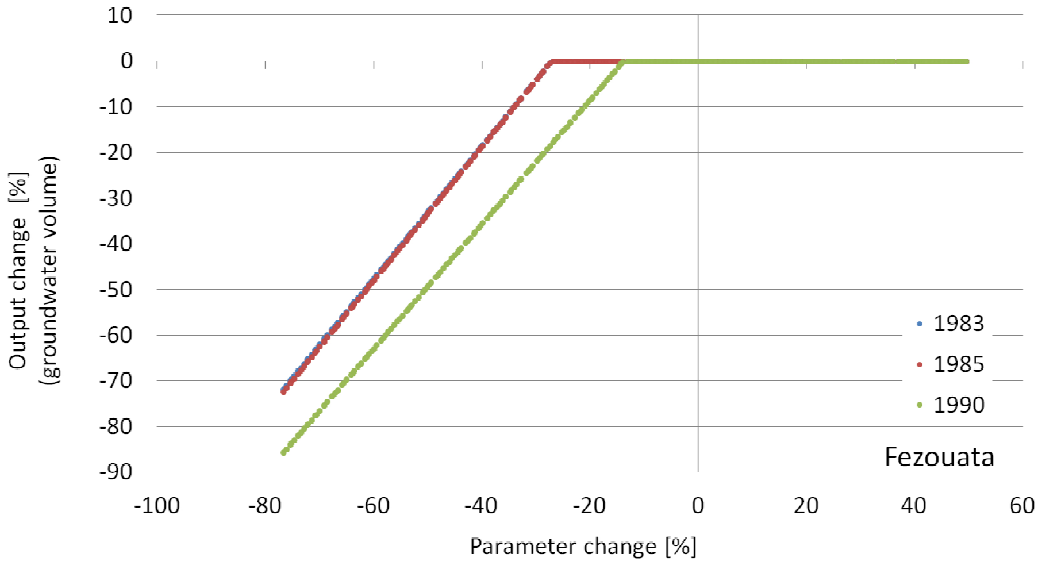

Figure 7-23: Medium model sensitivity for aquifer thickness at the Fezouata aquifer as an example.

Specific yield

The model sensitivity in terms of specific yield is medium and of linear nature. Only at Ternata the sensitivity is slightly moved to low and at Ktaoua to high, still being near medium (Table 7-14). The reason for that is similar as for the aquifer outcrop. The specific yield is factor of the estimation of the aquifer capacity and groundwater volume. As an example, the model sensitivity is narrow around the 1:1 ratio while the results for the humid period are lower and for the medium and dry period higher (Figure 7-24). Because of the high parameter uncertainty, the specific yield is of particular research interest.

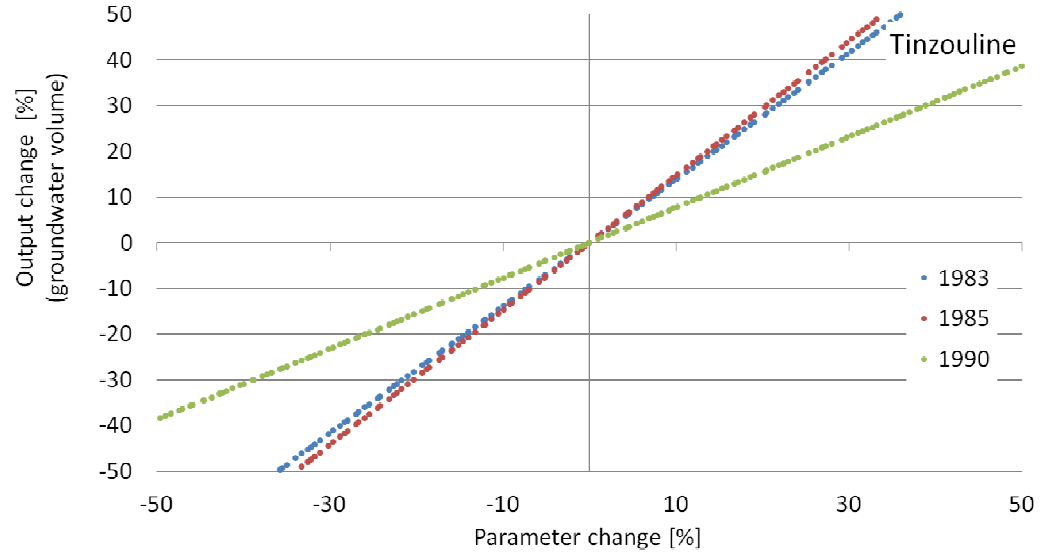

Figure 7-24: Medium model sensitivity for specific yield at the Tinzouline aquifer as an example.

Coefficient of recharge from wadi bed infiltration

The BIL model shows low to high sensitivity in terms of the recharge coefficient for wadi bed infiltration (Figure 7-25). Thereby, the model sensitivity decreases from upstream to downstream (Table 7-14). Because the recharge from wadi bed infiltration represents transmission losses, the residual stream flow reaching the respective next downstream aquifer is reduced increasingly with enhanced recharge coefficients. As the amount of stream flow is reduced downstream, the model sensitivity to recharge from stream flow infiltration decreases too. The comparison of the different behavior of the model sensitivity at the Drâa aquifers verifies the model set up in terms of the representation of stream flow management in the MDC (chapter 7.3). As an example, the groundwater volume at the Tinzouline rises relating to an increase of the recharge coefficient until a certain turning point. This turning point marks the state at which as much of the stream flow infiltrates in the upstream wadi bed, that the recharge from the residual stream flow cannot replenish the aquifer any more. From this point on, the more stream flow infiltrates in Mezguita, the less remains to recharge the Tinzouline aquifer. This turning point is observed at each Drâa aquifer except for Mezguita because this is the upper most aquifer representing the boundary condition of inflow from the reservoir Mansour Eddhabi.

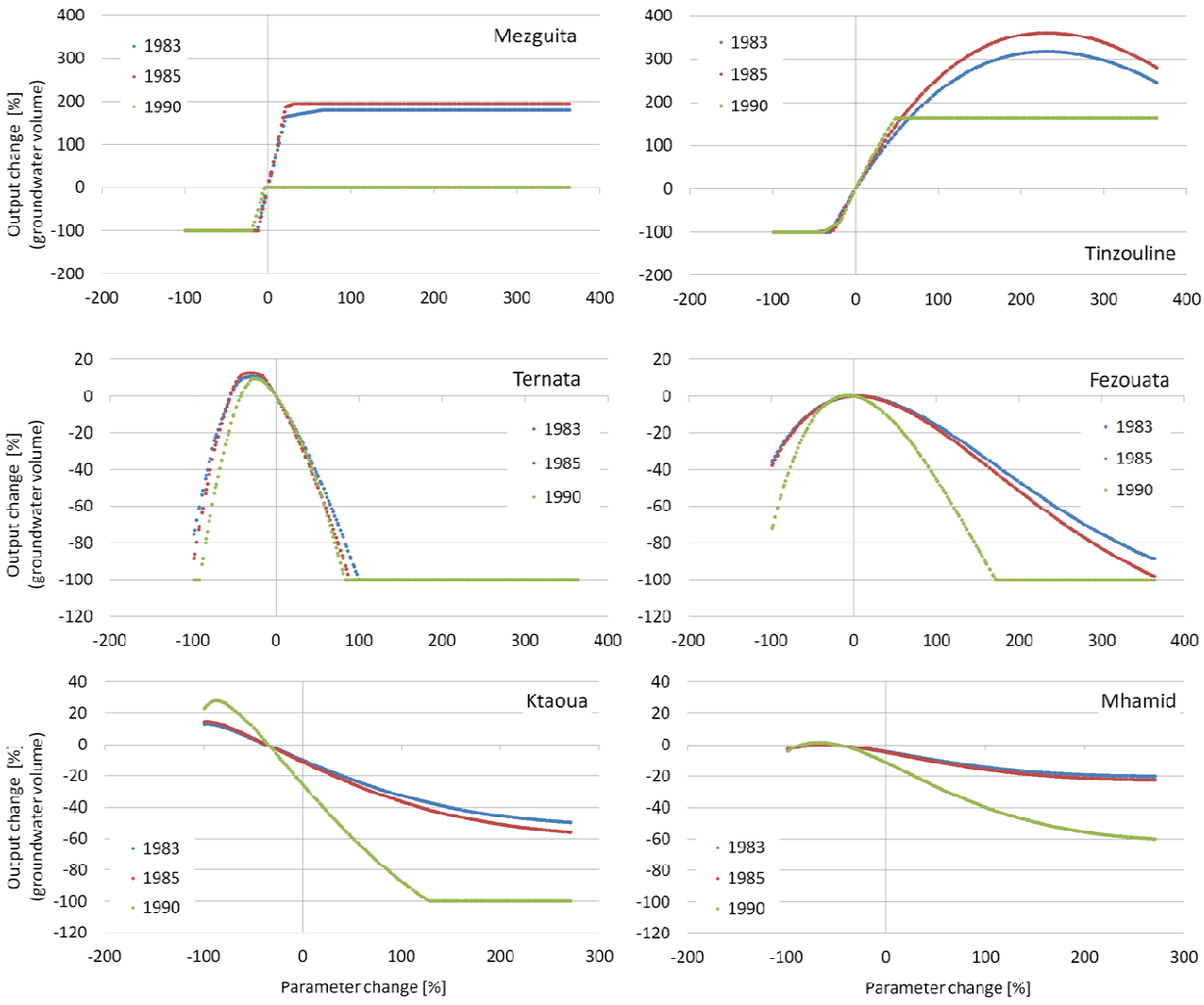

Figure 7-25: High model sensitivity for the recharge coefficient for wadi bed infiltration at all Drâa aquifers.

The model sensitivity is low in terms of the coefficient of recharge from infiltration of precipitation at the aquifer outcrop (direct recharge) because the amount of direct recharge is small in combination to the relatively small area of aquifer outcrop (Table 7-14).

The BIL model shows overall low sensitivity in relation of the coefficient of recharge from infiltration of irrigation water. Thereby, the three upper Drâa aquifers reveal higher sensitivity than the lower three. This is because the irrigation demand of the upper three Drâa aquifers is by far greater as in the lower three (Table 7-14; Table 7-11).

The sensitivity of the BIL model is low in terms of the catchment area of each Drâa aquifer because it is an input to the estimation of lateral groundwater inflow, which is overall of minor importance for the water balance (Table 7-14; Figure 7-13).

The model sensitivity in terms of the run-off coefficient for stream flow generating within the MDC mirrors the increasing aridity along the chain of the Drâa aquifers. According to the annual precipitation, the effect of the modification of the runoff coefficient is highest at the Mezguita aquifer and lowest at the Mhamid aquifer. Furthermore, the stream flow decreases downstream due to transmission losses (Table 7-14).

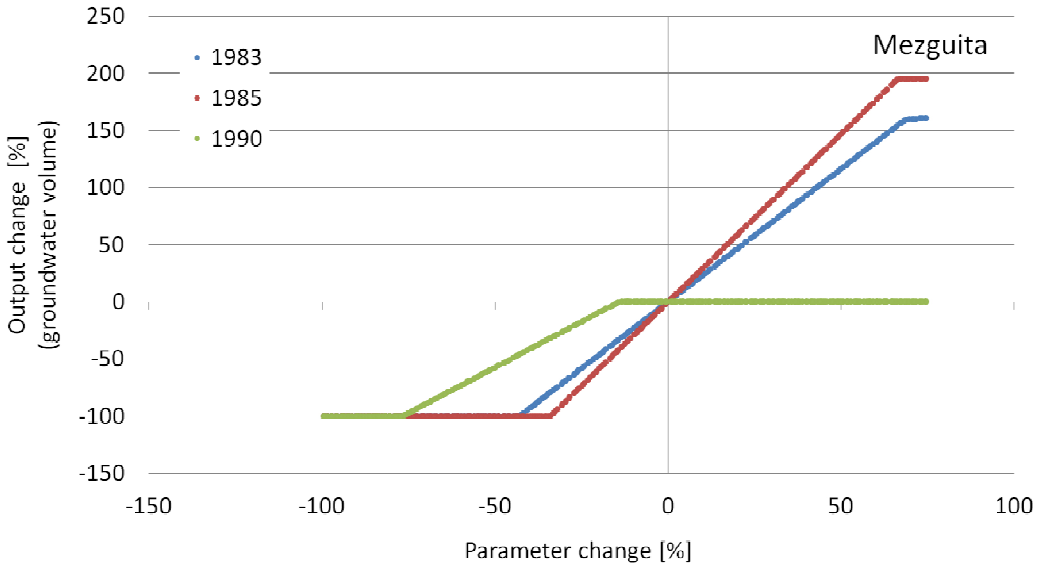

Figure 7-26: High model sensitivity for the run-off coefficient for stream flow generating within the MDC at the Mezguita aquifer.

The model sensitivity according to evaporation losses from stream flow is different at the Drâa aquifers. The successive increase in transmission losses and the resulting decrease in stream flow amount along the aquifer chain reduce the sensitivity against the modification of evaporation losses downstream the Wadi Drâa. This is of particular importance for the aquifers that depend strongly on irrigation from stream flow while irrigation is the most significant item of the water budget (Table 7-11; Figure 7-13). Accordingly, at the Ternata aquifer the model sensitivity against evaporation losses from stream flow is high. As the Tinzouline aquifer suffers from severe water scarcity the sensitivity is enhanced classifying to medium (Figure 7-17).

The results of the BIL model low sensitivity in terms of the all recession coefficients included in the linear storage estimations of lateral groundwater inflow, which is a minor item of the water budget (). However, a non-linear approach would better represent the lateral groundwater inflow.

Fractions of crops

The model sensitivity according to the fractions of crops constituting the crop mix of an oasis tends to be low mostly but remains differentiated in terms of wheat, alfalfa, henna and vegetables (Table 7-14). Accordingly, the sensitivity for wheat is the highest overall as it is high in the first four, medium in the fifth and low only in the sixth of the Drâa aquifers. This is due to the large proportion of wheat in the crop mix at each oasis (> 60 %). High model sensitivity found for alfalfa is due to relatively large cropping areas in combination to a high crop water demand. Henna and vegetables are highly water-consuming crops, so that the modification of their fraction in the crop mix can have an effect particularly in the three lower Drâa aquifers. (Table 7-14).
The modification of the number of date palms has generally a low effect on the model results (Table 7-14).

Irrigation efficiency

In terms of irrigation efficiency, the BIL model is highly sensitive because it is a factor for the crop water demand, which represents the most important discharge item of the groundwater balance (Table 7-14; Figure 7-11). Thereby, the aquifers with the greatest crop water demand reveal the highest sensitivity, such as Mezguita, Tinzouline and Ternata (Table 7-11). Taking Tinzouline as an example, the relation of parameter change and change in model output reveal a non-linear behavior reaching a plateau of filled up or run dry aquifers at different levels for dry, medium and humid periods. As expected, the plateau of the filled up aquifer is reached earlier referring to the humid periods because the antecedent filling level is higher in comparison to the dry and medium period (Figure 7-27). The irrigation efficiency is a very uncertain parameter because no data is available for the MDC. Furthermore, the determination of irrigation efficiency is subject of current scientific discussion. Accordingly, this parameter is calibrated in the modeling procedure and investigations on this field are highly recommended (chapter 7.5.2).

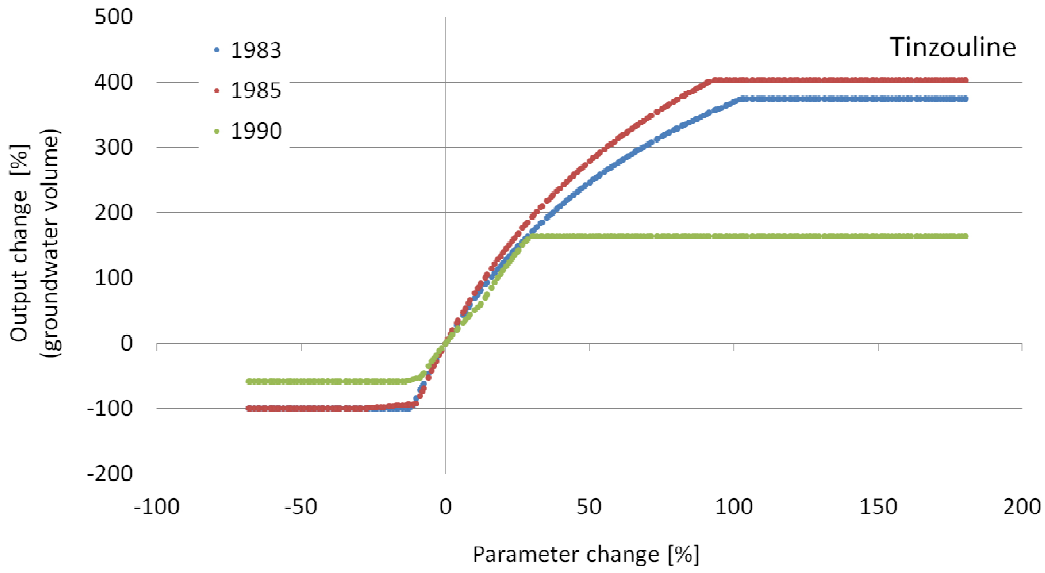

Figure 7-27: High model sensitivity for the irrigation efficiency at the Tinzouline aquifer as an example.

Repartition fraction of the irrigation water from the Wadi Drâa

The BIL model shows a differentiated sensitivity in terms of the repartition of the irrigation water from the Wadi Drâa to the fields at the different Drâa aquifers. Thereby, the sensitivity decreases from along the chain of Drâa aquifers downstream because the longer the course of the wadi the lower the amount of stream flow and thus amount of irrigation water (Table 7-14; chapter 7.3). Table 7-21 shows that the modification of the repartion of irrigation water from Wadi Drâa at a certain aquifer induces a change in groundwater volume at other Drâa aquifers too. This interdependence of sensitivities is evident for the next downstream aquifer and lowers with distance to the aquifer where the parameter is changed. This verifies the model set up in representing the connection of the Drâa aquifers via the Wadi Drâa and the stream flow respectively.

Table 7-21: Model sensitivities according the Drâa aquifer where the repartition fraction of irrigation water from the Wadi Drâa is modified (bold) and the induced sensitivity in all other aquifers (high, medium, low).

	Mezguita	Tinzouline	Ternata	Fezouata	Ktaoua	Mhamid
Mezguita	**High**	Medium	Medium	Low	Low	Low
Tinzouline	Low	**High**	Medium	Low	Low	Low
Ternata	High	Low	**High**	Medium	Medium	Low
Fezouata	Low	Low	Low	**Medium**	Low	Low
Ktaoua	High	Low	High	Low	**Medium**	Low
Mhamid	Low	Low	Low	Low	Low	**Low**

The BIL model reveals low sensitivities according to all parameters of demographic development and per capita domestic water consumption because they are included in the estimation of domestic groundwater extraction, which is a minor item of the water budget (Figure 7-11).

Initial saturated thickness

The model sensitivity is generally near medium in terms of the initial saturated thickness as initial condition of the aquifer filling level (Table 7-14; Figure 7-28). This is due to the lumped bucket model approach applied to the regional scale, which is inherently prone of modifications of lumped parameters representing a heterogeneous setting. A slight deviation occurs at Ternata with low model sensitivity and Ktaoua with high sensitivity. This may be the general trend in the development of the groundwater volumes and aquifer filling levels respectively. Thereby, the Ternata aquifer shows a positive trend whereas Ktaoua reveals a negative trend (Figure 7-18; Figure 7-20).

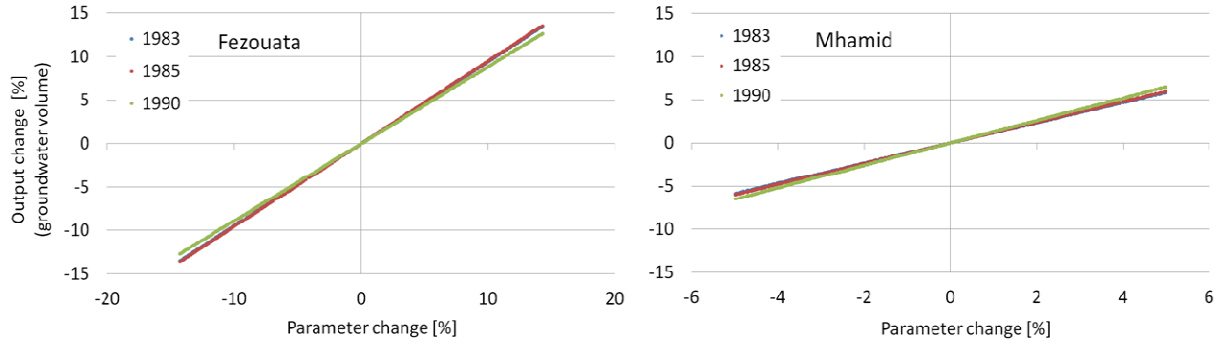

Figure 7-28: Medium model sensitivity for the initial saturated thickness at the Fezouata aquifer and at the Mhamid aquifer as examples (mind different scaling on the abscissa).

7.5.2 Calibration

The manual revisions of values of the irrigation efficiency and the initial aquifer filling level are the exclusive model calibration procedures.

Irrigation efficiency is calibrated because no field data are available. So, the calibration is based on the range of reasonable data given in literature. After Bos & Nugteren (1990) the irrigation efficiency ranges between 32 and 58 % for flood irrigation or rather basin irrigation, which is the widespread irrigation technique in the Middle Drâa Catchment (MDC). The BIL model uses the factor of irrigation inefficiency, which is the reciprocal value of the irrigation efficiency. The factor of irrigation inefficiency results in the multiple of the crop water demand reflecting the extraction of irrigation water, which is the most important item of the water balance (chapter 7.3). The BIL model uses the irrigation efficiency or rather irrigation inefficiency as modified field efficiency (modified from Bos & Nugteren, 1990). It includes aspects of the water use strategy and techniques of the farmers, for which precise data is lacking. The irrigation efficiency has an effect on the groundwater recharge as if more irrigation water is used percolation is enhanced. . Furthermore, the BIL model is highly sensitive to the modification of the irrigation efficiency at all Drâa aquifer.

Table 7-22: Calibrated 'modified irrigation efficiencies' starting from 40 % reference value for flood irrigation.

	Mezguita	Tinzouline	Ternata	Fezouata	Ktaoua	Mhamid
Calibrated irrigation efficiency [%]	31	32	61	62	80	75

The calibrated values for the modified irrigation efficiency touch the range of literature data referring to the Mezguita, Tinzouline, Ternata and Fezouata aquifer. So, water conflict between upstream and downstream users within Tinzouline may lead to e less effective use. The values referring to the Ktaoua and the Mhamid aquifer exceed the range of literature data, which may be due to a different farmer's water use strategy as implemented in the BIL model. Farmer's are supposed to use water more carefully due to increased aridity and significantly increased salinity in the southern most Drâa oases (chapter 6.3.3.3). Because salinity is not represented in the BIL model, the irrigation efficiency is the parameter incorporating a number of imponderable processes and uncertainties (chapter 7.5.4).

The initial saturated thickness is adjusted to meet the groundwater level observations at the end of the hydrological year of 1973/74 at the respective Drâa aquifer. Therefore, the observed groundwater levels are referred to the aquifer dimension as saturated thickness to calculate a lumped aquifer filling level (chapter 6.1.4, 7.3 & 7.5.3). As the sensitivity analysis shows, the calibration of the initial saturated thickness is delicate because its modification has an enhanced effect on the model result except for the Ternata aquifer (chapter 7.5.1).

Overall, the model calibration reveals differences in the aquifer response before and after the distinct humid period at the around 1990. This is due to the impact of operation of an increasing number of pumps since the 1980-ties. Therefore, the water use strategy of the farmers changed and hence the irrigation efficiency. Additionally, the differences are partly due to the non-linear effects of hysteresis in the vadose zone describing different hydraulic potentials at constant saturation (chapter 7.5.4).

7.5.3 Plausibility tests

The plausibility test is a comparison of observed groundwater levels at single sites and modeled lumped annual aquifer filling levels at the Drâa aquifers of Tinzouline, Ternata and Fezouata as groundwater lev-

el data is available. Therefore, the observed groundwater levels are referred to the aquifer dimension as saturated thickness to calculate a lumped aquifer filling level (chapter 6.1.4 & 7.3). So, the model results and the groundwater level measurements are comparable. The observed groundwater levels stem from the Moroccan observation program and reveal a fragmentary monthly or bi-monthly resolution (chapter 4.2 & 6.2.1). The mean root mean square error (RMSE) is chosen as absolute indicator for model deviations. It is commonly tested against the half of the standard deviation of the observed data. Accordingly, if the RMSE falls below the standard deviation of the observed data the model performance is good (Singh et al., 2005). This test is biased due to the fragmentary groundwater level observations and plausibility check of the model results against only one observation point in the aquifer. Consequently, a mean RMSE of up to 10 % represents a "slight model deviation" and thus good performance. The most important criterion is the consistency in the dynamic behavior of aquifer response between the modeled aquifer filling level and the selective groundwater level observations according to the sense of proportion.

The plausibility test cannot replace a model validation in terms of precise drainable groundwater volumes but the model capability of representing annual aquifer response is checked. The aquifer response relates to the drainable groundwater volume via the aquifer dimension and the specific yield. So, the drainable groundwater volume is verified indirectly. The phenomenon of equifinality cannot be excluded (Beven, 2006; chapter 7.5.4).

The modeled lumped annual filling level of the Tinzouline aquifer shows good accordance to the observed groundwater levels (at piezometer I.R.E. 767/73; Figure 6-9) in the period November 1974 – April 1999 including as well a distinct dry as a distinct humid period. The mean root mean square error (RMSE) of 6 % represents the slight model deviation (Figure 7-29). The model deviations are highest during the dry period around the year 1984 probably because the farmers' strategy of reducing the cropping area as a response on drought conditions is represented imprecisely (Figure 7-5; chapter 7.5.4)

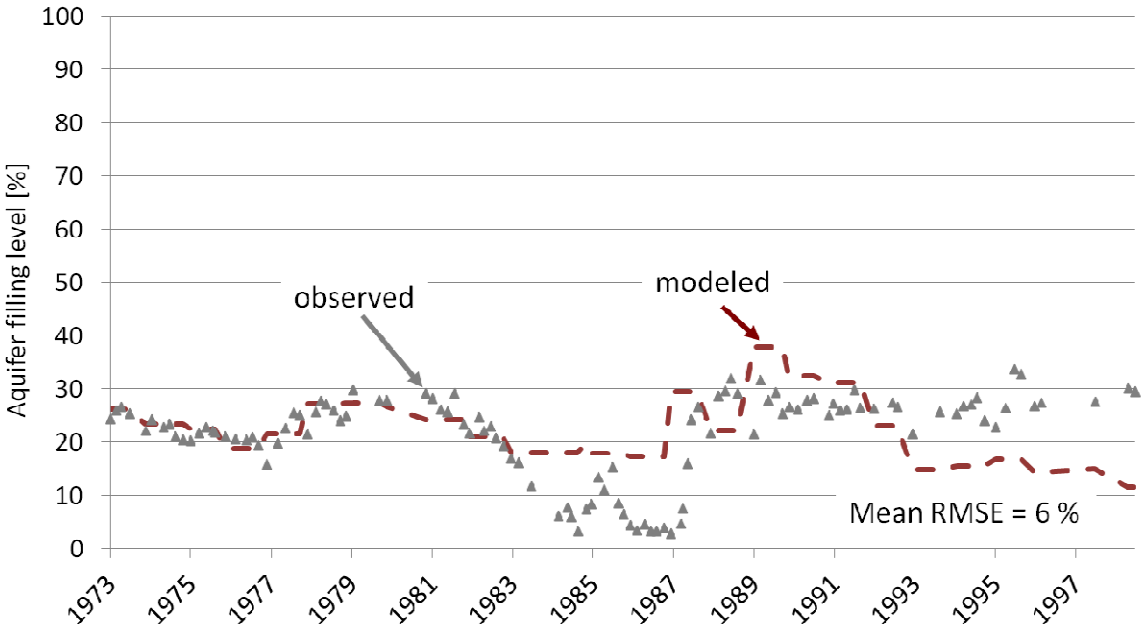

Figure 7-29: Plot of the modeled filling level of the Tinzouline aquifer versus groundwater level data (IRE 767/73) in the period November 1974 – April 1999 showing a model deviation of a mean root mean square error (RMSE) of 6 % for the period.

The compliance of modeled annual filling levels of the Ternata aquifer with the observed groundwater levels at the piezometer I.R.E. 904/73 (Ternata, Figure 6-9) in the period October 1986 to December 2000 is acceptable (Figure 7-30). The model deviation amounts to a mean RMSE of 16 %. The highest model deviations arise in the beginning of the modeling period due to data uncertainties concerning the initial filling level of the aquifer. Furthermore, the BIL model overestimates the period of declining groundwater levels between 1996 and 2000. This may be because the BIL model represents the variation of cropping area in relation to the surface water availability imprecisely.

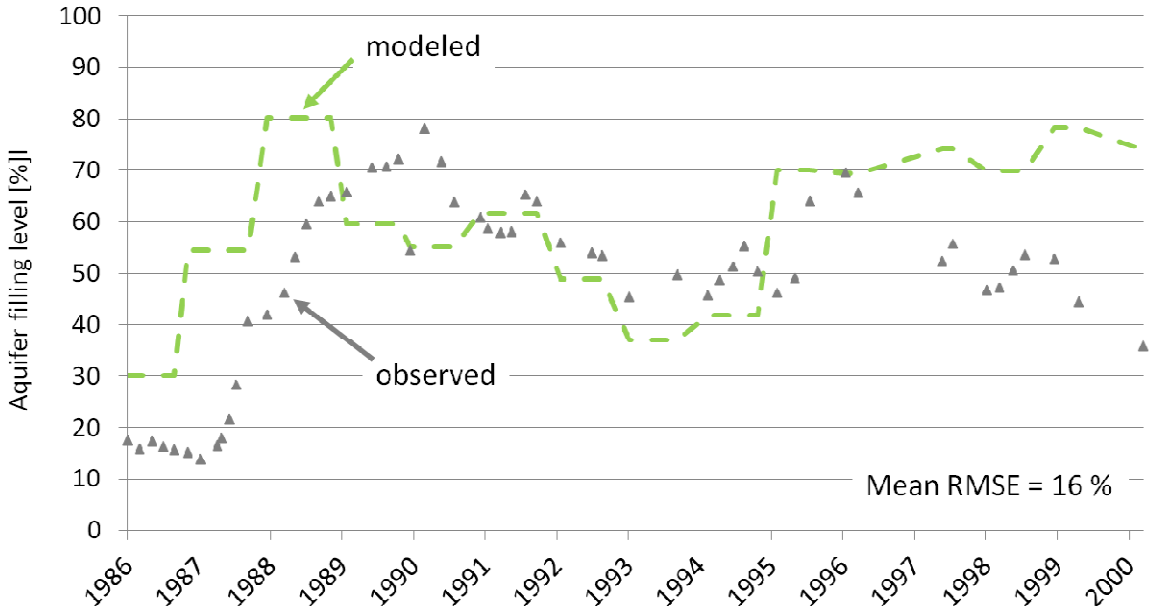

Figure 7-30: Plot of the modeled filling level of the Ternata aquifer versus groundwater level data (IRE 904/73) in the period October 1986 – December 2000 showing a model deviation of a mean root mean square error (RMSE) of 16 %.

The comparison of modeled filling levels and observed groundwater levels at the piezometer I.R.E. 134/73 (Fezouata) in the period November 1973 – August 2002 reveals good accordance (Figure 7-31). The model deviation is mean RMSE of 5 %. The divergence of modeling results versus observed data is widest in the period 1983 - 1990 when the BIL model overestimates aquifer filling levels for both courses of declining and courses of rising groundwater levels. In the period after 1993, the BIL model does both overestimating and underestimating the aquifer filling levels resulting in a subdued aquifer response. The reason for that may be the imprecise representation of water use in relation to the variation in cropping area.

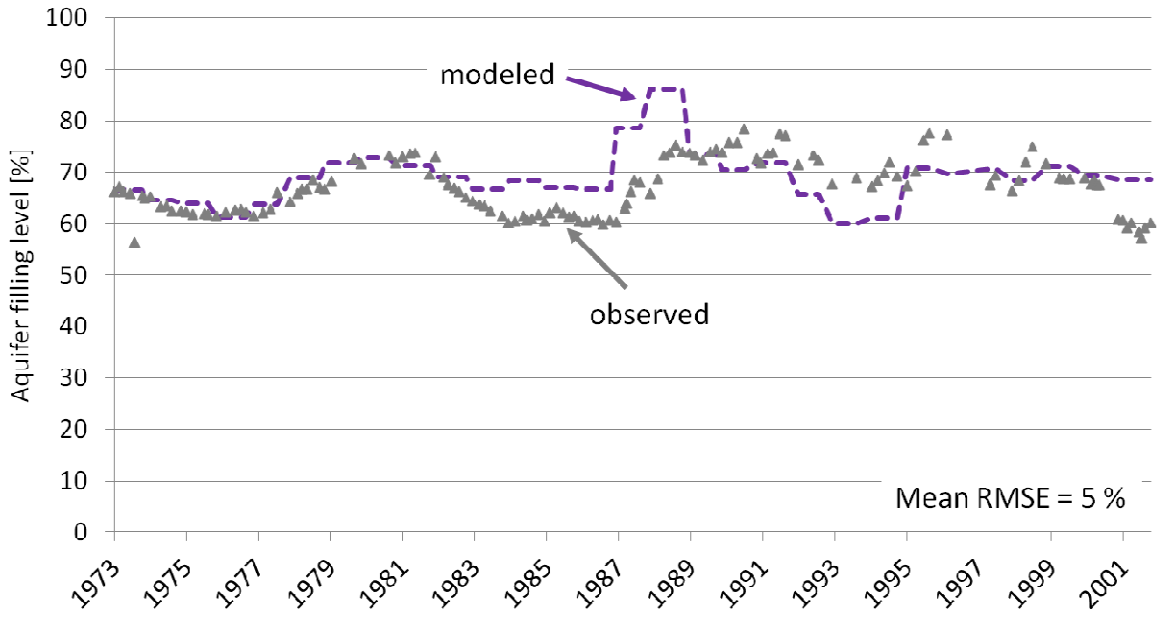

Figure 7-31: Plot of the modeled filling level of the Fezouata aquifer versus groundwater level data (IRE 134/73) in the period November 1973 – August 2002 showing a model deviation of a mean root mean square error (RMSE) of 5 %.

7.5.4 Uncertainty discussion

In the following sections, uncertainties of the data, the modeling concept and the model input are discussed because a precise quantification is difficult due to a lack of verifiying data and no least because the lumped parameter approach of the BIL model blurs some of the data uncertainty. Explanaition according to the uncertainty of specific parameters and processes is found in the respective previous chapters.

The data uncertainty refers to the e.g. deviations and errors in measurements of groundwater levels and analytical errors concerning the hydrochemical data. Particulary concerning the specific yield, the lithilogical description of the bore logs carry a high degree of uncertainty varying with the respective skilled worker and drilling master (chapter 4 and 6.1). Concerning the measured groundwater levels, the influence of pumping near the observation wells cannot be excluded (chapter 4, 5.2.1 and 6.2).

As lumped bucket concept applied to the regional scale, the BIL model is inherently prone of modifications of lumped parameters and input representing a heterogeneous setting. Furthermore, the groundwater budget is based on a difference equation that needs the aquifer filling level of the prior year. According to this, each modeled annual aquifer filling level has linear reference back to the antecedent filling level. Additionally, the differences are partly due to the non-linear effects of hysteresis in the vadose zone describing different hydraulic potentials at constant saturation. Therefore, inverstiagtions are needed because the model should represent the actual mechanisms at the respective scale (Kirchner, 2006). Also for other items of the model a non-linear representation of the processes would be preferable, e.g. of the lateral groundwater inflow. However, due to the low sensitivity of the BIL model against parameters related to lateral inflow (chapter 7.5.1; Table 7-23), the model uncertainty in terms of the linear storage model for lateral inflow is considered of minor importance. Differences in the modeled aquifer response before and after the distinct humid period at the around 1990 are due to the impact of operation of an increasing number of pumps since the 1980-ties. This means that, the model BIL cannot

represent the temporarily changing water use strategy of the farmers precisely. A lack of data on agricultural water consumption is the main reason for that. The parameters related to the farmers' water use strategy (repartition of surface water to the aquifers, crop mix and irrigation effeiciency) showed to be highly sensitive in most cases (chapter 7.5.1; Table 7-23). Accordingly, one of the most important uncertainties is the representation of any of the human actions such as the repartition of irrigation water or variation of cropping area.

The model input can be divided into fix parameters, e.g. aquifer dimension, and annually varaying input, e.g. precipitation and streamflow. The uncertainty in pramaters and variable model input is hard to quantifiy precisely why the sensitivity analysis is used to help the qualitative description of the uncertainty. In conclusion, the parameters to which the BIL model is the most sensitive are classified to high, medium or low uncertain based on expert knowledge (chapter 7.5.1). Therefore, the results of the sensitivity analysis are summed up for the overall chain of the Drâa aquifer to provide overview of the uncertainties compared ot the model sensitivity relating to selective parameters (Table 7-23). Furthermore, the resulting research need is estimated related to the presented parameters.

Some parameters reveal variable sensitivity to the model results because it changes from aquifer to aquifer. As an example, the BIL model shows high sensitivity to the modififcation of the recharge coefficient of wadi bed infiltration at the upper Drâa aquifers. In downstream direction, the sensitivity decreases because the stream flow decreases along the course of the Wadi Drâa due to transmission losses. Consequently, the recharge from wadi bed infiltration is less important at the lowermost Drâa aquifers compared to the upper ones. The uncertainty of the recharge coefficients is generally high (chapter (3.2.3). This leads in combination to the partly high sensitivity to an urgent research need.

Despite their high uncertainty, research on all parameters related to the lateral inflow is considered of low to medium priority, as the model results showe to be insensitive (chapter 7.5.1). This conclusion is also supported by the low importance of lateral groundwater inflow as recharge component (Figure 7-13: "gw afflux").

As stated above, both the model concept and the model input data concerning the representation of the farmers' agricultural water use strategy are highly uncertain and at the same time very sensitive (chapter 7.5.1; Table 7-23). Accordingly, the research need is considered high.

Furthermore, research concerning the parameters related to human water consumption is considered to play a minor role despite their partially high uncertainty (Table 7-23). The parameters are of low sensitivity (chapter 7.5.1; Table 7-23), which is apparently due to the low importance of domestic water consumption compared to agricultural water demand (Figure 7-11).

Table 7-23: Qualitative synthesis of model sensitivity, uncertainty and research need at the Drâa aquifers (high, medium, low).

Parameter	Sensitivtiy	Uncertainty	Research need
Aquifer outcrop	Low - medium	medium	Low - medium
Aquifer Thickness	Low - medium	High	Medium - high
Specific yield	Variable	High	Medium - high
Recharge coefficient -Wadi	Low - high	High	High
Recharge coefficient - Precipitation	Low	High	Low - medium
Recharge coefficient - Irrigation	Low	High	Low - medium
Catchment area	Low	Low	Low
Run-off coefficient	Variable	High	Medium -high
Evaporation loss –Surface water	Variable	High	Low - medium
Recharge coefficient – Regional recharge	Low	High	Low - medium
Recession coefficient – Lateral inflow fractured	Low	High	Low - medium
Recession coefficient – Lateral inflow fractured/karstic	Low	High	Low - medium
Recession coefficient – Lateral inflow porous	Low	High	Low - medium
Fraction of wheat per cropping area	High	High	High
Fraction of barley per cropping area	Low	High	Medium -high
Fraction of alfalfa per cropping area	Low - high	High	High
Fraction of henna per cropping area	Low - high	High	High
Fraction of vegetables per cropping area	Low - high	High	High
Fraction of maize per cropping area	Low	High	Medium -high
Number of date palms	Low	High	Medium - high
Irrigation efficiency	High	High	High
Repartition of irrigation water from Wadi Drâa (for respective aquifer;)	Low - high	High	High
Demographic development - rural	Low	Medium	Low - medium
Demographic development - urban	Low	Medium	Low - medium
Domestic water consumption – rural	Low	High	Low - medium
Domestic water consumption – urban	Low	High	Low - medium
Initial saturated thickness	Low - high	High	Medium -high

7.6 Scenario analysis

The lumped groundwater budget model BIL is used to assess scenarios of global change concerning the Drâa aquifers in the period 2007 – 2029. Accordingly, the probable future development of the lumped annual aquifer response and groundwater availability is analyzed in comparison to the base line model run covering 33 years in the period of 1974 to 2006 as a reference period (chapter 7.5).

The development of climate change scenarios is standardized via storylines provided by the IPCC (Intergovernmental Panel on Climate Change; e.g. Solomon et al., 2007). As part of the IMPETUS project, these storylines are applied to regional climate modeling using the REMO (Regional Model) model for tropi-

cal and northern Africa (30°W – 60°E; 15°S – 45°N) in the period 1960 – 2049 with a spatial resolution of 0.5°, i.e. approximately 50 km (Paeth et al., 2009; Christoph et al., 2010). Therefore, the REMO model is connected in series to global climate modeling using the ECHAM5/MPI-OM Global Circulation Model (GCM; Roeckner et al., 1996) including the greenhouse gas forcing according to the IPCC SRES (Intergovernmental Panel on Climate Change Special Report on Emissions Scenarios) A1B and B1 scenarios (Solomon et al., 2007; Paeth et al., 2009). The results of the REMO model form the basis of a downscaling procedure to make the climate scenarios applicable for the assessment of surface water and groundwater availability (Paeth, 2009; Born et al., 2008; Busche, (in prep.)).

The scenarios of climate change are combined to scenarios of socio-economic change resulting in the projection of global change. Therefore, storylines of socio-economic scenarios are developed as a part of the IMPETUS project (Reichert & Jaeger, 2010).

The assessment of the scenarios follows basically the DPSIR approach as a framework to determine and evaluate driving forces, pressures, states, impacts and responses (Stanners & Bourdeaux (eds), 1995). Accordingly, the storylines are implemented using system indicators.

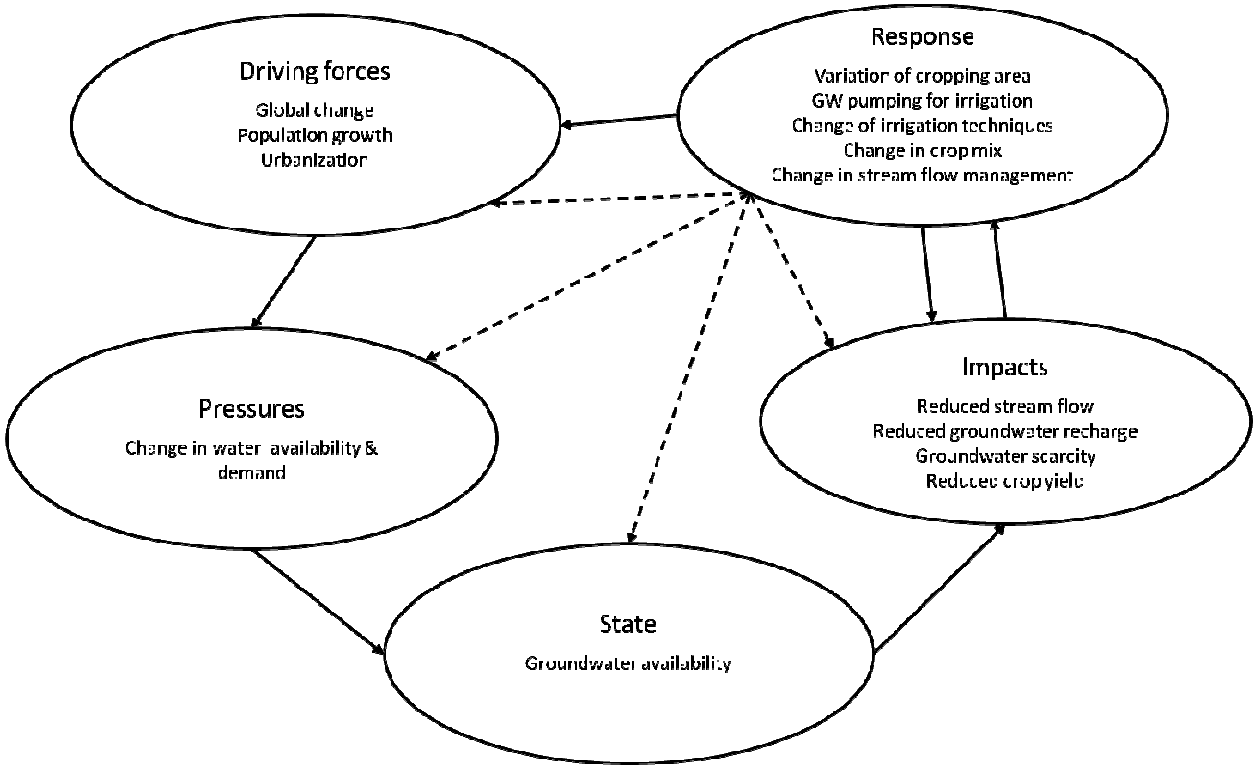

Figure 7-32: Scheme of the DPISR approach relating to groundwater availability of the Drâa aquifers (adapted to EEA (European Environmental Agency; http://www.eea.europa.eu/publications/92-9167-059-6-sum/page002.html, cited October 2012).

The lumped annual filling level of the Drâa aquifers is a major output of the BIL model and the indicator of the system's state. The increased temperature and reduced precipitation are indicators of the pressures of climate change. The reduced inflow from the reservoir Mansour Eaddahbi can indicate both climate change and socio-economic change combined to global change. Increased water demand stands for global change due to expansion of agriculture, urban agglomerations and increasing absolute population. The deviation between the mean filling level of the base line model run and the scenario projec-

tions is the indicator of impact on the groundwater availability. Therefore, the first ten years of the baseline model run are cut to have a comparable length of series (23 years) to the series of scenario results. The responses on changes and impacts are represented by the variation of cropping area and measures to enhance groundwater recharge (e.g. managed aquifer recharge, MAR).

7.6.1 Scenarios of climate change

In this study, the results of the climate modeling and the results of the hydrological modeling in the Upper Drâa Catchment as a part of the IMPETUS project provide trends of climate change in the period 2007 – 2029 (Paeth et al., 2009; Busche, (in prep.)). The average trends of precipitation and temperature in the period 2000 – 2029 represent the climate change scenario in comparison to the base line period (1960 – 2000; Born et al., 2008; Paeth et al., 2009; Busche, 2012):

- Average increase in temperature: 0.7°C
- Average decrease in precipitation: 8 %

Temperature trends are directly implemented in the BIL model by re-estimating the evapotranspiration of crops (crop water demand) using the FAO CropWat model (chapter 7.3). Changes in the precipitation input of the model lead to insignificant changes in the model output. The re-estimation of crop water demand is simplified by determining a monthly factor of increased evapotranspiration based on a reference calculation for the Mezguita oasis. The monthly factor is aggregated to a mean annual factor that is applied to the crop water demand of the baseline model run.

Furthermore, climate change trends referring to the inflow from the reservoir Mansour Eddahbi to the Wadi Drâa are imported from the hydrological modeling in the Upper Drâa Catchment (UDC) using the SWAT MAROC model (Soil and Water Assessment Tool; Busche, (in prep.)). Busche (in prep.) modeled the inflow to the reservoir Masnsour Eddahbi and the inflow to the Middle Drâa Catchment considering the siltation in the reservoir. Therefore, he approached a statistical downscaling of the climate scenarios to make the results of the REMO modeling applicable for hydrological modeling. This was necessary because of the coarse spatial resolution of the REMO-results. Moreover, the results of REMO base line simulations (1960-2000) reveal an invincible overestimation of precipitation by 20 % in comparison to observed data. Consequently, Busche (in prep.) applied the trends of the climate scenarios to the observed climate data based on statistical downscaling to obtain applicable absolute values. Three different downscaling techniques are used to determine a reasonable range of precipitation amount and temperature data while the variability of precipitation pattern remains the same as in the base line period (Busche, (in prep.)).

As the SWAT-MAROC model provides the outflow of the reservoir Mansour Eddahbi as a result, the BIL model takes this as inflow to the Wadi Drâa representing a very important input (boundary condition; chapter 7.3). Because of the scattered distribution of the climate change signal, the range between the 33 and 66 % percentile of the modeled inflow to the reservoir Mansour Eddahbi is assumed reasonable according to the IPCC terminology (Risbey & Kandlikar 2007; Solomon et al. 2007). Subsequently, Busche (in prep.) uses two model realizations representing the 33 and 66 % percentile of the hydrological scenario results to derive the outflow from the reservoir to the MDC. Accordingly, the modeled inflow to the reservoir Mansour Eddahbi is post-processed for estimating the inflow to the MDC by considering domestic water extractions and sedimentation in the reservoir.

As the variability of precipitation pattern remains the same as in the base line period, a procedure of shifting series is applied to artificially vary the succession of dry years and wet years. For each of the two scenario projections (33 and 66 % percentile of the scenario results), overall five model runs are realized with temporarily shifting series of inflow to reservoir and inflow to the MDC respectively. Therefore, the series is shifted for five years while the last five years are cut and added on top of the shifted part. Accordingly, the succession of dry and humid years varies arbitrary, but without changing their distribution in comparison to the base line scenario, which is a bias of the intention of the scenario projection.

Inflow to the MDC is compared for the climate change scenario for the period 2007-2029 and the base line model run for the period 1984-2006 (Table 7-24). Therefore, the mean and median values are depicted as most important inflow item of the water balance. Additionally, the number of years exceeding the mean value is presented. The mean inflow to the MDC is slightly lower in the climate change scenario while the median is higher. The decreased standard deviation in the base line model run proves that the distribution of inflow to MDC is more even than in the base line model run. The number of years exceeding the mean value is significantly lowered in the climate scenario. This hints on the impact of the climate change in relation to the decreased water availability in the Upper Drâa Catchment.

Table 7-24: Statistical measures of the inflow from reservoir Mansour Eddahbi to the MDC for the climate change scenario (2007-2029) and the base line model run (1974 – 2006).

Inflow Drâa [Mm³]	Climate change scenario (2007-2029)	Base line model run (1974-2006)	Base line model run (1974-1996)	Base line model run (1984-2006)
Mean	**258**	250	297	**268**
Median	**250**	210	219	**210**
SD	**250**	258	294	**301**
No. of years above mean	**5.4** (mean over 10 runs)	13	11	**10**

7.6.2 Impact of climate change on the Drâa aquifers

The filling level of the Drâa aquifers is the main indicator of the state of groundwater availability for the interpretation of the climate scenario. Its relative change from the mean value of the base line model run is the main indicator of impact of climate change. Figure 7-33 shows that all Drâa aquifers are affected by climate change regarding the exceedance probability of the mean values of the climate scenario compared to the base line model run. According to the absolute mean values of filling levels, Mezguita is the most affected aquifer, followed by the two lowermost aquifers. Fezouata and Tinzouline rank in the middle of the field while Ternata is the less affected aquifer (Table 7-25). The main reason for the impact is the enhanced irrigation demand determined by increased evapotranspiration amounts through increased temperature. In comparison to this, the slightly reduced inflow to the MDC from the reservoir Mansour Eddahbi contributes a minor impact (Table 7-25).

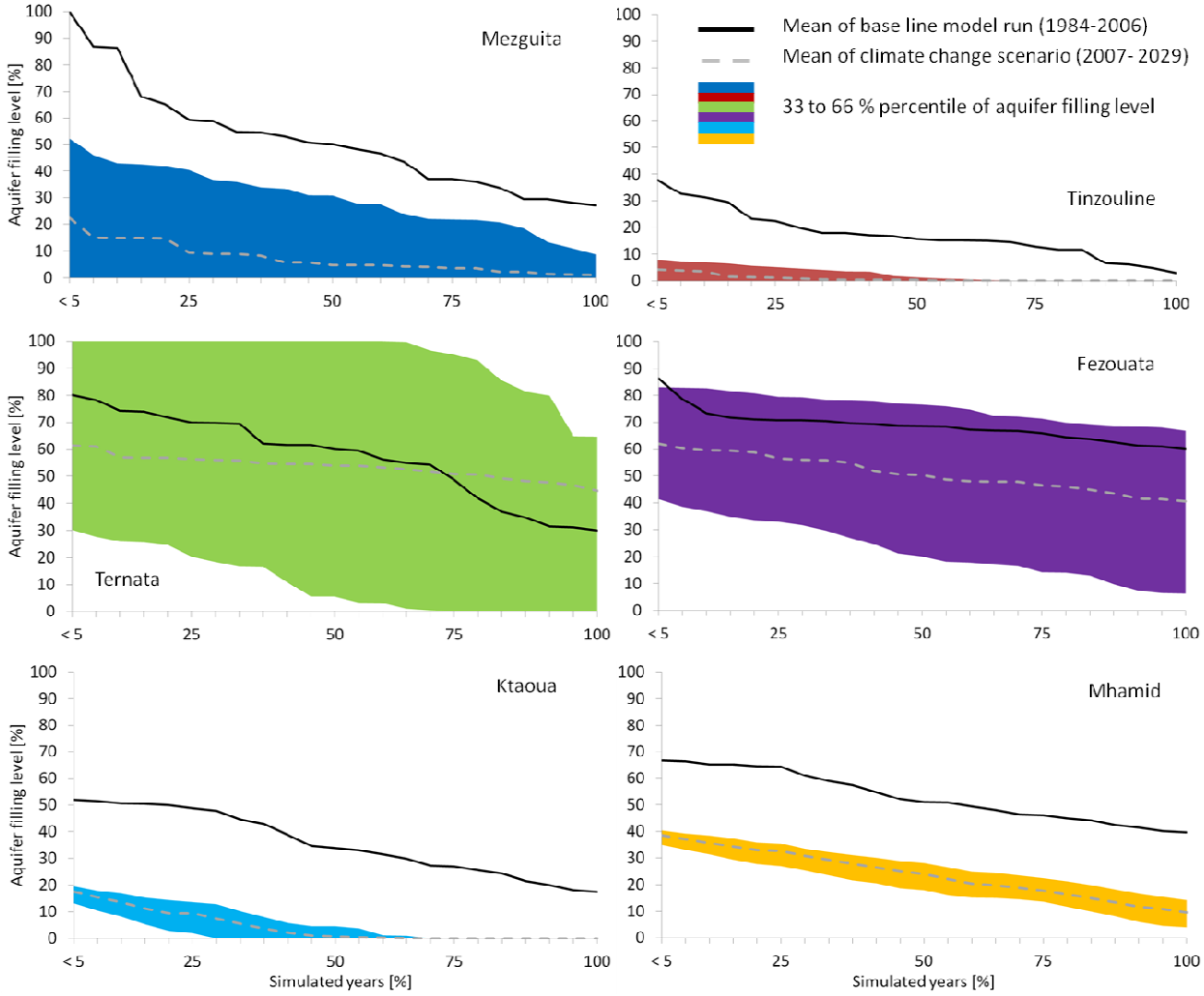

Figure 7-33: Projection of the climate change scenarios for all Drâa aquifer as exceedance probability with the mean (dashed grey line), the range of the 33 - 66 % percentile of the aquifer filling levels (colored area) and the mean of the base line model run (1984-2006, black line).

The Mezguita aquifer is strongly affected by climate change mainly because of the enhanced irrigation demand. Accordingly, the ratio of mean groundwater volume and mean irrigation demand decreases significantly compared to the base line model run falling from 0.9 to 0.1 (Table 7-25). The lower limit of the reasonable range of aquifer filling levels is zero in all years reflecting the threat of severe water scarcity. At the Tinzouline aquifer, the very low antecedent filling levels in combination to the climate change impact lead to a totally unmet of groundwater volumes in 50 % of the simulated years. The reason for this is the same as in Mezguita and the ratio of mean groundwater volume versus mean irrigation demand compared to the base line model run falls clearly from 0.9 to 0.0 (Table 7-25). So the two uppermost Drâa aquifers have to face a severe decline in groundwater availability due to climate change.

The mean value of the base line model run falls into the range of reasonable filling levels of the climate scenario at the Ternata and Fezouata aquifer. So, the signal of climate change is not significant and perishes in the band of the 33-66 % percentile of aquifer filling levels (Figure 7-33). The enhanced irrigation demand causes the subdued decline in mean annual filling level of the climate scenario. In the case of Ternata, the climate scenario reveals even increased groundwater availability for the filling levels be-

neath 50 % at the Ternata aquifer. This is due to the reduced meaning of groundwater as irrigation source and the compensation effect due to the reduction of cropping area as a response on dry conditions. At the Fezouata aquifer, the climate change impact is mitigated by the strong lateral inflow of groundwater (Table 7-25; chapter 7.5).

Ktaoua and Mhamid are also strongly affected by the increased irrigation demand due to increased temperature. Thereby, the buffer of the Mhamid aquifer against climate change is larger according to the absolute values of mean groundwater volume and the ratio of mean groundwater volume versus mean irrigation demand (Table 7-25).

Table 7-25: Results of the climate change scenario (2007-2029) compared to the results of the base line model run (1984-2006).

Base line model run (1984-2006)	Mezguita	Tinzouline	Ternata	Fezouata	Ktaoua	Mhamid
Mean aquifer filling level [%]	52	17	57	69	36	53
Sum of change in aquifer filling level [%]	0	-16	8	-6	-36	-28
Ratio of maximum aquifer volume versus mean irrigation demand	1.8	5.3	2.9	6.7	17.4	28.0
Ratio of mean groundwater volume versus mean irrigation demand	0.9	0.9	1.7	4.6	6.2	14.9
Climate change scenario (2007-2029)						
Mean aquifer filling level of climate change scenarios [%]	7	1	53	51	4	24
Difference in mean aquifer filling level [%l	-44	-16	-4	-18	-31	-29
Sum of change in aquifer filling level [%]	-28	-4	-5	-26	-20	-31
Ratio of maximum aquifer volume versus mean irrigation demand	1.6	4.6	2.8	6.5	16.6	26.8
Ratio of mean groundwater volume versus mean irrigation demand	0.1	0.0	1.5	3.3	0.7	6.4

7.6.3 Scenarios of global change

Three scenarios of global change are projected in this study. Therefore, socio-economic scenarios provided by the IMPETUS project are combined to the previously presented climate scenarios (Reichert & Jaeger, 2010). Thereby, the BIL model implements the story lines of probable socio-economical development in the Drâa region by both modification of indicative parameters and application of the results of global change in the Upper Drâa Catchment (UDC) as a boundary condition (Busche, (in prep.)). The three story lines portray the following types of scenario:

- **M1** – "Marginalization – non-support of the Drâa region"
- **M2** – "Rural development in the Drâa region through regional funds"
- **M3** – "Business as usual"

The BIL model implements socio-economic changes directly as modification of indicative parameters as follows:

- Variation of cropping area (M1 & M2 scenario)
- Demographic development
- Per capita water consumption
- Recharge from wadi bed infiltration (MAR option)

According to the **M1 scenario**, the variation of cropping area is limited to maximum 90 % referring to observed data (chapter 7.3). The limitation of cropping reflects the farmer's response on reduced opportunities to produce crops competitively due to further marginalization. In accordance to the scenarios of global change for the UDC, the inflow to the MDC from the reservoir is taken from the simulations with SWAT-MAROC (Busche, (in prep.)). These scenario simulations consider increased sediment delivery to the reservoir leading to reduced reservoir capacity as impact of intensified firewood extraction (A. Klose, 2009). This in turn leads to a decrease in inflow to the MDC. Moreover, the restricted urbanization is implemented via reduced population growth in the town Ouarzazate. This leads to less extraction of drinking water from the reservoir and thus to an increase in inflow to the MDC. Overall, the inflow to the MDC is slightly less compared to the base line model run (Table 7-26).

Table 7-26: Statistical measures of the inflow from reservoir Mansour Eddahbi to the MDC for the M1 scenario of global change (2007-2029) and the base line model run (1974–2006).

Inflow Drâa [Mm³]	M1 scenario (2007-2029)	Base line model run (1974-2006)	Base line model run (1974-1996)	Base line model run (1984-2006)
Mean	**264**	250	297	**268**
Median	**250**	210	219	**210**
SD	**263**	258	294	**301**
No. of years above mean	**6.9** (mean over 10 runs)	13	11	**10**

In the **M2 scenario** of rural development an upturn in agriculture is assumed represented by a minimum cropping area of 60 %. Simultaneously, the population is assumed to grow by 10 % until 2029 in both rural and urban areas. The per capita water consumption is raised to 120 L/d in the urban areas due to an increased standard of living and the development of small to medium industrial enterprises. The water management is assumed to benefit from the economical upturn being able to enhance groundwater recharge artificially and e.g. to realize installation of Managed Aquifer Recharge (MAR). Accordingly, the recharge coefficient from wadi bed infiltration increases by 2 % at each Drâa aquifer. Additionally, the M2 scenario of global change for the UDC is applied. Accordingly, the inflow to the MDC is influenced by an increase in sedimentation in the reservoir Mansour Eddahbi, increasing urbanization and enhanced per capita water consumption. Furthermore, the water demand relating to the reservoir increases due to the urban planning of the Ouarzazate Lake City focusing on the support of tourism (Busche, (in prep.)). Consequnetly, the simulated inflow to the MDC is slightly decreased compared to the inflow in the M1 scenario but overall still slightly reduced in comparison to the base line model run (Table 7-27).

Table 7-27: Statistical measures of the inflow from reservoir Mansour Eddahbi to the MDC for the M2 scenario of global change (2007-2029) and the base line model run (1974–2006).

Inflow Drâa [Mm³]	M2 scenario (2007-2029)	Base line model run (1974-2006)	Base line model run (1974-1996)	Base line model run (1984-2006)
Mean	**250**	250	297	**268**
Median	**250**	210	219	**210**
SD	**245**	258	294	**301**
No. of years above mean	**5.3** (mean over 10 runs)	13	11	**10**

The **M3 scenario** reflects the "business as usual" considering selective enhancement of artificial groundwater recharge. Therefore, the recharge coefficient from wadi bed infiltration increases by 2 % at Mezguita and Tinzouline as they are the aquifers mostly prone of water scarcity and the highest stream flow availability (chapter 7.2, 7.4, 7.4 & 7.5.1). Same as for the M1 ans M2 scanarios the simulated inflow to the MDC is taken from the respective scenario calculations with SWAT-MAROC. So, the input to the Wadi Drâa is influenced by the same factors as in the M2 scenario excluding decreased water availability in relation to the urban planning of the Ouarzazate Lake City (Busche, (in prep.)). Accordingly, the reduction in inflow to the MDC is insignificant in comparison to the base line model run (Table 7-28).

Table 7-28: Statistical measures of the inflow from reservoir Mansour Eddahbi to the MDC for the M3 scenario of global change (2007-2029) and the base line model run (1974–2006).

Inflow Drâa [Mm³]	M3 scenario (2007-2029)	Base line model run (1974-2006)	Base line model run (1974-1996)	Base line model run (1984-2006)
Mean	**255**	250	297	**268**
Median	**250**	210	219	**210**
SD	**249**	258	294	**301**
No. of years above mean	**5.4** (mean over 10 runs)	13	11	**10**

In conclusion, the reduction of inflow from the UDC to the MDC according to the global change scenario is of minor importance compared to the base line model run.

7.6.4 Impact of global change on the Drâa aquifers

According to the evaluation of impacts of climate change, the filling level of the Drâa aquifers is the main indicator of the state of groundwater availability. The relative deviation of aquifer filling levels from the mean value of the base line model run represents the main indicator of impact of global change.

The effects of Marginalization referring to the M1 scenario mitigate the climate change impact. This shows the significance of the management of cropping area (Figure 7-34). So, the irrigation demand is a very delicate item of the water balance and may be a starting point for adaptation to climate change if it is not in the line with further marginalization of the Drâa region. The impact of climate change is clearly mitigated in the first four Drâa aquifers as the mean annual filling levels of the base line model run fall within the band of the 33-66 % percentile. The relatively lowered mean aquifer filling levels of the M1

scenario show that there is still an impact of climate change except for Ternata. At the Ternata, aquifer the variation in cropping area appears to compensate the climate change impact leading even to increased mean filling levels compared to the base line model run (Figure 7-34; Table 7-29). The two lower most Drâa aquifer suffer from clear filling level decline that is very slightly mitigated in comparison to the climate change impact (Table 7-29).

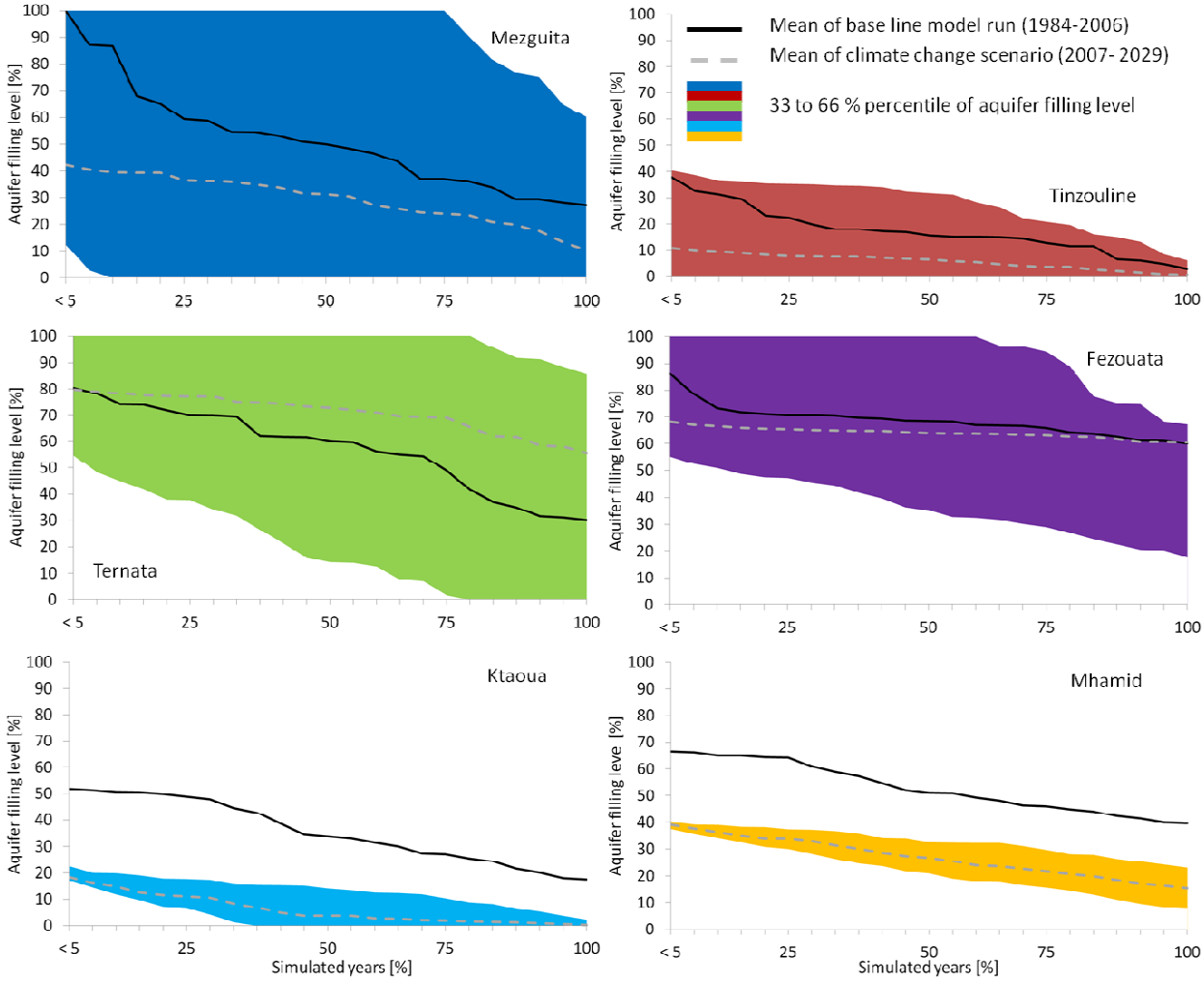

Figure 7-34: Results of the M1 scenario of global change for all Drâa aquifer as exceedance probability with the mean (dashed grey line), the range of the 33 - 66 % percentile of the aquifer filling levels (colored area) and the mean of the base line model run (1984-2006, black line).

According to the M2 scenario, rural development leads to differentiated effects at the Drâa aquifers (Figure 7-35; Table 7-29). The impact of climate change is mitigated at Mezguita and Tinzouline due to the enhanced recharge from wadi bed infiltration verified by the high model sensitivity to modifications of this parameter. At Mezguita, the mean aquifer filling level even perishes totally in the range of reasonable filling levels of the M2 scenario (Figure 7-35). At the Ternata aquifer, the permanent uplift of the lower limit of the cropping area leads to a decrease in groundwater resources as stream flow for irrigation is consumed and groundwater gains importance for irrigation. At the Fezouata aquifer, the increased urban water consumption at the town Zagora (Ternata oasis) has an effect too. The enhanced recharge from wadi bed infiltration looses significance compared to the Mezguita and Tinzouline aquifers as the sensitivity analysis confirms (chapter 7.5.1). At the Ktaoua and Mhamid aquifers, the decline

in filling levels is increased in comparison to the climate change scenario due to the relatively enlarged cropping area and the minor effect of mitigation by enhanced recharge from wadi bed infiltration (Table 7-29).

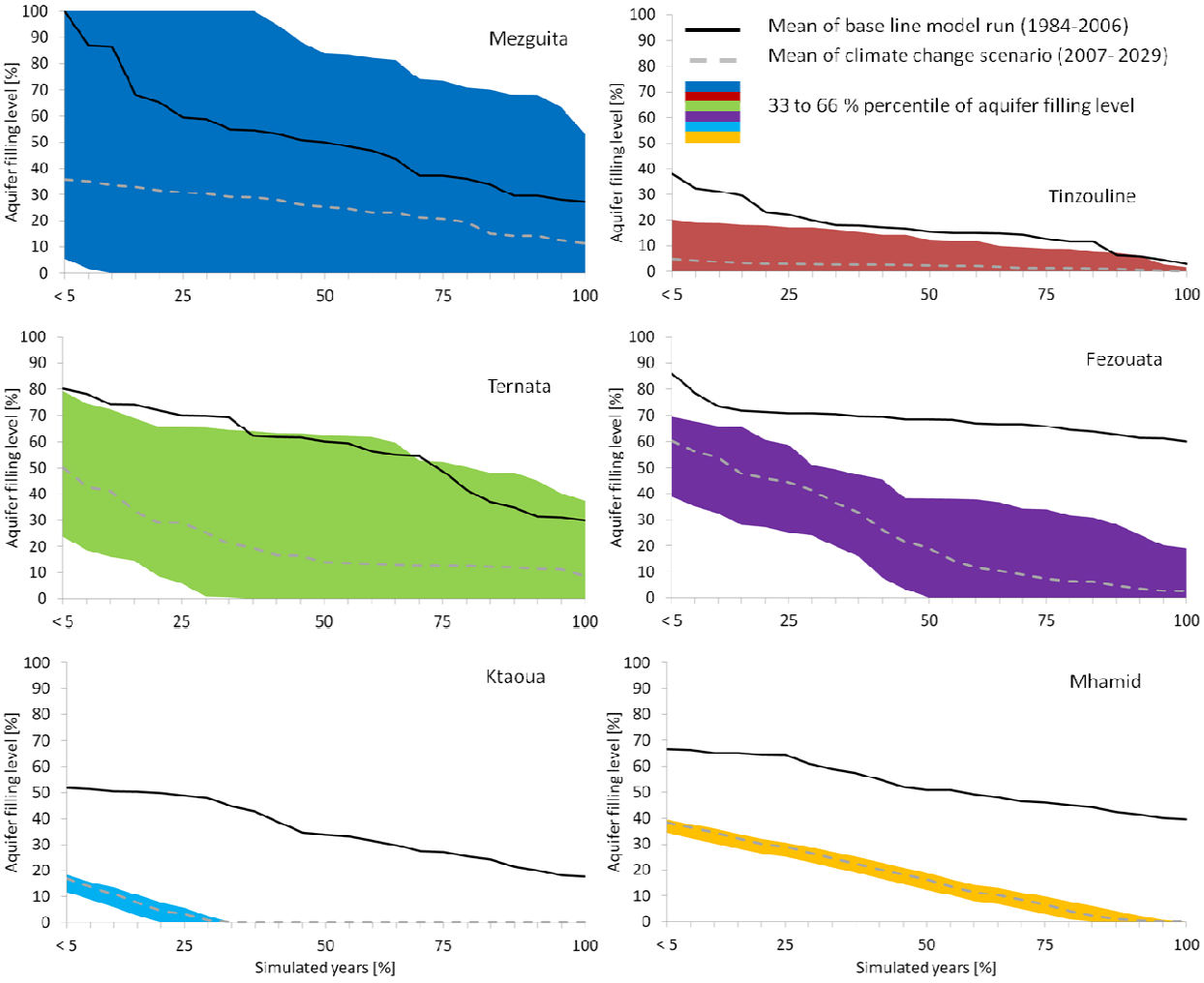

Figure 7-35: Results of the M2 scenario of global change for all Drâa aquifer as exceedance probability with the mean (dashed grey line), the range of the 33 - 66 % percentile of the aquifer filling levels (colored area) and the mean of the base line model run (1984-2006, black line).

The results of the M3 scenario reveal positive effects on the filling levels of the Mezguita and Tinzouline aquifers because only there the recharge from wadi bed infiltration is increased (Figure 7-36). Accordingly, less residual stream flow is left for the four lower Drâa aquifers leading to a tightening of the climate change impact (Table 7-29). Assuming that the M3 scenario represents “business as usual”, the two lowermost aquifers suffer from severe water scarcity and decline in groundwater availability. At the Ternata and Fezouata aquifer the filling levels never fall below 30 % representing the most stable conditions. The mitigation of climate change at Mezguita and Tinzouline shows that measures of managed aquifer recharge display a promising option of groundwater management.

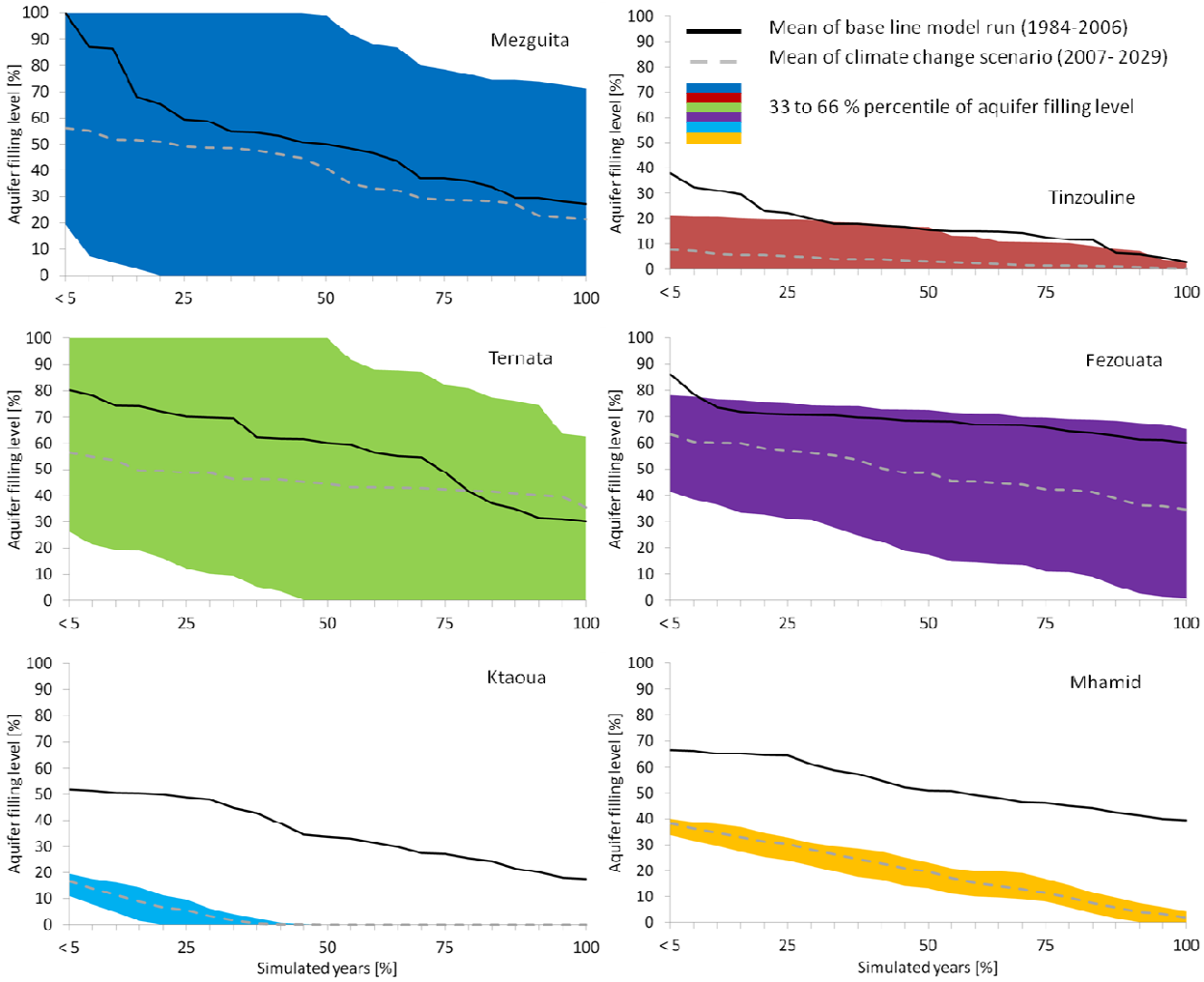

Figure 7-36: Results of the M3 scenario of global change for all Drâa aquifer as exceedance probability with the mean (dashed grey line), the range of the 33 - 66 % percentile of the aquifer filling levels (colored area) and the mean of the base line model run (1984-2006, black line).

In conclusion, the scenario simulations verify that useful results are gained to face the future pressures on groundwater resources in the MDC using the BIL model (chapter 9).

Table 7-29: Synthesis of the results of the global change scenarios and climate scenarios compared to the base line model run at all Drâa aquifers based on change in mean aquifer filling level, sum of change in aquifer filling level, ratio of maximum aquifer volume versus mean irrigation demand and ratio of mean groundwater volume versus mean irrigation demand.

Base line model run	Mezguita	Tinzouline	Ternata	Fezouata	Ktaoua	Mhamid
Mean aquifer filling level [%]	52	17	57	69	36	53
Sum of change in aquifer filling level [%]	0	-16	8	-6	-36	-28
Ratio of maximum aquifer volume versus mean irrigation demand	1.8	5.3	2.9	6.7	17.4	28.0
Ratio of mean groundwater volume versus mean irrigation demand	0.9	0.9	1.7	4.6	6.2	14.9
Climate change scenario						
Difference in mean aquifer filling level [%l	-44	-16	-4	-18	-31	-29
Sum of change in aquifer filling level [%]	-28	-4	-5	-26	-20	-31
Ratio of maximum aquifer volume versus mean irrigation demand	1.6	4.6	2.8	6.5	16.6	26.8
Ratio of mean groundwater volume versus mean irrigation demand	0.1	0.0	1.5	3.3	0.7	6.4
M1 scenario						
Difference in mean aquifer filling level [%l	-22	-11	-14	-4	-30	-26
Sum of change in aquifer filling level [%]	7	4	18	-2	-20	-25
Ratio of maximum aquifer volume versus mean irrigation demand	1.7	4.8	3.0	6.9	17.6	28.3
Ratio of mean groundwater volume versus mean irrigation demand	0.5	0.3	2.1	4.4	1.1	7.6
M2 scenario						
Difference in mean aquifer filling level [%l	-27	-15	-37	-44	-33	-36
Sum of change in aquifer filling level [%]	-1	-2	-48	-64	-20	-40
Ratio of maximum aquifer volume versus mean irrigation demand	1.5	4.2	2.5	5.9	15.0	24.2
Ratio of mean groundwater volume versus mean irrigation demand	0.4	0.1	0.5	1.4	0.4	4.1
M3 scenario						
Difference in mean aquifer filling level [%l	-12	-14	-12	-20	-33	-34
Sum of change in aquifer filling level [%]	27	0	-19	-33	-20	-38
Ratio of maximum aquifer volume versus mean irrigation demand	1.6	4.6	2.8	6.5	16.7	26.9
Ratio of mean groundwater volume versus mean irrigation demand	0.7	0.2	1.3	3.2	0.5	5.3

8 The IWEGS Spatial decision support system (SDSS)

The IWEGS spatial decision support system (Impact of Water Exploitation on Groundwater and Soil) is developed to help taking decisions on regional resource planning referring to groundwater and soil.

The development of the IWGS SDSS is based on the activities of an interdisciplinary work group within the IMPETUS project. The core of the working group constitutes of three disciplines as hydrogeology, agro-hydrology / soil science and ethnology. Each of the disciplines contributes expertise that is implemented in simulation models. Thereby, the SahysMod model simulates the lumped annual soil salinity for each Drâa oases. The BIL model estimates the lumped annual groundwater budget of each Drâa aquifer incorporating the C.E.M. Drâa and the CropDem modules. The C.E.M. Drâa module calculated the domestic water consumption based on the demographic dynamic and the daily per capita water use (chapter 7.3). The CropDem module assesses the crop water demand based on evapotranspiration calculations of the respective crop mix in the Drâa oases (chapter 7.3). So, the BIL model assesses the annual groundwater budget of the Drâa aquifers and SahysMod model estimates the soil salinity in the related Drâa oases. In the IWEGS SDSS, the SahysMod model is coupled to the BIL model based on the MS Excel ® software (Figure 8-1; ILRI, 2005; Laudien, 2008; IMPETUS, 2006).

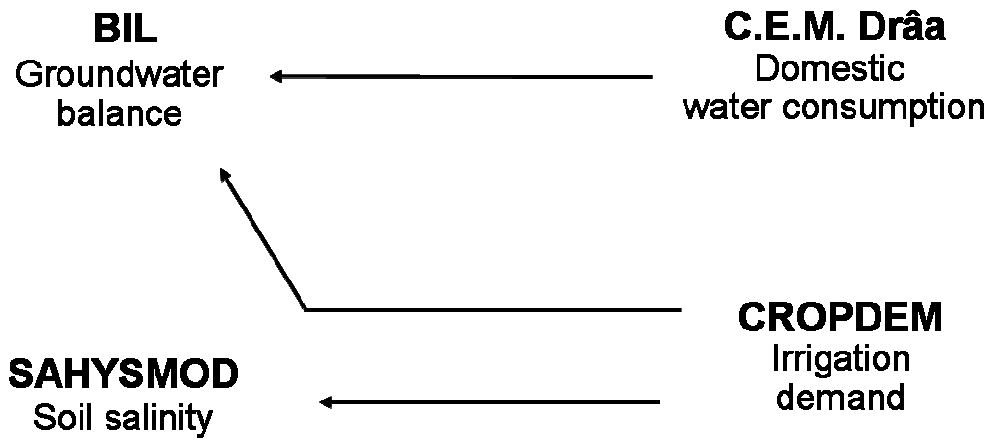

Figure 8-1: Principal of the model coupling in the SDSS IWEGS.

The interface of the IWEGS SDSS provides modification of selective parameters and model input to analyze scenarios of global change. The output is given as lumped annual percentage filling level of the Drâa aquifers and as lumped annual electric conductivity in the saturation paste of soil for each Drâa oasis. The results are visualized as tables and maps including a threshold query of the critical state of groundwater availability and soil salinity in the Drâa oases. The IWEGS SDSS is used to evaluate the need of further investigations on groundwater and soil. Against the background of the modeling, the most important parameters can be focused and investigations can be planned efficiently. As an example, if the model results reveal strong impacts of e.g. climate change for one oasis, the impact in this oasis can be further analyzed by scenario projections using the models and the IWEGS SDSS respectively (chapter 7.5 & 7.6). Consequently, the priority in management options can be evaluated referring to both groundwater availability and soil salinity.

The IWEGS SDSS is implemented in the IMPETUS SDSS Framework as an embracing interface of various SDSS and further tools developed as a part of the IMPETUS project. Technical details concerning the SDSS IWEGS are given in Enders et al. (2010).

9 Options for groundwater management in the Drâa aquifers

The Middle Drâa Catchment (MDC) is a marginal and rarely gauged basin so that well adapted investigation concepts and monitoring designs are needed to achieve an enhanced basis for groundwater management including technical, socio-political and economical aspects. The management options presented in this study are withdrawn from the regional hydrogeological analysis and the groundwater budget modeling. Thereby, the model simulations allow the assessment of the importance of parameters, water balance components and Drâa aquifers that should be targeted first according to the approach of this study.

The ratio of mean annual groundwater extraction for irrigation versus mean annual amount of irrigation water from the Wadi Drâa provides information on the importance of groundwater for irrigation. The higher the ration the more important is groundwater for irrigation over irrigation with surface water (Table 7-11). Accordingly, the priority of investigation demand concerning the Drâa aquifers is as follows:

1. Mhamid (ratio = 4.2)
2. Tinzouline (ratio = 2.8)
3. Mezguita (ratio = 2.6)
4. Ktaoua (ratio = 2.0)
5. Fezouata (ratio = 1.8)
6. Ternata (ratio = 0.7)

For the Ktaoua and Mhamid aquifer, field mapping, groundwater sampling and surveying of water consumption is recommended to better understand the aquifer response. Soil sampling can supplement the other observations because salinization is an urgent issue limiting agriculture (Heidecke, 2009; S. Klose et al., 2010).

In particular, the sensitivity analysis provides the set up of a priority list of investigations. The analyses of global change scenarios reveal some options for groundwater management through the influence of the modified indicators used to project the different scenarios (chapter 7.6.3). Accordingly, the feasibility of the following options should be checked:

- Selective installations for Managed Aquifer Recharge (MAR) to enhance the groundwater recharge from wadi bed infiltration (e.g. covered infiltration ditches, leaching basins)
- Regulation of arable land in combination to enhanced hydrometric observations and groundwater monitoring

Measures of MAR display an option even if groundwater pumping is costly whereas surface water is free of charge. So far, the infiltration of stream flow happens in the undeveloped wadi bed except of the minor barrages and branching of the irrigation channels. Technical installations of e.g. covered infiltration ditches may support the previous recharge from stream flow infiltration.

The regulation of arable land is largely a question of traditional rights and practice and requires an active dialogue with and within the agricultural sector. The introduction of water-saving techniques in urban households requires enlightenment among the population and cannot be evaluated in this study.

The variation of the crop mix in the Drâa oases has to be checked carefully as the sensitivity analysis of the groundwater budget modeling reveals that the existing crop mix represents a near-optimum state within narrow window of possible share.

The introduction of water-saving irrigation technique, such as drip irrigation, requires implicitly studies on soil salinization because the leaching of salts from the soil would be reduced in comparison to the established flood irrigation.

Furthermore, this study reveals some hints on technical and planning measures for a careful and cost effective groundwater management. Accordingly, the options for groundwater management derived from this study are divided in two issues:

- Research aspects
- Technical aspects

Research aspects

The state of research in the Middle Drâa Catchment requires enhancement. This study shows that methods should be kept robust and transparent against errors and uncertainties before highly parameterized model systems are applied for decision support and groundwater management (Kirchner, 2006). Comprehensible data based analysis of the mechanisms of aquifer response are recommended as particularly the sensitivity analysis within the BIL model reveals (Table 7-23; chapter 7.5.1; chapter 6.1, 6.2 & 6.2.3). According to the sensitivity analysis, a priority list of the Drâa aquifers is compiled:

1. Tinzouline
2. Mezguita
3. Fezouata
4. Ktaoua
5. Ternata
6. Mhamid

This list is not in accordance with the list given above that priorizes the aquifers concerning the importance of groundwater versus surface water for irrigation. So, decision makers should keep both aspects, groundwater importance as irrigation water source and research needs revealed by the sensitivity analysis, in mind when planning measures.

The investigation of distribution of geohydraulic parameters represents a promising advance in particular at the local scale.

Typical for dry environments, studies on groundwater availability in the MDC should handle surface water and groundwater closely related or even as one. Thereby, the vadose zone processes are one of the most precarious aspects. According to Kirchner (2006) the procedures to analyze and quantify water availability at the regional scale should be based on equations adapted to the mechanisms actually observed on site. Distributed groundwater flow modeling should be adapted to the prior outcomes of lumped groundwater modeling and the procedural abstraction of the actual mechanisms related to the respective temporal and spatial scale. Hydrogeochemical investigations in combination to groundwater

flow analysis are very important to understand the actual aquifer processes and to manage water quality issues. In particular, tracer and isotope analysis help to differentiate the currently renewable resources from “fossile” water. Furthermore, tracer and isotopic studies of should be used to check the plausibility of groundwater flow models, e.g. through groundwater residence time estimations. Groundwater studies in the MDC should implicitly be harmonized to agro-hydrological surveying of water use due to the dominating and partly uncontrolled water consumption for irrigation. Further hydro-meteorological observations are necessarily recommended in accordance with an adapted monitoring design.

Moreover, artificial recharge, managed aquifer recharge (MAR) and recovery as well as waste water reuse represent promising measures of groundwater management in dry environment (Bower 2002; Marsily; 2003; Flint & Ellet; 2004; Dillon; 2005; Gale (ed) 2005; Raju et al; 2006; Steenbergen & Tuinhof, 2009). For the Drâa aquifers, a discussion rose already about an enhanced artificial recharge and MAR along the course of the Wadi Drâa or at new installations. As the analysis of global change scenarios shows, the implementation of enhanced groundwater recharge from wadi bed in filtration leads to a significant mitigation of the impact of global change (chapter 7.6.3 & 7.6.4). Accordingly, studies on MAR should be focused based on integrated approaches such as the combination of hydro-geophysical and hydrogeochemical techniques.

Technical aspects

Most of all, the observation and monitoring of groundwater levels and water composition dominate the technical aspects of groundwater management options in the MDC. This study allows only to reveal technical recommendations with some reservations due to its regional approach. The investigation of the exemplary test sites Basin of Feija de Zagora and Plain of El Miyit provides the preliminary suggestions for the installation of piezometers and automatic groundwater level probes along the main flow paths (chapter 6.2.2; Figure 9-1). The choice of the observations points and measurement equipment is dependent on the current feasibility of the respective monitoring project.

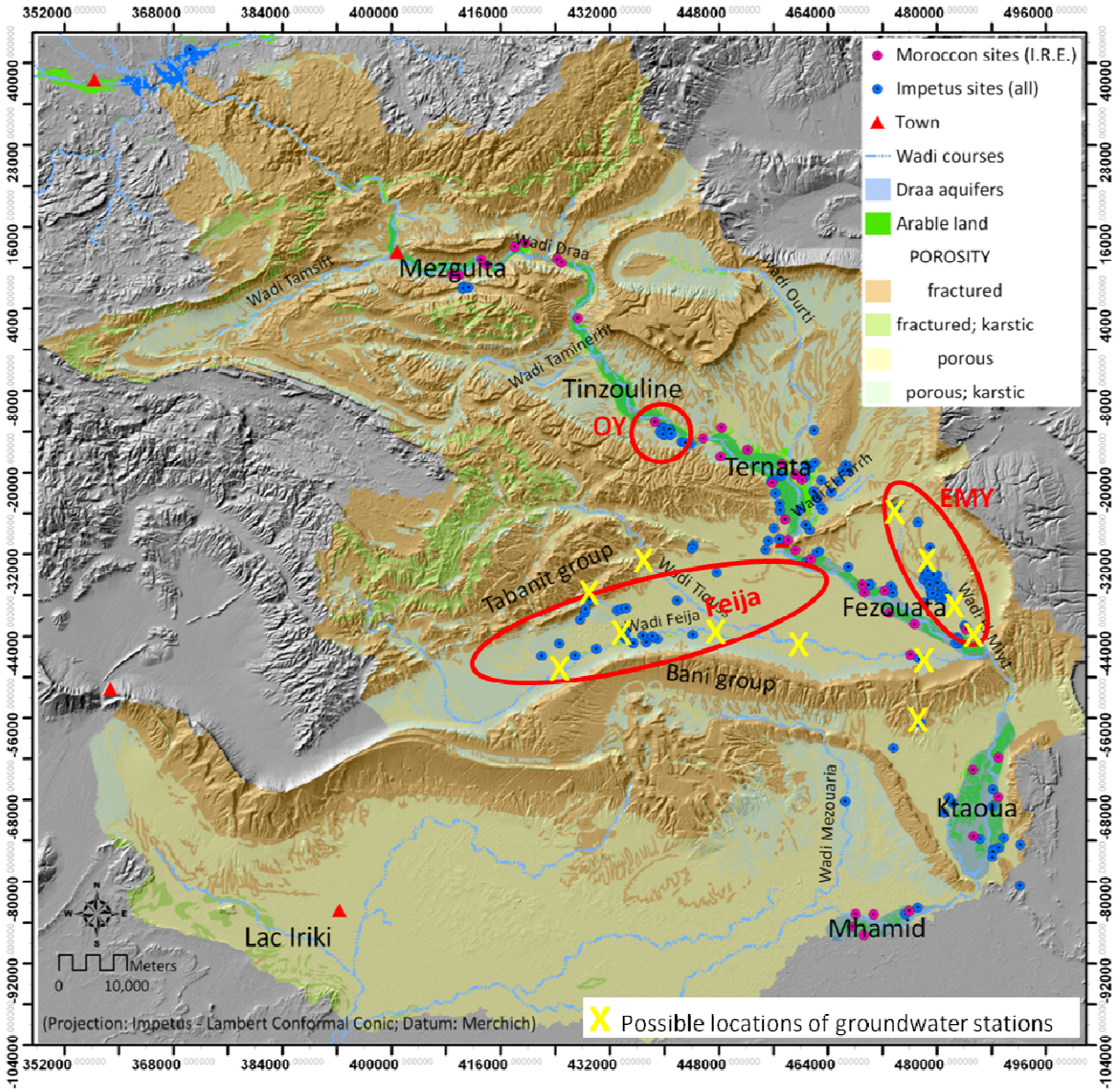

Figure 9-1: Overview map of Impetus groundwater observation points (blue circles), sites of the Service Eau Ouarzazate (pink circles) and possible locations of groundwater stations (yellow x) in the areas of the Basin of the Feija de Zagora and the Plain of El Miyit.

The groundwater budget modeling provides prioritization of the Drâa aquifers relating to the need of an enhanced base monitoring and eventually new specific monitoring networks (cf. Margane, 2004):

1. Tinzouline aquifer due to overexploitation
2. Mezguita aquifer due to high dynamic and uncertainties in aquifer response modeling

Groundwater level observations, groundwater sampling and field mapping is recommended for the Ktaoua and Mhamid aquifer because the data basis is very fragmentary and salinization of soil and groundwater is a severe problem for agriculture. So, soil sampling should be considered in planning observations and designing monitoring concepts (Heidecke, 2009; S. Klose et al. 2010).

Any monitoring network and the observation program should be harmonized to groundwater sampling, meteorological observations, hydrometric gauging, surveying of water consumption and field mapping. Thereby, the choice of site is a question that should be answered at the local scale, e.g. relating to drilling new observation wells.

The development of a drought early warning system appears to be a management option as the scenario analyses of global change reveal significant impact on water availability. The importance of a sound monitoring program is underlined, as it is the basis for a drought early warning system.

10 Conclusion & perspectives

This study gives a current state of knowledge on the regional groundwater resources of the Middle Drâa Catchment. Furthermore, it provides modeling of the lumped annual groundwater budget of the Drâa aquifers including the estimation of climate and global change scenarios using the BIL model. Therefore, a renewed data basis is created to characterize the aquifer setting, the groundwater system and composition in the Middle Drâa Catchment (MDC). Subsequently, the BIL model is developed. In order to answer the central research questions the results are concluded in the following sections.

Lithological information from mapping surveys and bore log descriptions form the basis of a hydrofacies framework refining the existing concept of the aquifer system in the MDC (chapter 6.1). Accordingly, the occurrence of the following aquifer compartments reveals:

1. Six alluvial shallow Drâa aquifers
2. Porous Basin Aquifers:
    - Thick Basin aquifers (> 10 m of mean thickness of sediments), e.g. Feija de Zagora,
    - Thin Basin aquifers (< 10 m of mean thickness of sediments), e.g. El Miyit (Figure 6-6)
3. Porous Tributary aquifers
4. Fractures Aquitard system

The groundwater level response of the Drâa aquifers relates to the re-interpreted distribution of specific yield values. The alternative specific yield data is higher and corresponds to the groundwater level dynamic of the individual Drâa aquifers in comparison to literature (chapter 6.2.1). So, it is more reliable than the data from former studies. According to the higher specific yield, the absolute values of potentially drainable aquifer volume are higher than found in literature, e.g. ORMVAO (1995) and Chamayou (1966) and Chamayou et al. (1977).
The recent recharge of the Drâa aquifers depends mostly on transmission losses from the regulated inflow from the Upper Drâa Catchment to the Wadi Drâa. Indirect recharge from floods generating after intense rainfall within the MDC is another source of aquifer replenishment (chapter 6.2.1).
The existing concept of groundwater flow is verified in terms of the overall southwards directed main path within Drâa aquifers. The evaluation of the main flow paths around the Ternata, Fezouata and Ktaoua aquifer results in the temporarily continuous lateral groundwater inflow towards the Drâa aquifers and a backwater effect in front of the aquitard outcrops at the lower end of the Drâa aquifers.
The analysis of inorganic groundwater composition provides a new characterization of the hydrochemistry in the MDC: In combination to the stable isotope signature, the hydrogeochemical analysis verifies the interpretation of the aquifer system and the main groundwater flow paths. The distribution of the hydrochemical facies and the state of hydrogeochemical evolution hint on significant influence of

groundwater pumping for irrigation. Accordingly, salinization is set up geogenically but enhanced by human activity, particulary groundwater return flow after irrigation (6.3.3.3).

The groundwater budget modeling provides the lumped annual groundwater avaiblabiltiy at the Drâa aquifers. The absolute values of the modeled groundwater volumes remain uncertain due data uncertainty and the lumped parameters approach (chapter 7.5.4). However, plausibility tests comparing single groundwater level observations to modeled aquifer response reveal good accordance for the Tinzouline, Ternata and Fezouata aquifers (chapter 7.5.3). Sufficient data for further comparable plausibility test are not available. The model results for the two lower aquifers, Ktaoua and Mhamid, are highly uncertain and suffer from data scarcity and conceptual uncertainty. Therefore, results for these aquifers are hardly interpretable.

Agricultural water abstraction is the most important negative item of the groundwater budget, domestic water extraction accounts for less than 3 %. However, uncertainties surround the representation of the agricultural water use strategies, as insufficient data on cropping area, crop mix, surface water repartition to the oases and irrigation efficiency is available. Groundwater discharge to the downstream oasis is of minor quantitative importance. Infiltrating river water (originating from the upstream reservoir Mansour Eddahbi and from streamflow generating within the MDC) is the main source of groundwater recharge, while lateral inflow and direct recharge from precipitation are of minor importance. The ratio between irrigation water demand covered by groundwater and by surface water reveals that Mhamid depends strongest and Ternata depends least on groundwater (Table 7-11). The ratio between mean groundwater availability and mean irrigation demand shows that the three uppermost Drâa aquifers suffer from severe water scarcity (Table 7-11).

The modeled aquifer response and the relative comparison of the base line model run and simulations of climate and global change lead to the deduction of options for groundwater management (7.5, 7.6 & 9). As a main outcome, the expected climate change causes a significant decrease in groundwater avaiblabitly in the Drâa aquifer accounting for reductions in mean aquifer filling levels of 4 to 44% up to the year 2029. The ratio of mean aquifer filling level to mean irrigation demand reveals an even enhanced water shortage (Table 7-29). Thereby, the artificially altered sequence of wet and dry years seems to have an important influence on groundwater availability as shown by the wide range of the results of the climate change scenario, while the total amount of inflow remains approximately the same (Figure 7-33).

In combination to the climate change scenario three scanarios of global change are estimated revealing the possibility of mitigating the impact of climate change. Thereby, the assumed impact responses representing socio-economic change in the BIL model lead to the overprint of the impact of global change in the Upper Drâa Catchment implemented via the inflow from the reservoir to the MDC. In conclusion, the scenario assumptions in the BIL model clarify the differences between the Drâa aquifers in response and buffer function against impact of global change.

As a perspective, further groundwater studies in the Middle Drâa Valley can help the resource management as the livelihood depends strongly on groundwater and the insight to the groundwater system is still at a basic level. Both scientific and applied investigations should represent integrated approaches as the interplay between groundwater and surface water resources and irrigation agriculture is decisive for the fragile equilibrium in the arid system functions.

The aquifer properties should be approached as often as possible in combination with the re-implementation of a monitoring network. Accordingly, the data coverage could be enhanced to form a basis for spatially discrete groundwater flow assessment. One of most important need relating to future investigations of the groundwater resources is an integrated approach considering the stream – aquifer interactions and the use of water for irrigation. Thereby, field mapping is highly recommended to better assess the irrigation demand and hopefully the farmers' response to impacts of hydro-meteoric variability and global change. However, the machanisms of aquifer response should be approached considering the scale and the respective need, or vice-versa (Kirchner, 2006).

References

Abbott, M.B. & Refsgaard, J.C. (1996): Distributed hydrological modeling. Dordrecht, Kluwer.

Abdalla, O.A.E. (2008): Groundwater discharge mechanism in semi-arid regions and the role of evapotranspiration. – Hydrological Processes, 22: 2993-3009.

Abdeljali, M., Marcais, J., Choubert, G. & Fallot, P. (1959): Carte Géologique 1:500000 – Feuille Ouarzazate.

Ad-Hoc-Arbeitsgruppe Hydrogeologie (1997) : Hydrogeologische Kartieranleitung. – Geologisches Jahrbuch – Information aus den Bund/Länder-Arbeitsgruppen der Staatlichen Geologischen Dienste, Reihe G, 2, Hannover.

Ait Hssaine, A. & Bridgland, D. (2009): Pliocene-Quaternary fluvial and aeolian records in the Souss Basin, southwest Morocco: A geomorphological model. – Global and planetary change, 68: 268-296.

Allen, R.G., Pereira, L., Raes, S. & Smith, D. (1998): Crop Evapotranspiration- Guidelines for Computing Crop Water Requirements. FAO Irrigation and Drainage Paper 56, FAO-Food and Agriculture Organization of the United Nations, Rome.

Allison, G.B. & Hughes, M.W. (1983): The use of natural tracers as indicators of soil-water movement in a temperate semi-arid region. – Journal of Hydrology, 60: 157-173.

Allison, G.B., Cook, P.G., Barnett, S.R., Walker, G.R., Jolly, I.D. & Hughes, M.W. (1990): Land clearance and river salinisation in the western Murray Basin, Australia. – Journal of Hydrogeology, 119: 1-20.

Anderson, M.P., Aiken, J.S., Webb, E.K. & Mickelson, D.M. (1999): Sedimentology and hydrogeology oft wo braided stream deposits. – Sedimentary Geology, 129: 187-199.

Aoubouazza, M. & El Meknassi, Y.E. (1996): Hydrologie et hydrogeologie du basin de la Feija de Zagora (Province de Ouarazate) – Etude sur la lutte contre la desertification dans la Vallee moyenne de l'Oued Drâa.

Appelo, C.A.J. & Postma, D. (2005): Geochemistry, groundwater and pollution. 2nd ed. Balkema, Amsterdam, 649 pp.

Appelo, C.A.J. & Postma, D. (2005): Geochemistry, groundwater and pollution. 3rd ed. Balkema, Amsterdam, 649 pp.

Arboyela, M.L., Babault, J., Owen, L.A., Teixell, A. & Finkel, R.C. (2008): Timing and nature of Quaternary fluvial incision in the Ouarzazate foreland basin, Morocco. – Journal of the Geological Society, London, 165: 1059-1073.

Arnold, J.G., Allen, P.M., Muttiah, R. &Bernhardt, G. (1995): Automated Base Flow Separation and Recession Analysis Techniques. – Ground Water, 33 (6): 1010-1018.

Awad, H. (1963): Some Aspects of the Geomorphology of Morocco Related to the Quaternary Climate. – The Geographical Journal, 129, No. 2: 129-139.

Ayers, R. & Westcott, D., (1994): Water quality for agriculture. FAO irrigation and drainage paper 29 Rev.1, Food and Agricultural Organisation of the United Nations.

Back, W. (1960): Origin of hydrochemical facies in groundwater in the Atlantic coastal plain. – Proceed. International Geological Congress I: 87-95. Copenhagen.

Bakalowicz, M. (1994): Water geochemistry: Water quality and dynamics. – Groundwater Ecology,
97- 127.

Bakker, M., Anderson, E.I., Olsthoorn, T.N. & Strack, O.D.L. (1999): Regional groundwater modelling of the Yucca Mountain site using analytic elements. – Journal of Hydrology, 226: 167-178.

Barica,. J (1972): Salinization of groundwater in arid zones. – Water resources research, 6(8): 925-933.

Batelaan, O. & De Smedt, F. (2001): WetSpass: a flexible, GIS based, distributed recharge methodology for regional groundwater modeling. – IAHS Publ., 269: 11-17.

Batelaan, O., De Smedt, F. & Otero Valle, M.N. (1993): Development and application of a groundwater model integrated in the GIS GRASS. – IAHS Publ., 211: 581-589.

Bazuhaire, A.S. & Wood W.W. (1996): Chloride mass-balance method for estimating ground water recharge in arid areas: examples from western Saudi Arabia. Journal of Hydrology 186: 153-159.

Bear, J., Beljin, M.S. & Ross, R.R. (2005): Fundamentals of Ground-Water Modeling. Technology Innovation Office, Office of Solid Waste and Emergency Response, US EPA, Washington, DC.

Beauchamp W., Allmendinger, R.W., Barazangi, M., Demnati, A., El Alji, M. & Dahmani, M. (1999): Inversion tectonics and the evolution of the High Atlas Mountains (Morocco), based on a geological-geophysical transect. – Tectonics, 18(2): 163-184.

Belfkih A.M., Azzimane, O., Barkaoui, M., Benhima, D., Benabdellah, B.R. Bourqia, R. Boutaleb, H., Chkili, T., Chraibi, S., de Casterle, E.D., Guessous, M., Hajoui, M., Lahjmori, A., Alami, A.L., M'jid, M., & Toufiq, A. (2006): 50 ans de développement humain et perpectives 2025. http://www.rdh50.ma (Accessed October 20. 2010).

Bellot, J., Sanchez, J.R., Chirino, E., Hernandez, N., Abdelli, F. & Martinez, J.M. (1999): Effect of Different Vegetation Type Cover on the Soil Water Balance in Semi-Arid Areas of South Eastern Spain. – Phys. Chem. Earth (B), 24, No. 4: 353-357.

Berkowitz, B. (2002): Charakterizing flow and transport in fractured geological media: A review. – Advances in Water Resources, 25: 861-884.

Beven, K. & Binley, A. (1992): The future of distributed models – Model calibration and uncertainty prediction. – Hydrological Processes, 6(3): 279-298.

Beven, K. & Freer, J. (2001): Equifinality, data assimilation, and uncertainty estimation in mechanistic modeling of complex environmental systems using the GLUE methodology. – Journal of hydrology, 249: 11-29.

Beven, K. (2006): A manifesto for the equifinality thesis. – Journal of Hydrology, 320: 18-36.

Beven, K., Smith, P.J. & Freer, J.E. (2008): So just why would a a modeler choose to be incoherent? – Journal of Hydrology, 354: 15-32.

Blöschl, G. & Sivapalan, M. (1995): Scale issues in hydrological modelling: A review. – Hydrological Processes, 9 (3-4): 251-290.

Boonstra, J. & De Ridder, N.A. (1990): Numerical modeling of groundwater basins. 2nd ed. International Institute for Land Reclamation and Improvement, Wageningen.

Born, K., Christoph, M., Fink, A.H., Knippertz, P., Paeth, H. & Speth, P. (2008): Moroccan Climate in the Present and Future: Combined View from Observational Data and Regional Climate Scenarios. In Zereini, F. & Hötzl, H. (eds.): Climatic Changes and Water Resources in the Middle East and in North Africa. Springer-Verlag, Wien.

Bos, M.G. & Nugteren, J. (1990): On irrigation efficiencies. ILRI, Wageningen.

Bouchaou, L., Chauve, P., Mania, J., Mudry, J. & Michelot, J.L. (1995): Apports des tracages artificiel et naturel à la connaissance des circulations et des zones de recharge en region semi-aride: cas de l'Atlas de Beni Mellal (Maroc). – Revue des Sciences de l'eau, 8: 43-55.

Bouchaou, L., Michelot, J.L., Qurtobi, M., Zine, N., Gaye, C.B., Aggarwal, P.K., Marah, H., Zerouali, A., Taleb, H. & Vengosh, A. (2009): Origin and residence time of groundwater in the Tadla basin (Morocco) using multiple isotopic and geochemical tools. – Journal of Hydrology, 379: 323-338.

Bouchaou, L., Michelot, J.L., Vengosh, A., Hsissou, Y., Qurtobi, M., Gaye, C.B., Bullen, T.D. & Zuppi, G.M. (2008): Application of multiple isotopic and geochemical tracers for investigation of recharge, salinization and residence time of water in the Souss-Massa aquifer, southwest of Morocco. – Journal of Hydrology, 325: 267-287.

Bouhlassa, S. & Aiachi, A. (2002): Groundwater dating with radiocarbon: application to an aquifer under semi-arid conditions in the south of Morocco (Guelmime). – Applied Radiation and Isotopes, 56: 637-647.

Bouhlassa, S., Ammary, B. & Elyahyaoui, A. (2007): Environmental tritium measurements and lumped parameter modeling in the Tafilalet aquifer, south-east Morocco. – Radiochim. Acta, 95: 607-616.

Bouidida, A. (1990): Salinité des eaux de la vallee du Drâa - situation actuelle et evolution. Diploma thesis Institut Agronomique et Veterinaire, Université Hassan II, Rabat.

Bouougri, E.H. & Saquaque, A. (2004): Lithostratigraphic framework and correlation of the Neoproterozoic northern West African Craton passice margin sequence (Siroua – Zenaga – Bouazzer Elgraara Inliers, Central Anti-Atlas, Morocco): an integrated approach. – Journal of African Earth Sciences, 39: 227-238.

Boutaleb, S., Bouchaou, L., Mudry, J., Hsissou, Y., Mania, J. & Chauve, P. (2000): Hydrogeologic effects on the quality of water in the Oued Issen watershed, western Upper Atlas Mountains, Morocco. – Hydrogeology Journal, 8: 230-238.

Bower, H. (2002): Artificial recharge of groundwater: hydrogeology and engineering. - Journal of Hydrology, 10:121-142.

Brancic, R. (1968): Sols de la palmeraie Fezouata. Ouarzazate: Organisation de mise en valeur agricole.

Bredehoeft, J. (2004): The conzeptualization model problem – surprise. – Hydrogeology Journal, 13: 37-46.

Breuer, S. (2007): Einfluss der Grundwasserbeschaffenheit auf die Bodenversalzung durch Bewässerung in S-Marokko - Modellierung mit SAHYSMOD. Unpublished Diploma thesis.University of Bonn.

Brodie, R.S. (1999): Integrating GIS and RDBMS technologies during construction of a regional groundwater model. – Environmental Modelling and Software, 14: 119-128.

Bromley, J., Edmunds, W.M., Fellman, E., Brouwer, J., Gaze, S.R., Sudlow, J. & Taupin, J.D. (1997): Estimation of rainfall inputs and direct recharge to the deep unsaturated zone of southern Niger using the chloride profile method. – Journal of Hydrology, 188-189: 139-154.

Burkhard, M., Caritg, S., Helg, U., Robert-Charrue, C. & Soulaimani, A. (2006): Tectonics of the Anti-Atlas of Morocco. – C. R. Geosciences, 338: 11-24.

Busche, H. (in prep.): Modeling hydrological processes in a semi-arid mountainous catchment at the regional scale. – PhD-Thesis. University of Bonn.

Bzioui, M. (2004) : Rapport nationale 2004 sur les ressources en eau au Maroc. - UN Water-Africa.

Cappy, S. (2006): Hydrogeological Charakterization of the Upper Drâa Catchment: Morocco. PhD-Thesis, University of Bonn, 190 pp.

Carillo-Rivera, J.J. (2000): Application of the groundwater-balance equation to indicate interbasin and vertical flow in two semi-arid drainage basins, Mexico. – Hydrogeology Journal, 8: 503-520.

Carrera-Hernández, J.J. & Gaskin, S.J. (2006): The groundwater modeling tool for GRASS (GMTG): Open source groundwater flow modeling. – Computers & Geosciences, 32: 339-351.

Cartig, S., Burkhard, M., Documum, R., Helg, U., Kopp, L. & Sue C. (2004): Fold interference patterns in the Late Paleozoic Anti-Atlas belt of Morocco. – Terra Nova, 16: 27-37.

Cartwright, I., Weaver, T.R., Fulton, S., Nichol, C., Reid, M. & Cheng, X. (2004): Hydrogeochemical and isotopic constraints on the origins of dryland salinity, Murray Basin, Victoria, Australia. – Applied Geochemistry, 19: 1233-1254.

Cavallar, W. (1950): Esquisse Préliminaire de la Carte des Sols du Maroc. 1:1,500,000, Rabat: Direction de l'Agriculture, du Commerce et des Forêts du Maroc. Division de l'Agriculture et de l'Elevage.

Chamayou, J. (1966): Hydrogéologie de la Vallée du Dra Moyen. PhD-Thesis. Rabat

Chamayou, J., Combe, M. & Dupuy, J.C. (1977) : Moyenne Vllee du Dra. In : Devision de la Geologie (ed.) : Ressources en eau du Maroc, Tome 3, Domaines atlasique et sud-atlasique, Notes et Mémoires du Service Géologique 231, Rabat.

Cherkaoui, H.D., Moussadek, R. & Sahbi, H. (2005): Apport des techniques geo-spatiales pour la caractérisation de la qualite des eaux sous-terraines des oasis de la Vallée du Draa-cas de la nappe de Fezouata. WASAMED, Project Publication, Rabat.

Christoph, M., Fink, A.H., Paeth, H., Born, K., Kerschgens, M. & Piecha, K., (2010): Climate Scenarios. - In P. Speth, M. Christoph, & B. Diekkrüger, eds. Impacts of Global Change on the Hydrological Cycle in West and Northwest Africa. Berlin: Springer, pp. 402–425.

Clark, I. & Fritz, P. (1997): Environmental Isotopes in Hydrogeology. New York: Lewis Publishers. 328 pp.

Collins, A.S. & Pisarevsky, S.A. (2005): Amalgamating eastern Gondwana: The evolution of the Circum-Indian Orogens. - Earth Sciences Reviews 71:229-270.

Compagnie Africain de Géophysique (1947) : Prospction electrique au Foum Takkat. Siège Social, Casablanca, 9pp.

Cook, P.G. & Herczeg, A.L. (2000): Einvironmental tracers in subsurface hydrology. CSIRO Land and Water, Glen Osmond, Austraial. Kluwer Academic Publisher, Boston. 529 pp.

Cook, P.G. (2003): A guide to regional groundwater flow in fractured rock aquifers. CSIRO Land and Water, Glen Osmond, Australia.

Coram, J., Bond, W., Dawes, W. & Stauffacher, M. (1999): Overview report: Groundwater and Farming Systems Water Balance Modelling. National Land and Water Resources Audit. CSIRO Land & Water, Canberra Bureau of Rural Sciences, Canberra.

Dahan, O., Tatarsky, B., Enzel, Y., Kulls, C., Seely, M. & Benito, G. (2008): Dynamics of flood-water infiltration and ground-water recharge in hyperarid desert. – Ground Water, 46(3): 450-461.

Darcy, H. (1857): Recherches expérimentales relatives au movement de l'eau dans les tuyaux. Mallet-Bachelier, Paris.

Davies, S.N. & De Wiest, R.J.M. (1976): Hydrogeology. 2nd ed., New York-London-Sidney, 463 pp.

De Roo, A.P.J., Offermans, R.J.E. & Cremers, N.H.D.T. (1996): Lisem: A single-event, physically based hydrological and soil erosion model for drainage basins. II: sensitivity analysis, validation and application. – Hydrological Processes, 10: 1119-1126.

De Roo, A.D.J. (1993): Modelling surface runoff and soil erosion in catchments using geographical information systems, Validity and applicability of the "ANSWERS" model in two catchments in the loess area of South Limburg (the Netherlands) and one in Deven (UK): 304 S.; Netherlands Geographical Studies 157.

De Vries, J.J. & Simmers, I. (2002): Groundwater recharge: an overwiev of processes and challenges. – Hydrogeology Journal 10: 5-17.

De Vries , J.J., Selaolo, E.T. & Beekman, H.E. (2000): Groundwater recharge in the Kalahari, with reference to paleo-hydrologic conditions. – Journal of Hydrology, 238: 110-123.

Delin, G.N., Healy, R.W., Lorenz, D.L. & Nimmo, J.R. (2007): Comparison of local- to regional-scale estimates of groundwater-recharge in Minnesota, USA. – Journal of Hydrology, 334: 231-249.

Destombes, J. (1985): Ordivician. In: Holland CH (ed.): Lower Palaeozoic of north-western and west central Africa. 1st ed., Chichester.

Dillon, P. (2005): Future management of aquifer recharge. – Hydrogeology Journal, 13(1): 313–316.

Dindane, K., Bouchaou, L., Hsissou, Y. & Krimissa, M. (2003): Hydrochemical and isotopic characteristics of groundwater in the Souss Upstream Basin, southwestern Morocco. – Journal of African Earth Sciences, 36: 315-327.

Domenico, P.A. & Schwartz, F.W. (1997): Physical and chemical hydrogeology. 2nd ed. Wiley and Sons, New York, 506 pp.

Dong, W., Yu, Z. & Weber, D. (2003): Simulations on soil water variation in arid regions. – Journal of Hydrology, 275: 162-181.

Doukkali, M.R. (2005): Water institutional reforms in Morocco. – Water Policy, 7(11): 71–88.

Dragoni, W. & Sukhija, B.S. (2008): Climate change and groundwater: a short review. – Geological Society, London, Special Publications, 288: 1-12.

DRE (Devision des Ressources en Eau) (1976): Étude des ressources en eau souterraine de l'Anti-Atlas Central (Région d'Ouarzazate). Programme spécial de recherche d'eau dans les zones déshéritées. Direction de l'Hydraulique, Ministère des Travaux Publics et des Communications. Royaume du Maroc, Rabat.

DRH (Direction de la Région Hydraulique d'Agadir de Souss Massa et Drâa) (2001): Étude d'approvisionnement en eau potable des populations rurales de la province de Zagora, Mission 1 : Analyse de la situation actuelle du service de l'eau et collecte des données de base, Volume 2, Etude des ressources en eau. Direction de la Recherche et de la Planification, Direction Générale de l'Hydraulique, Ministère de l'Equipement, Royaume du Maroc, Rabat.

DRPE (1998): Etude de plan Directeur De l'amenagement des eaux des bassins sud-atlasiques. Rabat: Direction de la recherche et de la planification de l'eau.

Dunkerley, D.L. (2002): Infiltration rates and soil moisture in a groved mulga community near Alice Springs, arid central Australia: evidence for complex internal rainwater redistribution in a runoff-runon landscape. – Journal of Arid Environments, 51: 199-219.

Dunkerley, D.L. (2008): Bank permeability in an Australian ephemeral dry-land stream: variation with stage resulting from mud deposition and sediment clogging. – Earth Surface Processes and Landforms, 33(2): 226–243.

Hötzl, H. & Witthüser, K. (1999): Methoden für die Beschreibung der Grundwasserbeschaffenheit - DVWK Schriften, 125: 113 S.; Wirtschafts- und Verlagsgesellschaft Gas und Wasser mbH, Bonn.

Earman, S., McPherson, B.J.O.L., Phillips, F.M., Ralser, S., Herrin, J.M., & Broska, J. (2008): Tectonic influences on groundwater quality: insight from complementary methods. - Ground Water, 46(3): 354–371.

Edmunds, W.M., Guendouz, A.H., A. Mamou, A., Moulla, A., Shand, P. &
Zouar, K. (2003): Groundwater evolution in the Continental Intercalaire aquifer of southern Algeria and Tunisia: trace element and isotopic indicators. - Applied Geochemistry 18: 805–822

Edmunds, W.M. (2003): Hydrogeochemical processes in semi-arid and arid regions – focus on North Africa. - In Simmers, I. (ed), Understanding water in a Dry Environment – Hydrological processes in arid and semi-arid zones. International Contributions to Hydrogeology. Balkema, Lisse.

El Ouali, A., Mudry, J., Mania, J., Chauve, P., Elyamine, N. & Marzouk, M. (1999): Present recharge of an aquifer in a semi-arid region: an example from the Turonian limestones of the Errachidia basin, Morocco. – Environmental Geology, 38(2): 171-176.

El Yaouti, F., El Mandour, A., Khattach, D., Benavente, J. & Kaufmann, O. (2009): Salinization processes in the unconfined aquifer of Bou-Areg (NE Morocco): A geostatistical, geochemical, and tomographic study. – Applied Geochemistry, 24: 16-31.

Enders, A., Diekkruger, B., Laudien, R., Gaiser, T. & Bareth G. (2010): The IMPETUS Spatial Decision Support Systems. - In P. Speth, M. Christoph, & B. Diekkrüger, eds. Impacts of Global Change on the Hydrological Cycle in West and Northwest Africa. Berlin: Springer, pp.

Ennih, N. & Liégeois, J.P. (2001): The Moroccan Anti-Atlas: the West African craton passive margin with limited Pan-African acitivity. Implications for the northern limit of the craton. – Precambrian Research, 112: 289-302.

Ewen, C. (2004): Geologishe Kartierung im Bereich der IMPETUS-Testsite Argioun (Drâa-Tal, Anti-Atlas, Marokko). Diploma mapping project. University of Bonn.

Fakir, Y., El Mernissi, M., Kreuser, T. & Berjami, B. (2002): Natural tracer approach to characterize groundwater in the coastal Sahel of Oualidia (Morocco). – Environmental Geology, 43: 197-202.

Farber, E., Vengosh, A., Gavrieli, I., Marie, A., Bullen, T.D., Mayer, B., Holtzman, R., Segal, M. & Shavit, U. (2004): The origin and mechanisms of salinization of the Lower Jordan River. – Geochimica et Cosmochimica Acta, 68(9): 1989-2006.

Fekkak, A., Boualoul, M., Badra, L., Amenzou, M., Saquaque, M. & El Amrani, I.E. (2000): Origine et contexte geotectonique des depots detritiques du Groupe Neoproterozoique inferieur de Kelaat Mgouna (Anti Atlas Oriental, Maroc). – Journal of African Earth Sciences, 30(2): 295-311.

Fetter, C.W. (2001): Applied hydrogeology. 4th ed. Prentice Hall Inc., New Jersey, 598 pp.

Finckh, M., & Poete, P. (2008): Vegetation map of the Drâa catchment. In O. Schulz & M. Judex, eds. IMPETUS Atlas Morocco. Research Results 2000–2007. Bonn: Department of Geography, University of Bonn, Germany., pp. 31–32.

Finckh, M. & Staudinger, M. (2002): Mikro- und makroskalige Ansätze zu einer Vegetationsgliederung des Drâa-Einzugsgebietes (Südmarokko). - Ber. d. Reinh.-Tüxen.-Ges. 14:81-92.

Fink, A., Piech, K., Brücher, T. & Knippertz, P. (2008): Precipitation Variability in Northwest Africa. In O. Schulz & M. Judex, eds. IMPETUS Atlas Morocco. – Research Results 2000–2007. Bonn: Department of Geography, University of Bonn, Germany: 11–12.

Fink, A.H. & Knippertz, P. (2003): An extreme precipitation event in southern Morocco in spring 2002 and some hydrological implications. – Weather, 8: 377-392.

Flint, A.L., & K.M. Ellett (2004): The role of the unsaturated zone in artificial recharge at San Gorgonio Pass, California. - Vadose Zone Journal, 3: 763–774.

Flint, A.L., Flint, L.E., Kwicklis, E.M., Fabryka-Martin, J.T. & Bodvarsson, G.S. (2002): Estimating recharge at Yucca Mountain, Nevada, USA: comparison of methods. – Hydrogeology Journal, 10: 180-204.

Folk, R.L. & Land, L.S. (1975): Mg/Ca ratio and salinity: two controls over crystallization of dolomite. Amer. Assoc. Petrol. Geol. Bull., 59: 60–68.

Fontes, J.C. & Edmunds, W.M. (1989): The use of environmental isotope techniques in arid zone hydrology – A critical view. Unesco, Paris.

Fontes, J.C. & Gasse, F. (1991): PALHYDAF (Palaeohydrology in Africa) program: objectives, methods, major results. – Palaeogeography, Palaeoclimatology, Palaeoecology, 84: 191-215.

Foster, S.S.D. & Perry, C.J. (2010): Improving groundwater resource accounting in irrigated areas: a prerequisite for promoting sustainable use. – Hydrogeology Journal, 18: 291-294.

Franke, O.L., Reilly, T.E. & Bennett, G.D. (1987): Techniques of water-resources investigations of the USGS – Chapter B5: Definition of boundary and initial conditions in the analysis of saturated

ground-water flow systems – an introduction. United States Government Printing Office, Washington.

Freeze, A.R. & Cherry, J.A. (eds.) (1979): Groundwater. 5th ed., Upper Saddle River, Prentice Hall.

Fritz, P. (1997): Saline groundwater and brines in crystalline rocks: the contributions of John Andrews and Jean-Charles Fontes to the solution of a hydrogeological and geochemical problem. – Applied Geochemistry, 12: 851-856.

Fritzsche, P. (2010): Development of a satellite-based dynamic regional vegetation model for the Drâa catchment.

Frizon de Lamotte, D., Michard, A. & Saddiqi, O. (2000): Quelques développements récents sur la geodynamics du Maghreb. – C.R. Geoscience, 338: 1-10.

Fryar, A.E. & Mullican, W.F. & Macko, S.A. (2001): Groundwater recharge and chemical evolution in the southern High Plains of Texas, USA. Hydrogeol. J., 9: 522–542.

Furtak, H. & Langguth, H.R. (1967): Zur hydrochemischen Kennzeichnung von Grundwässern und Grundwassertypen mittels Kennzahlen. - Int. Assoc. Hydrogeol. Mem., 7: 89-96. Hannover.

Gaaloul, N. & Cheng, A.H.D. (2003): Hydrogeological and Hydrochemical Investigation of Coastal Aquifers in Tunisia – Crisis in Overexploitation and Salinization. – Second International Conference on Saltwater Intrusion and Coastal Aquifers – Monitoring, Modeling and Management, Merida, Mexico.

Gale, I. (ed.) (2005): Strategies for Managed Aquifer Recharge (MAR) in semi-arid areas. Unesco IHP, Paris.

Gasquet, D., Levresse, G., Cheilletz, A., Azizi-Samir, M.R. & Moutaqi, A. (2005): Contribution to a geodynamic reconstruction of the Anti-Atlas (Morocco) during Pan-African times with the emphasis on inversion tectonics and metollogenic activity at the Precambrian-Cambrian transition. – Precambrian Research, 140: 157-182.

Gasquet, D., Ennih, N., Liegeois, J. P., Soulaimani, A. & Michard, A. 2008. The Pan-African Belt. - In Michard, A., Saddiqi, O., Chalouan, A., Frizon de Lamotte, D. (eds) (2008) Continental Evolution: The geology of Morocco – Structure, Stratigraphy and Tectonics of the African-Atlantic-Mediterranean Triple Junction. Springer, Berlin, 424 pp.

Gaye, C.B. & Edmunds, W.M. (1994): Estimating the spatial variability of groundwater recharge in the Sahel using chloride. - Journal of Hydrology 156(1–4): 47–59.

Gee, G.W. & Hillel, D. (1988): Groundwater recharge in arid regions: Review and critique of estimation methods. – Hydrological Processes, 2(3): 255–266.

Gehrels, H. & Gieske, A.S.M. (2003) Aquifer dynamics. - In Simmers, I. (ed), Understanding water in a Dry Environment – Hydrological processes in arid and semi-arid zones. International Contributions to Hydrogeology. Balkema, Lisse.

Gerrard, J. (1990): Mountain environments. MIT Press, Boston.

Glynn, P.D. & Plummer L.N. (2005): Geochemistry and the understanding of ground-water systems. – Hydrogeology Journal, 13: 263-287.

Goni, I.B., Fellman, E. & Edmunds, W.M. (2001): Rainfall geochemistry in the Sahel region of northern Nigeria. – Atmospheric Environment, 35: 4331-4339.

Goodrich, D.C., Lane, L.J., Shillito, R.M. & Miller, S.N. (1997): Linearity of basin response as a function of scale in a semiarid watershed. – Water Resources Research, 33(12): 2951–2965.

Graf, K. (2009): Drinking Water Supply in the middle Drâa Valley, South Morocco. Options for Action in the Context of Water Scarcity and Institutional Constraints. Diploma-Thesis, University of Bonn.

Gresens, F. (2006): Untersuchungen zum Wasserhaushalt ausgewählter Pflanzenarten im Draa-Tal - Südost Marokko. PhD-Thesis, University of Bonn.

Grossmann, J. & Lange, F. (1999): Eine Sensitivitätsanalyse zur Berechnung der Grundwasserneubildung aus Niederschlag. – Grundwasser, Zeitschrift der Fachsektion Hydrogeologie 1/99: 11-17.

Guendouz, A., Moulla, A.S., Edmunds, W.M., Zouari, K., Shand, P. & Mamou, A. (2003): Hydrogeochemical and isotopic evolution of water in the Complexe Terminal aquifer in the Algerian Sahara. – Hydrogeology Journal, 11: 483-495.

Guendouz, A., Moulla, A.S., Remini, B. & Michelot, J.L. (2006): Hydrochemical and isotopic behavior of a Saharan phreatic aquifer suffering severe natural and anthropic constraints (case of Oued-Souf region, Algeria). – Hydrogeology Journal, 14: 955-968.

Güler, C., Thyne, G.D., McCray, J.E. & Turner, A.K. (2002): Evaluation of graphical and multivariate statistical methods for classification of water chemistry data. – Hydrogeology Journal, 10(4), 455-474.

Haaken, K. (2008): Hydrogeologische Modellierung im südlichen Bereich der Oase Tinzouline (Süd-Marokko). Diploma-Thesis, University of Bonn.

Haitjema, H.M. (1995): On the residence time distribution in idealized groundwater sheds. – Journal of Hydrology, 172: 127-146.

Hamidi, E.M., Nahon, D., McKenzie, J.A., Michard, A., Colin, F. & Kamel, S. (1999): Marine Sr (Ca) inout in Quaternary volcanic rock weathering profiles from the Mediterranean coast of Morocco: Sr isotopic approach. – Terra Nova, 11(4): 157-161.

Hannappel, S., Fritsche, J.G. & Lessmann, B. (2003): Die Erstellung der hydrogeologischen Übersichtskarte (HÜK 200) in Hessen. – Hessischer Umweltmonitor, 4/03: 3-9.

Hatton, T. (1998): Catchment scale recharge modelling. The basics of recharge and discharge (Part 4). CSIRO, Collingwood.

Healy, R. & Cook, P. (2002): Using groundwater levels to estimate recharge. – Hydrogeology Journal, 10(1): 91–109.

Heidecke, C. (2009): Economic analysis of water use and management in the Middle Draa valley in Morocco. PhD-Thesis, University of Bonn.

Heinitz, W. (1984): Die Deformation des sedimentären Deckgebirges im zentralen Anti-Atlas (Südmarokko). – Berliner geowissenschaftliche Abhandlungen: Reihe A, Geologie und Paläontologie, 55.

Helg, U., Burkhard, M., Caritg, S. and Robert-Charrue, C. (2004): Folding and inversion tectonics in the Anti-Atlas of Morocco. – Tectonics, 23(4).

Hem, J.D. (1985): Study and Interpretation of the Chemical Characteristics of Natural Water; 3rd ed. U.S. Geological Survey Water Supply Paper 2254, 264 pp.

Hendrickx, J.M.H., Hong, S., Miller, T.W., Borchers, B. & Tobin, H. (2003): Soil effects on ground penetrating radar detection of buried nonmetallic mines. In Bristow, C.S. & Jol, H.M. (eds.) (2003): Ground Penetrating Radar in Sediments. – SP211, (Geological Society, London): 187-194.

Heppner, C.S. & Nimmo, J.R. (2005): A Computer Program for Predicting Recharge with a Master Recession Curve. – Scientific Investigtions Report, 2005-5172 (U.S. Geological Survey).

Herczeg, A.L. & Edmunds, W.M. (2000): Inorganic ions as tracers. In Cook, P.G. &Herczeg, A.L. (eds.) (2000): Environmental Tracers in Subsurface Hydrology, Kluwer Academic Publishers, Boston: 31-77.

Herczeg, A.L. & Leaney, F.W. (2011): Review: Environmental tracers in arid-zone hydrology. – Hydrogeology Journal, 19: 17-29.

Hibbs, B.J. (2008): Foreword: Ground Water in Arid Zones. – Ground Water, 46 (3): 345-348.

Hill, 1984;

Hogan, J.F., Phillips, F.M., Mills, S.K., Hendrickx, J.M.H., Ruiz, J., Chesley, J.T. & Asmerom, Y. (2007): Geologic origins of salinization in a semi-arid river: The role of sedimentary basin brines. – The Geological Society of America, 35(12): 1063-1066.

Hsissou, Y., Chauve, P. & Mania, J. (1996a): The aquifer of Turonian limestones (Tadla Basin, Morocco). Local and remote groundwater recharge from the Atlas. – Journal of Hydrology, 183: 433-443.

Hsissou, Y., Chauve, P., Mania, J., Mangin, A., Bakalowicz, M. & Gaiz, A. (1996b): Characterization of the groundwaters of the Turonian catchment of Tadla (Morocco) by the concentration ratios of Sr2+/Ca2+. Journal of Hydrology, 183: 445-451.

Huebner H, Schmidt M, Sogalla M & Kerschgens M (2004): Simulating evapotranspiration in a semi-arid environment. – Theoretical and Applied Climatology (published online first).

Hughes, D.A. & Sami, K. (1992): Transmission losses to alluvium and associated moisture dynamics in a semiarid ephemeral channel system in southern africa. – Hydrological Processes, 6: 45-53.

Hulme, M. (1992): Rainfall changes in Africa: 1931-1960 to 1961-1990. – International Journal of Climatology, 12: 685-699.

Hutchison, W.R. & Hibbs, B.J. (2008): Ground Water Budget Analysis and Cross-Formational Leakage in an Arid Basin. – Ground Water, 46 (3): 384-395.

IAEA (2001): Isotope techniques in water resource investigations in arid and semi-arid regions. – IAEA-TECDOC-1207.

IAEA (1996): Manual on mathematical models in isotope hydrogeology. – IAEA-TECDOC-910.

IMPETUS (2006): Second Final Report –1.5.2003 – 31.7.2007. University of Cologne and Bonn.
http://www.impetus.uni-koeln.de/content/download/EB2006/FinalReport2003_2006.pdf.

Ismat, Z. (2008): Folding kinematics expressed in fracture patterns: An example from the Anti-Atlas fold belt, Morocco. – Journal of Structural Geology, 30: 1396-1404.

Issar, A.S. & Resnick, S.D. (1996): Runoff, Infiltration and Subsurface Flow of Water in Arid and Semi-Arid Regions. Springer.

Jackson, T.J. (2002): Remote sensing of soil moisture: implications for groundwater recharge. – Hydrogeology Journal, 10: 40-51.

Ji, X., Kang, E., Chen, R., Zhao, W., Zhang, Z. & Jin, B. (2006): A mathematical model for simulating water balances in cropped sandy soil with conventional flood irrigation applied. – Agricultural Water Management, 87: 337-346.

Johnson, A.I. (1967): Specific yield – Compilation of specific yields for various materials: 74 S.; U.S. Geological Survey Water-Supply Paper 1662-D.

Jouzel, J., Hoffmann, G., Koster, R.D. & Masson, V. (2000): Water isotopes in precipitation: data/model comparison for present-day and past climates. – Quaternary Science Reviews, 19: 363-379.

Kamel, S., Younes, H., Chkir, N. & Kamel, Z. (2008): The hydro geochemical characterization of ground waters in Tunisian Chott's region. – Environ Geol, 54: 843-854.

Kattan, Z. (2008): Estimation of evaporation and irrigation return flow in arid zones using stable isotope ratios and chloride mass-balance analysis: Case of the Euphrates River, Syria. – Journal of Arid Environments, 72: 730-747.

Keefer, T.O., Moran, M.S. & Paige, G.B. (2008): Long-term meteorological and soil hydrology database, Walnut Gulch Experimental Watershed, Arizona, United States. – Water Resources Research, 44.

Kellgren N. (2002): Applicability of remote sensing techniques to groundwater exploration in semi-arid Hard Rock Terrain – a systematic approach, PhD Thesis, Chalmers University of Technology, Sweden.

Kendall, C. & Caldwell, E.A. (1998): Fundaments of isotope geochemistry. In Kendall, C. & McDonnell (eds.) (1998): Isotope tracers in catchment hydrology. Elsevier, Amsterdam.

Kendall, C. & McDonnel, J.J. (1998): Isotope tracers in catchment hydrology. Elsevier, Amsterdam.

Khayat, S., Hötzl, H., Geyer, S. & Ali, W. (2006): Hydrochemical investigation of water from the Pleistocene wells and springs, Jericho area, Palestine. – Hydrogeology Journal, 14: 192-202.

Kinzelbach, W. & Rausch, R. (1995): Grundwassermodellierung – Eine Einführung mit Übungen: 283 S.; Gebrüder Borntraeger Berlin, Stuttgart.

Kirchner, J.W. (2006): Getting the right answers for the right reasons: Linking measurements, analyses, and models to advance the science of hydrology. – Water Resources Research, 42.

Klemes, V. (1985): Sensivity of water resources systems to climate cariations, WCP Rep. 98, World Meteorological Organisation, Geneva.

Klemes, V. (1986): Operational testing of hydrological simulation models, Hydrol. Sci. J., 31(1): 13-24.

Klingbeil, R., Kleineidam, S., Asprion, U., Aigner, T. & Teutsch, G. (1999): Relating lithofacies to hydrofacies: ourcrop-based hydrgeological characterisation of Quarternary gravel deposits. – Sedimentary Geology, 129: 299-310.

Klingbeil, R. (1998): Outcrop Analogue Studies – Implications for Groundwater Flow and Contaminant Transport in Heterogeneous Glaciofluvial Quarternary Deposits. – Tübinger Geowissenschaftliche Arbeiten, Reihe C (43).

Klose, A. (2008a): Soil salinity – a case study from Ouled Yaoub. - In O. Schulz & M. Judex, eds. IMPETUS Atlas Morocco. Research Results 2000–2007. Bonn: Department of Geography, University of Bonn, Germany., pp. 31–32.

Klose, A. (2009): Soil characteristics and soil erosion by water in a semi-arid catchment (Wadi Drâa, South Morocco) under the pressure of global change. PhD-Thesis, University of Bonn.

Knighton, A.D. & Nanson, G.C. (1994): Flow transmission along an arid zone anastomosing river, Cooper Creek, Australia. – Hydrological Processes, 8: 137-154.

Knippertz, P., Christoph, M. & Speth, P. (2003): Long-term precipitation variability in Morocco and the link to the large-scale circulation in recent and future climates. – Meteorology and Atmosphere Physics, 83: 67–88.

Knippertz, P. (2003): Tropical-Extratropical Interactions Causing Precipitation in Northwest Africa: Statistical Analysis and Seasonal Variations. - Notes and Correspondence, Monthly Weather Review, 131: 3069-3076.

Knippertz, 2003b

Konikow, L.F. & Bredehoeft, J.D. (1992): Ground-water models cannot be validated. – Advances in Water Resources, 15: 75-83.

Köppen, W. (1963): Das geographische System der Klimate. In: Handbuch der Klimatologie, 1 (Part C), Gebr. Bornträger Verlag, Berlin.

Kovalevsky, V.S., Kruseman, G.P. & Rushton, K.R. (2004): Groundwater studies: an international guide for hydrogeological investigations. Unesco IHP, Paris.

Koziorovsky, G. (1985): Ermittlung der Transmissivität eines Lockergesteinsaquifers durch Kurzzeitpumpversuche in Grundwassermeßstellen. - Abh geol Landesamt Baden-Würtemberg, 11:45-75, Freiburg. i.B.

Krause, P., Boyle, D.P. & Bäse, F. (2005): Comparison of different efficiency criteria for hydrlogical model assessment. – Advances in Geoscienes, 5: 89-97.

Kresic, N. (2007): Hydrogeology and Groundwater Modeling, Second Edition. CRC Press/Taylor & Francis, Boca Raton, New York, London.

Krimissa, S., Michelot, J., Bouchaou, L., Mudry, J. & Hsissou, Y. (2004): Sur l'origine par alteration du substratum schisteux de la mineralization chlorurée des eaux d'une nappe côtière sous climat semi-aride (Chtouka-Massa, Maroc). – C.R. Geoscience, 336: 1363-1369.

Krusemann, G.P. & de Ridder, N.A. (2000): Analysis and Evaluation of Pumping Test Data. 2nd ed, International Institute for Land Reclamation and Improvement/lLRI, Printed by Veenman drukkers, Ede.

Külls, C. (2000): Groundwater of the North-Western Kalahari, Namibia – Estimation of Recharge and Quantification of the Flow Systems. – PhD Thesis, Julius-Maximilian University of Würzburg.

Kunert, A. (2008): Hydrogeologische Untersuchungen in der Palmoase Fezouata, Südmarokko. – Diploma-Thesis, Rheinische Friedrich-Wilhelms-Universität Bonn.

Kunkel, R., Wendland, F., Voigt, H.-J. & Hannappel, S. (2004): Die natürliche, ubiquitär überprägte Grundwasserbeschaffenheit in Deutschland. – Schriften des Forschungszentrum Jülich, Reihe Umwelt/Environment, 47.

Kutsch, U. (2008): Modellierung des Wasserhaushaltes in einem semi-ariden Einzugsgebiet im Süden Marokkos. Unpublished Diploma Thesis. University of Bonn.

Lange, J. & Leibundgut, Ch.: Surface runoff and sediment dynamics in arid and semi-arid regions. In Balkema, A.A. (2003): Understanding Water in a Dry Environment: Hydrological Processes in Arid and Semi-Arid Zones. pp. 115-150.

Lange, J. (2005): Dynamics of transmission losses in a large arid stream channel. – Journal of Hydrology, 306(1-4): 112–126.

Laudien, R. (2008): Verwendung von ArcGIS Engine zur räumlichen Entscheidungsunterstützung. – ArcAktuell, 1.

Le Bissonnais, Y., Cerdan, O., Lecomte, V., Benkhadra, H., Souchere, V. & Martin, P. (2005): Variability of soil surface characteristics influencing runoff and interrill erosion. - Catena 62(2-3): 111-124.

Le Houérou, H.N. (2001): Biogeography of the arid steppeland north of the Sahara. - Journal of Arid Environments Volume 48, Issue 2: 103–128

Leaney, F.W. & Herczeg, A.L. (1999): The origin of fresh ground water in the southwest Murray Basin and its potential for salinization. – CSIRO Land and Water Technical Rep., 7/99.

Leduc, C., Bromley, J. & Schroeter, P. (1997): Water table fluctuation and recharge in semi-arid climate: some results of the HAPEX-Sahel hydrodynamic survey (Niger). – Journal of Hydrology, 188-189: 123-138.

Lerner, D.N., Issar, A.S. & Simmers, I. (1990): Groundwater recharge: a guide to understanding and estimating natural recharge. Heise, Hannover.

Lerner, D.N. (2002): Identifying and quantifying urban recharge: a review. – Hydrogeology Journal, 10: 143-152.

Lewis, M.F. & Walker, G.R. (2002): Assessing the potential for significant and episodic recharge in southwestern Australia using rainfall data. – Hydrogeology Journal, 10: 229-237.

Lloyd, J.W. (1986): A Review of Aridity and Groundwater. – Hydrological Processes, 1:63-78.

Loucks, D.P. (1995): Developing and implementing decision support systems: A critique and a challenge. – Water Resources Bulletin, American Water Resources Association, 32(4): 571-582.

Maidment, D.R. (ed) (1993): Handbook of Hydrology. McGraw-Hill, Inc., New York.

Maley, J. (1997): Palaeoclimates of Central Sahara during the early Holocene. – Nature, 269: 573-577.

Mandle, R. J. (2002): Groundwater Modeling Guidance: 54 S.; Groundwater Modeling Program, Department of Environmental Quality, Michigan.

Marechal, J.C., Dewandel, B., Ahmed, S., Galeazzi, L. & Zaidi, F.K. (2006): Combined estimation of specific yield and natural recharge in a semi-arid groundwater basin with irrigated agriculture. – Journal of Hydrology, 329: 281-293.

Margane, A. (2003a): Management, protection and sustainable use of groundwater and soil resources in the Arab region: guideline for groundwater vulnerability mapping and risk assessment for the sustainability of groundwater resources to contamination. Vol. 4 — Arab Centre for the Study of the Arid Zones and Dry Lands (ACSAD) and Federal Institute for Geosciences and Natural Resources (BGR), Damascus.

Margane, A. (2003b): Management, protection and sustainable use of groundwater and soil resources in the Arab region: guideline for sustainable groundwater resources management. Vol. 6 — Arab Centre for the Study of the Arid Zones and Dry Lands (ACSAD) and Federal Institute for Geosciences and Natural Resources (BGR), Damascus.

Margane, A. (2004): Management, protection and sustainable use of groundwater and soil resources in the Arab region: guideline for groundwater monitoring. Vol.7 — Arab Centre for the Study of the Arid Zones and Dry Lands (ACSAD) and Federal Institute for Geosciences and Natural Resources (BGR), Damascus.

Margat, J. (1958) : Le probleme de l'eau et les etudes hydrgéologique a entreprendre dans la Vallee du Drâa. 21pp.

de Marsily, G. (2003): Importance of the maintenance of temporary ponds in arid climates for the recharge of groundwater. – C.R. Geoscience, 335: 933-934.

Martin, S. (2006): Influence du tourisme sur la gestion de l'eau en zone aride - Exemple de la vallée du Drâa (Maroc). PhD-Thesis, Université de Lausanne.

Masuch - Oesterreich, D., Schuster, S. & Villalobos, R. S. (2000): The Groundwater Data Base Hydrogis Linares. – Linares, Universidad Autónoma de Nuevo Leon, Facultad de Ciencias de la Tierra

Matter, J.M., Waber, H.N., Loew, S. & Matter, A. (2005): Recharge areas and geochemical evolution of groundwater in an alluvial aquifer system in the Sultanate of Oman. – Hydrogeology Journal, 14: 203-224.

Matthess, G. & Ubell, K.: 1. Allgemeine Hydrogeologie – Grundwasserhaushalt. Gebrüder Borntraeger, Berlin.

Matthes, G. (1990): Die Beschaffenheit des Grundwassers – Lehrbuch der Hydrogeologie, Band 2. 2nd ed. Bornträger, Berlin Stuttgart.

Merkel, B. & Planer-Friedrich, B. (2008): Grundwasserchemie – Praxisorientierter Leitfaden zur numerischen Modellierung von Beschaffenheit, Kontamination und Sanierung aquatischer Systeme. Springer, Berlin.

Meyboom, P.(1967): Mass-transfer studies to determine the groundwater regime of permanent lakes in Hummocky Moraine of Western Canada. – Journal of Hydrology, 5: 117-142.

Michard, A., Saddiqi, O., Chalouan, A. & Lamotte, D.F. (eds.) (2008): Continental Evolution: The Geology of Morocco: 424 S.; Springer-Verlag, Berlin.

Michard, A. (1976): Eléments de géologie marocaine. – Notes et Mémoires du Service Géologique du Maroc, 252.

Middleton, N. & Thomas, D. (eds.) (1997): World atlas of desertification. 2nd ed., Routledge, London.

Middleton, N.J. & Thomas, D.S.G. (1992): World Atlas of Desertification. Hodder Arnold, London.

Ministère des travaux publics (1998): Etude du plan directeur de l'aménagement des eaux des bassins sud-atlasiques, Mission 3: Etude des schémas d'aménagement, Volume 4: Unités du Draa, Rabat. 54 pp.

Misstear, B.D.R. (2000): Groundwater recharge assessment: A key component of river basin management. – National Hydrology Seminar.

Moench, A.F. (2008): Analytical and numerical analyses of an unconfined aquifer test considering unsaturated zone characteristics. – Water Resources Research, 44: 1-17.

Mook, W.G. (2000): Environmental isotopes in the hydrological cycle – principles and applications: Groundwater – Saturated and unsaturated zone. IHP-V Technical Documents in Hydrology 1 No. 39, Vol. IV UNESCO, Paris.

Morin, E., Grodek, T., Dahan, O., Benito, G., Kulls, C., Jacoby, Y., Langenhove, G.V., Seely, M. & Enzel, Y. (2009): Flood routing and alluvial aquifer recharge along the ephemeral arid Kuiseb River, Namibia.

Müller-Hohenstein, K. & H. Popp (1990): Marokko. Ein islamisches Entwicklungsland mit
kolonialer Vergangenheit. Stuttgart.

Nativ, R., Adar, E., Dahan, O. & Nissim, I. (1997): Water salinization in arid regions – observations from the Negev desert, Israel. – Journal of Hydrology, 196: 271-296.

Neumann, S.P. (1987): On Methods of Determining Specific Yield. – Ground Water, 25(6): 679-684.

Neumann, S. (2005): Trends, prospects and challenges in quantifying flowand transport through fractured rocks. - Hydrogeology Journal, 13: 124-147.

Nilsson, B., Hojberg, A.L., Refsgaard, J.C. & Troldborg, L. (2007): Uncertainty in geological and hydrogeological data. – Hydrol. Earth Syst. Sci., 11: 1551-1561.

Noetinger, B., Artus, V. & Zargar, G. (2005): The future of stochastic and upscaling methods in hydrogeology. – Hydrogeology Journal, 13: 184-201.

Nwankwor, G.I., Cherry, J.A. & Gillham, R.W. (1984): A Comparative Study of Specific Yield Determinations for a Shallow Sand Aquifer. – Ground Water, 22(6): 764-772.

ORMVAO (1995): Étude d'amélioration de l'exploitation des systèmes d'irrigation et de drainage del' ORMVAO: Phase 1 Diagnostique de la situation actuelle, Ouarzazate: Organistaion de mise en valeur agricole.

Gresens, F., 2006. Untersuchungen zum Wasserhaushalt ausgewählter Pflanzenarten im Draa-Tal - Südost Marokko, PhD thesis, University of Bonn.

ORMVAO (1981): Etablissement d'un plan directeur de mise en valeur agricole de la vallée du Drâa moyen. Ouarzazate.

Osterkamp, W.R., Lane, L.J. & Menges, C.M. (1995): Techniques of ground-water recharge estimates in arid/semi-arid areas, with examples from Abu Dhabi. – Journal of Arid Environments, 31: 349-369.

Oubalkace, M. (2007): Stratégie méditerranéenne pour le développement durable. Suivi des progrès dans le domaine de l'eau et promotion de politiques de gestion de la demande. Rapport final. Commission méditerranéenne du développement durable. Marco.

Ouhajou, L. (1996): Espace Hydraulique et Société au Maroc : Cas des Systèmes d'irrigation dans la vallée du Drâa. Thèse et Mémoire. Faculté des Lettres et des Sciences Humaines, Université Ibn Zohr. Agadir. Morocco.

Paeth, H., Born, K., Girmes, R., Podzun, R. & Jacob, D., (2009) : Regional Climate Change in Tropical and Northern Africa due to Greenhouse Forcing and Land Use Changes. Journal of Climate, 22(1) : 114–132.

Parissopoulos, G.A. & Wheater, H.S. (1992): Experimental and numerical infiltration studies in a wadi stream bed. – Hydrological Sciences -Journal- des Sciences Hydrologiques,37,1: 27-37.

Park, E. & Parker, J.C. (2008): A simple model for water table fluctuations in response to precipitation. – Journal of Hydrology, 356: 344-349.

Peck, A., Gorelick, S., Marsily, G.d., Foster, S., and Kovalevsky, V. (1988): Consequences of spatial variability in aquifer properties and data limitations for groundwater modelling practice: Wallingford, IAHS Press, 272 pp.

Petschick, R. (2000). MacDiff v4.x - Bedienungsanleitung. Johann Wolfgang Goethe-
Universität Frankfurt am Main.

Piper, A.M. (1944): A graphic procedure in the geochemical interpretation of water analyses. – American Geophysical Union Trans., 25: 914-923.

Piqué, A. (2001): Geology of Northwest Africa. – Beiträge zur regionalen Geologie der Erde 29: 310 S.; Gebrüder Borntraeger, Stuttgart.

Platt, S. (2008a): Current Development of the Population in the Provinces of Ouarzazate and Zagora.In O. Schulz & M. Judex, eds. IMPETUS Atlas Morocco. – Research Results 2000–2007, Department of Geography, University of Bonn: 33–36.

Platt, S. (2008b): Development of the Urbanized Regions in the Provinces of Ouarzazate and Zagora until 2020.In O. Schulz & M. Judex, eds. IMPETUS Atlas Morocco. – Research Results 2000–2007, Department of Geography, University of Bonn: 61–62.

Poesen, J. & Lavee, H. (1994): Rock fragments in top soils: significance and processes. – Catena, 23(1-2): 1–28.

Poeter, E.P. & Hill, M.C. (1997): Inverse Models: A Necessary Next Step in Ground-Water Modeling. – Ground Water, 35(2): 250-260.

Rademacher, C. (2010): Gehen, damit andere bleiben können? Migration, Geschlecht und sozio-ökonomischer Wandel in einem südmarokkanischen Oasendorf. PhD-Thesis, University of Cologne.

Raju, N.J., Reddy, T.V.K. & Munirathnam, P. (2006): Subsurface dams to harvest rainwater – a case study of the Swarnamukhi River basin, Southern India. – Hydrogeology Journal, 14: 526-631.

Refsgaard, J.C. & Knudsen, J. (1996): Operational validation and intercomparison of different types of hydrological models. – Water Resources Research, 32(7): 2189-2202.

Refsgaard, J.C. & Storm, B. (1996): Construction, Calibration and Validation of Hydrological Models. In: ABBOTT, M. B. & REFSGAARD, J. C. (Hrsg.): Distributed Hydrological Modelling: 321 S.; Kluwer, Dordrecht: 41-54.

Refsgaard, J.C. (1997): Parameterisation, calibration and validation of distributed hydrological models. – Journal of Hydrology, 198: 69-97.

Reichert, B., & Jaeger, A.K. (2010): Socio-economic scenarios. - In P. Speth, M. Christoph, & B. Diekkrüger, eds. Impacts of Global Change on the Hydrological Cycle in West and Northwest Africa. Berlin: Springer, pp. 426–441.

Reilly, T.E. (2001): System and Boundary Conceptualization in Ground-Water Flow Simulation: 29 S.; US Geological Survey, Virginia.

Renard, P. (2007): Stochastic Hydrogeology: What Professionals Really Need? – Ground Water, 45(5): 531-541.

Risbey, J.S. & Kandlikar, M. (2007): Expressions of likelihood and confidence in the IPCC-uncertainty assessment process. – Climatic Change, 85(1): 19-31.

Riser J (1988) Le Jbel Sarhro et sa retombée saharienne (Sud-Est Marocain) – Étude Géomorphologique. Notes et Memoires du service Géologique No. 317. Direction de la Géologie. Ministère de l'Énergie et des Mines, Royaume du Maroc. Rabat.

Robert-Charrue, C. & Burkhard, M. (2005): The Anti Atlas fold belt of Morocco: Variscan inversion tectonics and interference pattern of an "intracratonic" basin. – Proceedings of the 3rd Swiss Geoscience Meeting, 59-60, Zürich.

Rödiger, T., Sauter, M. & Büchel, G. (2009): Infiltration und Grundwasserströmung in geklüftet-porösen Buntsandsteingrundwasserleitern im Osten des Thüringer beckens. – Grundwasser, Zeitschrift der Fachsektion Hydrogeologie, 14: 21-32.

Roeckner, E., Arpe, K., Bengtsson, L., Christoph, M., Dümenil, L., Esch, M., Giorgetta, M., Schulzweida, U., Claussen, M. & Schlese, U. (1996): The atmospheric general circulation model ECHAM-4: Model description and simulation of present-day climate, Max Planck Institut, Hamburg.

Roth, A., (2009): Impact of climate change and stocking rates on pasture systems in SE Morocco–An Application of the SAVANNA Ecosystem Model. PhD-Thesis. University of Bonn.

Rozos, E., Efstratiadis, A., Nalbantis, I & Koutsoyiannis, D. (2004): Calibration of a semi-distributed model for conjunctive simulation of surface and groundwater flows. – Hydrological Sciences Journal, 49(5): 819-842.

Rueedi, J., Prtschert, R., Beyerle, U., Alberich, C. & Kipfer, R. (2005): Estimating groundwater mixing ratios and their uncertainties using a statistical multi parameter approach. – Journal of Hydrology, 305: 1-14.

Rushton, K.R. & Howard, K.W.F. (1983): The Unreliability of Open Observation Boreholes in Unconfined Aquifer Pumping Tests. – Ground Water, 20(5): 549-550.

Ruud, N., Harter, T. & Naugle, A. (2004): Estimation of groundwater pumping as closure to the water balance of a semi-arid, irrigated agricultural basin. – Journal of Hydrology, 297: 51-73.

Klose, S., Busche, H., Klose, A., Schulz, O., Diekkrüger, B., Reichert, B. & Winiger, M. (2010b): Impacts of Global Change on water resources and soil salinity in Southern Morocco. In P. Speth, M. Christoph, & B. Diekkrüger, eds. Impacts of Global Change on the Hydrological Cycle in West and Northwest Africa. Springer, Berlin, pp. 592–611.

Safriel, U.; Adeel, Z.; Niemeijer, D.; Puigdefabregas, J.; White, R.; Lal, R.; Winslow, M.; Ziedler, J.; Prince, S.; Archer, E.; King, C. (2005): Dryland systems. In Hassan, R., Scholes, R., Ash, N., eds., Ecosystems and human well-being: current state and trends. Washington Island Press, Washington.

Saltelli, A. (2002): Making best use of model evaluations to compute sensitivity indices. – Computer Physics Communications, 145: 280-297.

Sami, K. & Hughes, D.A. (1996): A comparison of recharge estimates to fractured sedimentary aquifer in South Africa from a chloride mass balance and an integrated surface-subsurface model. – Journal of Hydrology, 179: 111-136.

Sander, P. (2007): Lineaments in groundwater exploration: a review of applications and limitations. – Hydrogeology Journal, 15: 71-74.

Sanford, W. (2002): Recharge and groundwater models: an overview. – Hydrogeology Journal, 10: 110-120.

Sanford, W. & Pope, J.P. (2010): Current challenges using modelst o forecast seawater intrusion: lessons from the Eastern Shore of Virginia, USA. – Hydrogeology Journal, 18: 73-93.

Sanz, D., Gómez-Aldy, J.J., Castano, S., Moratalla, A., De las Heras, J. & Martinez-Alfaro, P.E. (2009): Hydrostratigraphic framework and hydrogeological behavior of the Mancha Oriental System (SE Spain). – Hydrogeology Journal, 17: 1375-1391.

Scanlon, B.R. (2000): Uncertainties in estimating water fluxes and residence times using environmental tracers in an arid unsaturated zone. – Water Resources Research, 36(2): 395-409.

Scanlon, B.R., Tyler, S.W. & Wierenga, P.J. (1997): Hydrologic issues in arid, unsaturated systems and implications for contaminant transport. – Reviews of Geophysics, 35(4): 461-490.

Scanlon, B.R., Healy, R.W. & Cook, P.G. (2002): Choosing appropriate techniques for quantifying groundwater recharge. – Hydrogeology Journal, 10: 18-39.

Scanlon, B.R., Mace, R.E., Barrett, M.E. & Smith, B. (2003): Can we simulate regional groundwater flow in a karst system using equivalent porous media models? Case study, Barton Springs Edwards aquifer, USA. – Journal of Hydrology, 276: 137-158.

Scanlon, B., Keese, K., Flint, A., Flint, L., Gaye, C., Edmunds, W. & Simmers, I. (2006): Global synthesis of groundwater recharge in semiarid and arid regions. – Hydrological Processes, 20(15): 3335–3370.

Scanlon, B.R., Jolly, I., Sophocleous, M. & Zhang, L. (2007): Global impacts of conversions from natural to agricultural ecosystems on water resources: Quantity versus quality. – Water Resources Research, 43: 1-18.

Schoeller; H. (1955) : Geochemie des eaux souterraines; Revue de l'Institute Français du petrole, 10:230-44.

Schulz, O., Busche, H. & Benbouziane, A. (2008): Decadal Precipitation Variances and Reservoir Inflow in the Semi-Arid Upper Drâa basin (South-Eastern Morocco).In F. Zereini & H. Hoetzl, eds. Climatic Changes and Water Resources in the Middle East and in North Africa. Springer, Wien: 165–178.

Schulz, O. (2006): Analyse schneehydrologischer Prozesse und Schneekartierung im Einzugsgebiet des Oued M'Goun, Zentraler Hoher Atlas (Marokko). PhD.-Thesis, University of Bonn.

Schulz, O. (2008): The IMPETUS climate monitoring network. - In O. Schulz & M. Judex, eds. IMPETUS Atlas Morocco. – Research Results 2000–2007, Department of Geography, University of Bonn: 17–18.

Schwarze, R., Herrmann, A. & Mendel, O. (1994): Regionalization of runoff components for Central European basins. – IAHS Publications, 221: 493-502.

Schwarze, R. (1999): Skalenwechsel über Parameter: Grundwasser. In H. Kleeberg, W. Mauser, G. Peschke, & U. Streit, eds., Hydrologie und Regionalisierung. DFG Research Report, Wiley,. Weinheim.p. 477

Sebrier, M., Siame, L., Zouine, E.M., Winter, T., Missenard, Y. & Leturmy, P. (2006): Active tectonics in the Moroccon High Atlas. – C. R. Geoscience, 338: 65-79.

Secréterait d'état charge de l'eau (2003) : Etat de la qualité des ressources en eau au Maroc – Année 2000-2001. Secréterait d'etat charge de l'eau, Royaume du Maroc. Rabat.

Seyfried, M.S., Schwinning, S., Walvoord, M.A., Pockmann, W.T., Newman, B.D., Jackson, R.B. & Phillips, F.M. (2005): Ecohydrological control of deep drainage in arid and semiarid regions. – Ecology, 86: 277-287.

Sharma, M.L. (1986): Measurement and prediction of natural groundwater recharge – An overview. – Journal of Hydrology, 25(1): 49-56.

Sharon, D. (1972): The spottiness of rainfall in a desert area. – Journal of Hydrology, 17: 161-175.

Sharp, A.L. & Saxton, K.E. (1962): Transmission Losses in Natural Stream Valleys.In: Cataldo, J., Behr, C., Montalto, F. & Pierce, R.J. (2004): A Summary of Published Reports of Transmission Losses in Ephemeral Streams in the U.S.. Report to the National Center for Housing and the Environment, Wetland Science Applications , Poolesville, 42 pp.

Shentsis, I., Meirovich, L., Ben-Zvi, A. & Rosenthal, E. (1999): Assessment of transmission losses and groundwater recharge from runoff events in a wadi under shortageof data on lateral inflow, Negev, Israel. – Hydrological Processes, 13: 1649-1663.

Sigg, L. & Stumm, W. (1996): Aquatische Chemie. 4th ed., Vdf Hochschulverlag, Zürich, 498 pp.

Simmers, I. (2003): Understanding Water in a Dry Environment – Hydrological Processes in Arid and Semi-arid Zones. 1st ed., A.A. Balkema Publishers, Lisse (Netherlands).

Simmers, .I, Hendrickx, J.M.H., Kruseman G.P. & Rushton, K.R. (eds.) (1997): Recharge of phreatic aquifers in (semi-)arid areas. – IAH International Contributions to Hydrogeology, 19, Balkema, Rotterdam, 277 pp.

Simmers, I. (1984): A systematic problem-oriented approach to hydrological data regionalization. – Journal of Hydrology, 73: 71-87.

Soletanche (1980): Forages de Reconnaissance .Palmeraie du Fezouata, Vallée du Draa. - Report, Office National des Irrigations Rabat.

Solomon, S., Qin, D., Manning, M., Alley, R.B., Berntsen, T., Bindoff, N.L., Chen, Z., Chithaisong, A., Gregory, J.M. & Hegerl, G.C. (2007): Climate change 2007: the physical science basis. Intergovernmental Panel on Climate Change, Cambridge.

Soltan, M.E. (1998): Characterisation, classification and evaluation of some groundwater samples in upper Egypt. – Chemosphere, 37(4): 735-745.

Sophocleous, M., & Perkins, S.P. (2000): Methodology and application of combined watershed and ground-water models in Kansas. – Journal of Hydrology, 236(3–4): 185-201.

Sophocleous, M. (1991): Combining the soilwater balance and water-level fluctuation methods to estimate natural groundwater recharge: Practical aspects. – Journal of Hydrology, 124: 229-241.

Sophocleous, M. (2002): Interactions between groundwater and surface water: the state of the science. – Hydrogeology Journal, 10(1): 52–67.

Sorman, A.U. & Abdulrazzak, M. J. (1995): Estimation of actual evaporation using precipitation and soil moisture records in arid climates. – Hydrological Processes, 9(7): 729–741.

USGS (2004): Shuttle Radar Topography Mission, Global Land Cover Facility, University of Maryland, College Park, Maryland, February 2000.

Stanners, D., & Bordeaux, P. (eds.) (1995): Europe's Environment; The Dobris Assessment. 1st ed., European Environment Agency, Copenhagen, 676 pp.

Steenbergen, F. van & Tuinhof, A. (2009): Managing the Water Buffer for Development and Climate Change Adaptation. – Groundwater Recharge, Retention, Reuse and Rainwater Storage.-

Steenpaß, C. (2007): Geologische Geländeaufnahme im ordovizischen Anti-Atlas bei Zagora, Süd-Marokko. Diploma Mapping Project, University of Bonn.

Stigter, T.Y., Carvalho Dill, A.M.M., Ribeiro, L. & Reis, E. (2006): Impact of the shift from groundwater to surface water irrigation on aquifer dynamics and hydrochemistry in a semi-arid region in the south of Portugal. – Agricultural water management, 85: 121-132.

Strosnider, W.H.J., Llanos López, F.S. & Nairn, R.W. (2010): Acid mine drainage at Cerro Rico de Potosí I: unabated high-strength discharges reflect a five century legacy of mining. – Environmental Earth, 64(4): 899-910.

Struckmeier, W. (2005): Hydrogeologische Karten von Deutschland, Europa und der Welt - ein deutscher Beitrag zum IHP der UNESCO. IHP/HWRP-Sekretariat, Bundesanstalt für Gewässerkunde. Koblenz.

Stuhldreher, G. (2008):Phytoindikation von Versalzungsprozessen in der Drâa-Oase, Südmarokko. Diploma-Thesis, University of Münster.

Stumpf, R. (2007): Hydrochemische Untersuchungen und Beschreibung der Grundwasserevolution in der Oase Fezouata, mittleres Drâa-Tal, S-Marokko. Diploma-Thesis, University of Bonn.

Sultan, M., Sturchio, N.,Hassan, F.A.,Hamdan, M.A.R., Mahmood, A.M.,Alfy, Z.E. &Stein, T. (1997): Precipitation Source Inferred from Stable Isotopic Composition of Pleistocene Groundwater and Carbonate Deposits in the Western Desert of Egypt. – Quartenary Research, 48 (1): 29-37.

Sumioka, S.S. & Bauer, H.H. (2004): Estimating Ground-Water Recharge from Precipitation on Whidbey and Camano Islands, Island County, Washington, Water Years 1998 and 1999. USGS, Water-Resources Investigations Report 03-4101, Tacoma.

Szaboa, B.J., Haynes Jr., C.V. & Maxwell, T.A. (1995): Ages of Quaternary pluvial episodes determined by uranium-series and radiocarbon dating of lacustrine deposits of Eastern Sahara. – Palaeogeography, Palaeoclimatology, Palaeoecology, 113: 227-242.

Tagma, T., Hsissou, Y., Bouchaou, L., Bouragba, L. & Boutaleb, S. (2009): Groundwater nitrate pollution in Souss-Massa basin (south-west Morocco). – African Journal of Environmental Science and Technology, Vol.3, 10: 301-309.

Tang, Y., Reed, P., Wagener, T., & van Werkhoven, K. (2007): Comparing sensitivity analysis methods to advance lumped watershed model identification and evaluation. – Hydrol. Earth Syst. Sci., 11: 793–817.

Taupin, J.D., Coudrain-Ribstein, A., Gallaire, R., Zuppi, G.M. & Filly, A. (2000): Rainfall characteristics (δ12O, δ2H, ΔT and ΔHr) in western Africa: Regional scale and influence of irrigated areas. – Journal of Geophysical Research, 105(D9): 11911-11924.

Taupin, J.D., Gaultier, G., Favreau, G., Leduc, C. & Marlin, C. (2002): Variabilité isotopique des précipitations sahéliennes à différentes échelles de temps à Niamey (Niger) entre 1992 et 1999: implication climatique. – C. R. Geoscience, 334: 43–50.

Martin, S. (2006): Influence de tourisme sur la gestion de l'eau en zone aride exemple de la vallée du Drâa (Maroc). Dissertation. University of Lausanne.

Thomas, R.J., Fekkak, A., Ennih, N., Errami, E., Loughlin, S.C., Gresse, P.G., Chevallier, L.P. & Liegeois, J.P. (2004): A new lithostratigraphic framework for the Anti-Atlas Orogen, Morocco. – Journal of African Earth Sciences, 39: 217–226.

Timlin, D., Starr, J., Cady, R. & Nicholson, T. (2003): Comparing ground-water recharge estimates using advanced monitoring techniques and models. US Nuclear Regulatory Commission Report NUREG/CR-6836, Washington, DC.

Tooth, S. (2000): Process, form and change in dryland rivers: A review of recent research. – Earth Science Reviews, 51: 67–107.

Toth, J. (1963): A theoretical analysis of groundwater flow in small drainage basins. – Journal of Geophysical Research, 68(16): 4795-4812.

Toth, J. (1995): Hydraulic continuitiy in large sedimentary basins. – Hydrogeology, 3(4): 4-16.

Tsang, C. (1991): The modeling process and model validation. – Ground Water, 29(6): 825-831.

Tweed, S.O., Leblanc, M, Webb, J.A. & Lubczynski, M.W. (2007): Remote sensing and GIS for mapping groundwater recharge and discharge areas in salinity prone catchments, southeastern Australia. – Hydrogeology Journal, 15: 75-96.

Uliana, M.M. & Sharp Jr., J.M. (2001): Tracing regional flow paths to major springs in Trans-Pecos Texas using geochemical data and geochemical models. – Chemical Geology, 179: 53-72.

Van Reeuwijk, L.P. van (1992): Procedure of soil analysis. – ISRIC. Wageningen. 100 pp.

Vengosh, A., Hening, S., Ganor, J., Mayer, B., Weyhenmeyer, C.E., Bullen, T.D. & Paytan, A. (2007): New isotopic evidence for the origin of groundwater from the Nubian Sandstone Aquifer in the Negev, Israel. – Applied Geochemistry, 22: 1052–1073.

Wahi, A., Hogan, J., James F. Hogan, Brenda Ekwurzel, Matthew N. Baillie Christopher J. Eastoe (2008): Geochemical Quantification of Semiarid Mountain Recharge. – Groundwater 46(3): 414-425.

Weber, B. (2004): Untersuchungen zum Bodenwasserhaushalt und Modellierung der Bodenwasserflüsse entlang eines Höhen- und Ariditätsgradienten (SE Marokko). – PhD-Thesis, University of Bonn.

Weismann, G.S., Yong, Z., Fogg, G.E., Blake, R.G., Noyes, C.D. & Maley, M. (2002): Modeling alluvial fan aquifer heterogeneity at multiple scales through stratigraphic assessment. – Proceedings of the International Groundwater Symposium, Lawrence Brekeley National Laboratory, Berkeley, California, March 25-28: 10 pp.

Wheater, H. & Al-Weshah, R.A. (2002): Hydrology of Wadi systems. IHP Regional Network on Wadi Hydrology in the Arab region. – Technical Documents in Hydrology, 55.

Wheater, H. (2002): Hydrological processes in arid and semi-arid regions. In Al-Weshah, R.A. & Wheater,H., eds.(2002): Hydrology of Wadi systems. IHP Regional Network on Wadi Hydrology in the Arab region. – Technical Documents in Hydrology, 55: 5–22.

Wilson, J.L. & Guan, H. (2004): Mountain-Block Hydrology and Mountain-Front Recharge. – Groundwater Recharge in A Desert Environment: The Southwestern United States Vol. 9. - edited by Hogan JF, Phillips FM, Scanlon BR. American Geophysical Union: 113–137. Washington, DC.

Winter, T.C. (1999): Relation of streams, lakes, and wetlands to groundwater flow systems. – Hydrogeology Journal, 7: 28-45.

Wittenberg, H. (1999): Baseflow recession and recharge as nonlinear storage processes. – Hydrological Processes, 13: 715-726.

Woessner, W.W. (2000): Stream and fluvial plain groundwater interactions: rescaling hydrogeological thought. – Ground Water, 38(3): 423–429.

Wood (1999)

Wood, W.W., Rainwater, K.A. & Thompson, D.B. (1997): Quantifying Macropore Recharge: Examples from a Semi-Arid Area. – Ground Water, 35, No. 6: 1097-1106.

Wood, W.W.,& Sanford, W.E. (1995): Chemical and Isotopic Methods for Quantifying Ground-Water Recharge in a Regional, Semiarid Environment. – U.S. Geological Survey

Xu, Y. & Beekman, H.E. (eds) (2003): Groundwater Recharge Estimation in Southern Africa. UNESCO IHP Series No. 64, Paris.

Yechieli, Y. & Wood, W. (2002): Hydrogeologic processes in saline systems: playas, sabkhas, and saline lakes. – Earth Science Reviews, 58:343-365.

Yu, Z. (2002): Hydrology: modeling and prediction. In: Encyclopedia of Atmospheric Science. – Academic Press, 3: 980-986.

Zagana, E., Obeidat, M., Kuells, Ch. & Udluft, P. (2007): Chloride, hydrochemical and isotope methods of groundwater recharge estimation in eastern Mediterranaen areas: a case study in Jordan. – Hydrological Processes, 21: 2112-2123.

Zuber, A. & Maloszewski, P. (2001): Lumped-parameter models. Environmental Isotopes in the Hydrological Cycle. – UNESCO, Tech. Doc. in Hydrology, 39: 5–35.

Zuppi, G.M. & Sacchi, G. (2004): Hydrogeology as a climate recorder: Sahara-Sahel (North Africa) and the Po Plain (Northern Italy). – Global and Planetary Change, 40: 79-91.

List of Publications

Heidecke, C., Kuhn, A. and Klose, S., 2008, Water pricing options for the Middle Drâa River Basin in Morocco. AfJARE, 2(2):170-187.

Klose, S., Reichert, B. and Lahmouri A., 2008, Management options for a sustainable groundwater use in the Middle Drâa Oases under the pressure of climatic changes. In: Zereini, F. and Hötzl, H. (eds): Climatic Changes and Water Resources in the Middle East and North Africa. Springer, Berlin, 552 pp.

Laudien, R., Klose, S., Klose, A., Rademacher, C. and Brocks, S., 2008, Implementation of non-Java based interfaces to embed existing models in Spatial Decision Support Systems - Case study: Integration of MS® Excel-models in IWEGS. - Proc. XXXVII, Part B2:527-532, Commission II (Edited by: Chen, J., Jiang J., Kainz, W.), ISPRS Congress, 3-11 July 2008, Beijing, China, ISSN 1682-1750.

Klose, S., 2008, Hydrogeological Map of the Drâa Basin. In: Schulz, O. and Judex, M. (ed.): IMPETUS Atlas Morocco. Research Results 2000–2007. 3. Edition. Department of Geography, University of Bonn, Germany.

Cappy, S., Klose, S., Hoffmann, H., Osterholt, V. and Bell, S., 2008, Hydrogeology of the Assif-n-Ait Ahmed catchment. In: Schulz, O. and Judex, M. (ed.): IMPETUS Atlas Morocco. Research Results 2000–2007. 3. Edition. Department of Geography, University of Bonn, Germany.

Klose, S. and Haaken, K., 2008, Groundwater quality in Ouled Yaoub. In: Schulz, O. and Judex, M. (ed.): IMPETUS Atlas Morocco. Research Results 2000–2007. 3. Edition. Department of Geography, University of Bonn, Germany.

A. Klose, H. Busche, S. Klose, O. Schulz, B. Diekkruger, B. Reichert and M. Winiger, 2010, Hydrological processes and soil degradation in Southern Morocco. In: P. Speth, M. Christoph and B. Diekkrüger, Impact of Global Change on the Hydrological Cycle in West and Northwest Africa. Springer publisher, ISBN 978-3-642-12956-8.

S. Klose, H. Busche, A. Klose, O. Schulz, B. Diekkrüger, B. Reichert and M. Winiger, 2010, Impacts of Global Change on water resources and soil salinity in Southern Morocco. In: P. Speth, M. Christoph and B. Diekkrüger, Impact of Global Change on the Hydrological Cycle in West and Northwest Africa. Springer publisher, ISBN 978-3-642-12956-8.

Annex

Adjoint to this work a medium of digitzed data is available that carries data of the following subjects:

- Bore logs
- Groundwater level data
- Anorganic hydrochemical data
- Geochemical data
- BIL model (including model input, output, and sensitivity analysis)